

**THE DEVELOPMENT OF IMMUNOASSAYS FOR THE  
DETECTION OF BOVINE BRUCELLOSIS AND  
AFLATOXIN B<sub>1</sub>**

**A thesis submitted for the degree of Ph.D.**

**by**

**Lynsey Dunne B.Sc. (Hons), M.Sc.**

**September 2004**



**Based on research carried out at  
School of Biotechnology, Dublin City University,  
Dublin 9, Ireland.**

**Under the supervision of Professor Richard O'Kennedy**

**This thesis is dedicated to my Mam and Dad**

**Declaration**

I hereby certify that the material, which I now submit for assessment on the programme of study leading to the award of Ph.D., is entirely my own work and has not been taken from the work of others save and to the extent that such work has been cited and acknowledged within the text of my work.

Signed: Lynsey Dunne

Date: 29/11/04

## **Acknowledgements**

Firstly, I would like to express my sincere gratitude and appreciation to my supervisor, Prof. Richard O’Kennedy, for his patience, guidance and support throughout the course of my Ph.D. His insight, experience and enthusiasm was greatly appreciated. I would also like to thank the members of the Applied Biochemistry Group, both past and present. A very special thanks to “The Girls” (Liz, Sharon, Joanne and Sinead L.) for their support, encouragement and above all their excellent friendship over the past few years. Thanks for all the laughs!!

The financial and technical support from the Department of Agriculture, Food and Fisheries was also greatly appreciated. I wish to extend a special word of thanks to Michael Sheehan and Michael Sheridan (Agriculture House, Dublin) and to Terry Heneghan, Seamus Power and Paddy Reilly (Blood Testing Laboratory, Cork) for the serum samples, *Brucella* cells, and above all the encouragement.

Special thanks to all my great friends from home (Amanda, Deirdre, Paula, Caitríona, Emma, Nicola and Niamh) and Maynooth (Maighréad, Ger, Diane, Claire, Cathy and Edel) who have always been there for me. Thanks for everything.

Above all I would like to express my sincere appreciation and thanks to my wonderful family. To my Mam and Dad who have always been there for me, encouraged me and believed in me, without whom this would never have been possible. I would also like to thank my brothers Lee, Simon and Emmet, my sisters in-law, Ciara and Georgina, and my adorable nephew Liam.

## Table of contents

<b>Declaration</b>	iii
<b>Acknowledgements</b>	iv
<b>Table of contents</b>	v
<b>Abbreviations</b>	xvi
<b>Units</b>	xix
<b>Publications</b>	xx
<b>Presentations</b>	xxi
<b>Abstract</b>	xxii
<b>Chapter 1: Introduction</b>	1
<b>1.1 Immunity to infection</b>	2
1.1.1 Innate immunity	2
1.1.2 Acquired Immunity	3
<i>1.1.2.1 Cell-mediated immunity</i>	3
<i>1.1.2.2 Humoral Immunity</i>	4
<b>1.2 Lymphatic system</b>	5
<b>1.3 Antibody structure</b>	8
<b>1.4 Genetic basis of antibody diversity</b>	12
<b>1.5 Antibody production</b>	16
1.5.1 Polyclonal antisera	16
1.5.2 Monoclonal antibody production	16
<b>1.6 Antibody fragments</b>	20
<b>1.7 Phage display technology</b>	22
1.7.1 The Filamentous Phage	22
1.7.2 Expression vectors	23
1.7.3 Library construction	24
1.7.4 Antibody repertoires	26
<i>1.7.4.1 Naïve repertoires</i>	26
<i>1.7.4.2 Immunised repertoires</i>	26
<i>1.7.4.3 Synthetic repertoires</i>	27

1.7.5	Isolation of specific antibody fragments from antibody repertoires	28
1.7.6	Soluble expression of antibody fragments	30
1.7.7	Purification of antibody fragments	31
1.7.8	Affinity maturation of antibody fragments	32
1.7.8.1	<i>Multivalent molecules</i>	32
1.7.8.2	<i>Site-directed mutagenesis</i>	32
1.7.8.3	<i>Error-prone PCR</i>	33
1.7.8.4	<i>Chain shuffling</i>	33
1.7.8.5	<i>Ribosomal display</i>	34
1.7.9	Krebber scFv phage display system	36
<b>1.8</b>	<b>Immunoassays</b>	39
1.8.1	Enzyme-linked immunosorbent assay (ELISA)	40
1.8.2	Lateral-flow immunoassay (LFIA)	44
<b>1.9</b>	<b>Biacore</b>	46
<b>1.10</b>	<b>Aims of research</b>	53
<b>Chapter 2:</b>	<b>Materials and methods</b>	54
<b>2.1</b>	<b>Material and equipment</b>	55
2.1.1	Material	55
2.1.2	Equipment	56
2.1.3	Composition of culture media	55
2.1.4	Buffers	59
2.1.5	Bacterial strains	60
<b>2.2</b>	<b>The production of genetically derived anti-aflatoxin B1 scFvs</b>	61
2.2.1	Aflatoxin B1 (AFB1) scFv Phage Display Library	61
2.2.2	Plasmid DNA purification using Wizard Plus SV miniprep DNA purification system	61
2.2.3	Sfi1 restriction enzyme digest	62
2.2.4	Agarose gel electrophoresis for DNA characterisation	62
2.2.5	DNA agarose gel purification	62
2.2.6	Ligation of scFv insert and pAK plasmid DNA	63
2.2.7	Preparation of competent <i>E.coli</i> cells	63

2.2.8	Transformation of JM83 <i>E.coli</i> with pAK vectors containing the scFv insert	64
2.2.9	Soluble scFv production	64
2.2.10	Isolation of scFvs from the periplasm	64
2.2.11	Sequence analysis on the gene encoding the AFB1-specific scFv	64
2.2.12	Sodium dodecyl sulphate – polyacrylamide gel electrophoresis (SDS-PAGE)	65
2.2.13	Coomassie blue staining	67
2.2.14	Western blot analysis	67
2.2.15	ELISA analysis of soluble anti-AFB1 scFv antibodies	68
	2.2.15.1 <i>Checkerboard ELISA for the determination of conjugate coating concentration and optimal scFv antibody dilution for use in a competitive ELISA</i>	68
	2.2.15.2 <i>Indirect competitive enzyme-linked immunosorbent assay (ELISA) for the detection of AFB1</i>	68
	2.2.15.3 <i>Direct competitive ELISA for the detection of AFB1 using the pAK600 alkaline phosphatase-labelled scFv</i>	69
	2.2.15.4 <i>Measurement of cross-reactions</i>	69
2.2.16	Development of a lateral flow immunoassay (LFIA) for the detection of AFB1	70
	2.2.16.1 <i>Physical adsorption of protein onto colloidal carbon particles</i>	70
	2.2.16.2 <i>Spraying and production of nitrocellulose strips</i>	71
	2.2.16.3 <i>Running test strips</i>	71
2.2.17	Development of a Biacore inhibition immunoassay for the detection of AFB1	74
	2.2.17.1 <i>AFB<sub>1</sub> Sensor Chip</i>	74
	2.2.17.2 <i>Sample Preparation for use in Inhibitive Assay</i>	74
	2.2.17.3 <i>Surface Regeneration</i>	74
	2.2.17.4 <i>Measurement of Cross-Reactivity</i>	74
<b>2.3</b>	<b>Cloning and expression of <i>Brucella</i>-specific proteins</b>	<b>75</b>
2.3.1	Isolation of <i>Brucella abortus</i> genomic DNA	75
2.3.2	Primer design	75
2.3.3	PCR amplification of genes encoding the <i>Brucella</i> -specific proteins	77

2.3.4	Ligation of PCR products and pCR2.1 plasmid	78
2.3.5	Transformation of INV $\alpha$ F' with pCR2.1, containing the cloned insert	78
2.3.6	BamH1 and Nco1 restriction analysis on pCR2.1, containing the cloned insert	79
2.3.7	Sub-cloning of cloned insert from pCR2.1 into pQE-60	79
2.3.8	Transformation of competent XL-10 Gold <i>E.coli</i> cells with pQE-60 containing the cloned inserts	80
2.3.9	BamH1/Nco1 restriction analysis on XL-10 Gold <i>E.coli</i> transformed with pQE-60	80
2.3.10	Sequencing of cloned inserts	80
2.3.11	Small-scale expression culture	80
2.3.12	Optimisation of IPTG concentration	81
2.3.13	Optimisation of sonication conditions	81
2.3.14	Time course expression cultures	81
2.3.15	Large-scale expression culture	81
2.3.16	IMAC purification of the 6xHis-tagged recombinant proteins	82
2.3.17	Bicinchoninic acid (BCA) assay	82
<b>2.4</b>	<b>Antibody production</b>	<b>84</b>
2.4.1	Antigen preparation	84
2.4.1.1	<i>Isolation of the crude cytoplasmic fraction from <u>Brucella abortus</u> 45/24</i>	84
2.4.1.2	<i><u>Brucella abortus</u> 45/20 cells</i>	84
2.4.2	Licencing	84
2.4.3	Rabbit immunisation protocol	84
2.4.4	Preparation of rabbit serum	85
2.4.5	Polyclonal antibody purification	85
2.4.5.1	<i>Saturated ammonium sulphate (SAS) precipitation</i>	85
2.4.5.2	<i>Protein G affinity-chromatography</i>	85
2.4.6	Determination of polyclonal antibody titre	86
2.4.7	Checkerboard ELISA for the determination of optimal cell-coating concentrations and optimal antibody dilution for use in a competitive ELISA	87

2.4.8	Indirect competitive enzyme-linked immunosorbent assay (ELISA) for the detection of <i>B. abortus</i>	87
2.4.9	Measurement of cross-reactions	88
<b>2.5</b>	<b>Screening for scFv phage display antibodies from a naïve phage display library</b>	<b>88</b>
2.5.1	Selection of antigen binders by panning in immunotubes	88
2.5.2	Re-infection of XL-1 Blue <i>E. coli</i> cells with eluted phage	88
2.5.3	Storage and rescue of phagemids antibodies after selection	89
2.5.4	Rescue of phagemids clones in microtitre trays for phage ELISA	89
2.5.5	Phage ELISA	90
2.5.6	Soluble ELISA	90
2.5.7	Sequence analysis on the gene encoding the bp26-specific scFvs	91
2.5.8	Checkerboard ELISA for the determination of optimal bp26 coating concentration and optimal scFv dilution for use in a competitive ELISA	91
2.5.9	Indirect competitive enzyme-linked immunosorbent assay (ELISA) for the detection of bp26	92
<b>2.6</b>	<b>Development of diagnostic assays for the detection of bovine brucellosis</b>	<b>92</b>
2.6.1	Indirect enzyme-linked immunosorbent assay for the detection of bovine brucellosis in serum samples	93
2.6.2	Sandwich enzyme-linked immunosorbent assay for the detection of bovine brucellosis in serum samples	93
<b>Chapter 3:</b>	<b>The production and characterisation of genetically derived scFv antibody fragments directed against aflatoxin B<sub>1</sub> (AFB<sub>1</sub>)</b>	<b>95</b>
<b>3.1</b>	<b>Introduction</b>	<b>96</b>
3.1.1	Chemical and physical properties of aflatoxins	96
3.1.2	Aflatoxin production and biosynthesis	98
3.1.3	Mode of action of aflatoxins	100
3.1.4	Toxicity of aflatoxins	102
3.1.5	Aflatoxin sampling and analysis	103

3.1.6	Methods of control and management of aflatoxins	106
3.1.7	Chapter outline	108
<b>3.2</b>	<b>Results</b>	109
3.2.1	Production of genetically derived scFv antibodies to Aflatoxin B <sub>1</sub>	109
3.2.1.1	<i>Construction of a pre-immunised phage display library for the isolation of functional scFvs against aflatoxin B<sub>1</sub></i>	109
3.2.1.2	<i>Isolation and nucleotide and amino acid sequence analysis on an AFB<sub>1</sub>-specific scFv</i>	109
3.2.1.3	<i>SfiI restriction digest on pAK100/400/500/600</i>	112
3.2.1.4	<i>Ligation and transformation of pAK400/500/600 into JM83 <u>E. coli</u></i>	113
3.2.1.5	<i>Soluble expression of the monomeric, dimeric and alkaline phosphatase-labelled scFvs</i>	113
3.2.1.6	<i>Western blot analysis on the monomeric, dimeric and bifunctional scFvs</i>	115
3.2.2	The use of genetically derived scFvs in the development of immunoassays for the detection of AFB <sub>1</sub>	116
3.2.2.1	<i>Development of Competitive ELISAs for the detection of aflatoxin B<sub>1</sub></i>	116
3.2.2.1.1	Optimisation of assay parameters for competitive ELISA for AFB <sub>1</sub>	116
3.2.2.1.2	Optimisation of methanol concentration for the preparation of free AFB <sub>1</sub>	120
3.2.2.1.3	Development of competitive ELISAs for AFB <sub>1</sub>	122
3.2.2.1.4	Cross-reactivity studies	126
3.2.2.2	<i>Development of Biacore inhibition assays for the detection of aflatoxin B<sub>1</sub></i>	130
3.2.2.2.1	Assessment of non-specific binding	130
3.2.2.2.2	Regeneration studies	133
3.2.2.2.3	Development of a Biacore inhibition assays for the detection of AFB <sub>1</sub>	137
3.2.2.2.4	Cross-Reactivity Studies	142
3.2.2.3	<i>Development of a lateral flow immunoassay (LFIA) for the detection of AFB<sub>1</sub></i>	145

3.2.2.3.1	Indirect competitive LFIA	145
3.2.2.3.2	Optimisation of flow-rate	147
3.2.2.3.3	Optimisation of control line	147
3.2.2.3.4	Development and optimisation of test line	149
3.2.2.3.5	Development of indirect competitive LFIA for the detection of AFB <sub>1</sub>	152
3.2.2.4	<i>Summary of results</i>	153
<b>3.3</b>	<b>Discussion</b>	154
<b>Chapter 4:</b>	<b>The cloning and expression of an 18kDa cytoplasmic and a 26kDa periplasmic <i>Brucella</i>-specific protein</b>	165
<b>4.1</b>	<b>Introduction</b>	166
4.1.1	TA cloning	166
4.1.2	QIAexpress cloning	167
4.1.3	Protein expression	169
4.1.3.1	<i>Protein solubility</i>	169
4.1.3.2	<i>Expression hosts</i>	170
4.1.3.2.1	<i>E. coli</i>	170
4.1.3.2.2	Yeast	172
4.1.3.2.3	Baculovirus	172
4.1.3.2.4	Mammalian cells	172
4.1.3.3	<i>The 6xHis tag</i>	173
4.1.4	Immobilised metal affinity chromatography (IMAC)	173
4.1.5	Chapter outline	176
<b>4.2</b>	<b>Results</b>	178
4.2.1	PCR amplification of the genes encoding p18 and bp26	178
4.2.2	TA cloning	180
4.2.3	Sub-cloning from pCR2.1 into pQE-60 and subsequent transformation into competent XL-10 Gold <i>E. coli</i>	182
4.2.4	Initial small-scale protein expression	184
4.2.5	Protein solubility determination	187

4.2.6	Optimisation of IPTG concentration for induction of protein expression	189
4.2.7	Optimisation of sonication conditions	192
4.2.8	Time-course analysis on the expression of p18 and bp26	195
4.2.9	Immobilised metal affinity chromatography (IMAC) purification of p18 and bp26	298
4.2.10	Nucleotide and amino acid sequence analysis on the recombinant p18 and bp26 proteins cloned in pQE-60	201
4.2.11	Immunogenicity studies on the recombinant p18 and bp26 expressed in XL-10 Gold <i>E. coli</i>	205
<b>4.3</b>	<b>Discussion</b>	<b>207</b>
 <b>Chapter 5: The production and characterisation of <i>Brucella</i>-specific polyclonal antibodies and scFv antibody fragments</b>		<b>214</b>
 <b>5.1 Introduction to <i>Brucella</i></b>		<b>215</b>
5.1.1	Taxonomy and classification of the genus <i>Brucella</i>	215
5.1.2	<i>Brucella</i> pathogenesis	217
5.1.3	Immunity and protection against <i>Brucella</i>	218
5.1.4	<i>Brucella abortus</i> 45/20	219
<b>5.2</b>	<b>Results</b>	<b>221</b>
5.2.1	Production and purification of polyclonal anti- <i>Brucella</i> antibodies	221
5.2.1.1	<i>Estimation of antibody titres in rabbit serum</i>	221
5.2.1.2	<i>Purification of polyclonal anti-sera</i>	223
5.2.1.3	<i>Characterisation of purified antibodies by SDS-PAGE</i>	224
5.2.1.4	<i>Western Blot analysis of purified antibodies</i>	224
5.2.1.5	<i>Development of competitive ELISAs for the detection of <i>B. abortus</i></i>	229
5.2.1.5.1	Optimisation of competitive ELISA for the detection of <i>B. abortus</i>	229
5.2.1.5.2	Development of competitive ELISAs for the detection of <i>B. abortus</i>	232
5.2.1.5.3	Cross-reactivity studies	237

5.2.1.6	<i>Antibody binding reactivity analysis on pAB1 and pAB2</i>	240
5.2.2	The isolation of <i>Brucella</i> -specific scFv antibody fragments from a naïve phage display library	243
5.2.2.1	<i>Panning procedure for the detection of scFv phage display antibodies directed against p18</i>	244
5.2.2.2	<i>Panning procedure for the detection of scFv phage display antibodies directed against bp26</i>	247
5.2.2.3	<i>Analysis on the soluble anti-bp26 scFvs for recognition of free bp26</i>	250
5.2.2.4	<i>Nucleotide and amino acid sequence analysis on clones B7, B11, C12 and D7</i>	252
5.2.2.5	<i>Western blot analysis on the specific detection of bp26 using the B7 scFv</i>	257
5.2.2.6	<i>ELISA analysis of the soluble B7 scFv antibody directed against bp26</i>	259
5.2.2.6.1	Checkerboard ELISA for the determination of the optimal scFv antibody dilution and bp26 concentration for use in a competitive ELISA	259
5.2.2.6.2	Intra- and inter-day assay variability studies of the B7 scFv antibody	261
5.2.2.6.3	Cross-reactivity studies on the anti-bp26 scFv	264
5.2.2.7	<i>Investigations on the use of the anti-bp26 scFv in the development of an immunoassay for the detection of <i>Brucella abortus</i></i>	265
<b>5.3</b>	<b>Discussion</b>	<b>266</b>
<b>Chapter 6:</b>	<b>The development and validation of immunoassay for the detection of bovine brucellosis in serum samples</b>	<b>276</b>
<b>6.1</b>	<b>Introduction to <i>Brucella</i></b>	<b>277</b>
6.1.1	Brucellosis	277
6.1.2	Brucellosis in Ireland	277
6.1.3	Conventional methods for the detection of Brucellosis	279

6.1.3.1	<i>Rose Bengal Plate Test (RBPT)</i>	279
6.1.3.2	<i>Complement Fixation Test (CFT)</i>	279
6.1.3.3	<i>Buffered Brucella Plate agglutination Test (BBAT)</i>	280
6.1.3.4	<i>Rapid Slide Agglutination Test (RSAT)</i>	280
6.1.3.5	<i>Serum Agglutination Test (SAT)</i>	280
6.1.4	Immunoassays for the diagnosis of brucellosis	280
6.1.4.1	<i>ELISAs for the diagnosis of brucellosis</i>	280
6.1.4.2	<i>Fluorescent polarisation assay (FPA) for the diagnosis of brucellosis</i>	281
6.1.5	Proteins as serological diagnostic markers of brucellosis	282
6.1.6	ELISA validation	284
<b>6.2 Results</b>		285
6.2.1	Feasibility studies	285
6.2.2	Assay development and standardisation	287
6.2.2.1	<i>Optimisation of blocking reagents and antibody diluent</i>	287
6.2.2.2	<i>Optimisation of antigen coating concentrations/dilutions for use in the indirect ELISAs</i>	291
6.2.2.3	<i>Optimisation of antibody coating dilutions for use in the sandwich ELISAs</i>	292
6.2.2.4	<i>Optimisation of antigen concentrations/dilutions for use in the sandwich ELISAs</i>	293
6.2.2.5	<i>Optimisation of serum dilutions for use in the indirect and sandwich ELISAs</i>	294
6.2.2.6	<i>Optimisation of anti-bovine secondary antibody dilution for use in the indirect and sandwich ELISAs</i>	295
6.2.2.7	<i>Initial estimates on the repeatability of the indirect and sandwich ELISAs</i>	296
6.2.3	Characterisation of assay performance	300
6.2.3.1	<i>Performance characterisation on the indirect and sandwich ELISAs</i>	300
<b>6.3 Discussion</b>		313

<b>Chapter 7: Conclusions</b>	319
<b>7.1 Overall conclusions and future work</b>	320
<b>Chapter 8: References</b>	324
<b>Appendix A</b>	354

## **Abbreviations**

<b>AFB<sub>1</sub></b>	<b>Aflatoxin B<sub>1</sub></b>
<b>AFB<sub>1</sub>-BSA</b>	<b>Aflatoxin B<sub>1</sub>-bovine serum albumin</b>
<b>AP</b>	<b>Alkaline phosphatase</b>
<b>APC</b>	<b>Antigen presenting cell</b>
<b>AT</b>	<b>Annealing temperature</b>
<b>BCA</b>	<b>Bicinchoninic acid</b>
<b>BIA</b>	<b>Biospecific interaction analysis</b>
<b>BSA</b>	<b>Bovine serum albumin</b>
<b>C</b>	<b>Constant</b>
<b>cDNA</b>	<b>Complementary deoxyribonucleic acid</b>
<b>CDR</b>	<b>Complementary determining regions of antibody</b>
<b>cfu</b>	<b>Colony forming unit</b>
<b>C<sub>H</sub></b>	<b>Constant heavy chain</b>
<b>C<sub>L</sub></b>	<b>Constant light chain</b>
<b>CM</b>	<b>Carboxyl-methyl</b>
<b>CTL</b>	<b>Cytotoxic T-lymphocyte</b>
<b>CTY</b>	<b>Crude cytoplasmic lysate</b>
<b>CV</b>	<b>Coefficient of variation</b>
<b>D</b>	<b>Diversity</b>
<b>DAFF</b>	<b>Department of Agriculture, Food and Fisheries</b>
<b>DNA</b>	<b>Deoxyribonucleic acid</b>
<b>DSn</b>	<b>Diagnostic sensitivity</b>
<b>DSp</b>	<b>Diagnostic specificity</b>
<b>EIA</b>	<b>Enzyme immunoassay</b>
<b>ELISA</b>	<b>Enzyme-linked immunosorbent assay</b>
<b>EU</b>	<b>European union</b>
<b>Fab</b>	<b>Antigen binding fragment of an antibody</b>
<b>FIA</b>	<b>Fluorescence immunoassay</b>
<b>FR</b>	<b>Framework region</b>
<b>Fv</b>	<b>Variable fragment</b>
<b>GC</b>	<b>Gas chromatography</b>
<b>GLC</b>	<b>Gas-liquid chromatography</b>
<b>H</b>	<b>Heavy chain</b>

HAT	Hypoxanthine, aminopterin and thymidine
HBS	Hepes buffered saline
HGPRT	Hypoxanthine guanine phosphoribosyl transferase
His	Histidine
HPLC	High performance liquid chromatography
HRP	Horse-radish peroxidase
IC <sub>50</sub>	50% inhibition concentration
IDA	Iminodiacetic acid
IFN	Interferon
Ig	Immunoglobulin
IL	Interleukin
IMAC	Immobilised metal affinity chromatography
IPTG	Isopropyl-β-D-galactopyranoside
J	Joining
L	Light chain
LB	Luria broth
LC	Lethal concentration
LD	Lethal dose
LDD	Least detectable dose
LED	Light emitting diode
LFIA	Lateral flow immunoassay
LPS	Lipopolysaccharide
MHC	Major histocompatibility complex
MRL	Maximum residue level
mRNA	Messenger ribonucleic acid
MS	Mass spectroscopy
MW	Molecular weight
NSS	National Standard Serum
NTA	Nitrilotriacetic acid
OD	Optical density
OIE	Organisation Internationale des Epizootics (World Organisation for Animal Health)
OPD	o-phenylenediamine dihydrochloride

PBS	Phosphate buffered saline
PBST	Phosphate buffered saline-tween
PCR	Polymerase chain reaction
PEG	Polyethylene glycol
PFGE	Pulse field gel electrophoresis
pH	Negative log of the hydrogen ion concentration
pI	Isoelectric point
pNPP	<i>para</i> -nitrophenyl phosphate
RIA	Radioimmunoassay
RT-PCR	Reverse transcription polymerase chain reaction
SAS	Saturated ammonium sulphate
scFv	Single chain variable fragment
SD	Standard deviation
SDS-PAGE	Sodium dodecyl sulphate polyacrylamide gel electrophoresis
SOC	Super Optimum Catabolite
SOE-PCR	Splice-by-overlap extension polymerase chain reaction
SPIA	Sol particle immunoassay
SPR	Surface plasmon resonance
TAE	Tris acetic acid-ethylene diamine tetra acetic acid
TBS	Tris buffered saline
Tc	Cytotoxic T-cell
TES	Tris-EDTA sucrose buffer
Th	T-helper
TIR	Total internal reflectance
TLC	Thin layer chromatography
TNF	Tumour necrosis factor
TY	Tryptone yeast extract
up	Ultra pure
UV	Ultra violet
V	Variable
V <sub>H</sub>	Variable heavy chain of antibody
V <sub>L</sub>	Variable light chain of antibody
X-gal	X-galactosidase

**Units**

<b>°C</b>	<b>degrees Celsius</b>
<b>μg</b>	<b>micrograms</b>
<b>(k)Da</b>	<b>(kilo) Daltons</b>
<b>μl</b>	<b>microlitres</b>
<b>μM</b>	<b>micromoles</b>
<b>bp</b>	<b>base pairs</b>
<b>cm</b>	<b>centimetres</b>
<b>g</b>	<b>grams</b>
<b>kb</b>	<b>kilobases</b>
<b>kg</b>	<b>kilograms</b>
<b>l</b>	<b>litres</b>
<b>m</b>	<b>metres</b>
<b>M</b>	<b>molar</b>
<b>mA</b>	<b>milliamps</b>
<b>mg</b>	<b>milligrams</b>
<b>min</b>	<b>minutes</b>
<b>ml</b>	<b>millilitres</b>
<b>mM</b>	<b>milimolar</b>
<b>mol</b>	<b>molar</b>
<b>nm</b>	<b>nanometres</b>
<b>nM</b>	<b>nanomolar</b>
<b>pg</b>	<b>picograms</b>
<b>ppb</b>	<b>parts per billion</b>
<b>rpm</b>	<b>revolutions per minute</b>
<b>RU</b>	<b>response units</b>
<b>sec</b>	<b>seconds</b>
<b>U</b>	<b>units</b>
<b>V</b>	<b>volts</b>
<b>v/v</b>	<b>volume per unit volume</b>
<b>w/v</b>	<b>weight per unit volume</b>

### Peer-reviewed journal publications

Daly, S., Dillon, P., Brennan, J., **Dunne, L.**, Fitzpatrick, J. and O'Kennedy R. (2001). Production and analytical applications of scFv antibody fragments. *Anal. Lett.*, 34(11), 1799 – 1827.

Daly, S., Dillon, P., Manning, B., **Dunne, L.**, and O'Kennedy, R. (2003) Production and characterisation of murine single chain Fv antibodies to Aflatoxin B<sub>1</sub> derived from a pre-immunised antibody phage display library system. *Food Agric. Immunol.* 14(4), 255 – 274.

**Dunne, L.**, Daly, S. and O'Kennedy, R. The use of monomeric, dimeric and bifunctional scFvs in the development of immunoassays for the detection of aflatoxin B<sub>1</sub> (AFB<sub>1</sub>). Submitted to the *Analyst* (2004).

**Dunne, L.**, Daly, S., Baxter A., Haughey, A. and O'Kennedy, R. (2004). The use of surface plasmon resonance-based scFv immunoassay for the detection of aflatoxin B<sub>1</sub> (AFB<sub>1</sub>). *Spectroscopy Letters* (In press).

Leonard, P., Hearty, S., Brennan, J., **Dunne, L.**, Quinn, J., Chakraborty, T. and O'Kennedy, R. (2003). Advanced in biosensors for detection of pathogens in food and water. *Enzyme and Microbiol Technology*, 32(1), 3 – 13.

## **Presentations**

Daly, S., Dillon, P., **Dunne, L.**, Manning, B.M. and O' Kennedy, R. (2001). Comparison of single chain Fv and polyclonal antibodies for 'real-time' biosensor-based assays for aflatoxin-B<sub>1</sub>. "Environ", Dublin City University, 27-28, January, p. 105.

Daly, S., Dillon, P., Wichers, J., van Amerongen, A., **Dunne, L.** and O'Kennedy, R. (2003). Rapid antibody-based technologies for aflatoxin B<sub>1</sub> detection. "The second World Mycotoxins Forum", Noordwijk aan Zee, Netherlands, 17 – 18 February.

**Dunne, L.** (2002). Immunoassay technology: ELISA and DELFIA. "Training of Trainer's Course: Production and application of antibodies and other immunological reagents incorporating web-based and practical approaches", Dublin City University, 12 – 13 February.

**Dunne, L.** and O'Kennedy R. (2001). Development of DELFIA and ELISA assays for the detection an 18kDa cytoplasmic protein specific to *Brucella abortus*. "Combined COST Meeting for Working Groups 1 (Epidemiology), 2 (Immunology / Diagnosis) and 3 (Harmonisation)", University of Navarra, Pamplona, Spain, 11-12 June.

**Dunne, L.** and O'Kennedy R. Development of ELISA and DELFIA assays for the diagnosis of bovine brucellosis. 6-monthly progress reports, Irish Department of Agriculture, 2001 – 2003.

**Dunne, L.** and O'Kennedy, R. (2003). The production and characterisation of two recombinant proteins, p18 and bp26, for use in the development of an immunoassay for the detection of bovine brucellosis in serum samples. "Brucellosis 2003 International Research Conference", University of Navarra, Pamplona, Spain, 15 – 17 September.

## **Abstract**

The research discussed in this thesis focuses on the development and characterisation of immunoassays for the detection of aflatoxin B<sub>1</sub> (AFB<sub>1</sub>), a toxic fungal metabolite, and for the diagnosis of bovine brucellosis, a highly contagious disease of cattle caused by *Brucella abortus*.

An AFB<sub>1</sub>-specific single chain fragment variable (scFv) was isolated from a pre-immunised phage display library and the gene encoding it sub-cloned into a range of different vectors for soluble expression of monomeric, dimeric and bifunctional scFvs. The genetically-derived scFvs were then applied to the development of competitive ELISAs and BIAcore-based inhibition assays for the detection of AFB<sub>1</sub>. A lateral flow immunoassay (LFIA) was developed for the detection of AFB<sub>1</sub> using an AFB<sub>1</sub>-specific monoclonal antibody. Each immunoassay format described was suitable for the detection of AFB<sub>1</sub>, with high levels of sensitivity, specificity and reproducibility achieved.

Several immunoassay formats for the diagnosis of bovine brucellosis, in serum samples, were investigated. Four antigens were selected as diagnostic markers for brucellosis and included whole *B. abortus* cells, a crude cytoplasmic lysate, an 18kDa cytoplasmic protein (p18) and a 26kDa periplasmic protein (bp26). Recombinant forms of the p18 and bp26 proteins were cloned and expressed using a high-level expression vector in *E. coli*. Two polyclonal antibodies, directed against whole *B. abortus* cells and the crude cytoplasmic lysate, were developed and a naïve phage display library was used to isolate scFvs directed against the recombinant bp26. Feasibility studies were carried out on the indirect ELISAs incorporating the four antigens and on the sandwich ELISAs with the polyclonal antibodies. The indirect and sandwich ELISAs, for the diagnosis of bovine brucellosis, were then validated using a panel of *Brucella*-positive and negative serum samples.

# CHAPTER 1

## Introduction

## **1.1 Immunity to infection**

Two cooperative defence systems have evolved to encounter foreign invasion from potentially dangerous viruses, bacteria and other pathogens. Firstly, the non-specific innate immunity provides two lines of defence and secondly the highly specific acquired immunity provides the third line of defence.

### **1.1.1 Innate immunity**

Non-specific innate immunity is present from birth and fundamentally is not affected by prior contact with foreign particles. Several factors, including physiological and chemical barriers, phagocytic white blood cells, the inflammatory response and complement pathway play critical roles in innate immunity.

The skin and mucous membranes act as the first line of defence against foreign invasion and prevent micro-organisms gaining entry. When intact, the skin is impermeable to infectious agents. The low pH of sweat and sebaceous secretions and the presence of hydrolytic enzymes and fatty acids inhibit microbial growth. Mucous membranes lining the inner surfaces of the body, such as the respiratory and gastrointestinal tracks, trap foreign particles, which are removed from the body by ciliary movement, coughing and sneezing. Pulmonary and alveolar macrophages in the respiratory tract and the hostile conditions within the gastrointestinal tract, such as presence of hydrolytic enzymes in saliva, the low pH of the stomach and proteolytic enzymes in bile, all aid in the elimination of micro-organisms.

Following penetration of the physiological and chemical barriers the second line of defence confronts the invading micro-organism. This involves various specialised cells that destroy the foreign micro-organism by phagocytosis or extracellular killing. Polymorphonuclear leukocytes, which include basophils, mast cells, eosinophils and neutrophils, facilitate in the destruction of invading micro-organisms. These short-lived phagocytic cells contain enzyme-rich lysosomes and produce toxic peroxide and superoxide radicals. Macrophages derived from blood monocytes also play a critical role in phagocytosis and subsequent destruction of the invading micro-organism. Natural killer cells lyse infected cells and tumour cells following the release of cytotoxic molecules.

The inflammatory response plays a critical role in both innate and acquired immunity. It is a complex process initiated by tissue damage that activates clotting, kinin-formation and fibrolytic pathways. It also induces fever, increased white blood cell production, increased synthesis of hydrocortisone and adrenocorticotrophic hormones and production of acute-phase proteins.

The complement system is also involved in innate immunity either by killing invading micro-organisms directly or stimulating ingestion and killing by phagocytic cells.

### **1.1.2 Acquired Immunity**

In contrast to innate immunity, acquired immunity is more specialized and specific. Two main cell types participate in acquired immunity, B-lymphocytes, which differentiate in the bone marrow and T-lymphocytes, which differentiate in the thymus. Acquired immunity can be further divided into cell-mediated immunity, which involves T-lymphocytes, and humoral immunity, which is mediated by B-lymphocytes.

#### **1.1.2.1 Cell-mediated immunity**

Following maturation of T-lymphocytes in the thymus they migrate to lymphoid organs such as the spleen and lymph nodes. T-lymphocytes or T-cells can be subdivided into  $CD4^+$  and  $CD8^+$  T-cells.  $CD4^+$  T-cells, with specific T-cell receptors (TCRs) recognise and bind foreign antigens presented on the surface of antigen presenting cells (APCs) in conjunction with an MHC class II molecule (Fig. 1.1). Stimulation of the  $CD4^+$  T-cell by the peptide-MHC complex results in the release cytokines, which affect the function of several cell types, including  $CD4^+$  and  $CD8^+$  T-cells, B-cells, macrophages and eosinophils. Based on the different cytokines secreted  $CD4^+$  T-cells, which are also known as T helper cells ( $T_H$ ), can be further divided into three subsets,  $T_{H0}$ ,  $T_{H1}$  and  $T_{H2}$ .  $T_{H0}$  cells synthesise IL-2, interferon  $\gamma$  (IFN- $\gamma$ ) and IL-4.  $T_{H1}$  and  $T_{H2}$  cells are produced following the antigen driven differentiation of  $T_{H0}$  cells.  $T_{H1}$  cells release IL-2, IFN- $\gamma$  and tumour necrosis factor beta (TNF- $\beta$ ). These cytokines result in the activation of  $CD8^+$  T-cells, natural killer cells and macrophages, which are involved in cell-mediated immunity.  $T_{H2}$  cells

synthesise IL-4, IL-5, IL-10 and IL-13. The cytokines released by  $T_H2$  cells trigger B-cells to class switch to IgE production and result in the activation of eosinophils.

In contrast to  $CD4^+$  T-cells, the  $CD8^+$  T-cells function in the direct killing of infected cells.  $CD8^+$  T-cells or cytotoxic T lymphocytes (CTLs) recognise a foreign peptide in conjunction with an MHC class I molecule. Interaction between the TCR, on the  $CD8^+$  T-cell, and the peptide-MHC class I complex results in the direct killing of the antigen-presenting cell. Activated  $CD8^+$  CTLs release perforin and granzymes, which perforate the target-cell membrane and induce apoptosis, respectively.  $CD8^+$  T-cells also synthesise the cytokines IFN- $\gamma$  and TNF- $\beta$ , which are associated with a  $T_H1$  response, and IL-4, which is linked with a  $T_H2$  response.

Following antigen stimulation,  $CD4^+$  and  $CD8^+$  T-cells divide into effector cells (as discussed above) and memory cells. The memory cells persist within the body and will multiply and mature if they are re-exposed to the antigen-MHC complex.

### **1.1.2.2 Humoral Immunity**

Humoral immunity is mediated by B-cells and circulating antibodies. Interaction between membrane bound immunoglobulins (Ig), on the surface of B-cells, and a specific antigen results in the activation of B-cells, which start secreting antigen-specific antibodies (Fig. 1.2).  $CD4^+$  T-cells also play a role in the activation of a humoral immune response. Following antigen binding at the B-cell surface the antigen-immunoglobulin complex is internalised and degraded in acid compartments. In conjunction with an MHC class II molecule the processed peptides of the antigen are displayed on the surface of the B-cell and, therefore, enable interaction with a  $CD4^+$  T-cell, expressing the appropriate TCR. Interaction between the peptide-MHC class II complex on the B-cell surface and the TCR on the  $CD4^+$  T-cell is accompanied by key cell surface interactions at the surface of the B and T-cells, which result in activation of the B and T-cells. The activated T-cells synthesise and release cytokines and B-cell activation results in the synthesis and release of antigen-specific antibodies. Several paired interactions are involved in T-cell/B-cell (T-B) cooperation. One important interaction occurs between CD40 on the surface of the B-cell and CD154 on the T-cell surface. This interaction promotes upregulation of B7, a

co-stimulatory molecule on the B-cell surface, which in turn interacts with CD28 on the T-cell surface increasing the effectiveness of the B-cell as an APC. CD40-CD154 interaction also promotes proliferation and antibody class switching. Following T-cell activation, the B-cells differentiate into either antibody secreting plasma cells or memory B-cells, which are capable of being activated for a subsequent and more rapid response to the antigen. B-cell activation can also occur in the absence of T-cells and cytokines produced by T-cells. Generally only large polymeric antigens such as bacterial cell wall components are capable of these T-independent responses. The B-cells are activated following extensive cross-linking between the multivalent antigen and B-cell surface immunoglobulins. However, T-independent responses primarily generate IgM antibodies and fail to give rise to memory.

## **1.2 Lymphatic system**

The lymphatic system comprises the organs in which lymphocyte maturation, differentiation and proliferation occur. The lymphatic organs are subdivided into primary lymphoid organs, in which B-cell and T-cell maturation occurs, and secondary lymphoid organs where antigen driven proliferation and differentiation occurs (Male *et al.*, 1996). The primary lymphoid organs include the bone marrow and thymus where B-cells and T-cells develop, respectively. Embryonic B-cell differentiation occurs in hematopoietic stem cells. However, following birth this function migrates to the bone marrow, where mature B-lymphocytes, expressing antigen-specific immunoglobulins, are developed. T-cell differentiation occurs in the thymus, following migration of progenitor cells from the bone marrow. The thymus consists of epithelial cells organised into cortical and medullary areas, which contain thymocytes. Following T-cell maturation, in the cortex, they migrate to the medulla, where they encounter macrophages and dendritic cells. Development of mature T-cells is completed following thymic selection. Mature T-cells are capable of responding to specific foreign epitopes using specific T-cell receptors. Antigen stimulation of mature T-cells and B-cells occurs in the secondary lymphoid organs, which include the spleen, lymph nodes, tonsils, appendix, Peyer's Patches (small intestine), and lymphoid aggregates throughout the mucosal tissue. The secondary lymphoid organs function in trapping foreign particles and are the main areas for antibody production and activation of antigen-specific T-lymphocytes.

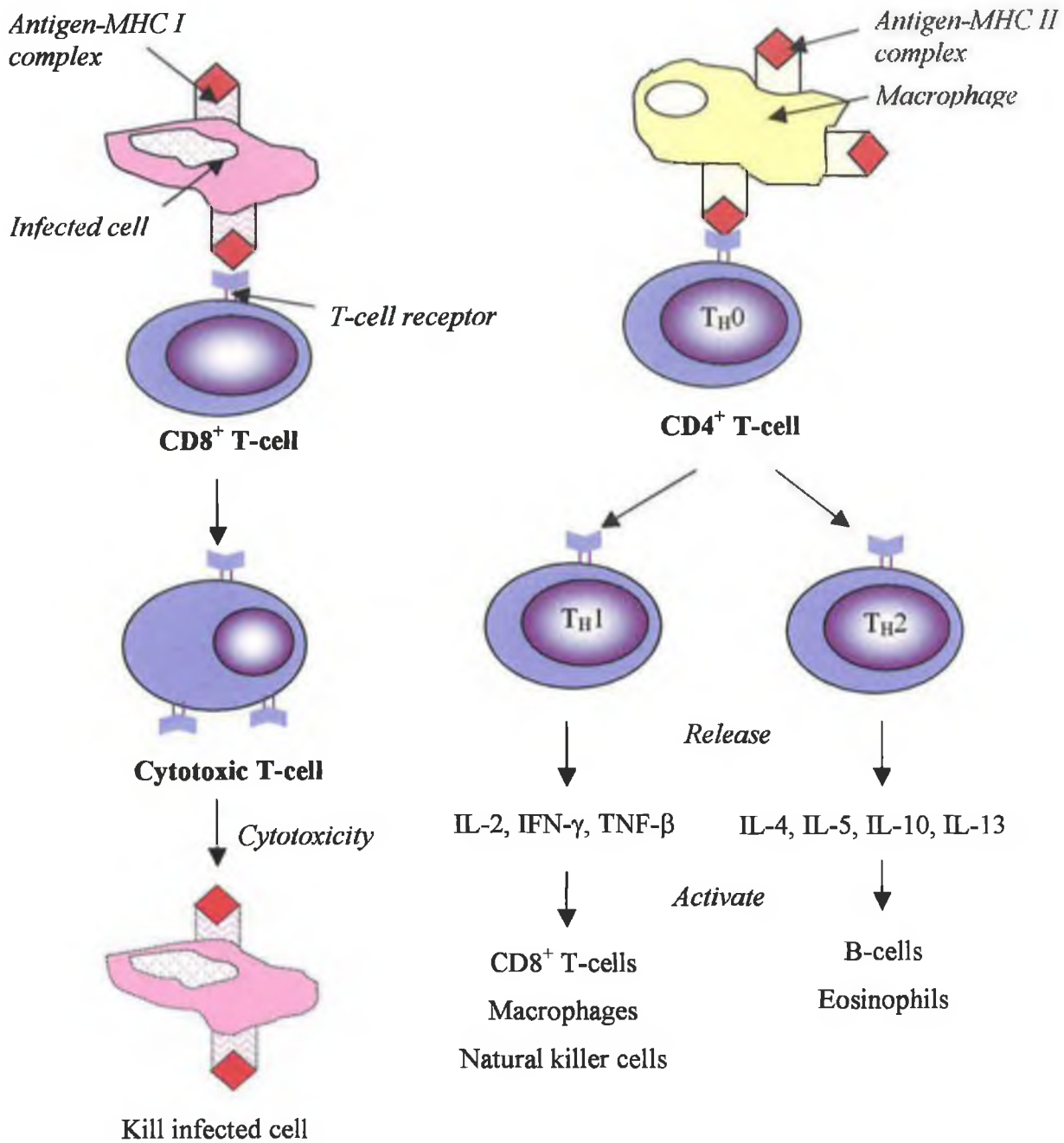


**Figure 1.1:** Overview of the cell-mediated immunity. The cell-mediated immune response operates through the generation of cytotoxic T-cells from CD8<sup>+</sup> T-cells and T-helper cells (T<sub>H</sub>) from CD4<sup>+</sup> T-cells. Following interaction between the T-cell receptor, on the CD4<sup>+</sup> T-cells, and the antigen-MHC class II complex, on the antigen-presenting cell, the CD4<sup>+</sup> T-cell differentiates into T<sub>H1</sub> or T<sub>H2</sub> cells, which secrete different cytokines. The CD8<sup>+</sup> T-cell differentiates into a cytotoxic T-cell, following interaction between its T-cell receptor and the antigen-MHC class I complex on the infected cell.

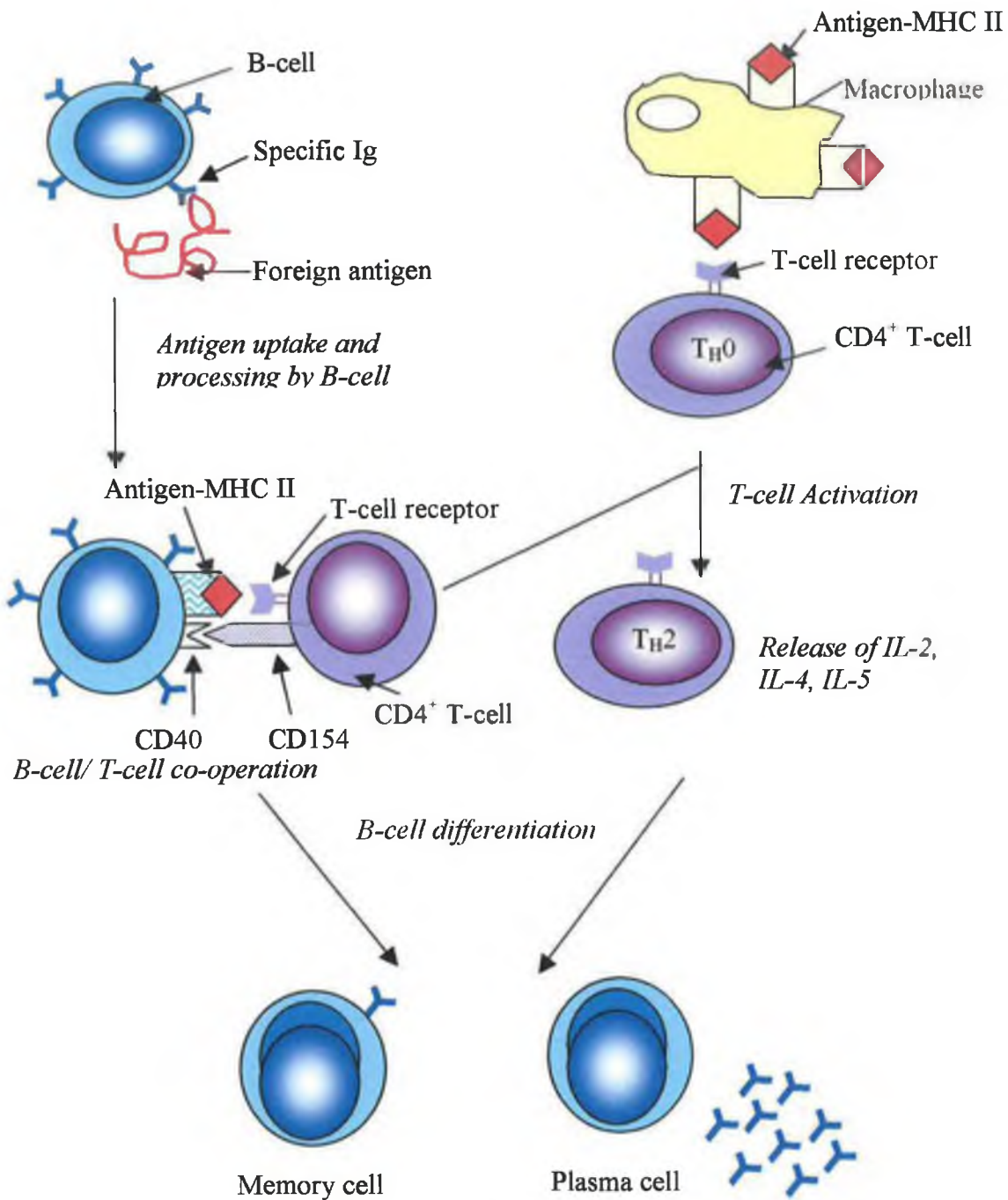


**Figure 1.2:** Overview of T-cell dependent humoral immunity. Initially an antigen-presenting cell internalises the foreign antigen by phagocytosis. The antigen is then processed and displayed on the cell surface complexed with an MHC class II molecule.  $T_H$  cells directly activate B-cell differentiation through cell-to-cell contact via several paired interactions or indirectly through the release of  $T_H2$  cytokines following interaction between the T-cell receptor on the  $CD4^+$  T-cell and the antigen-MHC class II complex on the surface of a macrophage. Ultimately B-cell differentiation results in the formation of memory cells and antibody-secreting plasma cells.

### 1.3 Antibody structure

Antibodies comprise a class of glycoproteins known as the immunoglobulins (Igs) that are produced by the immune system in response to foreign antigens. Five major structural classes of immunoglobulins exist, which include IgG, IgM, IgA, IgD and IgE. The five classes differ from each other depending on the type of heavy chain they possess. However, IgG is generally used to represent the typical antibody structure (Fig. 1.3).

IgG is a monomeric subunit composed of four polypeptide chains, two identical  $\gamma$  heavy chains and two identical  $\kappa$  or  $\lambda$  light chains. The IgG molecule has an apparent molecular weight of 150kDa, with each light chain weighing 25kDa and each heavy chain 50kDa. A heavy chain consists of one variable domain ( $V_H$ ) and three constant domains ( $C_{H1}$ ,  $C_{H2}$  and  $C_{H3}$ ). Each light chain is composed of one variable domain ( $V_L$ ) and one constant domain ( $C_L$ ). The light chain consists of 212 amino acid residues and each heavy chain is composed of 450 amino acid residues (Killard *et al.*, 1995). The hinge region is a short amino acid sequence positioned on the heavy chain between the  $C_{H1}$  and  $C_{H2}$  domains, which permits flexibility between the antigen-binding arms. Each monomeric antibody molecule has two antigen binding sites that bind to an epitope or antigenic determinant on the corresponding antigen.

The variable regions of the immunoglobulin are important for antigen-antibody binding and the generation of diversity. Within the variable region is a considerable amount of amino acid sequence diversity. The sequence variability is concentrated in several hypervariable regions known as complementarity-determining regions (CDRs). Each variable light domain and each variable heavy region contains three CDRs (CDR1, CDR2 and CDR3). Each CDR is flanked on either side by framework regions (FRs), which have little or no sequence variability. The CDRs on the heavy and light chain result in the formation of a specific 3-D structure, which acts as an antigen-binding site. Electrostatic forces, hydrogen bonds, hydrophobic interactions and Van der Waals forces are the main non-covalent forces, which give rise to antibody-antigen interactions.

Intra-chain disulphide bonds are present on the heavy and light chains with inter-chain disulphide bridges linking the two heavy chains and linking the heavy chain and light chain. The inter-chain and intra-chain disulphide bonds play an important role in the globular nature of the immunoglobulin. The individual domains of the immunoglobulin chains all form globular structures, which are constructed of a  $\beta$ -Barrel.  $\beta$ -Barrels consist of specific arrangement of two  $\beta$ -Sheets packed together and linked by a disulphide bond resulting in the formation a cylindrical shape. These specific  $\beta$ -Barrels are known as the immunoglobulin fold, a structure that plays important roles in antibody function (Rees *et al.*, 1994). The immunoglobulin folds are also found in several other molecules of the immune and nervous systems as well as in other proteins (Porter, 1991).

Immunoglobulins are glycosylated at conserved positions in the constant regions of the heavy chain with each isotype possessing a distinct array of N-linked carbohydrate structures. The carbohydrates protect against proteolytic degradation and affect protein assembly, secretion and functional activity (Wright and Morrison, 1997). In the case of IgG<sub>1</sub> there are two carbohydrate-binding domains located on the C<sub>H</sub>2 fragment.

The stem of the antibody (or the Fc portion) is responsible for the effector function of the antibody and it allows contact with the rest of the immune system. The immunoglobulin communicates with the rest of the immune system via Fc receptors, which are located on the majority of cells involved in the immune response. The Fc receptors enable accessory cells (e.g. macrophage, mast cells, eosinophils etc.) to detect pathogens through antibody-bound molecules. Different cells express different types of Fc receptors, which in turn bind different immunoglobulin isotypes. Fc $\gamma$ RII receptors are found on mast cells, B-cells and neutrophils. Aggregated binding of IgG molecules to Fc $\gamma$ RII receptors triggers phagocytosis and the oxidative burst in neutrophils. Fc $\gamma$ RIII receptors on the surface of natural killer cells, eosinophils, macrophages, neutrophils and mast cells mediate phagocytosis or antibody dependent cellular cytotoxicity following the binding of aggregated IgG or IgG antigen complexes. Binding of antigen to IgE-Fc $\epsilon$ R1 complexes on the surface of mast cells, eosinophils and basophils triggers the release of histamines and various inflammatory

mediators. Fc $\alpha$ RI receptors on the surface of macrophages, eosinophils and neutrophils bind IgA and are involved in antibody dependent cell killing and in the clearance of immune complexes.

There are five distinct types of heavy chains,  $\gamma$ ,  $\mu$ ,  $\alpha$ ,  $\delta$ , and  $\epsilon$ , which define the five classes of immunoglobulins, IgG, IgM, IgA, IgD and IgE, respectively. IgG is the most abundant antibody found circulating in the serum and accounts for 70 –75% of the total Ig pool (Roitt *et al.*, 1998). There are four subclasses of IgG in humans, IgG<sub>1</sub>, IgG<sub>2</sub>, IgG<sub>3</sub> and IgG<sub>4</sub>, and four subclasses in mice, IgG<sub>1</sub>, IgG<sub>2a</sub>, IgG<sub>2b</sub> and IgG<sub>3</sub>. The number of inter-chain disulphide bonds distinguishes the different subtypes of IgG. IgG functions in activation of the classical complement pathway, thereby attracting phagocytic cells. IgG molecules also bind to Fc receptors on the surface of macrophages and polymorphs and cross the placenta by passive transfer, thus conferring immunity to the foetus. IgM occurs naturally as a pentamer, with an additional J-chain for polymerisation, and has a molecular weight of 900 kDa. IgM is involved in the activation of the complement cascade and in the activation of macrophages. IgA exists as a dimer and is mainly produced at mucosal surfaces. There are two IgA isotypes, IgA<sub>1</sub> and IgA<sub>2</sub>. IgA<sub>1</sub> is predominant in the serum where IgA<sub>2</sub> is found in secretions such as saliva and tears. IgA functions in preventing the attachment of viruses and bacteria to the epithelial. IgD appears in the serum as a monomer and is a surface component of B-cells. Although the function of IgD is still poorly understood it is believed to act as an antigen receptor on B-cells and be involved in lymphocyte differentiation. IgE also appears as a monomer in the serum and defends the body against parasitic invasion. IgE interacts with mast cells and eosinophils and stimulates mast cells to release histamine. However, the interaction between IgE and the mast cells and eosinophils can lead to hypersensitivity reactions such as hay fever, asthma, hives and anaphylaxis.

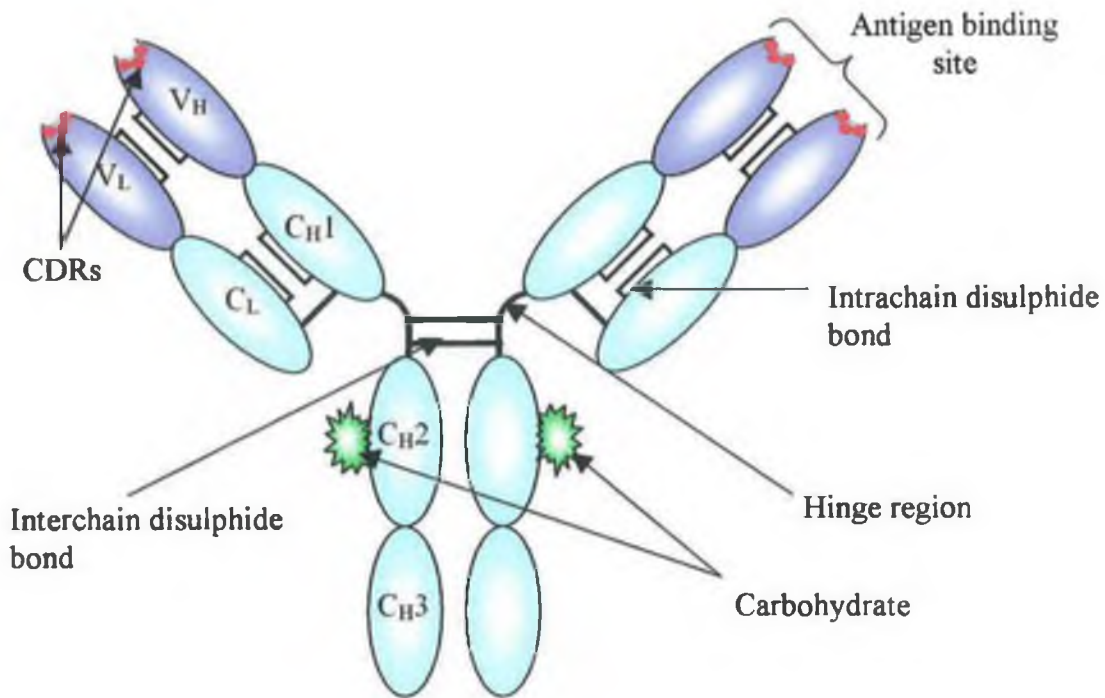


**Figure 1.3:** Diagrammatic representation of an immunoglobulin G (IgG) molecule. The IgG molecule is composed of two identical light chains and two identical heavy chains. The light chains comprise of a variable ( $V_L$ ) and constant ( $C_L$ ) domain. The heavy chain consists of one variable ( $V_H$ ) and three constant ( $C_{H1}$ ,  $C_{H2}$  and  $C_{H3}$ ) domains with a hinge region connecting the  $C_{H1}$  and  $C_{H2}$  regions. The heavy and light chains are connected via disulphide bonds; disulphide bonds are also present in the constant and variable regions. The CDRs within the variable domains confer antigenic specificity and contain considerable amino acid sequence variation.

#### 1.4 Genetic basis of antibody diversity

In humans, there is an estimated  $10^8$  antibody molecules, each with a different antigenic specificity (French *et al.*, 1989). The variable regions of the antibody encode the diversity. The  $\kappa$  and  $\lambda$  light chains and the heavy chains are encoded by separate multi-gene families, which are situated on different chromosomes. The gene family encoding the  $\kappa$  light chain are located on chromosome 2, those for the  $\lambda$  chain are located on chromosome 22 and the gene segments encoding the heavy chain are positioned on chromosome 14. In all cells, except B cells and lymphocytes, a considerable distance separates the genes encoding the variable and constant domains of an immunoglobulin. During B-cell differentiation DNA rearrangements occur that bring the constant and variable regions closer together (Davies *et al.*, 1999).

The variable regions of the  $\kappa$  and  $\lambda$  light chains are encoded by two separate gene fragments. The  $V_L$  (variable) segment encodes the first 95 amino acids and the  $J_L$  (joining) segment encodes 13 amino acids at the carboxy-terminal. (Fig. 4). During DNA rearrangement the  $V_L$  and  $J_L$  gene segments are combined (VJ recombination) to produce a continuous piece of DNA that encodes for the variable domain of the light chain. Following transcription, RNA splicing combines the V-J segment and constant ( $C_L$ ) domain.

The gene arrangement of the heavy chain is similar to that of the light chain (Fig. 1.5). In contrast with the light chain four gene segments,  $C_H$ ,  $V_H$ ,  $J_H$  and  $D_H$ , encode the heavy chain. Thus, in addition to the V and J segments, genes encoding the variable region of the heavy chain also include a  $D_H$  (diversity) segment. The  $D_H$  gene segment is situated between the  $V_H$  and the  $J_H$  gene segments. Multiple genes encoding the  $C_H$  domain are also present in the germline, which determine the antibody class. There are two recombination steps involved in the generation of the heavy chain, firstly the  $D_H$  segment is joined to the  $J_H$  segment and then the  $V_H$  segment is joined to the DJ segment, which gives rise to the  $V_H$  domain. RNA splicing then joins the  $V_H$  segment to the  $C_H$  region (Lewis, 1994).

Although the molecular events leading to recombination are not completely understood several factors involved in the rearrangement of the antibody gene

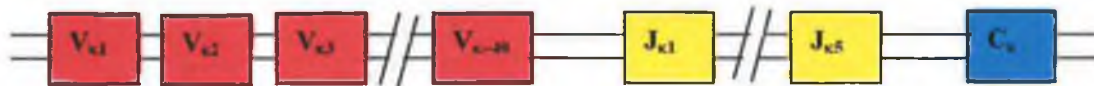
segments have been identified. An enzyme complex, V(D)J recombinase, mediates the rearrangement of receptor genes in B and T cells. Two recombination activation genes (RAG), RAG-1 and RAG-2 have been identified, the products of which are exclusively expressed in lymphocytes and critical for the development of T and B-cells. RAG-1 and RAG-2 proteins cut double stranded DNA at recombinational signal sequences (RSS) forming double-stranded breaks. The RSS are non-coding DNA sequences, which are critical for recombination of antibody genes. The RSS are conserved sequences located at the 3' side of the V segments, the 5' side of the J segments and on both sides of the D<sub>H</sub> segments. Each RSS consists of seven nucleotides (heptamer) and a block of nine nucleotides (nonamer), which are separated by a 12 or 23 base pair spacer. The heptamer is a conserved sequence, which can be CACAGTG or the inverse complement and the conserved nonamer sequence can be ACAAAAACC or the inverse complement.

Several factors, such as the presence of multiple variable (V) genes, combinatorial association, random assortment of heavy (H) and light (L) chains, junctional and insertional diversity and somatic hypermutations are all involved in generating antibody diversity. The number of different genes encoding the variable region in the germ line constitutes the baseline from which antibodies are derived. Initially, diversity results from the formation of a complete variable-region gene following the random recombination of separate V, D and J gene segments. Additional diversity is introduced during random assortment of the H and L chains during which any H chain may associate with any L chain. Inaccuracies also occur at the precise positions at which the V, D and J segments join, resulting in junctional diversity. The absence of precision in joining the gene segments during DNA rearrangement leads to deletions or amino acid changes, which result in the generation of diversity. In addition small sets of nucleotides can also be inserted at the V-D and D-J junctions. This is referred to as insertional diversity and is mediated by the enzyme terminal deoxynucleotidyltransferase (TdT). Somatic hypermutations, which occur in the V genes of heavy and / or light chains during the lifetime of the B cell, also increase antibody diversity. These somatic hypermutations are predominantly point mutations in the V(D)J recombined segment of the antibody V genes, and lead to amino acid changes. These mutations occur at a rate at least ten-fold higher than the normal rate

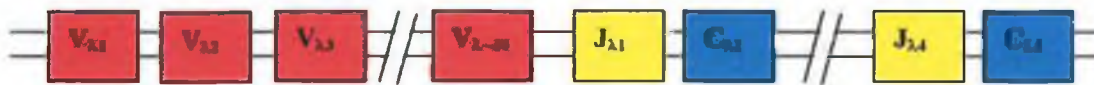
of mutation and results in the generation of antibodies with increased affinities (Benjamini *et al.*, 2000).

Following antigenic stimulation, a B-cell can rearrange its DNA and switch to make a different class of antibody, which retains the same antigenic specificity. This phenomenon is known as class or isotype switching and involves further DNA rearrangement, combining the VDJ genes with different heavy chain C genes. Each C<sub>H</sub> region gene contains a 5' end stretch of repeating bases called the switch (S) region, which permits any C<sub>H</sub> gene (except  $\delta$ , which contains no S region) to associate with the VDJ segment. Following stimulation a B-cell with a VDJ segment linked to C $\mu$  rearranges its DNA to link the VDJ region to an S region in front of an alternative C gene. In doing so the intervening C region DNA is removed, and therefore, the B-cell loses its ability to revert to making this class of antibody. This mechanism is regulated by antigen and T-cell derived cytokines and allows an antibody with a single antigenic specificity to associate with a variety of different effector functions.

**$\kappa$  light chain genes**



**$\lambda$  light chain genes**



**Heavy chain genes**



*Figure 1.4: Germline DNA arrangement of the genes encoding the heavy and light chains. The three sets of genes are encoded for on distinct chromosomes. Modified from Benjamini *et al.* (2000).*

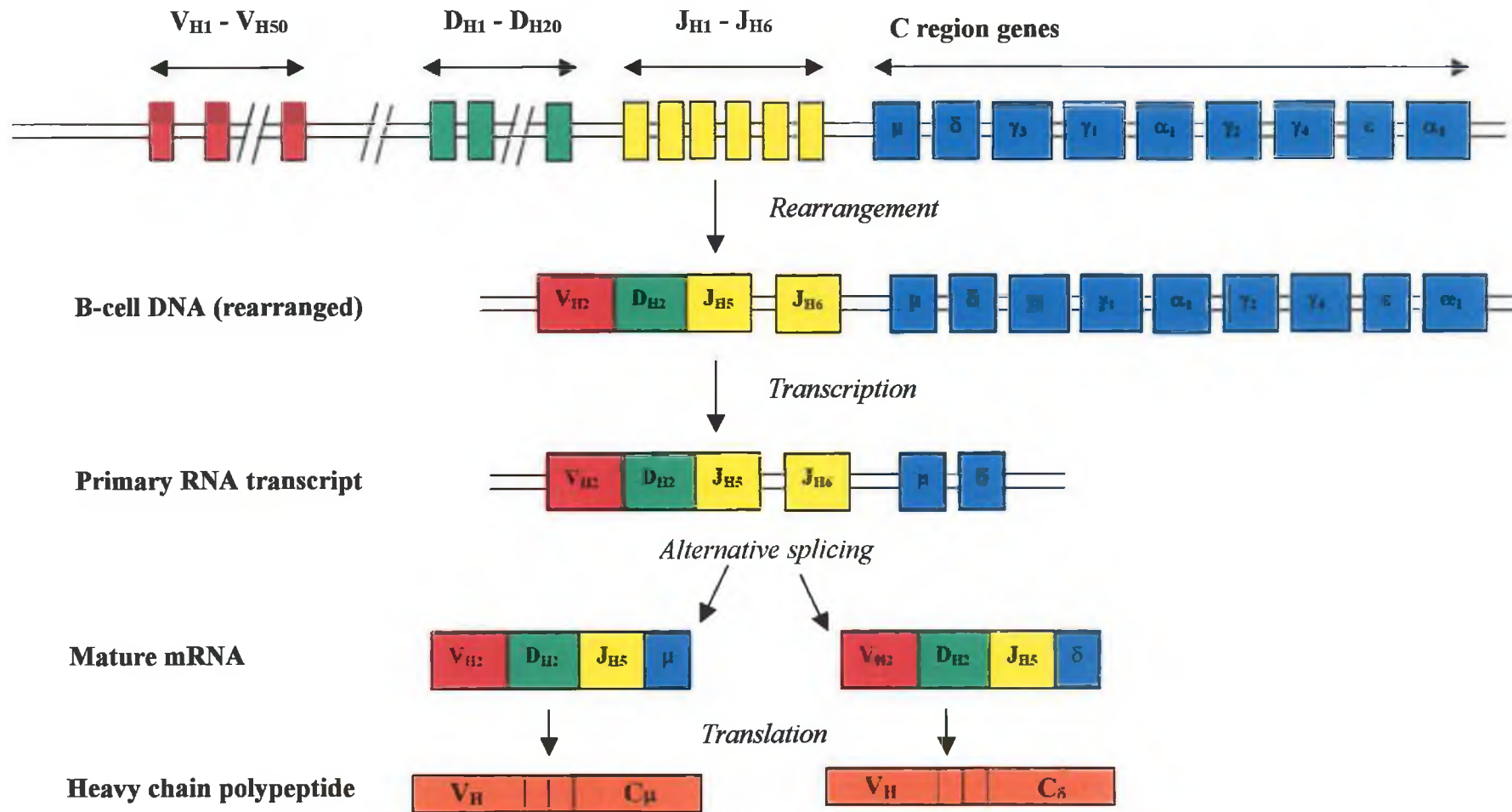


**Figure 1.5:** Schematic representation of the events leading up to heavy chain synthesis. Germline DNA is rearranged into B-cell DNA following two-recombination steps, which result in VJD joining. The DNA is then transcribed into mRNA, which is translated into the heavy chain polypeptide. Modified from Benjamini *et al.* (2000).

## **1.5 Antibody production**

### **1.5.1 Polyclonal antisera**

Following immunisation of an animal with a particular immunogen, an immune response is induced against the foreign antigen. Polyclonal antiserum can be recovered from the immunized subject and should contain several antibody populations, with different epitope specificities, against the particular immunogen. Relatively large animals such as rabbits, goats, sheep, guinea pigs, donkeys and fowl have all been used for the generation of polyclonal antisera. The chosen subject used for the immunization depends on the type and quantity of antiserum required, on the previous success of the particular animal and on the cost and welfare of the animal. Rabbits are frequently used for the production of polyclonal antiserum because they are cheap and easy to handle for immunisation and bleeding purposes. Polyclonal antisera production is relatively cost effective and does not involve laborious techniques. However, the heterogeneous antibody population may cross-react with structurally related molecules and there is little consistency between batches. Small molecules or haptens (i.e. < 1000 Daltons) must be covalently attached to a large carrier molecule such as bovine serum albumin (BSA), prior to immunisation, to elicit an immune response against it. The protein conjugate is required during the production, screening and characterisation of antibodies.

### **1.5.2 Monoclonal antibody production**

The first system for the production of monoclonal antibodies was reported by Kohler and Milstein (1975). It provided an alternative method for antibody production, resulting in the isolation of a homogenous antibody population. Plasma cells are the end product of B cell differentiation and they produce antibodies of a single specificity. However, plasma cells can only last a few days under cultured conditions. On the other hand myeloma cells are immortalised cancerous cells that can survive extended periods of time in culture and are non-antibody producers. Somatic cell hybridisation allows the fusion of the antibody secreting plasma cell and the immortalised myeloma cell. The resulting hybridoma (*hybrid-myeloma*) displays characteristics from both parental cell types. It exhibits the immortality of the

myeloma cell and the antibody producing properties of the splenocyte, resulting in a virtually unlimited supply of the specific antibody.

The B-lymphocytes are generally isolated from an immunised animal, such as a mouse or rat. Following several intra-peritoneal and a final intravenous immunisation with the specific antigen or hapten-carrier conjugate the spleen, which is then rich in antibody-secreting B-lymphocytes, is removed and the splenocytes recovered.

The myeloma cells used are derived from tumourogenic murine plasma cells (Van Emon *et al.*, 1989). Commonly used myeloma cell lines include X63-Ag8.653 and Sp2/0-ag14. The myeloma cells lack the enzyme hypoxanthine guanine phosphoribosyl transferase (HGPRT). The absence of this enzyme renders the myeloma cell incapable of synthesising purines and pyrimidines when grown in the presence of HAT (hypoxanthine, aminopterin and thymidine)-supplemented media. The aminopterin blocks DNA synthesis via the *de novo* pathway and in the absence of the enzyme HGPRT, the myeloma cells are unable to synthesise purines and pyrimidines using the salvage pathway (Fig. 1.6). Splenocytes have the enzyme HGPRT and in the presence of aminopterin convert to the salvage pathway for DNA synthesis. However, *in vitro* the splenocytes are unable to proliferate and die off within days. Following the myeloma and splenocyte fusion the resulting hybridoma will proliferate in the presence of HAT, as it will have inherited the HGPRT enzyme from the splenocyte. This HAT selection system, employed by Kohler and Milstein (1975), was previously described by Littlefield (1964).

Figure 1.7 outlines the principle of monoclonal antibody production. The splenocytes and myeloma cells are fused in the presence of polyethylene glycol (PEG), which is a polywax that promotes cell fusion and transfer of nuclei. The resulting hybridomas are immortalised and produce specific antibodies, expressing properties from both parental cell lines. However, the fusion event occurs with an extremely low frequency of  $10^{-5}$ . This means that approximately  $10^8$  spleen cells are required to produce 1000 hybrid cells and out of the hybrid cells produced only a small number will secrete the desired antibody (Wild and Davies, 1994). After the fusion has taken place, a mixed population of hybridomas, unfused lymphocytes and unfused myelomas remain. The hybridoma cells are positively selected for when grown in the presence of HAT. The

myeloma cells, lacking the enzyme HGPRT, die off in the presence of HAT and the spleenocytes die within a few days in culture, regardless of the growth medium. Then, using limiting dilution, hybridomas from a single cell parent, secreting the specific antibody, are isolated (Goding, 1996).

Alternatively, monoclonal antibodies can be produced following an *in vitro* immunisation (Borrebaeck *et al.*, 1983). Naïve spleenocytes are isolated from a non-immunised mouse and exposed to the antigen in culture for a period of 5 – 9 days. The activated spleenocytes are then fused with the myeloma cells as described above. An *in vitro* immunisation leads to a primary immune response and the resulting antibodies produced are predominately IgM, which have lower affinities than IgG antibodies. Previously, an initial *in vivo* immunisation, prior to the secondary *in vitro* boost, has led to an increase in the production of IgG antibodies (De Boer *et al.*, 1989).

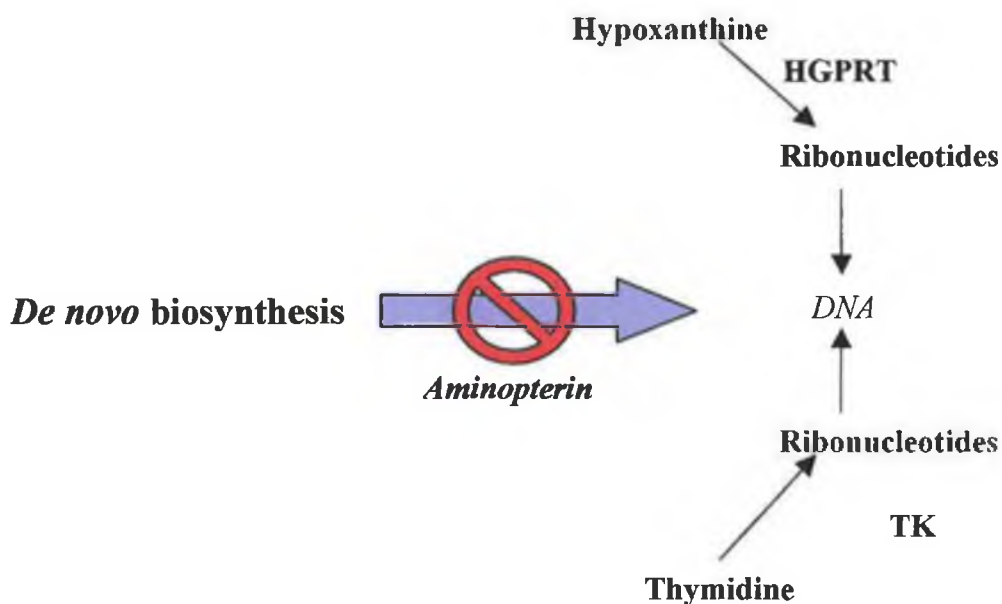


**Figure 1.6:** The *de novo* biosynthesis of purines and pyrimidines is blocked in the presence of aminopterin. In the absence of *de novo* synthesis, cells containing the enzymes hypoxanthine-guanine phosphoribosyl transferase (HGPRT) and thymidine kinase (TK), convert to the salvage pathway for nucleic acid synthesis, in the presence of hypoxanthine and thymidine. However, cells lacking the enzyme HGPRT will die off in the presence HAT because they are unable to produce purines and pyrimidines for nucleic acid synthesis.

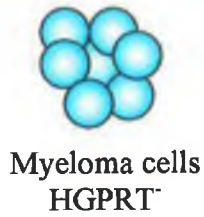
Immunise mouse with antigen of interest



Spleen extracted

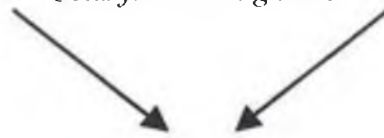


Extracted splenocytes  
HGPRT<sup>+</sup>



Myeloma cells  
HGPRT<sup>-</sup>

*Cells fused using PEG*

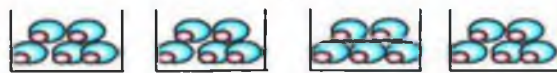


Fused hybridomas  
HGPRT<sup>+</sup>

*Hybridoma selection in HAT media*



*Propagation of selected hybridomas*



*Cloning by limiting dilution to achieve monoclonality*



Antibody purification and characterisation

**Figure 1.7:** Schematic representation showing the principle of monoclonal antibody production.

## 1.6 Antibody fragments

The Ig molecule can be broken into several fragments using chemical, enzymatic or genetic means. Research conducted by Porter and associates (1966) demonstrated that proteolytic treatment of the Ig with the enzyme papain resulted in the formation of three fragments. Papain cleaves the two heavy chains above the interchain disulphide bridge, resulting in the formation of two individual antibody-binding fragments (Fab) and the Fc portion. Treatment of the Ig with the enzyme, pepsin, cleaves the two heavy chains below the interchain disulphide bond and results in the formation of an antibody fragment containing two binding arms (F(ab')<sub>2</sub>).

Various antibody fragments, including the Fab, Fv and scFv, can also be produced using recombinant DNA technology. The smallest antibody fragment required for complete antigen binding is the Fv fragment. This truncated Fab fragment consists of one V<sub>L</sub> domain and one V<sub>H</sub> domain. The Fv fragment can be very unstable for use in therapeutics or immunanalysis because it lacks the inter-chain disulphide bond, which is present in the Fab fragment. A synthetic peptide linker, or in some cases the insertion of cysteine residues to form a disulphide bridge, has been incorporated into the Fv fragment to produce a more stable single chain Fv fragment (scFv) (Brinkmann *et al.*, 1993; Reiter *et al.*, 1994 and Young *et al.*, 1995). Other antibody fragments have been engineered that have the ability to bind antigen, these include the Fd, which consists of one V<sub>H</sub> and one C<sub>H1</sub> domain, and CDR, the smallest antibody fragment capable of binding to an antigen (Fig. 1.8).

The scFv is one of the most commonly used antibody fragments, with many analytical and therapeutic applications. Recombinant scFvs with specific affinities have been produced and applied to the detection of illicit drugs (Brennan *et al.*, 2002 and Dillon *et al.*, 2003), residues (Garrett *et al.*, 1997; Alcocer *et al.*, 2000 and Strachan *et al.*, 2000) and food contaminants (Daly *et al.*, 2001). The small size and stability of the scFv fragments makes it particularly applicable to therapeutics (Arakawa *et al.*, 2002 and Suzuki *et al.*, 2003). The attachment of a toxin or label has also enabled the use of scFv in drug therapy (Sun *et al.*, 2003) and tumour imaging (Demartis *et al.*, 2001).

Recombinant phage display technology (Section 1.7) is now routinely utilised in the generation of scFv antibody fragments.

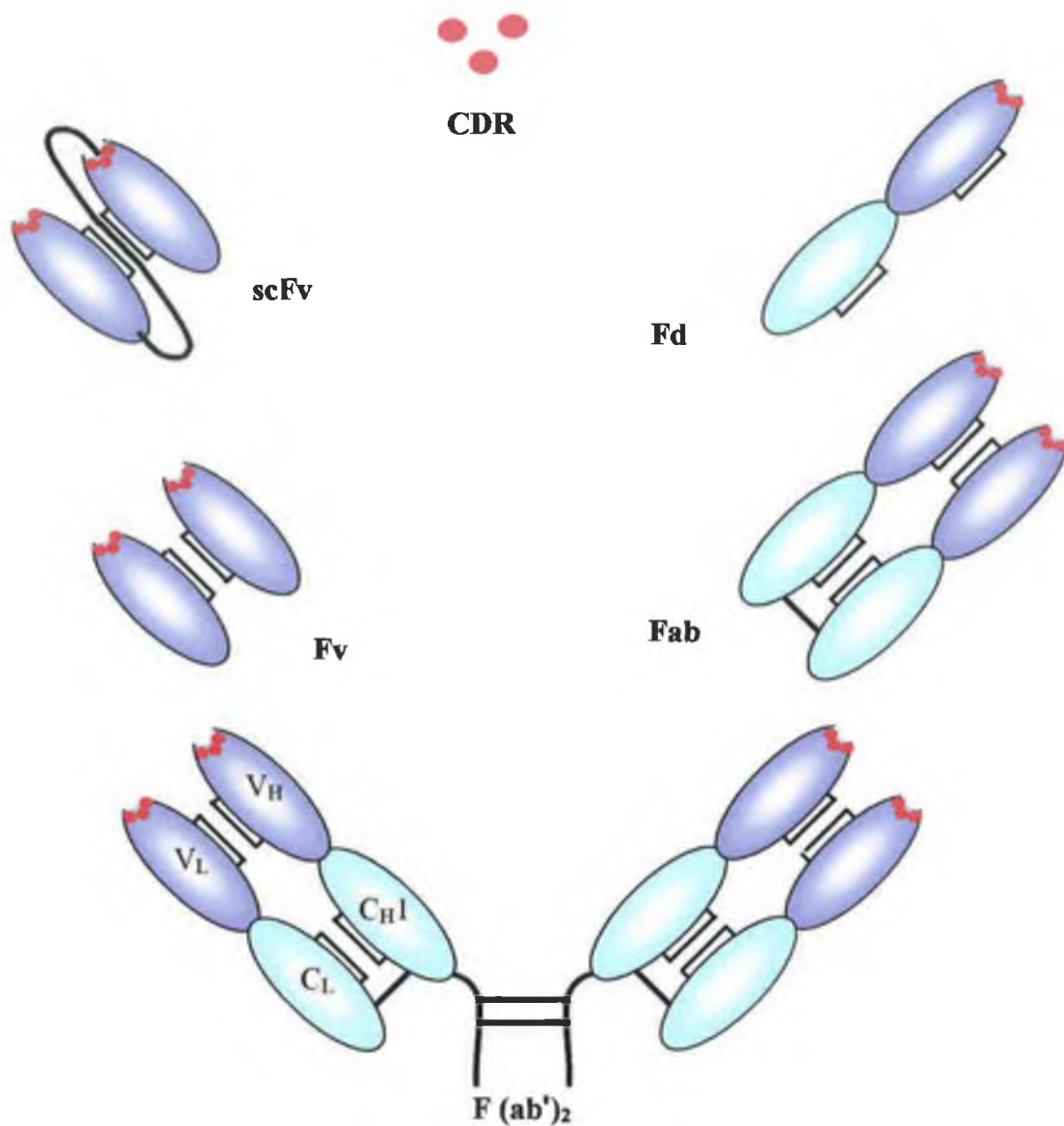


**Figure 1.8:** Structure of the various IgG antibody fragments, which may be generated through genetic, enzymatic or chemical manipulations. The  $F(ab')_2$  consists of two antigen binding fragments linked at the hinge regions, with the Fab fragment consisting of one antigen binding domain and the Fd comprising one  $V_H$  and one  $C_H$  domain. The Fv fragment consists of one  $V_H$  and one  $V_L$ , which following stabilisation by a synthetic linker results in the formation of the scFv fragment. The CDR represents the smallest antibody fragment capable of antigen binding.

## 1.7 Phage display technology

The introduction of phage display technology, in 1985 by Smith, paved the way for an alternative method of antibody production *in vitro* (Smith *et al.*, 1985). Phage display technology enabled the expression of antibody fragments on the surface of filamentous phage as a fusion partner to a phage coat protein. Phage particles displaying an antibody fragment of interest could then be subsequently selected using a method known as panning (See Section 1.7.5), which has enabled the isolation of high affinity antibodies (Barbas, *et al.*, 1991; Breitling *et al.*, 1991; Garrard *et al.*, 1991; Hoogenboom *et al.*, 1991 and McCafferty *et al.*, 1990). Fab (Hoogenboom *et al.*, 1991) and single chain Fv (scFv) (McCafferty *et al.*, 1990) antibody fragments have been displayed on filamentous phage attached to either the N-terminus (McCafferty *et al.*, 1991) or C-terminus (Barbas *et al.*, 1991) of the minor phage coat protein g3p. Large antibody repertoire libraries can be generated from a variety of naïve, immunized and synthetic sources.

### 1.7.1 The Filamentous Phage

The filamentous phage are routinely used in phage display technology. They belong to the genus *Inivirus* and infect a variety of gram-negative bacteria. They are metabolically inactive in their extra-cellular form and only capable of reproduction within their host. The Ff bacteriophage (f1, fd and M13) are the most extensively studied and, as their name would suggest, they infect host cells via attachment to the F pili, present on male *E. coli* such as TG1. The phage particle is comprised of a single strand of circular DNA encapsulated in a protein coat. The single stranded genome contains 11 genes, which encode the proteins required for DNA replication, the protein capsid and phage assembly. The filamentous phage replicate within the host cells without inducing a lytic infection. The Ff bacteriophage attach to the F pilus on the *E. coli* host via the gene III-encoded coat protein (g3p) and the single stranded DNA enters the cell. Within the host the single stranded DNA is replicated via a double stranded intermediate, which is produced using the host's genetic machinery. The replicated single stranded genome serves as a template for expression of the phage proteins. The phage coat proteins are expressed as integral membrane proteins and the single stranded phage genome is packaged into the protein capsid at the bacterial membrane and released. Figure 1.9 represents the structure of a phage particle displaying an scFv fused to the pIII coat protein.

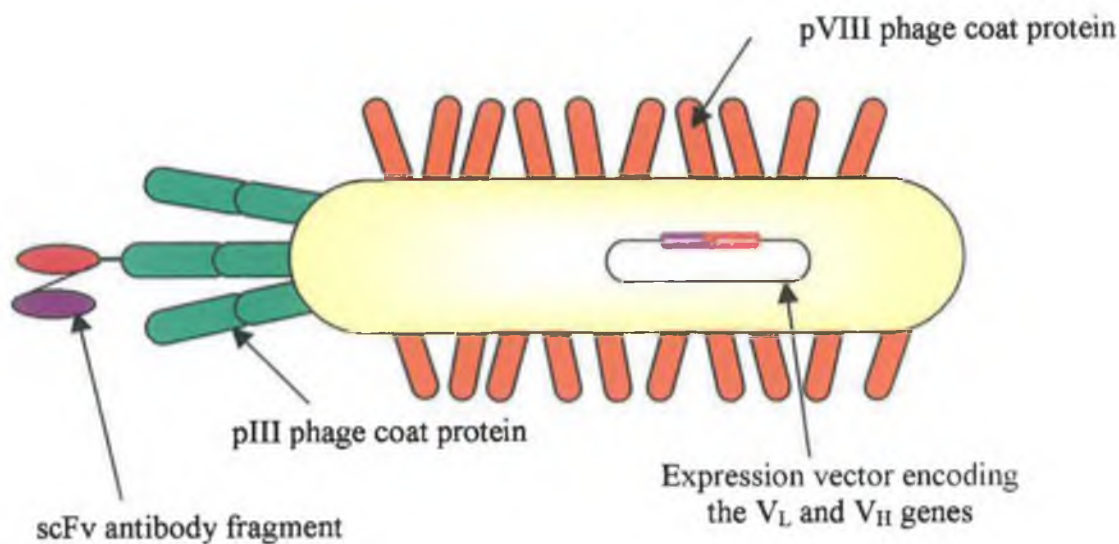


**Figure 1.19:** Schematic representation of a filamentous phage particle displaying an scFv antibody fragment. The scFv is displayed attached to the pIII phage coat protein, with the genes encoding the variable heavy and light chains encoded for on an expression vector, within the filamentous phage.

### 1.7.2 Expression vectors

There are a variety of phage and phagemids vectors available for the expression of antibody fragments on the surface of filamentous phage. Phage vectors encode the g3p-antibody fusion along with all the genes required for replication, packaging and bacterial infection. Phagemids vectors encode the g3p-antibody fusion, the phage and *E. coli* origins of replication and an antibiotic resistance for selection. However, unlike the phage vector, they lack all structural and non-structural genes. Therefore, they require rescue with a helper phage that encodes the appropriate proteins for phage replication and packaging. Suitable helper phage that are routinely used in phage display are VCSM13 and M13K07, which both encode a kanamycin resistance gene for selection. Rondot and associates (2001) have described a helper phage called hyperphage that increased antibody phage display particles by more than two fold. These hyperphage have a wild-type pIII phenotype and are capable of infecting F' *E. coli* cells with high efficiency. However, they lack a functional pIII gene so that the phagemid-encoded pIII antibody fusion is the sole source of pIII in phage assembly. Therefore, this results in a considerable increase in the number of phage displaying

the antibody fragment on their surface. Promoter regions and tags, to aid in purification and detection, are also coded for on the phagemid vector.

### 1.7.3 Library construction

Initial stages of library construction involve the isolation of a genetic source from which total RNA is extracted (Fig. 1.10). The genetic material can be sourced from a variety of locations including peripheral blood lymphocytes, lymph nodes, the spleen, bone marrow and hybridomas. The mRNA is then reverse transcribed into cDNA and the  $V_H$  and  $V_L$  genes PCR amplified using universal primer sets that in theory enable the amplification of the entire antibody repertoire. Several universal primer sets have been described for the production of antibody phage display libraries, which have been species specific and degenerate, and have enabled the construction of V-gene repertoires from several species including humans (Marks *et al.*, 1991) and mice (Clackson *et al.*, 1991; Kettleborough *et al.*, 1993 and Krebber *et al.*, 1997). The  $V_H$  and  $V_L$  chains are then assembled into the scFv fragment by SOE-PCR (slicing by overlap polymerase chain reaction). The SOE-PCR is carried out using specific primers with restriction sites that aid in the later stages of cloning. Depending on the cloning strategy and display vector of choice, the restriction sites may be engineered outside the V-region or within the scFv sequence. The scFv fragment is then cloned into the appropriate vector, following restriction of the scFv insert and display vector. The vector containing the scFv insert is transformed into  $CaCl_2$  competent or electro-competent *E. coli* cells, for antibody expression. The ligation and transformation efficiency are crucial steps in library construction and they can directly influence library size (Azzazy and Highsmith, 2002). The transformed bacterial cells are then infected with a helper phage (VCSM13 or M13K07), which results in the production of antibody displaying phage particles. Transformation efficiencies of bacterial cells have limited library size to approximately  $1 \times 10^8$ . However, larger phage repertoires of approximately  $1 \times 10^{10}$  clones have been reported (Griffiths *et al.*, 1994) following combinatorial infection and *in vivo* recombination (Waterhouse *et al.*, 1993). More recently, techniques involving *in vitro* display and the introduction of mutagenesis steps into the antibody-encoding RNA sequence (See Section 1.7.8.5) have enabled the construction of antibody libraries containing  $> 10^{12}$  clones (Hanes *et al.*, 2000).

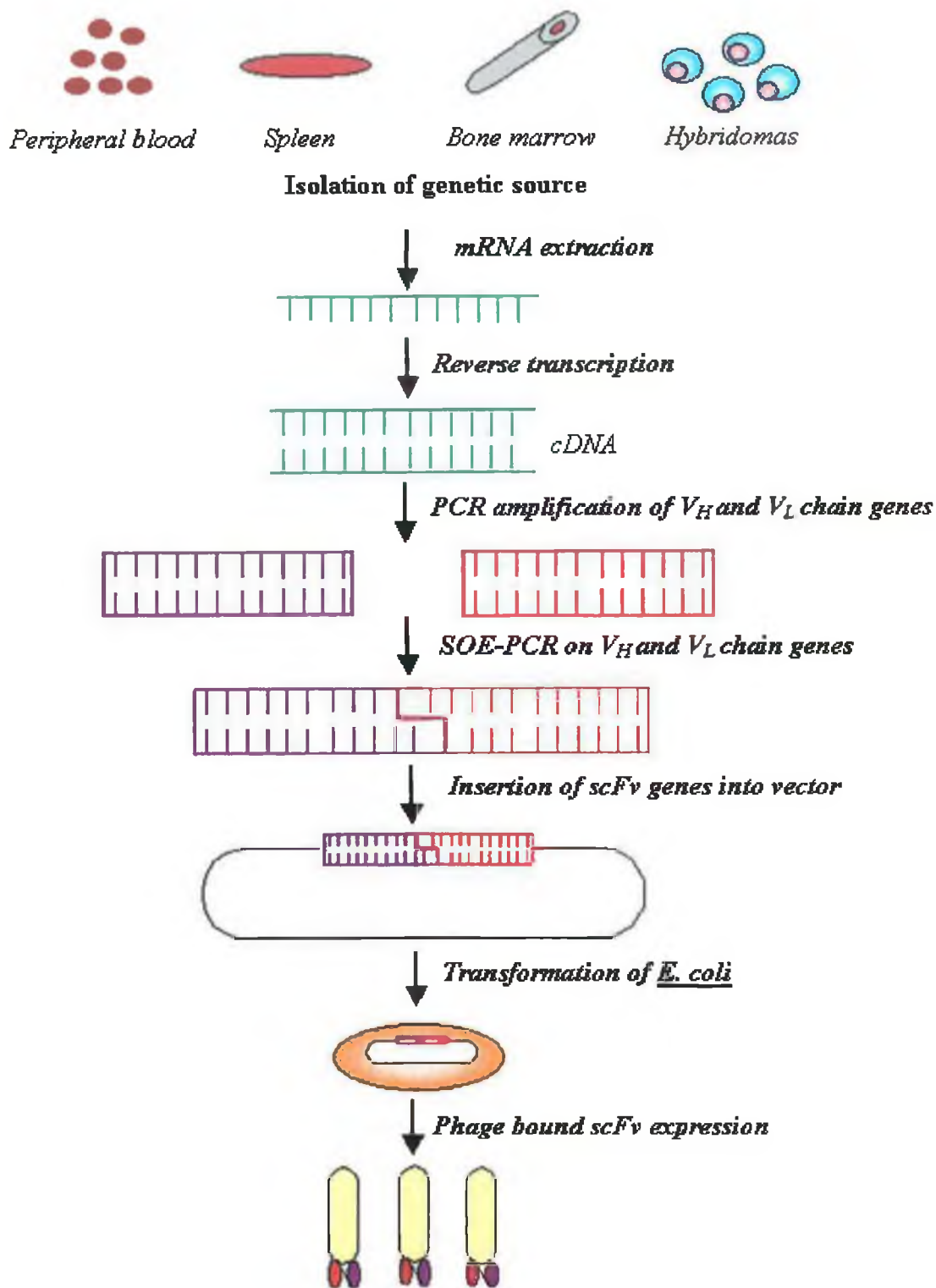


**Figure 1.10:** Schematic representation illustrating the production of an antibody phage display library. Genes encoding the antibody fragment are amplified by PCR, following mRNA isolation and reverse transcription. The DNA insert is ligated into a phagemid vector that is then transformed into *E. coli*. Antibody fragments are then expressed on the surface of phage particles, following super-infection with helper phage.

## 1.7.4 Antibody repertoires

### 1.7.4.1 Naïve repertoires

Naïve antibody repertoires are constructed using B-lymphocytes from non-immunised human or animal donors. The IgM mRNA is isolated from peripheral blood lymphocytes, bone marrow or spleen cells. Naïve antibody repertoires enable the isolation of high affinity antibodies against self, non-immunogenic and toxic antigens and they can be used for the isolation of antibodies against numerous antigens in a relatively short period of time.

Numerous large naïve repertoires have been reported and have enabled the isolation of antibodies against a variety of antigens. Non-immunised human donors (43) were used to construct a repertoire of  $1.4 \times 10^{10}$  scFv-phage display particles (Vaughan *et al.*, 1996). This library provided a source of specific, high affinity human monoclonal antibodies against a variety of antigens including fluorescein, and the haptens DTPA and oestradiol. A naïve human Fab repertoire containing  $3.7 \times 10^{10}$  clones has also been reported (de Haard *et al.*, 1999). Naïve human repertoires have also enabled the isolation of antibody fragments against antigens associated with *Chlamydia trachomatis* (Lindquist *et al.*, 2002) and small haptens such as aflatoxin B<sub>1</sub> (Moghaddam *et al.*, 2001).

### 1.7.4.2 Immunised repertoires

Antibody repertoires can also be constructed from IgG genes isolated from B-lymphocytes from immunised animals and immune donors. Pre-immunised libraries are enriched with antigen-specific antibodies, some of which will have been affinity matured within the host. However, this method of library construction may be time-consuming if animal immunisation is required, antibodies against self or toxic antigens cannot be isolated, individual libraries must be constructed for different antigens and the immune response against different antigens is unpredictable.

Immunised or pre-immunised repertoires have been constructed following immunisation of mice (Daly *et al.*, 2002 and Dillon *et al.*, 2003), chicken (Davies *et al.*, 1995 and Yamanaka *et al.*, 1996), rabbits (Lang *et al.*, 1996), sheep (Charlton *et al.*, 2001), camels (Arbabi *et al.*, 1997) and sharks (Dooley *et al.*, 2003). Immunised

phage display libraries have been used for the isolation of antibody fragments against small haptens such as morphine-3-glucuronide (Dillon *et al.*, 2003), the mycotoxins zearalenone (Yuan *et al.*, 1997) and aflatoxin B<sub>1</sub> (Daly *et al.*, 2002) and bacterial cells including *B. melitensis* (Hayhurst *et al.*, 2003).

#### 1.7.4.3 Synthetic repertoires

Synthetic antibody libraries are constructed artificially by *in vitro* assembly of V gene fragments and D/J segments. Synthetic repertoires are made following randomisation of the CDR regions using oligonucleotide-directed mutagenesis or PCR-based techniques. The CDR3 of the heavy chain is most central to the antigen-binding site and encodes the majority of the structural and sequence diversity, with the other five CDRs encoding limited variation. Therefore, it has been targeted for introducing diversity in synthetic libraries. Synthetic repertoires have been constructed using randomised light and heavy chain CDR3s (Akamatsu *et al.*, 1993) and V-gene segments in which all three CDRs have been diversified (Garrard and Henner, 1993). Synthetic libraries enable control over the contents, local variability and overall diversity of the antibody repertoire.

Hoogenboom and Winters (1992) reported the construction of one of the first synthetic antibody repertoires. Human V<sub>H</sub> fragments (49), containing short CDR3 regions encoding either 5 or 8 amino acids and a J-region, were assembled using PCR and cloned for scFv display with a human lambda light chain. Subsequently, more diversity was introduced following enlargement of the CDR3-region, which ranged from 4 – 12 amino acids (Nissim *et al.*, 1994). The largest synthetic library constructed to date consists of  $6.5 \times 10^{10}$  Fab-displaying phage (Griffiths *et al.*, 1994). This library was constructed using the 49 human V<sub>H</sub> fragments (Hoogenboom and Winters, 1992), which were combined with 47 human kappa and lambda light chain fragments containing partially randomised CDR3 regions. Synthetic libraries have been reported for the isolation of antibody fragments against a variety of antigens such as haptens, foreign antigens and human antigens (Griffiths *et al.*, 1994) and environmental contaminants including microcystin-LR a cyanobacterial hepatotoxins (McElhiney *et al.*, 2000) and *Streptococcus suis* (de Greeff *et al.*, 2000).

### 1.7.5 Isolation of specific antibody fragments from antibody repertoires

The isolation of specific-phage clones, expressing the antibody fragment of interest, enables the sequential enrichment of specific binding phage from a large repertoire of non-binding clones. Figure 1.11 outlines the bio-panning process, which involves multiple rounds of selection during which specific phage are bound to the immobilised antigen and non-specific phage are washed away. Bound phage are eluted and reinfected into bacteria for further rounds of selection and enrichment. Selection can be performed against the antigen absorbed onto plastic surfaces such as immunotubes and ELISA plates (Marks *et al.*, 1991) or against the antigen immobilised on a Biacore sensor surface (Malmberg *et al.*, 1996). The bound phage can be eluted from the specific antigen using acidic solutions such as HCl or glycine buffer (Krebber *et al.*, 1997), with basic solutions, such as triethylamine (Marks *et al.*, 1991 and de Bruin *et al.*, 1999), following enzymatic cleavage of a protease-sensitive site engineered between the antibody and gp3 (Ward *et al.*, 1996) or by competition with excess antigen (Clackson *et al.*, 1991).

Selection using antigens in solution have also been described (Hawkins *et al.*, 1992 and Griffiths *et al.*, 1994). Following incubation of the phage antibody repertoire with biotinylated antigen, phage bound to the labelled antigen are recovered using avidin or streptavidin-coated paramagnetic beads. Panning can also be performed on monolayers of adherent cells or on cells in suspension for the isolation of antibodies against cell surface antigens (de Kruif *et al.*, 1995 and Cai and Garen, 1995). *In vivo* selection methods have also been described, which involves the direct injection of antibody repertoires into animals followed by tissue isolation and examination of bound phage (Pasqualini and Ruoslahti, 1996).

Following each round of selection, eluted phage are analysed for specific-antigen binding. Phage ELISAs are commonly used during which the antigen of interest is immobilised on an immunoplate and incubated with the antibody-displaying phage clones. Bound phage particles are then detected using an enzyme-labelled secondary antibody specific for either the phage or a phagemid-encoded tag (e.g. c-myc).

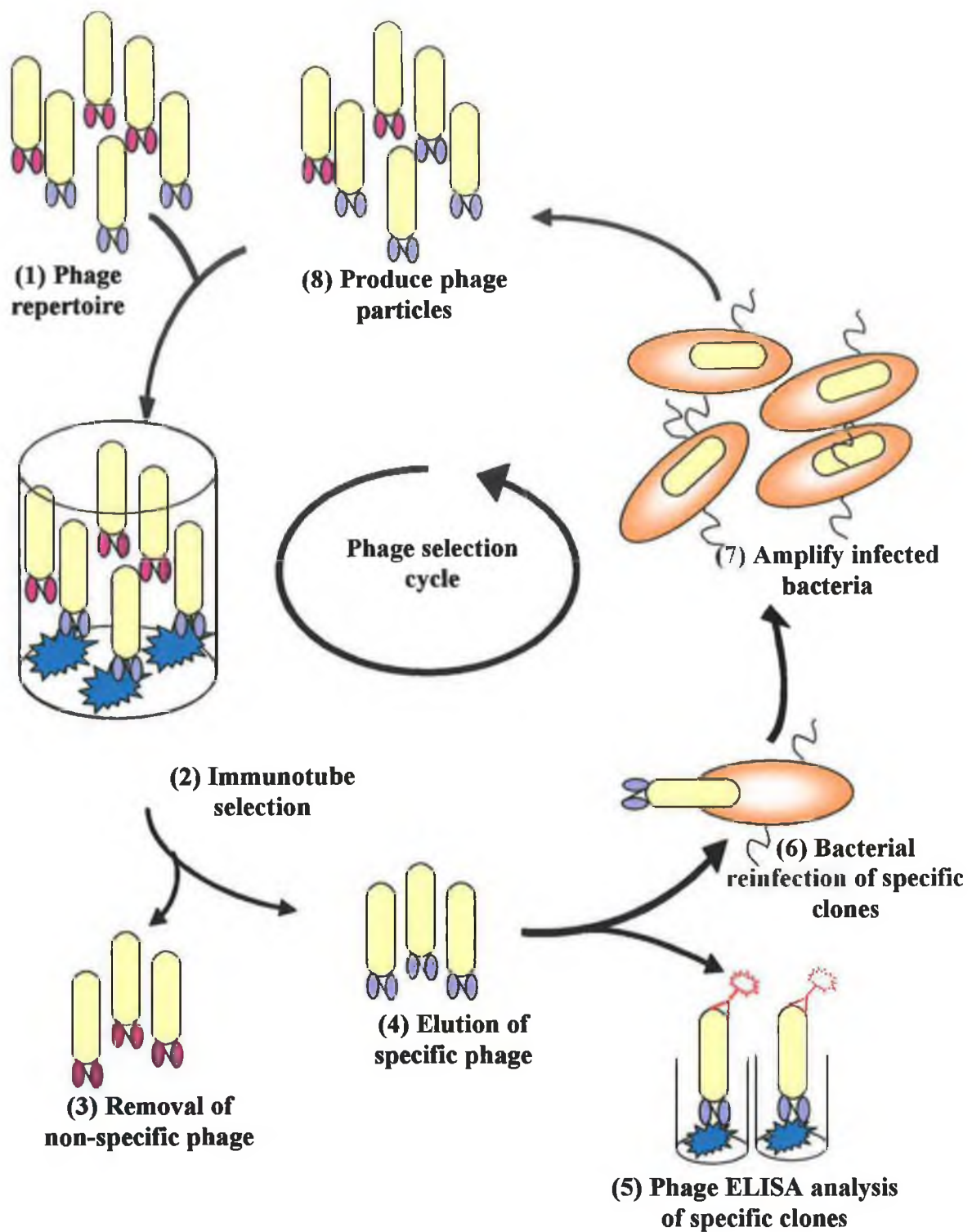


*Figure 1.11: Schematic representation of the selection process for the isolation of specific phage clones. The phage repertoire is incubated with the antigen of interest. Phage displaying the antigen-specific antibodies bind and non-specific phage are washed away. Positive phage are then eluted and reinfect into bacterial for further rounds of selection and enrichment.*

### 1.7.6 Soluble expression of antibody fragments

Following selection, the antigen-positive phage are infected into a non-suppressor *E. coli* strain (e.g. TG1 and JM83) for soluble scFv production. These bacterial strains recognise the phagemid encoded amber stop codon situated between the scFv gene segment and the g3p coat protein. Therefore, they express the scFv without the g3p protein. Phagemid vectors can also encode tags such as 6xHis and c-myc tags, that following soluble expression, are fused to the scFv to aid in detection and purification. Depending on the isolated clone, the soluble antibodies can be expressed into the culture supernatant, the bacterial periplasm or both. Phagemids incorporating pelB leader sequences enable the *E. coli* cell mimic the eukaryotic secretory pathway for proteins resulting in appropriate refolding and relocation of the expressed antibody to the periplasm (Leumeulle *et al.*, 1998).

Bacterial expression systems are most commonly used for the soluble production of functional antibody fragments because they are easy to manipulate, fermentation is rapid and inexpensive and high-levels of protein production can be achieved (up to several hundred milligrams). Fully functional antibody fragments can be expressed in *E. coli* because, unlike whole antibody molecules, they do not require any complex post-translational modifications.

Eukaryotic expression systems have also been described for expression of antibody fragments and are capable of performing post-translational modifications such as glycosylation. Yeast expression systems offer the distinct advantage that their codon usage and protein folding pathways mimic that of mammalian cells. Expression of scFvs has been reported in several strains of yeast including *Schizosaccharomyces pombe* (Davis *et al.*, 1991), *Pichia pastoris* (Freyre *et al.*, 2000), *Trichoderma reesei* (Eldin *et al.*, 1997) and *Saccharomyces cerevisiae* (Shusta *et al.*, 1998). Insect expression systems in conjunction with the baculovirus have also enabled the expression and secretion of correctly folded scFvs (Kretzschmar *et al.*, 1996; Brocks *et al.*, 1997 and Lemeulle *et al.*, 1998). Mammalian cells have provided an alternative system for high-level expression of antibody fragments. Antibody fragments have been successfully expressed in Chinese Hamster ovary (CHO) cells (Dorai *et al.*, 1994), myeloma cells (Dorai *et al.*, 1994) and COS cells (Jost *et al.*, 1994 and Ridder *et al.*, 1995). Rapid eukaryotic expression vectors have also enabled the conversion of

scFv and Fab fragments into fully assembled and functional whole antibody molecules (Mahler *et al.*, 1997; Persic *et al.*, 1997 and Boel *et al.*, 2000). Plant expression systems have also proved useful for the expression of antibody fragments. Plant expression systems do not require large sterile fermentation processes, the expressed fragments are free from bacterial toxins and mammalian viruses and the plants are capable of storing the expressed antibody fragments for a short period of time within the leaf and over a longer time period within the seeds. The tobacco plant using *Agrobacterium*-mediated transfection has been widely reported for soluble expression of antibody fragments (Owen *et al.*, 1992; Fiedler and Conrad, 1995 and Hendy *et al.*, 1999).

#### **1.7.7 Purification of antibody fragments**

Several purification strategies have been described for scFvs, which include antigen affinity chromatography (Owen *et al.*, 1992; Casey *et al.*, 1995 and Cho *et al.*, 2000), ion exchange and size exclusion chromatography (Kretzschmar *et al.*, 1996), human constant light chain tagging (Ridder *et al.*, 1995 and Longstaff *et al.*, 1998) and immobilised metal affinity chromatography (IMAC) (Kipriyanov *et al.*, 1997 and Freyre *et al.*, 2000).

IMAC is now routinely used for the purification of recombinant proteins including antibody fragments. This method ensures high ligand stability, high protein loading, mild elution conditions, relatively low cost, and complete ligand recovery following regeneration (Arnold *et al.*, 1991). The theory behind IMAC is discussed further in Section 4.1.3. Kipriyanov and associates (1997) demonstrated that IMAC could be successfully applied for the purification of functional scFvs from *E. coli* periplasmic lysates. IMAC is now frequently used for the purification of his-tagged scFvs and it has recently been applied to the purification of scFvs against the mycotoxin deoxynivalenol (Choi *et al.*, 2004) and scFvs against the transmembrane envelope glycoproteins gp46 of maedi-visna virus (MVV) (Blazek *et al.*, 2004).

### **1.7.8 Affinity maturation of antibody fragments**

Although antibody fragments selected from immune and single-pot repertoires have proven to be extremely useful, their affinity is often not sufficient for therapeutic applications in immunotherapy, viral neutralisation, or for use in sensitive diagnostics (Hoogenboom *et al.*, 1998). To date, several methods have been described for affinity maturation of antibody fragments.

#### **1.7.8.1 Multivalent molecules**

Decreases in apparent affinity have been reported with scFvs, when compared to the parental monoclonal antibody (Huston *et al.*, 1988). The reduced levels of affinity observed can be due to the decrease in the number of antibody binding sites. One of the easiest methods to improve scFv-binding affinity is the creation of a multimer. Several multivalent scFv-based structures have been reported, including miniantibodies (Pack and Pluckthun, 1992), dimeric miniantibodies (Muller *et al.*, 1998), minibodies (Hu *et al.*, 1996), diabodies (Holliger *et al.*, 1993) and triabodies (Iliades *et al.*, 1998; Lawrence *et al.*, 1998; Hudson and Kortt, 1999). Non-covalent diabodies and triabodies are among the easiest to engineer and are produced by shortening the polypeptide linker connecting the variable heavy and light chains from 15 amino acids to 5 for the diabodies and 0 – 3 for the triabodies. The compatible vector series described by Krebber and associates (1997) allows for the production of dimeric scFvs (as discussed in Section 1.7.9).

#### **1.7.8.2 Site-directed mutagenesis**

Site-directed mutagenesis involves amino acid substitutions within one or more of the CDRs followed by the subsequent selection of clones with higher affinity for the target antigen. Schier and associates (1996) reported a 16-fold increase in affinity of an scFv directed against HER2/neu following randomisation of the light chain CDR3. The resulting affinity mutant was then used as a starting molecule for the manipulation of the heavy chains. Following selection on the subsequent V<sub>H</sub> CDR3 libraries, containing randomised amino acids, a 1200-fold increase in affinity over the parental scFv was observed. An alternative method of site-directed mutagenesis, termed “parsimonious mutagenesis” was described by Balint and Larrick (1993). This method involves screening the entire CDR sequence and identifying the amino acids that are actively involved in antigen binding. First, the number of codons introduced is

limited so that each amino acid is only coded for by a single codon. The amino acids at each position are then manipulated to favour the parental sequence, conservative changes and those that appear more frequently in CDR regions of the antibody. PCR-based site-directed mutagenesis has been described for the affinity maturation of an scFv against Venezuelan equine encephalitis virus (VEE), during which a five-fold increase in reactivity against VEE was observed in ELISA over the parental clone (Alvi *et al.*, 2003).

#### **1.7.8.3 Error-prone PCR**

Error-prone PCR is a random mutagenesis technique used to introduce amino acid changes into proteins. Mutations are deliberately introduced during PCR amplification of the specific genes through the use of error-prone DNA polymerase reaction conditions. Taq DNA polymerase is commonly used because it lacks proofreading activity and the error rate is further increased by employing reaction buffers containing  $Mn^{2+}$  and unbalanced dNTP concentrations (Leung *et al.*, 1989; Cadwell and Joyce, 1992). Error-prone PCR has been successfully applied to the affinity maturation of an scFv directed against cardiac glycoside digoxigenin (Daugherty *et al.*, 2000). More recently error-prone PCR has been described in conjunction with an additional affinity maturation process. Zahnd and associates (2004) have described a method involving ribosomal display, error-prone PCR and DNA shuffling for the affinity maturation of a peptide binding scFv, which lead to a 500-fold affinity improvement over its potential germ line precursor.

#### **1.7.8.4 Chain shuffling**

Chain shuffling mutagenesis involves alterations to the intrinsic affinity of the monovalent antibody fragment. During chain shuffling the scFv is subjected to a series of manipulations during which the gene for one chain (e.g.  $V_H$ ) of the scFv is cloned into a repertoire for the second chain (e.g.  $V_L$ ) (Marks *et al.*, 1992). The resulting antibody library consists of phage encoding an scFv containing  $V_H$  chains specific for the target antigen and random  $V_L$  chains. The resulting library is then panned against the specific antigen and clones with improved binding properties are identified. The cycle is then repeated except this time the new  $V_L$  gene is shuffled into a  $V_H$  repertoire. However, in order to maintain the specificity of the parent scFv, the CDR3 (that contains most of the contact residues to the antigen) is conserved.

Therefore, only the V<sub>H</sub> segment from frameworks 1 to 3, including CDRs 1 and 2 are replaced. Using this method the affinity of a naïve human scFv directed against the glycoproteins tumour antigen c-erbB-2 was increased six-fold following light chain shuffling and five-fold by heavy-chain shuffling (Schier *et al.*, 1996).

#### 1.7.8.5 Ribosomal display

Ribosomal display is an *in vitro* technique aimed at the simultaneous selection and evolution of proteins from diverse libraries without the need for any bacterial transformations. Ribosomal display of scFv antibody fragments has been described in prokaryotic (Hanes and Pluckthun, 1997) and eukaryotic (He and Taussig, 1997) systems.

Figure 1.12 illustrates the principal of *in vitro* ribosomal display. Initially the DNA encoding the scFv library is PCR amplified, whereby a T7 promoter, a ribosome-binding site and stem loops are introduced, and then transcribed, *in vitro*, into mRNA. The T7 promoter ensures efficient transcription by T7 RNA polymerase, the ribosome binding sites enable initiation of translation *in vitro* and the stem loop structure prevents RNase E degradation. Following purification the mRNA is translated *in vitro*, whereby the mRNA is retained on the ribosome as a result of an absent stop codon (Hanes and Pluckthun, 1997 and He *et al.*, 1999) resulting in the formation of a tertiary mRNA-ribosome-scFv complex. The tertiary complex is stabilised at low temperature (4°C) and in buffer containing magnesium (Hanes and Pluckthun, 1997 and Schaffitzel *et al.*, 1999). The mRNA-ribosome-scFv complexes are then affinity selected from the translation mixture through binding of the native scFv to the specific immobilised antigen. Non-specific binders are eliminated following stringent wash steps and specific binders are eluted following dissociation with EDTA or upon addition of free antigen (Hanes and Pluckthun, 1997 and Schaffitzel *et al.*, 1999). The mRNA can then be isolated from the specific binder and reverse transcribed into cDNA for use in the next enrichment cycle. Ribosomal display is an entirely cell free system that does not require the need for bacterial transformations. Therefore, large antibody repertoires can be constructed and used for selection. Further diversity can be introduced either before starting or in between ribosomal display cycles via DNA shuffling (Stemmer, 1994) or error-prone PCR (Cadwell and Joyce, 1994). Ribosome

display methods have been successfully applied to *in vitro* affinity maturation of an scFv against bovine insulin during which up to a 40-fold increase in affinity was observed (Hanes *et al.*, 2000).

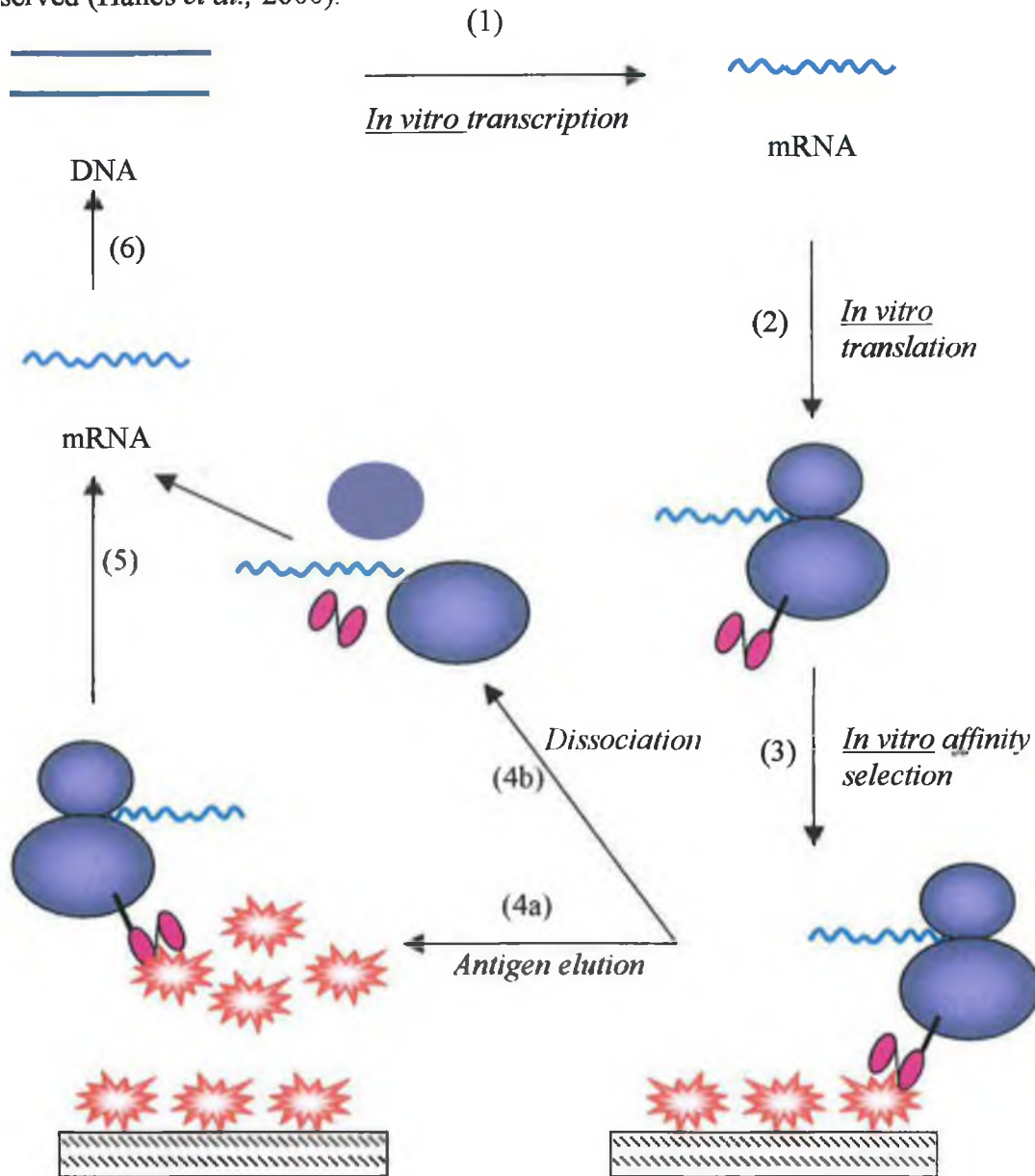


**Figure 1.12:** Illustration of the principal of ribosomal phage display technology. DNA encoding the scFv library is PCR amplified, and transcribed into mRNA (1). The mRNA is then translated *in vitro* in such a way that a mRNA-ribosome-scFv complex is formed (2). Ribosome complexes, containing the scFv of interest, are affinity selected, with non-specific complexes being removed following stringent wash steps (3). Affinity selected complexes are eluted using free antigen (4a) or following EDTA dissociation (4b). The mRNA is isolated (5) and reverse transcribed into cDNA (6) for the next round of selection / enrichment. (Modified from Hanes and Pluckthun, 1997.)

### 1.7.9 Krebber scFv phage display system

Krebber and co-workers (1997) have developed and optimised a phage display system for the expression of scFv antibody fragments. This system offers robustness, vector stability and tight control of scFv expression fused to the wild type geneIII coat protein of filamentous phage, primer usage for PCR amplification of variable region genes, scFv assembly strategy and subsequent directional cloning using a single rare cutting restriction enzyme (SfiI). The Krebber system also offers a compatible vector series to simplify modification, detection, multimerization and rapid purification. The pAK vector series, described by Krebber *et al.* (1997), consists of 6 vectors (pAK100 – pAK600), which can be used for the expression of scFvs on the surface of phage (pAK100/200) or in soluble form (pAK300 – 600) (Fig. 1.13).

Each vector contains a chloramphenicol resistance marker and a tetracycline resistance gene. The tetracycline gene is flanked on either side by an SfiI restriction site that allows the *tet* gene to be removed and replaced with the genes encoding the variable heavy and light genes of the antibody. All vectors also contain *pelB* leader sequence, a strong upstream  $t_{HP}$  terminator, between the *lacI* gene and the *lac* promoter/operator region, which in combination with glucose repression of the *lac* promoter prevents background expression prior to IPTG induction. The pAK100 vector contains a truncated version of gIII phage coat protein in order to avoid immunity to superinfection, a c-myc tag for detection and an amber codon, that allows the switching between phage-bound and soluble scFv expression by simply changing the expression host. The primers engineered for the amplification of the variable regions encode a truncated version of the FLAG sequence, which enables detection and purification of the expressed scFv. The pAK400 vector contains a C-terminal hexa-His tag for purification using immobilised metal affinity chromatography (IMAC) and detection using an anti-His tag antibody and a strong Shine Dalgarno sequence (SDT7g10) for increased scFv expression. The pAK500 vector contains a single chain double helix (dHLX) for scFv dimerisation followed by a penta-His tag. The pAK600 contains a bacterial alkaline phosphatase gene that allows direct detection and results in dimerisation of the scFv. A schematic representation of the soluble scFvs expressed from pAK400/500/600 can be seen in Figure 1.14.

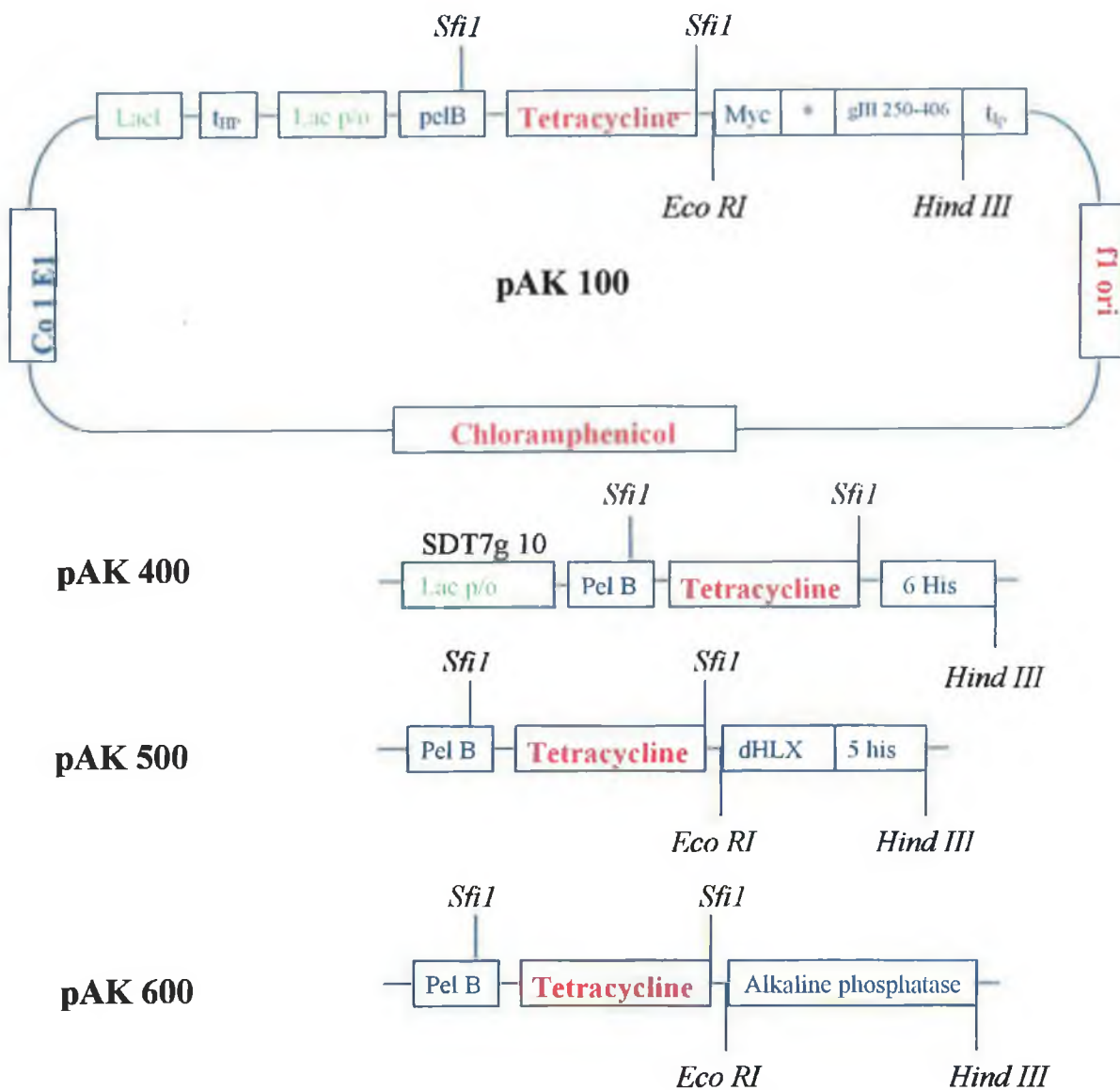


**Figure 1.13:** pAK compatible vector series. Phage display vector (pAK100) and its related vectors (pAK400 – 600) are used to construct various scFv modifications. The pAK vectors contain the same elements as detailed for pAK100 except for the modified cassettes shown above. The pAK vectors encode tetracycline and chloramphenicol antibiotic resistance genes, the lacI repressor gene (LacI), a strong upstream terminator ( $T_{HP}$ ), the lac promoter / operator (Lac p/o), the pelB leader sequence (pelB), modified to contain an SfiI site and a downstream terminator ( $t_{1p}$ ). Additionally, pAK100 encodes a truncated version of the gIII phage coat protein (gIII<sub>250 - 406</sub>), a c-myc tag (myc) and an amber codon (\*). pAK400 encodes hexa-His tag for purification and detection and a strong Shine Dalgarno sequence (SDT7g10) for increased scFv expression. pAK500 encodes penta-His tag and a helix for dimerisation (Park *et al.*, 1993). pAK600 encodes an alkaline phosphatase label for direct detection and dimerisation (Lindner *et al.*, 1997). Modified from Krebber *et al.*, 1997.

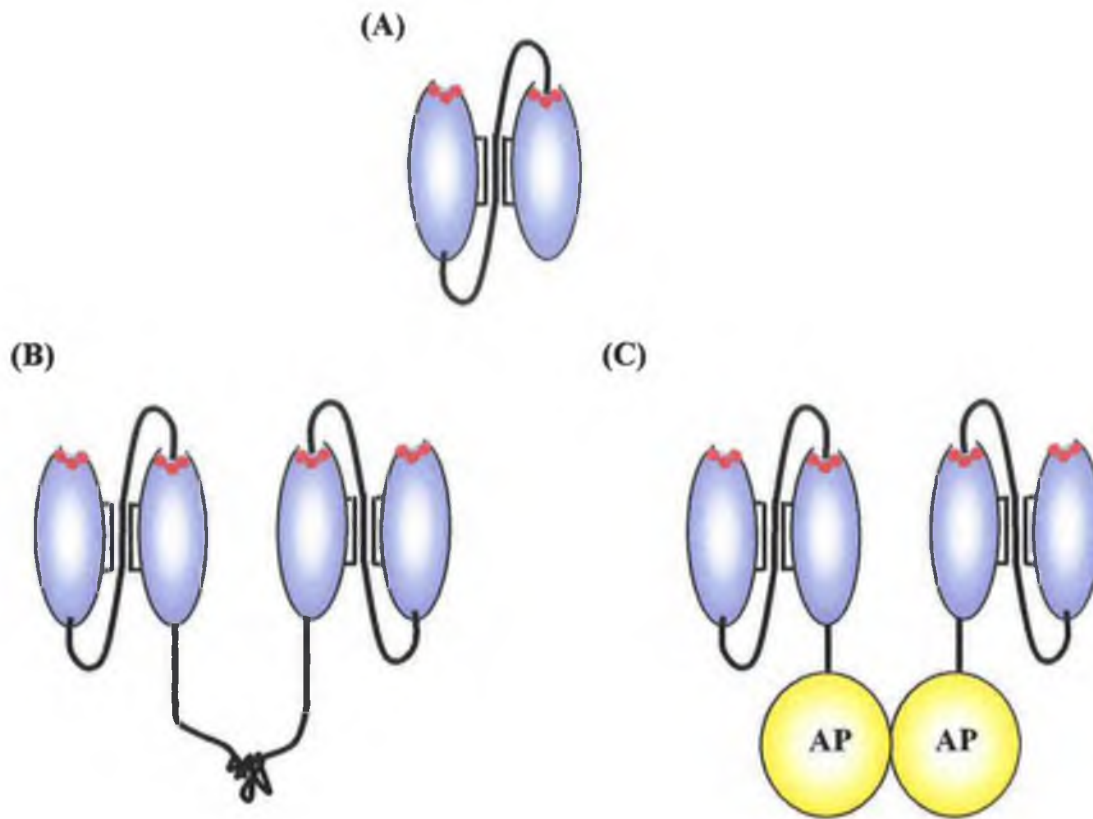


**Figure 1.14:** Schematic representation of the monomeric (A), dimeric (B) and bifunctional scFvs (C). The monomeric scFv consists of a variable heavy and light chain domain stabilised with a serine-glycine linker; the dimeric scFv comprises two scFv fragments dimerised via a double helix and the bifunctional scFv consists of two alkaline phosphatase-labelled scFvs fused via the alkaline phosphatase (AP).

## 1.8 Immunoassays

An immunoassay is an analytical technique that relies on the use of antibody molecules for the detection of a specific compound present in a complex sample or matrix. The first immunoassay was introduced by Yalow and Berson (1959) and it was used to detect the presence of insulin in blood samples.

Immunoassays have numerous advantages over the conventional analytical methods such as mass spectrometry, gas chromatography and liquid chromatography. In contrast to such techniques, immunoassays do not require the use of expensive equipment, which requires highly skilled technical expertise to operate and the analysis of samples using immunoassays is relatively quick. Immunoassays can be performed easily, they are relatively economical, sensitive and highly specific. The selectivity of an immunoassay is based on the innate selectivity of the antibody-antigen reaction and the sensitivity is determined by the detection limit of the label and by the affinity of the specific antibody (Van Emon *et al.*, 1989).

Immunoassay can be defined as homogeneous or heterogeneous depending on whether the assay is carried out in solution (fluid phase) or on the surface of plastic (solid-phase). Homogeneous immunoassays are performed in a single step, in solution, and do not require the separation of the free and bound labelled antibody. However, heterogeneous immunoassays involve the immobilisation of either the antigen or antibody onto a solid support matrix, in such a way that the immunogenicity of the molecule is not affected. Immunoassays can also be further classified depending on the label used to detect the antibody-antigen interaction. Radioisotopes are used in a radioimmunoassay format (RIA), enzymes in an enzyme immunoassay format (EIA or ELISA) and fluorescent labels are used in a fluorescent immunoassay format (FIA).

Several different immunoassay formats have been described with the most commonly used including the non-competitive or indirect and the competitive immunoassays. Non-competitive immunoassays can be used to determine the concentration of an antibody in the sample being analysed during which the analyte is adsorbed onto the solid support matrix and the antiserum allowed to react with the immobilised analyte. Antibody-antigen interactions can then be indirectly quantified using a labelled

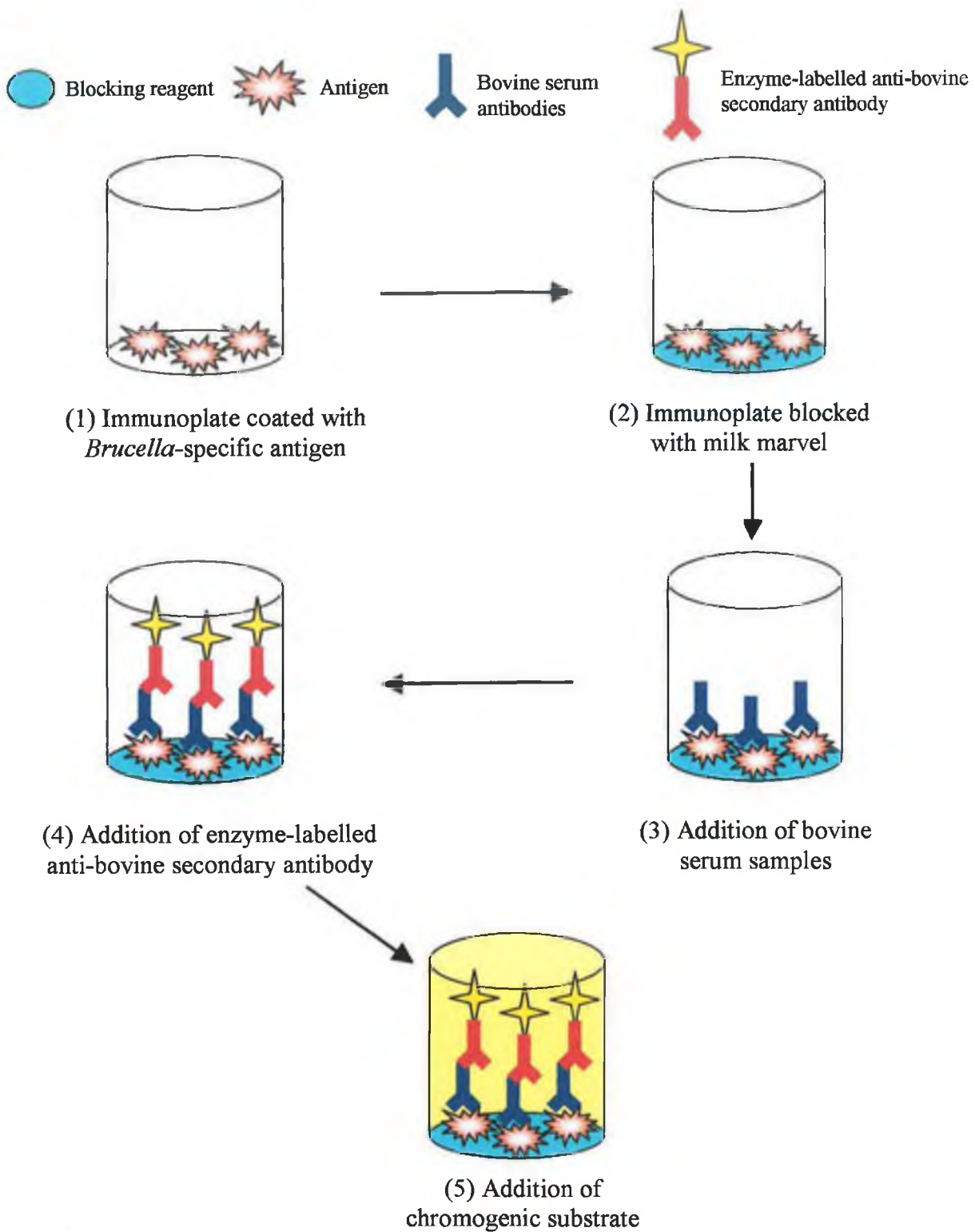
secondary antibody. However, a competitive immunoassay measures competition in binding to antibody between a fixed amount of antigen and an unknown quantity of antigen (analyte) in the sample. In a competitive immunoassay format the response obtained is inversely proportional to the concentration of analyte in the sample mixture.

### **1.8.1 Enzyme-linked immunosorbent assay (ELISA)**

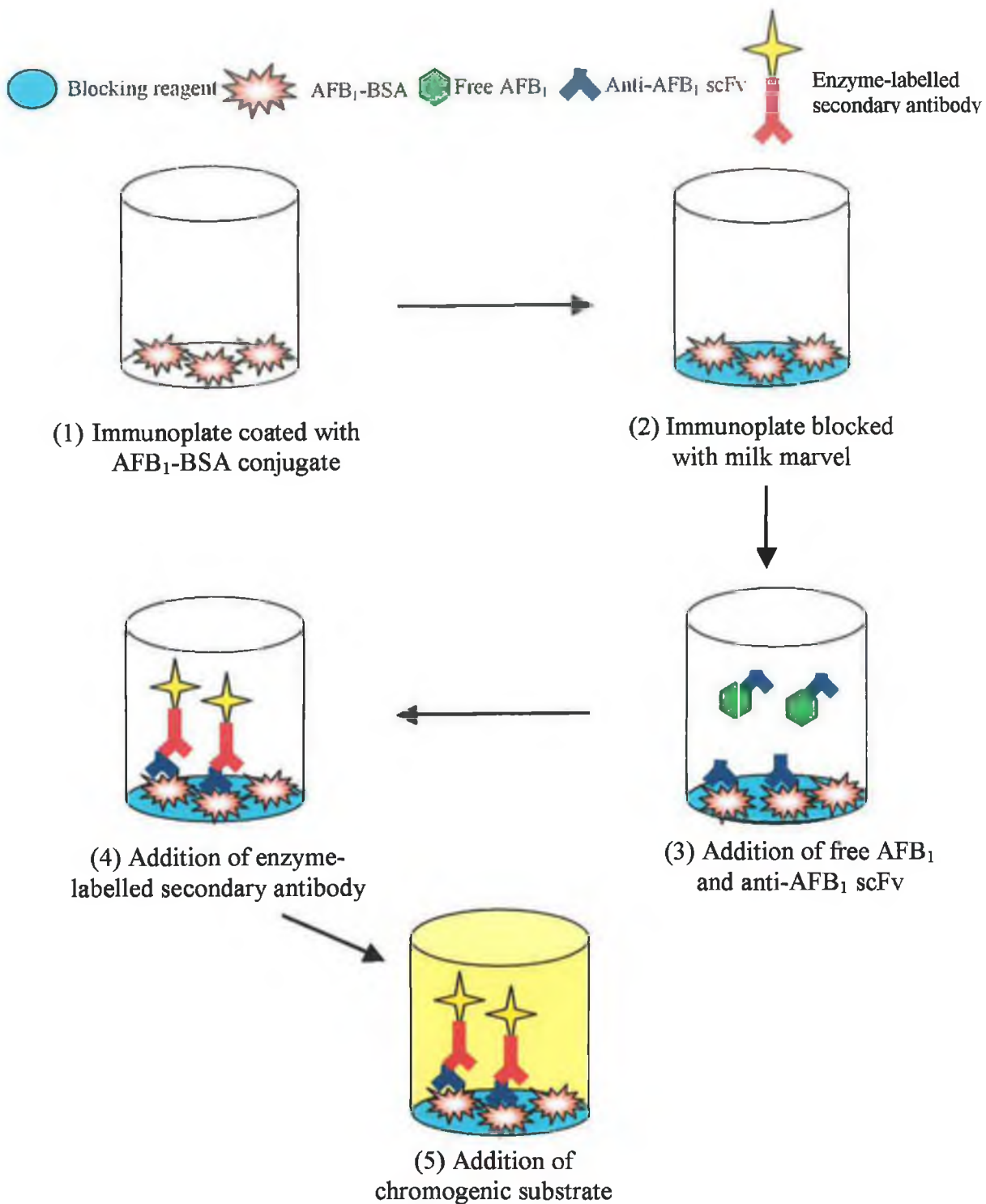
The ELISA technique is one of the most commonly used immunoassay formats for detecting antigen-antibody interaction and is routinely used for the detection of many important analytes including dangerous residues in meat products (Pou *et al.*, 1994) and pesticide residues in food (Franek *et al.*, 1995). In this type of immunoassay format either the antigen or antibody is immobilised onto a solid support matrix in such a way that the immunogenicity of the molecule is not affected. The immunosorbent refers to the solid support onto which the antigen or antibody is adsorbed. An enzyme label is attached to the antigen or antibody and this is used to detect bound antigen-antibody complexes. The most commonly used enzymes in ELISAs are horseradish peroxidase and alkaline phosphatase.

Figure 1.15 illustrates a schematic representation of an indirect non-competitive ELISA. Initially, the antigen of interest is absorbed onto the solid support matrix through hydrophobic interactions. Following suitable incubation (i.e. 1 hour at 37°C) the plate is washed three times with phosphate-buffered saline (PBS) and 3 times with PBS – 0.05% (v/v) tween. Non-specific binding interactions are then eliminated following blocking with milk marvel dissolved in PBS, which binds any uncoated absorption sites. Following appropriate incubation the plate is washed, as before, and serial dilutions of the specific antibody / serum samples are added to each well and allowed interact with the immobilised antigen. After incubation any unbound antibodies are removed following a wash step. An enzyme-labelled anti-species secondary antibody is added and incubated. The plate is then washed and following addition of a chromogenic substrate the colour intensity is determined at the appropriate wavelength use a spectrophotometer. The colour produced is directly proportional to the concentration of the specific antibody and can be used to quantitatively measure antigen – antibody binding.

Figure 1.16 displays a schematic representation of a competitive ELISA. This assay format is similar to that of the indirect non-competitive ELISA. The antigen of interest, in this case an aflatoxin B<sub>1</sub>-BSA conjugate, is absorbed onto an immunoplate, which is blocked using milk marvel. A solution containing a constant amount of the specific antibody and varying concentrations of free antigen (AFB<sub>1</sub>) is added to the wells of the immunoplate and incubated. The immunoplate is washed and the enzyme-labelled anti-species secondary antibody added. Following incubation the plate is washed and the chromogenic substrate added. The colour produced in this assay format is inversely proportional to the concentration of free antigen added. Therefore, this assay format can be used for the quantitative detection of an antigen following reference to a standard curve.



**Figure 1.15:** Schematic representation of an indirect non-competitive ELISA. Each step requires an appropriate incubation period and any unbound material is removed following a wash procedure. The plate is coated with the antigen of interest (1) and any unbound sites are blocked with casein to prevent any non-specific interactions (2). The specific antibody is then incubated with the immobilised antigen (3) and any antigen – antibody interactions are detected using an enzyme-labeled species-specific antibody (4) following addition of the chromogenic substrate (5).



**Figure 1.16:** Schematic representation of an indirect competitive ELISA. Each step requires an appropriate incubation period and any unbound material is removed following a wash procedure. The plate is coated with the antigen of interest (1) and any unbound sites are blocked with casein to prevent any non-specific interactions (2). Free and immobilised antigen compete for binding to the specific antibody (3) and any antibodies bound to the immobilised antigen are detected using an enzyme-labelled species-specific antibody (4) following addition of the chromogenic substrate (5).

### 1.8.2 Lateral-flow immunoassay (LFIA)

The lateral flow immunoassay (LFIA) is an immunochromatographic technique studying antibody-antigen interaction as components of a sample are separated using a chromatographic technique. These membrane immunoassays have been developed for a variety of applications including the detection of several antigens including aflatoxins (Sibanda *et al.*, 1999 and Niessen *et al.*, 1998); human chorionic gonadotropin (van Amerongen *et al.*, 1994); cannabinoids, cocaine and opiates in urine (Wenning *et al.*, 1998) and *Fusarium* T-2 toxin in wheat (de Saeger and Peteghem, 1996). The first commercially successful LFIA was the pregnancy test, which was based on the rapid detection of human chorionic gonadotropin in urine (May, 1991).

LFIA involves the unidirectional flow of pre-impregnated antibody or antigen-coated particles (e.g. latex, carbon, colloidal gold or silica) along a membrane. Interactions between the particle-coated antigen / antibody and the target molecule occur as the sample flows along the membrane and, if present, are subsequently detected and captured by a specific antibody immobilised in a defined area on the membrane. Figure 1.17 illustrates the principle behind the lateral flow immunoassay whereby the capture ligand is spotted or immobilised onto the nitrocellulose strips in a line-format. The sample droplet containing a detection ligand coupled to colloidal carbon particles is applied to the tip of the strip and allowed chromatographically run through the membrane by capillary action. Upon passing the immobilised capture ligand the detection ligand, bound to the specific antigen, can specifically bind, resulting in the formation of a visual signal (i.e. a black line).

Surface-modified hydrophilic membrane supports that covalently bind protein are used in a LFIA format. These retain the immobilised protein in its native conformation (Pfund and Bourdage, 1990). The basic chemistry of the solid phase can affect the immobilisation of the capture reagent and the release and flow of the mobile samples (Price *et al.*, 1997). Nitrocellulose is the most suitable membrane for LFIA development because it possesses high protein binding, low non-specific binding, a smooth white surface that gives better visibility of results and, typically, it is of uniform thickness. Protein binds to nitrocellulose by electrostatic mechanisms. The porosity of the nitrocellulose can influence protein binding with increasing pore size

resulting in a decrease in the polymer surface area and consequently the membrane binds less protein. Increased pore size can however result in increased flow rates (Harvey, 1991). Although faster flow rates decrease the assay time the sensitivity of the assay may be affected, as the molecules in the sample have less time to interact.

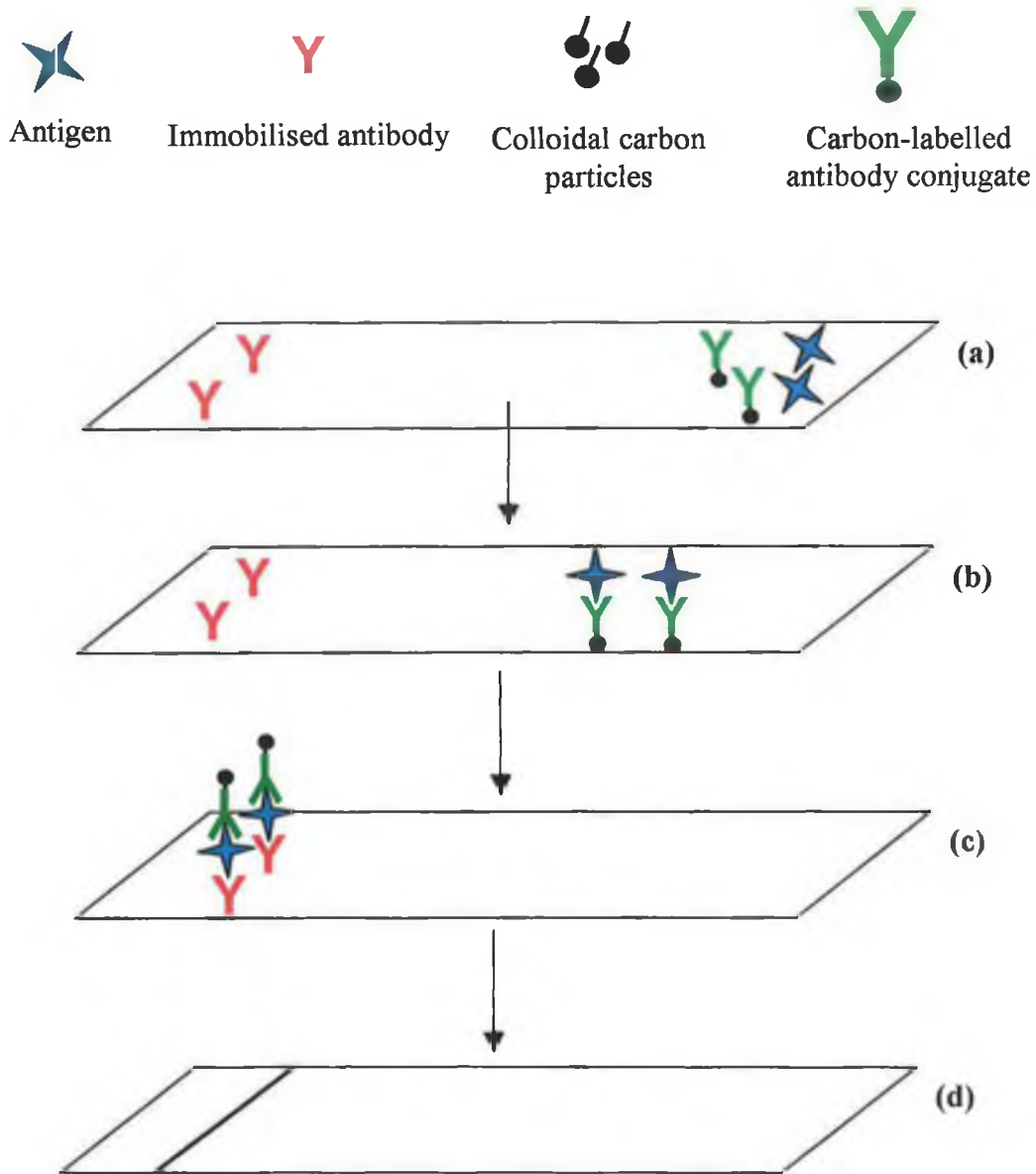


**Figure 1.17:** Schematic representation of a lateral flow immunoassay device. Following sample addition (a) the carbon-labelled antibody interacts with the antigen as the sample flows along the membrane. The antigen-antibody interaction is then captured by the antibody immobilised on the membrane (c). Concentration of the antigen-antibody-coated particle complex in a defined area on the membrane results in the generation of a signal, which is visible by the naked eye (d).

## 1.9 Biacore

The Biacore is a commercially available biosensor system that has been applied to the development immunoassays for the detection of several analytes including aflatoxin B<sub>1</sub> (Van der Gaag *et al.*, 1998 and Daly *et al.*, 2000) and morphine 3-glucuronide (Brennan *et al.*, 2002 and Dillon *et al.*, 2003). Biacore systems detect binding events using the phenomenon of surface plasmon resonance (SPR) (Liedberg *et al.*, 1995; Salamon *et al.*, 1999 and Quinn and O’Kennedy, 1999). The Biacore sensor uses continuous flow technology that enables biospecific interaction analysis (BIA) such as antigen-antibody binding in “real-time”. The Biacore system offers several advantages over conventional biomolecular interaction techniques. It provides real-time monitoring, label free detection, a reusable sensor surface, flexible-experimental design, rapid analysis, exact sample handling and a complete integrated analytical system.

SPR is an optical technique that utilises the principle of total internal reflection (TIR). When a plane-polarized light beam propagates a medium of higher refractive index (e.g. glass prism) and meets an interface with a medium of lower refractive index (e.g. sample solution) the light is totally internally reflected, above a certain critical angle. Under these conditions an evanescent wave, an electromagnetic field component of the light, penetrates into the low refractive media to a magnitude of one wavelength (Fig. 1.18). If the TIR interface is coated with a thin metal film (which is gold in the case of the Biacore) and the light is monochromatic and p-polarised (i.e. the electric vector component is parallel to the plane of incidence) the evanescent wave interacts with the electrons on the metal layer. The electron clouds on the surface of the metal layer are also known as plasmons and following propagation of the evanescent wave the plasmons begin to resonate forming a quantum mechanical wave known as the surface plasmon wave. At a particular angle of incidence, some of the energy of the reflected light causes excitation of the surface plasmons, resulting in a decrease in intensity of the reflected light. The specific angle at which SPR occurs is known as the SPR angle. The SPR angle is dependent on the refractive index of the medium close to metal film. Therefore, changes in the refractive index of the buffer solution (i.e. an increase in the surface concentration of solutes) can alter the SPR angle. Continuous monitoring of the SPR angle enables the quantification of changes in the refractive index of the medium adjacent to the metal layer. Therefore, SPR can be

used to monitor biological interactions on the metal film because changes in the refractive index of the media are directly proportional to changes in mass or concentration on the surface of the metal layer.

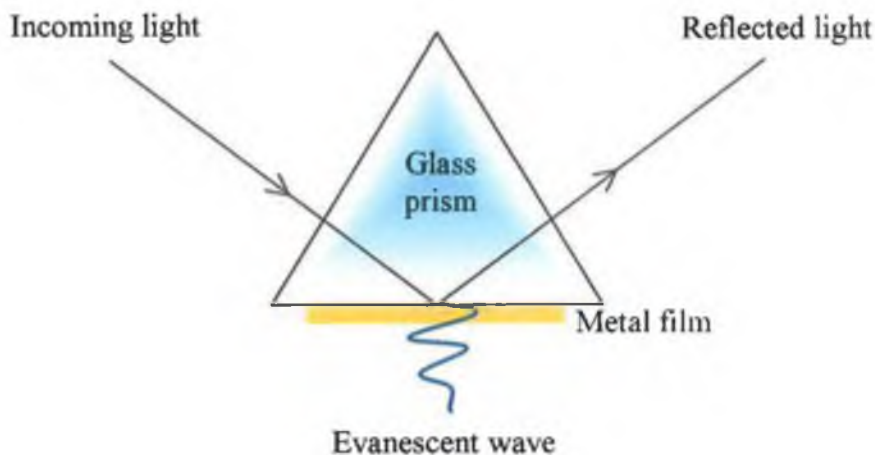


**Figure 1.18:** *Principle of surface plasmon resonance. Under conditions of total internal reflection at a metal-coated interface an electromagnetic field component of the light, known as the evanescent wave, propagates into the medium of lower refractive index on the non-illuminated side.*

The SPR angle is dependent on a number of factors, including the properties of the metal film (e.g. thickness, optical constants and uniformity), the wavelength of the incident light and the refractive index of the media on either side of the metal film. The refractive index of the medium into which the evanescent wave propagates, on the non-illuminated side of the surface, is affected by the surface concentration of solutes, so that monitoring the SPR angle provides a real-time measure of changes in the surface concentration. A shift in the SPR angle is observed when biomolecules bind to the immobilised surface and changes the refractive index of the surface layer (Fig. 1.19). The change in SPR angle is plotted against time in a sensogram, which displays the progress of the interaction at the sensor surface as it occurs (Fig. 1.20).

Biacore systems utilise a high-efficiency near-infrared light emitting diode, at a wavelength of 760nm, which focuses light, in a wedge-shaped beam, onto the sensor surface providing a fixed range of incident angles. The SPR response in the reflected light is monitored using a fixed array of light-sensitive 2-dimensional diodes, from which the angle at which minimal reflection occurs (the SPR angle or resonance) is calculated.

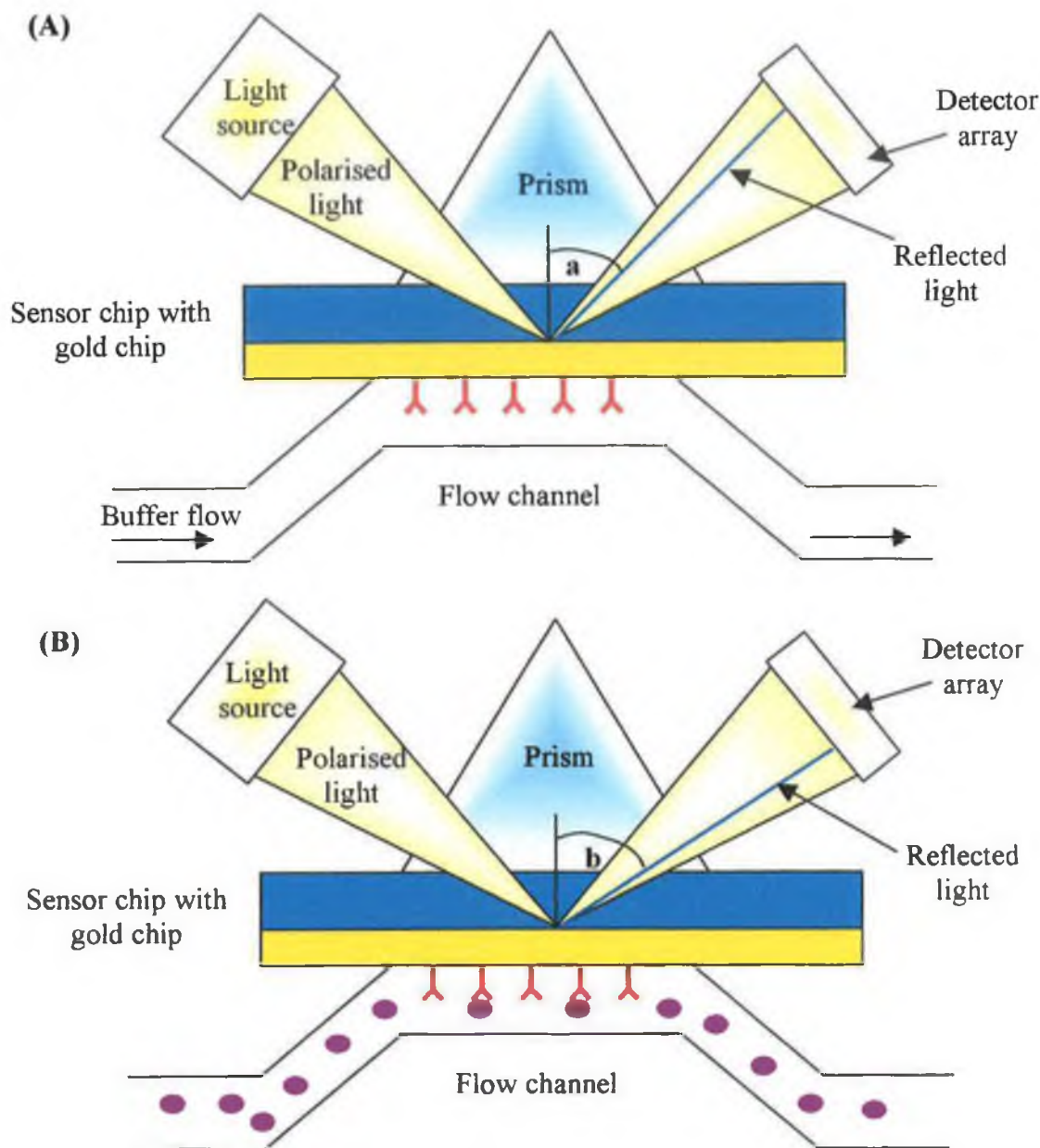


**Figure 1.19:** Diagrammatic representation of surface plasmon resonance occurring at the surface of a Biacore sensor chip. (A) The sensor surface is immobilised with an antibody (Y) using EDC/NHS chemistry. Light from a light-emitting diode is focused on the sensor and the reflected light is detected using a 2-dimensional photo-diode array. Under conditions of total internal reflection an evanescent wave propagates into the medium of lower refractive index, which results in a dip in the intensity of the reflected light at a particular angle known as the SPR angle ( $a$ ). (B) Following injection of the antigen (●), a shift in the surface plasmon resonance angle ( $b$ ) occurs following specific interaction between the immobilised antibody and antigen. The change in the SPR angle is as a direct result of changes in the mass concentration at the immobilised sensor surface.

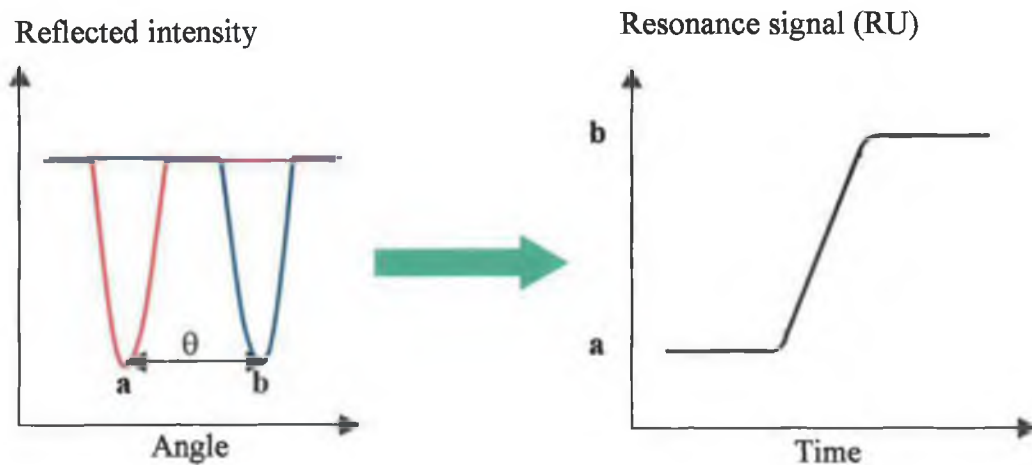


**Figure 1.20:** The sensogram is used to display the progress of interactions at the sensor surface. Changes in the SPR angle ( $\theta$ ) are continuously monitored and displayed as a function of time on a sensogram as the antibody-antigen interactions occur. Binding interactions on the sensor surface result in a change in the mass concentration, which causes an increase in the SPR angle. The increase in the SPR angle is seen as a gradual increase in signal on the sensogram. Resonance units (RU) are used to express the SPR signal on the sensogram.

Changes in the SPR angle occur due to changes in the refractive index of the surface layer, which in turn is as a result of both the bulk solution and interactions on the surface matrix. In the majority of Biacore applications the contribution of the bulk solution is eliminated because the measured parameter is either the rate of change of the signal, which is the case in binding kinetics, or the difference in signal between response units before and after injection is used, as with binding interaction studies. Figure 1.21 represents a schematic sensogram after sample injection. Following injection a significant increase in the refractive index is observed due to the bulk solution. A steady increase in the binding response is then seen as the antigen interacts with the immobilised antibody and, on completion of sample injection, a large decrease in the refractive index is observed as running buffer begins to pass over the surface. The difference between the resonance units before and after sample injection is used to determine binding interactions on the immobilised surface. A binding response of 1000 RU is equivalent to a change of approximately  $1\text{ ng/mm}^2$  in surface protein concentration or of about  $6\text{ mg/ml}$  in bulk protein concentration (Stenberg *et al.*, 1991).

The quantitative analysis on the binding interactions between biomolecules is dependent on the immobilisation of a target molecule on the sensor chip surface (Fig. 1.22). The sensor chip surface consists of a glass layer coated with a thin gold film. Gold is selected because of its chemical inertness and good SPR response. The gold layer is covered with a covalently attached matrix (attached through a linker layer), onto which biomolecules can be immobilised. The CM5 sensor chip is the most widely used and consists of the gold surface modified with a carboxymethylated dextran layer. The carboxymethylated dextran provides a hydrophilic environment for the immobilisation of biomolecules. Sensor chips for specialised applications are also available. These include Sensor Chip SA, which is covalently immobilised with streptavidin to capture biotinylated molecules, Sensor Chip NTA, for the capture of His-tagged molecules and the Sensor Chip HPA, which enables the attachment of lipid monolayers for membrane biochemistry and the study of membrane-associated receptors.

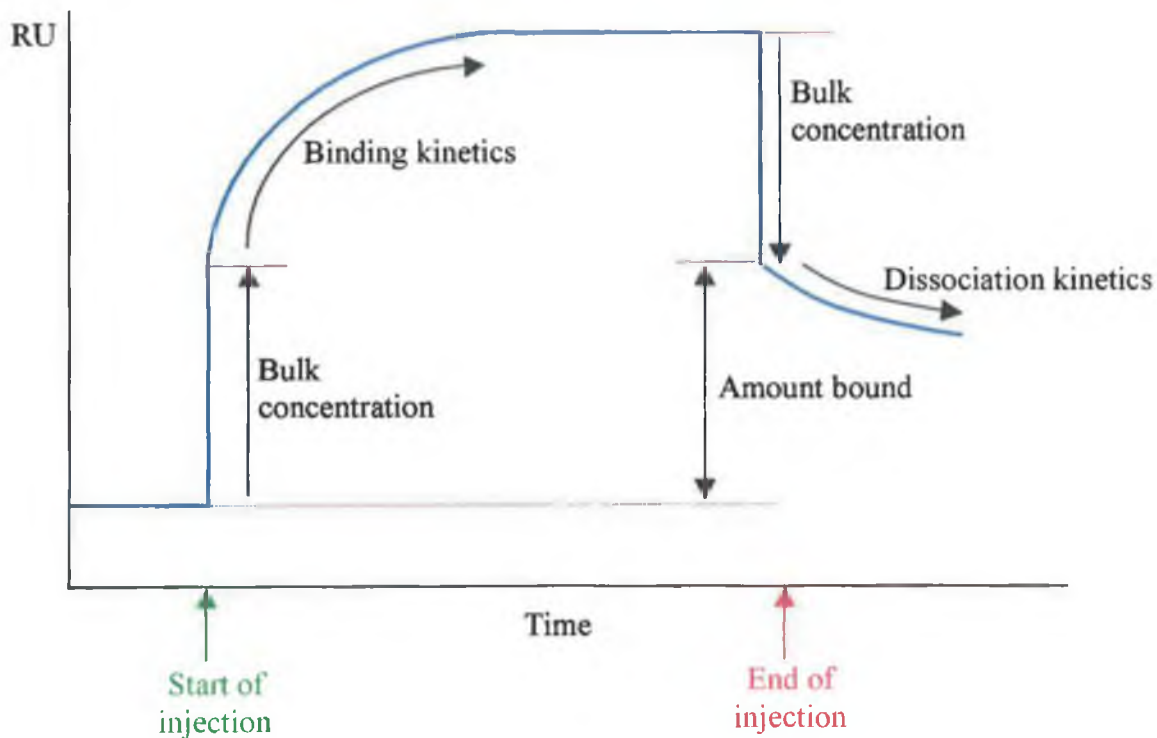


**Figure 1.21:** Schematic representation of a sensogram following injection of antigen over an antibody immobilised surface. Initially a steady baseline is observed as running buffer is passed over the surface. Following injection of the sample an initial change in the refractive index is observed due to the bulk solution. This is followed by a steady increase in the SPR signal as binding interactions occur at the sensor surface. On completion of sample injection there is a rapid decrease in the bulk refractive index as running buffer is passed over the surface. The amount of bound antigen is then determined as the difference in response units observed before and after sample injection.

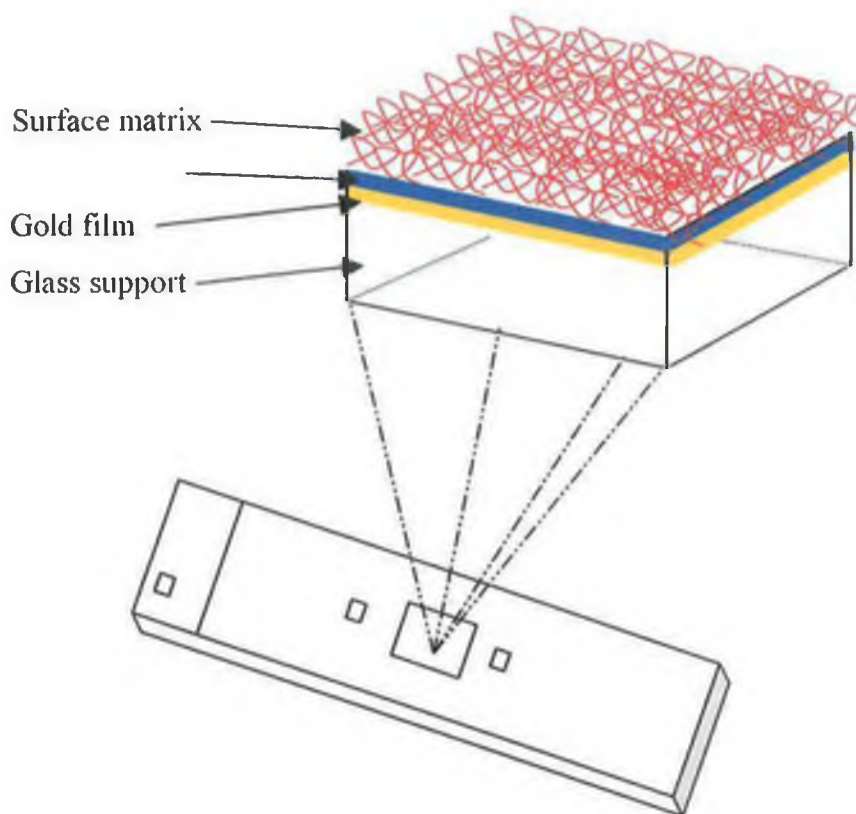


**Figure 1.22:** Diagrammatic representation of the surface of a carboxymethylated 5 (CM5) sensor chip. The chip consists of three layers: glass, a thin gold film and a matrix layer. The matrix layer is attached to the gold film through an inert linker layer. In the case of the CM5 chip the matrix layer is carboxymethylated dextran, which allows the covalent immobilisation of molecules onto the sensor surface.

### 1.10 Aims of research

The main aims of this research project were the development of rapid immunoassays for the detection of aflatoxin B<sub>1</sub>, using novel antibody fragments, and the development of a highly sensitive and specific immunoassay for the detection of a *Brucella* infection in bovine serum samples.

Chapter 3 describes the production and characterisation of a monomeric, a dimeric and an alkaline phosphatase-labelled scFv against aflatoxin B<sub>1</sub>. The scFvs were applied to the development of competitive ELISAs and Biacore inhibition immunoassays for the detection of aflatoxin B<sub>1</sub>. A rapid sol particle immunoassay was also developed for the detection of aflatoxin B<sub>1</sub>, using a monoclonal antibody obtained from collaborators (IFR Norwich, UK.).

Chapter 4 describes the production and characterisation of two *Brucella*-specific recombinant proteins. p18, an 18kDa cytoplasmic protein, and bp26, a 26kDa periplasmic protein, were cloned from *B. abortus* 45/20 cells. Following high-level expression, the recombinant proteins were purified using immobilised metal affinity chromatography (IMAC), characterised and investigated for use as serological diagnostic markers of bovine brucellosis.

Chapter 5 described the production and characterisation of polyclonal and recombinant *Brucella*-specific antibodies. Polyclonal antibodies were raised against *B. abortus* 45/20 cells, and following purification the antibodies were applied to the development of a competitive immunoassay for the detection of whole *B. abortus* cells. A naïve human phage display library was also panned against the p18 and bp26 recombinant proteins.

Chapter 6 describes the optimisation and validation of immunoassays for the detection of a *Brucella* infection in bovine serum samples. Several indirect and sandwich immunoassay formats were developed, using the antigens and antibodies described in chapters 4 and 5, and validated using a pool of known positive and negative serum samples.

# CHAPTER 2

## Materials and Methods

## 2.1 Material and equipment

### 2.1.1 Material

All reagents and chemicals were of analytical grade and supplied by Sigma-Aldrich Co. (Poole, Dorset, U.K.), unless listed below (Table 2.1).

*Table 2.1: Reagents and chemicals used and the relevant suppliers.*

Reagent	Supplier
Acetic acid Hydrochloric acid	Riedel de-Haen AG, Wunstorfer, Strabe 40, D-30926, Hannover, Germany.
Anti-bovine-HRP antibody	DakoCytomation Denmark A/S, Golstrup, Denmark.
BamHI enzyme NcoI enzyme T4 DNA ligase	Biosciences, 13 Charlemont Tce., Crofton Rd., Dun Laoghaire, Co. Dublin.
Bicinchoninic acid assay (BCA) kit	Pierce and Warner (UK) Ltd., Chester UK.
Colloidal carbon	ATO BV, Postbus 17, NL-6700, AA, Wageningen, The Netherlands.
M13K07 Helper phage	Stratagene, North Torrey Pines Rd., La Jolla, USA.
Ni-NTA resin pQE-60	QIAGEN, QIAGEN House, Fleming Way, Crawley, West Sussex, UK.
Nitrocellulose membrane	Schleicher and Schuell Bioscience GmbH, Hahnestrasse 3, D-37586, Dassel, Germany.

---

PCR primers Sequencing	MWG-Biotech Ltd., Milton Keynes, MK12 5RD, UK.
SfiI enzyme	New England Biolabs, 73 Knowl Piece, Wibury Way, Hitchin, Hertfordshire, UK.
TA cloning kit	Invitrogen, 9704-CH-Groningen, Netherlands.

---

### 2.1.2 Equipment

*Table 2.2: List detailing equipment used and the relevant suppliers.*

---

Equipment	Supplier
3015 pH meter	Jenway Ltd., Gransmore Green, Felsted, Dunmow, Essex, UK.
Atto dual minislab AE-6450 Atto Ae-6100 Titertek Twinreader PLUS Sterile universal tubes Hybrid PCR express	Medical Supply Company (MSC), Damastown, Mulhuddart, Dublin 15, Ireland.
Beckman ultracentrifuge (L8-70M) Beckman centrifuge (J2-21)	Beckman-Coulter Inc., 4300N Harbour Boulevard, Fullerton, CA 92834-3100, USA.
BIACORE 3000	Biacore International AB, Uppsala, Sweden.
Biometra PCR machine	Anachem Ltd., Anachem House, Charles St., Luton, Bedfordshire, UK.

---

---

BioRad wet blotter	BioRad, BioRad House, Maylands Ave., Hemel Hempstead, Hertfordshire, UK.
Eppendorf centrifuge (5810 R)	Eppendorf AG, 10 Signet Court, Swann Rd., Cambridge, UK.
Eppendorf tubes	Sarstedt, Wexford, Ireland.
Grant waterbath (Y6)	Grant Instruments (Cambridge) Ltd., 29 Station Rd., Shepreth, Royston, Hertfordshire, UK.
Hermle centrifuge Z 200 M/H)	Hermle Labortechnik, 78564-Wehingen, Gosheimerstr. 56, Germany.
Image Master VSD gel documentation system	Pharmacia Biotech, Uppsala, Sweden.
Linomat 5	Camag, Muttenz, Switzerland.
Sintered glass filtration system	Millipore, 900 Middlesex Tpk., Billerica, MA 01821, USA.
NUNC Maxisorb plates	NUNC, Kamstrup DK, Roskilde, Denmark.
Orbital incubator	Sanyo Gallenkamp plc., Monarch Way, Belton Park, Loughborough, Leicester, UK
SB1 blood tube rotator	Stuart Scientific, Holmethrope Industrial Est., Redhill, Surrey, UK.

---

Stuart platform shaker (STR 6)	Lennox, John F Kennedy Industrial Est., Naas Rd., Dublin 12, Ireland.
Tomy autoclave (SS 325)	Mason Technology, Greenville Hall, 228 South Circular Rd., Dublin 8, Ireland.
UV-160A spectrophotometer	Shimadzu Corp., Albert-Hahn-Str. 6-10, 47269 Duisburg, Germany.

### 2.1.3 Composition of culture media

**Table 2.3: Composition of culture media used.**

2x Tryptone yeast extract (2x TY) medium	Tryptone	16g/l
	Yeast extract	10g/l
	NaCl	5g/l
Luria broth (LB) medium	Tryptone	10g/l
	Yeast extract	5g/l
	NaCl	10g/l
Super optimal catabolite (SOC) medium	Tryptone	20g/l
	Yeast extract	5g/l
	NaCl	0.5g/l
	KCl	2.5mM
	*MgCl <sub>2</sub>	20mM
	*Glucose	20mM
	pH	7.0
* Added separately following autoclaving		

#### 2.1.4 Buffers

*Table 2.4: Composition of buffers used.*

---

<b>Hepes buffered saline (HBS)</b>	10mM HEPES 150mM NaCl 3.4mM EDTA 0.05% (v/v) Tween 20 pH 7.4
<b>Phosphate buffered saline (PBS)</b>	0.15M NaCl 2.5mM KCl 10mM Na <sub>2</sub> HPO <sub>4</sub> 1.8mM KH <sub>2</sub> PO <sub>4</sub> pH 7.3
<b>Tris-acetate / EDTA electrophoresis buffer (TAE)</b>	40mM Tris-acetate 1mM EDTA pH 8.0
<b>Tris-EDTA sucrose buffer (TES)</b>	100mM Tris-HCl, 0.5M Sucrose 0.5mM EDTA pH 8.0

---

## 2.1.5 Bacterial strains

*Table 2.5: Bacterial host strains and their genotypes.*

Bacterial strain	Genotype
XL-1 Blue <i>E. coli</i>	<i>RecA endA1 gyrA96 thi-1 hsdR17 supE44 relA1 lac [F'proAB lacI<sup>q</sup> ZΔM15 Tn10 (Tet<sup>r</sup>)]</i>
JM83 <i>E. coli</i>	<i>Ara Δlac-proAB rpsL φ80 dlacZΔM15</i>
INVαF' <i>E. coli</i>	<i>F'endA1 recA1 hsdR17 (r<sub>k</sub><sup>-</sup>, m<sub>k</sub><sup>+</sup>) supE44 thi-1 gyrA96 relA1 φ80lacZΔM15 Δ(lacZYA-argF)U16 λ</i>
XL-10 Gold <i>E. coli</i>	<i>Tet<sup>R</sup> Δ(mcrA) 183Δ(mcrCB-hsdSMR-mrr) 173 endA1 supE44 thi-1 recA1 gyrA96 relA1 lac Hie [F' proAB lacI<sup>q</sup>ZΔM15 Tn10 (Tet<sup>R</sup>) Amy Cam<sup>R</sup>]</i>
DH5α <i>E. coli</i>	<i>F' φ80 dlacZΔM15 Δ(lacZTA-argF)U169 deoR recA1 endA1 hsdR17(r<sub>k</sub><sup>-</sup>, m<sub>k</sub><sup>+</sup>) phoA supE44 λ thi-1 gyrA96 relA1</i>

## **2.2 The production of genetically derived anti-aflatoxin B<sub>1</sub> scFvs**

### **2.2.1 Aflatoxin B<sub>1</sub> (AFB<sub>1</sub>) scFv Phage Display Library**

A pre-immunised phage display library was constructed by Dr. Stephen Daly, Dublin City University. An AFB<sub>1</sub>-specific clone was isolated (following third round panning on the pre-immunised phage display library). The clone consisted of XL-1 Blue *E. coli* harbouring pAK100 plasmid DNA encoding an AFB<sub>1</sub>-specific scFv.

### **2.2.2 Plasmid DNA purification using Wizard Plus SV miniprep DNA purification system**

Single colonies of *E. coli* cells harbouring the appropriate plasmid were inoculated in 5ml of 2x TY, containing the appropriate antibiotics, and grown while shaking at 37°C overnight. The overnight culture was centrifuged at 4000rpm for 20 min. The supernatant was discarded and the tube was blotted on tissue paper to remove any remaining supernatant. The bacterial pellet was completely resuspended in 250µl of the cell suspension solution (50mM Tris-HCl, pH 7.5, 10mM EDTA and 100µg/ml Rnase A). The resuspended pellet was then transferred to a sterile 1.5ml microcentrifuge tube. Cell lysis solution (0.2M NaOH and 1% (w/v) SDS) (250µl) was added and mixed gently by inverting the tube four times. The suspension was then incubated at room temperature for approximately 1-5 min, until the cell suspension cleared to ensure complete cell lysis. Alkaline protease solution (10µl) was then added and mixed by inverting the tube four times. This was then incubated at room temperature for 5 min. Neutralisation solution (4.09M guanidine-HCl, 0.759M potassium acetate and 2.12M glacial acetic acid, pH 4.2) (350µl) was added and mixed by inverting the tube four times. The bacterial lysate was then centrifuged at 14,000rpm for 10 min at room temperature. The cleared bacterial lysate was transferred to a spin column by decanting and centrifuged at 14,000rpm for 1 minute at room temperature. The spin column was removed, the flow through discarded and the spin column re-inserted. Column wash solution (60% (v/v) ethanol, 60mM potassium acetate, 8.3mM Tris-HCl and 0.04mM EDTA) (750µl), previously diluted with 95% (v/v) ethanol, was added to the spin column. The column was then centrifuged at 14,000rpm for 1 min at room temperature and the flow through discarded. Column wash solution (250µl) was added to the column, which was then

centrifuged at 14,000rpm for 2 min at room temperature. The spin column was then transferred to a sterile 1.5ml microcentrifuge tube and the plasmid DNA was eluted from the column by adding 100µl of autoclaved upH<sub>2</sub>O. The column was centrifuged at 14,00rpm for 1 min at room temperature. The eluted plasmid DNA was then stored at -20°C.

### 2.2.3 SfiI restriction enzyme digest

An SfiI restriction enzyme digest was set up as follows:

Plasmid DNA	10µl
SfiI Buffer (10X)	2µl
SfiI (20U/µl)	2µl
BSA (10mg/ml)	0.5µl
upH <sub>2</sub> O	5.5µl

The restriction digest reaction was incubated at 50°C overnight.

### 2.2.4 Agarose gel electrophoresis for DNA characterisation

DNA was analysed by running on agarose gels in an Atto horizontal gel apparatus. Gels were prepared by dissolving agarose in 1xTAE (40mM Tris-acetate, 1mM EDTA, pH 8.0) containing 400µg/ml of ethidium bromide, to the required concentration (typically 0.7 – 1.2% (w/v)) and boiling until the solution went clear. The 1xTAE, containing 400µg/ml of ethidium bromide, was also used as the running buffer. A tracker dye was incorporated into the DNA samples (1µl of dye to 5µl of sample) to facilitate loading of samples. Mini- and maxi-gels were run at 100V for 1 hour or until the tracking dye reached the base of the gel. Gels were then visualised on a UV transilluminator and photographed using a UV image analyser.

### 2.2.5 DNA agarose gel purification

DNA samples were gel-purified using a Wizard PCR-prep purification kit. DNA was electrophoresed on a 1% (w/v) low melt agarose gel at 70V for approximately 1 - 2 hours. The gel was then visualised under ultra violet (UV) light and the bands of interest excised from the gel using a sterile scalpel and placed in a sterile 1.5ml microcentrifuge tube. The gel bands were then incubated in a 70°C water bath until

the gel was completely melted. Immediately after the gel melted 1ml of resin was added. The gel resin-mix was then flushed through the wizard mini-column using 5ml syringe barrel. The mini-column was then washed with 2ml of 80% (v/v) propanol. The syringe barrel was then removed and the mini-column placed in a fresh 1.5ml eppendorf tube. The column and eppendorf were then centrifuged at 14,000 rpm for 2 min, to remove the propanol. The column was once again transferred to a fresh 1.5ml microcentrifuge tube and then 50µl of upH<sub>2</sub>O added to the column. This was incubated at room temperature 1 min and the column was then centrifuged at 14,000 rpm for 20 sec. The eluted DNA was collected in a sterile microcentrifuge tube and stored at -20°C.

### 2.2.6 Ligation of scFv insert and pAK plasmid DNA

Gel-purified DNA encoding pAK plasmid and scFv were ligated as follows:

pAK plasmid	3.0µl
scFv insert	2.6µl
Ligation buffer (10X)	1.0µl
Water	2.4µl
T4 DNA ligase (1U/µl)	1.0µl

The ligation reaction was incubated at 15°C overnight.

### 2.2.7 Preparation of competent *E. coli* cells

A single *E. coli* colony was inoculated in 5ml of 2x TY, containing the appropriate antibiotics, and grown overnight at 37°C shaking. The overnight culture was used to inoculate 100ml of 2x TY and the culture incubated, shaking at 37°C, until the optical density at 550nm (OD<sub>550</sub>) was between 0.3 and 0.4. The cells were then left on ice for 15 min and centrifuged at 4000rpm for 20 min at 4°C. The supernatant was decanted and the pellet was resuspended in 20ml of cold 100mM MgCl<sub>2</sub>. The cells were centrifuged at 4000rpm for 20 min at 4°C and the pellet was resuspended in 20ml of cold 50mM CaCl<sub>2</sub>. The cells were incubated on ice for 30 min and collected by centrifugation at 4000rpm for 20 min at 4°C. The supernatant was decanted and the cells were resuspended in 2ml of CaCl<sub>2</sub>. The CaCl<sub>2</sub>-competent *E. coli* were flash frozen in 200µl aliquots and stored at -80°C.

### **2.2.8 Transformation of JM83 *E. coli* with pAK vectors containing the scFv insert**

Ligated DNA (50ng) was added to a 200µl aliquot of CaCl<sub>2</sub>-competent JM83 *E. coli*. The transformation was incubated on ice for 60 min. The cells were then heat-shocked in a 42°C water bath for 45 sec and then immediately placed back on ice. SOC media (700µl) was then added to the heat-shocked cells, which were then incubated shaking at 37°C for one hour. The heat-shocked transformation (150µl) was plated out onto 2x TY agar plates containing 1% (v/v) glucose, 25µg/ml chloramphenicol and 50µg/ml streptomycin sulphate. The plates were then incubated, inverted, overnight at 37°C. 2x TY (1.5ml) was added to each plate and the cells were scraped off and collected. The collected cells were suspended in 15% (v/v) glycerol, flash frozen and stored at -80°C.

### **2.2.9 Soluble scFv production**

An overnight culture of JM83 *E. coli*, harbouring the pAK vector containing the scFv gene of interest, was used to inoculate 200ml of 2x TY containing 25µg/ml chloramphenicol. The culture was incubated at 37°C, with vigorous shaking, until the OD<sub>550nm</sub> reached 0.5 – 0.6. The culture was then induced using 1mM isopropylthiogalactopyranoside (IPTG) and incubated for a further 4 hours, for pAK400 (or 16 hours for pAK500 and pAK600), at 26°C, with vigorous shaking, and then centrifuged at 4000rpm for 20 min.

### **2.2.10 Isolation of scFvs from the periplasm**

Following scFv expression the bacterial pellet was resuspended in 10ml of TES (100mM Tris-HCl, pH 8, 0.5M sucrose, 0.5mM EDTA) and incubated on ice for 1 hour. Cellular debris was then removed following centrifugation at 4000rpm for 20 min and the supernatant (crude periplasmic lysate) dialysed against phosphate-buffered saline (PBS: 0.15M NaCl, pH 7.3) overnight at 4°C.

### **2.2.11 Sequence analysis on the gene encoding the AFB<sub>1</sub>-specific scFv**

Plasmid DNA for sequencing was purified from overnight cultures using the Promega Wizard Plasmid DNA Purification Kit (See Section 2.2.2). The plasmid DNA was quantified using an ultra-violet (UV) spectrophotometer at 260nm and 20µg of DNA was transferred to a fresh 1.5ml microcentrifuge tube and vacuum dried. The linear

nucleotide sequence was determined by MWG-Biotech and analysed using a variety of web-based bioinformatic tools (Table 2.6).

**Table 2.6:** *Web-based bioinformatic tools, and their source location, used during the sequence analysis of cloned inserts.*

<b>Tool</b>	<b>Source</b>
Translate tool	<a href="http://www.expasy.org">www.expasy.org</a>
BLAST	<a href="http://www.expasy.org">www.expasy.org</a>
Swiss-model	<a href="http://swissmodel.expasy.org">http://swissmodel.expasy.org</a>
Deep View	<a href="http://ca.expasy.org/spdbv">http://ca.expasy.org/spdbv</a>
ClustalW	<a href="http://www.ch.embnet.org/software/ClustalW.html">www.ch.embnet.org/software/ClustalW.html</a>
ESPrpt	<a href="http://prodes.toulouse.inra.fr/ESPrpt/cgi-bin/ESPrpt.cgi">http://prodes.toulouse.inra.fr/ESPrpt/cgi-bin/ESPrpt.cgi</a>
Kabat rules	<a href="http://acrmwww.biochem.ucl.ac.uk/abs">http://acrmwww.biochem.ucl.ac.uk/abs</a>

### **2.2.12 Sodium dodecyl sulphate – polyacrylamide gel electrophoresis (SDS-PAGE)**

SDS-PAGE analysis was used to assess protein purity and determine the apparent molecular mass of proteins. Protein electrophoresis was performed using an Atto dual minislab AE-6450 gel under reducing conditions, by the method previously described by Laemmli (1970). Table 2.7 details the composition of the gels, running buffer and sample loading buffer. Samples for analysis (approx. 1mg/ml) were diluted with the sample loading dye (4:1, sample: buffer) and boiled for 10 min. The sample (20µl) was added to the gel and electrophoresed alongside appropriate molecular weight markers. Prestained molecular weight markers were also electrophoresed when the gels were being prepared for western blot analysis (See Section 2.2.13). Initially the gels were electrophoresed at 15mA per plate until the samples migrated through the stacking gel and then they were electrophoresed at 20mA per plate until the sample had migrated to the end of the gel (approximately 90 min).

**Table 2.7: Composition of SDS-PAGE gels and buffer.**

---

Stacking gel	5% (w/v) acrylamide
	0.13% (w/v) bis acrylamide
	125mM Tris
	0.1% (w/v) SDS
	0.15% (w/v) ammonium persulphate
	0.25% (v/v) TEMED
Separating gel	10% (w/v) acrylamide
	0.27% (w/v) bis acrylamide
	375mM Tris
	0.1% (w/v) SDS
	0.08% (w/v) ammonium persulphate
	0.08% (v/v) TEMED
Sample loading buffer	60mM Tris
	25% (v/v) glycerol
	2% (v/v) SDS
	14.4 mM 2-mercaptoethanol
	0.1% (w/v) bromophenol blue
Electrophoresis buffer	25mM Tris
	192mM glycine
	0.1% (w/v) SDS

---

### 2.2.13 Coomassie blue staining

SDS-PAGE gels were stained for 4 hours using Coomassie blue staining solution (Table 2.8) and then destained overnight in destaining solution (Table 2.8).

*Table 2.8: Composition of Coomassie blue staining and destaining solutions.*

---

Coomassie blue staining solution	0.1% (w/v) Coomassie Brilliant Blue R-250 25% (v/v) methanol 10% (v/v) acetic acid
Destaining solution	14% (v/v) methanol 10% (v/v) acetic acid

---

### 2.2.14 Western blot analysis

Proteins were transferred from SDS-PAGE gels (Section 2.2.11) to nitrocellulose membrane by electrophoretic means using a BioRad wet blotter in electrophoresis buffer containing 20% (v/v) methanol, for 90 min at 72V. The membrane was blocked using PBS-5% (w/v) milk marvel overnight at 4°C. The blocked membrane was then washed using 3 x 10 min PBS washes. The membrane was probed with the primary antibody, to the appropriate dilution with PBS-1% (w/v) milk marvel, for 1.5 hours at room temperature and washed as before. An alkaline phosphatase (AP)-labelled secondary antibody diluted to 1/2000 with PBS-1% (w/v) milk marvel was added and the blot incubated and washed as before. Colour development was then observed following addition of the substrate, BCIP-NBT, and the reaction stopped by addition of 50mM EDTA.

## **2.2.15 ELISA analysis of soluble anti-AFB<sub>1</sub> scFv antibodies**

### **2.2.15.1 Checkerboard ELISA for the determination of conjugate coating concentration and optimal scFv antibody dilution for use in a competitive ELISA**

A 96-well microtitre plate (Nunc Immunoplate Maxisorp, Gibco Ltd., Paisley, UK) was coated with different concentration of the AFB<sub>1</sub>-BSA conjugate ranging from 0 to 50µg/ml, at 100µl/well. The plate was incubated for 1 hour at 37°C and the contents emptied. The plate was then washed three times with PBS - 0.05% (v/v) Tween and three times with PBS. The plate was blocked using 150µl of PBS - 4% (w/v) milk marvel and incubated at 4°C overnight. Serial scFv dilutions ranging from undiluted to 1/128 were then prepared in PBS - 1% (w/v) milk marvel and 100µl of each dilution added per well. The plate was incubated at 37°C for 1 hour and washed as before. 100µl of anti-FLAG antibody, diluted to 1/400 in PBS - 1% (w/v) milk marvel, was added to each well and the plate incubated at 37°C for 1 hour. After washing, 100µl of horseradish peroxidase (HRP)-conjugated anti-mouse antibody, diluted to 1/2000 in PBS - 1% (w/v) milk marvel, was added to each well. The plate was once again incubated at 37°C for 1 hour and washed as before. The substrate (100µl), *o*-phenylenediamine (*o*-PD), was added to each well and incubated for 30 min at 37°C. Absorbance values at 405nm were then read using a Titertek plate reader.

### **2.2.15.2 Indirect competitive enzyme-linked immunosorbent assay (ELISA) for the detection of AFB<sub>1</sub>**

Microtitre plates were coated with 100µl of AFB<sub>1</sub>-BSA conjugate prepared in PBS at 25µg/ml and 12.5µg/ml for the monomeric and dimeric scFv, respectively, and incubated for 1 hour at 37°C. The plates were then emptied and washed 3 times with PBS - 0.05% (v/v) Tween and three times with PBS. The plates were then blocked by adding 150µl/well of PBS - 4% (w/v) milk marvel and incubated at 4°C overnight. Free AFB<sub>1</sub> standards were prepared in PBS - 5% (v/v) methanol in concentrations ranging from 1.5 - 12500ng/ml. The plates were washed as before and 50µl of the anti-AFB<sub>1</sub> scFv was added to each well along with 50µl of the AFB<sub>1</sub> standard. After washing 100µl of anti-FLAG antibody, diluted to 1/400 in PBS - 1% (w/v) milk

marvel, was added to each well and the plate incubated at 37°C for 1 hour. After washing, 100µl of horseradish peroxidase (HRP)-conjugated anti-mouse antibody, diluted to 1/2000 in PBS - 1% (w/v) milk marvel, was added to each well. The plate was once again incubated at 37°C for 1 hour and washed as before. The substrate (100µl), *o*-phenylenediamine (*o*-PD), was added to each well and incubated for 30 min at 37°C. Absorbance values at 405nm were then read using a Titertek plate reader.

#### **2.2.15.3 Direct competitive ELISA for the detection of AFB<sub>1</sub> using the pAK600 alkaline phosphatase-labelled scFv**

Microtitre plates were coated with 100µl of AFB<sub>1</sub>-BSA conjugate dissolved in PBS 6.25µg/ml and incubated for 1 hour at 37°C. The plates were then emptied and washed 3 times with PBS - 0.05% (v/v) Tween and three times with PBS. The plates were then blocked by adding 150µl/well of PBS - 4% (w/v) milk marvel and incubated at 4°C overnight. Free AFB<sub>1</sub> standards were prepared in PBS - 5% (v/v) methanol in concentrations ranging from 1.5 – 12500ng/ml. The plates were washed as before and 50µl of the alkaline phosphatase-labelled scFv was added to each well along with 50µl of the AFB<sub>1</sub> standard. The plates were incubated at 37°C for 1 hour and washed as before. The substrate (100µl), *para*-nitrophenyl phosphate (pNPP), was added to each well and incubated for 30 min at 37°C. Absorbance values at 405nm were then read using a Titertek plate reader.

#### **2.2.15.4 Measurement of cross-reactions**

The monomeric, dimeric and bifunctional scFv antibodies were assayed against a range of standards of aflatoxins B<sub>1</sub>, B<sub>2</sub>, M<sub>1</sub>, M<sub>2</sub>, G<sub>1</sub> and G<sub>2</sub>. Stock solutions of the aflatoxins were prepared in methanol and diluted using PBS - 5% (v/v) methanol. The assays were carried out as for the competitive ELISAs (Sections 2.2.14.2 and 2.2.14.3) except the aflatoxin standards were added to the immunoplate with the anti-AFB<sub>1</sub> scFvs.

### 2.2.16 Development of a lateral flow immunoassay (LFIA) for the detection of AFB<sub>1</sub>

Buffers used during the development of a lateral flow immunoassay are detailed in Table 2.9.

*Table 2.9: Buffers used during the development of a lateral flow immunoassay.*

Buffer	Composition
Colloidal carbon suspension	1% (w/v) in demineralised water
Carbon conjugate wash solution	5mM borate buffer, pH 8.5 1% (w/v) BSA 0.02% (v/v) NaN <sub>3</sub>
Carbon conjugate storage solution	100mM borate buffer, pH 8.5 1% (w/v) BSA 0.02% (v/v) NaN <sub>3</sub>
LFIA Running buffer	100mM borate buffer, pH 8.5 0.1% (w/v) BSA 0.05% (v/v) Tween 20 0.01% (v/v) Triton-X-100 0.02% (v/v) NaN <sub>3</sub>

#### 2.2.16.1 Physical adsorption of protein onto colloidal carbon particles

The 1% (w/v) colloidal carbon stock solution was diluted to a final concentration of 0.2% (w/v) using 5mM borate buffer pH 8.5. A 1ml suspension was sonicated for 5 – 10 min and the pH adjusted to 0.5 – 1 pH unit above the pI of the protein. The protein was dissolved in 5mM borate buffer and the pH also adjusted to 0.5 – 1 pH unit above the pI of the protein. The protein (350µg in as small a volume as possible) was added to the 1ml colloidal carbon suspension and allowed to mix, gently stirring, overnight at 4°C. The protein-sol suspension was then centrifuged at 13,000rpm for 15 min and the pellet washed four times using 1.5ml of carbon conjugate wash solution. After the

final wash step the pellet was resuspended in 1 ml of carbon conjugate storage solution and stored in a glass vial at 4°C in the dark.

#### **2.2.16.2 Spraying and production of nitrocellulose strips**

Lateral flow strips (10) were prepared using a piece of nitrocellulose with plastic backing cut 10cm wide and 4.5cm long. Samples were sprayed onto the nitrocellulose using a Linomat 5 (Fig. 2.1), with the control and test lines sprayed 3 and 2.7cm, respectively, from the bottom of the nitrocellulose. A 70mm band was sprayed for the test and control lines at a rate of 400nl/sec. The nitrocellulose strips were dried for at least one hour at 37°C and stored in closed laminated foil pouches with a 0.25g silica minipax at room temperature.

#### **2.2.16.3 Running test strips**

The nitrocellulose strips were stuck to a perspex bridge (Figure 2.2) using double sided sticky tape across the bridge. A small piece of filter paper was stuck to the top of each strip and a piece of parafilm placed beneath the strips to allow for sample application (Figure 2.3). Carbon conjugates were sonicated for 20 sec before use. Samples consisting of 100µl of running buffer containing 1µl of the carbon conjugate and any additional solutions were placed on the parafilm and allowed to run up the nitrocellulose strip for 10 –15 min. The strips were then washed by adding 100µl of running buffer and signal observed.

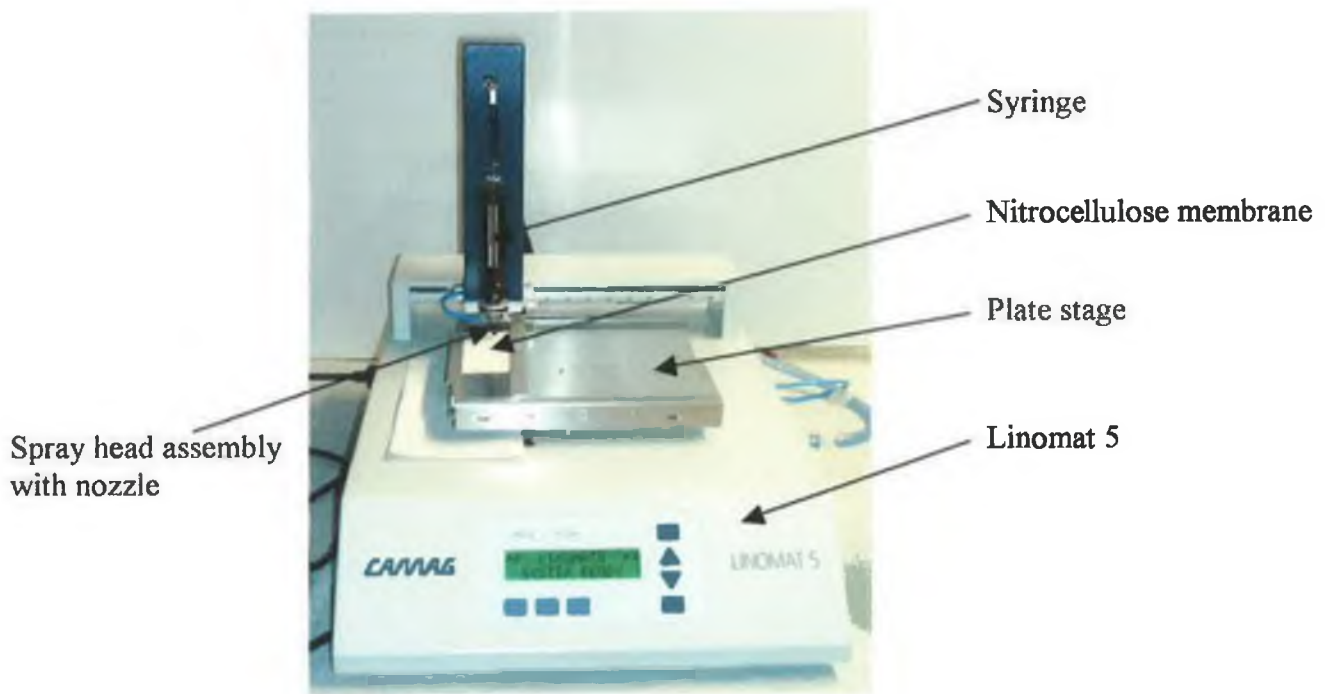


*Figure 2.1: Photograph of the Linomat 5 sprayer showing a piece of nitrocellulose in place for spraying.*

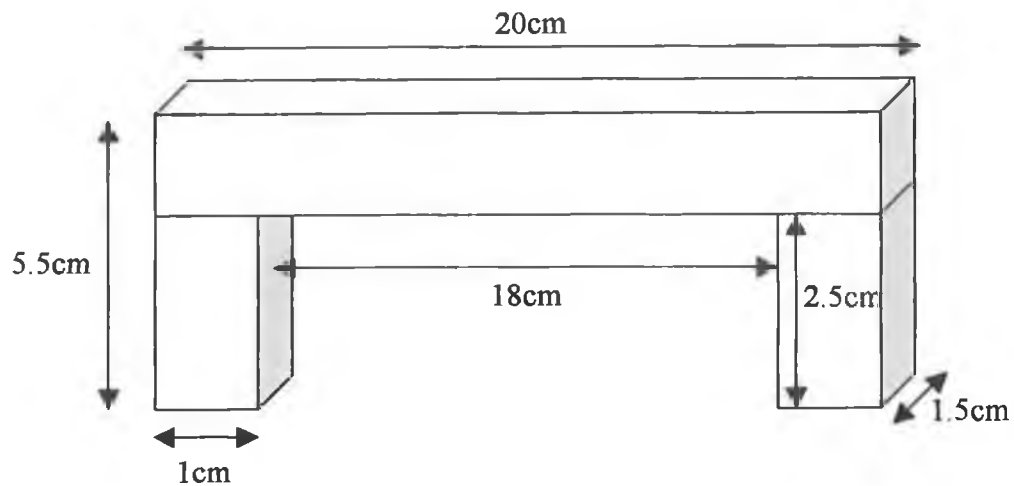


**Figure 2.2:** Dimensions of the perspex bridge used during the development of a lateral flow immunoassay.

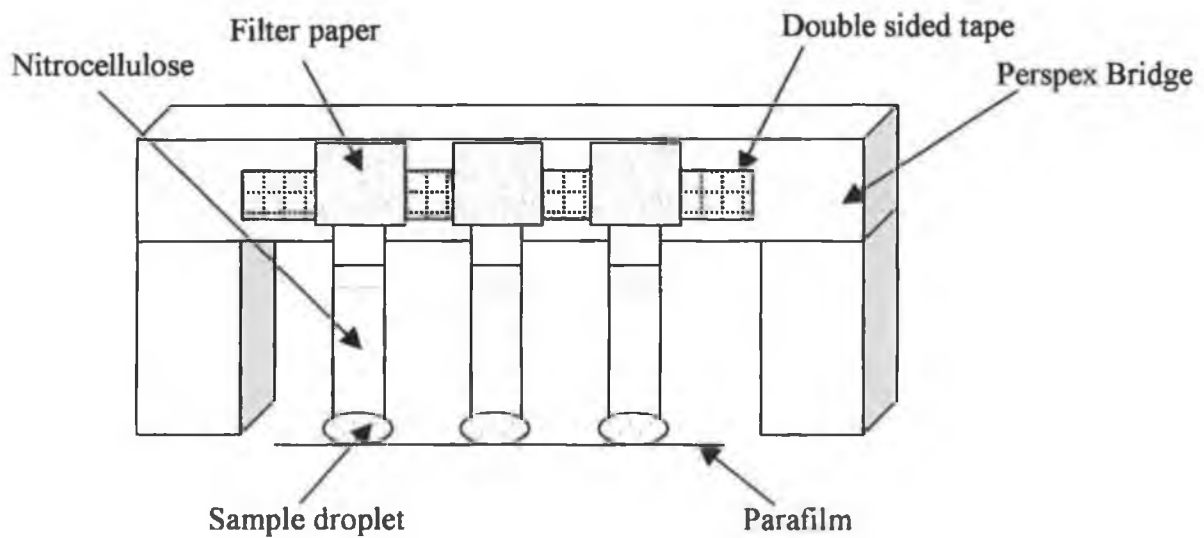


**Figure 2.3:** Schematic representation of running nitrocellulose strips for the development of a lateral flow immunoassay.

### **2.2.17 Development of a Biacore inhibition immunoassay for the detection of AFB<sub>1</sub>**

Biacore inhibition assay development was carried out using a Biacore 3000<sup>TM</sup> supplied by Biacore International AB (Uppsala, Sweden). HEPES buffered saline (HBS) buffer, pH7.4 (10mM HEPES, 150mM NaCl, 3.4mM EDTA, 0.05% (v/v) Tween 20) was used for all Biacore experiments. All solutions were filtered using 0.22µm syringe filters and the running buffer degassed using a Millipore sintered glass filtration system.

#### **2.2.17.1 AFB<sub>1</sub> Sensor Chip**

A Biacore CM5 chip immobilised with an AFB<sub>1</sub> derivative was kindly donated by XenoSense Ltd., c/o Qubis, North Lanyon, Queen's University Belfast, University Rd., Belfast, BT7 1NN.

#### **2.2.17.2 Sample Preparation for use in Inhibitive Assay**

A 1mg/ml of free AFB<sub>1</sub> was prepared in 100% methanol. Standards, ranging in concentrations from 190 – 24000pg/ml, were prepared in PBS containing 5% (v/v) methanol. Each AFB<sub>1</sub> standard was then pre-incubated with an equal volume of a 1/4 dilution for the monomeric scFv and a dilution of 1/35 for the dimeric scFv for 30 min at 37°C. Each concentration was then passed over the sensor surface three times. Regeneration of the sensor surface was carried out as described in Section 2.2.17.3.

#### **2.2.17.3 Surface Regeneration**

Regeneration of the AFB<sub>1</sub> sensor surface was carried out using 10mM NaOH, for the monomeric scFv and 25mM NaOH, for the dimeric scFv.

#### **2.2.17.4 Measurement of Cross-Reactivity**

Both the monomeric and dimeric scFv were assayed with a range of structurally related aflatoxin molecules, which included aflatoxin B<sub>2</sub>, M<sub>1</sub>, M<sub>2</sub>, G<sub>1</sub> and G<sub>2</sub>, in order to determine potential cross-reactivity in a Biacore inhibition assay format. Stock solutions of each aflatoxin were prepared in methanol and diluted in PBS - 5% (v/v) methanol to a range of concentrations ranging from 780 – 6250 pg/ml.

## **2.3 Cloning and expression of *Brucella*-specific proteins**

Heat-killed *Brucella abortus* 45/20 cells were kindly donated by the Blood Testing Laboratory, Department of Agriculture and Food (DAFF), Model Farm Rd., Cork.

### **2.3.1 Isolation of *Brucella abortus* genomic DNA**

The heat-killed *B. abortus* cells (5ml) were washed three times in PBS and resuspended in PBS to a final volume of 5ml. The resuspended cells (1.5ml) were transferred to a sterile 1.5ml microcentrifuge tube and centrifuged at 13,000rpm for 5 min. The bacterial pellet was resuspended in 1.5ml of TES (10mM Tris, 1mM EDTA, 50mM NaCl, pH8.0) and centrifuged at 13,000rpm for 5 min. The pellet was then resuspended in 700µl of TE (10mM Tris, 1mM EDTA, pH8.0). Lysozyme (50µl of 2 mg/ml prepared in TE), made up freshly, was added. The culture was incubated at 30° for 20 min. Sarkosyl/proteinase (50µl of 10% (v/v) sarkosyl in TE, with 5mg/ml proteinase) was added. The culture was then incubated at 37° for 60 min. 3M sodium acetate (70µl) was added and mixed by flicking. Kirby mix (49% (v/v) phenol, 49% (v/v) chloroform, 1.9% (v/v) isoamyl alcohol, 0.39% (w/v) 8-hydroxy quinolone) (600µl) was added and the mix was then centrifuged at 13,000rpm for approximately 4 min. The aqueous phase was removed to a fresh microcentrifuge tube and a further 600µl of Kirby mix was added. The solution was mixed and then centrifuged at 13,000rpm for 4 min. The aqueous phase was removed to a fresh microcentrifuge tube and 700µl of chloroform: isoamylalcohol (24:1) was added. The mixture was then centrifuged at 13,000rpm for 4 min. The aqueous phase was removed and added to an equal volume of isopropanol. The mixture was centrifuged at 13,000rpm for 5 min (or until a pellet formed). The supernatant was discarded and the pellet was washed twice with 70% (v/v) ethanol. The pellet was centrifuged at 13,000rpm for 5 min and any excess liquid removed. The pellet was then left to air dry for approximately 5 min. The dried pellet was then resuspended in 100 - 200µl of TE buffer and stored at 4°C.

### **2.3.2 Primer design**

Forward and reverse DNA primers were designed for the genes encoding the p18 and bp26 proteins based on DNA sequences previously submitted to GenBank. The p18 primers were based on the sequence of the recombinant p18 protein cloned and

expressed by Hemmen and associates (1995) from *B. abortus* (Accession number Z46864). The bp26 specific primers were also based on a recombinant form of the protein, which was cloned and expressed by Cloeckert and associates (1996) from *B. melitensis* (Accession number U45996). NcoI and BamHI restriction enzyme sites were incorporated into the forward and reverse primers, respectively, for subsequent directional cloning into the high-level expression vector pQE-60. The DNA sequences of the forward and reverse primers for the p18 and bp26 genes are detailed in Table 2.10.

*Table 2.10: The nucleotide sequences of the p18 and bp26-specific forward and reverse primers.*

Primer	DNA sequence
	NcoI
p18 forward	5' <b>CC ATG</b> GGA AAC CAA AGC TGT CCG AAC AAG AC 3' Start codon
	BamHI
p18 reverse	5' <b>GGA TCC</b> GAC AAG CGC GGC GAT GCG G 3'
	NcoI
bp26 forward	5' <b>CC ATG</b> GGA AAC ACT CGT GCT AGC AAT 3' Start codon
	BamHI
bp26 reverse	5' <b>GGA TCC</b> CTT GAT TTC AAA AAC GAC ATT G 3'

### 2.3.3 PCR amplification of genes encoding the *Brucella*-specific proteins

Standard polymerase chain reactions (PCRs) were used to amplify the genes encoding p18 and bp26 (Table 2.11) using the PCR cycle detailed in Table 2.12.

**Table 2.11:** *The components for a standard PCR reaction.*

Component	PCR reaction
dNTP mix (10mM)	1µl
Thermo buffer, containing Mg <sup>2+</sup> (10X)	5µl
Forward primers (0.5nM/µl)	1µl
Reverse primers (0.5nM/µl)	1µl
Template DNA	1µl
Sterile upH <sub>2</sub> O	38.5µl
Taq polymerase (1U/µl)	2.5µl

**Table 2.12:** *The stages and steps for a standard PCR reaction.*

Stage	Step	Number of cycles
1	Step 1: 95°C for 10 min	
2	Step 1: 95°C for 1 min Step 2: 55°C for 30 sec Step 3: 72°C for 1 min	30
3	Step 1: 72°C for 10 min	

### 2.3.4 Ligation of PCR products and pCR2.1 plasmid

The ligation of the Taq DNA polymerase amplified PCR products and the pCR2.1 vector reaction was set up as follows:

Sterile upH <sub>2</sub> O	5µl
Ligation buffer (10X)	1µl
pCR2.1 vector (25ng/µl)	2µl
Fresh PCR product	1µl
T4 DNA ligase (4U/µl)	1µl

The ligation reaction was incubated at 14°C for at least 4 hours, but preferably overnight. The ligation was then centrifuged briefly and stored at -20°C.

### 2.3.5 Transformation of INVαF' with pCR2.1, containing the cloned insert

Vials containing the ligation reaction were centrifuged briefly and then placed on ice. The overnight ligation reaction (2µl) was added to 50µl of 'One Shot' competent INVαF' *E.coli* cells and mixed gently. The vials were then incubated on ice for 30 min. The transformation reaction was then treated with a heat shock, by placing the vials in a 42°C water bath for 30 sec and then directly back on ice. SOC media (250µl) was then added to each transformation reaction. The transformation reaction was then incubated at 37°C for 1 hour, while shaking at 225rpm. Each transformation reaction (150µl) was then spread onto LB agar plates containing X-Gal and 50µg/ml of kanamycin. The plates were then incubated, inverted, at 37°C for at least 18 hours. The plates were then shifted to 4°C for 2 - 3 hours to allow further colour development.

### 2.3.6 BamH1 and Nco1 restriction analysis on pCR2.1, containing the cloned insert

Overnight cultures of the clones for analysis were inoculated in 5ml of 2x TY containing 50µg/ml of kanamycin and grown shaking at 37°C overnight. The plasmid DNA was purified from each clone using the Wizard Plus SV Minipreps DNA Purification System as described in Section 2.2.2. BamH1/Nco1 restriction enzyme digests were set up as follows:

NE buffer 2 (10X)	2µl
BSA (10mg/ml)	0.5µl
Plasmid DNA	10µl
UpH <sub>2</sub> O (Sterile)	30.5µl
BamH1 (10U/µl)	2µl
Nco1 (10U/µl)	2µl

The restriction digest was incubated at 37°C for two hours.

### 2.3.7 Sub-cloning of cloned insert from pCR2.1 into pQE-60

A single DH5α *E. coli* colony harbouring pQE-60 was grown overnight in 5ml of LB broth containing 100µg/ml ampicillin shaking at 37°C. The pQE-60 plasmid DNA purified using the Promega Wizard Plus Miniprep DNA Purification System (See section 2.2.2). The pQE-60 plasmid DNA was then linearised using a BamH1 / Nco1 restriction digest as described in Section 2.3.6 and the linearised plasmid was gel purified, following agarose gel electrophoresis, using the Wizard PCR-prep purification kit (See Section 2.2.6). A BamH1/Nco1 restriction digest was also carried out on the pCR2.1 plasmid DNA containing the cloned gene of interest (See Section 2.3.6). The restriction digest was electrophoresed on a 1% (w/v) low melt agarose gel and the bands corresponding to the gene of interest was gel purified using the Promega Wizard PCR Preps DNA Purification System (See Section 2.2.5). The DNA encoding the gene of interest was then directionally cloned into the linearised pQE-60 using T4 DNA ligase.

The ligation reaction was set up as follows:

pQE-60 DNA	4 $\mu$ l
Gene of insert	4 $\mu$ l
T4 DNA ligase (1U/ $\mu$ l)	1 $\mu$ l
Ligation buffer (10X)	1 $\mu$ l

The ligation reaction was incubated at 14° overnight.

### **2.3.8 Transformation of competent XL-10 Gold *E.coli* cells with pQE-60 containing the cloned inserts**

CaCl<sub>2</sub>-competent XL-10 Gold *E coli* were prepared as described in Section 2.2.7. The competent XL-10 Gold *E coli* were then transformed with the pQE-60, containing the gene of interest, as described in Section 2.2.8.

### **2.3.9 BamH1/Nco1 restriction analysis on XL-10 Gold *E coli* transformed with pQE-60**

BamH1/Nco1 restriction enzyme analysis was carried out on the pQE-60 plasmid DNA isolated from the transformed XL-10 Gold *E coli* as described in Section 2.3.6.

### **2.3.10 Sequencing of cloned inserts**

Plasmid DNA for sequencing was purified from overnight cultures using the Promega Wizard Plasmid DNA Purification Kit (See Section 2.2.2). The plasmid DNA was quantified using a UV spectrophotometer at 260nm and 20 $\mu$ g of DNA was aliquoted into a fresh 1.5ml microcentrifuge tube and vacuum dried. Sequence analysis was then conducted as detailed in Section 2.2.11.

### **2.3.11 Small-scale expression culture**

Overnight cultures of the XL-10 Gold *E. coli* harbouring the pQE-60 plasmid were inoculated in 2x TY (5ml) containing 100 $\mu$ g/ml ampicillin, 10 $\mu$ g/ml tetracycline and 25 $\mu$ g/ml chloramphenicol. The culture were grown shaking at 37°C overnight. The overnight culture was then used to inoculate 20ml of 2x TY containing 100 $\mu$ g/ml ampicillin, 10 $\mu$ g/ml tetracycline and 25 $\mu$ g/ml chloramphenicol. The culture was

incubated shaking at 37°C until the optical density at 550nm (OD<sub>550</sub>) reached 0.5. Protein expression was then induced following addition of 1mM IPTG. The culture was incubated shaking at 37°C for 4 hours and then centrifuged at 4000rpm for 20 min. The supernatant was discarded and the pellet resuspended in 1ml of denaturing buffer (8M Urea, 100mM NaH<sub>2</sub>PO<sub>4</sub>, 10mM Tris, pH8.0) and sonicated for 30 sec with 6 sec pulses at 220W. The lysed cells were then centrifuged at 13,000rpm for 15 min and the supernatant analysed using SDS-PAGE (Section 2.2.11) for protein expression.

### **2.3.12 Optimisation of IPTG concentration**

Several small-scale expression cultures were carried out as described in Section 2.3.11, except various IPTG concentrations, ranging from 0 – 1mM, were used for induction of protein expression.

### **2.3.13 Optimisation of sonication conditions**

Several small-scale expression cultures were carried out as described in Section 2.3.11, except a range of sonication times, from 0 – 60 seconds, were analysed for optimal protein isolation.

### **2.3.14 Time course expression cultures**

Small-scale expression cultures were carried out as described in Section 2.3.11, except following IPTG induction 1ml samples were taken at hourly intervals for up to five hours and then following overnight induction. A non-induced sample was also taken before IPTG addition.

### **2.3.15 Large-scale expression culture**

Overnight cultures of the XL-10 Gold *E. coli* harbouring the pQE-60 plasmid were inoculated in 2x TY (10ml) containing 100µg/ml ampicillin, 10µg/ml tetracycline and 25µg/ml chloramphenicol. The culture were grown shaking at 37°C overnight. The overnight culture was then used to inoculate 500ml of 2x TY containing 100µg/ml ampicillin, 10µg/ml tetracycline and 25µg/ml chloramphenicol. The culture was incubated shaking at 37°C until the optical density at 550nm (OD<sub>550</sub>) reached 0.5. Protein expression was then induced following addition of 0.5mM IPTG. The culture

was incubated shaking at 37°C for 4 hours and then centrifuged at 4000rpm for 20 min. The supernatant was discarded and the pellet resuspended in 25ml of denaturing buffer and sonicated for 30 sec followed by a 30 sec interval and this was repeated three times. The lysed cells were then centrifuged at 4000rpm for 15 min and the supernatant analysed using SDS-PAGE (See Section 2.2.11) for protein expression and the his-tagged recombinant proteins purified using IMAC (See Section 2.3.16).

### **2.3.16 IMAC purification of the 6xHis-tagged recombinant proteins**

IMAC running buffer (10ml) (Table 2.13) was added to 1ml of Ni-NTA resin. The resin mix was centrifuged at 4000rpm for 1 min. The cell lysate (4ml) was added to the equilibrated resin and incubated on an over-end rotor for 90 min at room temperature. The resin mix was then centrifuged for at 4000rpm for 1 min and the supernatant removed. Wash buffer (10ml) (Table 2.13) was added to the resin and mixed. Following centrifugation at 4000rpm for 1 min the supernatant was removed. This wash step was then repeated twice more and followed by three elutions steps, which involved addition of 1ml of elution buffer (Table 2.13) followed by centrifugation at 4000rpm for 1 min. The eluted fractions were then pooled and dialysed in PBS overnight at 4°C. The concentration of the purified protein was then determined using a BCA assay (See Section 2.3.17) and stored in 1ml fractions at -20°C.

### **2.3.17 Bicinchoninic acid (BCA) assay**

Bovine serum albumin (BSA) protein standards ranging in concentration from 0.75 – 2mg/ml were prepared in PBS. Each standard (10µl) was added to a 96-well immunoplate along with 200µl of the BCA reagent, in triplicate. The plate was allowed develop at 37°C for 30 min and the absorbance values obtained at 560nm using a Titertek Plate reader. A standard curve was constructed and used to calculate the protein concentration of samples.

**Table 2.13:** *Composition of buffers used during the IMAC purification of his-tagged proteins.*

<b>Solution</b>	<b>Composition</b>
Running buffer	8M Urea 100mM NaH <sub>2</sub> PO <sub>4</sub> 10mM Tris pH 8.0
Wash buffer	8M Urea 100mM NaH <sub>2</sub> PO <sub>4</sub> 10mM Tris pH 6.3
Elution buffer	8M Urea 100mM NaH <sub>2</sub> PO <sub>4</sub> 10mM Tris pH 4.5

## **2.4 Antibody production**

### **2.4.1 Antigen preparation**

#### **2.4.1.1 Isolation of the crude cytoplasmic fraction from *Brucella abortus* 45/20**

The crude cytoplasmic lysate was isolated from *Brucella abortus* 45/20 cells using a method previously described by Goldbaum *et al.* (1995). Washed *B. abortus* 45/20 cells were centrifuged at 16,000g for 10 min. The cells were then washed three times, which involved resuspension of the bacterial pellet in 1ml of Tris buffer (10mM Tris-HCl, pH8.0) followed by centrifugation at 16,000g for 5 min. The cells were then resuspended in 1ml of Tris buffer (per 0.1g dry weight) and sonicated with three 2 min pulses. The cells were then digested with 10µg/ml of RNase and 10µg/ml of DNase and incubated for one hour at room temperature. Unbroken cells were separated by centrifugation at 16,000g for 5min. The supernatant was then centrifuged at 360,000g for 2 hours. The resulting supernatant / cytoplasmic fraction was dialysed in PBS at 4°C overnight and stored in 1ml aliquots at -20°C.

#### **2.4.1.2 *Brucella abortus* 45/20 cells**

Heat-killed *B. abortus* 45/20 cells were washed three times in PBS and resuspended to a final concentration of  $1.6 \times 10^8$  cells/ml in PBS.

### **2.4.2 Licensing**

All animal procedures were approved and licensed by the Department of Health and Children, with steps taken to minimise levels of distress caused to the animals.

### **2.4.3 Rabbit immunisation protocol**

New-Zealand white rabbits were immunised by subcutaneous injection with an emulsion (1ml) consisting of a 1mg/ml solution of antigen mixed 1:1 with Freund's complete adjuvant. 21 days following the initial immunisation the rabbits were re-immunised with 1ml of the same concentration of antigen mixed 1:1 with Freund's incomplete adjuvant. A blood sample was taken from the marginal ear vein 14 days after the second immunisation and an antibody titre determined (See section 2.4.7). The cycle of boosts and test bleeds were continued until an antibody titre in excess of

1/100,000 was obtained. The rabbit was then exsanguinated and serum recovered as described in Section 2.4.5.1

#### **2.4.4 Preparation of rabbit serum**

Blood samples were allowed to clot at room temperature for two hours. They were then stored overnight at 4°C to allow the clot to tighten and centrifuged at 4000rpm for 20 min. The supernatant (serum) was gently removed and stored at -20°C.

#### **2.4.5 Polyclonal antibody purification**

Polyclonal antibodies were initially purified from rabbit serum using saturated ammonium sulphate precipitation followed by protein G affinity chromatography.

##### **2.4.5.1 Saturated ammonium sulphate (SAS) precipitation**

SAS (3.6ml) was added drop wise to 3.6ml of the rabbit serum, on ice. The mixture was then left stirring on ice for one hour. The precipitated mixture was then centrifuged at 3000rpm for 20 min at 4°C. The supernatant was discarded and the pellet was resuspended in 3.6ml of 45% (w/v) SAS. The resuspended pellet was then centrifuged at 3000rpm for 20 min at 4°C. The supernatant was, once again, discarded and the pellet resuspended in 3.6ml of 45% (w/v) SAS. The resuspended pellet was then centrifuged at 3000rpm for 20 min at 4°C. The pellet was finally resuspended in 1.8ml of PBS and the solution was dialysed overnight at 4°C in PBS.

##### **2.4.5.2 Protein G affinity-chromatography**

A pre-poured protein G column was washed with 25ml of running buffer (Table 2.14) containing 0.05% (v/v) azide. The column was then equilibrated with 20ml of running buffer, with the flow rate set at 1.5ml/min. The column was stoppered when the running buffer reached the top of the column. The sample (1.5ml) was added to the column and the flow rate was set at 0.5ml/min. The effluent was monitored at 280 nm and fractions containing protein (i.e.  $OD_{280nm} \geq 0.05$ ) were collected. Running buffer was continually added to prevent the column running dry. After all the protein was collected the fractions were passed over the column two more times. The gel was washed with 20ml of wash buffer (Table 2.14), with the flow rate set at 1.5ml/min. (any protein collected at this stage was collected and stored in 0.01% (v/v) azide). The

column was then equilibrated using running buffer, which was allowed to pass through the column for five min at 1.5ml/min. The running buffer was allowed reach the top of the column and then 1.5ml of elution buffer (Table 2.14) was added. The elution buffer was allowed to run into the column. Then the column was stoppered and the elution buffer was left within the column for five min. The flow rate was set at 0.5ml/min and 500µl fractions of protein were collected into tubes containing 50 µl of neutralising buffer (Table 2.14), once protein was detected. Fractions were collected until no further protein was detected (i.e.  $OD_{280} \leq 0.05$ ). The fractions were then analysed at 280nm in quartz cuvettes and fractions containing the majority of protein were pooled and stored in 0.01% (w/v) azide. The protein G column was then washed using running buffer and stored in 20% (v/v) methanol.

*Table 2.14: Composition of buffers used during the protein G purification of rabbit IgG polyclonal antibodies.*

Running buffer	PBS – 0.05% (v/v) Tween, 0.15M NaCl
Wash buffer	PBS – 0.05% (v/v) Tween, 0.35M NaCl
Elution buffer	0.1M Glycine/HCl, pH 2.7
Neutralising buffer	2M Tris/HCl, pH 8.6

#### **2.4.6 Determination of polyclonal antibody titre**

A 96-well microtitre plate was coated with 100µl/well of the appropriate antigen (approximately  $1 \times 10^8$  cells/ml or 10µg/ml of protein) and incubated at 37°C for 1 hour. The plates were washed 3 times with PBS and 3 times with PBS - 0.05%(v/v) Tween and then blocked with 150µl/well of PBS - 4% (w/v) milk marvel. Following overnight incubation at 4°C the plate was washed as before. Dilutions of the appropriate antibody, ranging from 1/1000 – 1/5000000, were prepared in PBS - 1% (w/v) milk marvel and 100µl of each added to the immunoplate (in duplicate). The plates were then incubated for 1 hour at 37°C and washed as before. A goat anti-rabbit horseradish peroxidase-labelled antibody, previously diluted to 1/5000 with PBS-1% (w/v) milk marvel, was added to the plate (100µl/well) and the plate incubated at 37°C for 1 hour. Following the wash step 100µl/well of *o*-PD substrate was added

and, after 30 min incubation at 37°C, absorbances at 405nm were determined using a Titertek plate reader. The results obtained were then graphed using Excel and the antibody titre was defined as the highest antibody dilution with an absorbance value that was greater than 2 standard deviations (SD) above the mean absorbance value for the zero control.

#### **2.4.7 Checkerboard ELISA for the determination of optimal cell-coating concentrations and optimal antibody dilution for use in a competitive ELISA**

A 96-well microtitre plate was coated with different cell concentrations, ranging from 0 to  $1.6 \times 10^9$  cells/ml, by adding 100µl of each concentration per well. The plate was incubated for 1 hour at 37°C and the contents emptied. The plate was then washed three times with PBS - 0.05% (v/v) Tween and three times with PBS. The plate was blocked using 150µl of PBS - 4%(w/v) milk marvel and incubated at 4°C overnight. Serial antibody dilutions ranging from 1/10 – 1/1000000 were then prepared in PBS – 1% (w/v) milk marvel and 100µl of each dilution added per well. The plate was incubated at 37°C for 1 hour and washed as before. Goat anti-rabbit-horseradish peroxidase-labelled antibody, previously diluted to 1/5000 with PBS - 1% (w/v) milk marvel, was added to the plate (100µl/well) and the plate incubated at 37°C for 1 hour. Following the wash step, 100µl/well of *o*-PD substrate was added and, after 30 min incubation at 37°C, absorbances at 405nm were determined using a Titertek plate reader.

#### **2.4.8 Indirect competitive enzyme-linked immunosorbent assay (ELISA) for the detection of *B. abortus***

Microtitre plates were coated with 100µl of the appropriate *B. abortus* cell concentration and incubated for 1 hour at 37°C. The plates were then emptied and washed 3 times with PBS - 0.05% (v/v) Tween and three times with PBS. The plate were then blocked by adding 150µl/well of PBS - 4% (w/v) milk marvel and incubated at 4°C overnight. Free *B. abortus* cell concentrations, ranging from  $1.95 \times 10^6$  and  $1 \times 10^9$  cells/ml, were prepared in PBS. The plate was washed as before and 50µl of each cell concentration was added to each well along with 50µl of the *Brucella*-specific polyclonal antibody previously diluted to 1/5000 with PBS - 2% (w/v) milk marvel. The plate was incubated at 37°C for 1 hour and washed as before.

Goat anti-rabbit-horseradish peroxidase-labelled antibody, previously diluted to 1/5000 with PBS - 1% (w/v) milk marvel, was added to the plate (100µl/well) and the plate incubated at 37°C for 1 hour. Following the wash step 100µl/well of *o*-PD substrate was added and, after 30 min incubation at 37°C, absorbances at 405nm were determined using a Titertek plate reader.

#### **2.4.9 Measurement of cross-reactions**

The *Brucella*-specific polyclonal antibodies were assayed against a variety of gram-negative and positive bacterial strains. The assays were carried out as for the competitive ELISAs (Section 2.4.9) except the bacterial strains were added to the immunoplate with the *Brucella*-specific polyclonal antibodies.

### **2.5 Screening for scFv phage display antibodies from a naïve phage display library**

#### **2.5.1 Selection of antigen binders by panning in immunotubes**

An immunotube was coated with 0.5ml of the appropriate antigen at 10µg/ml overnight at 4°C. Following incubation the immunotube was washed three times with PBS and then blocked with 3% (w/v) milk marvel, for 2 hours at room temperature. Meanwhile, a 500µl sample of phage, at a concentration of approximately  $1 \times 10^{12}$  cfu/ml, was pre-blocked with 3% (w/v) milk marvel. The blocking solution was removed from the immunotube, which was washed three times with PBS. The pre-blocked phage were then added to the immunotube and incubated for 90 min at 37°C. The immunotube was then rinsed 10 times with PBS - 0.05% (v/v) Tween and 10 times with PBS. Bound phage were then eluted using 0.5ml of freshly prepared 100mM glycine-HCl, pH 2.2. The eluted phage was neutralised upon addition of 100µl of Tris-HCl, pH 8.0. XL-1 Blue cells were then infected with the eluted phage and the output titre determined (Section 2.5.2).

#### **2.5.2 Re-infection of XL-1 Blue *E. coli* cells with eluted phage**

A 20ml culture of 2x TY was inoculated with a single colony of XL-1 Blue *E. coli* and incubated shaking for 4 hours at 37°C, until OD<sub>550</sub> was approximately 0.5. Exponentially growing XL-1 Blue (5ml) were placed in a Falcon tube and 300µl of

the eluted phage were allowed infect the *E. coli* at 37°C for 30 min, while stationary, and for 30 min while shaking at 200rpm. Four ten-fold dilutions of the infected *E. coli* were prepared in 2x TY and 100µl of each dilution plated on 2x TY agar plates containing 100µg/ml ampicillin, 10µg/ml tetracycline and 2% (w/v) glucose. The remaining cells were centrifuged at 3500rpm for 10 min and then resuspended in 500µl of 2x TY and spread on 2x TY agar plates containing 100µg/ml ampicillin, 10µg/ml tetracycline and 2% (w/v) glucose. The agar plates were then incubated at 37°C overnight, while inverted.

### **2.5.3 Storage and rescue of phagemid antibodies after selection**

Colonies were scraped from the stock plates into 10ml of 2x TY in a 50ml Falcon tube. Sterile 50% (v/v) glycerol (5ml) was added to the cell suspension and 1ml aliquots were flash frozen using liquid nitrogen and stored at -70°C. 25ml of 2x TY containing 100µg/ml ampicillin, 10µg/ml tetracycline and 2% (w/v) glucose was inoculated with 100µl of the plate scrape and grown at 37°C to mid-log phase ( $OD_{550} = 0.5$ ). M13KO7 helper phage (200µl) were then added and allowed to infect the cells at 37°C for 30 min stationary and 30 min at 200rpm. The infected cells were then centrifuged at 3500rpm for 10 min and the bacterial pellet resuspended in 25ml of 2x TY containing 100µg/ml ampicillin, 10µg/ml tetracycline and 25µg/ml kanamycin. The resuspended pellet was then transferred to a sterile 250ml flask and grown for either 3.5 hours at 30°C or overnight at 25°C at 300rpm. For each selection, 1ml of culture was centrifuged for 5 min at 13000rpm. The phage-containing supernatant (10µl) was then used to infect mid-log phase XL-1 Blue *E. coli*, in order to determine the input phage titre.

### **2.5.4 Rescue of phagemid clones in microtitre trays for phage ELISA**

Colonies (95) were selected from the selection output agar plates and inoculated into 100µl of 2x TY containing 100µg/ml ampicillin, 10µg/ml tetracycline and 2% (w/v) glucose in a 96-well immunoplate plate and grown at 37°C with shaking at 120rpm. This was the master plate. A replica plate was then prepared by inoculating 100µl of 2x TY containing 100µg/ml ampicillin, 10µg/ml tetracycline and 2% (w/v) glucose with 20µl of the overnight cultures from the master plate. The replica plate was grown

at 37°C for 5 - 6 hours at 120rpm and 50µl of 50% (v/v) glycerol was added to each well of the master plate, which was stored at -20°C. M13KO7 helper phage (10µl) was then added to each well of the replica plate and allowed to infect the cells at 37°C for 60 min at 125rpm. The replica plate was centrifuged at 2000rpm for 10 min and the pellets resuspended in 100µl of 2x TY containing 100µg/ml ampicillin, 10µg/ml tetracycline and 25µg/ml kanamycin. The plate was then grown at 37°C overnight at 120rpm to produce phage particles.

### **2.5.5 Phage ELISA**

A 96-well plate was coated with the appropriate antigen at 10µg/ml, with 100µl/well and incubated overnight at 4°C. The coated immunoplate was then washed three times with PBS and blocked with 4% (w/v) milk marvel (150µl/well). The phage was then pre-blocked by centrifuging the replica plate at 2000 rpm for 10 min and transferring the supernatant to a fresh immunoplate containing 50µl of 9% (w/v) milk marvel in each well. The phage were pre-blocked for 30 min at room temperature and then added to the coated and blocked immunoplates and incubated at 37°C for 1 hour. The plate was washed three times with PBS - 0.05% (v/v) Tween and three times with PBS. The anti-fd bacteriophage, previously diluted to 1/5000 with PBS, was added (100µl/well) and the plate incubated at 37°C for 1 hour. The plate was washed as before and 100µl of a 1/5000 dilution of the HRP-labelled anti-rabbit Ig antibody added and the plate incubated at 37°C for 1 hour. The plate was re-washed, 100µl of *o*-PD substrate added to each well and then incubated for 30 min at 37°C. Absorbance values were then recorded at 405nm.

### **2.5.6 Soluble ELISA**

Colonies (95) were chosen from the selection output agar plates and inoculated into 100µl of 2x TY containing 100µg/ml ampicillin, 10µg/ml tetracycline and 2% (w/v) glucose in a 96-well immunoplate plate and grown at 37°C with shaking at 120rpm. This was the master plate. A replica plate was then prepared by inoculating 100µl of 2x TY containing 100µg/ml ampicillin, 10µg/ml tetracycline and 2% (w/v) glucose with 20µl of the overnights cultures from the master plate. The replica plate was grown at 37°C for 5 - 6 hours at 120rpm and 50µl of 50% (v/v) glycerol was added to

each well of the master plate, which was stored at  $-20^{\circ}\text{C}$ . The replica plate was centrifuged at 2000rpm for 10 min and the pellets resuspended in 100 $\mu\text{l}$  of 2x TY containing 100 $\mu\text{g/ml}$  ampicillin, 10 $\mu\text{g/ml}$  tetracycline and 1mM IPTG. The plate was then grown at  $30^{\circ}\text{C}$  overnight at 120rpm to induce antibody expression.

A 96-well plate was coated with the appropriate antigen (100 $\mu\text{l}$  of a 10 $\mu\text{g/ml}$  concentration) and incubated overnight at  $4^{\circ}\text{C}$ . The coated immunoplate was then washed three times with PBS and blocked with 150 $\mu\text{l/well}$  of 4% (w/v) milk marvel. The soluble scFvs were then pre-blocked by centrifuging the replica plate at 2000 rpm for 10 min and transferring the supernatant to a fresh immunoplate containing 50 $\mu\text{l}$  of 9% (w/v) milk marvel in each well. This was incubated for 30 min at room temperature. The pre-blocked scFvs were then added to the previously coated and blocked immunoplate and incubated at  $37^{\circ}\text{C}$  for 1 hour. The plate was washed three times with PBS - 0.05% (v/v) Tween and then three times with PBS. An anti-c-myc-HRP antibody, previously diluted to 1/1000 in PBS was added (100 $\mu\text{l/well}$ ) and the plate incubated at  $37^{\circ}\text{C}$  for 1 hour. Once again the plate was washed and 100 $\mu\text{l}$  of *o*-PD substrate added to each well and incubated for 30 min at  $37^{\circ}\text{C}$ . Absorbance values were then recorded at 405nm.

#### **2.5.7 Sequence analysis on the gene encoding the bp26-specific scFvs**

Nucleotide and amino acid sequence comparisons were carried out on the bp26-specific scFvs as previously described in Section 2.2.11.

#### **2.5.8 Checkerboard ELISA for the determination of optimal bp26 coating concentration and optimal scFv dilution for use in a competitive ELISA**

A 96-well microtitre plate was coated with different bp26 concentrations, ranging from 0 to 50 $\mu\text{g/ml}$ , by addition of 100 $\mu\text{l}$  of each concentration per well. The plate was incubated for 1 hour at  $37^{\circ}\text{C}$  and the contents emptied. The plate was then washed three times with PBS - 0.05% (v/v) Tween and three times with PBS. The plate was blocked using 150 $\mu\text{l}$  of PBS - 4% (w/v) milk marvel and incubated at  $4^{\circ}\text{C}$  overnight. Serial scFv dilutions ranging from undiluted to 1/1000 were then prepared in PBS – 1% (w/v) milk marvel and 100 $\mu\text{l}$  of each dilution added per well. The plate was

incubated at 37°C for 1 hour and washed as before. Anti-c-myc-horseradish peroxidase-labelled antibody, previously diluted to 1/1000 with PBS - 1% (w/v) milk marvel, was added to the plate (100µl/well) and the plate incubated at 37°C for 1 hour. The plate was washed, as before, and *o*-PD substrate added (100µl/well). After 30 min incubation at 37°C absorbances at 405nm were determined using a Titertek Plate reader.

### **2.5.9 Indirect competitive enzyme-linked immunosorbent assay (ELISA) for the detection of bp26**

Microtitre plates were coated with 100µl of the bp26 at 12.5µg/ml and incubated for 1 hour at 37°C. The plates were then emptied and washed 3 times with PBS - 0.05% (v/v) Tween and three times with PBS. The plate were then blocked by adding 150µl/well of PBS - 4% (w/v) milk marvel and incubated at 4°C overnight. Free bp26 concentrations, ranging from 24 – 25000ng/ml, were prepared in PBS. The plate was washed as before and 50µl of each bp26 concentration was added to each well along with 50µl of the bp26-specific scFv previously diluted to 1/8 with PBS - 2% (w/v) milk marvel. The plate was incubated at 37°C for 1 hour and washed as before. Anti-c-myc-horseradish peroxidase-labelled antibody, previously diluted to 1/1000 with PBS-1% (w/v) milk marvel, was added to the plate (100µl/well) and the plate incubated at 37°C for 1 hour. The plate was washed, as before, and *o*-PD substrate added (100µl/well). After 30 min incubation at 37°C absorbances at 405nm were determined using a Titertek plate reader.

### **2.6 Development of diagnostic assays for the detection of bovine brucellosis**

All serum samples used in the development of the diagnostic assays for the detection of bovine brucellosis were kindly donated by Blood Testing Laboratory, Department of Agriculture and Food (DAFF), Model Farm Rd., Cork. A set of three standard serum samples were provided, which included the two *Brucella*-positive standards, which displayed significantly high antibody titres against *Brucella abortus*, the DeVeere Hunt Serum and the National Standard Serum (NSS), and the standard *Brucella*-negative serum. A panel of *Brucella*-positive and negative serum samples were also obtained, which consisted of 18 positive serum samples, which were previously identified as positive for a *Brucella* infection using the conventional LPS-

indirect ELISA, and 50 serum samples, which were previously identified as negative for a *Brucella* infection.

### **2.6.1 Indirect enzyme-linked immunosorbent assay for the detection of bovine brucellosis in serum samples**

Wells of a 96-well immunoplate were coated with the appropriate antigen diluted in PBS. The immunoplate was then incubated at 37°C for 1 hour. The plate was washed three times with PBS - 0.05% Tween and three times with PBS. Milk marvel (4% (v/v)) in PBS was added to each well (150µl / well) and the plates were incubated at 4°C overnight. The *Brucella*-positive and negative bovine serum samples diluted to 1/50 in PBS - 0.05% (v/v) Tween containing 4% (w/v) milk marvel were pre-incubated at 37°C for 1 hour. The immunoplate was washed as before and 100µl of each serum dilution was added to each well, in duplicate. The plate was incubated at 37°C for one hour and washed as before. The anti-bovine horseradish peroxidase-labelled antibody (100µl), previously diluted to 1/2000 and pre-incubated in PBS-0.05% (v/v) Tween containing 4% (w/v) milk marvel, was added to each well. The plate was then incubated at 37°C for one hour. The plate was washed, as before, and *o*-PD substrate added (100µl/well). After 30 min incubation at 37°C absorbances at 405nm were determined using a Titertek plate reader.

### **2.6.2 Sandwich enzyme-linked immunosorbent assay for the detection of bovine brucellosis in serum samples**

A 1/500 dilution of the purified polyclonal antibody was prepared in carbonate buffer, pH 9.6, and 100µl added to a 96-well immunoplate. The plate was incubated at 37°C for one hour and washed three times with PBS - 0.05% (v/v) Tween and three with PBS. 150µl of 4% (w/v) milk marvel in PBS was added to each well and the plates were incubated at 4°C overnight. The plates were washed as before and 100µl of the appropriate antigen, diluted in PBS, added to each well. The plate was then incubated at 37°C for 1 hour. The *Brucella*-positive and negative bovine serum samples, diluted to 1/50 in PBS - 0.05% (v/v) Tween containing 4% (w/v) milk marvel, were pre-incubated at 37°C for 1 hour. The immunoplate were washed as before 100µl of each serum dilution was added to each well, in duplicate. The plate was incubated at 37°C for one hour and washed as before. The anti-bovine horseradish peroxidase-labelled

antibody (100 $\mu$ l), previously diluted to 1/2000 and pre-incubated in PBS - 0.05% (v/v) Tween containing 4% (w/v) milk marvel was added to each well. The plate was then incubated at 37°C for one hour. The plate was washed, as before, and *o*-PD substrate added (100 $\mu$ l/well). After 30 min incubation at 37°C absorbances at 405nm were determined using a Titertek plate reader.

## CHAPTER 3

**The production and characterisation of genetically  
derived scFv antibody fragments directed against  
aflatoxin B<sub>1</sub> (AFB<sub>1</sub>)**

### 3.1 Introduction

The discovery of aflatoxins stems from 1960 following the death of several thousand-turkey poults in East Anglia (Hartley *et al.*, 1963). Aflatoxins consist of a group of approximately 20 related fungal metabolites that occur in *Aspergillus* species (O’Kennedy and Thornes, 1997). High humidity, in tropical and sub-tropical climates favours fungal growth and the production of aflatoxins. Contamination is widespread in agricultural commodities including maize, cottonseed, peanuts and tree nuts and occurs during growth and, to greater extent, storage. They can also occur in a wide range of important raw food produce including spices, figs and dried fruit. Aflatoxins are members of the coumarin family and are the most widely spread group of toxins from naturally occurring moulds that results in contamination of food products. Aflatoxins B<sub>1</sub>, B<sub>2</sub>, G<sub>1</sub> and G<sub>2</sub> are normally found in food, with additional metabolites, aflatoxins M<sub>1</sub> and M<sub>2</sub>, found in milk. Aflatoxin B<sub>1</sub> (AFB<sub>1</sub>), which is produced by *A. flavus* and *A. parasiticus*, is the most predominant and toxic. AFB<sub>1</sub> is considered to be one of the most potent naturally occurring carcinogens, is linked to human hepatocellular carcinoma and is regarded as a human carcinogen by the International Agency for Research on Cancer (Ward *et al.*, 1990).

#### 3.1.1 Chemical and physical properties of aflatoxins

Aflatoxins are crystalline structures that fluoresce under UV radiation. Aflatoxins are hydrophobic in nature and soluble in solvents such as chloroform, methanol and dimethyl sulfoxide (DMSO), and in water to the extent of 10 – 20mg/l. They are extremely stable in the absence of light and UV radiation, even at temperatures in excess of 100°C. The presence of the lactone moiety makes them susceptible to alkaline hydrolysis. However, this hydrolysis appears to be reversible following acidification. Aflatoxins are broken down in the presence of oxidising agents, such as sodium hypochlorite, potassium permanganate and hydrogen peroxide, resulting in the loss of fluorescence. In acid solutions aflatoxins B<sub>1</sub> and G<sub>1</sub> are converted to aflatoxins B<sub>2a</sub> and G<sub>2a</sub> due to the acid-catalysed addition of water across the double bond of the furan ring. Figure 3.1 illustrates the structure of AFB<sub>1</sub> and its structural analogues.

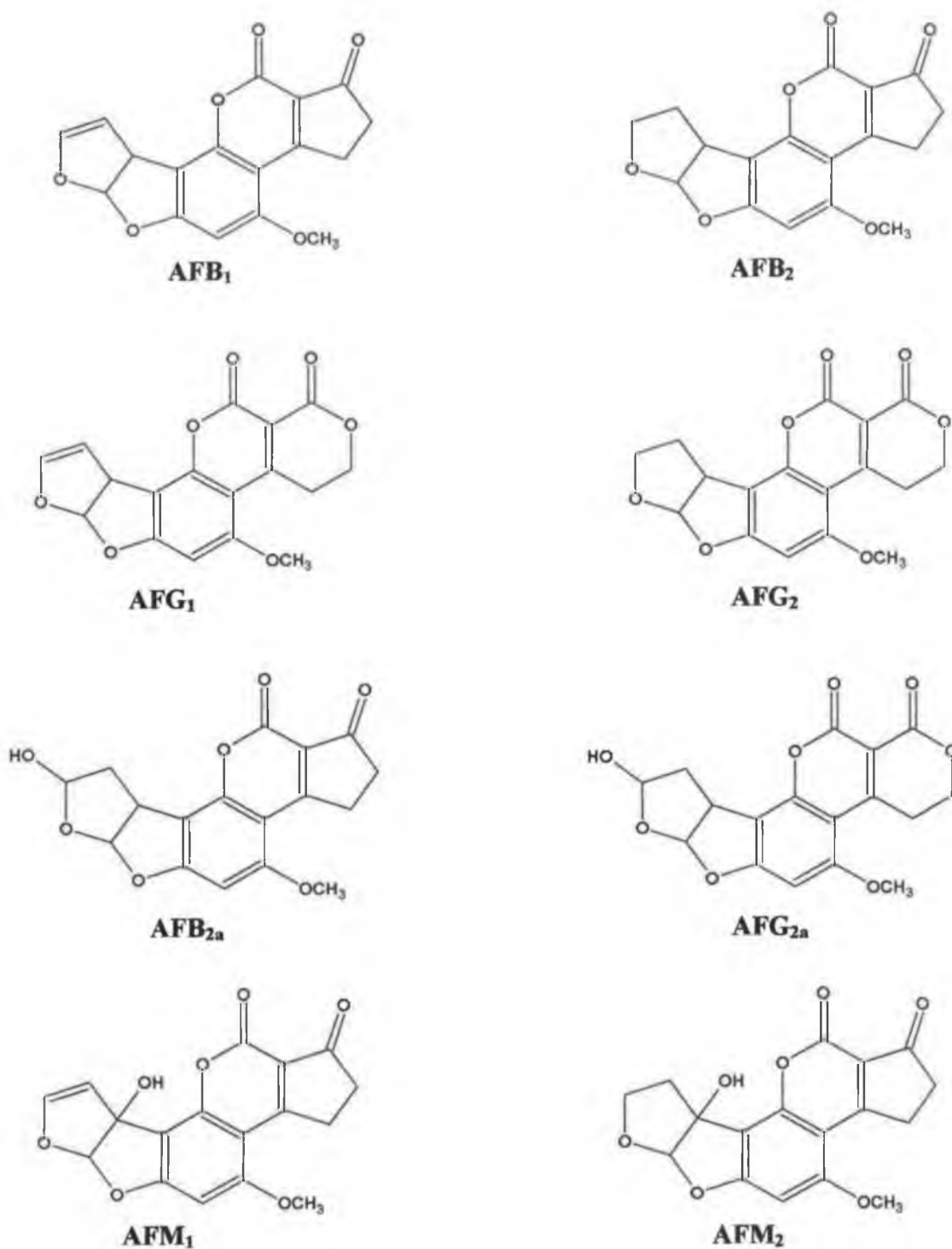


**Figure 3.1:** Chemical structure of aflatoxin B<sub>1</sub> (AFB<sub>1</sub>) and its structural analogues: aflatoxin B<sub>2</sub> (AFB<sub>2</sub>), aflatoxin G<sub>1</sub> (AFG<sub>1</sub>), aflatoxin G<sub>2</sub> (AFG<sub>2</sub>), aflatoxin M<sub>1</sub> (AFM<sub>1</sub>), aflatoxin M<sub>2</sub> (AFM<sub>2</sub>), aflatoxin B<sub>2a</sub> (AFB<sub>2a</sub>) and aflatoxin G<sub>2a</sub> (AFG<sub>2a</sub>).

### 3.1.2 Aflatoxin production and biosynthesis

*A. flavus*, *A. parasiticus* and *A. nomius* are widely distributed moulds that share the ability to produce aflatoxins (Gourama and Bullerman, 1995). Aflatoxins are secondary metabolites of these fungal species and are not essential for growth. Several factors, including fungal species, substrate and environment contribute to aflatoxin production. The optimal growth temperature for *A. flavus* is 25°C and 25 -35°C for *A. parasiticus* and the optimum temperature for aflatoxin production is generally accepted to be 25 - 28°C. Maximum levels of aflatoxin production are linked to the exhaustion of sugars in the medium and the onset of mycelial autolysis. Relative humidity levels of at least 83 – 88% are required for aflatoxin production. Aflatoxin yields increase as the relative humidity increases, up to 99%. Since fungal growth and aflatoxin production are aerobic, CO<sub>2</sub> concentrations from 20 – 100% gradually inhibit aflatoxin production. Zinc and magnesium are essential for aflatoxin biosynthesis and a mix of cadmium and iron was found to stimulate production. However, iron has been found to inhibit fungal growth and, therefore, aflatoxin production. Other substances such as nitrate, ethylene, sorbic acid and competing mycoflora, such as *A. niger* and *Rhizopus oligosporus*, also inhibit aflatoxin production.

The majority of genes involved in the biosynthesis of aflatoxins are contained within a single cluster on a chromosome, which in *A. flavus* and *A. parasiticus* is estimated to be 75kb (Woloshuk and Prieto, 1998). The main precursors of aflatoxins are acetate polyketides. Aflatoxins are produced from the acetate building blocks, which are produced during the idiophase of the fungal life-cycle. Aflatoxin B<sub>1</sub> biosynthesis is complex and involves numerous intermediate compounds, including norsolorinic acid, averantin, averufin, versiconal hemiacetal acetate, versicolorin A and sterigmatocystin (Fig. 3.2).

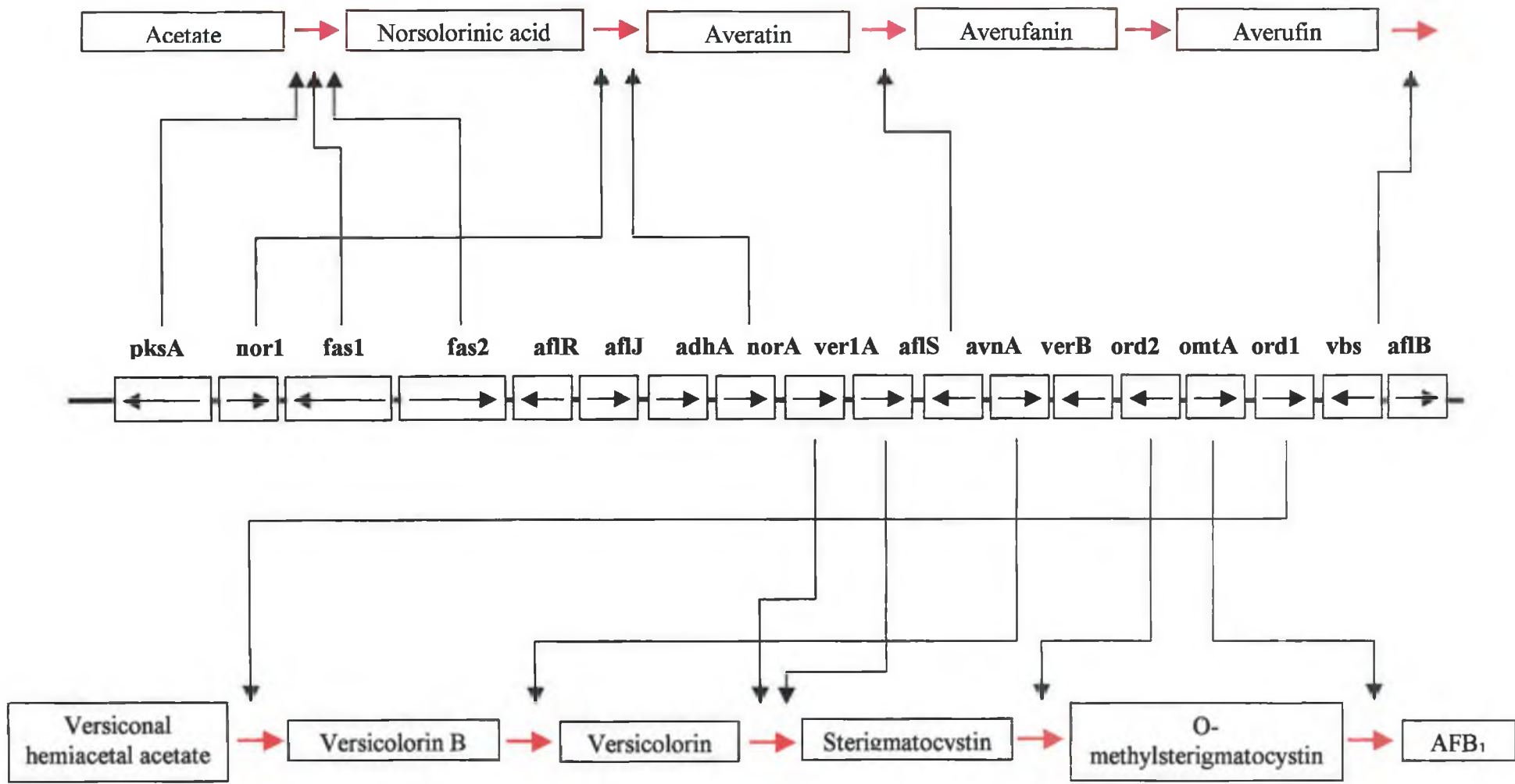


**Figure 3.2:** Biosynthetic pathway of aflatoxin B<sub>1</sub>, detailing the major intermediates and the genetic organisation of the aflatoxin gene cluster (after Woloshuk and Prieto, 1998).

### 3.1.3 Mode of action of aflatoxins

The most toxic and carcinogenic effects associated with aflatoxin B<sub>1</sub> are as a result of metabolic activation. Several cytochrome P450 enzymes including 1A2, 2A, 3A and 2A5, are involved in the biotransformation of aflatoxin B<sub>1</sub> (Pelkonen *et al.*, 1997). Cytochrome P450 can metabolise AFB<sub>1</sub> to both an *exo*- and *endo*-AFB<sub>1</sub>-8,9-epoxide. In an attempt to rid the body of aflatoxin the cytochrome P450 enzymes add a highly reactive epoxide group, making it highly mutagenic (Goodsell, 2001). The resulting *exo*-epoxide reacts covalently with DNA to form adducts that ultimately result in heritable genetic change (Smela *et al.*, 2001). The activated epoxide forms covalent attachments with the N7 of guanine resulting in the formation of a number of adducts (Hussein and Brasel, 2001). 8,9-dihydro-8-(N7-guanyl)-9-hydroxyaflatoxin B<sub>1</sub> (AFB<sub>1</sub>-N7-Gua) is the most abundant, both *in vivo* and *in vitro* (Smela *et al.*, 2001). Other adducts formed include an apurinic (AP) site, resulting following depurination by the positively charged imidazole ring of the principal adduct, and a more chemically and biologically stable AFB<sub>1</sub> formamidopyrimidine (AFB<sub>1</sub>-FAPY), which is produced when the imidazole ring on the AFB<sub>1</sub>-N7-Gua opens (Smela *et al.*, 2001). All three adducts represent the chemical precursors that account for the genetic effects of AFB<sub>1</sub>, which are dominated by G-T transversions. The epoxide has been linked to G-T transversions at codon 249 of the p53 tumour suppressor gene, which is associated with many human cancers (Smela *et al.*, 2001). Hydroxylation of the epoxide results in the formation of AFB<sub>1</sub>-8-9-dihydrodiol, which inhibits *in vivo* and *in vitro* protein synthesis presumably explaining the cause of liver necrosis and resulting death (Gourama and Bullerman, 1995). Figure 3.3 details the metabolic pathway of AFB<sub>1</sub> leading to covalent adduct formation.

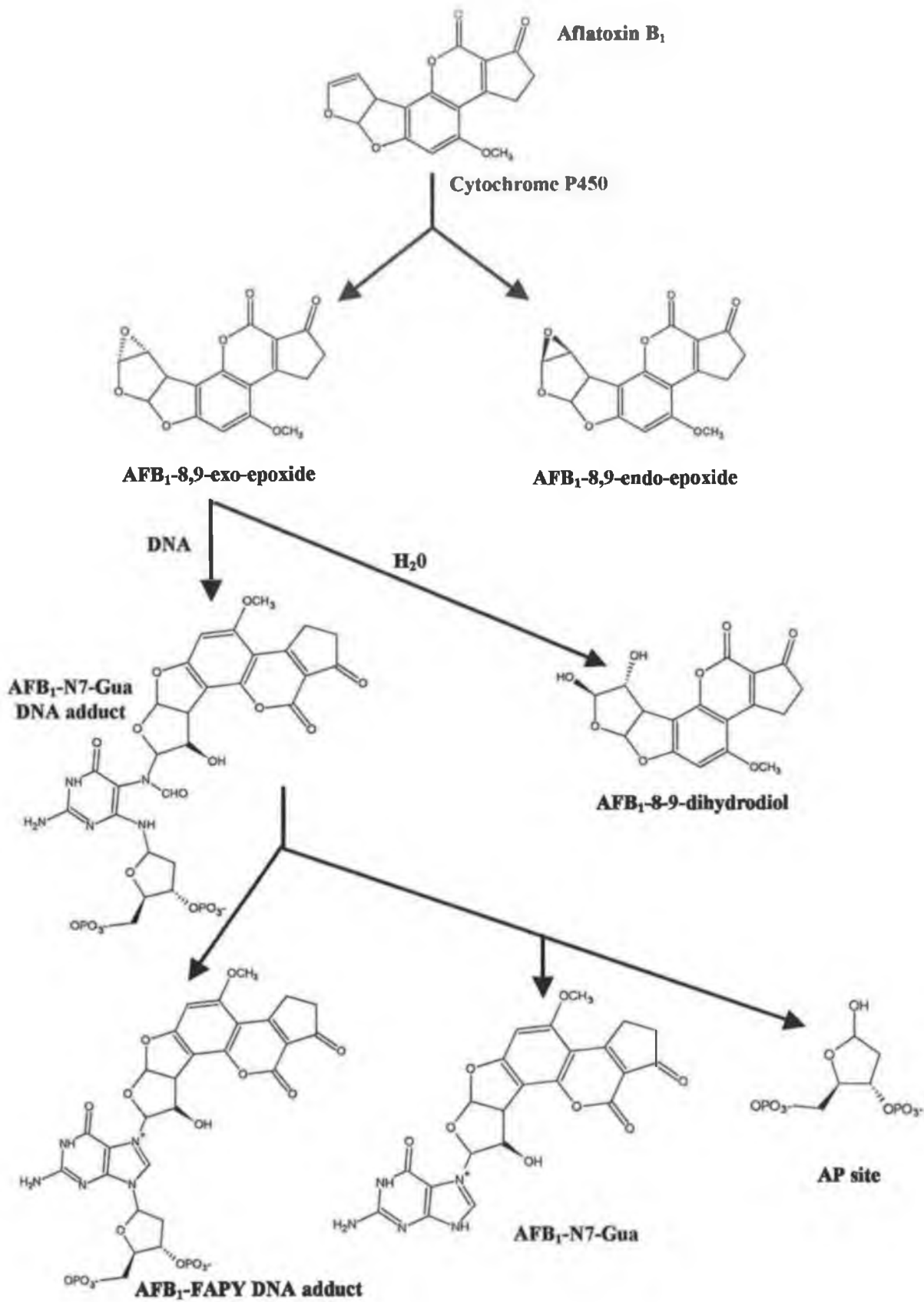


**Figure 3.3:** Pathway detailing the metabolic activation of aflatoxin B<sub>1</sub> leading to the formation of DNA adducts.

### 3.1.4 Toxicity of aflatoxins

Aflatoxins are potent, carcinogenic, mutagenic, immunosuppressive agents that can be both acutely and chronically toxic. AFB<sub>1</sub> is considered to be one of the most potent naturally occurring carcinogens, is linked to human hepatocellular carcinoma and is regarded as a human carcinogen by the International Agency for Research on Cancer (Ward *et al.*, 1990). Acute aflatoxin poisoning in man is extremely unlikely and in animals is rare in temperate developed areas. However, the outbreak of Turkey X disease, in the 1960s highlighted the potential devastating effects of mycotoxin contamination, in particular the aflatoxins.

The susceptibility of animals to acute mycotoxin poisoning is determined from the LD<sub>50</sub> (mg/kg of body weight), which in turn is dependent on several factors including species, age, sex and nutrition. In general LD<sub>50</sub> for animals range between 0.5 – 10mg/kg of body weight. Clinical signs of aflatoxosis in animals include gastrointestinal dysfunction, reduced reproducibility, reduced feed utilisation and efficiency, anaemia and jaundice. The effects of aflatoxin poisoning varies from species to species with calves, chicks, ducklings, guinea pigs and pigs being susceptible to aflatoxin B<sub>1</sub> and goats, rats, mice and sheep being relatively resistant (Gourama and Bullerman, 1995).

Cases of acute aflatoxin poisoning in humans have been reported sporadically, mainly in Africa and Asia. In the majority of reported cases the humans become exposed to aflatoxins by consuming contaminated food such as maize, rice or cereal products. A broad range of symptoms can be found, including vomiting, abdominal pain, pulmonary edema, acute liver damage, loss of function of the digestive tract, convulsions, cerebral edema and death, depending on dose consumed. The onset of symptoms is relatively slow (i.e. > 8 hours post exposure). In general our understanding on the affects of aflatoxin poisoning on humans is limited to case studies on sporadic outbreaks of aflatoxosis. Studies on human outbreaks suggest a minimum dose of 50µg/kg/day is required for clinically significant effects. A woman who attempted suicide by ingesting 5.5mg over 2 days and 35mg over two weeks (6 months later) of aflatoxin B<sub>1</sub> recovered completely with no significant signs of liver damage (Hussein and Brasel, 2001). This suggests that extended subacute doses, as

seen in dietary exposure in certain countries, are necessary for inducing lethal acute effects.

One of the most significant accounts of aflatoxin poisoning occurred in India in 1974. 397 people were affected following consumption of contaminated corn. The corn was contaminated with aflatoxin at levels ranging from 0.25 – 15mg/kg. It is estimated that the daily aflatoxin B<sub>1</sub> intake was at least 55µg/kg of body weight, for an undetermined number of days. Patients experienced several symptoms including high fever, jaundice, vomiting, pain and swollen livers and out of the infected people 108 died. In Malaysia in 1990 approximately 40 people were affected and 13 children died following the consumption of noodles highly contaminated with aflatoxin and boric acid. In this case autopsy results later revealed high levels of aflatoxin in the liver, lung, kidney heart, brain and spleen.

Aflatoxins have also been found in tissue specimens taken from children suffering from Kwashiorkor and Reye's syndrome suggesting that aflatoxins may be a contributing factor to these diseases (Hussein and Brasel, 2001). Studies, carried out in Asia and Africa, have demonstrated the positive association between dietary aflatoxin exposure and liver cell cancer. In 1987 the International Agency for Research on Cancer (IARC) classified aflatoxin B<sub>1</sub> as a class I human carcinogen (Ward *et al.*, 1990). Although less studies have been conducted on aflatoxins G<sub>1</sub> and M<sub>1</sub> they appear to be toxicologically similar to aflatoxin B<sub>1</sub>. However, they are slightly less potent liver carcinogens and slightly more potent kidney carcinogens.

### **3.1.5 Aflatoxin sampling and analysis**

As previously discussed aflatoxin contamination can occur in a wide range of agricultural commodities including corn, peanuts and maize. The aflatoxin concentration in grains or nuts can vary from less than 1ppb to more than 12ppb with the aflatoxin highly concentrated in individual kernels (Gourama and Bullerman, 1995). Therefore, it is essential to select an analytical sample that is truly representative of the consignment. Polar solvents such as methanol, chloroform and acetonitrile are used extract the aflatoxins from food and animal feed. Sample clean-up using solid phase extraction techniques and immunoaffinity columns may also be

required for the traditional methods of detection for AFB<sub>1</sub>, which include thin-layer chromatography (TLC), high-pressure liquid chromatography (HPLC), gas-liquid chromatography (GLC) and mass spectrometry (Nawaz *et al.*, 1995). These conventional analytical techniques have offered good resolution, a high degree of precision, reproducibility and sensitivity in the detection of aflatoxins. Hunt *et al.* (1978) describes a HPLC system combined with the use of a fluorescence detection system for the detection of aflatoxins and ochratoxin in food. This system offered detection limits of 2.5µg/ml for AFB<sub>1</sub>. A gas chromatography / mass spectrometry / selected ion monitoring system has also been described for the confirmation of aflatoxin B<sub>1</sub> and B<sub>2</sub> with limits of detection for aflatoxin B<sub>1</sub> and B<sub>2</sub> at 0.1ppb (Rosen *et al.*, 1984). Although these techniques may offer good sensitivity extensive sample clean up is required making them time-consuming and costly. Therefore, attention has focused on immunoanalytical techniques incorporating AFB<sub>1</sub>-specific antibodies, which offer increased sensitivity and specificity for AFB<sub>1</sub> detection. AFB<sub>1</sub> has a relatively small molecular mass of approximately 312 Daltons and in order to elicit an immune response it must be covalently attached to a large carrier molecule such as bovine serum albumin (BSA), for immunisation. The protein conjugate is required during the production, screening and characterisation of antibodies. A variety of immunoassay formats have been described for aflatoxin detection with varying degrees of sensitivity and specificity. The more conventional immunoassays incorporate either polyclonal or monoclonal antibodies and, more recently, developments in recombinant antibody techniques have provided novel antibody fragments, with desirable affinities and specificities.

One of the first immunoassays described for the detection of AFB<sub>1</sub> was a radioimmunoassay incorporating an AFB<sub>1</sub>-specific polyclonal antibody (Langone and Van Vunakis, 1976). This immunoassay was capable of detecting AFB<sub>1</sub> in crude extracts of corn and peanut butter, supplemented with AFB<sub>1</sub>, at levels as low as 1µg/kg. Recently, a more sensitive radioimmunoassay was described for the detection of AFB<sub>1</sub>, in a variety of agricultural commodities, using a polyclonal antibody (Korde *et al.*, 2003). Separation systems, incorporating PEG (liquid phase) or antibody-coated beads (solid phase), resulted in increased sensitivity levels, over the

radioimmunoassay described by Langone and Van Vunakis (1976), with limits of detection for AFB<sub>1</sub> at 0.2ng/ml.

However, there are several drawbacks to the use of radioimmunoassay, the radioisotopes used are hazardous, labile and expensive. Therefore, the majority of immunoassays developed for aflatoxin detection incorporate enzymes. Several enzyme-linked immunosorbent assays (ELISAs) have been developed for the detection of aflatoxin. Candlish *et al.* (1985) describes the development of a competitive ELISA for AFB<sub>1</sub> detection using a monoclonal antibody. This was one of the first reported cases on the development and use of monoclonal antibodies against AFB<sub>1</sub>. This competitive ELISA offered limits of detection for AFB<sub>1</sub> at 0.2ng/ml. Ward *et al.* (1990) has described the development of competitive ELISAs for AFB<sub>1</sub> using both polyclonal and monoclonal antibodies, raised against an aflatoxin B<sub>1</sub> oxime-BSA conjugate. The polyclonal antibodies offered the lowest sensitivity levels with limits of detection for AFB<sub>1</sub> at 0.1pg/well. The monoclonal antibodies developed offered limits of detection for AFB<sub>1</sub> as low as 1 pg/well. Polyclonal antibodies have also been applied to the development of competitive ELISAs for the detection of AFB<sub>1</sub> in peanut at levels as low as 0.25ppb (Aldao *et al.*, 1995). Polyclonal antibodies have also been applied to the development of Biacore inhibition assays for the detection of AFB<sub>1</sub> with limits of detection for AFB<sub>1</sub> at 3 ng/ml (Daly *et al.*, 2000). More recently, scFv antibody fragments directed against AFB<sub>1</sub> have been isolated from a phage display library (Daly *et al.*, 2002). The library was constructed using a method previously described by Krebber *et al.* (1997) and the specific scFvs applied to the development of competitive ELISAs and Biacore inhibition assays. The competitive ELISA offered limited sensitivity with a limit of detection for AFB<sub>1</sub> at 98ng/ml. Increased levels of sensitivity were observed with the Biacore inhibition assay format with limits of detection for AFB<sub>1</sub> at 3 and 0.75ng/ml in PBS and spiked grain, respectively. A Biacore-based inhibition assay, incorporating a commercial monoclonal antibody, has also been described for AFB<sub>1</sub> detection with limits of detection of 0.2ppb (ng/ml) (Van Der Gaag *et al.*, 1998). Other immunoanalytical techniques described for aflatoxin detection include a dipstick enzyme immunoassay for the simultaneous detection of 5 mycotoxins with a lower limit of detection for AFB<sub>1</sub> at 2ng/ml (Schneider *et al.*, 1995) and an immunoaffinity fluorometric biosensor with a lower limit of detection at 0.1ppb (Carlson *et al.*, 2000). A sol-

particle lateral flow immunoassay (LFIA) with limits of detection of for AFB<sub>1</sub> 0.1ppb in buffer and 10ppb in grain samples has also been developed (Niessen *et al.*, 1998). Research has also focused on the development of on-site immunoassays for the detection of aflatoxins. Pal and Dhar (2004) have developed a nitrocellulose-based immunoassay using an improved catalysed reporter deposition method of signal amplification involving biotinylated tyramine and avidin-horseradish peroxidase conjugates. This system is capable of analysing 12 extracted samples in a single test within 12 minutes and offers detection limits of 0.01ng/ml.

### **3.1.6 Methods of control and management of aflatoxins**

Aflatoxins are considered unavoidable contaminants of food for both human and animal consumption, irrespective of good manufacturing practice. Therefore, several international agencies have established specific guidelines on acceptable levels of aflatoxins in food and feed. In the US the Federal Food Drug and Cosmetic Act Sec. 402 (a) and the FDA have established specific action levels set at 20ppb total aflatoxins in food and 0.5ppb for aflatoxin M<sub>1</sub> in milk (Hussein and Brasel, 2001). The EU has also established guidelines on maximum residue limits for aflatoxins in a range of commodities (Table 3.1). However, several countries within the EU have proposed their own maximum residue limits with some degree of variation observed from country to country. Table 3.2 details the maximum limits for aflatoxin B<sub>1</sub> in various European countries. The FAO in conjunction with the WHO Joint Expert Committee on Food Additives and Contaminants have established programs to ensure proper sampling and analysis for mycotoxins in developing countries (Hussein and Brasel, 2001).

Numerous detoxification strategies for aflatoxins, including chemical and physical treatments, have also been investigated. Physical treatments including blending, heat, microwaves, gamma waves, X-rays, UV light and adsorption have all been used to reduce aflatoxins levels in animal feed in an attempt to reduce aflatoxin M<sub>1</sub> yields in milk. Ammoniation appears to be the most successful chemical method for degrading aflatoxins and appears to result in 95 – 98% decomposition of AFB<sub>1</sub> (Creppy, 2002). This procedure is used in various countries for the detoxification of animal feed. However, detoxification of aflatoxin-contaminated food for human consumption may

result in undesirable alterations in the nutritional and organoleptic qualities of the food (Das and Mishra, 2000).

*Table 3.1: Maximum levels for aflatoxins in a variety of food types established as guidelines by the EU set out in Commission Regulation (EC) No 466/2001.*

<b>Products</b>	<b>B<sub>1</sub> (ppb)</b>	<b>B<sub>1</sub> + B<sub>2</sub> + G<sub>1</sub> + G<sub>2</sub> (ppb)</b>	<b>M<sub>1</sub> (ppb)</b>
Groundnuts, nuts and dried fruit, for direct human consumption	2	4	-
Groundnuts, nuts and dried fruit, subject to sorting or physical treatment	8	15	-
Cereals for direct human consumption	2	4	-
Milk	-	-	0.05

*Table 3.2: Maximum limits for aflatoxin B<sub>1</sub> in foods established by various countries within the European Union (Creppy, 2002).*

<b>Country</b>	<b>Maximum limit of AFB<sub>1</sub> (ppb)</b>	<b>Foods</b>
Finland	2	All
Germany	2	All
The Netherlands	5	All
Belgium	5	All
Portugal	25	Peanuts
	5	Children's food
	20	Others
Austria	1	Alls
	2	Cereals, nuts
Switzerland	1	All
	2	Maize, cereals
Spain	5	All
Luxemburg	5	All
Ireland	5	All
Denmark	5	All
Greece	5	All

### **3.1.7 Chapter outline**

This chapter focuses on the production and characterisation of three genetically derived scFv antibody fragments, a monomeric, dimeric and alkaline phosphatase-labelled scFv, directed against aflatoxin B<sub>1</sub> (AFB<sub>1</sub>). The scFvs were applied to the development of several immunoassay formats, including competitive ELISAs and Biacore inhibition assays, for the detection of AFB<sub>1</sub>. A lateral flow immunoassay was also developed for the detection of AFB<sub>1</sub>, which incorporated an anti-AFB<sub>1</sub> rat monoclonal antibody.

## **3.2 Results**

### **3.2.1 Production of genetically derived scFv antibodies to aflatoxin B<sub>1</sub>**

#### **3.2.1.1 Construction of a pre-immunised phage display library for the isolation of functional scFvs against aflatoxin B<sub>1</sub>**

An aflatoxin B<sub>1</sub> recombinant antibody library was constructed by Dr. Stephen Daly, DCU (Daly *et al.*, 2002). The pre-immunised scFv phage display library was developed using a method previously described by Krebber *et al* (1997). Basically, Balb/C mice were immunised with a commercially available AFB<sub>1</sub>-BSA conjugate and when sufficient titres were obtained the splenic RNA was isolated and reverse transcribed into cDNA. The mouse heavy and light chain genes were then amplified by multiplex PCR and annealed together using a splice by overlap extension PCR (SOE-PCR). The 800bp SOE-PCR product was then ligated into the phage display vector, pAK100, and the ligated vector transformed into supercompetent XL-1 Blue *E. coli*. The resulting phage display library consisted of  $5 \times 10^3$  clones and following three rounds of panning six clones recognising free AFB<sub>1</sub> were isolated.

#### **3.2.1.2 Isolation and nucleotide and amino acid sequence analysis on an AFB<sub>1</sub>-specific scFv**

Following three rounds of panning on the pre-immunised phage-display library a positive clone (D1) was selected and used for the production of soluble scFvs specific to AFB<sub>1</sub>. Plasmid DNA, encoding the AFB<sub>1</sub>-specific scFv, was purified from XL-1 Blue *E. coli*, as described in Section 2.2.2. The plasmid DNA was quantified and sent to MWG-Biotech (Germany) for sequencing. Comfort reads were obtained in both directions on the scFv insert, using primers specific to the multiple cloning site of the pAK100 vector. The nucleotide sequence of the scFv gene was determined and used to deduce the amino sequence (Fig. 3.4). The deduced amino acid sequence was compared with variable regions of immunoglobulins found in the SwissProt database and used along with the Kabat rules to identify the loops corresponding to the CDRs within the variable heavy and variable light domains. The 3-D structure of the scFv was also predicated, using SwissModel, based on structurally related proteins (Fig. 3.5).

gaatctgcactcaccacatcacctggtgaaacagtcacactcacttgtcgtcaagtact  
 E S A L T T S P G E T V T L T C\* R S S T  
 ggggctgttacaactagtaactatgccaaactgggtccaagaaaaccagatcatttattc  
G A V T T S N Y A | N W V Q E K P D H L F  
**CDR-L1**  
 actggtctaataaggtggtaccaacaaccgagctccaggtgttctctgagattctcagggc  
 T G L I G | G T N N R A P | G V P A R F S G  
**CDR-L2**  
 tcctgattggagacaagggtgccctcaccatcacaggggacagactgaggatgaggca  
 S L I G D K A A L T I T G A Q T E D E A  
 atatatttctgtgctctatggtacagcaaccattgggtgttcggtggaggaaccaaactg  
 I Y F C\* | A L W Y S N H W V | F G G G T K L  
**CDR-L3**  
 actgtcctaggtggtggtggtggttctgggtggtggttctggcggcggcggctccggt  
 T V L G G G G G S G G G G S G G G G S G  
 ggtggtgatcccaggtccagctgcagcagctctgggctgagctggtgaggcctggggct  
 G G G S Q V Q L Q Q S G P E L V R P G A  
 tccgtgaagatgtcctgcaagtcttctggctacagctttaccagctactggttgcactgg  
 S V K M S C\* K S S | G Y S F T S Y W L H W  
**CDR-H1**  
 gtaaacagaggcctggacagggctctagaatggattggtgctatttatcctggaaatagt  
V K Q R P G Q G L E | W I G | A I Y P G N S  
 gatactaggtacaaccagaaattcaagggcaagggtcaaactgactgcagtcacatccgcc  
D T R Y N Q K F K G K V | K L T A V T S A  
**CDR-H2**  
 agcactgcctacatggagctcagcagcctgacaaatgaggactctgcggctctattactgt  
 S T A Y M E L S S L T N E D S A V Y Y C\*  
 acaagaggggaggcctactataggtacgacgggatctggtttgcttactggggccaaggg  
 T R | G E A Y Y R Y D G I W F A Y | W G Q G  
**CDR-H3**  
 agtctggtcactgtctct  
 S L V T V S

**Figure 3.4:** The nucleotide and deduced amino acid sequences of the gene encoding the AFB<sub>1</sub> specific scFv. The amino acid sequences representing the CDRs are underlined and in bold and were defined according to Kabat et al. (1991). The four conserved cystine residues are indicated with an asterisk.

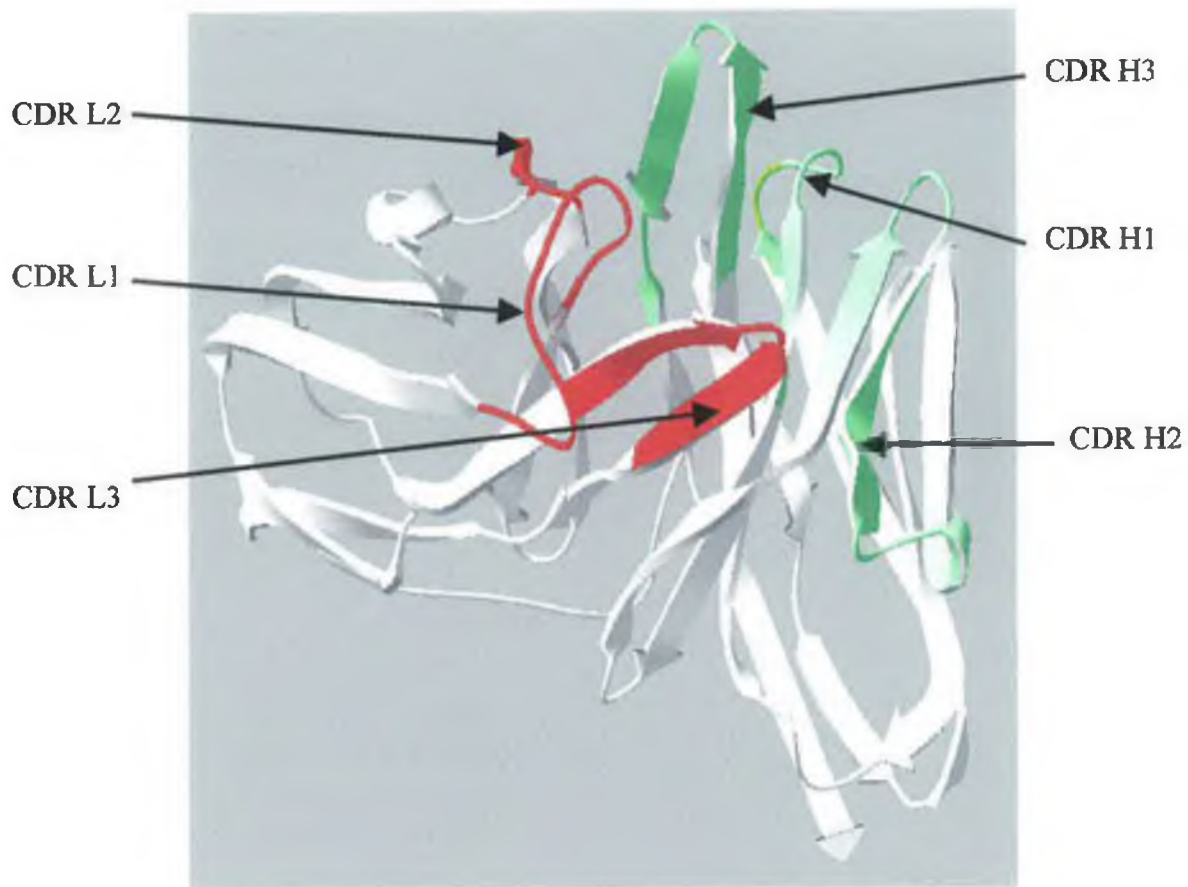


**Figure 3.5:** *The 3-D structure of the monomeric scFv, which was predicted using SwissModel. The complementary determining regions (CDRs) are shown in red on the light chain and in green on the heavy chain.*

### 3.2.1.3 SfiI restriction digest on pAK100/400/500/600

In order to produce soluble scFvs the gene encoding the scFv was sub-cloned from pAK100 into a variety of soluble expression vectors, pAK400, 500 and 600. This involved purifying the D1 plasmid DNA from XL-1 Blue *E. coli* as described in Section 2.2.2. The plasmid DNA was then restricted using SfiI and electrophoresed on an agarose gel. The soluble expression vectors, pAK400, 500 and 600 were also digested using SfiI and electrophoresed alongside the pAK100 (Fig. 3.6). A band at approximately 800bp, representing the scFv insert, was isolated following restriction of the pAK100 and bands representing the excised tetracycline stuffer gene were visible at 2101bp following digestion of the pAK400, 500 and 600. The bands representing the scFv insert and the restricted pAK400, 500 and 600 plasmid DNA were then gel purified as described in Section 2.2.5.

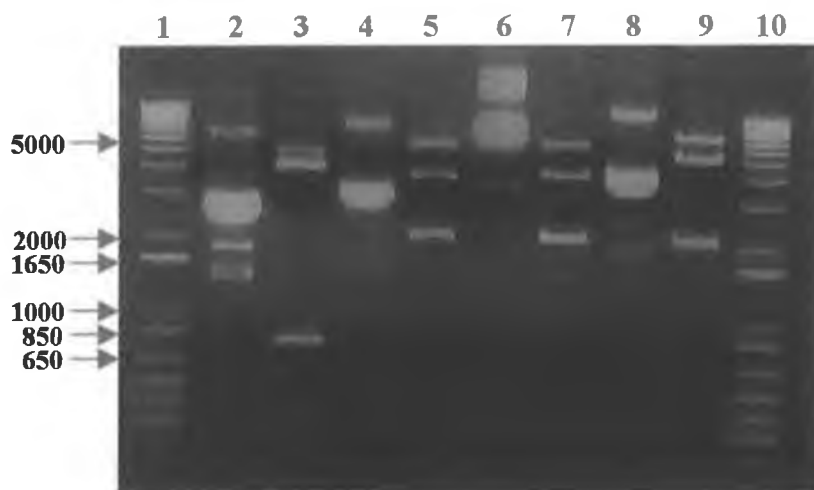


**Figure 3.6:** Restriction enzyme digest on pAK100, 400, 500 and 600 using SfiI. Lanes 1 and 10: 1Kb PLUS DNA ladder (Gibco-BRL); Lane 2: Purified pAK100 plasmid DNA containing the scFv insert; Lane 3: SfiI restriction digest on pAK100 plasmid DNA with scFv insert at 800bp; Lane 4: Purified pAK400 plasmid DNA; Lane 5: SfiI restricted pAK400 with 2101bp tetracycline insert; Lane 6: Purified pAK500 plasmid DNA; Lane 7: SfiI restricted pAK500 with 2101bp tetracycline insert; Lane 8: Purified pAK600 plasmid DNA; Lane 9: SfiI restricted pAK600 with 2101bp tetracycline insert.

#### **3.2.1.4 Ligation and transformation of pAK400/500/600 into JM83 *E. coli***

The gene encoding the AFB<sub>1</sub>-specific scFv was ligated into pAK400, 500 and 600, as described in Section 2.2.6. Following ligation, the vectors encoding the scFv gene were transformed into calcium-competent JM83 *E. coli*.

#### **3.2.1.5 Soluble expression of the monomeric, dimeric and alkaline phosphatase-labelled scFvs**

Following selection of JM83 *E. coli* positively transformed with the appropriate vector (pAK400/500/600), single colonies were isolated, grown in 2x TY and soluble scFv expression induced upon addition of IPTG, as described in Section 2.2.9. Optimum induction periods were determined for each scFv, with 4 hours post induction proving sufficient for the monomeric scFv, and a 16 hour induction period required for the dimeric and alkaline phosphatase-labelled scFvs (Data not shown). The alkaline phosphatase-labelled scFv is referred to as the bifunctional scFv, throughout this chapter, due to its ability to bind aflatoxin and act as a reporter antibody with the enzyme label. Following IPTG induction the cellular distribution of each scFv was determined. Figure 3.7 shows the ELISA analysis on the culture supernatant and periplasmic lysate following expression of the monomeric and dimeric scFvs. High-levels of soluble expression into the periplasm were observed with the monomeric and dimeric scFvs. Figure 3.8 shows the ELISA analysis of the culture supernatant and periplasmic lysate following expression of the bifunctional scFv. Minimal expression levels were observed in the culture supernatant and high-levels of expression were observed in the periplasm. For subsequent characterisation the soluble scFvs were isolated from the periplasm.

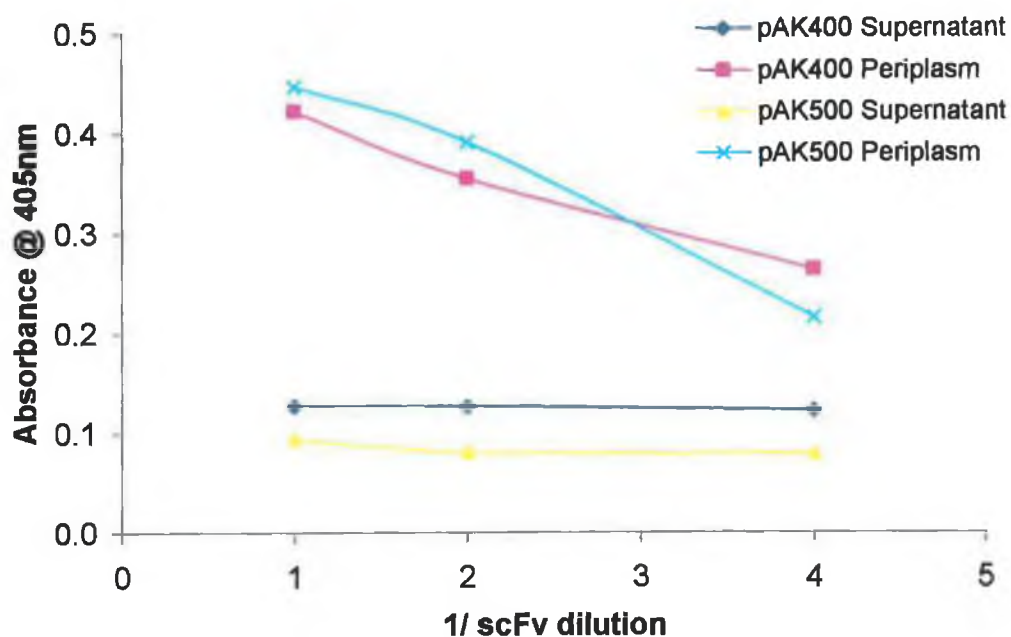


*Figure 3.7: ELISA analysis on the culture supernatant and periplasmic lysate following soluble expression of the monomeric and dimeric scFvs. Results indicated that high-levels of the monomeric and dimeric scFvs were expressed into the periplasm.*

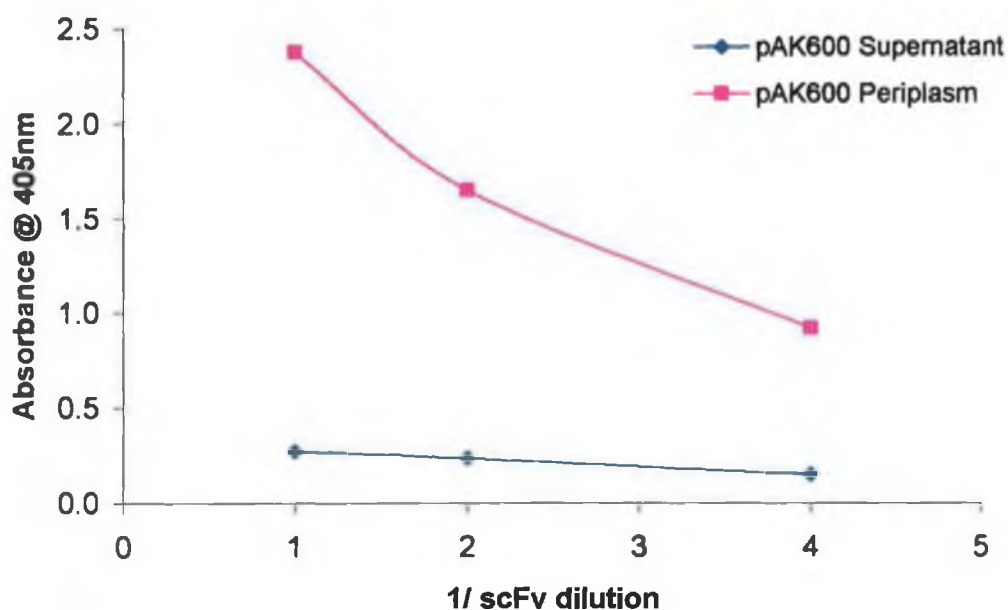


*Figure 3.8: ELISA analysis of the culture supernatant and periplasmic lysate following soluble expression of the bifunctional scFv. The bifunctional scFv was isolated into the periplasm.*

### 3.2.1.6 Western blot analysis on the monomeric, dimeric and bifunctional scFvs

Western blot analysis was carried out on the scFvs in order to demonstrate that the secondary (anti-FLAG) and tertiary (anti-mouse) antibodies could specifically detect the scFvs from the crude periplasmic lysate. The crude lysates containing the expressed scFvs were electrophoresed using SDS-PAGE and then transferred onto nitrocellulose, which was probed using anti-FLAG followed by an alkaline phosphatase-labelled anti-mouse antibody. Figure 3.9 indicates that the secondary and tertiary antibodies enabled specific detection of the scFvs. A single band at approximately 32kDa was visible following expression from pAK400, which represented the monomeric scFv. A single band was also visible following expression using the pAK500. However, this band appeared at approximately 35kDa representing the cleaved dimeric scFv, consisting of a monomeric scFv attached to a portion of the double helix. Following expression from the pAK600 vector two bands were visible at approximately 85kDa and 32kDa, representing the alkaline phosphatase-scFv fusion, and the monomeric scFv, respectively.

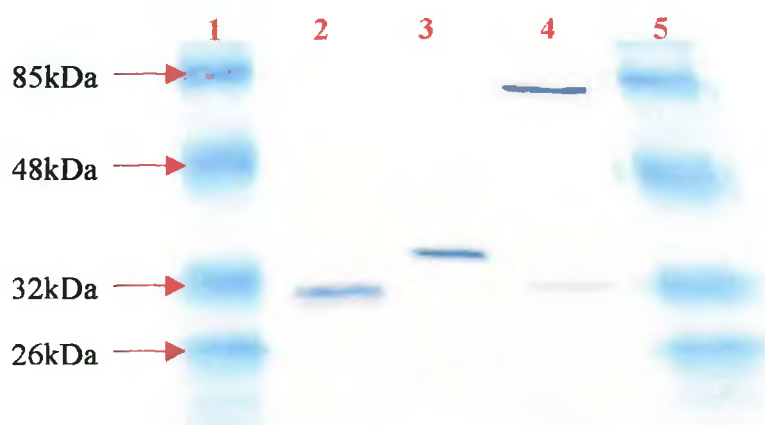


**Figure 3.9:** Western blot analysis on the monomeric, dimeric and bifunctional scFvs. The membrane containing the transferred scFvs was probed using the anti-FLAG monoclonal M1 antibody followed by an alkaline phosphatase-labelled anti-mouse antibody and visualised upon addition of BCIP/NBT substrate. Lanes 1 and 5: BlueRanger prestained protein molecular weight markers (Pierce); Lane 2: Monomeric scFv expressed from pAK400; Lane 3: Dimeric scFv expressed from pAK500; Lane 4: Bifunctional scFv expressed from pAK600.

### **3.2.2 The use of genetically derived scFvs in the development of immunoassays for the detection of AFB<sub>1</sub>**

Following the successful expression and initial characterisation of the three genetically derived scFvs several immunoassay formats, incorporating the scFvs, were investigated for the detection of AFB<sub>1</sub>.

#### **3.2.2.1 Development of Competitive ELISAs for the detection of aflatoxin B<sub>1</sub>**

##### **3.2.2.1.1 Optimisation of assay parameters for competitive ELISA for AFB<sub>1</sub>**

Initial checkerboard ELISA was carried out in order to determine the optimal conjugate coating concentrations and scFv antibody dilutions for use in competitive ELISAs. Varying AFB<sub>1</sub>-BSA coating concentrations ranging from 0 – 50µg/ml and scFv antibody dilutions ranging from undiluted – 1/64 were assayed for the monomeric, dimeric and bifunctional scFvs. The optimal conjugate coating concentration for the monomeric scFv was found to be 25µg/ml of the AFB<sub>1</sub>-BSA and the optimum scFv dilution determined to be 1/4 (Fig. 3.10). For the dimeric scFv the optimal coating concentration was 12.5µg/ml of the AFB<sub>1</sub>-BSA with a 1/8 dilution of the scFv (Fig. 3.11), and for the bifunctional scFv 6.25µg/ml of the AFB<sub>1</sub>-BSA and a 1/4 dilution of the scFv were determined to be optimal (Fig. 3.12).

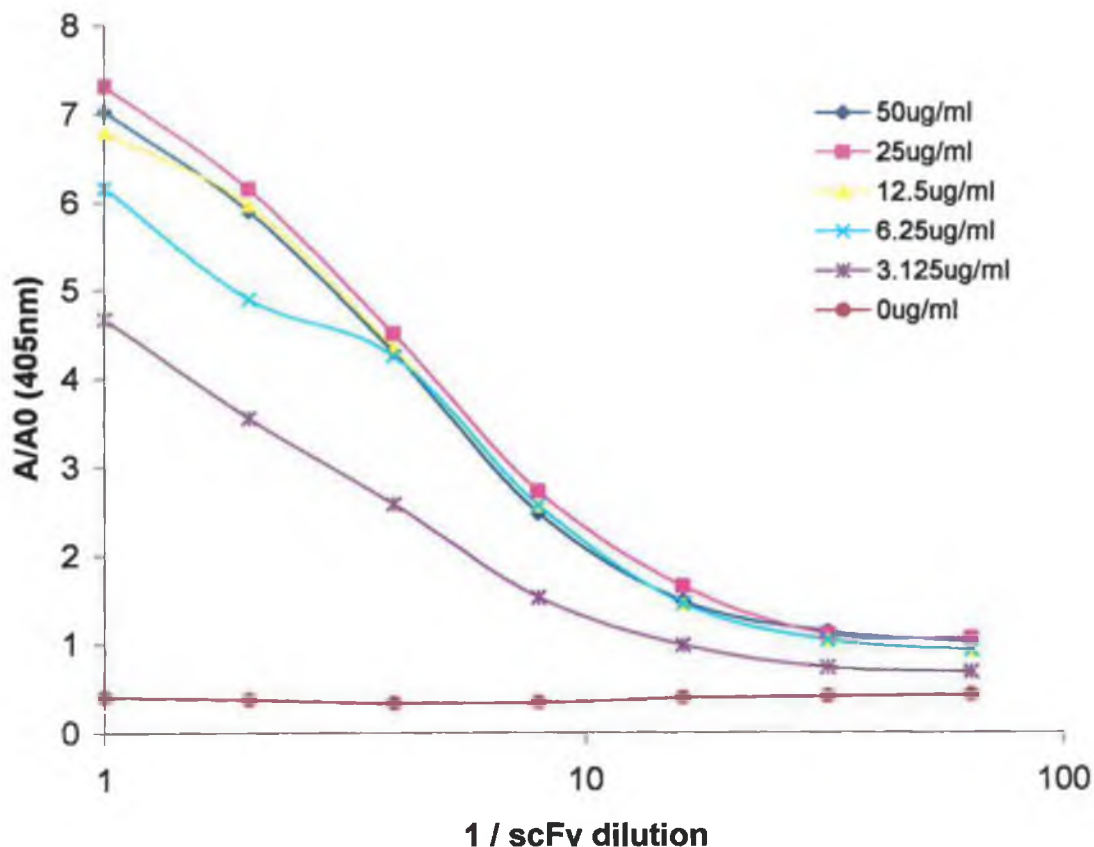


**Figure 3.10:** Checkerboard ELISA for determination of optimal conjugate coating concentration and monomeric scFv antibody dilution for use in a competitive ELISA. Varying AFB<sub>1</sub>-BSA coating concentrations ranging from 0 – 50µg/ml and scFv antibody dilutions from undiluted to 1/64 dilution were assayed. A 25µg/ml conjugate concentration and a 1/4 scFv antibody dilution was chosen for use in the competitive ELISA.

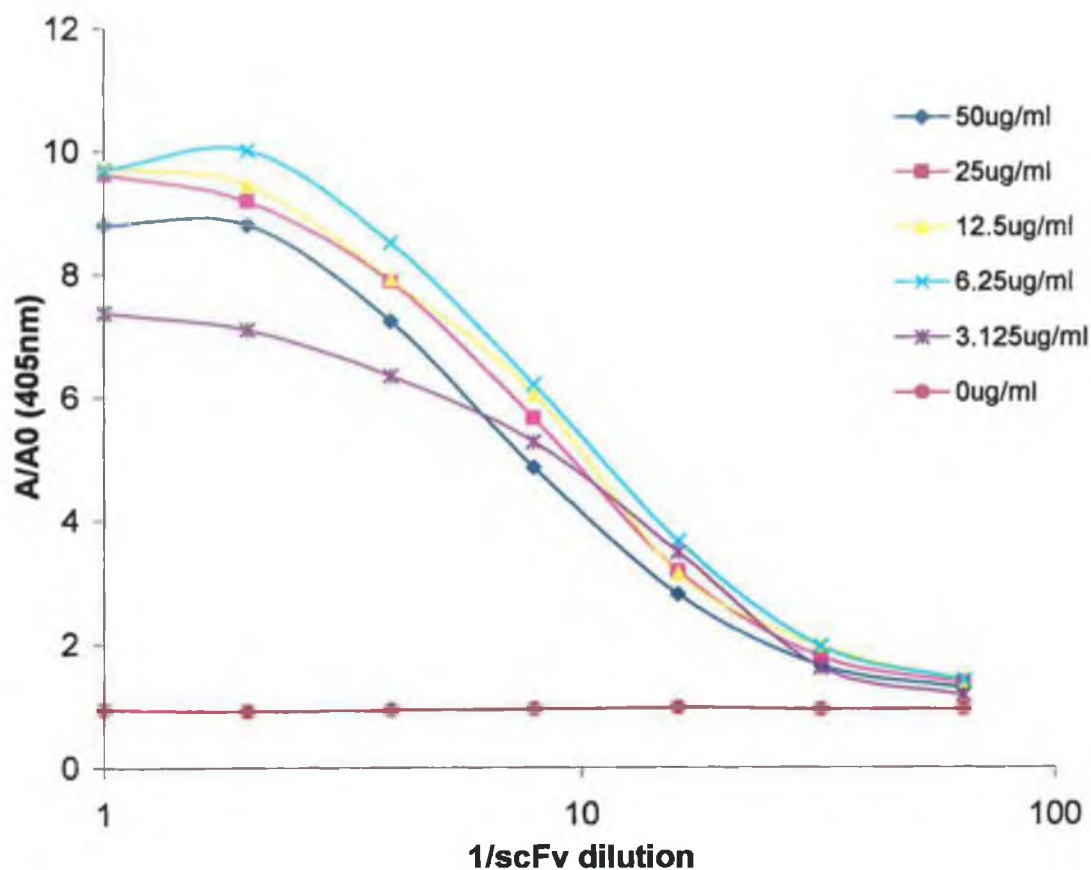


**Figure 3.11:** Checkerboard ELISA for determination of optimal conjugate coating concentration and dimeric scFv antibody dilution for use in a competitive ELISA. Varying AFB<sub>1</sub>-BSA coating concentrations ranging from 0 – 50µg/ml and scFv antibody dilutions from undiluted to 1/64 dilution were assayed. A 12.5µg/ml conjugate concentration and a 1/8 scFv antibody dilution were chosen for use in the competitive ELISA.

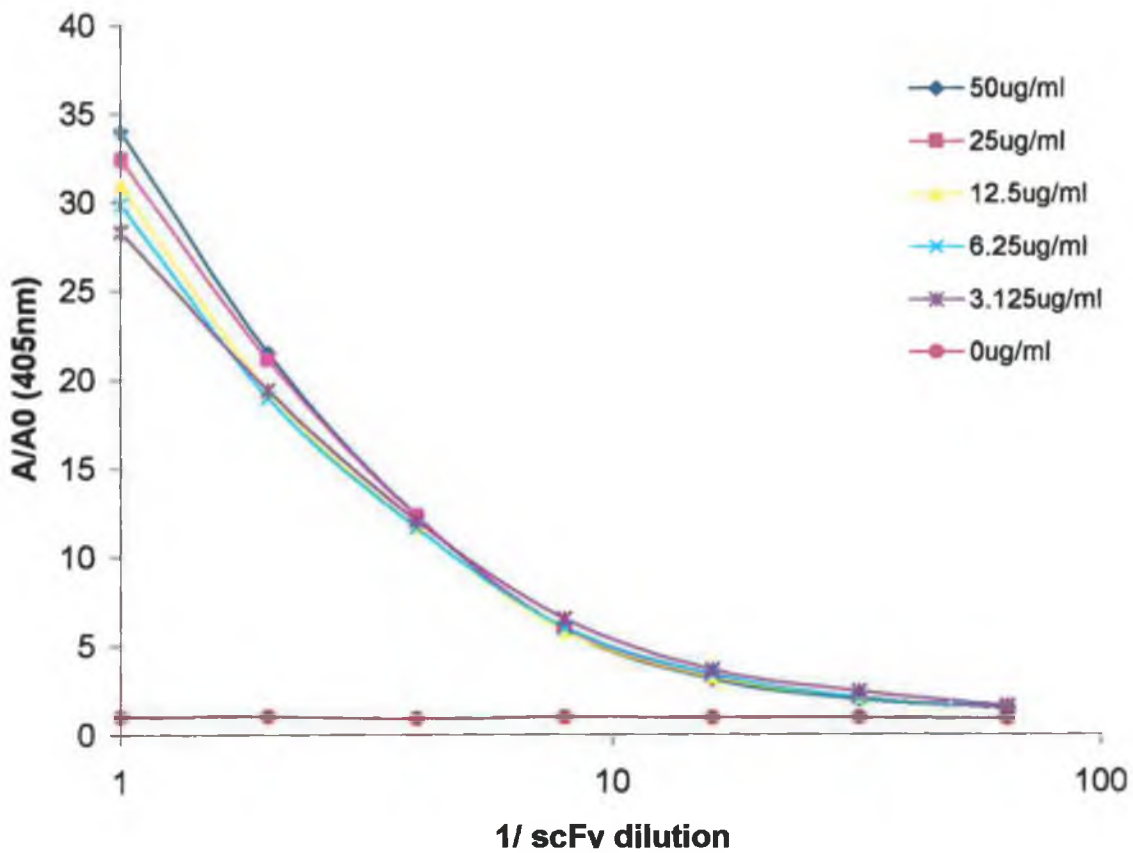


**Figure 3.12:** Checkerboard ELISA for determination of optimal conjugate coating concentration and bifunctional scFv antibody dilution for use in a competitive ELISA. Varying AFB<sub>1</sub>-BSA coating concentrations ranging from 0 – 50µg/ml and scFv antibody dilutions from undiluted to 1/64 dilution were assayed. A 6.25µg/ml conjugate concentration and a 1/4 scFv antibody dilution was chosen for use in the competitive ELISA.

### 3.2.2.1.2 Optimisation of methanol concentration for the preparation of free AFB<sub>1</sub>

Due to its strong hydrophobic nature it is necessary to prepare free AFB<sub>1</sub> standards in methanol. However, methanol can have an inhibitory effect on an assay's sensitivity. In order to determine the optimal methanol concentration competitive ELISAs were carried out with each scFv using varying methanol concentrations to prepare the free AFB<sub>1</sub> standards. A series of AFB<sub>1</sub> standards ranging in concentration from 6 – 6250ng/ml were prepared in PBS containing varying methanol concentrations from 2.5 to 40% (v/v). 50µl of each of these standards were then added to an AFB<sub>1</sub>-BSA-coated plate along with 50µl of the appropriate scFv dilution. Fig. 3.13, 3.14 and 3.15 show the graphs obtained for the methanol concentration optimisation with the monomeric, dimeric and bifunctional scFvs, respectively. In each case 5% (v/v) methanol appeared optimal for the preparation of the free AFB<sub>1</sub> standards.

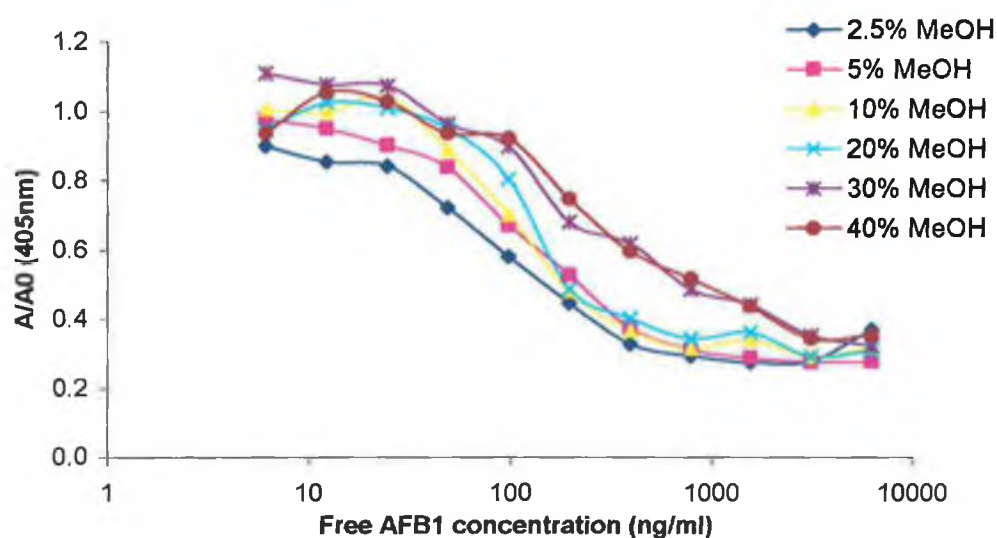


**Figure 3.13:** Competition ELISA using the monomeric scFv, to determine optimum methanol concentration for preparation of free AFB<sub>1</sub>. AFB<sub>1</sub> standards ranging from 6 to 6250ng/ml were prepared in PBS containing varying methanol concentrations ranging from 2.5 to 40% (v/v). 5% (v/v) methanol appeared to cause the least inhibitory effect on the assay and was therefore chosen to be the optimum methanol concentration for the preparation of free AFB<sub>1</sub>.

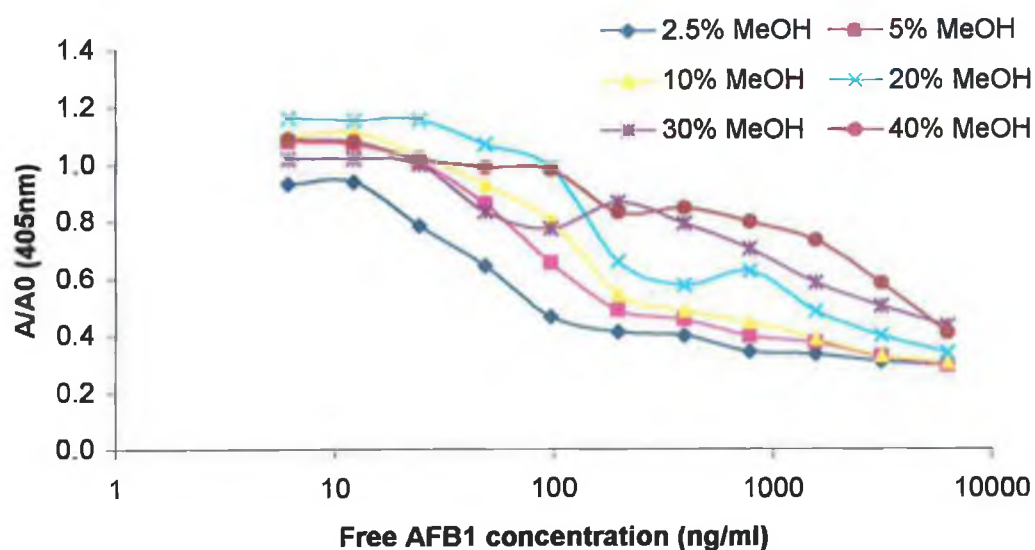


*Figure 3.14: Competition ELISA using the dimeric scFv, to determine optimum methanol concentration for preparation of free AFB<sub>1</sub>. AFB<sub>1</sub> standards ranging from 6 to 6250ng/ml were prepared in PBS containing varying methanol concentrations ranging from 2.5 to 40% (v/v). 5% (v/v) methanol appeared to cause the least inhibitory effect on the assay and was therefore chosen to be the optimum methanol concentration for the preparation of free AFB<sub>1</sub>.*

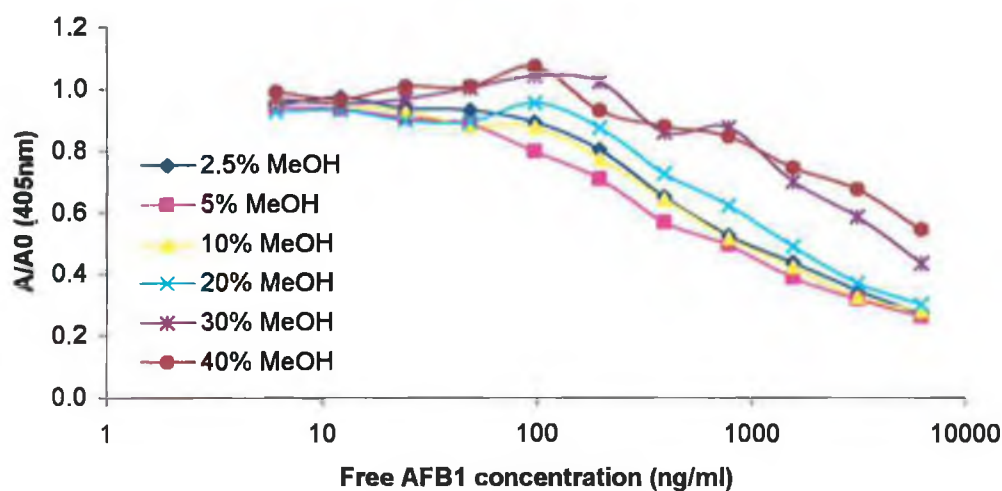


*Figure 3.15: Competition ELISA using the bifunctional scFv, to determine optimum methanol concentration for preparation of free AFB<sub>1</sub>. AFB<sub>1</sub> standards ranging from 6 to 6250ng/ml were prepared in PBS containing varying methanol concentrations ranging from 2.5 to 40% (v/v). 5%(v/v) methanol appeared to cause the least inhibitory effect on the assay and was therefore chosen to be the optimum methanol concentration for the preparation of free AFB<sub>1</sub>.*

### **3.2.2.1.3 Development of competitive ELISAs for AFB<sub>1</sub>**

Following optimisation of the various assay parameters, competitive ELISAs were developed for the detection of AFB<sub>1</sub> using the monomeric, dimeric and bifunctional scFvs. Immunoplates coated with 25µg/ml, 12.5µg/ml and 6.25µg/ml of AFB<sub>1</sub>-BSA for the monomeric, dimeric and bifunctional scFvs, respectively, were used to determine the range of detection of free AFB<sub>1</sub> for each scFv. AFB<sub>1</sub> standards ranging in concentration from 3 – 781ng/ml were prepared in PBS-5% (v/v) methanol and added to an equal volume of the optimal scFv dilution. Intra and inter-day variability studies were carried out the monomeric, dimeric and bifunctional scFvs, in order to estimate assay reproducibility.

In order to determine intra-day assay variation, each AFB<sub>1</sub> concentration was assayed five times on one day and the mean absorbance of bound antibody at each AFB<sub>1</sub> concentration was plotted against the free AFB<sub>1</sub> concentration. Intra-day studies showed the monomeric scFv had a range of detection between 12 and 781ng/ml and the coefficients of variation (C.V.'s) obtained ranged from 1.22 to 11.5%. The dimeric scFv had a range of detection between 3 and 781ng/ml and CVs remained below 11.98%. The bifunctional scFv yielded a range of detection between 3 and 390ng/ml with CVs between 0.20 and 8.28%.

Inter-day assay variability studies were also carried out on the each scFv by performing the assays over five separate days. The coefficients of variation (CVs) were determined for each assay by expressing the standard deviation as a percentage function of the mean. The inter-day assay on the monomeric scFv displayed a range of detection between 12 and 781ng/ml (Fig. 3.16) and as can be seen in Table 3.3 the coefficients of variation ranged from 2.72 to 11.35%. The inter-day assay on the dimeric scFv had a range of detection between 3 and 781ng/ml (Fig. 3.17) and the coefficients of variation for the inter-day assay ranged from 1.25 to 6.99% (Table 3.4). The inter-day assay on the bifunctional scFv displayed a range of detection between 3 and 390ng/ml (Fig. 3.18) and as can be seen in Table 3.5 the coefficients of variation ranged from 3.01 to 5.25%, indicating that the three assays were reproducible over the five days.

**Table 3.3:** Inter-day assay coefficients of variation for the detection of free AFB<sub>1</sub> using the monomeric scFv. Five sets of seven standards were assayed on five different days and the C.V.'s were calculated as the standard deviation (S.D.) expressed as a percentage of the mean values for each standard.

AFB <sub>1</sub> concentration (ng/ml)	Calculated mean ± S.D., A/A0	Coefficient of variation (%)
781.2	0.27 ± 0.02	6.25
390.6	0.32 ± 0.02	6.05
195.3	0.44 ± 0.05	11.35
97.7	0.61 ± 0.05	8.97
48.8	0.79 ± 0.05	5.83
24.4	0.90 ± 0.04	4.26
12.2	0.96 ± 0.03	2.72

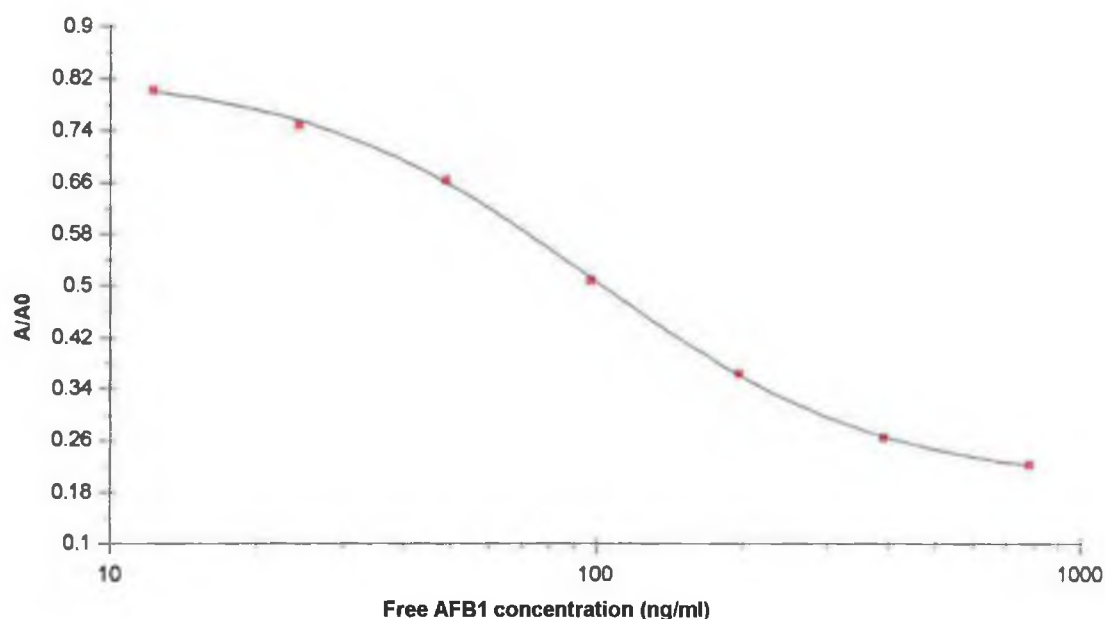


**Figure 3.16:** Inter-day competitive ELISA for the determination of the range of detection for free AFB<sub>1</sub> using the monomeric scFv. A 25 µg/ml AFB<sub>1</sub>-BSA conjugate coating concentration was used with a 1/4 dilution of the monomeric scFv. The range of detection was found to be between 12 and 781 ng/ml.

*Table 3.4: Inter-day assay coefficients of variation for the detection of free AFB<sub>1</sub> using the dimeric scFv. Five sets of nine standards were assayed on five different days and the C.V.'s were calculated as the standard deviation (S.D.) expressed as a percentage of the mean values for each standard.*

<b>AFB<sub>1</sub> concentration (ng/ml)</b>	<b>Calculated mean ± S.D., A/A0</b>	<b>Coefficient of variation (%)</b>
781.2	0.61 ± 0.043	6.99
390.6	0.60 ± 0.008	1.36
195.3	0.68 ± 0.028	4.18
97.7	0.70 ± 0.026	3.69
48.8	0.74 ± 0.009	1.25
24.4	0.84 ± 0.035	4.14
12.2	0.89 ± 0.004	0.49
6.1	0.92 ± 0.027	2.99
3.0	0.93 ± 0.035	3.72

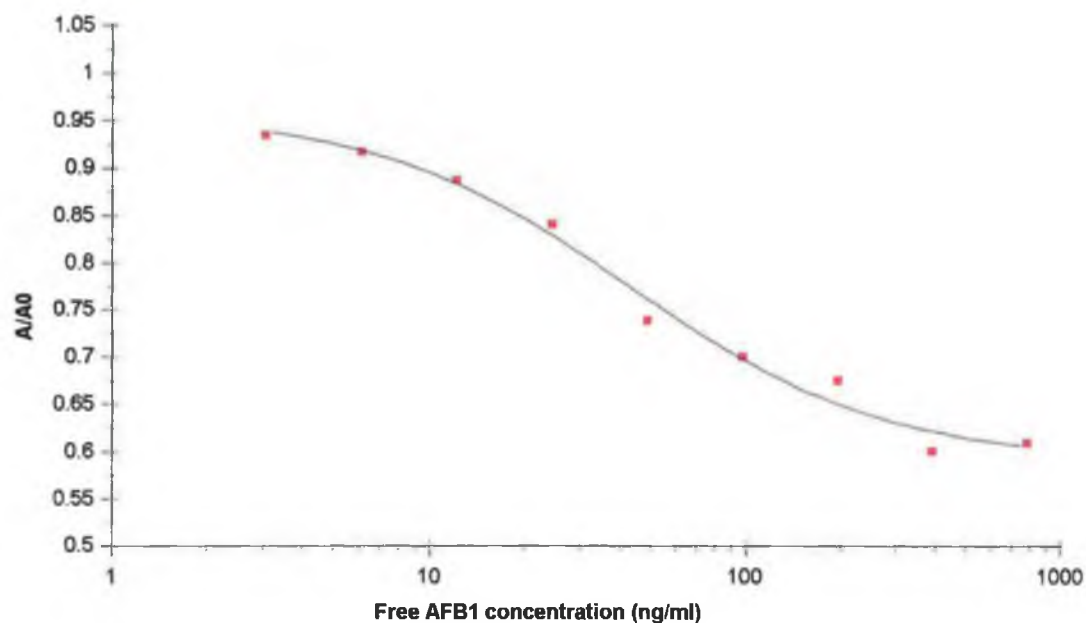


*Figure 3.17: Inter-day competitive ELISA for the determination of the range of detection for free AFB<sub>1</sub> using the dimeric scFv. A 12.5 µg/ml AFB<sub>1</sub>-BSA conjugate coating concentration was used with a 1/8 dilution of the dimeric scFv. The range of detection was found to be between 3 and 781 ng/ml.*

**Table 3.5:** Inter-day assay coefficients of variation for the detection of free AFB<sub>1</sub> using the bifunctional scFv. Five sets of eight standards were assayed on five different days and the C.V.'s were calculated as the standard deviation (S.D.) expressed as a percentage of the mean values for each standard.

AFB <sub>1</sub> concentration (ng/ml)	Calculated mean ± S.D., A/A0	Coefficient of variation (%)
390	0.17±0.008	4.52
195	0.23±0.009	4.00
97	0.31±0.010	3.32
48	0.47±0.024	5.11
24	0.67±0.023	3.45
12	0.81±0.042	5.25
6	0.90±0.031	3.44
3	0.98±0.029	3.01

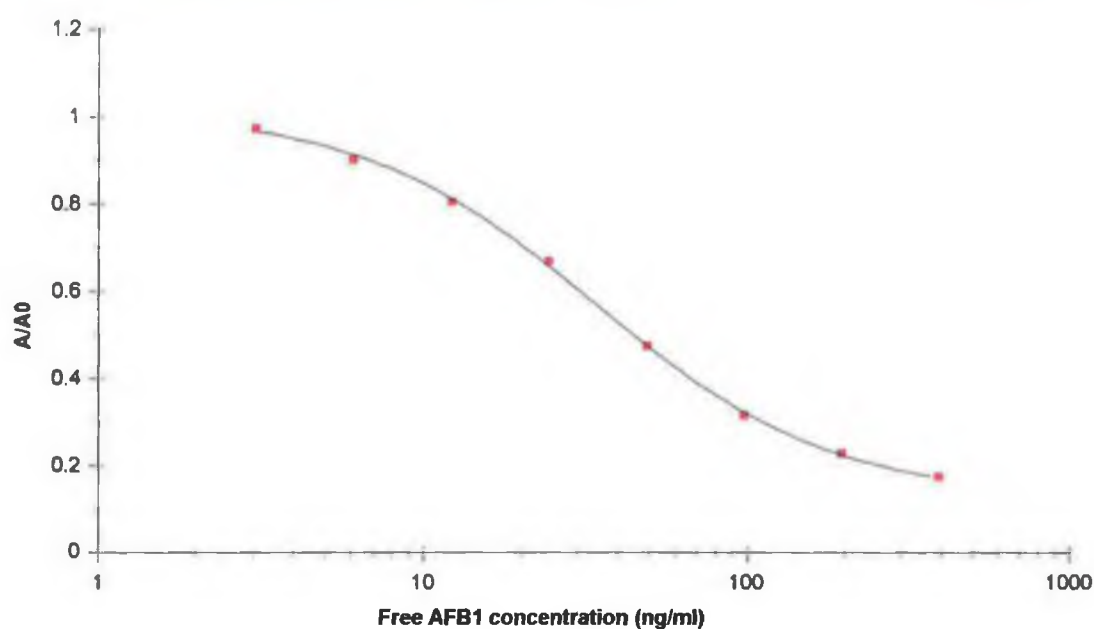


**Figure 3.18:** Inter-day competitive ELISA for the determination of the range of detection for free AFB<sub>1</sub> using the bifunctional scFv. A 6.25 µg/ml AFB<sub>1</sub>-BSA conjugate coating concentration was used with a 1/4 dilution of the bifunctional scFv. The range of detection was found to be between 3 and 390 ng/ml.

#### 3.2.2.1.4 Cross-reactivity studies

Cross reactivity studies were then carried out on the monomeric, dimeric and bifunctional scFvs in relation to various structurally related aflatoxins. The least detectable dose (LDD) and IC<sub>50</sub> values were determined for each aflatoxin as 90% A/A0 and 50% A/A0, respectively. The percentage cross reactivities were then estimated at the LDD (CR<sub>90</sub>) and at the IC<sub>50</sub> (CR<sub>50</sub>) by expressing 100-fold the ratio of the aflatoxin B<sub>1</sub> and of the cross-reacting aflatoxin.

Table 3.6 summarizes the specificity and cross reactivity studies on the monomeric scFv with the structurally related aflatoxins B<sub>2</sub>, G<sub>1</sub>, G<sub>2</sub>, M<sub>1</sub> and M<sub>2</sub>. The monomeric scFv displayed some degree of cross-reactivity with aflatoxins B<sub>2</sub>, G<sub>1</sub> and G<sub>2</sub> (i.e. < 12.5%) and low-levels of cross-reactivity against aflatoxins M<sub>1</sub> and M<sub>2</sub> (i.e. < 3%) at the LDD. Whereas slightly higher levels of cross-reactivity (19%) were obtained at the IC<sub>50</sub> values with aflatoxins B<sub>2</sub>, G<sub>1</sub> and G<sub>2</sub> and low-levels of cross-reactivity was observed against aflatoxins M<sub>1</sub> and M<sub>2</sub> (i.e. < 3%). The dimeric scFv offered greater specificity towards aflatoxin B<sub>1</sub>, in comparison with the monomeric scFv, with the percentage cross reactivity against the various aflatoxins remaining below 3% at the LDD and 8% at the IC<sub>50</sub> (Table 3.7). The bifunctional scFv displayed high levels of cross-reactivity towards aflatoxins B<sub>2</sub>, G<sub>1</sub> and G<sub>2</sub> (i.e. > 30%) and low-levels of cross-reactivity towards aflatoxins M<sub>1</sub> and M<sub>2</sub> (i.e. < 3%) at the LDD (Table 3.8). The bifunctional scFv also cross-reacted with the aflatoxins B<sub>2</sub>, G<sub>1</sub> and G<sub>2</sub> and to a lesser extent with aflatoxins M<sub>1</sub> and M<sub>2</sub> (i.e. < 6%), at the IC<sub>50</sub>.

**Table 3.6:** Cross reactivity and specificity studies on the monomeric scFv against various aflatoxins. The cross-reactivity potential was approximated at the least detectable dose (LDD), which was estimated at 90% A/A0, and at the IC<sub>50</sub> value, which was estimated at 50% A/A0. The CR<sub>90</sub> and CR<sub>50</sub> were then expressed as 100-fold the ratio of the antigen and of the cross-reactant.

Aflatoxin	LDD <sup>a</sup> (ng/ml)	IC <sub>50</sub> <sup>b</sup> (ng/ml)	CR <sub>90</sub> <sup>c</sup> (%)	CR <sub>50</sub> <sup>d</sup> (%)
B <sub>1</sub>	6	150	100	100
B <sub>2</sub>	48	781	12.5	19
G <sub>1</sub>	120	781	5	19
G <sub>2</sub>	48	781	12.5	19
M <sub>1</sub>	195	6250	3	2.4
M <sub>2</sub>	50000	50000	<0.1	0.3

<sup>a</sup> Least detectable dose calculated at 90% A/A0

<sup>b</sup> 50% inhibition concentration (50% A/A0)

<sup>c</sup> Percentage cross-reactivity determined at IC<sub>50</sub>

<sup>d</sup> Percentage cross-reactivity determined at LDD

**Table 3.7:** Cross reactivity and specificity studies on the dimeric scFv against various aflatoxins. The cross-reactivity potential was approximated at the least detectable dose (LDD), which was estimated at 90% A/A0, and at the IC<sub>50</sub> value, which was estimated at 50% A/A0. The CR<sub>90</sub> and CR<sub>50</sub> were then expressed as 100-fold the ratio of the antigen and of the cross-reactant.

Aflatoxin	LDD <sup>a</sup> (ng/ml)	IC <sub>50</sub> <sup>b</sup> (ng/ml)	CR <sub>90</sub> <sup>c</sup> (%)	CR <sub>50</sub> <sup>d</sup> (%)
B <sub>1</sub>	3	97	100	100
B <sub>2</sub>	97	12500	3	0.8
G <sub>1</sub>	97	1200	3	8
G <sub>2</sub>	390	12500	0.8	0.8
M <sub>1</sub>	390	50000	0.8	0.2
M <sub>2</sub>	50000	50000	<0.1	0.2

<sup>a</sup> Least detectable dose calculated at 90% A/A0

<sup>b</sup> 50% inhibition concentration (50% A/A0)

<sup>c</sup> Percentage cross-reactivity determined at IC<sub>50</sub>

<sup>d</sup> Percentage cross-reactivity determined at LDD

**Table 3.8:** Cross reactivity and specificity studies on the bifunctional scFv against various aflatoxins. The cross-reactivity potential was approximated at the least detectable dose (LDD), which was estimated at 90% A/A0, and at the IC<sub>50</sub> value, which was estimated at 50% A/A0. The CR<sub>90</sub> and CR<sub>50</sub> were then expressed as 100-fold the ratio of the antigen and of the cross-reactant.

Aflatoxin	LDD <sup>a</sup> (ng/ml)	IC <sub>50</sub> <sup>b</sup> (ng/ml)	CR <sub>90</sub> <sup>c</sup> (%)	CR <sub>50</sub> <sup>d</sup> (%)
B <sub>1</sub>	6	45	100	100
B <sub>2</sub>	20	97	30	46
G <sub>1</sub>	6	97	100	46
G <sub>2</sub>	20	195	30	23
M <sub>1</sub>	195	781	3	6
M <sub>2</sub>	3125	>3125	0.2	<1.5

<sup>a</sup> Least detectable dose calculated at 90% A/A0

<sup>b</sup> 50% inhibition concentration (50% A/A0)

<sup>c</sup> Percentage cross-reactivity determined at IC<sub>50</sub>

<sup>d</sup> Percentage cross-reactivity determined at LDD

### **3.2.2.2 Development of Biacore inhibition assays for the detection of aflatoxin B<sub>1</sub>**

This section focuses on the development of a Biacore inhibition assay for AFB<sub>1</sub> using a Biacore CM5 chip immobilised with an AFB<sub>1</sub> derivative, which was kindly donated by Andrew Baxter, XenoSense Ltd., Queen's University Belfast. Both the monomeric and dimeric scFv were applied for the development of inhibition assays. For the successful development of an inhibition assay for the detection of AFB<sub>1</sub>, the optimisation of a number of parameters was required. These included optimal antibody dilution, removal of non-specific interactions and surface regeneration conditions.

#### **3.2.2.2.1 Assessment of non-specific binding**

The degree of non-specific binding of the monomeric and dimeric scFvs to the CM5 dextran layer was assessed. This was achieved by passing the monomeric and dimeric scFvs over an unactivated CM dextran surface, diluted to 1/8 and 1/70, respectively. Figure 3.19 and 3.20 show the overlay plots obtained following injection of the monomeric and dimeric scFvs, respectively, over the AFB<sub>1</sub> surface and an unactivated CM dextran layer. Negligible binding to the dextran (i.e. < 10 RU) was observed with each scFv and as a result there was no need to incorporate dextran into the diluent buffer.

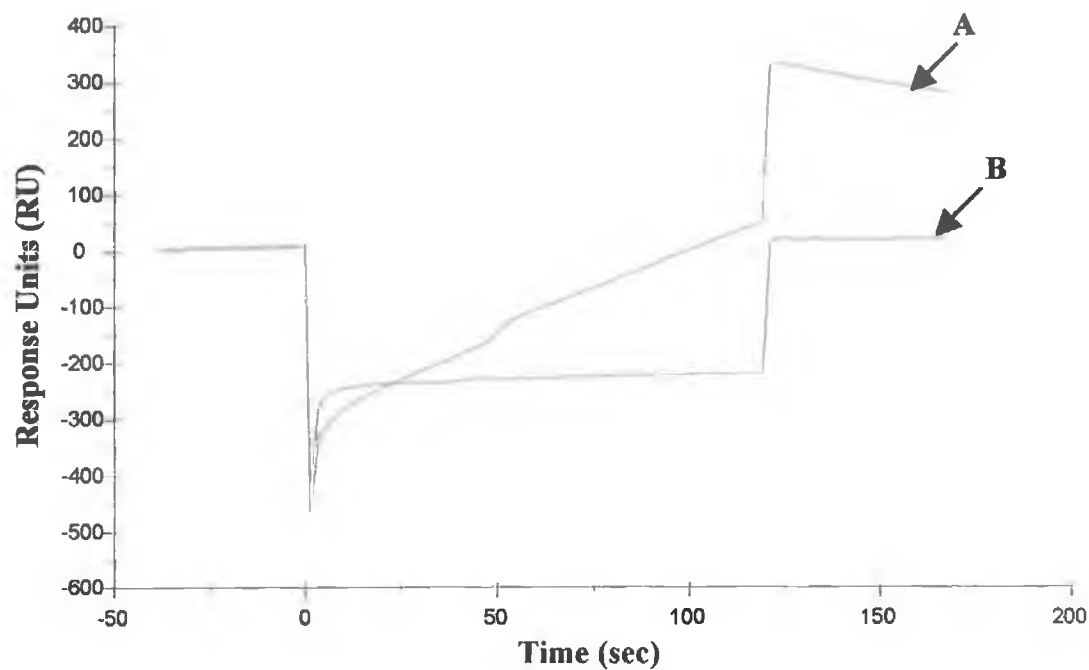


**Figure 3.19:** Overlay plot demonstrating binding of the monomeric scFv to the immobilised AFB<sub>1</sub> surface (A) and an unactivated dextran surface (B). Negligible binding of the monomeric scFv was observed to the unactivated dextran. However, approximately 350 response units (RU) of the monomeric scFv bound to the directly immobilised AFB<sub>1</sub> surface. This indicates the specificity of the monomeric scFv towards AFB<sub>1</sub>.

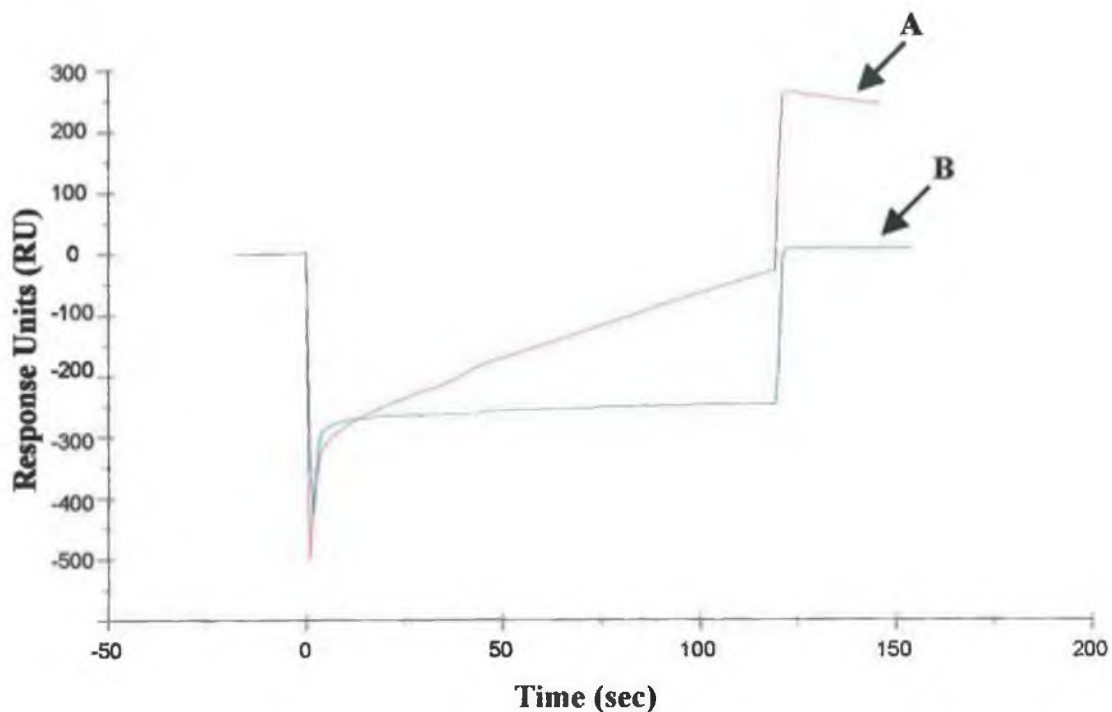


*Figure 3.20: Overlay plot demonstrating binding of the dimeric scFv to the immobilised AFB<sub>1</sub> surface (A) and an unactivated dextran surface (B). Negligible binding of the dimeric scFv was observed to the unactivated dextran. However, approximately 250 response units (RU) of the dimeric scFv bound to the directly immobilised AFB<sub>1</sub> surface. This indicates the specificity of the dimeric scFv towards AFB<sub>1</sub>.*

### 3.2.2.2.2 Regeneration studies

Optimisation of scFv antibody dilution and effective regeneration conditions was also required. The monomeric scFv was diluted to 1/8 and the dimeric to 1/70 with HBS running buffer and 20µl was injected over the immobilised AFB<sub>1</sub> surface at a flow-rate of 10µl/min. Initial studies showed little dissociation of the scFv from the immobilised surface. A regeneration solution consisting of 10mM NaOH enabled complete removal of the bound monomeric scFv and 25mM NaOH was sufficient for removing the dimeric scFv (Fig. 3.21). In each case a 0.5-min pulse at a flow-rate of 10µl/min was sufficient to regenerate the AFB<sub>1</sub> surface.

The efficiency of the regeneration process was then evaluated by performing multiple (i.e. 75) binding-regeneration cycles on the AFB<sub>1</sub> surface. Figure 3.22 shows the regeneration studies using the monomeric scFv. The monomeric scFv diluted to 1/8 was passed over the surface using a 2-minute pulse at 10µl/min. The bound scFv was completely removed using a 0.5-min pulse of 10mM NaOH at 10µl/min. Over the 75 binding-regeneration cycles the antibody binding capacity varied slightly but it did not significantly affect the assay performance. Figure 3.23 shows the regeneration studies on the dimeric scFv, which was diluted to 1/70 and passed over the surface using a 2-min pulse at 10µl/min. The bound scFv was completely removed using a 0.5-min pulse of 25mM NaOH at 10µl/min. Once again, over the 75 binding-regeneration cycles, the antibody binding capacity slightly oscillated without significantly affecting the performance of the assay. In each case binding of the scFv to the AFB<sub>1</sub> surface was highly reproducible, with approximately 400RU of the monomeric scFv and 280 RU of the dimeric scFv binding to the surface each time. This indicates that the regeneration solutions, 10mM NaOH for the monomeric scFv and 25mM NaOH for the dimeric scFv, did not affect antibody binding throughout the regeneration study.

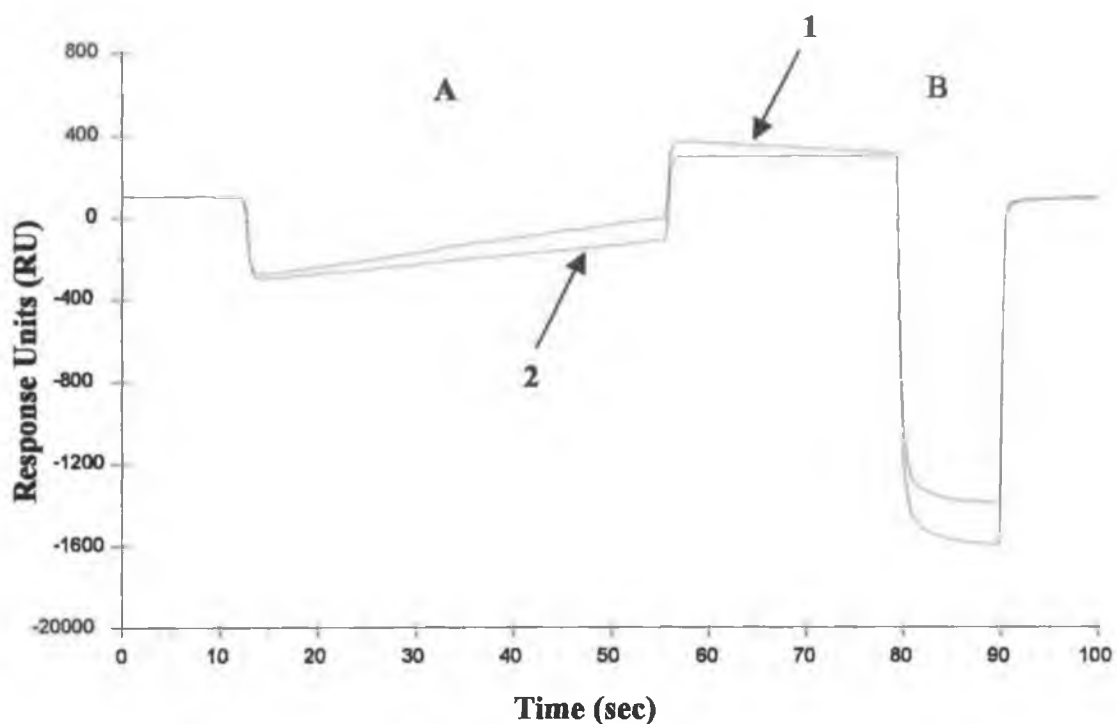


*Figure 3.21: Typical sensorgram showing the binding and regeneration of the monomeric scFv (1) and the dimeric scFv (2) on the AFB<sub>1</sub> surface. A 1/8 and a 1/35 dilution of the monomeric and dimeric scFvs, respectively, was passed over the sensor surface at 10  $\mu$ l/min for 4 min with approximately 400 and 350 response units of the monomeric and dimeric scFv binding, respectively (A). The surface was then completely regenerated using a 0.5 min pulse of 10 and 25mM NaOH for the monomeric and dimeric scFvs, respectively (B).*

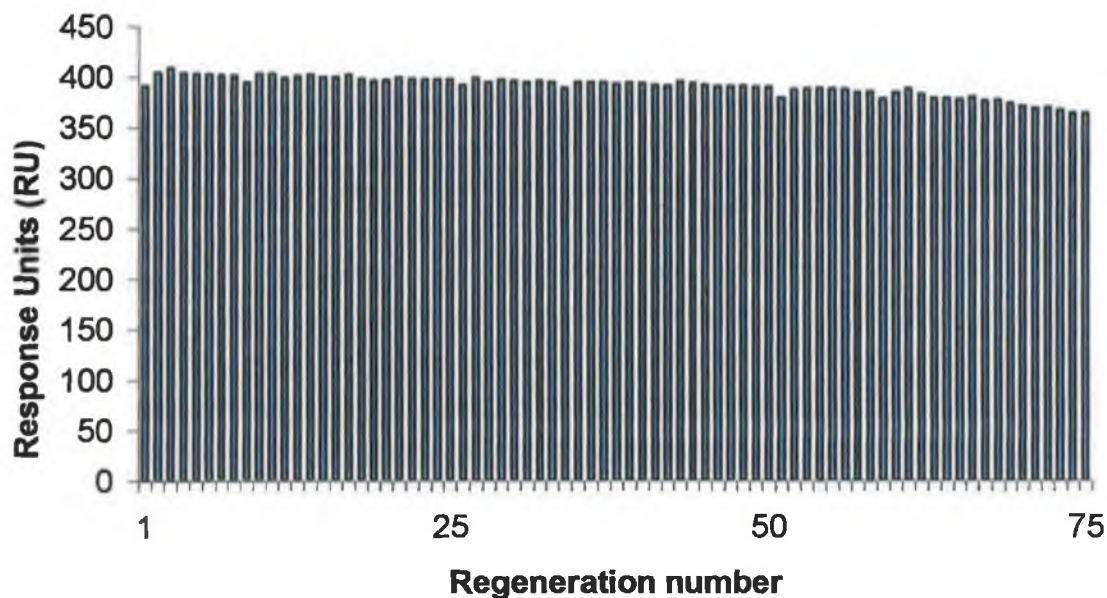


*Figure 3.22: Graph showing the regeneration studies on the immobilised AFB<sub>1</sub> sensor surface. Seventy-five consecutive regeneration cycles were carried out with the monomeric anti-AFB<sub>1</sub> scFv. A 2-min pulse of the monomeric scFv was followed by a 0.5-min injection of 10mM NaOH, as the regeneration solution. This regeneration solution enabled the complete removal of all bound scFv after each binding cycle. Resulting in highly reproducible binding cycles, as can be seen with no significant decrease in the binding response measured over the course of the regeneration studies.*

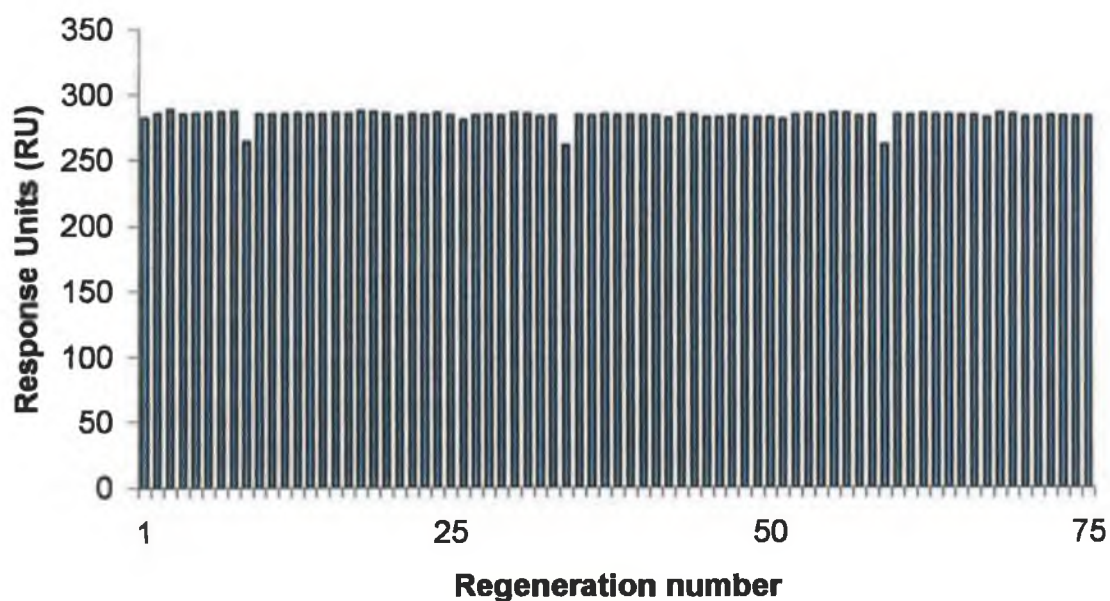


**Figure 3.23:** Graph showing the regeneration studies on the directly immobilised AFB<sub>1</sub> sensor chip. Seventy-five consecutive regeneration cycles were carried out with the dimeric anti-AFB<sub>1</sub> scFv. A 2-min pulse of the dimeric scFv was followed by a 0.5-min injection of 25mM NaOH, as the regeneration solution. This regeneration solution enabled the complete removal of all bound scFv after each binding cycle. Resulting in highly reproducible binding cycles, as can be seen with no significant decrease in the binding response measured over the course of the regeneration studies.

### 3.2.2.2.3 Development of a Biacore inhibition assays for the detection of AFB<sub>1</sub>

Following optimisation of the various assay parameters, inhibition assays, incorporating the monomeric and dimeric scFvs, were developed for the detection of AFB<sub>1</sub> using the Biacore CM5 chip immobilised with an AFB<sub>1</sub> derivative. Free AFB<sub>1</sub> standards, ranging in concentration from 375 - 12,000pg/ml for the monomeric scFv and 190 - 24,000pg/ml for the dimeric scFv, were prepared in PBS containing 5%(v/v) methanol. Each free AFB<sub>1</sub> concentration was incubated with an equal volume of the monomeric scFv diluted to 1/4 (to ensure a final dilution of 1/8) and a 1/35 dilution (to ensure a final dilution of 1/70) of the dimeric scFv and allowed to equilibrate for 30 min at 37°C. The equilibrated samples were then passed over the sensor surface, in random order, and followed by regeneration of the AFB<sub>1</sub> sensor surface using the appropriate regeneration solution. Figs. 3.24 and 3.25 show a typical overlay sensorgram showing the antibody binding responses of the monomeric and dimeric scFvs, respectively, in the presence of a range of free AFB<sub>1</sub> standards.

Intra and inter-day variability studies were carried out on the inhibition assays with monomeric and dimeric scFvs, in order to estimate the reproducibility of the assays. In order to determine intra-day assay variation, each concentration was assayed three times on one day and the mean response units of bound antibody for each AFB<sub>1</sub> concentration was plotted against the free AFB<sub>1</sub> concentration. Intra-day variability studies showed the monomeric scFv had a range of detection for free AFB<sub>1</sub> from 375 - 12,000pg/ml with coefficients of variation (CVs) remaining below 0.61% and the dimeric scFv had a range of detection between 190 and 24,000pg/ml with CVs below 3.37%. The inter-day assay variation was then estimated by performing the assay over three separate days, and a separate calibration curve plotted for each normalised response unit (response units / response units 0 (R/R0)) value versus the respective AFB<sub>1</sub> concentration for each assay carried out on each day. Fig. 3.26 and 3.27 show the inter-day assay curves for the monomeric and dimeric scFvs, respectively, where the range of detection of free AFB<sub>1</sub> was 375 - 12,000pg/ml for the monomeric and 190 and 24,000pg/ml for the dimeric scFv. The CVs obtained for the inter-day variability studies on the monomeric scFv ranged between 1.9 and 4.18% (Table 3.9) and between 3 and 11.53% for the dimeric scFv (Table 3.10), indicating that both assays were reproducible over the 3 days.

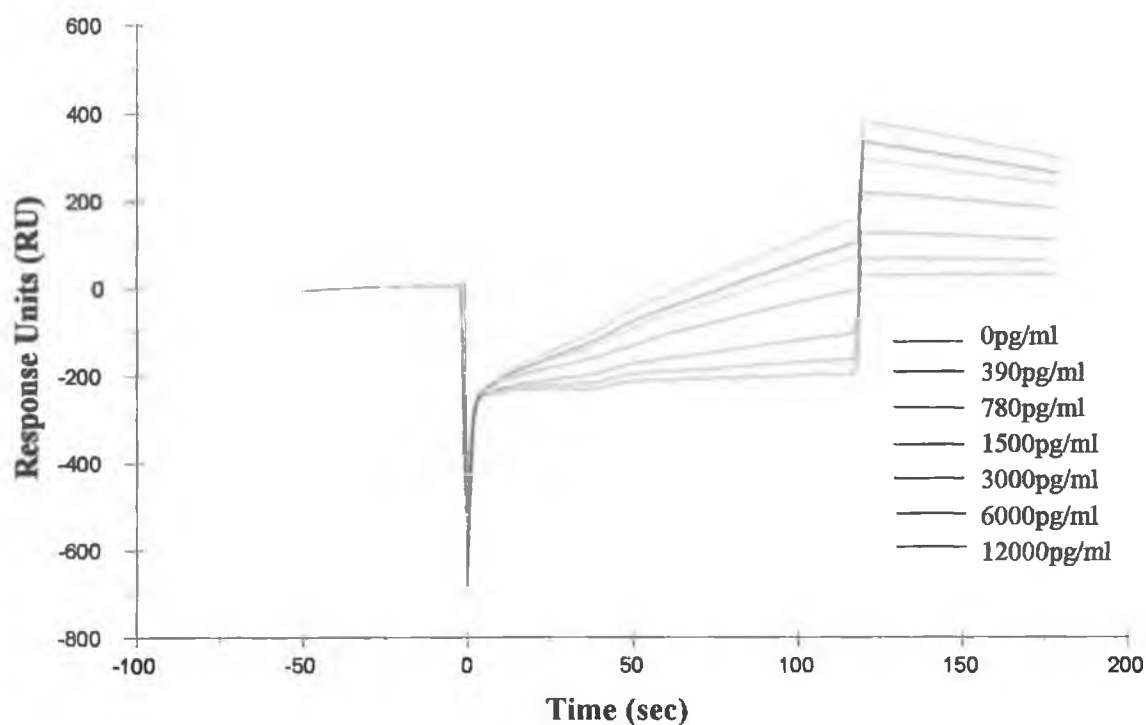


*Figure 3.24: Typical overlay sensorgram showing the antibody binding responses of the monomeric scFv in the presence of a range of free AFB<sub>1</sub> standards. Free AFB<sub>1</sub> concentration, ranging in concentration from 0 – 12000pg/ml, were pre-incubated with an equal volume of the monomeric scFv and passed over the sensor surface. The sensor surface was regenerated using 10mM NaOH.*

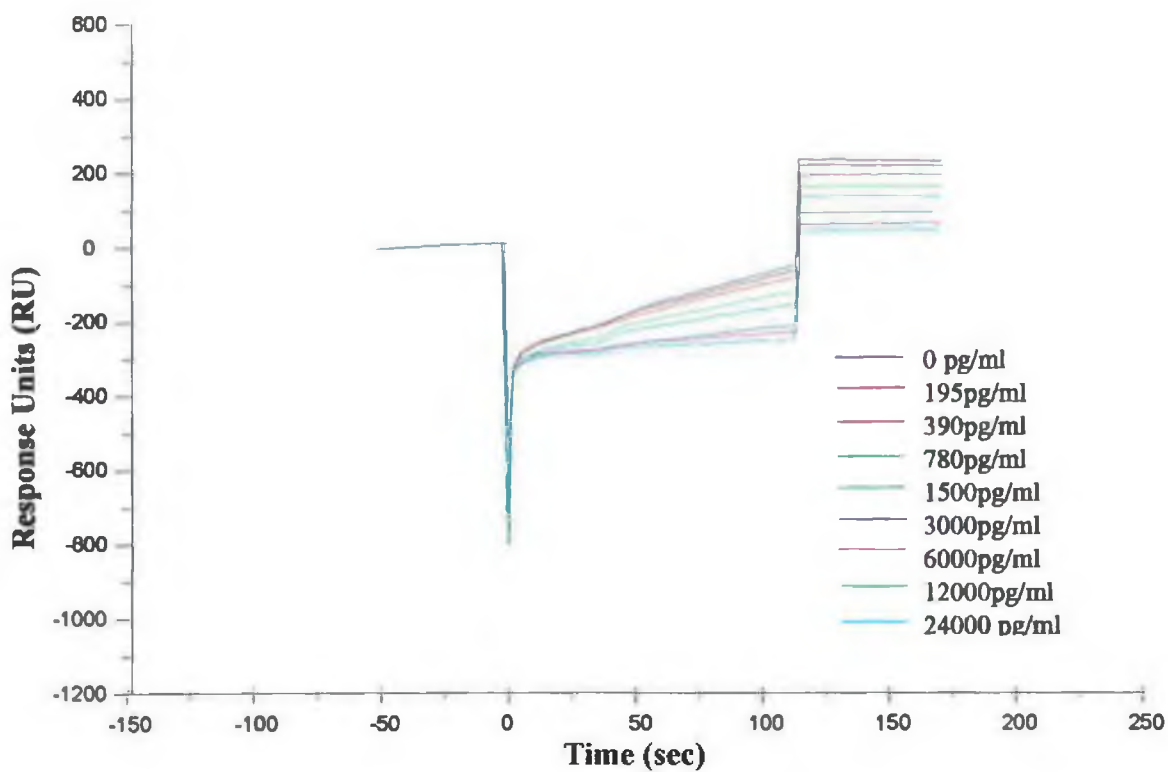


*Figure 3.25: Typical overlay sensorgram showing the antibody binding responses of the dimeric scFv in the presence of a range of free AFB<sub>1</sub> standards. The AFB<sub>1</sub> standards, ranging in concentration 0 – 24000pg/ml, were pre-incubated with an equal volume of the dimeric scFv and passed over the sensor surface. The sensor surface was regenerated using 25mM NaOH.*

**Table 3.9:** Inter-day assay co-efficients of variation for the Biacore inhibition assay for the detection of AFB<sub>1</sub> using the monomeric scFv. Three sets of six standards were assayed on three different days and the C.V.'s were calculated as the standard deviation (S.D.) expressed as a percentage of the mean values for each standard.

AFB <sub>1</sub> concentration (pg/ml)	Calculated mean ± S.D.	Coefficient of variation (%)
12000	0.11 ± 0.004	3.75
6000	0.19 ± 0.006	3.16
3000	0.35 ± 0.015	4.18
1500	0.59 ± 0.020	3.40
750	0.77 ± 0.012	1.58
375	0.88 ± 0.017	1.90

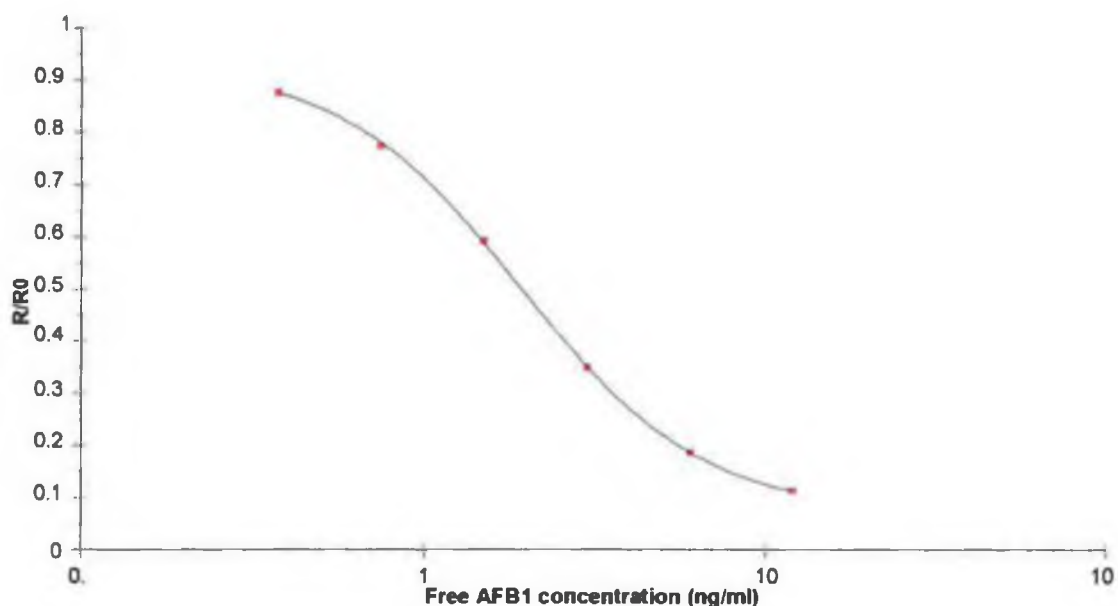


**Figure 3.26:** Inter-day Biacore inhibition assay for the determination of the range of detection of free AFB<sub>1</sub> using the monomeric scFv. The range of detection was found to be between 375 and 12000 pg/ml.

*Table 3.10: Inter-day assay co-efficients of variation for the Biacore inhibition assay for the detection of AFB<sub>1</sub> using the dimeric scFv. Three sets of eight standards were assayed on three different days and the C.V.'s were calculated as the standard deviation (S.D.) expressed as a percentage of the mean values for each standard.*

<b>AFB<sub>1</sub> concentration (pg/ml)</b>	<b>Calculated mean ± S.D.</b>	<b>Coefficient of variation (%)</b>
24000	0.16 ± 0.013	7.95
12000	0.19 ± 0.017	8.89
6000	0.26 ± 0.030	11.53
3000	0.39 ± 0.020	5.27
1500	0.58 ± 0.048	8.28
750	0.72 ± 0.055	7.66
375	0.85 ± 0.054	6.36
190	0.98 ± 0.029	3.00

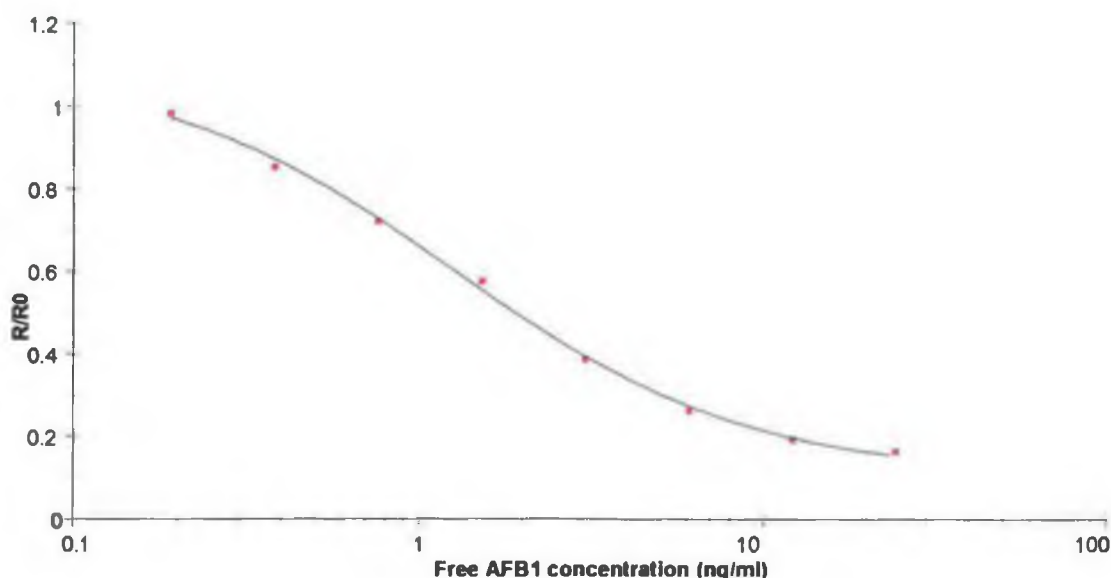


*Figure 3.27: Inter-day Biacore inhibition assay for the determination of the range of detection of free AFB<sub>1</sub> using the dimeric scFv. The range of detection was found to be between 190 and 24000pg/ml.*

#### 3.2.2.2.4 Cross-Reactivity Studies

Cross-reactivity potential of the scFvs were determined against five structurally related aflatoxins, B<sub>2</sub>, G<sub>1</sub>, G<sub>2</sub>, M<sub>1</sub> and M<sub>2</sub>, in a Biacore inhibition assay format. Comparisons of the LDD and IC<sub>50</sub> values were used to accurately estimate levels of cross-reactivity, with the IC<sub>50</sub> value defined as the analyte concentration that results in 50% inhibition and the least detectable dose (LDD) as the analyte concentration that results in 90% inhibition or as the smallest concentration of analyte that produces a response that can be significantly distinguished from zero. Levels of cross-reactivity were estimated at the LDD (CR<sub>90</sub>) and at the IC<sub>50</sub> (CR<sub>50</sub>) as 100-fold the ratio between the LDD and IC<sub>50</sub> values of the antigen and of the cross reactant, respectively. Table 3.11 shows the results obtained with the monomeric scFv, which displayed highest level of cross-reactivity with aflatoxin M<sub>1</sub> and G<sub>1</sub> at the LDD (12.5%) and aflatoxin G<sub>1</sub> at the CR<sub>50</sub> (13%). Low-levels of cross-reactivity was observed with the monomeric scFv against aflatoxins B<sub>2</sub>, G<sub>2</sub>, M<sub>1</sub> and M<sub>2</sub> at the IC<sub>50</sub> (i.e. ≤ 5%) and against aflatoxins B<sub>2</sub>, G<sub>2</sub>, and M<sub>2</sub> at and LDD (i.e. ≤ 3%). The dimeric scFv displayed low-levels of cross-reactivity with aflatoxins B<sub>2</sub>, G<sub>2</sub>, M<sub>1</sub> and M<sub>2</sub> at the IC<sub>50</sub> and LDD (i.e. ≤ 5%) (Table 3.12). Slightly higher-levels of cross-reactivity were observed with aflatoxin G<sub>1</sub> at the IC<sub>50</sub> (10%) and LDD (20%). This suggests that both the monomeric and dimeric scFvs appear to specifically bind to AFB<sub>1</sub> with relatively low-levels of cross-reactivity (i.e. ≤ 20%) observed at the IC<sub>50</sub> and LDD.

**Table 3.11:** Cross reactivity studies on the monomeric scFv in a Biacore inhibition assay format. The cross reactivity potential was approximated at the least detectable dose (LDD), which is estimated at 90% A/A0, and at the IC<sub>50</sub> value, which is estimated at 50% A/A0. The CR<sub>90</sub> and CR<sub>50</sub> were then expressed as 100-fold the ratio of the antigen and of the cross-reactant.

Aflatoxin	LDD <sup>a</sup> (ng/ml)	IC <sub>50</sub> <sup>b</sup> (ng/ml)	CR <sub>90</sub> <sup>c</sup> (%)	CR <sub>50</sub> <sup>d</sup> (%)
B <sub>1</sub>	375	2000	100	100
B <sub>2</sub>	12500	200000	1	3
M <sub>1</sub>	3000	40000	5	12.5
M <sub>2</sub>	31250	> 250000	< 1	1.2
G <sub>1</sub>	3000	15000	13	12.5
G <sub>2</sub>	12500	200000	1	3

<sup>a</sup> Least detectable dose calculated at 90% A/A0

<sup>b</sup> 50% inhibition concentration (50% A/A0)

<sup>c</sup> Percentage cross-reactivity determined at IC<sub>50</sub>

<sup>d</sup> Percentage cross-reactivity determined at LDD

**Table 3.12:** Cross reactivity studies on the dimeric scFv in a Biacore inhibition assay format. The cross reactivity potential was approximated at the least detectable dose (LDD), which is estimated at 90% A/A0, and at the IC<sub>50</sub> value, which is estimated at 50% A/A0. The CR<sub>90</sub> and CR<sub>50</sub> were then expressed as 100-fold the ratio of the antigen and of the cross-reactant.

Aflatoxin	LDD <sup>a</sup> (ng/ml)	IC <sub>50</sub> <sup>b</sup> (ng/ml)	CR <sub>90</sub> <sup>c</sup> (%)	CR <sub>50</sub> <sup>d</sup> (%)
B <sub>1</sub>	300	2000	100	100
B <sub>2</sub>	25000	300000	<1	1.2
M <sub>1</sub>	20000	200000	1	1.5
M <sub>2</sub>	125000	> 250000	<1	<1
G <sub>1</sub>	1500	20000	10	20
G <sub>2</sub>	25000	250000	<1	1.2

<sup>a</sup> Least detectable dose calculated at 90% A/A0

<sup>b</sup> 50% inhibition concentration (50% A/A0)

<sup>c</sup> Percentage cross-reactivity determined at IC<sub>50</sub>

<sup>d</sup> Percentage cross-reactivity determined at LDD

### **3.2.2.3 Development of a lateral flow immunoassay (LFIA) for the detection of AFB<sub>1</sub>**

This section focuses on the development of a lateral flow immunoassay (LFIA) for the detection of AFB<sub>1</sub>, which incorporates colloidal carbon labels to generate the signals in the assay.

#### **3.2.2.3.1 Indirect competitive LFIA**

A lateral flow immunoassay (LFIA) is a one-step sol particle immunoassay (See Section 1.8.2). Carbon particles are physically adsorbed onto an antibody or hapten-protein conjugate, which are then used as the detection ligand. This section describes the development of an indirect competitive LFIA, which incorporates an anti-AFB<sub>1</sub> rat monoclonal antibody, for the detection of AFB<sub>1</sub>. Colloidal carbon was absorbed onto an AFB<sub>1</sub>-BSA conjugate and used to generate the test signal.

Mouse anti-rat antibodies were sprayed onto a nitrocellulose membrane as the test line, 3mm below the control line, which consisted of anti-horse antibodies sprayed onto the nitrocellulose. A droplet of running buffer containing free AFB<sub>1</sub>, the AFB<sub>1</sub>-BSA-carbon-conjugate, the anti-AFB<sub>1</sub> rat monoclonal antibody and a carbon-conjugated horse antibody was mixed and allowed to flow along the nitrocellulose. The free AFB<sub>1</sub> and the AFB<sub>1</sub>-BSA-carbon conjugate compete for binding to the anti-AFB<sub>1</sub> rat monoclonal antibody, as the sample droplet travels along the membrane. The intensity of the generated signal increases, as the concentration of free AFB<sub>1</sub> in the sample droplet decreases, because the numbers of antibodies available for binding the AFB<sub>1</sub>-BSA-carbon conjugate increases. Figure 3.28 shows a schematic representation of the indirect competitive LFIA developed using the anti-AFB<sub>1</sub> rat monoclonal antibody, for the detection of AFB<sub>1</sub>.

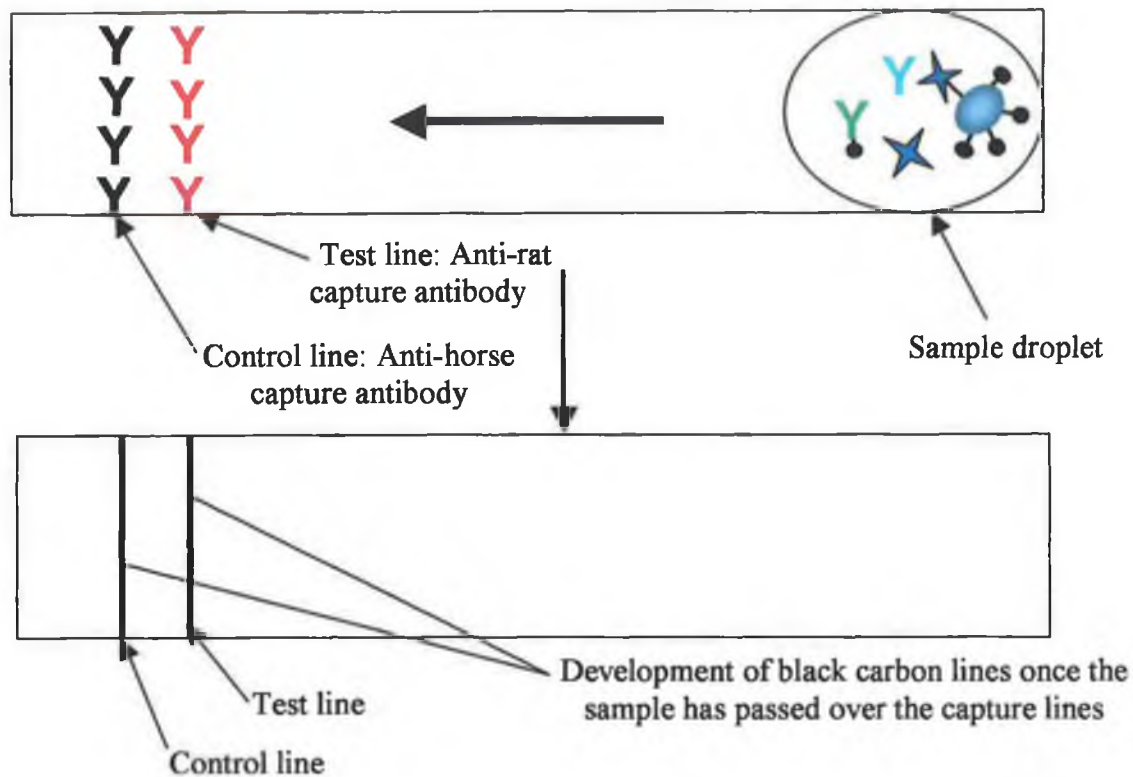
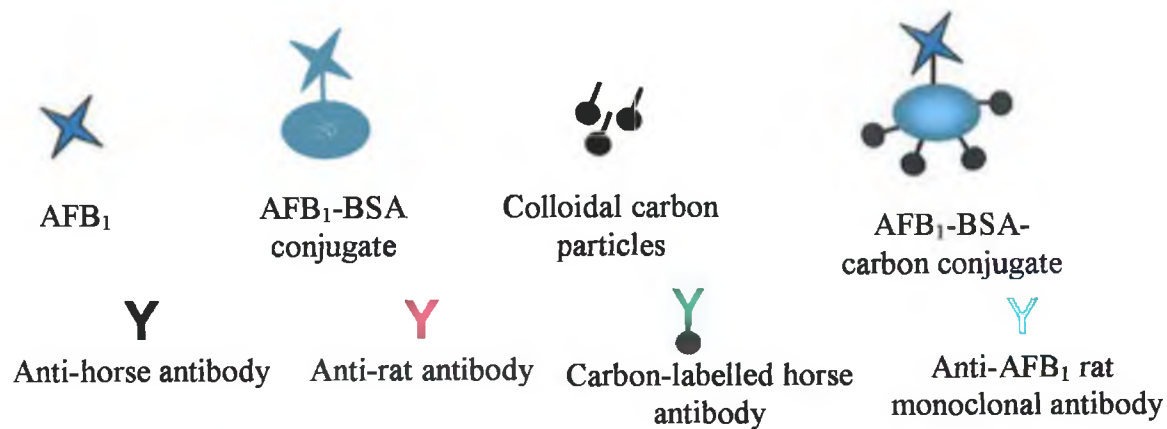


**Figure 3.28:** Schematic representation of an indirect competitive LFIAs for the detection of AFB<sub>1</sub>. Test lines and control lines consisting of an anti-rat antibody and anti-horse antibody, respectively, were sprayed onto nitrocellulose. A sample droplet consisting of free AFB<sub>1</sub>, an AFB<sub>1</sub>-BSA-carbon conjugate, the anti-AFB<sub>1</sub> rat monoclonal antibody and the carbon-conjugated horse antibody in running buffer was allowed travel along the nitrocellulose. Free AFB<sub>1</sub> and the AFB<sub>1</sub>-BSA-carbon conjugate compete for binding to the anti-AFB<sub>1</sub> rat monoclonal antibody as the sample travels along the nitrocellulose. Signals are generated as the carbon conjugates bind to the captured antibodies immobilised on the nitrocellulose. The intensity of the generated signal decreases as the concentration of free AFB<sub>1</sub> increases.

### **3.2.2.3.2 Optimisation of flow-rate**

From a safety point of view it was necessary to develop the LFIA assay format that involved spraying either anti-AFB<sub>1</sub> antibodies or species-specific antibodies, designed to capture the anti-AFB<sub>1</sub> antibodies, directly onto the nitrocellulose. Significant safety concerns were envisaged spraying the AFB<sub>1</sub>-BSA conjugate directly onto the nitrocellulose. The antibodies in question were sprayed onto the nitrocellulose membrane using a Linomat 5 sample application device. The flow-rate used to deposit the antibodies onto the nitrocellulose membrane was initially optimised. Various flow-rates, ranging from 100 – 500nl/sec, were tested by spraying 500µg/ml of anti-horse antibody. Signals were developed using a carbon-conjugated horse antibody in running buffer, which was allowed run up the nitrocellulose strip. A flow-rate of 400nl/sec was chosen for use in subsequent assays, as it produced a definite line with minimal dispersion (Fig. 3.29).

### **3.2.2.3.3 Optimisation of control line**

The incorporation of an appropriate control line is essential for the development of a LFIA. The control line is sprayed approximately 3mm above the test line and signals are only generated when the sample has travelled along the nitrocellulose over the test line and then over the control line, confirming that the sample droplet has passed over the test line. It is essential, when selecting an appropriate control line, to ensure that the carbon-labelled antigen used to generate the signals for the control line does not interact non-specifically with the capture antibodies sprayed onto the nitrocellulose for the test line. This would result in false-positive results. Colloidal carbon was adsorbed onto a mouse antibody, a horse antibody and a rabbit antibody. The three carbon-conjugates were investigated for use in the generation of the signal for the control line. Nitrocellulose strips were sprayed with a several capture antibodies, including the anti-AFB<sub>1</sub> monomeric and dimeric scFvs, the anti-AFB<sub>1</sub> rat monoclonal antibody, a mouse anti-FLAG antibody and a mouse anti-rat antibody. Each of the three carbon-conjugated antibodies was passed over the capture antibodies in order to ensure they did not interact non-specifically. The carbon-conjugated horse antibody was selected for use in subsequent assays, as negligible non-specific interactions were observed between it and the capture antibodies. Therefore, control lines consisting of

goat anti-horse antibodies, sprayed onto the nitrocellulose, and a carbon-conjugated horse antibody were incorporated into subsequent assays.

The concentration of the goat anti-horse antibody for use in the development of the control line was then optimised. Various concentrations of the goat anti-horse antibody, ranging from 0 – 750 $\mu$ g/ml, were sprayed onto nitrocellulose. Signals were generated using 100 $\mu$ l of running buffer containing the carbon-conjugated horse antibody (Fig. 3.30). It was found that 500 $\mu$ g/ml of the goat anti-horse antibody sprayed onto the nitrocellulose was sufficient for the development of an acceptable control line.

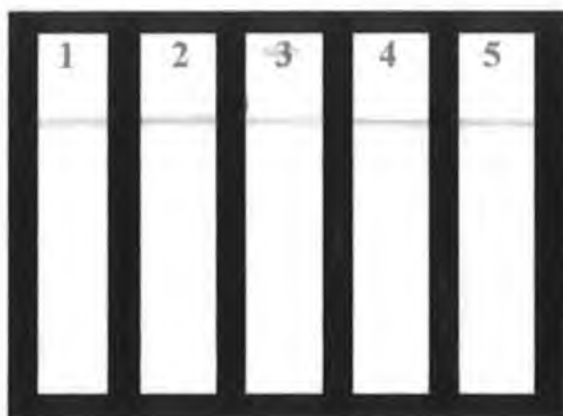


**Figure 3.29:** *Optimisation of flow-rate used to spray the nitrocellulose strips. The goat anti-horse antibody (500 $\mu$ g/ml) was sprayed onto the nitrocellulose with various flow-rates. Signals were generated using the carbon-conjugated horse antibody. Strips 1, 2, 3, 4 and 5 represent flow-rates of 500, 400, 300, 200 and 100nl/sec, respectively. 400nl/sec was chosen for subsequent assay development.*

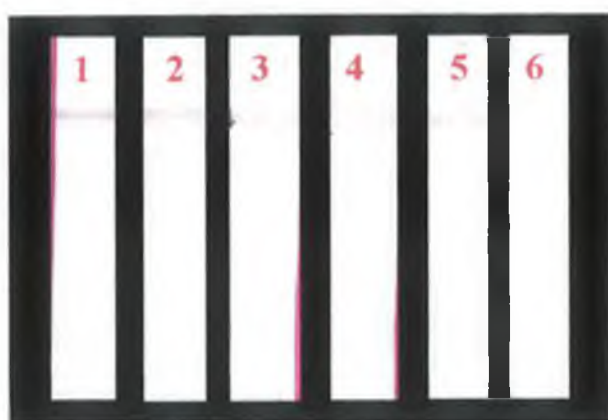


*Figure 3.30: Optimisation of the concentration of goat anti-horse antibody sprayed on the nitrocellulose for development of the control line. Strips 1, 2, 3, 4, 5 and 6 were sprayed with 750, 500, 250, 125, 62.5 and 0 $\mu$ g/ml of the anti-horse antibody, respectively. 500 $\mu$ g/ml of the goat anti-horse antibody was found to be optimal.*

#### **3.2.2.3.4 Development and optimisation of test line**

Initially attempts were made to develop a competitive LFIA incorporating the AFB<sub>1</sub>-specific monomeric and dimeric scFvs. Test lines, consisting of the monomeric or dimeric scFvs sprayed onto the nitrocellulose, were investigated for use in the development of a direct competitive LFIA for AFB<sub>1</sub>. However, following addition of the sample droplet, which consisted of running buffer, free AFB<sub>1</sub> and the AFB<sub>1</sub>-BSA carbon conjugate, no test line developed. Attempts were then made to develop an indirect competitive LFIA where strips were sprayed with a mouse anti-FLAG antibody, to capture the FLAG-tagged scFvs. However, once again no signals were generated for the test line, following addition of the sample droplet, containing the monomeric or dimeric scFv, free AFB<sub>1</sub> and the AFB<sub>1</sub>-BSA carbon conjugate.

Due to the difficulties encountered trying to develop a LFIA incorporating the monomeric and dimeric scFvs, an indirect LFIA was developed using an anti-AFB<sub>1</sub> rat monoclonal antibody, which was kindly donated by the Institute of Food Research (Norwich, U.K). This assay format consisted of spraying nitrocellulose strips with a mouse anti-rat capture antibody and allowing the sample droplet, containing the rat anti-AFB<sub>1</sub> monoclonal antibody, free AFB<sub>1</sub> and the AFB<sub>1</sub>-BSA carbon conjugate, run

up the strip (Fig. 3.28). A control line consisting of immobilised goat anti-horse antibody and the carbon-conjugated horse antibody was incorporated. The optimisation of several assay parameters was also required for the development of the test line.

Initially four AFB<sub>1</sub>-BSA carbon conjugates were developed for use with the LFIA. They four carbon conjugates were produced using different quantities of the AFB<sub>1</sub>-BSA, 50, 150, 250 and 350µg, absorbed onto the colloidal carbon. The optimum conjugate for use in the development of the indirect LFIA was determined. Strips were sprayed with 500µg/ml of the goat anti-horse antibody as the control line and with 500µg/ml of the mouse anti-rat antibody as the test line. Allowing the sample droplet, containing the carbon-conjugated horse antibody and the various AFB<sub>1</sub>-BSA carbon-conjugates, travel along the strips enabled the generation of the signals. Minimal difference was observed between the four AFB<sub>1</sub>-BSA carbon conjugates (Fig. 3.31). Therefore, subsequent assay development was carried out using the 350µg AFB<sub>1</sub>-BSA conjugate.

Optimisation of the concentration of the mouse anti-rat antibody for use in the development of the test line was also carried out. Various concentrations of the mouse anti-rat antibody, ranging from 0 – 750µg/ml, were sprayed onto nitrocellulose along with the anti-horse antibody as the control line, at 500µg/ml. Signals were then generated using a sample droplet containing the AFB<sub>1</sub>-BSA-carbon conjugate (test line) and a carbon-conjugated horse antibody (control line) (Fig. 3.32). It was found that 500µg/ml of the mouse anti-rat antibody sprayed onto the nitrocellulose was sufficient for the development of an acceptable test line.

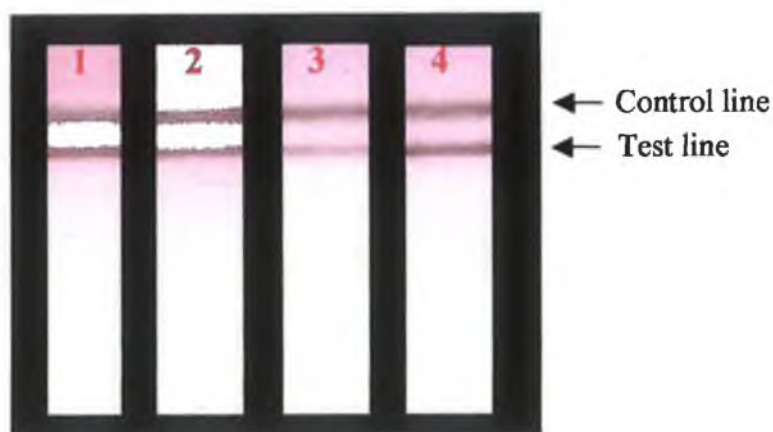


**Figure 3.31:** Optimisation of the amount of AFB<sub>1</sub>-BSA absorbed to the colloidal carbon for the development of the test line. Strips 1, 2, 3 and 4 were sprayed 500 µg/ml of the mouse anti-rat antibody and developed using the carbon-conjugates produced using 350, 250, 150 and 50 µg/ml of the AFB<sub>1</sub>-BSA conjugate. A control line consisting of and goat anti-horse antibody sprayed at 500 µg/ml, developed using a carbon-conjugated horse antibody, was also incorporated.



**Figure 3.32:** Optimisation of the concentration of mouse anti-rat antibody sprayed onto the nitrocellulose for the development of the test line. Strips 1, 2, 3, 4, 5 and 6 were sprayed with 750, 500, 250, 125, 62.5 and 0 µg/ml of the mouse anti-rat antibody, respectively. 500 µg/ml of the mouse anti-rat antibody was found to be optimal. A control line consisting of a goat anti-horse antibody sprayed at 500 µg/ml, developed using a carbon-conjugated horse antibody, was also incorporated.

### 3.2.2.3.5 Development of indirect competitive LFIA for the detection of AFB<sub>1</sub>

Following optimisation of the various parameters required for the control and test lines an indirect competitive LFIA for the detection of AFB<sub>1</sub> was developed using the anti-AFB<sub>1</sub> rat monoclonal antibody. Nitrocellulose stripes were sprayed with 500µg/ml of the mouse anti-rat antibody (test line) and 500µg/ml of the goat anti-horse antibody (control line). Standards of free AFB<sub>1</sub>, ranging in concentration from 390 – 25000pg/ml, were prepared in running buffer. 50µl of each AFB<sub>1</sub> standard was then mixed with 50µl of running buffer containing the anti-AFB<sub>1</sub> rat monoclonal antibody, the AFB<sub>1</sub>-BSA-carbon conjugate and carbon-conjugated horse antibody. The mixed samples were allowed travel along the nitrocellulose membrane followed by 100µl of running buffer to wash the strips. The limit of detection of the assay was found to be 1.5ng/ml (Fig. 3.33).

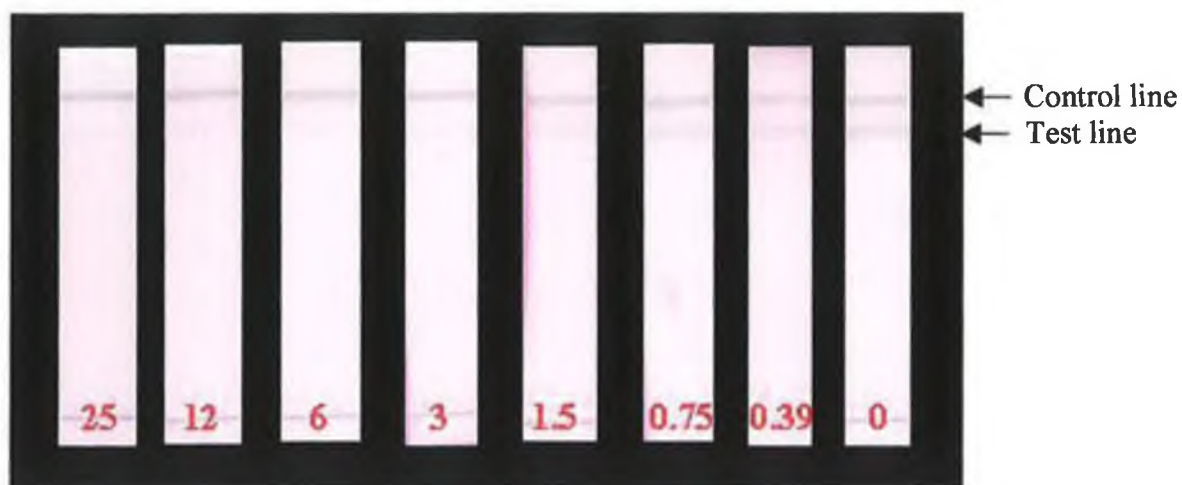


*Figure 3.33: Competitive LFIA for the detection of AFB<sub>1</sub>, using an anti-AFB<sub>1</sub> rat monoclonal antibody. The numbers below the strips represent the concentration of free AFB<sub>1</sub> added to the sample in ng/ml. The lower limit of detection for the assay was 1.5ng/ml. A control line consisting of an anti-horse antibody sprayed at 500µg/ml, developed using a carbon-conjugated horse antibody, was also incorporated.*

### 3.2.2.4 Summary of results

Table 3.13 summarises the limits of detection obtained with each immunoassay format developed in this chapter.

*Table 3.13: Summary of the limits of detection, for free AFB<sub>1</sub>, using a variety of immunoassay formats incorporating AFB<sub>1</sub>-specific, scFv and monoclonal, antibodies.*

<b>Anti-AFB<sub>1</sub> antibody</b>	<b>Competitive ELISA</b>	<b>Biacore inhibition assay</b>	<b>Competitive LFIA</b>
Monomeric scFv	12ng/ml	0.39ng/ml	N/A
Dimeric scFv	3ng/ml	0.19ng/ml	N/A
Bifunctional scFv	3ng/ml	N/A	N/A
Rat monoclonal	N/A	N/A	1.5ng/ml

### 3.3 Discussion

The main focus of this chapter was the production and characterisation of genetically derived scFv antibody fragments specific for AFB<sub>1</sub>. The gene encoding an AFB<sub>1</sub>-specific scFv was isolated from a phage display library. The nucleotide sequence was determined and used to deduce the amino acid sequence (Fig. 3.4). The complementary determining regions (CDRs) regions were then identified on the heavy and light chains according to Kabat *et al.* (1991) and the 3-D structure of the scFv predicted using SwissModel (Fig. 3.5).

The scFv gene was sub-cloned into pAK400 for the soluble expression of a monomeric scFv, pAK500 for the soluble expression of a dimeric scFv and into pAK600 for the soluble expression of an alkaline phosphatase-labelled bifunctional scFv. SfiI restriction digestion was used to directionally clone the scFv insert the restricted plasmid (Fig. 3.6). Soluble expression of each scFv was induced using 1mM IPTG. Sufficient levels of expression of the monomeric scFv were observed following a 4 hour induction period and 16 hours was required for the dimeric and bifunctional scFvs. The cellular distribution of the expressed scFvs was then determined following ELISA analysis on the culture supernatant and periplasmic lysate. High-levels of soluble expression, of the monomeric, dimeric and bifunctional scFvs, were observed into the periplasm (Fig. 3.7 and 3.8).

Following expression from pAK400 and 500 a C-terminal his-tag was incorporated in the monomeric and dimeric scFvs, respectively. Immobilised metal affinity chromatography was employed for the purification of the his-tagged scFvs. However, following purification SDS-PAGE analysis showed the presence of several contaminating *E. coli* proteins. Western blot analysis was carried out on the scFvs in order to demonstrate the specificity of the secondary and tertiary antibodies and to confirm the contaminating protein within the periplasmic lysates did not result in non-specific binding. Western blot analysis was also used to confirm the monomeric or dimeric nature of the expressed scFvs (Fig. 3.9). Following expression from pAK400 a band at approximately 32kDa represented the monomeric scFv. Expression from pAK500 yielded a band at approximately 35kDa representing the reduced monomeric fusion, confirming the dimeric nature of the scFv expressed from pAK500. Two bands were visible, at 85kDa and 32kDa, following scFv expression from pAK600,

representing the alkaline-phosphatase-labelled scFv, and the monomeric scFv, respectively. Brennan *et al.* (2002) also reported similar finding using the pAK vector series for the expression of scFvs against M3G.

Following the successful expression and initial characterisation of the three genetically derived scFvs several immunoassay formats were investigated for the detection of AFB<sub>1</sub>. Competitive ELISAs and Biacore inhibition assays, incorporating the genetically derived scFvs, were developed and a lateral flow immunoassay (LFIA) was developed using an anti-AFB<sub>1</sub> rat monoclonal antibody.

Initially, attention focused on the development of three competitive ELISAs for the detection of AFB<sub>1</sub>. Two indirect competitive ELISAs were developed, with the monomeric and dimeric scFvs, and a direct competitive ELISA was developed using the alkaline phosphatase-labelled (bifunctional) scFv. In order to develop a sensitive competitive ELISA for AFB<sub>1</sub> several parameters were optimised. The limit of detection of a competitive ELISA can be affected by an antibodies affinity and the equilibrium between free and immobilised hapten. If the concentration of the immobilised hapten-conjugate were too high than there would be an unfair binding bias towards the immobilised conjugate. For similar reasons the optimal scFv dilution used must be the limiting factor because excess would result in binding to both free and immobilised AFB<sub>1</sub> to a higher degree affecting the assay limit of detection. Checkerboard ELISAs were carried out with each scFv to determine the optimal conjugate coating concentration and scFv dilution for use in a competitive ELISA (Fig. 3.10, 3.11 and 3.12). AFB<sub>1</sub>-BSA coating concentrations of 25, 12.5 and 6.25µg/ml were found to be optimal for the monomeric, dimeric and bifunctional scFvs, respectively. The optimal scFv dilutions, which displayed between 50 –70% of maximum binding, were found to be 1/4, 1/8 and 1/4 for the monomeric, dimeric and bifunctional scFvs, respectively. Due to its strong hydrophobic nature it was necessary to prepare standards of AFB<sub>1</sub> in methanol. However, methanol can have an inhibitory effect on the limit of detection of an assay. Therefore, the optimal methanol concentration for use with each scFv was also optimised by carrying out competitive ELISA on each scFv using varying concentrations of methanol ranging from 2.5 –

40% (v/v). 5% (v/v) methanol appeared optimal for each scFv (Figs. 3.13, 3.14 and 3.15).

Optimisation of the various assay parameters was then followed by the development of three competitive ELISAs. The range of detection for the monomeric, dimeric and bifunctional scFvs were determined and ranged between 12 and 781ng/ml, 3 and 781ng/ml and 3 and 390ng/ml, respectively (Fig. 3.16, 3.17, 3.18). Intra- and inter-day variability studies were conducted to determine the reproducibility of the assays. The coefficients of variation (CVs) for intra-day assay with the monomeric, dimeric and bifunctional scFvs remained below 11.5, 11.98 and 8.28%, respectively. Inter-day CVs for the monomeric, dimeric and bifunctional scFvs were less than 11.35, 6.99 and 5.25%, respectively (Tables 3.3, 3.4 and 3.5). The results discussed above suggest that the monomeric, dimeric and bifunctional scFvs offer excellent sensitivity and reproducibility for a model assay system for AFB<sub>1</sub>.

Cross-reactivity studies were then carried out on each scFv, in a competitive ELISA format; in order to determine the cross-reactivity potential of the scFvs against five structurally related aflatoxins, B<sub>2</sub>, G<sub>1</sub>, G<sub>2</sub>, M<sub>1</sub> and M<sub>2</sub> (Tables 3.6, 3.7 and 3.8). Hennion *et al.* (1998) recommends the comparison of two sets of values, the LDD and IC<sub>50</sub>, in order to accurately estimate cross reactivity over the measurement range. The least detectable dose (LDD) is defined as the smallest concentration of analyte that produces a response that can be significantly distinguished from zero (Hennion *et al.*, 1998) and the IC<sub>50</sub> is defined as the analyte concentration that results in 50% inhibition. The cross-reactivity is then estimated at the LDD (CR<sub>90</sub>) and at the IC<sub>50</sub> (CR<sub>50</sub>) as 100-fold the ratio between the LDD and IC<sub>50</sub> values of the antigen and of the cross reactant, respectively. The dimeric scFv displayed low-levels of cross-reactivity with each of the structurally related aflatoxins at both the LDD (i.e. ≤ 3%) and CR<sub>50</sub> (i.e. ≤ 8%). In comparison with the dimeric scFv the monomeric scFv displayed slightly higher levels of cross-reactivity at the LDD (i.e. ≤ 12.5%) and IC<sub>50</sub> (i.e. ≤ 19%). The bifunctional scFv appeared to cross-react with the aflatoxins to a greater extent with levels as high as 100% and 46% observed at the LDD and IC<sub>50</sub>, respectively. However, it must be noted that each scFv displayed minimal cross-reactivity with aflatoxins M<sub>1</sub> and M<sub>2</sub>, suggesting that both the monomeric and dimeric

scFvs appear to specifically bind to AFB<sub>1</sub> with low-levels of cross-reactivity (i.e. ≤ 20%). Non-specific interactions, with high-levels of cross-reactivity, were observed with the bifunctional scFv against aflatoxins B<sub>2</sub>, G<sub>1</sub> and G<sub>2</sub>.

Attempts made to develop a sandwich ELISA for AFB<sub>1</sub> incorporating the dimeric scFv, as the capture antibody, and the alkaline-phosphatase labelled antibody, for detection, were unsuccessful (Data not shown). Brennan *et al.* (2002) also carried out a similar study that was unsuccessful. The difficulties encountered are probably due to the size of AFB<sub>1</sub> (312Da), whereby once an antibody binds the AFB<sub>1</sub> molecule the other epitopes are inaccessible.

The development of a Biacore inhibition assay was then investigated for the detection of AFB<sub>1</sub>. In the past several difficulties have been encountered during the development of Biacore assays for AFB<sub>1</sub>. Problems have been encountered when trying to immobilise anti-AFB<sub>1</sub> antibodies to a sensor surface, either directly or indirectly (Keating 1998). When directly immobilising the antibodies to the sensor surface the coupling chemistry affected the antibodies binding capacity and indirectly immobilising the antibodies, using either protein A or species specific antibodies, resulted in no binding between the captured antibody and the protein conjugate. Daly *et al.* (2000) also encountered difficulties developing a Biacore assay for the detection of AFB<sub>1</sub> using polyclonal antibodies. In this case a sensor surface immobilised with an AFB<sub>1</sub>-BSA conjugate was used in the development of an inhibition assay format but difficulties were encountered when trying to regenerate the sensor surface. Therefore, this study focused on the use of a CM5 chip immobilised with an AFB<sub>1</sub> derivative for the development of assays for the detection of AFB<sub>1</sub>. The monomeric and dimeric scFvs were applied to the development of Biacore inhibition assays for the detection of AFB<sub>1</sub>.

For the successful development of an inhibition assay for the detection of AFB<sub>1</sub>, the optimisation of a number of parameters was required. These included optimal antibody dilution, removal of non-specific interactions and surface regeneration conditions. Several scFv dilutions were passed over the AFB<sub>1</sub> surface and the dilution resulting in the binding of approximately 300 – 400RU was selected as optimal. A 1/8

dilution of the monomeric and a 1/70 dilution of the dimeric scFv were found to produce binding responses of approximately 380 and 280RU, respectively. Non-specific binding analysis was carried out on the monomeric (Fig. 3.19) and dimeric scFvs (Fig. 3.20) to ensure any observed binding was due specifically to the interaction between the scFv and immobilised AFB<sub>1</sub>. Negligible binding was observed with each scFv to the dextran and, as a result, there was no need to incorporate dextran into the diluent buffer.

The regeneration of the sensor surface is a major factor affecting the development of Biacore assays. The regeneration conditions for the removal of the monomeric and dimeric scFv from the AFB<sub>1</sub> sensor surface were optimised. A 0.5 min pulse of 10mM NaOH and 25mM NaOH enabled complete removal of the monomeric and dimeric scFvs, respectively. Figure 3.21 show a typical sensogram for the binding and regeneration of the monomeric and dimeric scFvs, respectively, on the AFB<sub>1</sub> sensor surface. Previous studies have encountered problems regenerating the sensor surface immobilised with hapten – protein conjugates following injection of specific polyclonal antibodies. The need for stringent regeneration conditions were required, including 1M ethanolamine, pH 13.6 for the regeneration of an M3G-OVA surface (Dillon<sup>a</sup> *et al.* 2003) and 1M ethanolamine with 20% (v/v) acetonitrile, pH 12.0 for the regeneration of an AFB<sub>1</sub>-BSA surface (Daly *et al.* 2000). In the case of this study the use of 10 and 25mM NaOH for the monomeric and dimeric scFvs, respectively, enabled the complete regeneration of the AFB<sub>1</sub> surface. The need for a higher NaOH concentration with the dimeric scFv suggests that the two binding sites increase the avidity of the scFvs for AFB<sub>1</sub>. Recent publications on the development of Biacore assays with monomeric scFvs have also reported the need for less stringent regeneration conditions in comparison with the use of polyclonal antibodies (Brennan *et al.*, 2002; Daly *et al.*, 2002 and Dillon<sup>b</sup> *et al.*, 2003). Multiple regenerations of the sensor surface is essential in the development of an assay in order to enable the analysis of multiple samples, making the biosensor a more cost effective method of detection. Multiple binding – regeneration cycles were carried out on the sensor surface to determine the binding capacities of the monomeric and dimeric scFvs. Over the course of the binding-regeneration cycles the binding capacity of the scFv to AFB<sub>1</sub> should not decrease by more than 20% (Wong *et al.*, 1997). Following optimisation of the regeneration solution for use with the monomeric and dimeric scFv regeneration

studies were conducted. This involved repeatedly injecting the scFv over the AFB<sub>1</sub> sensor surface and regenerating it with the appropriate regeneration solution. It was possible to regenerate the sensor surface at least 75 times using the monomeric scFv, before a decrease of 12% in the ligand binding capacity was observed (Fig. 3.22). The sensor surface could also be regenerated at least 75 times using the dimeric scFv, with a decrease in the ligand binding capacity of 10% being observed (Fig. 3.23). These results suggest excellent reproducibility of the AFB<sub>1</sub> sensor surface and the decrease in ligand binding capacity remains well below the limits suggested by Wong *et al.* (1997). It should also be noted at this point that the majority of the Biacore work carried out in this chapter was done using only one flow-cell, making it possible to carry out at least 530 regenerations on one CM5 surface immobilised with the AFB<sub>1</sub> derivative.

Following optimisation of the various assay parameters, inhibition assays, incorporating the monomeric or dimeric scFvs, were developed for the detection of AFB<sub>1</sub> using the CM5 chip immobilised with an AFB<sub>1</sub> derivative. Intra- and inter-day studies were conducted for each assay to give an indication on the assay's reproducibility. Studies on the intra-day variability showed that the monomeric scFv had a range of detection for free AFB<sub>1</sub> from 375 – 12,000pg/ml (Fig. 3.24) with coefficients of variation (CVs) remaining below 0.61%. The intra-day variability assay with the dimeric scFv had a range of detection between 190 and 24,000pg/ml (Fig. 3.25) and the CVs remained below 3.37%. Inter-day variability studies were also carried out in order to determine the reproducibility of the assay over three days. Figures 3.26 and 3.27 show the inter-day assay curves for the monomeric and dimeric scFvs, respectively, where the range of detection for free AFB<sub>1</sub> was 375 – 12,000pg/ml for the monomeric and 190 and 24,000pg/ml for the dimeric scFv. The CVs obtained for the inter-day variability studies on the monomeric scFv ranged between 1.9 and 4.18% (Table 3.9) and between 3 and 11.53% for the dimeric scFv (Table 3.10), indicating that both assays were reproducible over the 3 days. The results show that both the monomeric and dimeric scFvs offer excellent specificity and reproducibility for a model Biacore inhibition assay system for AFB<sub>1</sub>.

Cross-reactivity studies were then carried out on each scFv in an inhibition assay format on the Biacore. Cross-reactivity potential of the scFvs were determined against

five structurally related aflatoxins, B<sub>2</sub>, G<sub>1</sub>, G<sub>2</sub>, M<sub>1</sub> and M<sub>2</sub> at the LDD and IC<sub>50</sub>. The monomeric scFv displayed highest level of cross-reactivity against aflatoxin M<sub>1</sub> and G<sub>1</sub> at the LDD (12.5%) and aflatoxin G<sub>1</sub> at the CR<sub>50</sub> (13%) (Table 3.11). The monomeric scFv displayed low-levels of cross-reactivity against aflatoxins B<sub>2</sub>, G<sub>2</sub>, M<sub>1</sub> and M<sub>2</sub> at the IC<sub>50</sub> (i.e. ≤ 5%) and against aflatoxins B<sub>2</sub>, G<sub>2</sub>, and M<sub>2</sub> at and LDD (i.e. ≤ 3%). The dimeric scFv displayed low-levels of cross-reactivity against aflatoxins B<sub>2</sub>, G<sub>2</sub>, M<sub>1</sub> and M<sub>2</sub> at the IC<sub>50</sub> and LDD (i.e. ≤ 5%) (Table 3.12). Slightly higher-levels of cross-reactivity were observed against aflatoxin G<sub>1</sub> at the IC<sub>50</sub> (10%) and the LDD (20%). This suggests that both the monomeric and dimeric scFvs appear to specifically bind to AFB<sub>1</sub> with low-levels of cross-reactivity (i.e. ≤ 20%) observed at the IC<sub>50</sub> and LDD.

The development of a lateral flow immunoassay (LFIA) was also investigated as a rapid assay for the detection of AFB<sub>1</sub>. Direct and indirect assay configurations, incorporating the monomeric and dimeric scFvs, were investigated. The direct assay format involved spraying the anti-AFB<sub>1</sub> scFvs directly onto nitrocellulose and the indirect format involved immobilising a capture antibody onto the nitrocellulose. Usually it is possible to spray hapten-protein conjugates directly onto nitrocellulose. However, from a safety point it was envisaged that spraying the AFB<sub>1</sub>-protein conjugate might result in the release of hazardous vapours. The optimisation of numerous parameters was required. Initially the flow-rate at which strips was sprayed was optimised to give a definite line with minimal dispersal. Flow-rates ranging from 100 – 500nl/sec were used to spray strips with 500µg/ml of an anti-horse antibody. Upon development of the lines using a sample droplet consisting of running buffer and a carbon-conjugated horse antibody it was apparent that 400nl/sec was optimal (Fig. 3.29). This flow-rate enabled a quick spraying time and resulted in minimal dispersion of the line. The development of a specific control line is an essential part in the development of a LFIA. The use of three carbon-labelled antibodies, a mouse antibody, a horse antibody and a rabbit antibody, was investigated. The carbon-conjugated horse antibody was selected for subsequent assay development because it did not non-specifically interact with immobilised antibodies used with the test lines. The concentration of the anti-horse antibody sprayed onto the nitrocellulose, for use in the control line, was then optimised. Various concentrations of the anti-horse

antibody, ranging from 0 – 750µg/ml, were investigated. 500µg/ml was sufficient for the development of a sufficient control line (Fig. 3.30).

Initially attempts were made to develop a competitive LFIA incorporating the AFB<sub>1</sub>-specific monomeric and dimeric scFvs. Test lines, consisting of the monomeric and dimeric scFvs sprayed directly onto the nitrocellulose, were investigated for the development of a direct competitive LFIA for AFB<sub>1</sub>. However, upon development no test line appeared. Attempts were also made to develop an indirect competitive LFIA where strips were sprayed with an anti-FLAG antibody, to capture the FLAG-tagged scFvs. However, once again no test line developed. Observations on the optimisation of the control line suggested the need for spraying lines at relatively high concentrations (500µg/ml). Therefore, the scFvs were concentrated 10-fold, using an Amicon filter, and re-applied to each assay format. Once again no test line developed. Difficulties were previously encountered trying to purify the his-tagged scFvs. SDS-PAGE analysis on the IMAC purification confirmed the presence of a large number of contaminating *E. coli* proteins. Therefore, attempts made to concentrate the scFvs would also have resulted in the concentration of the contaminating proteins, which may have resulted in an inhibitory effect on the development of the test line. The porosity of the nitrocellulose can affect the sensitivity of a LFIA. Highly concentrated solutes may result in clogging of the nitrocellulose, preventing the sample running up over the test line and control line. The concentrated scFv, containing the concentrated contaminating proteins, may have clogged the nitrocellulose preventing the sample passing over the control and test lines. Suggesting the need for nitrocellulose with a larger pore size or the need for a relatively pure antibody stock for the development of the LFIA for the detection of AFB<sub>1</sub>.

Therefore, the use of a purified rat monoclonal antibody, specific for AFB<sub>1</sub> was employed for the development of an indirect competitive LFIA for the detection of AFB<sub>1</sub>. This assay format consisted of spraying nitrocellulose strips with a anti-rat capture antibody and allowing the sample droplet, consisting of running buffer, the rat anti-AFB<sub>1</sub> antibody, free aflatoxin and the AFB<sub>1</sub>-BSA carbon conjugate, run up the strip (Fig. 3.28). The quantity of the AFB<sub>1</sub>-BSA conjugate absorbed onto the colloidal

carbon was initially optimised. Carbon conjugates containing 50, 150, 250 and 350 $\mu$ g of AFB<sub>1</sub>-BSA absorbed onto the colloidal carbon were developed. Minimal difference between the four conjugates was observed (Fig. 3.31). Therefore the conjugate containing 350 $\mu$ g of the AFB<sub>1</sub>-BSA conjugate was selected for subsequent assays. The concentration of anti-rat sprayed onto the nitrocellulose for the development of the test line was also optimised. Various concentrations of the anti-rat, ranging from 0 – 750 $\mu$ g/ml, were investigated. 500 $\mu$ g/ml was sufficient for the development of a sufficient test line (Fig. 3.32).

Following optimisation of the various parameters required for the control and test lines an indirect competitive LFIA for the detection of AFB<sub>1</sub> was developed using the rat anti-AFB<sub>1</sub> monoclonal antibody. Nitrocellulose stripes were sprayed with the anti-rat (test line) and the anti-horse (control line). Standards of free AFB<sub>1</sub>, ranging in concentration from 0.39 – 25ng/ml, were prepared and mixed with an equal quantity of running buffer containing the AFB<sub>1</sub>-BSA and horse carbon conjugates. The mixed samples were allowed travel along the nitrocellulose membrane followed by 100 $\mu$ l of running buffer to wash the strips. The signal intensity of the test line increased as the concentration of free hapten decreased (Fig. 3.33). The control line remained constant on each strip. The limit of detection was then selected as the highest concentration that produced a test line and in this case was found to be 1.5ng/ml.

This chapter focused on the development of several immunoassay formats, incorporating the genetically derived scFvs, for the detection of AFB<sub>1</sub>. Table 3.13 summarises the limits of detection obtained with each immunoassay format. The limits of detection obtained using the competitive ELISAs compare favourably with published literature. Daly *et al.* has described competitive ELISAs for the detection of AFB<sub>1</sub> incorporating both polyclonal antibodies (2000) and monomeric scFvs (2002) with limits of detection of 3ng/ml and 98ng/ml, respectively. However, more sensitive ELISAs have been described by Candlish *et al.* (1985), Aldao *et al.* (1995) and Abouzied *et al.* (1998) with limits of detection at 0.2ng/ml, 0.25 $\mu$ g/kg (ppb), and 0.5ng/ml, respectively. Limits of detection described with the Biacore inhibition assays also compare positively with published literature on Biacore-based inhibition assays for the detection of AFB<sub>1</sub>. Van der Gaag *et al.* (1999) developed an assay in

spiked grain samples using a monoclonal antibody with similar detection limits of 0.2 ppb. Daly and collaborators developed an assay using a polyclonal antibody in PBS with a limit of detection of 3ng/ml (Daly *et al.*, 2000) and an scFv-based assay with a limit of detection of 3ng/ml in PBS and 0.75ng/ml in spiked grain (Daly *et al.*, 2002). The limits of detection described in this chapter also compare favourably with several other immunoassay formats including a fluorescence polarization assay for aflatoxins with a range of detection between 5 and 200ppb (Korde *et al.*, 2003) and a dipstick assay with a limit of detection of 2ng/ml (Schneider *et al.*, 1995). However, analytical techniques, including a HPLC detection system described by Kussak *et al.* (1995) with limits of detection for aflatoxins B<sub>1</sub>, B<sub>2</sub>, G<sub>1</sub> and G<sub>2</sub> at 6.8pg/ml in urine and an immunoaffinity fluorometric biosensor with a lower limit of detection at 0.1ppb (Carlson *et al.*, 2000) have offered greater levels of sensitivity. In the case of the lateral flow immunoassay, a sol-particle lateral flow immunoassay with limits of detection for AFB<sub>1</sub> at 0.1ppb in buffer and 10ppb in grain samples (Niessen *et al.*, 1998), has offered improved sensitivity, for the detection of AFB<sub>1</sub> in buffer, over the lateral flow developed using the AFB<sub>1</sub>-specific monoclonal antibody.

Although some assay formats described in the literature may offer lower limits of detection it must be noted that the assays described in this chapter are highly reproducible, with acceptable levels of sensitivity and specificity. The competitive ELISAs described are relatively cheap and cost effective, with the bifunctional scFv eliminating the need for secondary and tertiary detection antibodies, further reducing the cost and time of the assay. The ELISAs developed using the dimeric and bifunctional scFvs are also capable of detecting AFB<sub>1</sub> levels below the EU maximum residue level, which is set at 8ppb (ng/ml) in nuts and dried fruit subjected to sorting, or other physical treatment, for human consumption. The development of the Biacore inhibition assays enabled results to be viewed in real-time and offered in excess of a 10-fold increase in sensitivity over the competitive ELISAs. The Biacore inhibition assays also enabled detection of AFB<sub>1</sub> below the EU maximum residue level, which is set at 2ppb (ng/ml) in nuts, dried fruit and cereals for direct human consumption or as ingredients in foodstuffs. The lateral flow immunoassay described in this chapter is also relatively cheap and results are obtained within 5 – 10 min. The LFIA is also capable of detecting AFB<sub>1</sub> at levels below the EU maximum residue limits of 2ppb, in

nuts, dried fruit and cereals for direct human consumption or as ingredients in foodstuffs.

This chapter focused on the development of several immunoassays for the detection of AFB<sub>1</sub> using recombinant scFv antibodies and throughout the course of this study several advantages of recombinant antibody technology have been highlighted. Recombinant antibody techniques have provided an alternative unlimited source of antibodies with desirable affinity and specificity. Initially, a monomeric scFv was expressed using an antibody phage display library and used in the development of a competitive ELISA for AFB<sub>1</sub>. Although this scFv was specific for AFB<sub>1</sub> it was unable to detect levels as low as the EU maximum residue level, which is set at 8ppb (ng/ml) in nuts and dried fruit subjected to sorting, or other physical treatment, for human consumption. Using recombinant antibody technology the scFv was expressed as a dimeric fusion, altering the scFvs affinity and specificity for AFB<sub>1</sub>. In the competitive ELISA format the dimeric scFv offered increased affinity and specificity with a decrease in the limit of detection, enabling detection for AFB<sub>1</sub> below the EU maximum residue level, and a decrease in cross-reactivity levels with structurally related aflatoxins. The AFB<sub>1</sub>-specific scFv was also expressed as a dimerised form fused to an alkaline phosphatase enzyme and used in the development of a direct competitive ELISA. This also resulted in a lower limit of detection, enabling detection below the EU maximum residue level. The presence of the alkaline phosphatase label on the scFv eliminated the need for secondary and tertiary detection antibodies, reducing the cost and time of the assay. Similar results were noted following comparisons on the Biacore inhibition assays incorporating the monomeric and dimeric scFvs, with the dimeric scFv assay offering increased sensitivity over the monomeric assay.

## CHAPTER 4

The cloning and expression of an 18kDa cytoplasmic and  
a 26kDa periplasmic *Brucella*-specific protein

## 4.1 Introduction

The cloning and subsequent expression of recombinant *B. abortus* proteins offers several advantages over the isolation of native proteins from whole *B. abortus* cells. Cloning eliminates the need for growing large-scale cultures of this class III pathogen and provides an unlimited supply of the recombinant proteins that may have incorporated affinity tags enabling one-step purification.

### 4.1.1 TA cloning

The Original TA cloning kit provides a one step cloning strategy that allows the direct insertion of a Taq-polymerase-amplified PCR product into the pCR2.1 plasmid (Figure 4.1).

Following PCR with Taq-polymerase a non-template-dependent terminal transferase activity adds a single deoxyadenosine (A) to the 3' ends of the amplified PCR product. The PCR product can then be efficiently ligated into the linearised pCR2.1 plasmid because it has been engineered to contain 3' deoxythymidine (T) overhanging residues.

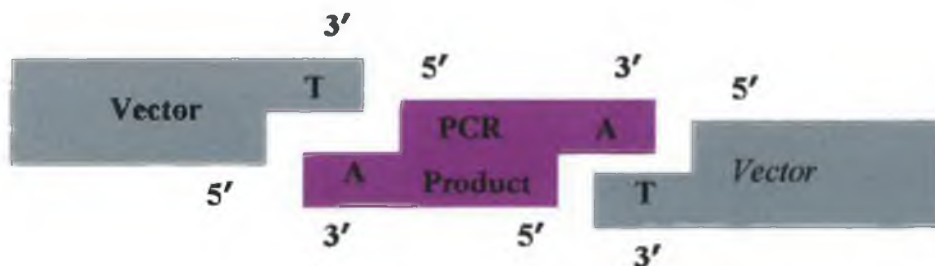


**Figure 4.1:** Schematic representation of the concept behind the TA cloning kit. The PCR product with its 3' single deoxyadenosine (A) overhang can be efficiently ligated into the linearised pCR2.1 vector with its 3' deoxythymidine (T) overhang.

#### 4.1.2 QIAexpress cloning

The QIAexpress system (Qiagen) provides a complete system for the cloning, expression, purification and detection of heterologous proteins. High-level expression of 6x-His-tagged proteins in *E. coli* is achieved using the QIAexpress pQE vectors, which in turn can be purified using nickel-nitrilotriacetic acid (Ni-NTA).

The pQE plasmids were derived from the plasmids pDS56/RBSII and pDS781/RBSII-DHFRS (Stuber *et al.*, 1990) and belong to the pDS plasmid family (Bujard *et al.*, 1987). Depending on the intended use of the expressed protein pQE vectors incorporating C- or N-terminal 6xHis tags can be used. When incorporating C-terminal His tags the cloned insert must be in-frame with the ATG start codon and the 6xHis tag. The use of a C-terminal His tag ensures only full-length proteins are purified.

pQE-60 results in the incorporation of a C-terminal 6xHis tag. A number of features present on this low-copy plasmid contribute to the efficient high-level expression of recombinant proteins (Fig. 4.2). The plasmid has a phage T5 promoter, which is recognised by the RNA polymerase from *E. coli* and two lac operator sequences, which cause an increase in lac repressor binding allowing for efficient repression of the T5 promoter. The plasmid also harbours a synthetic ribosomal binding site, RBSII, that increases the rate of translation and a sequence coding a 6xHis-tag 3' to the cloning region. pQE-60 also has a multiple cloning site (Fig. 4.3) and translational stop codons in all reading frames for convenient preparation of the expression construct. Two robust transcriptional terminators,  $t_0$  from phage lambda and T1 from the *rrnB* operon of *E. coli* are also encoded on the plasmid, which prevent read-through transcription and increase construct stability. The  $\beta$ -lactamase gene (*bla*), which confers ampicillin resistance at 100 $\mu$ g/ml, and the *colE1* origin of replication are also important features encoded for on the pQE-60 plasmid.

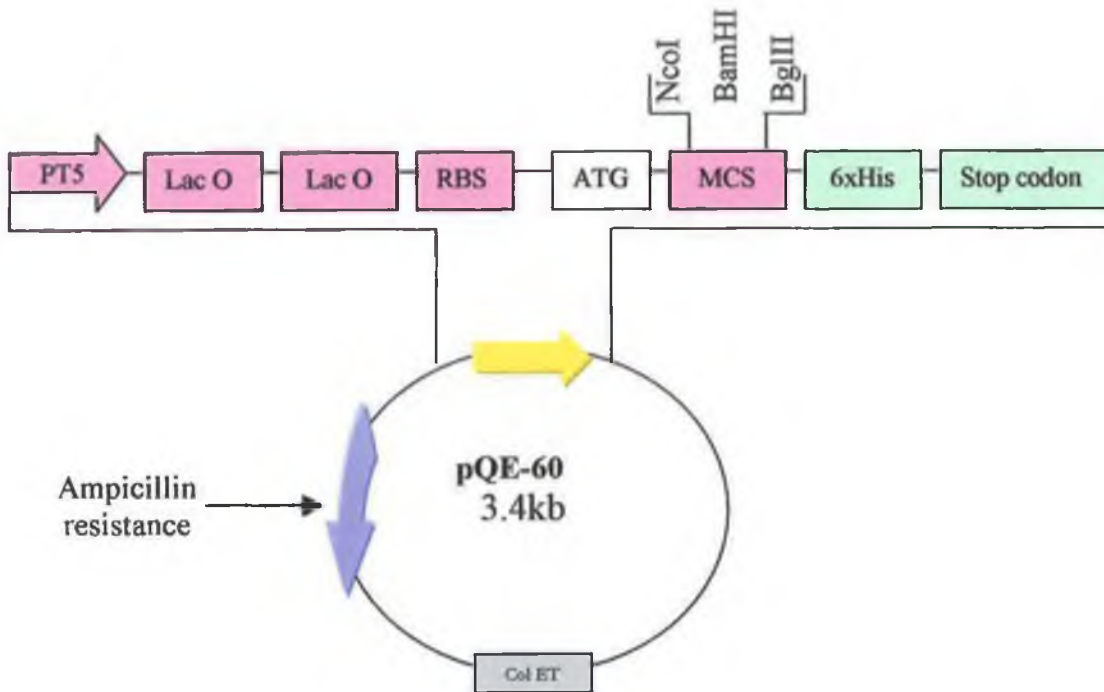


**Figure 4.2:** *pQE-60* vector used for C-terminal 6xHis tag constructs. PT5: T5 promoter, lacO: lac operator, RBS: ribosome binding site, ATG: start codon, 6xHis: 6xHis tag sequence, MCS: multiple cloning site with *Nco* I, *Bam* HI and *Bgl* III restriction sites, stop codons: Stop codons in all three reading frames, Col E1: Col E1 origin of replication.

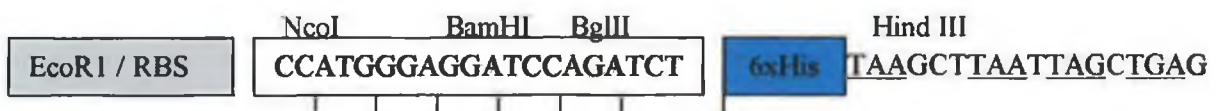


**Figure 4.3:** Multiple cloning site of *pQE-60* vector containing *Nco*I, *Bam*HI and *Bgl*III restriction sites.

### **4.1.3 Protein expression**

High-level recombinant protein expression using pQE-60 is induced upon addition of isopropyl- $\beta$ -D-thiogalactoside (IPTG). IPTG binds to the lac repressor protein resulting in its inactivation. This allows the host strains RNA polymerase to transcribe the sequence downstream of the promoter sequence with the resultant transcript being translated into the recombinant protein.

#### **4.1.3.1 Protein solubility**

Heterologous protein expression in *E. coli* can result in the formation of insoluble inclusion bodies. Although the QIAexpress system enables purification of inclusion bodies, following solubilisation with denaturing buffer, several approaches for the isolation of functional proteins have been described.

Several factors, including growth temperature, the promoter, plasmid copy number and inducer concentration, affect protein expression levels. Increased levels of protein expression can result in the formation of insoluble inclusion body. Therefore, reducing the rate of protein synthesis can lead to increased levels of soluble protein production. The ratio of soluble to insoluble protein can also be increased using non-metabolisable sugars such as sucrose, that have been shown to directly effect the folding of the protein (Bowden and Georgiou, 1990). Periplasmic expression can also increase the levels of soluble protein obtained. The periplasm offers an oxidising environment, which allows formation of disulphide bonds, exhibits reduced proteolysis, allows accumulation of toxic proteins and it contains two foldases (disulfide oxidoreductase (DsbA) and disulfide isomerase (DsbC)). These factors all play a role in protein solubility. Levels of soluble protein expression can also be increased with the co-expression of chaperones (Georgiou and Valax, 1996), which aid in protein folding, and the use of gene fusions, which consist of the target protein fused to a carrier protein such as *E. coli* thioredoxin (TRX) (LaVallie *et al.*, 1993) and glutathione S-transferase (GST) (Ghosh *et al.*, 1995 and Smith and Johnson, 1988).

#### 4.1.3.2 Expression hosts

Recombinant protein expression can be produced in a variety of expression hosts including *E. coli*, mammalian cells, insect cells using baculovirus, vectors, yeast and plants. The selection of the expression host depends on the intended use of the protein, with *E. coli* incapable of performing post-translational modifications.

##### 4.1.2.2.1 *E. coli*

Up until the mid-90's *E. coli* was the preferred host strain due to its ease of handling and detailed working knowledge available on its capacity and performance. *E. coli* was the first host strain for recombinant protein expression when used for the expression of human insulin (Swartz, 2001).

The QIAexpress system recommends the use of the *E. coli* strain M15 [pREP4], when using pQE-60 for high-level protein expression. M15 [pREP4] contain a low copy number of the pREP4 plasmid, which encodes a gene, *lacI*, for the constitutive expression of the *lac* repressor protein. High levels of the *lac* repressor protein are required to control the exceptionally high transcription rate, which is initiated by the T5 promoter. *E. coli* host strains, such as XL1 Blue, TG1 and XL-10 Gold, harbouring the *lacI<sup>q</sup>* mutation also produce enough *lac* repressor to efficiently regulate and repress protein expression.

When using *E. coli* for the expression of recombinant proteins it is important to take into account the fact that the tRNAs that recognise certain codons are rarely found. For example the tRNAs that recognise the codons AGG and AGA, which encode arginine, are among the least abundant in *E. coli*. If the recombinant protein being expressed contains several of this rare codons a truncated version of the protein is likely to be produced. For this reason it is necessary to establish the number of rare codons within the protein sequence. If several rare codons are located within the sequence it maybe necessary to express the protein in a host strain, which contains an extra plasmid that encodes these rare tRNAs. The bacterial host strains Rosetta and RosettaBlue have been engineered to contain a chloramphenicol resistant plasmid, pRARE that encodes tRNAs for the codons AUA, AGG, AGA, CUA, CCC, and GGA (Fig. 4.4), therefore, allowing the universal expression of proteins, which would otherwise be limited by the codon usage of *E. coli*.

XL 10-Gold cells are derivatives of Stratagene's highest-efficiency competent cell line XL2-Blue MRF' and contain the Hte phenotype, which increases transformation efficiency of ligated DNA molecules. XL 10-Gold cells also grow faster than XL1 and XL2-Blue cells, resulting in larger colonies. XL 10-Gold cells are endonuclease-deficient (*endA1*), which greatly improves the quality of plasmid miniprep DNA, and recombination-deficient (*recA*), which ensures insert stability. The *mcrA*, *mcrCB* and *mrr* mutations prevent cleavage of the cloned DNA that carries cytosine and/or adenine methylation, which is often present in eukaryotic DNA and cDNA. The *hsdR* mutation prevents the cleavage of the cloned DNA by the EcoK endonuclease system.

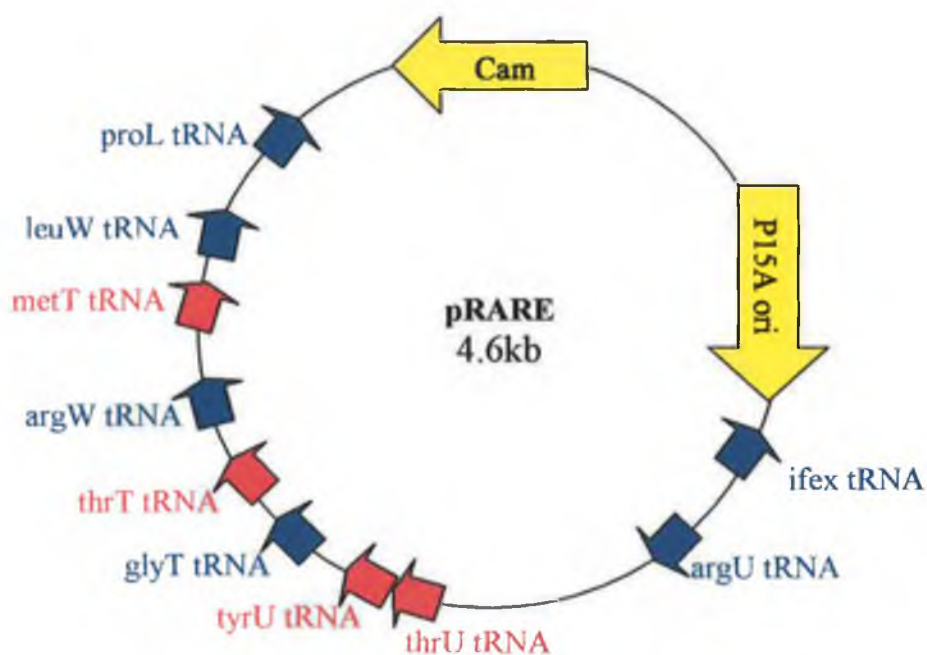


**Figure 4.4:** Map of the pRARE plasmid family. A chloramphenicol resistance gene (*Cam*), a replicon (*P15A ori*) and tRNA genes, with the rare *E. coli* codons in blue, are encoded on the pRARE plasmid.

#### 4.1.2.2.2 Yeast

Eukaryotic protein expression in yeast offers the distinct advantage of providing most eukaryotic post-translational modifications with the protein folding pathways and codon usage mimicking that of mammalian cells (Cho *et al.*, 1998). The ease of

handling also makes the use of yeast as expression hosts appealing. The two most commonly used yeast expression systems involve *Saccharomyces cerevisiae* and *Pichia pastoris*. *P. pastoris* has been successfully applied to the expression of human chitinase (Goodrick *et al.*, 2001), insulin precursors (Wang *et al.*, 2001) and recombinant scFv antibody fragments (d'Anjou and Daugulis, 2001 and Hellwig *et al.*, 2001). *E. coli* / yeast shuttle plasmids are the most commonly used expression vectors (Baldarini and Cesareni, 1985 and Clare *et al.*, 1991). The expression vectors are easily introduced into the yeast cells using either electroporation or transformation into competent cells. Protein expression is induced using either the galactosidase-inducible system in *S. cerevisiae* or the methanol-driven induction in the methylotropic, *P. pastoris*.

#### **4.1.2.2.3 Baculovirus**

The baculovirus is capable of infecting and multiplying within cultured insect cells making it possible to express heterologous proteins within insect cells. Insect cells offer comparative advantages to mammalian cells, which include ease of culture, higher expression-levels and higher osmolality and by-product concentration tolerance (Ikonomou *et al.*, 2003). Insect cells are also capable of performing post-translational modification such as glycosylation, phosphorylation, precursor processing and targeting. *Autographa californica* nuclear polyhedrosis virus (AcMNPV), a lytic virus that infects lepidopterans, is the most widely used virus. The most frequently used insect cell lines are Sf9 and Sf21. Following cloning of the gene into a plasmid transfer vector, the DNA is co-transferred into the insect cell along with a double stranded baculovirus DNA. The gene of interest is incorporated into the viral genome following homologous recombination of the plasmid and insert DNA with the viral DNA.

#### **4.1.2.2.4 Mammalian cells**

Although expression levels from mammalian cells are generally low they provide the same post-translational modifications and recognise the same synthesis, processing and secretion signals for recombinant vertebrate proteins. Several mammalian systems have been developed for the high-level expression of recombinant proteins with Chinese hamster ovary (CHO), human embryonic kidney (HEK) and baby hamster kidney dominating the field (Wurm and Bernard, 1999). The expression vectors

contain a strong promoter such as the cytomegalovirus (CMV) for transcription initiation, mRNA processing signals such as mRNA cleavage and polyadenylation sequences and markers for the selection of cells containing the stably integrated DNA. Mammalian expression vectors can also contain sequences for the controlled induction of expression using an external stimulus such as  $\beta$ -interferon, heavy metal ions, glucocorticoids and heat shock. A number of plasmid DNA delivery systems for mammalian cells have been described, which include calcium phosphate DNA co-expression (Graham and Van der Eb, 1973), polyethyleneimine (PEI) DNA complexes (Boussif *et al.*, 1995) and electroporation (Chu *et al.*, 1987).

#### **4.1.3.3 The 6xHis tag**

The 6xHis tag is relatively small (0.84kDa) in comparison to other affinity tags such as glutathione-S-transferase (26kDa) and maltose-binding protein (40kDa). Its small size, low immunogenicity and absence of charge at pH8.0 means it does not usually interfere with protein secretion, compartmentalisation or folding within the host strain. The 6xHis tag also allows the linkage of the tagged protein to a metal chelating surface enabling immobilised metal affinity chromatography (IMAC) (See Section 4.1.3.1). Detection of the expressed protein is easily achieved using anti-His antibodies.

#### **4.1.4 Immobilised metal affinity chromatography (IMAC)**

Porath and associates (1975) were first to introduce the use of immobilised metal affinity chromatography (IMAC), while working on the fractionation of proteins from human serum. Since then hundreds of papers have been published detailing the use of IMAC for group purification and the highly selective purification of target proteins from complex biological samples. Hochuli and co-workers (1987 and 1988) were first to apply IMAC for the purification of recombinant proteins containing engineered N- or C-terminus histidine tags.

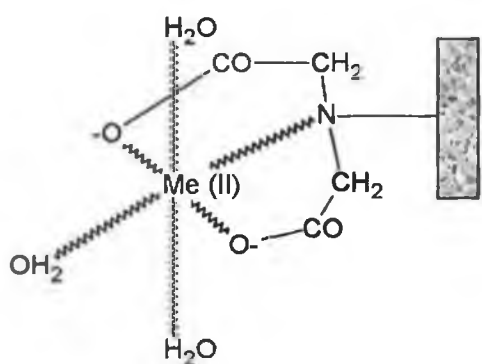
The principle of IMAC is based on the affinity of proteins for immobilised metal ions. The interaction between the immobilised metal ions and the side chains of amino acids is reversible under mild conditions. IMAC offers a number of advantages over conventional biospecific chromatographic techniques, including low cost, ligand

stability, mild elution conditions, simple regeneration and high protein loading (Arnold, 1991). IMAC also offers the distinct advantage of its applicability to protein purification under both native and denaturing conditions since the interaction between the Ni-NTA and the 6xHis tagged recombinant protein does not depend on the tertiary structure.

Protein adsorption during IMAC is based on the coordination between an immobilised metal ion and electron donor groups on the protein surface. Transition metal ions including Zn (II), Cu (II), Co (II) Ni (II) and Fe (III), which act as electron-pair acceptors, are most commonly used. The metal ions are attached to the chromatographic support via electron donor atoms (N, S, O) in the chelating compounds forming metal chelates, which may be bidentate, tridentate etc., depending on the number of occupied coordination bonds (Gaberc-Porekar and Menart, 2001). The remaining coordination sites, generally occupied by water molecules, can then be exchanged with suitable electron-donor groups from the target protein. Several amino acids such as Glu, Asp, Tyr, Cys, His, Arg, Lys and Met can participate in metal adsorption, with IMAC primarily focusing on the availability histidine residues. In neutral or slightly basic solutions the nonprotonated imidazole nitrogens in the histidine residues adsorb the IMAC support, with the reduction in non-specific electrostatic interactions observed using relatively high-ionic strength buffers (0.1 – 1M NaCl). Elution of the immobilised protein can be achieved by means of protonation using a pH shock, ligand exchange using imidazole or metal ion chelation using a strong chelator such as EDTA. The affinity of a protein for metal chelates depends strongly on the metal ion involved, with  $\text{Cu (II)} > \text{Ni (II)} > \text{Zn (II)} \geq \text{Co (II)}$  showing increasing affinities. There are several commercially available chelating ligands, which include iminodiacetic acid (IDA) (Amersham Pharmacia Biotech, TosoHaas, Sterogene), nitrilotriacetic acid (NTA) (Qiagen), carboxymethylated aspartic acid (CM-Asp) (Clontech) and tris-carboxymethyl ethylene diamine (TED) (Inovata), with the IDA offering tri-dentate, the NTA and CM-Asp offering tetra-dentate and the TED adsorbent offering penta-dentate complexes with the corresponding metal ion (Fig. 4.5). The tetra-dentate chelators offer higher affinities for metal ions than the tri-dentate ligands but may exhibit decreased protein binding due to the loss of one coordination site. The lower binding

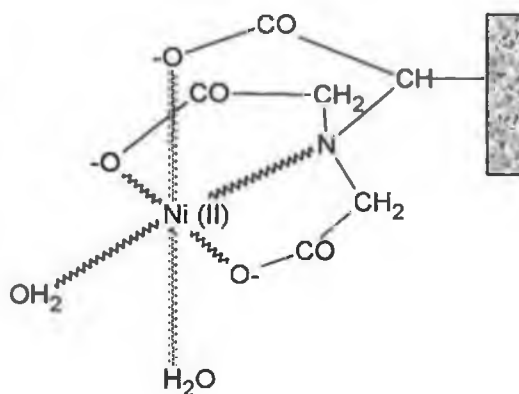
capacity is even more evident with the penta-dentate ligands with only one protein binding coordination site remaining. However, the use of the tri-dentate IDA chelator results in weak binding to the metal ions, which leads to the leaching of strongly chelating peptides and proteins. This results in low protein yields, impurities and metal ion contamination following purification. The QIAexpress system recommends the use of the nitrilotriacetic acid (NTA) containing the four metal-chelating sites because it binds to the metal ions more stably and retains them under stringent washing and eluting conditions.

(A)



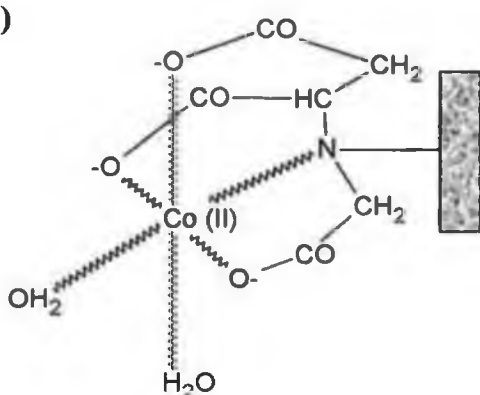
IDA-Me (II)

(B)



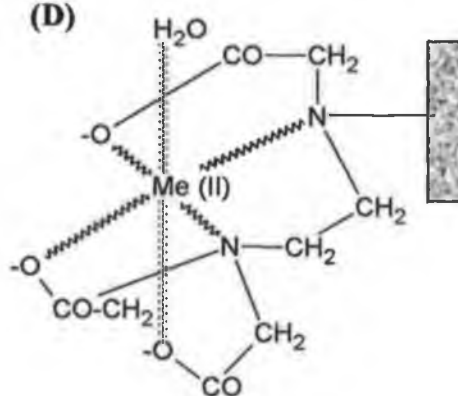
NTA-NI (II)

(C)



CM-Asp-Co (II)

(D)



TED-Me (II)

**Figure 4.5:** Structures of commercially available immobilised metal affinity chromatography (IMAC) chelators complexed with metal ions. Me (II) represents Cu (II), Ni (II), Zn (II) or Co (II). A: Iminodiacetic acid (IDA) (Amersham Pharmacia Biotech, TosoHaas, Sterogene); B: Nitrilotriacetic acid (NTA) (Qiagen); C:

*Carboxymethylated aspartic acid (CM-Asp) (Clontech); D: Tris-carboxymethyl ethylene diamine (TED) (Inovata).*

#### **4.1.5 Chapter outline**

This chapter focuses on the cloning and expression of two recombinant *B. abortus* proteins, p18 and bp26. A two step cloning strategy incorporating TA cloning and subsequent QIAexpress cloning enabled the successful cloning and expression of the two recombinant proteins (Fig. 4.6).

Total genomic DNA was isolated from heat-killed *B. abortus* 45/20 cells and used as template DNA for the PCR amplification of the p18 and bp26 specific genes. The Taq DNA polymerase amplified PCR products containing the deoxyadenosine (A) overhangs was then ligated into the linearised pCR2.1 plasmid containing the deoxythymidine (T) overhanging residues. The pCR2.1 plasmid DNA encoding the gene of interest was purified (following the identification of a successfully transformed INV $\alpha$ F' *E. coli*). The cloned insert gene was isolated from the pCR2.1 plasmid following a BamH1/Nco1 restriction digest and then directionally ligated into the high-level expression vector pQE-60, that was previously linearised following a BamH1/Nco1 restriction digest. The ligated pQE-60 and cloned insert were then transformed into competent XL-10 Gold *E. coli* for subsequent protein expression.

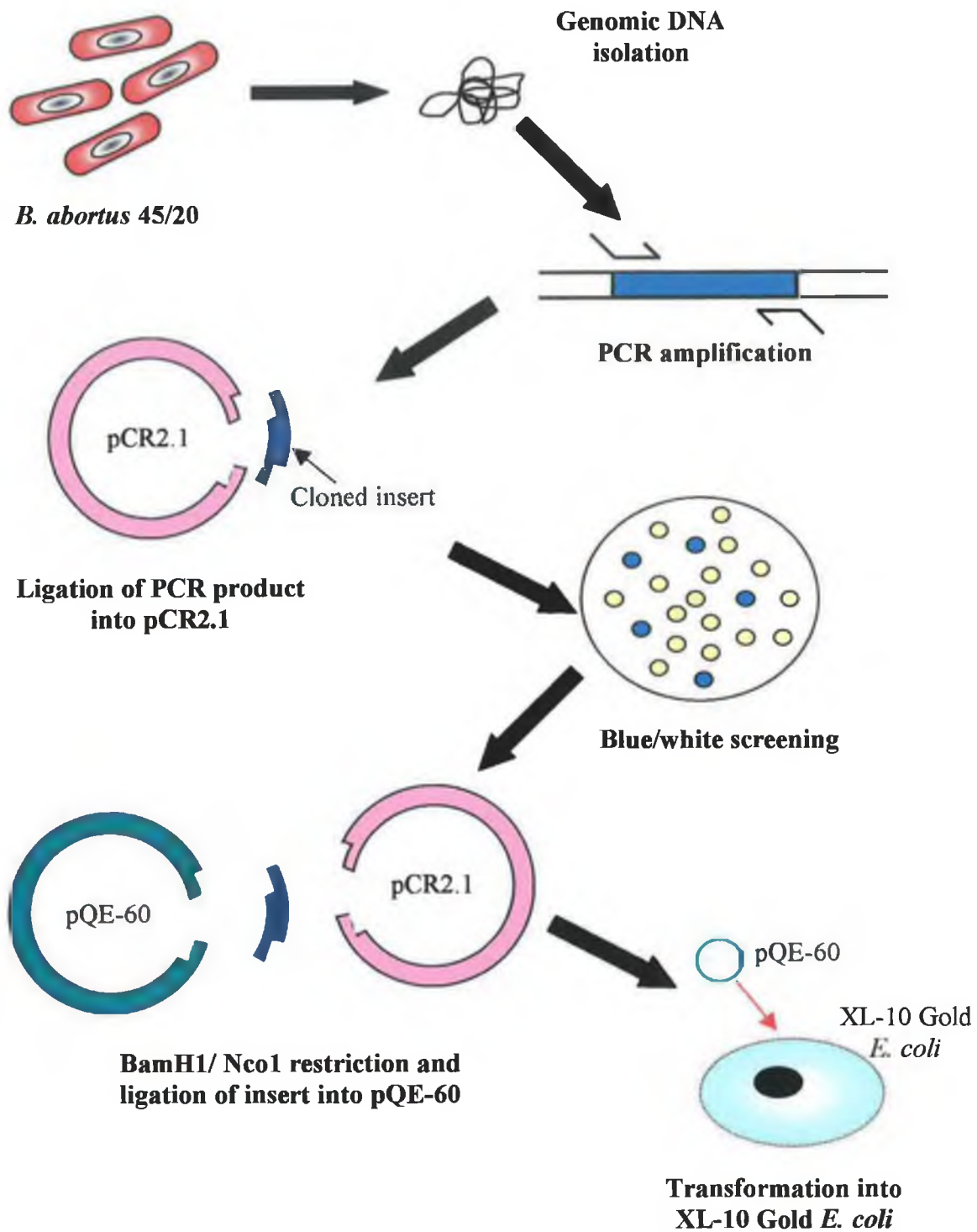


**Figure 4.6:** Schematic representation of the two-step cloning strategy. Following PCR amplification of the DNA sequence encoding the recombinant protein, the DNA insert is ligated into the vector pCR2.1. From there the insert is sub-cloned into the high-level expression vector pQE-60. The recombinant protein is then expressed in XL10 Gold *E. coli* cells, with a 6xHis tag attached to the C-terminus to aid in purification and detection.

## 4.2 Results

### 4.2.1 PCR amplification of the genes encoding p18 and bp26

Total genomic DNA was extracted from heat-killed *Brucella abortus* 45/20 cells as described in Section 2.3.1 and electrophoresed on an agarose gel (Fig. 4.7). The genomic DNA was used as a template for the amplification of the p18 and bp26 genes. Forward and reverse primers were engineered for each gene with NcoI and BamHI restriction sites incorporated for the subsequent directional cloning into the high-level expression vector pQE-60. The optimum annealing temperature for use with each gene was determined using a temperature gradient PCR. This involved carrying out several standard PCR reactions with varying annealing temperatures, ranging from 58 - 65°C. The optimum annealing temperature for the amplification of each gene was found to be 65°C (Fig. 4.8). Following optimisation of the conditions for PCR the p18 and bp26 genes were amplified for ligation onto the pCR2.1 plasmid. Figure 4.9 shows the optimised PCR amplification of the genes encoding p18 (Lane 2) and bp26 (Lane 4) with bands visible at approximately 485 and 785bp, respectively.

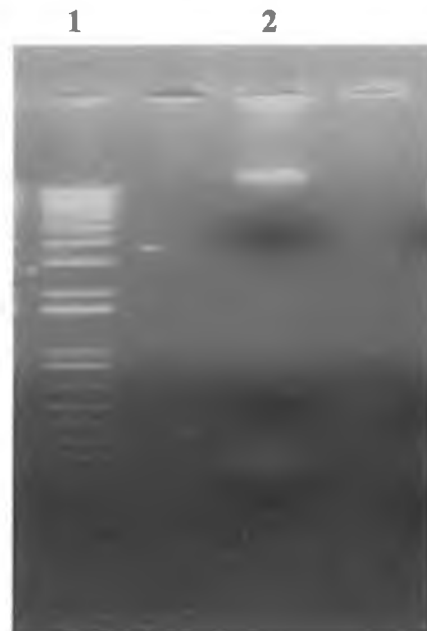


**Figure 4.7:** Total genomic DNA isolated from *Brucella abortus* 45/20. Lane 1: 1Kp DNA plus Ladder. Lane 2: Total genomic DNA from *B. abortus* 45/20.

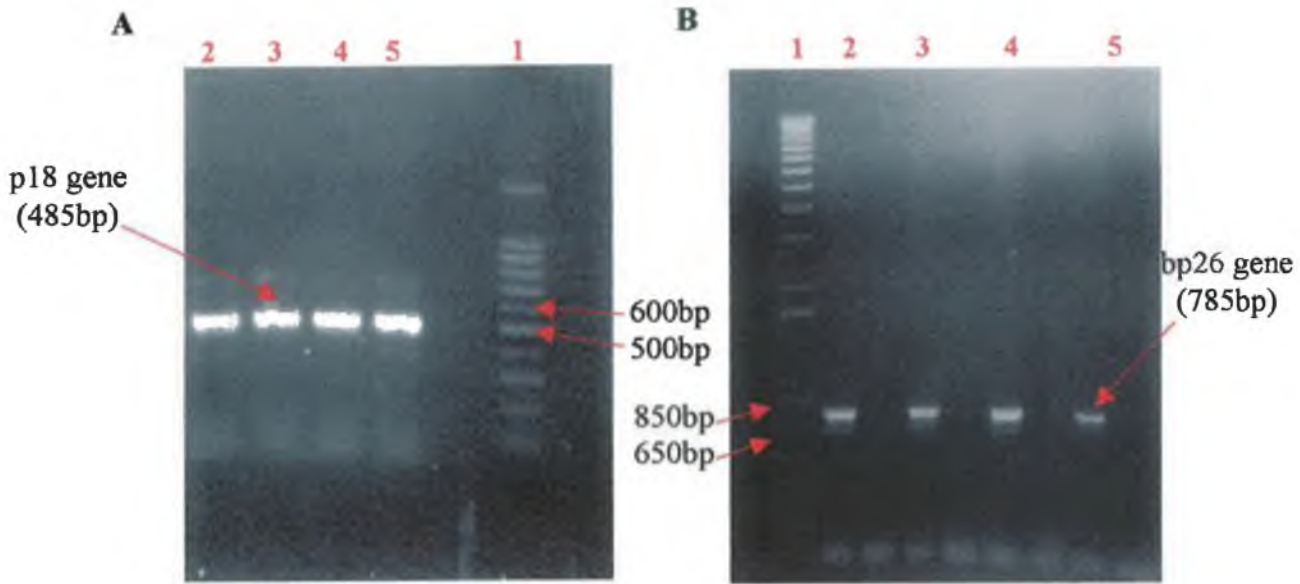


**Figure 4.8:** Optimisation of annealing temperature for use in the PCR amplification of the genes encoding p18 and bp26. **A:** Temperature gradient PCR for p18. Lane 1: 100bp DNA ladder; Lane 2: Annealing temperature (AT) of 58 °C; Lane 3: AT of 60 °C; Lane 4: AT of 62 °C; Lane 5: AT of 65 °C. **B:** Temperature gradient PCR for bp26. Lane 1: 1Kb plus DNA ladder; Lane 2: Annealing temperature (AT) of 58 °C; Lane 3: AT of 60 °C; Lane 4: AT of 62 °C; Lane 5: AT of 65 °C.

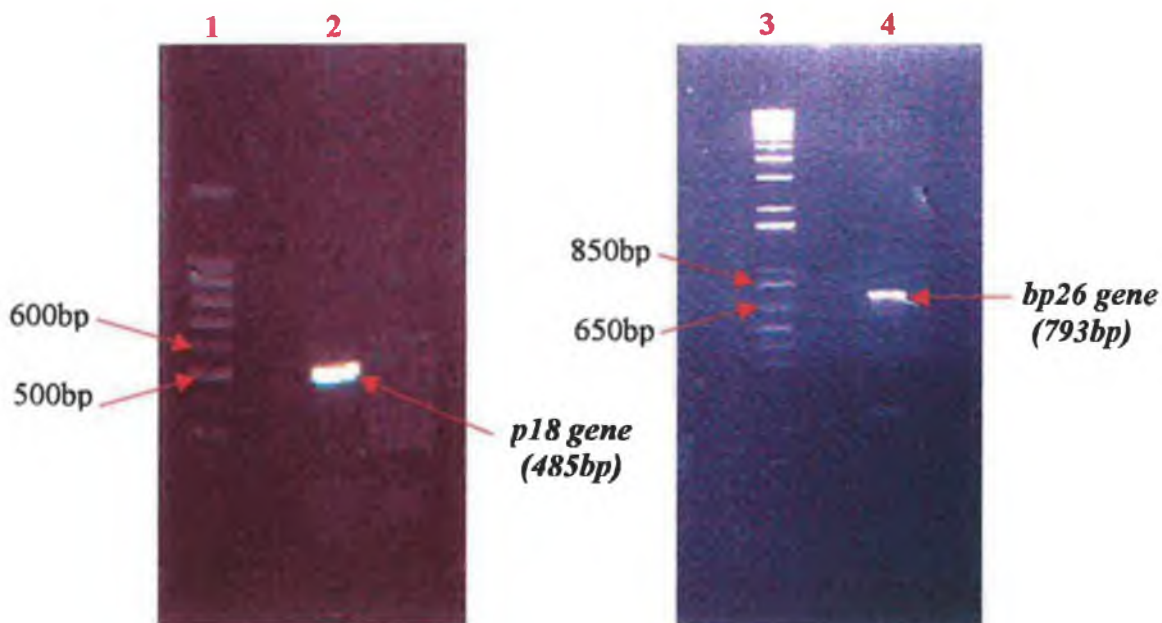


**Figure 4.9:** Optimised PCR on the genes encoding p18 and bp26. The PCR products were amplified using an optimised annealing temperature of 65 °C. Lane 1: 100bp DNA ladder; Lane 2: PCR amplification of the gene encoding p18; Lane 3: 1Kb plus DNA ladder Lane 4: PCR amplification of the gene encoding bp26.

#### 4.2.2 TA cloning

The Original TA cloning kit provides a one step cloning strategy that allows the direct insertion of a Taq-polymerase-amplified PCR product into the pCR2.1 plasmid (as described in Section 4.1.1). The PCR amplified genes encoding p18 and bp26 were ligated into the pCR2.1 and the ligation transformed into competent INV $\alpha$ F' *E. coli*, which were provided with the Original TA Cloning Kit. The presence of the multiple cloning sites within the LacZ gene of the pCR2.1 vector enables blue/white colony selection. The LacZ gene encodes the enzyme beta-galactosidase, which metabolises X-gal resulting in the formation of blue colonies. However, positive transformants containing the cloned insert disrupt the LacZ gene and colonies appear colourless, when screened on X-gal plates following transformation. Five positive transformants (white colonies) were selected for each gene and grown up individually. The pCR2.1 plasmid DNA was isolated from each clone and analysed using a BamHI / NcoI restriction digest for the presence of the 485bp or 793bp insert. Figure 4.10 shows the agarose gel analysis for the restriction analysis on the p18 clone bp26 clones, with bands clearly visible at 485 and 793bp, respectively.

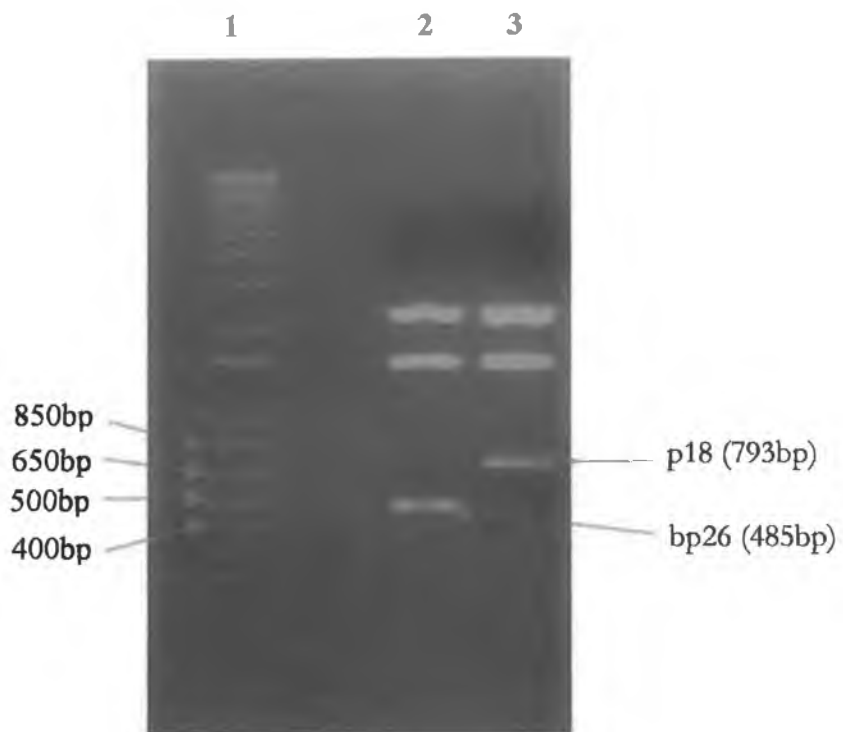


**Figure 4.10:** *Bam*HI and *Nco*I restriction digest on the p18 and bp26 pCR2.1 clones. Lane 1: 1Kb plus DNA ladder; Lane 2: *Bam*HI/*Nco*I restriction digest on the pCR2.1 vector containing the gene encoding p18; Lane 3: *Bam*HI/*Nco*I restriction digest on the pCR2.1 vector containing the gene encoding bp26.

#### **4.2.3 Sub-cloning from pCR2.1 into pQE-60 and subsequent transformation into competent XL-10 Gold *E. coli***

The next stage of the cloning strategy involved sub-cloning the p18 and bp26 genes from the pCR2.1 vector into the high-level expression vector pQE-60. Protein expression from pQE-60 results in the incorporation of a C-terminal 6xHis tag for ease in purification and analysis. Initially, a BamHI / NcoI restriction digest was carried out on the pCR2.1 vector containing the genes encoding p18 and bp26 (See Section 2.3.6). The 485 and 793bp fragments encoding the p18 and bp26, respectively, were then gel-purified as described in section 2.2.5. A BamHI / NcoI restriction digest was used to linearise the pQE-60, which was also gel purified (See Section 2.3.6). The p18 and bp26 genes were directionally cloned into the pQE-60 vector using T4 DNA ligase and the ligated pQE-60 transformed into CaCl<sub>2</sub> competent XL-10 Gold *E. coli* cells. Screening for positive transformants was performed on LB agar plates containing ampicillin and kanamycin. Figure 4.11 shows the BamHI/NcoI restriction digests on the pQE-60 plasmid DNA. pQE-60 plasmid DNA containing no cloned insert was restricted (Lanes 2&3) along with pQE-60 plasmid DNA containing the cloned p18 (Lanes 4&5) and bp26 (Lanes 6&7) genes. Bands clearly visible at 485 and 793bp represent the cloned p18 and bp26 genes, respectively.

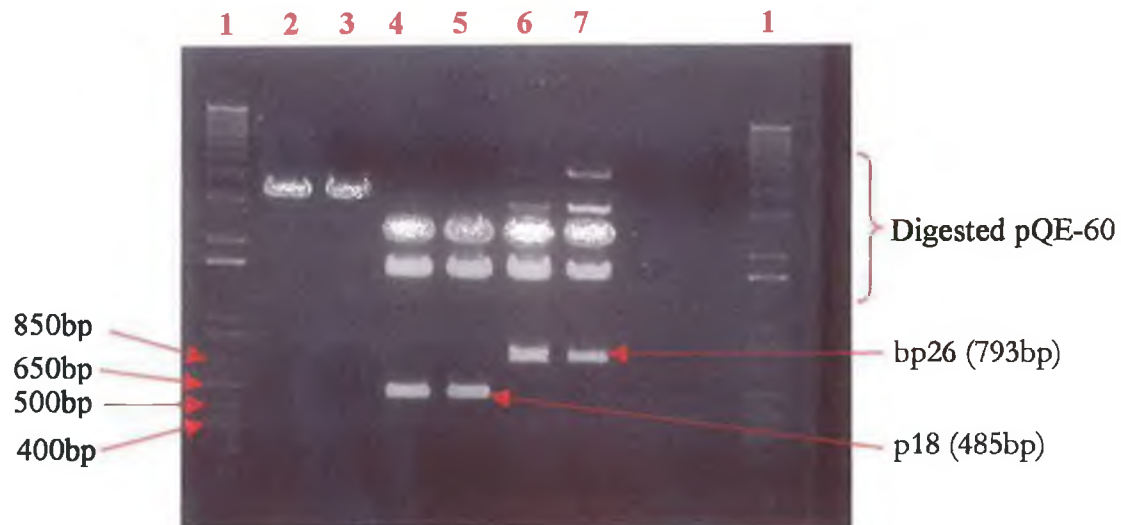


**Figure 4.11:** *Bam*H1 and *Nco*I restriction analysis on the pQE-60 clones following transformation into XL-10 Gold *E. coli*. Lane 1: 1Kb plus DNA ladder; Lane 2 & 3: *Bam*H1/*Nco*I digested on pQE-60 plasmid DNA containing no cloned insert; *Bam*H1/*Nco*I digested on pQE-60 plasmid DNA containing the p18 cloned insert; Lanes 6 & 7: *Bam*H1/*Nco*I digested on pQE-60 plasmid DNA containing the bp26 cloned insert.

#### 4.2.4 Initial small-scale protein expression

Following the successful transformation of the competent XL-10 Gold *E. coli* with the pQE-60 vectors containing the appropriate genes, small-scale expression cultures were carried out on a number of clones, to determine host strain suitability as described in Section 2.3.11.

Single colonies were picked from a freshly streaked plate and used to inoculate 5ml of 2x TY containing the appropriate antibiotics. The culture was grown overnight at 37°C overnight and used to inoculate a 20ml culture of 2x TY containing the appropriate antibiotics. The culture was incubated at 37°C, while shaking, until OD<sub>550</sub> reached approximately 0.5. Protein expression was then induced upon addition of 1mM IPTG. The induced culture was then further incubated for 4 hours at 37°C, while shaking. The bacterial cells were then pelleted following centrifugation, at 4000rpm for 20 min, and the supernatant discarded. The bacterial pellet was then resuspended in 1ml of denaturing buffer and sonicated for 30 secs at 220W. Cell debris was then removed following centrifugation, at 13,000rpm for 15 min, and the supernatant analysed by SDS-PAGE in order to confirm protein expression.

SDS-PAGE analysis on the p18 and bp26 initial expression cultures yielded the appropriate bands at 18kDa and 26kDa. The SDS-PAGE analysis on the initial small-scale expression cultures of p18 can be seen in Figure 4.12. A band at 18kDa is clearly visible in 4 out of 5 clones analysed, which represents the expressed p18 protein. Figure 4.13 shows the SDS-PAGE obtained following the initial expression cultures on the bp26 protein in XL-10 Gold. A band at 26kDa is clearly visible in each of the 5 clones analysed, which represents the expressed bp26 protein. Indicating that the two recombinant proteins, p18 and bp26, were successfully expressed in XL-10 Gold from the high-level expression vector pQE-60.

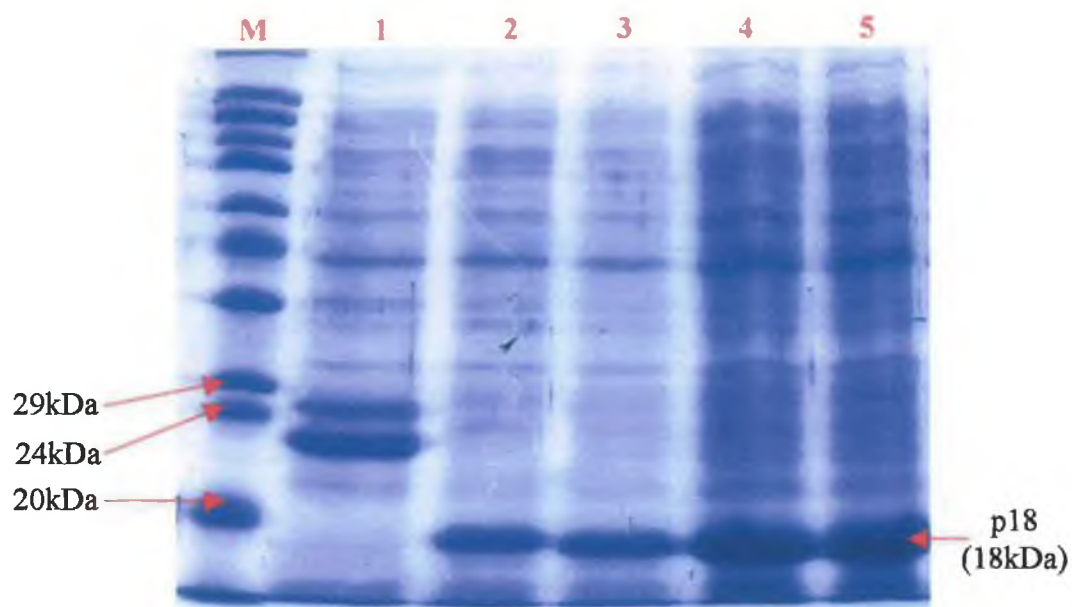


**Figure 4.12:** SDS-PAGE analysis on the small-scale expression cultures of p18. Following the transformation of XL-10 Gold *E. coli*, with the ligated pQE-60 and p18 gene, 5 clones were analysed post IPTG induction. Lane M: Sigma wide-range molecular weight markers; Lane 1: Small-scale expression cultures on p18 clone 1; Lane 2: Small-scale expression cultures on p18 clone 2; Lane 3: Small-scale expression cultures on p18 clone 3; Lane 4: Small-scale expression cultures on p18 clone 4; Lane 5: Small-scale expression cultures on p18 clone 5. A band at 18kDa is clearly visible following induction of protein expression in clones 2-5.

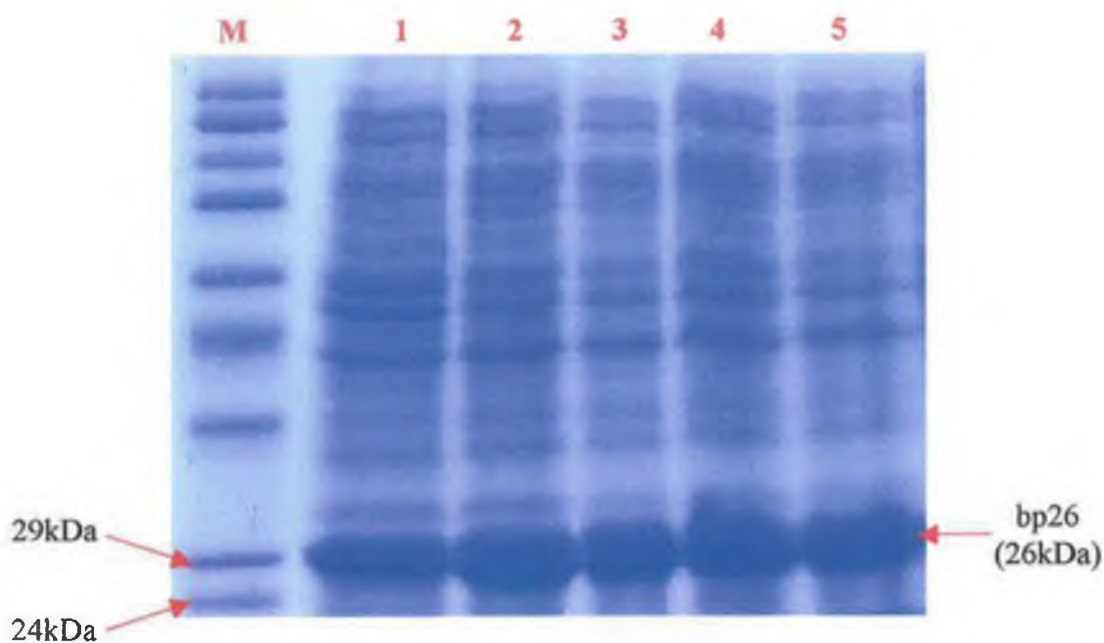


**Figure 4.13:** SDS-PAGE analysis on the small-scale expression cultures of bp26. Following the transformation of XL-10 Gold *E. coli*, with the ligated pQE-60 and bp26 gene, 5 clones were analysed post IPTG induction. Lane M: Sigma wide-range molecular weight markers; Lane 1: Small-scale expression cultures on bp26 clone 1; Lane 2: Small-scale expression cultures on bp26 clone 2; Lane 3: Small-scale expression cultures on bp26 clone 3; Lane 4: Small-scale expression cultures on bp26 clone 4; Lane 5: Small-scale expression cultures on bp26 clone 5. A band at 26kDa is clearly visible following induction of protein expression in each of the 5 clones.

#### 4.2.5 Protein solubility determination

The high-level expression of recombinant proteins in *E. coli* may result in the formation of insoluble inclusion bodies, consisting of aggregates of the expressed protein (See section 4.1.3.1). Protein solubility determination enables high-level recombinant protein recovery, following optimisation of the buffer required for protein isolation.

Single colonies of XL-10 Gold *E. coli*, harbouring pQE-60 encoding the p18 or bp26 proteins, were picked from a freshly streaked plate and used to inoculate 5ml of 2x TY containing the appropriate antibiotics. The culture was grown at 37°C overnight and used to inoculate a 10ml culture of 2x TY containing the appropriate antibiotics. The culture was incubated at 37°C, while shaking, until the OD<sub>550</sub> reached approximately 0.5. Protein expression was then induced upon addition of 1mM IPTG. The induced culture was then further incubated for 4 hours at 37°C, while shaking. The bacterial cells were then pelleted by centrifugation, at 4000rpm for 20 mins, and the supernatant discarded. The bacterial pellet was resuspended in 1ml of dH<sub>2</sub>O and sonicated for 30sec. at 220W. Following centrifugation, at 13,000rpm for 15 mins, the supernatant (soluble protein) was analysed by SDS-PAGE. The pellet was resuspended in 1ml of denaturing buffer and sonicated for 30sec 220W. Following centrifugation, at 13,000rpm for 15 mins, the supernatant (insoluble protein) was analysed using SDS-PAGE.

The protein solubility determination for p18 and bp26 can be seen in Figure 4.14. Although, some soluble expression of p18 and bp26 was observed (Lanes 2 and 4, respectively), the majority of the expressed p18 and bp26 forms insoluble inclusion bodies, which were solubilised using 8M urea (Lanes 2 and 4, respectively). This suggests the need for denaturing buffer (containing 8M urea) for the subsequent isolation of recombinant p18 and bp26, following high-level expression in XL-10 Gold *E. coli*. A web-based bioinformatics program was also used to determine the solubility of the recombinant proteins (Harrison, 2000). Based on the amino acid sequence of the protein this model uses the approximate charge average, which accounts for the differences in the numbers of Asp plus Glu verses Lys plus Arg residues, and the turn-forming residue content, which accounts for the total number of

Asn, Gly, Pro, and Ser residues, to determine the protein solubility. This program estimated that the p18 protein had a 62% chance of solubility and that the bp26 protein had an 80% chance of insolubility, therefore, confirming the need for denaturing buffer, containing 8M urea, for the solubilisation and isolation of the recombinant p18 and bp26 proteins, following expression in XL-10 Gold *E. coli*.

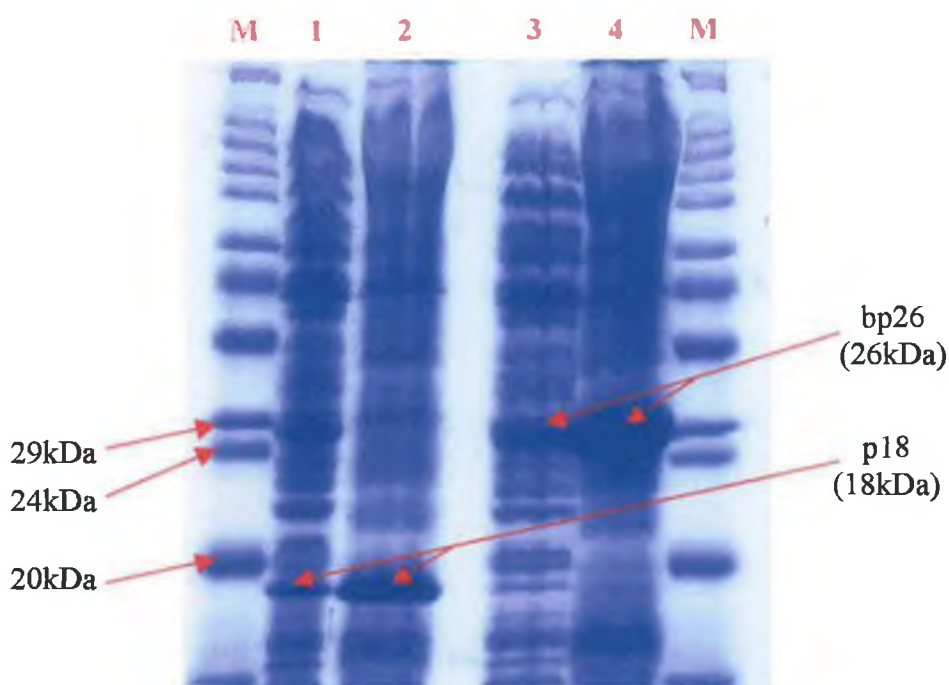


**Figure 4.14:** SDS-PAGE analysis on the solubility determination following p18 and bp26 expression in XL-10 Gold. Lane M: Sigma wide-range molecular weight markers; Lane 1: Isolation of soluble p18 under native conditions; Lane 2: Isolation of insoluble p18 under denaturing conditions; Lane 3: Isolation of soluble bp26 under native conditions; Lane 4: Isolation of insoluble bp26 under denaturing conditions.

#### 4.2.6 Optimisation of IPTG concentration for induction of protein expression

Expression of p18 and bp26, from pQE-60, is rapidly induced upon addition of isopropyl- $\beta$ -D-thiogalactoside (IPTG). The IPTG binds to the *lac* repressor protein and inactivates it. Once the *lac* repressor is inactivated, the host cell's RNA polymerase can transcribe the sequence downstream from the promoter. The transcript produced can then be translated into the recombinant protein either for p18 or bp26. However, the concentration of IPTG required for induction must be optimised, so that the highest level of protein expression is achieved without the level of protein expression and IPTG concentration becoming toxic to the cell. IPTG concentrations ranging from 0.01 – 1mM were used in order to determine the optimal concentration required for the high-level protein expression in XL 10-Gold.

Expression cultures of the XL-10 Gold *E. coli*, harbouring pQE-60 encoding the p18 or bp26 proteins, were prepared, as described in Section 4.2.5, except that individual cultures were induced using varying IPTG concentrations ranging from 0 – 1mM. Following induction, the cultures were incubated for 4 hours at 37°C and then the bacteria were pelleted by centrifugation, at 4000rpm for 20 mins. The resulting pellets were resuspended in 2ml of denaturing buffer and sonicated for 30 secs at 220W. The lysed cells were centrifuged, at 13,000rpm for 15 mins, and the supernatants analysed by SDS-PAGE.

Figures 4.15 and 4.16 show the gel pictures obtained for the expression of p18 and bp26, respectively, in XL 10-Gold *E. coli*, following induction with the various IPTG concentrations. In each case 0.5mM IPTG appeared to be the optimal concentration for the expression of p18 and bp26. The levels of p18 and bp26 expression were estimated, at each IPTG concentration, using ImageJ software, which monitors the band intensities on an SDS-PAGE. Tables 4.1 and 4.2 display the expression levels of p18 and bp26, respectively, as a percentage of the total protein content. The levels of p18 and bp26 expressed at each IPTG concentration suggested that 0.5mM IPTG was optimal for the induction of p18 and bp26, with the highest levels of recombinant protein expression observed. Basal level expression of the p18 and bp26 was visible following induction with zero concentration of IPTG.

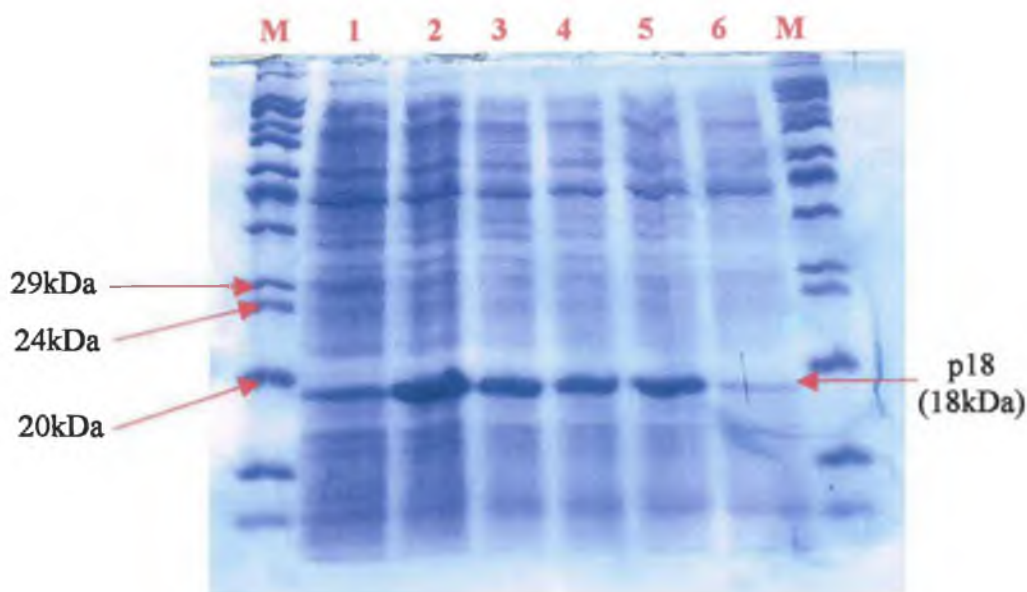


**Figure 4.15:** IPTG concentration optimisation for induction of p18 expression in XL-10 Gold *E. coli*. Lane M: Sigma wide-range molecular weight markers; Lane 1: p18 induction using 1mM IPTG; Lane 2: p18 induction using 0.5mM IPTG; Lane 3: p18 induction using 0.1mM IPTG; Lane 4: p18 induction using 0.05mM IPTG; Lane 5: p18 induction using 0.01mM IPTG; Lane 6: p18 induction using 0mM IPTG. A band at 18kDa is clearly visible following induction with each of the IPTG concentrations.

**Table 4.1:** IPTG concentration optimisation for use with the expression of p18. The levels of p18 expression, expressed as a percentage of the total protein concentration, are shown at each IPTG concentration.

IPTG concentration (mM)	1	0.5	0.1	0.05	0.01	0
p18 expression (% of total protein)	6	17	13	13	14	10

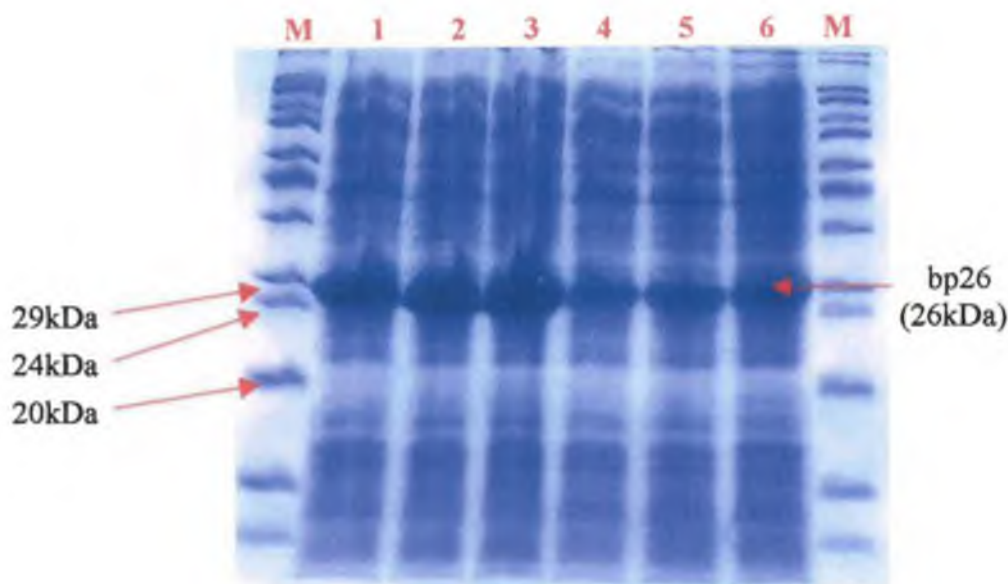


**Figure 4.16:** IPTG concentration optimisation for induction of bp26 expression in XL-10 Gold *E. coli*. Lane M: Sigma wide-range molecular weight markers; Lane 1: bp26 induction using 1mM IPTG; Lane 2: bp26 induction using 0.5mM IPTG; Lane 3: bp26 induction using 0.1mM IPTG; Lane 4: bp26 induction using 0.05mM IPTG; Lane 5: bp26 induction using 0.01mM IPTG; Lane 6: bp26 induction using 0mM IPTG. A band at 26 kDa is clearly visible following induction with each of the IPTG concentrations.

**Table 4.2:** IPTG concentration optimisation for use with the expression of bp26. The levels of bp26 expression, expressed as a percentage of the total protein concentration, are shown at each IPTG concentration.

IPTG concentration (mM)	1	0.5	0.1	0.05	0.01	0
bp26 expression (% of total protein)	24	32	29	18	19	18

#### 4.2.7 Optimisation of sonication conditions

Following intracellular protein expression the bacterial cells must be lysed to isolate the recombinant protein. For the isolation of inclusion bodies the pelleted bacteria were resuspended in denaturing buffer, containing 8M urea, and then sonicated. Sonication involves pulsing the cells with a high voltage current, which perforates the cell membrane and allows the cell contents to be released. However, the bacterial cells should only be sonicated for the minimum time necessary because prolonged sonication may destroy the protein and cleave the 6xHis tag. Therefore, the optimum sonication time for the isolation of the p18 and bp26 proteins from XL 10-Gold *E. coli* was determined.

Expression cultures of the XL-10 Gold *E. coli*, harbouring pQE-60 encoding the p18 or bp26 proteins, were prepared, as described in Section 4.2.6, except the cultures were induced upon addition of 0.5mM IPTG and incubated at 37°C for four hours. 1ml samples were taken and following centrifugation, at 13,000rpm for 15 mins, the pelleted bacteria were resuspended in 200µl of denaturing buffer. The resuspended bacteria were then sonicated with at 220W, for between 0 – 60 secs and the supernatants (following centrifugation at 13,000rpm for 15 mins) were analysed by SDS-PAGE.

Fig. 4.17 shows the optimisation of sonication conditions for the isolation of p18 from XL 10-Gold *E. coli*. The intensity of the 18kDa band gradually increased as the sonication time increased up until 30 seconds, after which time the band intensities levelled off. Suggesting that a 30 second sonication pulse was optimal for the isolation of p18. Determining the levels of p18 expression for each sonication time, using ImageJ, also confirmed 30 secs was optimal (Table 4.3).

Fig. 4.18 shows the optimisation of sonication conditions for the isolation of bp26 from XL 10-Gold *E. coli*. The intensity of the 26kDa band also gradually increased as the sonication time increased, with a 20 second sonication appearing optimum. ImageJ analysis on the levels of protein expression at each sonication time also confirmed that a 20 second sonication was optimal for the isolation of bp26 (Table 4.4).

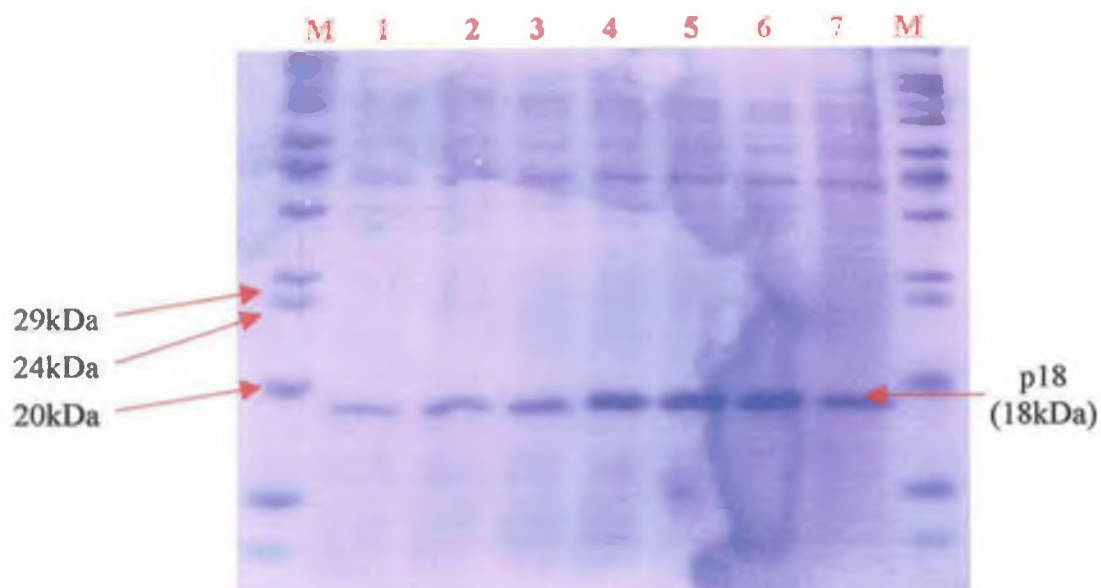


**Figure 4.17:** Optimisation of sonication conditions for the isolation of p18 from XL-10 Gold. Lane M: Sigma wide-range molecular weight markers; Lane 1: Isolation of p18 using 0 sec sonication; Lane 2: Isolation of p18 using 10 secs sonication; Lane 3: Isolation of p18 using 20 secs sonication; Lane 4: Isolation of p18 using 30 secs sonication; Lane 5: Isolation of p18 using 40 secs sonication; Lane 6: Isolation of p18 using 50 secs sonication; Lane 7: Isolation of p18 using 60 secs sonication. A band representing the p18 is clearly visible at 18kDa.

**Table 4.3:** Optimisation of sonication conditions for the isolation of p18 from XL-10 Gold *E. coli*. The levels of p18 expression, expressed as a percentage of the total protein concentration, are shown at varying sonication times ranging from 0 – 60 seconds.

Sonication time (seconds)	0	10	20	30	40	50	60
p18 expression (% of total protein)	10	13	14	17	17	17	15

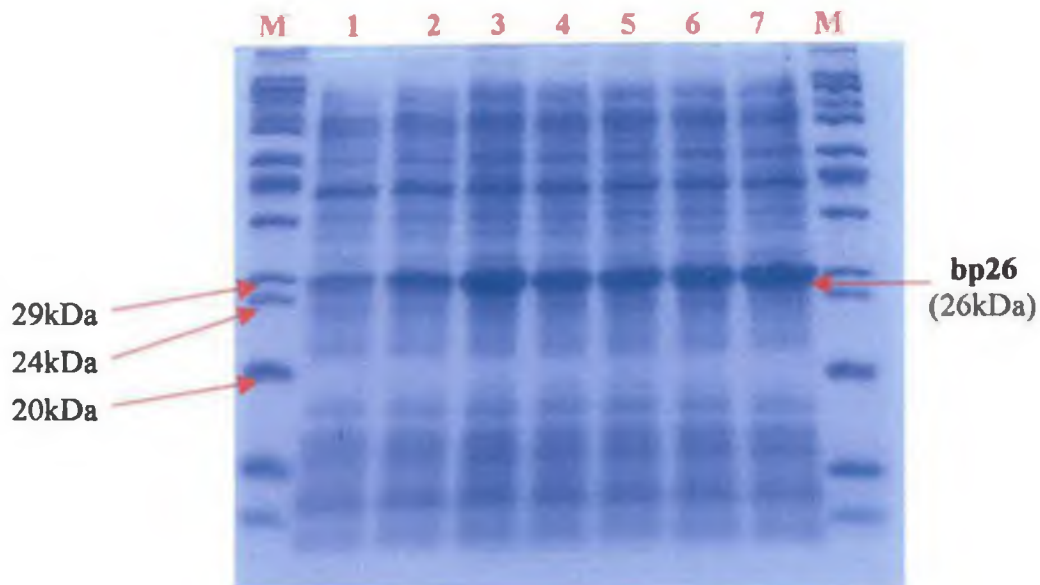


**Figure 4.18:** *Optimisation of sonication conditions for the isolation of bp26 from XL-10 Gold E. coli. Lane M: Sigma wide-range molecular weight markers; Lane 1: Isolation of bp26 using 0 sec sonication; Lane 2: Isolation of bp26 using 10 secs sonication; Lane 3: Isolation of bp26 using 20 secs sonication; Lane 4: Isolation of bp26 using 30 secs sonication; Lane 5: Isolation of bp26 using 40 secs sonication; Lane 6: Isolation of bp26 using 50 secs sonication; Lane 7: Isolation of bp26 using 60 secs sonication. A band representing the bp26 is clearly visible at 26kDa.*

**Table 4.4:** *Optimisation of sonication conditions for the isolation of bp26 from XL-10 Gold E. coli. The levels of bp26 expression, expressed as a percentage of the total protein concentration, are shown at varying sonication times ranging from 0 – 60 seconds.*

<b>Sonication time (seconds)</b>	0	10	20	30	40	50	60
<b>bp26 expression (% of total protein)</b>	10	15	20	16	16	16	19

#### 4.2.8 Time-course analysis on the expression of p18 and bp26

Following optimisation of the various parameters for protein expression a time-course analysis on the level of protein expression was carried out in order to determine the optimal induction time for protein expression. This is important in order to get a balance between the amount of soluble protein in the cells, the formation of inclusion bodies, and protein degradation. By checking the recombinant protein present at various times after IPTG induction, the optimal induction period can be established. This section describes the time-course analysis on p18 and bp26 expression in XL 10-Gold *E. coli*.

Expression cultures of the XL-10 Gold *E. coli*, harbouring pQE-60 encoding the p18 or bp26 proteins, were prepared, as described in Section 4.2.7, except that following IPTG induction, 1ml samples were taken every hour, for up to five hours, and then following overnight (20 hours) induction. A 1ml non-induced control sample was also taken prior to IPTG addition. Each of the 1ml samples was centrifuged, at 13,000rpm for 15 mins and the pelleted bacteria resuspended in 200µl of denaturing buffer. The resuspended bacteria were then sonicated for 30 secs for p18 or for 20 secs for bp26, at 220W, and the supernatants analysed by SDS-PAGE.

SDS-PAGE analysis on the time course analysis for p18 and bp26 suggested the optimal induction period for protein expression was 4 hours, after which no major difference in the levels of protein expression were observed (Figs. 4.19 and 4.20). ImageJ analysis on the band intensities of the SDS-PAGE was used to determine the level of p18 and bp26 expression, as a percentage of the total protein content (Tables 4.5 and 4.6). The ImageJ analysis confirmed that a 4-hour induction period was sufficient with levels of p18 and bp26 expression at 25% and 19%, respectively, of the total protein content. Although slightly higher levels of p18 (28%) and bp26 (21%) expression were observed following a 5-hour induction period, 4 hours was selected to minimise proteolytic degradation of the proteins and 6xHis tag cleavage.

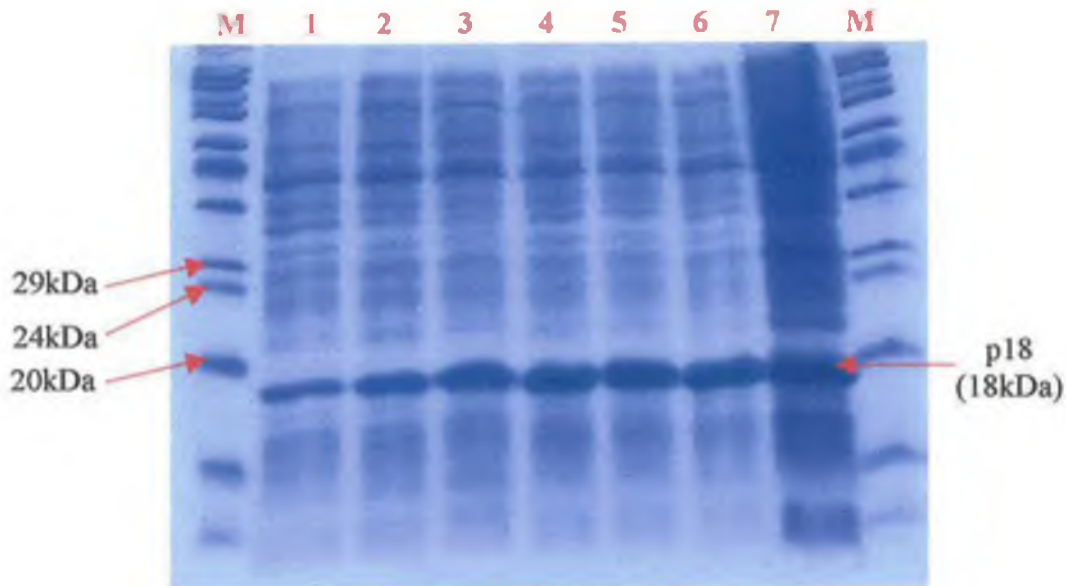


**Figure 4.19:** Time course expression analysis on p18 in XL-10 Gold *E. coli*. Lane M: Sigma wide-range molecular weight marker; Lane 1: Non- induced control; Lane 2: p18 expression 1 hour post IPTG induction; Lane 3: p18 expression 2 hours IPTG post induction; Lane 4: p18 expression 3 hours post IPTG induction; Lane 5: p18 expression 4 hours post IPTG induction; Lane 6: p18 expression 5 hours post IPTG induction; Lane 7: p18 expression following overnight induction using IPTG. A band representing the p18 is clearly visible at 18kDa.

**Table 4.5:** Time course expression to determine optimum induction period for the expression of p18 from XL-10 Gold *E. coli*. The levels of p18 expression, expressed as a percentage of the total protein concentration, are shown at varying time intervals following IPTG induction.

Induction time (hours)	0	1	2	3	4	5	20
p18 expression (% of total protein)	10	14	18	22	25	28	16

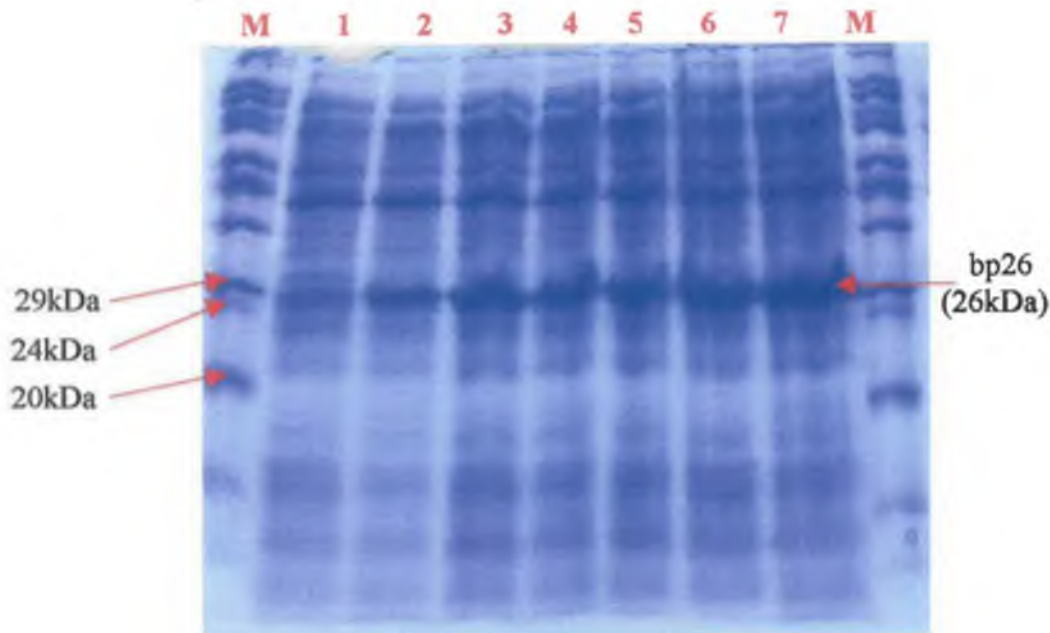


**Figure 4.20:** Time course expression analysis on bp26 in XL-10 Gold *E. coli*. Lane M: Sigma wide-range molecular weight marker; Lane 1: Non- induced control; Lane 2: bp26 expression 1 hour post IPTG induction; Lane 3: bp26 expression 2 hours post IPTG induction; Lane 4: bp26 expression 3 hours post IPTG induction; Lane 5: bp26 expression 4 hours post IPTG induction; Lane 6: bp26 expression 5 hours post IPTG induction; Lane 7: bp26 expression following overnight induction using IPTG. A band representing the bp26 is clearly visible at 26kDa.

**Table 4.6:** Time course expression to determine optimum induction period for the expression of bp26 from XL-10 Gold *E. coli*. The levels of bp26 expression, expressed as a percentage of the total protein concentration, are shown at varying time intervals following IPTG induction.

Induction time (hours)	0	1	2	3	4	5	20
bp26 expression (% of total protein)	10	11	14	19	19	21	22

#### **4.2.9 Immobilised metal affinity chromatography (IMAC) purification of p18 and bp26**

Following expression of the p18 and bp26 from pQE-60 a C-terminal 6xHis-tag was incorporated into the recombinant proteins (See section 4.1). This enables the use of immobilised metal chelating affinity chromatography for the purification of the His-tagged recombinant proteins. This section describes the use of Ni-NTA (nickel-nitrilotriacetic acid) resin (QIAGEN) for the purification of the 6xHis-tagged p18 and bp26, from XL-10 Gold *E. coli* lysates under denaturing conditions.

A batch purification method was chosen for the purification of the recombinant p18 and bp26 proteins as described in section 2.3.16. 5ml of the Ni-NTA resin was incubated with 20ml of the cytoplasmic lysate from the XL-10 Gold cells for 90 min at room temperature on an over-end rotor. The resin was then washed three times with 20ml denaturing buffer, pH 6.3, and the immobilised recombinant proteins eluted in 3 x 3ml fractions using denaturing buffer, pH 4.5. The purified fractions were pooled and then dialysed into PBS, overnight at 4°C.

Fractions from each stage of the purification process, including the wash steps, were analysed using SDS-PAGE. Figure 4.21 shows the IMAC purification of p18 with the eluted fragments pooled and analysed in Lane 9. The gel picture clearly shows that the purity of the p18 greatly increased following the IMAC purification with one main band visible at 18kDa. Figure 4.22 represents the SDS-PAGE analysis on the IMAC purification of bp26, with the eluted fragments pooled and analysed in Lane 9. The purity of the bp26 is greatly improved following the IMAC purification when compared with the cell lysate (Lane 1). However, the pooled eluted fractions contained some contaminating *E. coli* proteins.

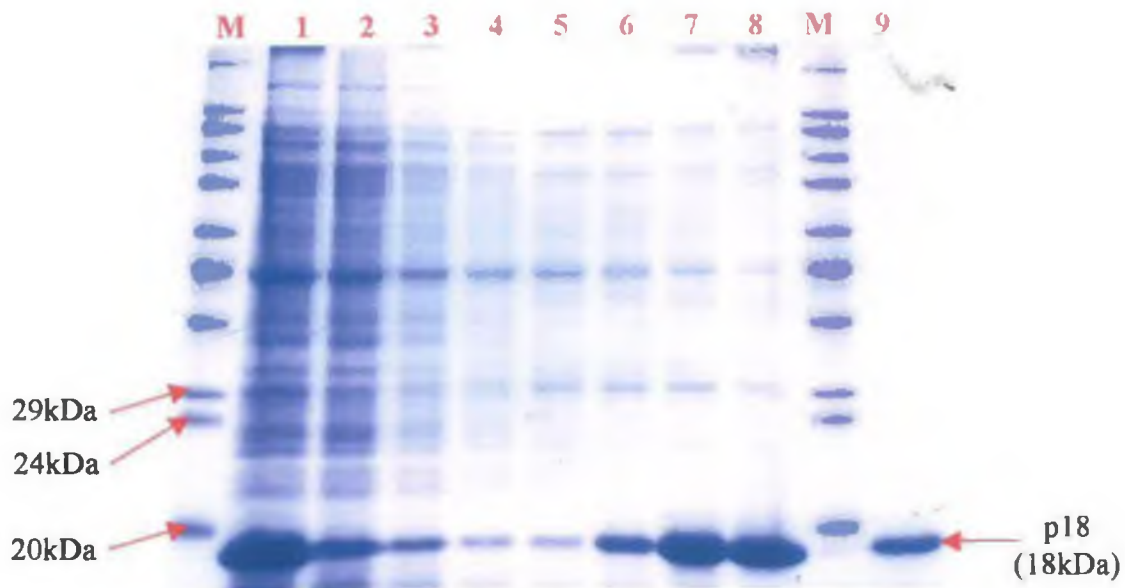


**Figure 4.21:** SDS-PAGE analysis on the IMAC purification of p18 using a pH shock elution. Lane M: Sigma wide-range molecular weight markers; Lane 1: Crude cytoplasmic lysate from XL-10 Gold following p18 expression; Lane 2: Flow-through from IMAC column following application of crude lysate; Lane 3, 4 and 5: Wash fractions 1, 2 and 3, respectively; Lane 6, 7 and 8: Elutions 1, 2 and 3, respectively; Lane 9: Purified p18, consisting of elutions 1, 2 and 3 pooled. A band at 18kDa is clearly visible in each of the 3 elutions and in the purified sample.

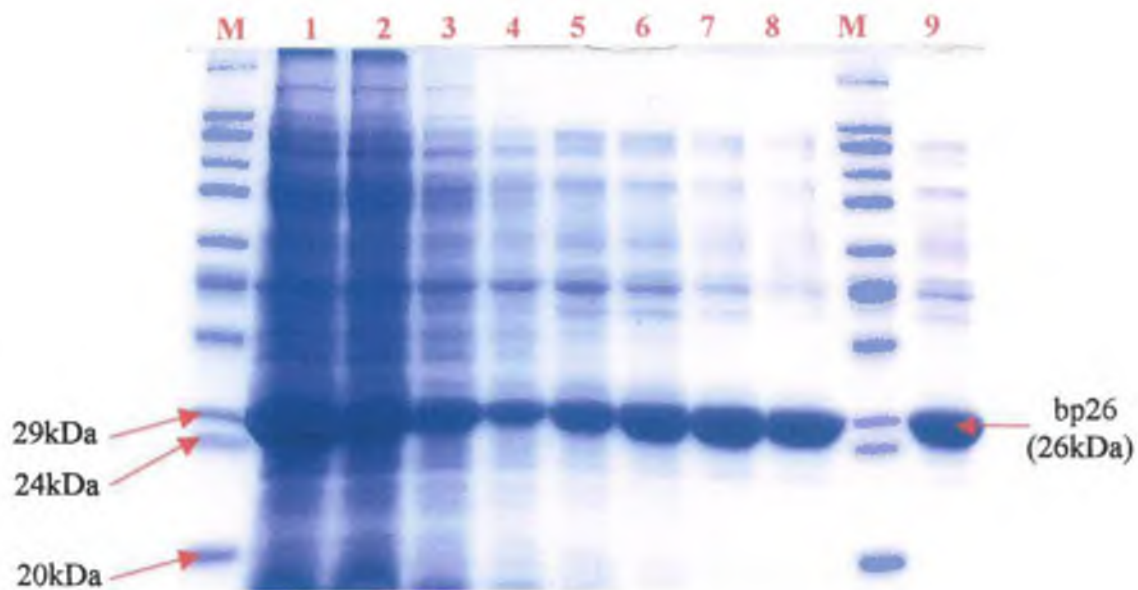


**Figure 4.22:** SDS-PAGE analysis on the IMAC purification of bp26 using a pH shock elution. Lane M: Sigma wide-range molecular weight markers; Lane 1: Crude cytoplasmic lysate from XL-10 Gold following bp26 expression; Lane 2: Flow-through from IMAC column following application of crude lysate; Lane 3, 4 and 5: Wash fractions 1, 2 and 3, respectively; Lane 6, 7 and 8: Elutions 1, 2 and 3, respectively; Lane 9: Purified bp26, consisting of elutions 1, 2 and 3 pooled. A band at 26kDa is clearly visible in each of the 3 elutions and in the purified sample.

#### **4.2.10 Nucleotide and amino acid sequence analysis on the recombinant p18 and bp26 proteins cloned in pQE-60**

The nucleotide sequence of the cloned p18 and bp26 genes were obtained as described in section 2.3.10. The pQE-60 plasmid DNA containing the p18 and bp26 inserts was purified from the XL-10 Gold *E. coli*. A Comfort read (in both directions) was then obtained from MWG-Biotech on each plasmid and the nucleotide sequence returned. The amino acid sequences were then deduced from the nucleotide sequences using a web-based translate tool (See section 2.2.11).

Nucleotide sequence comparisons between the cloned p18 and the previously sequenced p18 genes revealed that the cloned p18, the *B. melitensis* p18 and the *B. abortus* p18 were identical with only a two base pair difference with the *B. suis* p18 (Fig. 4.23) suggesting 99.6% homology between the 4 analysed nucleotide sequences. However, amino acid sequence analysis revealed that the four proteins were identical (Fig. 4.24) suggesting 100% homology between the four aligned amino acid sequences.

Nucleotide sequence comparisons between the recombinant bp26 and the previously sequenced bp26 genes revealed a 3 base pair difference between the cloned bp26 and two *B. melitensis* sequences (U30815 and U45996), a 4 bp difference with the *B. suis* sequence and a 6 bp difference with *B. melitensis* 16M gene (Fig. 4.25) suggesting 99.1% homology with the 5 aligned sequences. Whereas, amino acid sequence analysis suggested that the cloned bp26 displayed 99.6% homology with the previously sequenced genes (Fig. 4.26).

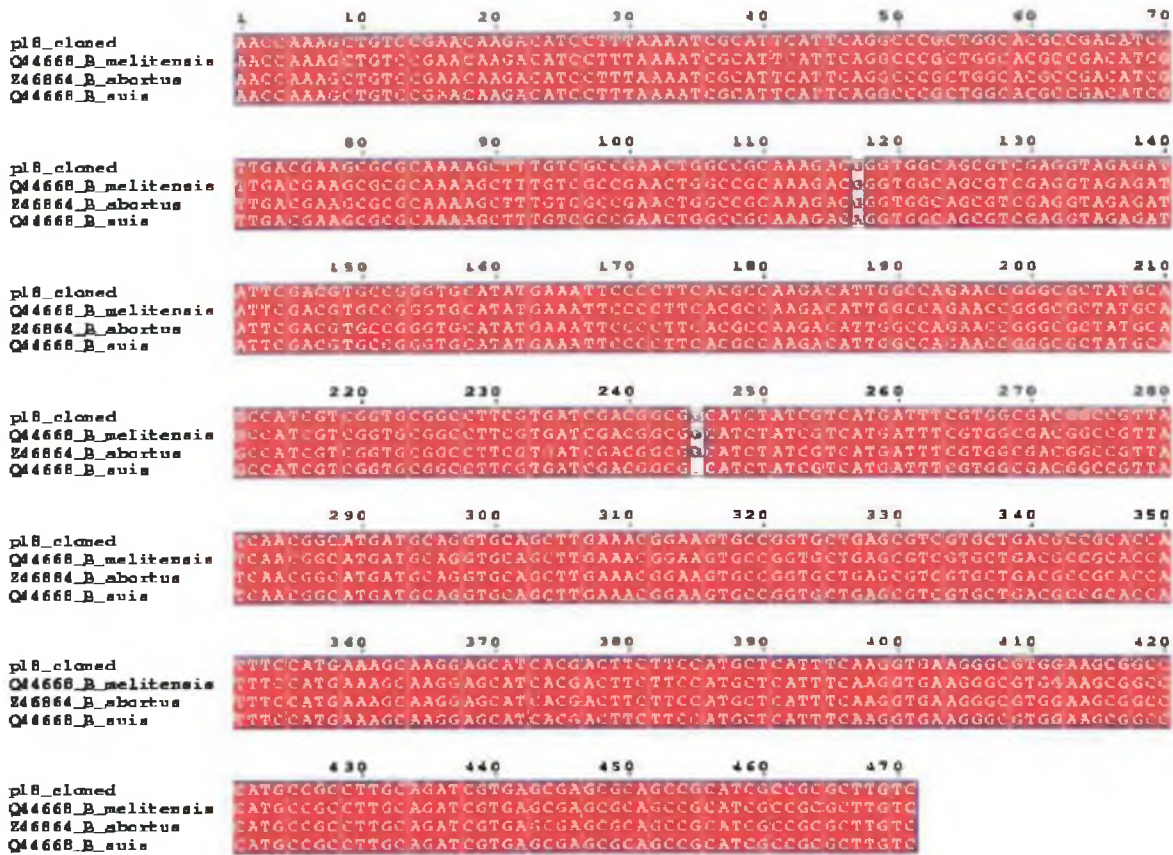


Figure 4.23: Nucleotide sequence alignment on the cloned p18. The p18 nucleotide sequence was aligned with 3 previously sequenced p18 genes from *B. melitensis* (Q44668), *B. abortus* (Z46864) and *B. suis* (Q44668).

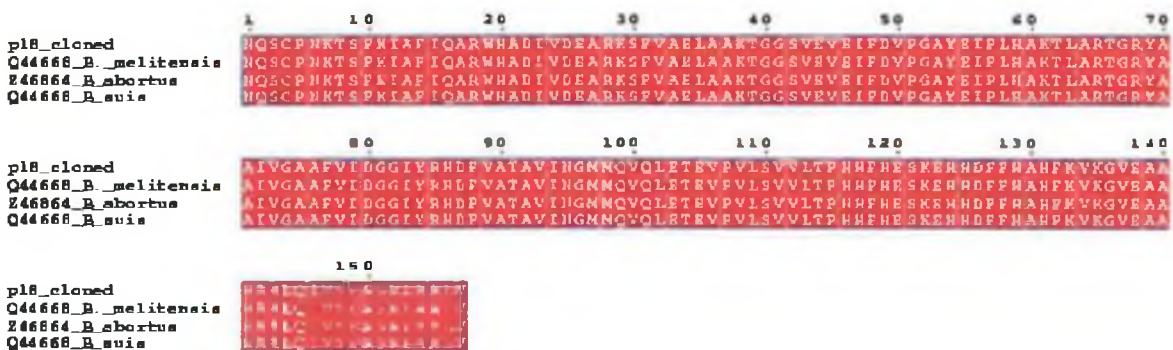


Figure 4.24: Amino acid sequence alignment on the cloned p18. The p18 amino acid sequence was aligned with 3 previously sequenced p18 proteins from *B. melitensis* (Q44668), *B. abortus* (Z46864) and *B. suis* (Q44668).

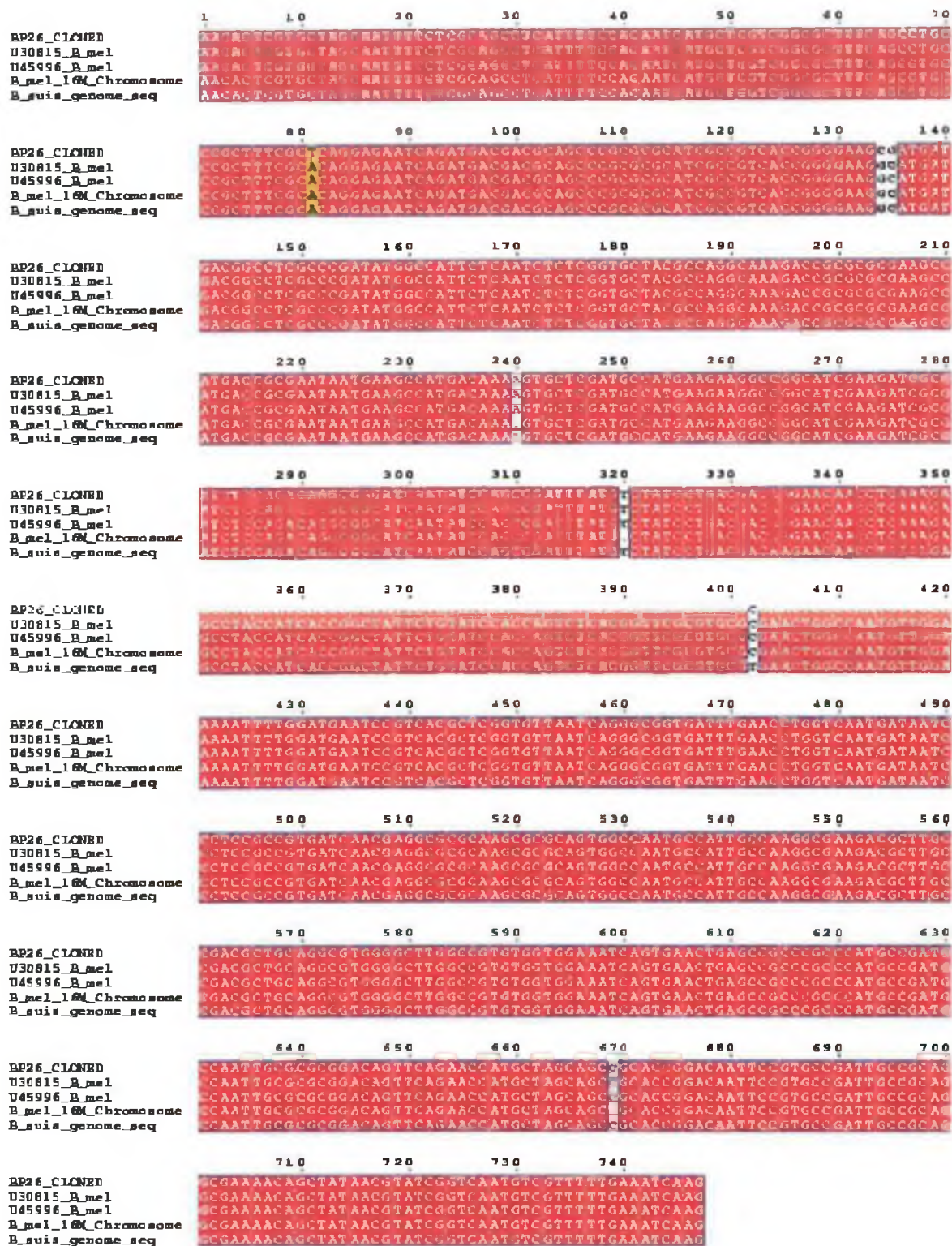


Figure 4.25: Nucleotide sequence alignment on the cloned bp26. The bp26 nucleotide sequence was aligned with 4 previously sequenced bp26 genes from *B. melitensis* (U30815, U45996 and B\_mel\_16M), and *B. suis* (*B\_suis\_genome*).

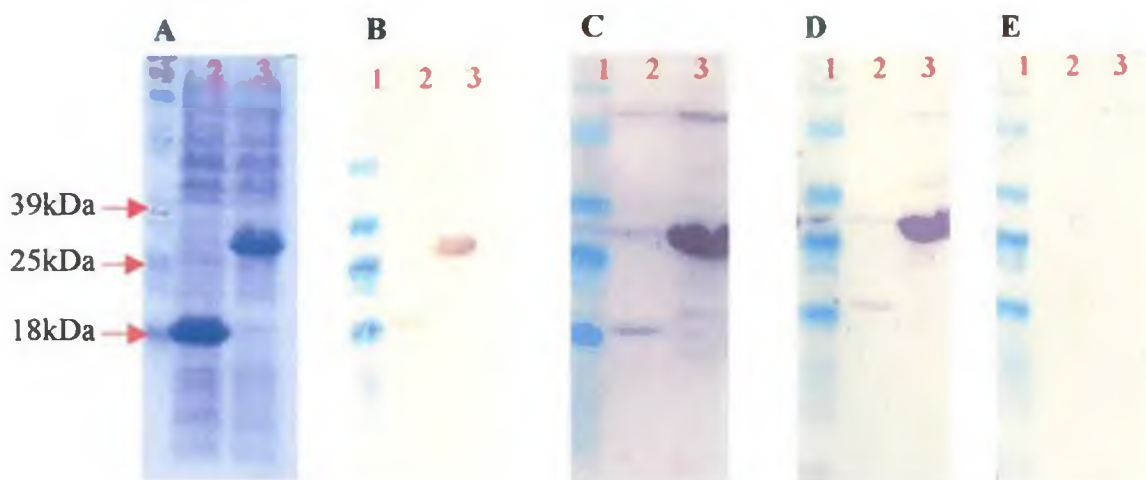
	10	20	30	40	50	60	70
bp26_cloned	MTRALNPLAASPESTINLVGAFSLPAPAFQENQMTTOPARIAVTGEINMTASPDNAILLNLSVLRQARTARE						
U30815_B_mel	MTRALNPLAASPESTINLVGAFSLPAPAFQENQMTTOPARIAVTGEINMTASPDNAILLNLSVLRQARTARE						
U45996_B_mel	MTRALNPLAASPESTINLVGAFSLPAPAFQENQMTTOPARIAVTGEINMTASPDNAILLNLSVLRQARTARE						
B_mel_16M_Chromosome	MTRALNPLAASPESTINLVGAFSLPAPAFQENQMTTOPARIAVTGEINMTASPDNAILLNLSVLRQARTARE						
B_suis_genome_seq	MTRALNPLAASPESTINLVGAFSLPAPAFQENQMTTOPARIAVTGEINMTASPDNAILLNLSVLRQARTARE						
	80	90	100	110	120	130	140
bp26_cloned	MTANHEAMTKVLDANKKAGIEDRDLQTTGGINIQPIYVYVYDDKNNLEKPTITGYSVSTSLTVRVRELAVG						
U30815_B_mel	MTANHEAMTKVLDANKKAGIEDRDLQTTGGINIQPIYVYVYDDKNNLEKPTITGYSVSTSLTVRVRELAVG						
U45996_B_mel	MTANHEAMTKVLDANKKAGIEDRDLQTTGGINIQPIYVYVYDDKNNLEKPTITGYSVSTSLTVRVRELAVG						
B_mel_16M_Chromosome	MTANHEAMTKVLDANKKAGIEDRDLQTTGGINIQPIYVYVYDDKNNLEKPTITGYSVSTSLTVRVRELAVG						
B_suis_genome_seq	MTANHEAMTKVLDANKKAGIEDRDLQTTGGINIQPIYVYVYDDKNNLEKPTITGYSVSTSLTVRVRELAVG						
	150	160	170	180	190	200	210
bp26_cloned	KILDESVTLCVHQGGDLNLYVHNPISAVINEARKRAVANAIKAKTLAGAAGVGLGRVVEISELSRPPMPK						
U30815_B_mel	KILDESVTLCVHQGGDLNLYVHNPISAVINEARKRAVANAIKAKTLAGAAGVGLGRVVEISELSRPPMPK						
U45996_B_mel	KILDESVTLCVHQGGDLNLYVHNPISAVINEARKRAVANAIKAKTLAGAAGVGLGRVVEISELSRPPMPK						
B_mel_16M_Chromosome	KILDESVTLCVHQGGDLNLYVHNPISAVINEARKRAVANAIKAKTLAGAAGVGLGRVVEISELSRPPMPK						
B_suis_genome_seq	KILDESVTLCVHQGGDLNLYVHNPISAVINEARKRAVANAIKAKTLAGAAGVGLGRVVEISELSRPPMPK						
	220	230	240				
bp26_cloned	PIARGNPTNLAAPFHSVPTAAGEQYNVSMVVFETI						
U30815_B_mel	PIARGNPTNLAAPFHSVPTAAGEQYNVSMVVFETI						
U45996_B_mel	PIARGNPTNLAAPFHSVPTAAGEQYNVSMVVFETI						
B_mel_16M_Chromosome	PIARGNPTNLAAPFHSVPTAAGEQYNVSMVVFETI						
B_suis_genome_seq	PIARGNPTNLAAPFHSVPTAAGEQYNVSMVVFETI						

Figure 4.26: Amino acid sequence alignment on the cloned bp26. The bp26 amino acid sequence was aligned with 4 previously sequenced bp26 proteins from *B. melitensis* (U30815, U45996 and B.mel\_16M), and *B. suis* (B\_suis\_genome).

#### **4.2.11 Immunogenicity studies on the recombinant p18 and bp26 expressed in XL-10 Gold *E. coli***

Western blot analysis was then carried out on the two recombinant proteins, p18 and bp26, to establish the antibody binding activity and immunogenicity of the recombinant proteins.

The recombinant proteins were electrophoresed alongside a prestained molecular weight marker using SDS-PAGE as described in Section 2.2.11. Figure 4.27 A shows the Coomassie stained gel with bands representing the p18 (Lane 2) and bp26 (Lane 3) clearly visible at 18 and 26kDa, respectively. The electrophoresed proteins were transferred to nitrocellulose for western blot analysis as described in Section 2.2.13. The nitrocellulose blots were then probed with an anti-His antibody and three standard serum samples, the DeVeere Hunt serum, the National Standard Serum (NSS) and a standard negative serum. Initially, a Western blot was carried out using an anti-His antibody to ensure the 6xHis tag remained in place following IMAC purification and to confirm that the recombinant proteins were expressed in the correct reading-frame. Figure 4.21 B represents the blot probed with the anti-His antibody with bands are clearly visible at 18kDa and 26kDa representing the p18 and bp26, respectively. The usefulness of the recombinant proteins as diagnostic markers for a bovine brucellosis infection was also initially investigated using Western blotting. The nitrocellulose containing the transferred recombinant proteins was probed using two *Brucella*-positive serum standards, the DeVeere Hunt Serum and the National Standard Serum (NSS) and one standard negative serum. Bands at 18kDa and 26kDa are clearly visible following Western blot analysis with the two positive sera, the DeVeere Hunt Serum (Figure 4.21 C) and the NSS (Figure 4.21 C). However, no bands were visible on the Western blot using the standard negative serum (Figure 4.21 E), thus, indicating the discriminatory capabilities of the recombinant proteins between *Brucella*-positive and negative serum samples.



**Figure 4.27:** SDS-PAGE and Western blot analysis on the high-level expression of p18 (Lane 2) and bp26 (Lane 3) in XL10 Gold *E. coli* (with prestained molecular weight markers in Lane 1). (A) SDS-PAGE analysis on the expression of p18 and bp26, with bands clearly visible 18kDa and 26kDa, respectively. (B) Western blot analysis on the expression of p18 and bp26 using an anti-His antibody to probe the nitrocellulose, with bands clearly visible at 18kDa and 26kDa, respectively. (C) Western blot analysis on the expression of p18 and bp26 using the DeVeere Hunt Serum, a *Brucella*-positive standard sera, to the probe the nitrocellulose, with bands clearly visible at 18kDa and 26kDa, respectively. (D) Western blot analysis on the expression of p18 and bp26 using the National Standard Serum, a *Brucella*-positive standard sera, to the probe the nitrocellulose, with bands clearly visible at 18kDa and 26kDa, respectively. (E) Western blot analysis on the expression of p18 and bp26 using the *Brucella*-negative standard sera, to the probe the nitrocellulose, with no bands visible at either 18kDa or 26kDa.

### 4.3 Discussion

The main focus of this chapter was the cloning and expression of two *Brucella*-specific proteins, p18, an 18kDa cytoplasmic protein, and bp26, a 26kDa periplasmic protein. The recombinant proteins were then investigated for use as diagnostic markers of bovine brucellosis. Their subsequent use in the development of an immunoassay for the detection of bovine brucellosis will also be investigated (See Chapter 6).

Total genomic DNA was isolated from heat-killed *B. abortus* 45/20 cells and used as the template DNA for PCR amplification of the specific genes. Studies using pulse-field gel electrophoresis (PFGE) have revealed that the *Brucella* genomes consist of two circular chromosomes of 2.1Mb and 1.15Mb (Jumas-Bilak *et al.*, 1998 and Michaux *et al.*, 1993). The quality of the isolated genomic DNA was assessed by agarose gel electrophoresis (Figure 4.7) with only one distinct band visible. The extremely large size of the two chromosomes makes it impossible to separate them using conventional gel electrophoresis. However, the presence of only one band confirmed that the DNA was of good quality and that no shearing of the DNA occurred during the isolation process.

The genes encoding the p18 and bp26 *Brucella*-specific proteins were then PCR amplified using the total genomic DNA as the template. Forward and reverse primers were engineered for each gene based on nucleotide sequences previously submitted to GenBank. The p18-specific primers were based on the nucleotide sequence (Accession number Q4468) of an 18kDa *Brucella*-specific lumazine synthase previously submitted to GenBank by Goldbaum and associates (1999). The bp26-specific primers were based on the nucleotide sequence of a 26kDa periplasmic protein from *B. melitensis* (Accession number U45996) previously submitted to GenBank by Cloeckaert and associates (1996). An NcoI restriction site was engineered into the forward primers and a BamHI site into the reverse to enable the directional cloning into pQE-60. Since proteins expressed from pQE-60 contain a C-terminal 6xHis tag the genes were cloned in frame with the 3' sequence encoding the 6xHis tag. The authentic ATG start codons within the protein sequences were used to initiate protein expression using the optimised Shine Dalgarno region of the pQE-60.

The sequence of the forward and reverse primers are given in Table 2.10 with the BamH1 / Nco1 restriction sites and the authentic start codons highlighted.

A standard PCR reaction was then used to amplify the genes encoding the p18 and bp26 proteins. Initially, a temperature gradient PCR was carried out in order to determine the optimum annealing temperature for use with the specific primers. Standard PCR reactions were carried out with varying annealing temperatures ranging from 58 – 65°C. An annealing temperature of 65°C was found to be optimum for the specific amplification of the genes encoding p18 and bp26 (Figure 4.8). Failure to optimise the annealing temperature would result in non-specific amplifications, which would interfere in the later stages of cloning. Following PCR optimisation the genes encoding the p18 and bp26 genes were amplified using DNA Taq polymerase as described in Section 2.3.3 (Fig. 4.9). The PCR amplified genes were then cloned using the TA cloning kit, which provides a one step cloning strategy that allows the direct insertion of a Taq-polymerase-amplified PCR product into the pCR2.1 plasmid. The fresh PCR products, containing the deoxyadenosine (A) overhangs, were ligated into the linearised pCR2.1 vector containing the 3' deoxythymidine (T) overhanging residues and transformed into competent INV $\alpha$ F' *E. coli*. The presence of the multiple cloning sites within the LacZ gene of the pCR2.1 vector enables blue/white colony selection. The LacZ gene encodes the enzyme beta-galactosidase, which metabolises X-gal resulting in the formation of blue colonies. However, positive transformants containing the cloned insert disrupt the LacZ gene and when grown in the presence of X-gal appear colourless. Following the selection of positive transformants the presence of the 485bp and 793bp cloned inserts (encoding p18 and bp26, respectively) within the pCR2.1 vector were confirmed following a BamH1/Nco1 restriction digest (Figure 4.10). The BamH1/Nco1 restricted genes encoding the p18 and bp26 were then gel-purified and directionally cloned into the high-level expression vector pQE-60, which was previously linearised using a BamH1 / Nco1 restriction digest. The pQE-60 plasmids containing the cloned inserts were then transformed into CaCl<sub>2</sub>-competent XL-10 Gold *E. coli*, which are fast growing *E. coli* that allow a sufficiently high transformation rate. Once again the presence of the 485bp and 793bp cloned insert were confirmed following a BamH1/Nco1 restriction digest of the pQE-60 plasmid (Fig. 4.11).

Following the successful cloning of the p18 and bp26 genes into the high-level expression vector pQE-60 the suitability of the XL-10 Gold *E. coli* host strain was determined. Initial small-scale expression cultures were carried out on the p18 and bp26 XL-10 Gold *E. coli* clones as described in Section 2.3.11. Following protein expression the cell lysates were analysed using SDS-PAGE. Figures 4.12 and 4.13 show the small-scale expression cultures on the p18 and bp26, respectively. A strong band at 18kDa is visible in 4 out of the 5 p18 clones and a band at 26kDa is clearly visible in each of the 5 bp26 clones analysed, confirming the suitability of the XL-10 Gold *E. coli* as a host strain for the expression of p18 and bp26 from the high-level expression vector pQE-60.

High-level protein expression within *E. coli* host strains may result in the formation of insoluble aggregated folding intermediates. These inclusion bodies must be solubilised using strong denaturants such as 8M urea or 6M guanidine hydrochloride, resulting in an inactive protein. Active proteins can be isolated from inclusion bodies but following isolation under denaturing conditions the denaturant must be removed under optimal conditions for protein re-folding. However, following the refolding process the yield of renatured protein can be relatively low. Other approaches for the expression of soluble proteins include the co-expression of chaperones (Georgiou and Valax, 1996 and Hannig and Makrides, 1998), which aid in protein folding and the use of gene fusions, which consist of the target protein fused to a carrier protein such as *E. coli* thioredoxin (TRX); (LaVallie *et al.*, 1993) and glutathione S-transferase (GST); (Ghosh *et al.*, 1995 and Smith and Johnson, 1988). However, protein re-folding, co-expression with chaperones and gene fusions can be time-consuming, ineffective and in some cases, depending on the desired use, unnecessary. Solubility determination studies on the recombinant p18 and bp26 proteins (Fig. 4.14) indicated that the high-level expression of p18 and bp26 resulted in the formation insoluble exclusion bodies, which could be solubilised using 8M urea (Lanes 3 and 5, respectively). A web-based bioinformatics program, to determine the solubility of the recombinant proteins (Harrison, 2000), predicted that the p18 protein had a 62% chance of solubility and that the bp26 protein had an 80% chance of insolubility, confirming the need for denaturing buffer, containing 8M urea, to ensure high-level recovery of p18 and bp26 following expression in XL-10 Gold *E. coli*.

Following confirmation on the suitability of the XL-10 Gold as an expression host and the need for denaturing buffer for the isolation of each recombinant protein factors affecting the expression and recovery levels of the recombinant proteins were optimised individually for the p18 and the bp26. These parameters included IPTG concentrations, sonication conditions and incubation time post induction.

Expression of recombinant proteins from pQE-60 is under the control of an optimised promoter-operator element consisting of the phage T5 promoter, which is recognised by *E. coli* RNA polymerase, and two *lac* operator sequences, which increase *lac* repressor binding. The extremely high transcription rate initiated at the T5 promoter can be effectively regulated and repressed by the presence of high levels of the *lac* repressor. The *lacI<sup>q</sup>* gene contained on the F' episome of XL-10 Gold *E. coli* ensures the production of high levels of the *lac* repressor protein and tightly regulates recombinant protein expression. High-level protein expression from pQE-60 is rapidly induced upon addition of isopropyl- $\beta$ -D-thiogalactoside (IPTG), which binds to the *lac* repressor protein and inactivates it. However, previous studies have demonstrated the need to optimise the concentration of IPTG so that the levels of protein expression and IPTG concentration are not toxic to the host cell (Liu *et al.*, 1999). Therefore, the optimal IPTG concentration for the induction of p18 and bp26 expression in XL-10 Gold *E. coli* was determined. Varying IPTG concentrations ranging from 0.01 – 1mM were investigated for the high-level expression of p18 and bp26. Figures 4.15 and 4.16 show the SDS-PAGE analysis on p18 and bp26 expression, respectively, with the highest-levels of expression observed following induction with 0.5mM IPTG. The band intensities on an SDS-PAGE were monitored, using ImageJ software, and used to estimate the concentration (as a percentage of the total protein content) of p18 and bp26 expressed at each IPTG concentration. Tables 4.1 and 4.2 indicate p18 and bp26 expression levels, respectively, which confirmed 0.5mM IPTG was optimal for the induction of p18 and bp26 production. Basal level expression of the p18 and bp26 was visible with zero concentration of IPTG.

High-level expression of the recombinant p18 and bp26 proteins in XL-10 Gold *E. coli* resulted in the formation of insoluble intracellular inclusion bodies. Recovery of the intracellular proteins involved resuspending the pelleted bacteria in denaturing

buffer and pulsing the resuspension with an electrical current using a sonicator. Sonication results in the perforation of the cell membrane and allows the cell contents to be released. However, Ausubel and co-workers (1996) have reported that prolonged sonication can lead to co-purification of *E. coli* host proteins and breakdown of fusion proteins. SDS-PAGE (Figs. 4.17 and 4.18) and Image J (Tables 4.3 and 4.4) analysis on the optimisation of sonication time suggested that a 30 and 20 sec sonication pulse was optimal for the isolation of p18 and bp26, respectively, from XL-10 Gold *E. coli*.

Time-course expression cultures were also carried out to determine the optimal induction period, post IPTG addition, for p18 and bp26 expression. Intracellular protein content is a balance between the amount of soluble protein in the cells, the formation of inclusion bodies and protein degradation. Analysis on the levels of protein expression at hourly intervals post IPTG induction was used to determine the optimal induction period. SDS-PAGE (Figs. 4.19 and 4.20) and ImageJ (Tables 4.5 and 4.4) analysis on the time-course expression cultures for p18 and bp26 suggested that a 4-hour induction period enabled sufficient levels of protein production. Slightly higher levels of p18 and bp26 expression were observed following a 5-hour induction period. However, the 4-hour induction period appeared satisfactory and minimised the risk of potential proteolytic degradation and 6xHis tag cleavage.

The optimised parameters, as discussed above, were then applied for the large-scale production of the p18 and bp26 recombinant proteins. Immobilised metal affinity chromatography (IMAC) was then used for the purification of the recombinant proteins, which contained C-terminal 6xHis tags. Figures 4.21 and 4.22 show the IMAC purification of the p18 and bp26, respectively, where the use of a pH shock elution enabled the one-step purification of the recombinant proteins. The highest levels of purity were obtained for the p18 protein with some contaminating proteins remaining following the purification of bp26. Certain *E. coli* proteins have been identified that may bind to IMAC columns under certain conditions. These proteins include superoxide dismutase, chloramphenicol acetyl-transferase, camp receptor protein, heat shock protein, host factor-1 protein and wondrous histidines-rich protein which contain 8, 12, 6, 14, 5 and 18 native histidines residues, respectively (Muller *et al.*, 1998) and may account for the impurities obtained following the IMAC purification of the bp26. However, the IMAC purification did provide a suitable one-

step purification strategy for the p18 and bp26 proteins with the purity of the proteins greatly increasing following pH elution (Lanes 9) in comparison to the denatured cell lysate (Lanes 1). The concentration of the purified proteins was then estimated using a BCA assay. A standard curve was constructed using BSA and concentration values for the purified protein obtained from it. The final concentration of the purified p18 and bp26 was 62.5µg/ml and 500µg/ml, respectively.

The genes encoding the p18 and bp26 recombinant proteins were then sequenced and used to deduce the amino acid sequence. The 18kDa cytoplasmic protein p18 was previously identified as lumazine synthase and a possible diagnostic marker for brucellosis (Hemmen *et al.*, 1995 and Goldbaum *et al.*, 1999) (See section 4.1). Nucleotide and amino acid sequences of the p18 have been submitted to GenBank and NCBI, from different *Brucella* species. Hemmen and associates cloned and expressed the p18 gene from *B. abortus* and submitted the sequence to NCBI (Accession number Z46864). Nucleotide and amino acid sequences of the p18 were also submitted to GenBank following completion of the genomic sequence of *B. melitensis* (Accession number AE009695 / Q44668) and *B. suis* (Accession number AE014565 / Q44668). A 26kDa outer membrane protein Omp26 was initially identified as a useful diagnostic marker for brucellosis (Lindler *et al.*, 1996). Linder and associates cloned and expressed this 26kDa and submitted the sequence to GenBank (Accession number U30815). The protein was later cloned and expressed and then re-identified as 26kDa cytoplasmic protein (Cloeckert *et al.*, 1996) (Accession number U45996). Nucleotide and amino acid sequences of the bp26 were also submitted to GenBank following completion of the genomic sequence of *B. melitensis* (Accession number AE009496) and *B. suis* (Accession number AE014442). Nucleotide and amino acid sequence alignments were then used to compare the cloned p18 and bp26 described in this chapter with the sequences previously submitted to GenBank and the NCBI database. Nucleotide (Figure 4.23) and amino acid (Figure 4.24) sequence analysis on the p18 showed 100% homology between the cloned p18 and the recombinant 17kDa protein previously identified by Hemmen *et al.*, 1995 (Accession no. Z46864) and the *B. melitensis* sequence, submitted to GenBank following genome sequencing (Accession number AE009695 / Q44668), with the *B. suis* sequence, submitted to GenBank following genome sequencing (Accession number AE014565 / Q44668) showing a

2bp difference. Suggesting 99.6% homology between the 4 nucleotide sequences and 100% between the corresponding amino acid sequences. Nucleotide (Fig. 4.25) and amino acid (Fig. 4.26) sequence alignments on the bp26 suggest 99.1% and 99.6% homology, respectively. With a 3 base pair difference between the cloned bp26 and two of the *B. melitensis* sequences (U30815 and U45996), a 4 bp difference with the *B. suis* sequence and a 6 bp difference with *B. melitensis* 16M gene.

The bioreactivity and immunogenicity of the two recombinant proteins were then determined using Western blotting. The two recombinant proteins were electrophoresed using SDS-PAGE (Fig. 4.27 A) and the bands representing the expressed p18 and bp26 were clearly visible at 18 and 26kDa, respectively. The proteins were then transferred to nitrocellulose for Western blotting. Initially the nitrocellulose was probed with an anti-His antibody to ensure the recombinant proteins were expressed in frame. The presence of the bands at 18kDa (Lane 2) and 26kDa (Lane 3) confirm the proteins were fully expressed in frame with a 6xHis tag (Fig. 4.27 B). The ability of the recombinant proteins to discriminate between standard positive sera, the DeVeere Hunt Serum and the NSS, and the standard negative serum, was also investigated using Western blotting. Nitrocellulose containing the transferred proteins was probed with the two standard positive sera and the standard negative serum. The presence of the bands at 18kDa (Lane 2) and 26kDa (Lane 3) on the nitrocellulose probed with the DeVeere Hunt Serum (Fig. 4.27 C) and the National Standard Serum (Fig. 4.27 D) and their absence on the nitrocellulose probed using the standard negative serum suggests the recombinant proteins are capable of distinguishing between *Brucella*-positive and negative serum samples.

This chapter focused on the cloning and subsequent high-level expression of two *Brucella*-specific proteins, p18 an 18kDa cytoplasmic protein and bp26 a 26kDa periplasmic protein, from *B. abortus* cells. Following optimisation of the various parameters required for high-level protein expression the recombinant proteins were purified using IMAC. The ability of the proteins to discriminate between *Brucella*-positive and negative serum samples was then confirmed using Western blotting. The recombinant proteins were then applied to the development of an indirect ELISA for the diagnosis of bovine brucellosis in serum samples (See Chapter 6).

## CHAPTER 5

The production and characterisation of *Brucella*-specific polyclonal antibodies and scFv antibody fragments

## 5.1 Introduction to *Brucella*

The genus *Brucella* consists of a group of gram-negative facultative intracellular pathogenic bacteria. These non-motile bacteria may be rods or coccobacilli with an approximate size of 0.5-0.7µm x 0.6-1.5µm and they may become pleomorphic. These non-sporing bacteria are strictly aerobic, they may produce urease and they are oxidase-positive and catalase-positive. *Brucellae* grow best on trypticase, soy-based or other enriched media and have a doubling time of 2 hours (Hoover and Friedlander, 2004). They are the causative agent of Brucellosis, which is an infectious disease affecting several animal species that can be transmitted to man (See Chapter 6). *Brucella* spp. are classified as class III pathogens and are regarded as a potential bioterrorist agent (Kortepeter and Parker, 1999; Robinson-Dunn, 2002 and Rotz *et al.*, 2002).

### 5.1.1 Taxonomy and classification of the genus *Brucella*

*Brucellae* belong to the alpha-*Proteobacteria* and are phylogenetically related to plant pathogens and symbionts such as *Rhizobium* and *Agrobacterium*, intracellular animal parasites including *Bartonella* and *Rickettsia* and to the opportunistic and free-living bacteria *Ochrobacterum* and *Caulobacter* (Moreno *et al.*, 2002).

The genus *Brucella* is subdivided into six species, *B. abortus*, *B. canis*, *B. melitensis*, *B. neotomae*, *B. ovis* and *B. suis* based mainly on pathogenicity and host preference (Table 5.1). *B. abortus* is mainly responsible for bovine brucellosis, *B. canis* for canine brucellosis, *B. ovis* causes ram epididymitis, *B. suis* is responsible for swine brucellosis, *B. melitensis* causes ovine and caprine brucellosis and *B. neotomae* has been isolated from desert rats. Three of the six *Brucella* species include several biovars. *B. abortus* includes biovars 1, 2, 3, 4, 5, 6, and 9, biovars 1, 2 and 3, are defined for *B. melitensis* and *B. suis* includes biovars 1, 2, 3, 4 and 5. Distinction between the *Brucella* species and their biovars are based on metabolic and antigenic properties, phage typing, CO<sub>2</sub> requirement, H<sub>2</sub>S production, and dye sensitivity (Alton *et al.*, 1988). *Brucella* species can also be further classified according to their colony morphology. *Brucellae* can present themselves with either a smooth or rough colonial morphology. Smooth species have lipopolysaccharide (LPS) molecules containing a polysaccharide O-chain, while rough organisms lack this chain on their

LPS molecule. In some strains the O-chain plays an important role in virulence, with rough species of *B. abortus* being non-virulent.

DNA polymorphisms have enabled molecular typing of the *Brucella* species and their biovars. In particular the *omp2* locus encoding the 36kDa major porin OMP has enabled distinction between all *Brucella* species and some of their biovars (Cloeckert *et al.*, 1995).

DNA-DNA hybridisation studies have revealed that the *Brucella* genus comprises a highly homogeneous group of bacteria with greater than 90% DNA homology between all six species (Cloeckert *et al.*, 1996). During the mid-1980s it was suggested that the genus should represent only one genomic species, *B. melitensis*, and that the classical species should be considered as biovars. However, to date, no agreement has been made by the Subcommittee on the Taxonomy of *Brucella* of the International Committee on Systematic Bacteriology and thus the six species classification is still used (Cloeckert *et al.*, 2000).

More recently, several *Brucella* strains that do not fit into the classical species have been isolated from several marine mammals such as seals, porpoises and dolphins (Ross *et al.*, 1994 and Foster *et al.*, 1996). It was suggested that these new isolates should comprise a new nomen species to be called *B. maris* (Jahans *et al.*, 1997). DNA polymorphism studies at the *omp2* locus of 33 *Brucella* strains isolated from marine mammals suggest that grouping the isolates from marine mammals into one species, *B. maris*, would be inappropriate (Cloeckert *et al.*, 2001). Based on the current classification system, Cloeckert *et al.* (2001), has proposed that marine mammal *Brucella* isolates should in fact comprise at least two new *Brucella* species, *B. pinnipediae* (for seal isolates) and *P. cetaceae* (for cetacean isolates). However, this is yet to be confirmed by the Subcommittee on the Taxonomy of *Brucella* of the International Committee on Systematic Bacteriology.

**Table 5.1: Overview of the taxonomy of the *Brucella* genus.**

Species	Biovars	Host preference	Human pathogenicity
<i>B. abortus</i>	1, 2, 3, 4, 5, 6, 9	Cattle	Intermediate
<i>B. melitensis</i>	1, 2, 3	Goats and sheep	High
<i>B. suis</i>	1, 2, 3, 4, 5	Swine	High
<i>B. neotomae</i>	N/A	Desert rats	None
<i>B. ovis</i>	N/A	Rams	None
<i>B. canis</i>	N/A	Dogs	Intermediate

### 5.1.2 *Brucella* pathogenesis

*Brucellae* gain entry in mammalian hosts via skin abrasions and cuts, the conjunctiva, the gastrointestinal tract and the respiratory tract. Once within in the host the *Brucellae* survive and replicate within macrophages and non-professional phagocytes. *Brucellae* have also been shown to survive and replicate within non-phagocytic cells (Detilleux *et al.*, 1990). The ability to survive and replicate within macrophages enables the bacteria to evade the extracellular mechanisms of the host defense systems, which is a key aspect of *Brucella* virulence (Liautard *et al.*, 1996 and Sangari and Aguero, 1996). *Brucellae* create a novel intracellular environment in which to multiply by modifying the process of phagosome maturation. Porte *et al.* (1999) have demonstrated that following uptake of the *Brucella* the phagosome is rapidly acidified to a pH of 4.0, which inhibits fusion of the early phagosome and lysosome. Phagosome acidification has been shown as the major signal that induces expression of *Brucella* virulence factors (Boschioli *et al.*, 2002). A type IV secretion system has been identified as critical for the intracellular survival and multiplication of *Brucella*. The proteins encoded by the *virB* operon, which consists of 12 genes, are essential for *Brucella* virulence in mice and culture cells (Boschioli *et al.*, 1999). Transcription of the *virB* operon is induced specifically within macrophages, with phagosome acidification being the key intracellular signal (Boschioli *et al.*, 2002). Virulence factors are responsible for the interaction and fusion that occurs between the phagosome and the endoplasmic reticulum (ER), where a sub-compartment within the ER is the final destination for *Brucella*. Currently the genes involved in transporting the bacteria from the phagosome to the ER are unknown.

Studies carried out by Riley and associates suggest that the intracellular survival of *Brucella* in human and bovine polymorphonuclear leukocytes is aided by the ability of *Brucella* to resist intraleukocytic killing systems (1984). In contrast to the non-virulent *B. abortus* 45/20 rough strain the *B. abortus* 45/0 smooth strain does not stimulate an effective level of degranulation following bacterial ingestion.

Rafie-Kolpin and associates (1996) have identified 42 *Brucella* proteins that are upregulated and over 100 that are down regulated in bovine macrophages. Many of the genes involved in the protein regulation are metabolic and probably involved in the adaptation to the intracellular environment. Two interesting genes *manB/ppm*, which is involved in LPS biosynthesis and essential for virulence, and *mtgA*, which is involved in peptidoglycan metabolism, are upregulated suggesting that restructuring of the bacterial envelope occurs (Boschioli *et al.*, 2001). These molecules play a critical role in remodelling the phagosome and bacterial envelope creating a unique intracellular compartment in which the *Brucella* replicates. Ultimately the bacteria destroy the host cell and infect additional cells.

The completion of the *B. melitensis* (DelVecchio *et al.*, 2002), *B. suis* (Paulsen *et al.*, 2002) and *B. abortus* (Sanchez *et al.*, 2001) genome projects will give further insight into the intracellular behaviour and pathogenicity of *Brucella*.

### **5.1.3 Immunity and protection against *Brucella***

Immunity and protection against *Brucella* involves the entire repertoire of the immune system. In the early stages of infection, non-specific, innate immunity is involved. The classical complement pathway, neutrophils, natural killer cells and macrophages all play a role in reducing the number of bacteria and providing the environment for generating a Th1 immune response (Fig. 5.1). Adaptive immunity then provides protection against *Brucella* and is critical for providing memory function, which plays an important role in vaccination. Antigen specific T-cell activation, CD4+ and CD8+ T-cells and humoral responses are all involved (Oliveira *et al.*, 2002). Protection against *Brucella* is primarily mediated by a Th1 type immune response (Zhan *et al.*, 1993). *Brucella* trigger release of interleukin 12 (Il-12) by antigen presenting cells, which results in differentiation of Th0 cells into Th1 cells. INF- $\gamma$  has been shown to

play an important role in mediating resistance to primary and secondary *Brucella* infection (Zhan and Cheers, 1993). Up-regulation of macrophage killing is then initiated following secretion of gamma interferon (INF- $\gamma$ ) from Th1 cells. In addition, *Brucella* infected macrophages are killed by the INF- $\gamma$  secreting CD8<sup>+</sup> cytotoxic T cells, which is critical in the fight against a *Brucella* infection.

#### 5.1.4 *Brucella abortus* 45/20

The need for a successful vaccine against *B. abortus* has been extensively investigated since the early 1920's (See chapter 6). The use of a live, attenuated rough strain would offer protective immunity and due to the lack of the smooth LPS would not result in virulence. The smooth strain *B. abortus* 45/0 was isolated from a cow in 1922 and a rough derivative was obtained following 20 passages in guinea pigs (Schurig *et al.*, 2002). This phenotypically rough strain was named *B. abortus* 45/20. This strain enabled protective immunity in guinea pigs and cattle but when used as a live vaccine it was unstable and tended to revert back to the virulent smooth strain.

Current immunoassays for the detection of *B. abortus* focus on the immunodominant lipopolysaccharide (LPS) antigen. However, several bacterial species share the immunologically distinguishing 0.9 epitope on the O-chain. In particular, *Yersinia* strains have cross-reacted with anti-*Brucella* sera (Caroff *et al.*, 1984). Distinction between *Brucella* and *Yersinia* cells is critical since double infections can be common (Kittelberger *et al.*, 1995) and because *Yersinia* are also considered biological warfare agents. Throughout the course of this chapter *B. abortus* 45/20 cells are used. These cells were chosen for use because of their rough morphology and, therefore, lack the LPS O-chain. This rules out the cross-reactivity potential with structurally related bacterial cells containing the LPS O-chain.

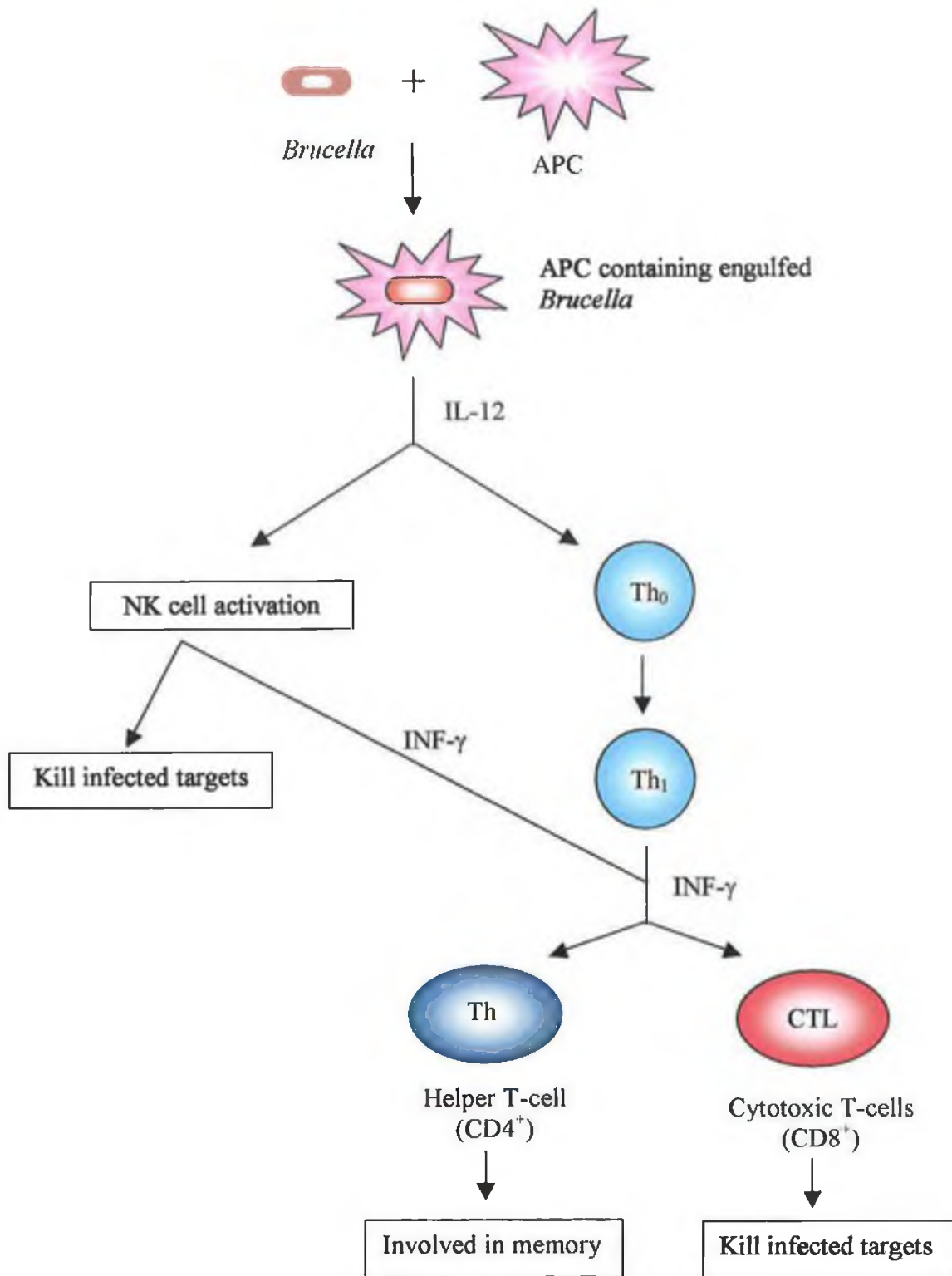


**Figure 5.1:** An overview of protection and immunity against *Brucella*. *Brucella* trigger antigen presenting cells (APCs) to release IL-12, which recruits natural killer cells (NK) to kill infected targets. It causes Th0 cells to differentiate into Th1 cells, resulting in a Th1 immune response, which involves the cytotoxic T-cell (CTL) killing of infected cells.

## 5.2 Results

This chapter focuses on the production and characterisation of *Brucella*-specific antibodies for use in the development of immunoassays for the detection of *Brucella abortus*. The antibodies described in this chapter will also be investigated for use in the development of a diagnostic immunoassay for bovine brucellosis (See Chapter 6). Polyclonal antibodies were raised against the crude cytoplasmic lysate from *B. abortus* 45/20 and whole *B. abortus* 45/20 cells. *Brucella*-specific scFv antibody fragments were also isolated from a naïve scFv phage display library, which was panned using the recombinant *Brucella*-specific proteins, p18 and bp26 (See Chapter 4).

### 5.2.1 Production and purification of polyclonal anti-*Brucella* antibodies

Polyclonal antibodies were raised against *Brucella abortus* 45/20 cells in two rabbits, rabbit 1 and rabbit 2. Antibodies were raised against the crude cytoplasmic lysate from the *B. abortus* 45/20 cells in rabbit 1 and against whole *B. abortus* 45/20 cells in rabbit 2. The polyclonal antibodies were purified from the rabbit serum by saturated ammonium sulphate precipitation followed by protein G affinity chromatography. The purification process was investigated using SDS-PAGE and Western Blots. The two polyclonal antibodies were then investigated for use in the development of competitive ELISAs for the detection of *B. abortus*.

#### 5.2.1.1 Estimation of antibody titres in rabbit serum

New Zealand white female rabbits were immunised with the appropriate immunogen by sub-cutaneous injection as described in Section 2.4.3. Rabbit 1 was immunised with the crude cytoplasmic lysate from *Brucella abortus* 45/20 cells and rabbit 2 was immunised with whole *Brucella abortus* 45/20 cells. Each rabbit was sacrificed 72 days after the initial immunisation and the serums recovered. Antibody titres against the crude cytoplasmic lysate and whole *Brucella abortus* 45/20 cells were determined for each rabbit, as detailed in Section 2.4.6. The antibody titre was defined as the highest antibody dilution with an absorbance value that was greater than 2 standard deviations (SD) above the mean absorbance value for the zero control. The resulting titres were greater than 1/327,6800 and are shown in Figures 5.2 and 5.3 for rabbit 1 and 2, respectively.

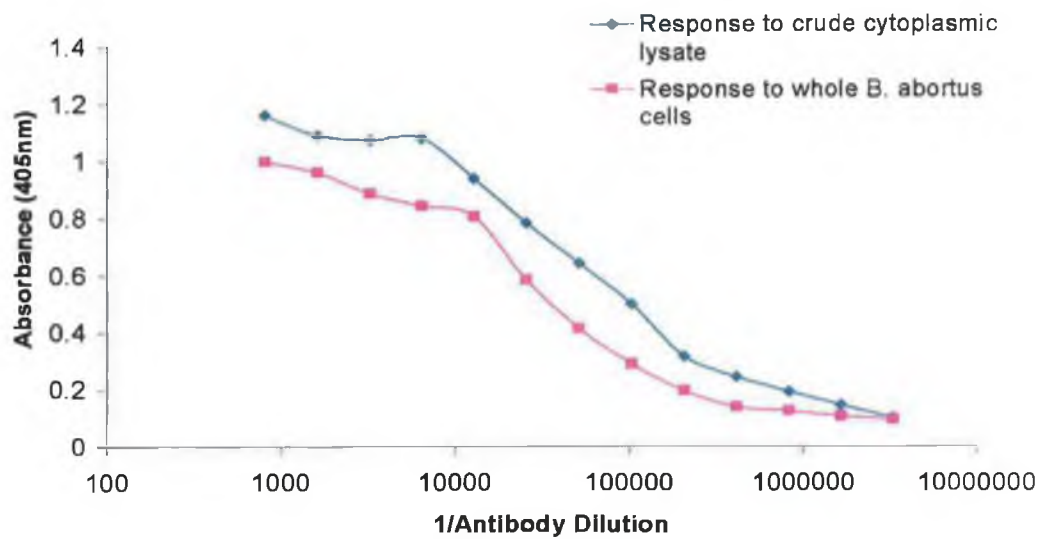


**Figure 5.2:** Graphical representation of the final serum titres obtained from rabbit 1 against the crude cytoplasmic lysate from *B. abortus* 45/20 and whole *B. abortus* 45/20 cells. Serial dilutions of the serum ranging from 1/800 – 1/327,6800 were prepared in PBS and added to wells of a microtitre plate coated with the crude cytoplasmic or whole *B. abortus* cells. The final serum titre obtained was 1/327,6800 against the crude cytoplasmic lysate and 1/163,8400 against *B. abortus* 45/20 cells.

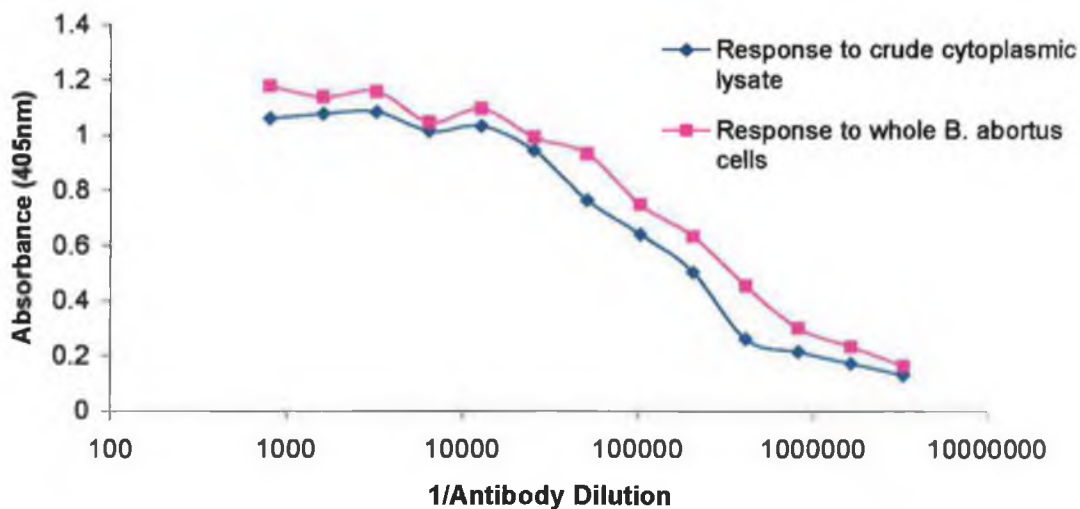


**Figure 5.3:** Graphical representation of the final serum titres obtained from rabbit 2 against the crude cytoplasmic lysate from *B. abortus* 45/20 and whole *B. abortus* 45/20 cells. Serial dilutions of the serum ranging from 1/800 – 1/327,6800 were prepared in PBS and added to wells of a microtitre plate coated with the crude cytoplasmic or whole *B. abortus* cells. The final serum titre obtained was 1/327,6800 against the crude cytoplasmic lysate and 1/163,8400 against *B. abortus* 45/20 cells.

### 5.2.1.2 Purification of polyclonal anti-sera

The purification of polyclonal anti-*Brucella* antibodies from the rabbit serum was achieved using a saturated sulphate ammonium sulphate (SAS) precipitation followed by protein G affinity chromatography, as described in Section 2.4.5. The partially purified antibodies from the SAS precipitation were affinity purified using a protein G column. The rabbit IgG antibodies were eluted from the protein G, following extensive washing, using glycine buffer at pH 2.2. The absorbances of the eluted fractions were analysed at 280nm to monitor the protein content. Figure 5.4 shows the typical elution profile of the IgG antibodies from the protein G column, for rabbit 1 and rabbit 2. Results suggest that the majority of antibody was eluted in the first three fractions, which were pooled and dialysed in PBS. Titres of the affinity-purified antibodies were then determined for rabbit 1 (pAB1) and rabbit 2 (pAB2). Titres in excess of 1/400,000 were obtained for pAB1 and pAB2 against the crude cytoplasmic lysate and whole *B. abortus* cells.

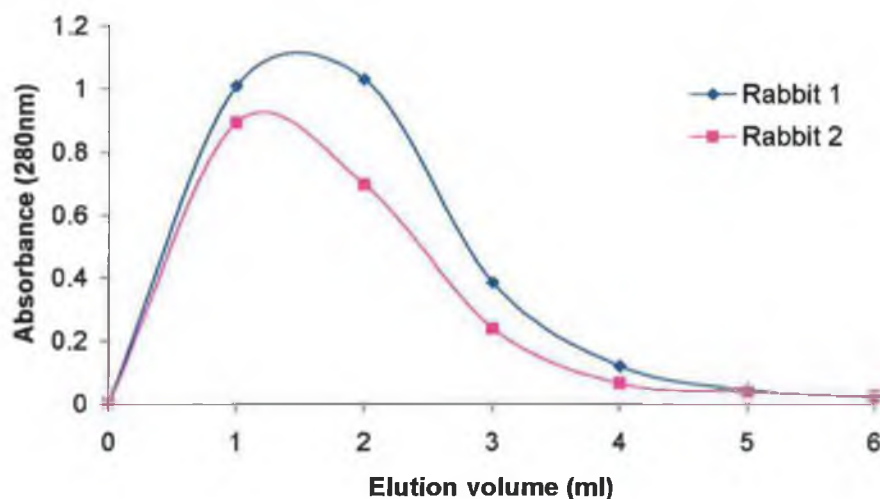


**Figure 5.4:** Typical elution profile for polyclonal antibodies from rabbit 1 and rabbit 2 from a 1ml protein G affinity chromatography column. The purified IgG antibodies were eluted from the protein G column using 0.2 M glycine, pH 2.2. 1ml fractions were collected and the protein content estimated by measuring absorbance at 280nm. In the case of rabbits 1 and 2 fractions 1-3 contained the majority of the eluted IgG antibodies and were collected and pooled.

### **5.2.1.3 Characterisation of purified antibodies by SDS-PAGE**

The purification process was investigated by sodium dodecyl sulphate polyacrylamide gel electrophoresis (SDS-PAGE) as described in Section 2.2.22. The antibodies, at each stage of the purification process, were electrophoresed under reducing conditions, which separated the proteins and their components on the basis of molecular weights. The level of purity obtained was assessed by comparisons between the serum, SAS precipitated and the protein G-purified antibodies. Figures 5.5 and 5.6 show the acrylamide gels obtained for rabbit 1 and rabbit 2, respectively. In each case, two bands were clearly visible following the protein G affinity chromatography. One band with a molecular weight of 50kDa corresponds to the heavy chain and the second band with a molecular weight of 25kDa indicates the presence of the light chain.

### **5.2.1.4 Western blot analysis of purified antibodies**

As previously discussed in Section 5.2.1.3, the purification process was assessed using SDS-PAGE, which separates the proteins according to the molecular weights. However, the SDS-PAGE cannot be probed with antibodies to confirm the presence of rabbit IgG antibody molecules. Therefore, the proteins were transferred from the polyacrylamide gels to nitrocellulose by electrophoretic means. The nitrocellulose was probed using an alkaline phosphatase labelled anti-rabbit IgG secondary antibody. The presence of rabbit IgG antibodies was then confirmed upon addition of a chromogenic substrate. Figures 5.7 and 5.8 show the Western blots for rabbits 1 and 2, respectively. Two bands are visible on each blot for the protein G-purified antibody. A band at 50kDa represents the heavy chain and one at 25kDa represents the light chain.

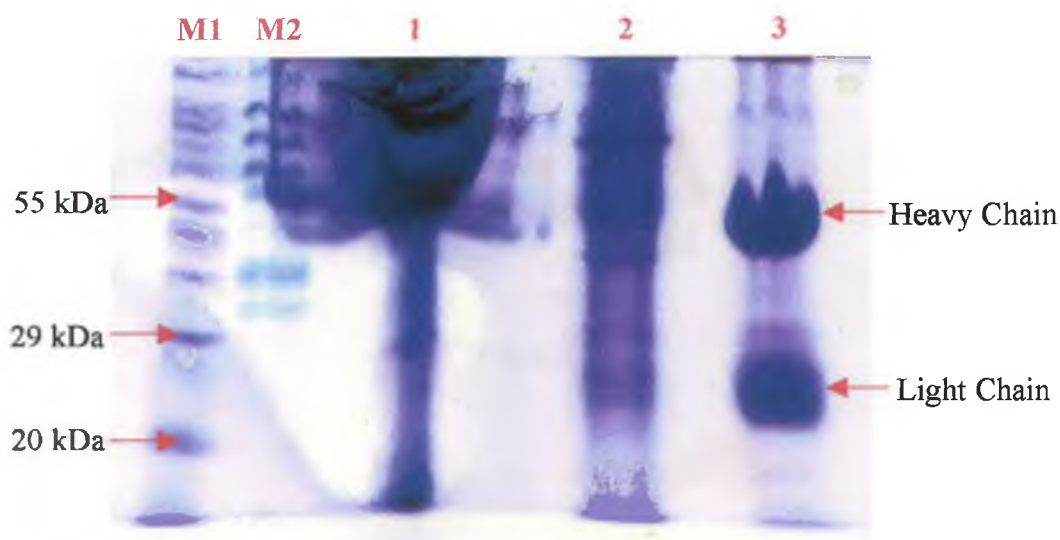


**Figure 5.5:** SDS-PAGE analysis on the purification of the anti-*Brucella* antibodies from serum isolated from rabbit 1. Lane M1: Sigma wide-range molecular weight marker; Lane M2: Sigma prestained molecular weight markers; Lane 1: Unpurified anti-*Brucella* antibodies from rabbit serum, which was diluted 1 in 5 with PBS; Lane 2: Partially purified rabbit antibodies following sodium sulphate precipitation, which was diluted 1 in 2 with PBS; Lane 3: Purified rabbit antibodies obtained following protein G affinity chromatography. The protein G-purified sample in lane 3 has two distinct bands, at approximately 25 and 50kDa, which are consistent with the presence of antibody heavy and light chains, respectively.

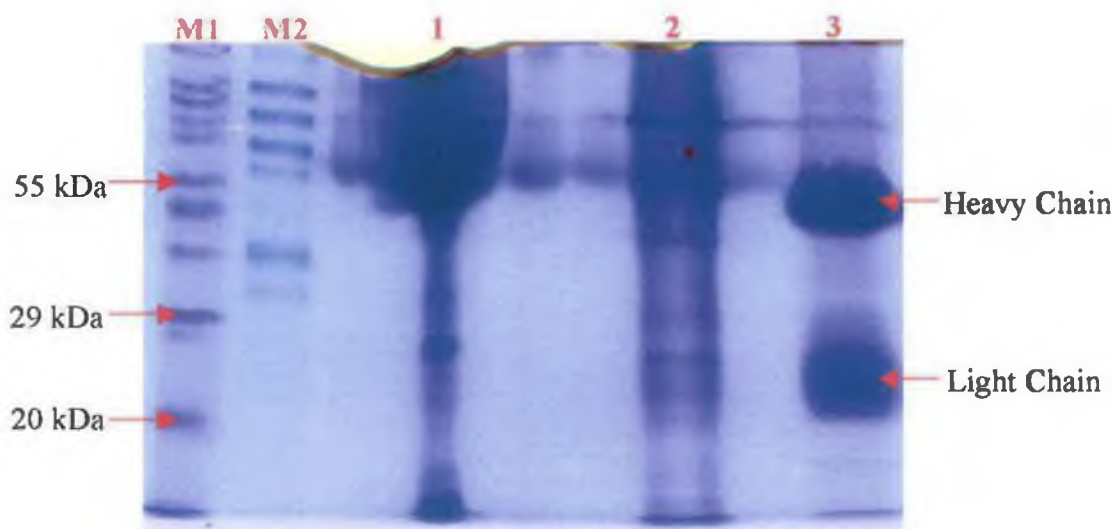


**Figure 5.6:** SDS-PAGE analysis on the purification of the anti-*Brucella* antibodies from serum isolated from rabbit 2. Lane M1: Sigma wide-range molecular weight marker; Lane M2: Sigma prestained molecular weight markers; Lane 1: Unpurified anti-*Brucella* antibodies from rabbit serum, which was diluted 1 in 5 with PBS; Lane 2: Partially purified rabbit antibodies following sodium sulphate precipitation, which was diluted 1 in 2 with PBS; Lane 3: Purified rabbit antibodies obtained following protein G affinity chromatography. The protein G-purified sample in lane 3 has two distinct bands, at approximately 25 and 50kDa, which are consistent with the presence of antibody heavy and light chains, respectively.

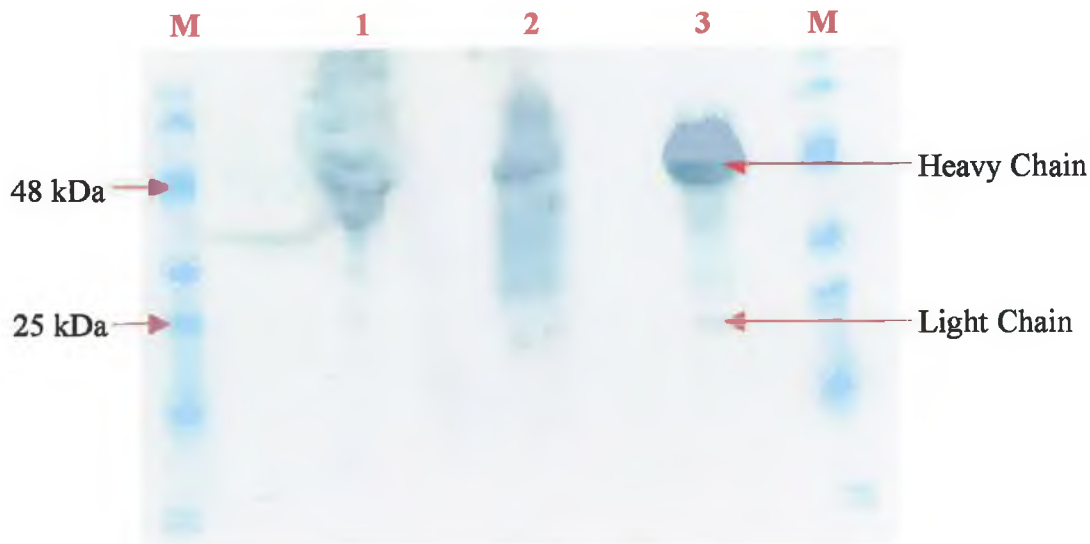


*Figure 5.7: Western blot analysis on the purification of the anti-Brucella antibodies from serum isolated from rabbit 1. The proteins were electrophoresed using SDS-PAGE and then transferred to nitrocellulose membrane, which was probed using an alkaline phosphatase-labelled anti-rabbit antibody to confirm the presence of rabbit antibodies. Lane M: Pierce Blue Ranger prestained molecular weight markers; Lane 1: Unpurified anti-Brucella antibodies from rabbit serum, which was diluted 1 in 5 with PBS; Lane 2: Partially purified rabbit antibodies following sodium sulphate precipitation, which was diluted 1 in 2 with PBS; Lane 3: Purified rabbit antibodies obtained following protein G affinity chromatography. The protein G-purified antibody sample in lane 3 has two distinct bands, at approximately 25 and 50kDa, which are consistent with the presence of antibody heavy and light chains, respectively.*

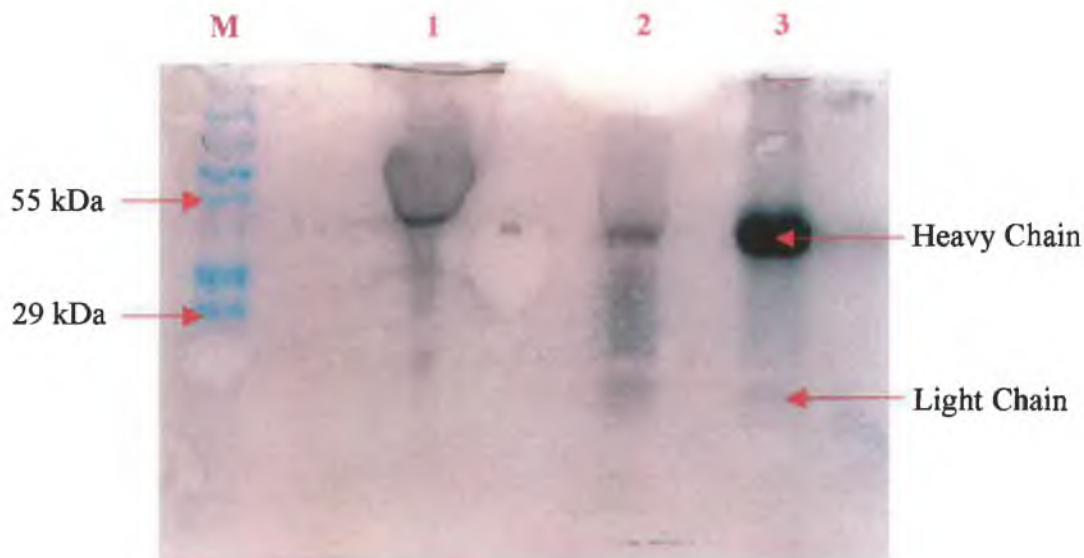


**Figure 5.8:** Western blot analysis on the purification of the anti-*Brucella* antibodies from serum isolated from rabbit 2. The proteins were electrophoresed using SDS-PAGE and then transferred to nitrocellulose membrane, which was probed using an alkaline phosphatase-labelled anti-rabbit antibody to confirm the presence of rabbit antibodies. Lane M: Sigma prestained molecular weight markers; Lane 1: Unpurified anti-*Brucella* antibodies from rabbit serum, which was diluted 1 in 5 with PBS; Lane 2: Partially purified rabbit antibodies following sodium sulphate precipitation, which was diluted 1 in 2 with PBS; Lane 3: Purified rabbit antibodies obtained following protein G affinity chromatography. The protein G-purified antibody sample in lane 3 has two distinct bands, at approximately 25 and 50kDa, which are consistent with the presence of antibody heavy and light chains, respectively.

### **5.2.1.5 Development of competitive ELISAs for the detection of *B. abortus***

Competitive ELISAs were then developed for the detection of *B. abortus* using the affinity purified polyclonal antibodies from rabbit 1 and 2, which were designated pAB1 and pAB2, respectively.

#### **5.2.1.5.1 Optimisation of competitive ELISA for the detection of *B. abortus***

Initial checkerboard ELISAs was carried on the pAB1 and pAB2 to determine the optimal antibody dilution and cell-coating concentration for use in a competitive ELISA. Several *B. abortus* 45/20 cell coating concentrations, ranging from 0 to  $1.6 \times 10^{10}$  cells/ml and antibody dilutions between 1/100 and 1/1000000, of pAB1 and pAB2, were assayed. The optimal cell-coating concentration for pAb1 was found to be  $1.6 \times 10^8$  cells/ml and the optimum antibody dilution determined to be 1/5000 (Fig. 5.9). The optimal cell-coating concentration for pAB2 was also found to be  $1.6 \times 10^8$  cells/ml, with a 1/5000 antibody dilution (Fig. 5.10).

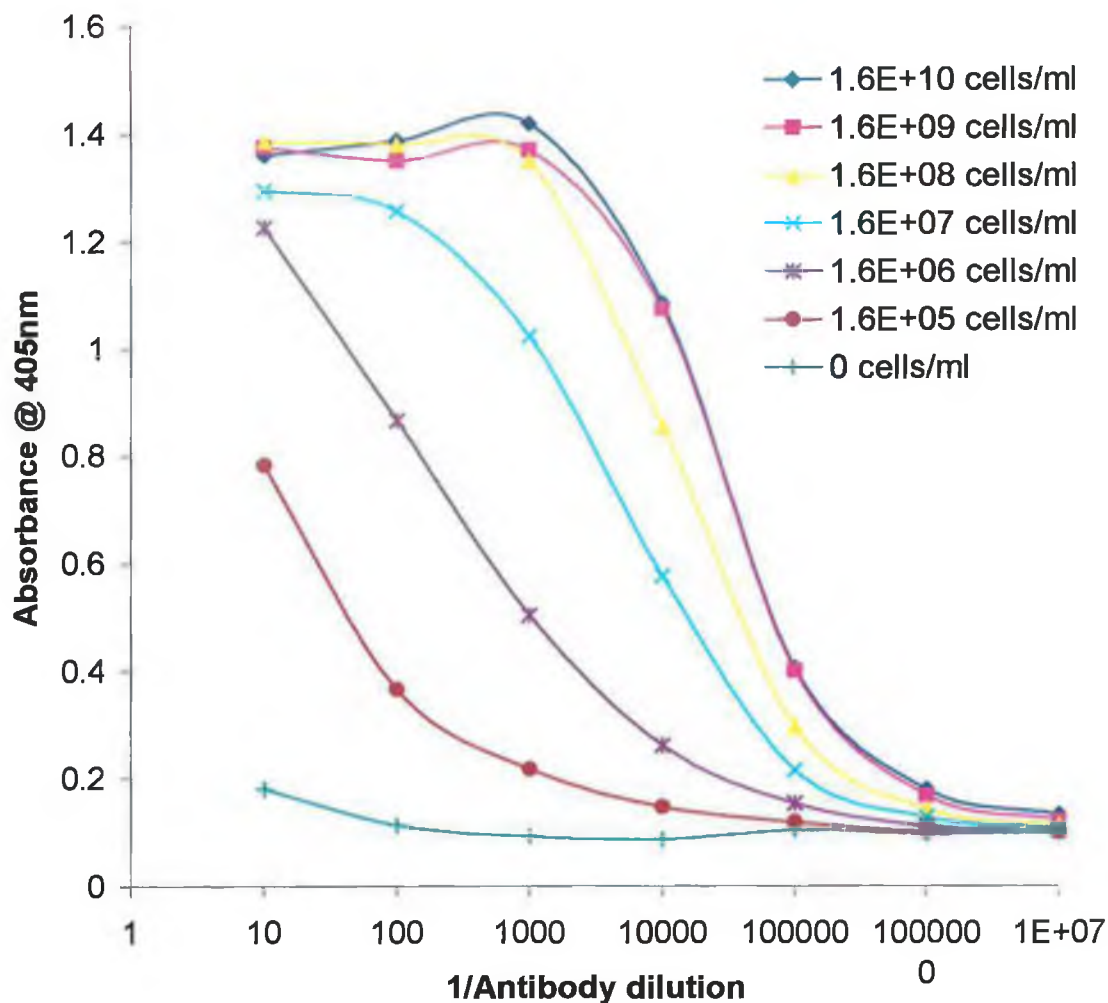


**Figure 5.9:** Checkerboard ELISA on pAB1, for determination of the optimal cell-coating concentration and antibody dilution, for use in a competitive ELISA for the detection of *B. abortus*. The optimal cell coating concentration chosen was  $1.6 \times 10^8$  cells/ml and the optimal antibody dilution, which gave 70% of the maximum absorbance, was 1/5000.

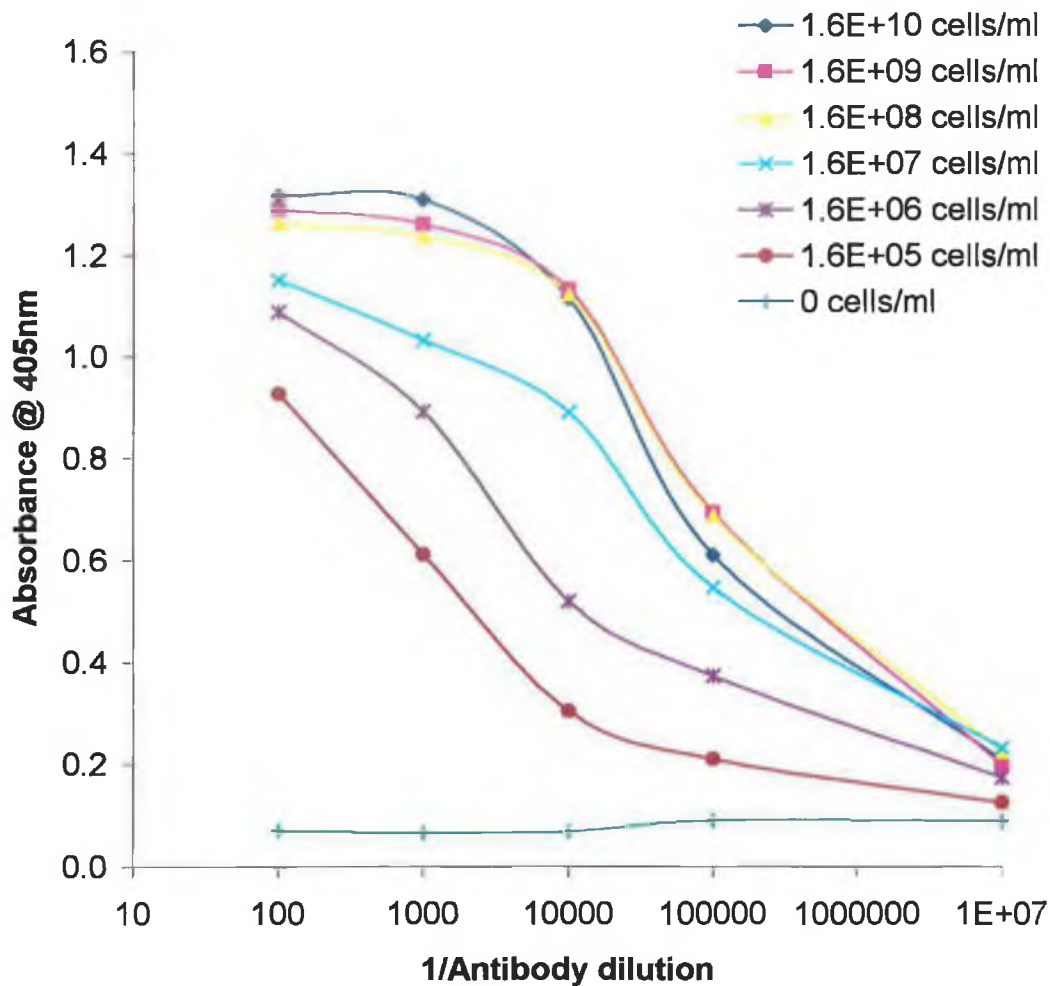


**Figure 5.10:** Checkerboard ELISA on pAB2, for determination of the optimal cell-coating concentration and antibody dilution for use in a competitive ELISA for the detection of *B. abortus*. The optimal cell coating concentration chosen was  $1.6 \times 10^8$  cells/ml and the optimal antibody dilution, which gave 70% of the maximum absorbance, was 1/5000.

#### 5.2.1.5.2 Development of competitive ELISAs for the detection of *B. abortus*

Following optimisation of the various assay parameters, competitive ELISAs were developed for the detection of *B. abortus*. The range of detection for each antibody was determined using immunoplates coated with  $1.6 \times 10^8$  cells/ml of *B. abortus*. *B. abortus* standards ranging from  $9.77 \times 10^5$  to  $1.00 \times 10^9$  cells/ml were added to the immunoplate with an equal volume of the pAB1 or pAB2 antibody diluted to 1/5000. Intra- and inter-day variability studies were then carried out on the polyclonal antibodies in order to estimate assay reproducibility.

In order to determine the intra-day assay variation each *B. abortus* cell concentration was assayed five times on one day and the mean absorbance of bound antibody at each cell concentration plotted against the cell concentration. Using Biaevaluation 3.1 software the calibration curve was plotted using the four-parameter equation with the range of detection for free *B. abortus* 45/20 cells found to be between  $1.95 \times 10^6$  and  $1.00 \times 10^9$  cells/ml for pAB1 and  $9.77 \times 10^5$  to  $1.00 \times 10^9$  cells/ml for pAb2 (Data not shown). The coefficients of variation (CVs) between the five replicates at each cell concentration were determined by expressing the standard deviation as a percentage function of the mean. The intra-day coefficients of variation (CVs) ranged from 1.32 to 8.96% and 0.32 and 8.97% for pAB1 and pAB2, respectively.

The inter-day assay variations were then calculated for each of the antibodies by performing the same assay over five separate days. The normalised mean values, which were calculated as the mean absorbance at each antigen concentration / absorbance in the presence of zero antigen concentration ( $A/A_0$ ), over the five days were used to construct a separate calibration curve for the inter-day assay. The inter-day assay on pAB1 had a range of detection for *B. abortus* cells between  $1.95 \times 10^6$  and  $1.00 \times 10^9$  cells/ml (Fig. 5.11). The C.V.'s for this inter-day assay were determined and ranged between 0.73 and 5.85% (Table 5.2). The inter-day assay obtained for pAB2 had a range of detection for *B. abortus* cells between  $9.77 \times 10^5$  and  $1.00 \times 10^9$  cells/ml (Fig. 5.12) and CVs between 1.14 and 6.40% (Table 5.3), indicating that the two competitive ELISAs were reproducible over five days.

*Table 5.2: Inter-day assay coefficients of variation for the detection of B. abortus 45/20 cells using pAB1. Five sets of ten standards were assayed on five different days and the coefficients of variation calculated.*

<b><i>B. abortus</i> 45/20 cells/ml</b>	<b>Calculated mean ± S.D. (A/A<sub>0</sub>)</b>	<b>Coefficient of variation (%)</b>
1.00x10 <sup>9</sup>	0.219 ± 0.005	2.33
5.00x10 <sup>8</sup>	0.250 ± 0.007	3.11
2.50x10 <sup>8</sup>	0.306 ± 0.014	4.70
1.25x10 <sup>8</sup>	0.380 ± 0.022	5.85
6.25x10 <sup>7</sup>	0.520 ± 0.020	3.85
3.13x10 <sup>7</sup>	0.594 ± 0.004	0.73
1.56x10 <sup>7</sup>	0.700 ± 0.023	3.31
7.81x10 <sup>6</sup>	0.769 ± 0.013	1.68
3.90x10 <sup>6</sup>	0.894 ± 0.018	2.05
1.95x10 <sup>6</sup>	0.946 ± 0.013	1.40

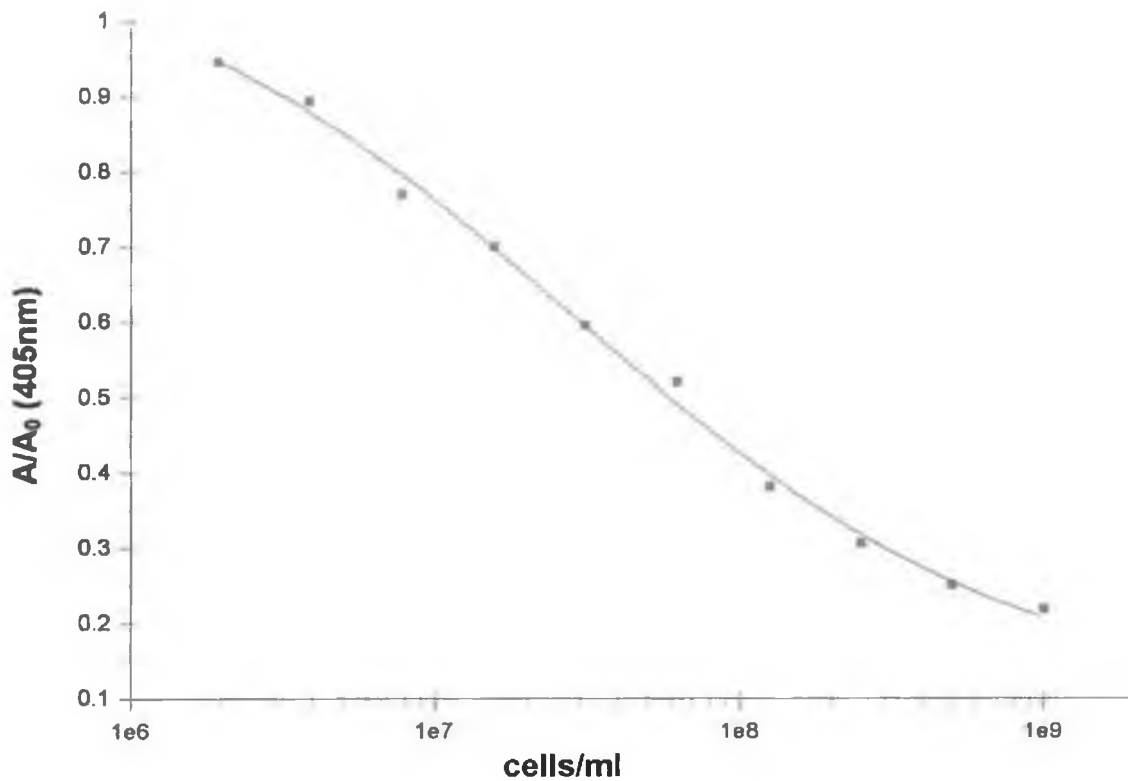


**Figure 5.11:** Inter-day assay curve for the detection of *B. abortus* 45/20 cells using pAB1 in a competitive ELISA format. The range of detection of the antibody for *B. abortus* was between  $1.95 \times 10^6$  and  $1 \times 10^9$  cells/ml. The calibration curve was plotted using Biaevaluation software 3.1 and represents the average normalised ( $A/A_0$ ) results obtained over five individual days.

**Table 5.3:** Inter-day assay coefficients of variation for the detection of *B. abortus* 45/20 cells using pAB2. Five sets of eleven standards were assayed on five different days and the coefficients of variation calculated.

<i>B. abortus</i> 45/20 cells/ml	Calculated mean $\pm$ S.D. (A/A <sub>0</sub> )	Coefficient of variation (%)
1.00x10 <sup>9</sup>	0.232 $\pm$ 0.015	6.40
5.00x10 <sup>8</sup>	0.276 $\pm$ 0.012	4.33
2.50x10 <sup>8</sup>	0.324 $\pm$ 0.018	5.65
1.25x10 <sup>8</sup>	0.393 $\pm$ 0.010	2.36
6.25x10 <sup>7</sup>	0.501 $\pm$ 0.006	1.14
3.13x10 <sup>7</sup>	0.575 $\pm$ 0.025	4.26
1.56x10 <sup>7</sup>	0.664 $\pm$ 0.016	2.42
7.81x10 <sup>6</sup>	0.715 $\pm$ 0.019	2.68
3.90x10 <sup>6</sup>	0.809 $\pm$ 0.021	2.64
1.95x10 <sup>6</sup>	0.841 $\pm$ 0.025	2.97
9.77x10 <sup>5</sup>	0.911 $\pm$ 0.014	1.49

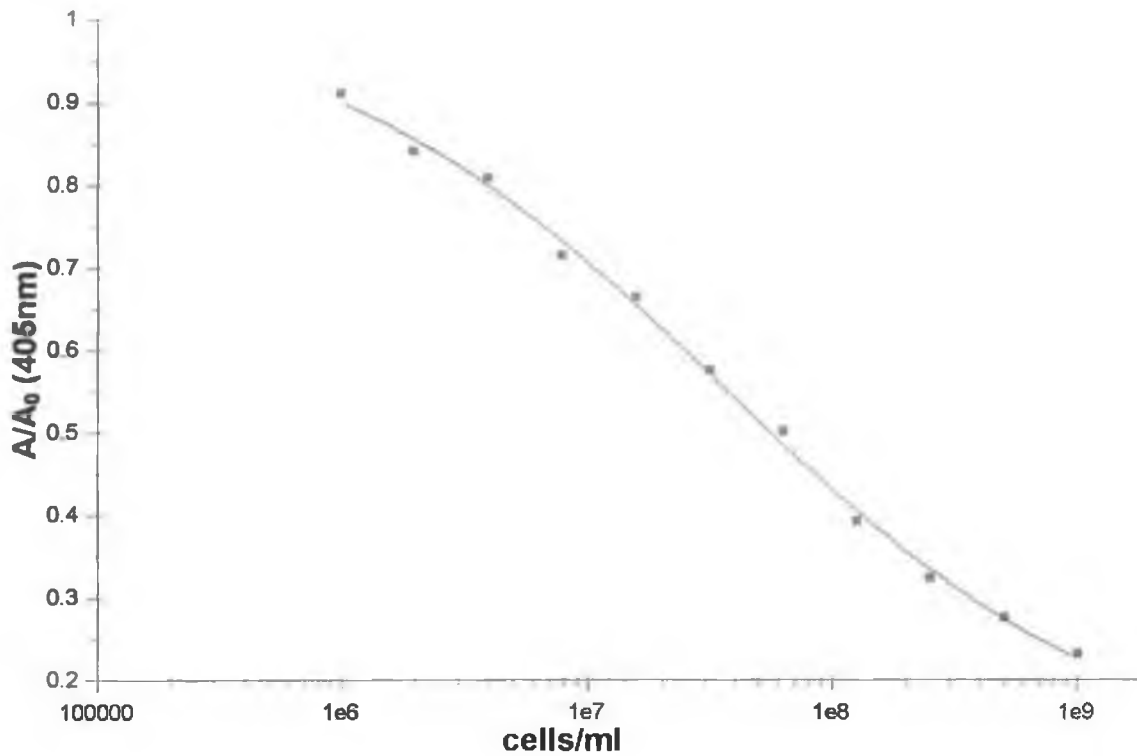


*Figure 5.12: Inter-day assay curve for the detection of B. abortus 45/20 cells using pAB2 in a competitive ELISA format. The range of detection of the antibody for B. abortus was between  $5.77 \times 10^5$  and  $1 \times 10^9$  cells/ml. The calibration curve was plotted using Biaevaluation software 3.1 and represents the average normalised ( $A/A_0$ ) results obtained over five individual days.*

### 5.2.1.5.3 Cross-reactivity studies

Cross reactivity studies were then carried out on the polyclonal antibodies to determine the antibody specificity towards *B. abortus* in relation to ubiquitous gram-positive and gram-negative bacteria (as described in Section 2.4.9). The assays were carried out as for the competitive ELISAs except the cross-reactants were added to the immunoplate with the *Brucella*-specific polyclonal antibodies. Separate calibration curves were plotted for each bacterial strain and the least detectable dose (LDD) and IC<sub>50</sub> values were determined for each as 90% A/A<sub>0</sub> and 50% A/A<sub>0</sub>, respectively. The percentage cross reactivities were then estimated at the LDD (CR<sub>90</sub>) and at the IC<sub>50</sub> (CR<sub>50</sub>) by expressing 100-fold the ratio of *B. abortus* and the cross-reacting bacterial strain.

Table 5.4 summarises the specificity and cross reactivity studies on the pAb1 against 5 gram-negative and 5 gram-positive bacterial strains. pAB1 did not display any specificity towards the gram-positive bacteria *B. subtilis*, *L. invanovii*, *L. welshimeri*, *L. innocua* and *L. swligeri* at either the LDD or IC<sub>50</sub> values with minimal levels of cross-reactivity observed (i.e. < 0.2%). Minimal levels of cross-reactivity (i.e. < 1%) were also observed between the gram-negative bacteria *E. coli*, *S. marcescens*, *E. aerogenes*, *Ps. aeruginosa* and *P. vulgaris* and pAB1 at both the LDD and IC<sub>50</sub> values. Minimal cross-reactivity was also seen with pAb2 against the gram-positive and negative bacterial strains (Table 5.5). The gram-positive bacteria displayed < 0.01% cross-reactivity with pAB2 at the LDD and IC<sub>50</sub> and < 0.02% cross-reactivity was observed between pAB2 and the gram-negative bacteria at the LDD and IC<sub>50</sub>.

*Table 5.4: Cross-reactivity and specificity studies on pAB1 against various ubiquitous bacterial strains. The cross-reactivity potential was approximated at the least detectable dose (LDD) and at the IC<sub>50</sub> value.*

<b>Bacterial strain</b>	<b>Gram stain</b>	<b>LDD<sup>a</sup></b> <b>(cells/ml)</b>	<b>IC<sub>50</sub><sup>b</sup></b> <b>(cells/ml)</b>	<b>CR<sub>90</sub><sup>c</sup></b> <b>(%)</b>	<b>CR<sub>50</sub><sup>d</sup></b> <b>(%)</b>
<i>B. abortus</i>	Negative	1.9 x 10 <sup>6</sup>	3.1 x 10 <sup>7</sup>	100	100
<i>B. subtilis</i>	Positive	>2.5 x 10 <sup>10</sup>	>2.5 x 10 <sup>10</sup>	< 0.01	< 0.2
<i>E. coli</i>	Negative	> 5.0 x 10 <sup>9</sup>	> 5.0 x 10 <sup>9</sup>	< 0.04	< 1
<i>L. invanovii</i>	Positive	4.0 x 10 <sup>11</sup>	> 8.0 x 10 <sup>11</sup>	0.01	< 0.01
<i>L. welshimeri</i>	Positive	2.7 x 10 <sup>10</sup>	> 5.5 x 10 <sup>10</sup>	< 0.01	< 0.1
<i>L. innocua</i>	Positive	>1.0 x 10 <sup>11</sup>	>1.0 x 10 <sup>11</sup>	< 0.01	< 0.1
<i>L. swligeri</i>	Positive	5.0 x 10 <sup>10</sup>	> 1.0 x 10 <sup>11</sup>	< 0.01	< 0.1
<i>S. marcescens</i>	Negative	>1 x 10 <sup>11</sup>	> 1 x 10 <sup>11</sup>	< 0.01	< 0.01
<i>E. aerogenes</i>	Negative	> 1 x 10 <sup>10</sup>	> 1 x 10 <sup>10</sup>	< 0.01	< 0.01
<i>Ps. aeruginosa</i>	Negative	> 1 x 10 <sup>10</sup>	> 1 x 10 <sup>10</sup>	< 0.01	< 0.01
<i>P. vulgaris</i>	Negative	> 1 x 10 <sup>10</sup>	> 1 x 10 <sup>10</sup>	< 0.01	< 0.01

<sup>a</sup> Least detectable dose calculated at 90% A/A<sub>0</sub>

<sup>b</sup> 50% inhibition concentration (50% A/A<sub>0</sub>)

<sup>c</sup> Percentage cross-reactivity determined at IC<sub>50</sub>

<sup>d</sup> Percentage cross-reactivity determined at LDD

**Table 5.5: Cross-reactivity and specificity studies on pAB2 against various ubiquitous bacterial strains. The cross-reactivity potential was approximated at the least detectable dose (LDD) and at the IC<sub>50</sub> value.**

<b>Bacterial strain</b>	<b>Gram stain</b>	<b>LDD<sup>a</sup></b> <b>(cells/ml)</b>	<b>IC<sub>50</sub><sup>b</sup></b> <b>(cells/ml)</b>	<b>CR<sub>90</sub><sup>c</sup></b> <b>(%)</b>	<b>CR<sub>50</sub><sup>d</sup></b> <b>(%)</b>
<i>B. abortus</i>	Negative	9.7 x 10 <sup>5</sup>	6.3 x 10 <sup>7</sup>	100	100
<i>B. subtilis</i>	Positive	>2.5 x 10 <sup>10</sup>	>2.5 x 10 <sup>10</sup>	< 0.01	< 0.01
<i>E. coli</i>	Negative	> 5.0 x 10 <sup>9</sup>	>5.0 x 10 <sup>9</sup>	< 0.02	< 0.01
<i>L. invanovii</i>	Positive	2.0 x 10 <sup>11</sup>	> 8.0 x 10 <sup>11</sup>	< 0.01	< 0.01
<i>L. welshimeri</i>	Positive	6.9 x 10 <sup>9</sup>	> 5.5 x 10 <sup>10</sup>	< 0.02	< 0.01
<i>L. innocua</i>	Positive	2.5 x 10 <sup>10</sup>	> 1.0 x 10 <sup>11</sup>	< 0.01	< 0.01
<i>L. swligeri</i>	Positive	2.5 x 10 <sup>11</sup>	>1.0 x 10 <sup>11</sup>	< 0.01	< 0.01
<i>S. marcescens</i>	Negative	>1 x 10 <sup>11</sup>	> 1 x 10 <sup>11</sup>	< 0.01	< 0.01
<i>E. aerogenes</i>	Negative	> 1 x 10 <sup>10</sup>	> 1 x 10 <sup>10</sup>	< 0.01	< 0.01
<i>Ps. aeruginosa</i>	Negative	> 1 x 10 <sup>10</sup>	> 1 x 10 <sup>10</sup>	< 0.01	< 0.01
<i>P. vulgaris</i>	Negative	> 1 x 10 <sup>10</sup>	> 1 x 10 <sup>10</sup>	< 0.01	< 0.01

<sup>a</sup> Least detectable dose calculated at 90% A/A<sub>0</sub>

<sup>b</sup> 50% inhibition concentration (50% A/A<sub>0</sub>)

<sup>c</sup> Percentage cross-reactivity determined at IC<sub>50</sub>

<sup>d</sup> Percentage cross-reactivity determined at LDD

#### 5.2.1.6 Antibody binding reactivity analysis on pAB1 and pAB2

The antibody binding reactivity of pAB1 and pAB2 was determined against the crude cell lysate from *B. abortus* 45/20 cells and against the *Brucella*-specific recombinant proteins, p18 and bp26, using Western blot analysis as described in Section 2.2.23.

*B. abortus* 45/20 cells were disrupted by sonication and the crude cell lysate electrophoresed using SDS-PAGE. The electrophoresed proteins were then transferred to nitrocellulose, which was probed using pAB1 and pAB2 followed by an alkaline phosphatase-labelled anti-rabbit antibody. Figure 5.12 shows the Western blots obtained for the crude cell lysate, which was probed using pAB1 (A) and pAB2 (B). pAB1 recognised two main proteins from the crude cell lysate with molecular weights of approximately 18 and 45kDa (Fig. 5.13 A). The pAB2 antibody, which was raised against whole *B. abortus* 45/20 cells, recognised four main proteins, with apparent molecular weights of 15, 18, 38 and 45kDa (Fig. 5.13 B).

The specificity of pAB1 and pAB2 towards p18 and bp26 was established using Western blot analysis. The recombinant proteins were electrophoresed alongside a prestained molecular weight marker using SDS-PAGE and then transferred to nitrocellulose for Western blot analysis. The transferred proteins were probed using pAB1 and pAB2 followed by an alkaline phosphatase-labelled anti-rabbit antibody. Figure 5.14 represents the Western blots obtained using pAB1 (A) and pAB2 (B). Both polyclonal antibodies were capable of detecting p18 (Lane 1) with a band clearly visible at 18kDa. However, the polyclonal antibodies failed to detect the 26kDa periplasmic protein, bp26 (Lane 2).

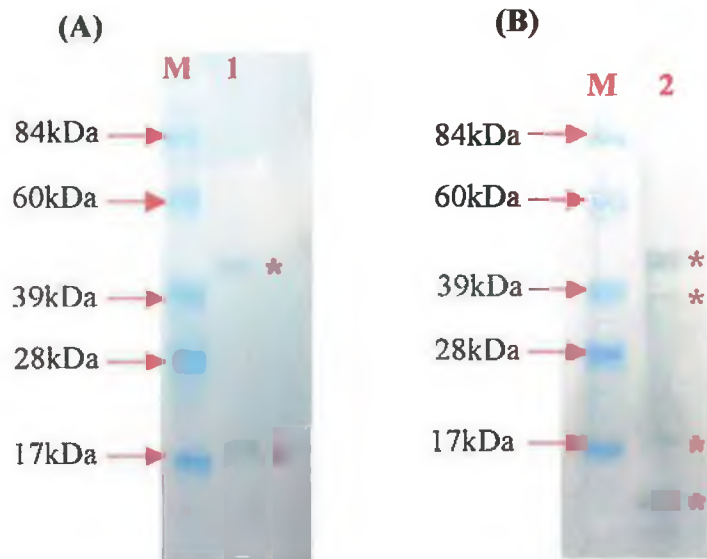


**Figure 5.13:** Antibody binding reactivity analysis on pAB1 and pAB2 against the crude cell lysate from *B. abortus* 45/20. The crude cell lysate was electrophoresed using SDS-PAGE and transferred to nitrocellulose, which was then probed using pAB1 and pAB2. (A) Represents Western blot analysis on the crude cell lysate probed using pAB1. Lane M: Pierce Blue Ranger prestained molecular weight markers; Lane 1: Crude cell lysate from *B. abortus* 45/20 cells. (B) Represents the Western blot analysis on the crude cell lysate probed using pAB2. Lane M: Pierce Blue Ranger prestained molecular weight markers; Lane 1: Crude cell lysate from *B. abortus* 45/20 cells. Specific-proteins detected with pAB1 and pAB2 denoted with an asterisks.

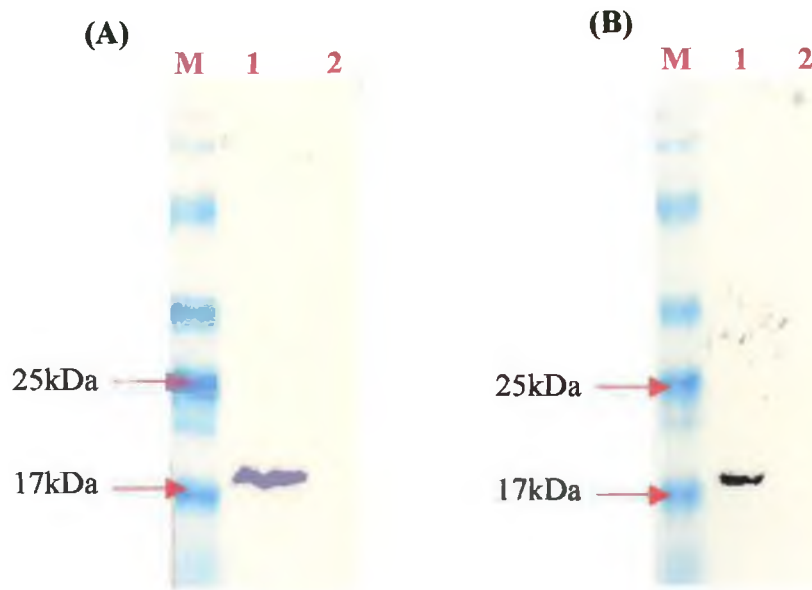


**Figure 5.14:** Antibody binding reactivity analysis on pAB1 and pAB2 against the two recombinant proteins p18 and bp26. The recombinant proteins were electrophoresed using SDS-PAGE and transferred to nitrocellulose, which was then probed using pAB1 and pAb2. (A) Represents Western blot analysis on the recombinant proteins probed using pAB1. Lane M: Pierce Blue Ranger prestained molecular weight markers; Lane 1: p18; Lane 2: bp26. (B) Represents the Western blot analysis on the recombinant proteins probed using pAB2. Lane M: Pierce Blue Ranger prestained molecular weight markers; Lane 1: p18; Lane 2: bp26. pAB1 and pAB2 are capable of detecting p18 with bands clearly visible at 18kDa (Lanes 1). However, the polyclonal antibodies are unable to detect the bp26 with no corresponding bands at 26kDa visible in Lanes 2.

### **5.2.2 The isolation of *Brucella*-specific scFv antibody fragments from a naïve phage display library**

The BMV library is a large non-immunised scFv phage display library that was developed by Vaughan *et al.* (1996) and kindly donated by Cambridge Antibody Technology (CAT) (Cambridge, England). Functional V-gene segments were isolated from 43 non-immunised human donors and used to construct a repertoire of  $1.4 \times 10^{10}$  single-chain Fv (scFv) displayed on the surface of phage. The scFv fragments were cloned into a phagemid vector, pCANTAB6, which enables the production of phage-displayed scFv in the presence of a helper phage (M13 K07) or soluble scFv in the presence of IPTG in the growth media. scFvs expressed from the pCANTAB vector contain a stretch of six histidines (6xHis) for immobilised metal affinity chromatography (IMAC) purification and a sequence derived from c-myc for detection.

BMV library stocks were panned against the p18 and bp26 recombinant proteins, for the selection of specific-phage clones, displaying scFvs directed against the recombinant proteins. Generally, 4-6 rounds of panning are required for the successful selection of positive clones from a non-immunised library (Vaughan *et al.*, 1996). This section details six rounds of panning carried out on the BMV library against the p18 and bp26 recombinant proteins and the subsequent isolation and characterisation of soluble scFvs.

### **5.2.2.1 Panning procedure for the detection of scFv phage display antibodies directed against p18**

Six rounds of panning were carried out on the BMV library stocks against the recombinant p18. Table 5.6 gives a summary of the phage titres obtained and the number of positive clones isolated that recognised p18.

The BMV library stocks received consisted of  $1.4 \times 10^{10}$  cfu/ml of scFv-displaying phage particles. These were initially used for the first round of panning against p18. Panning was carried out in immunotubes coated with  $10\mu\text{g/ml}$  of p18 (as described in Section 2). Following the first round of selection panned library stocks were prepared and the output phage titre obtained (as described in Section 2.5.1).  $5.6 \times 10^4$  cfu/ml of phage were produced following the first round of panning. These were then used for the second round of panning, where a phage titre of  $2 \times 10^2$  cfu/ml was obtained. 95 random clones were selected from the second round of panning and the scFv-displaying-phage produced from each were analysed, using a phage ELISA, for recognition of p18. No positive phage recognising p18 were isolated. A third round of panning was then carried out and a phage titre of  $1.6 \times 10^6$  cfu/ml obtained. 95 random clones screened did not recognise p18. Following the fourth round of panning, which yielded a phage titre of  $5.6 \times 10^5$  cfu/ml, 5 positive phage recognising p18 were isolated. However, attempts made to express soluble p18-specific scFvs were unsuccessful. Therefore, a fifth and sixth round of panning was carried out with phage titres of  $3.7 \times 10^4$  and  $3.7 \times 10^3$  cfu/ml obtained, respectively. Phage ELISAs were carried out on 95 random clones from each round of panning and 8 positive clones recognising p18 were selected following the fifth round of panning and 10 were selected following the sixth round (Fig. 5.15). However, once again attempts made to isolate soluble p18-specific scFvs were unsuccessful. Figure 5.16 shows the results obtained for the soluble ELISA on the supernatant and periplasmic lysate, following the sixth round of panning, with no soluble scFvs directed against the p18 isolated.

**Table 5.6:** Data obtained following six rounds of panning on the naïve BMV library against p18.

Pan	Input Titre (cfu/ml)	Output Titre (cfu/ml)	# Clones assayed	# Positive phage clones	# Clones recognising free protein
1	$1 \times 10^{13}$	$5.6 \times 10^4$	-	-	-
2	$7.2 \times 10^{10}$	$2 \times 10^2$	95	0	0
3	$2.4 \times 10^8$	$1.6 \times 10^6$	95	0	0
4	$4.9 \times 10^9$	$5.6 \times 10^5$	95	5	0
5	$1.9 \times 10^8$	$3.7 \times 10^4$	95	8	0
6	$8.1 \times 10^7$	$3.7 \times 10^3$	95	10	0

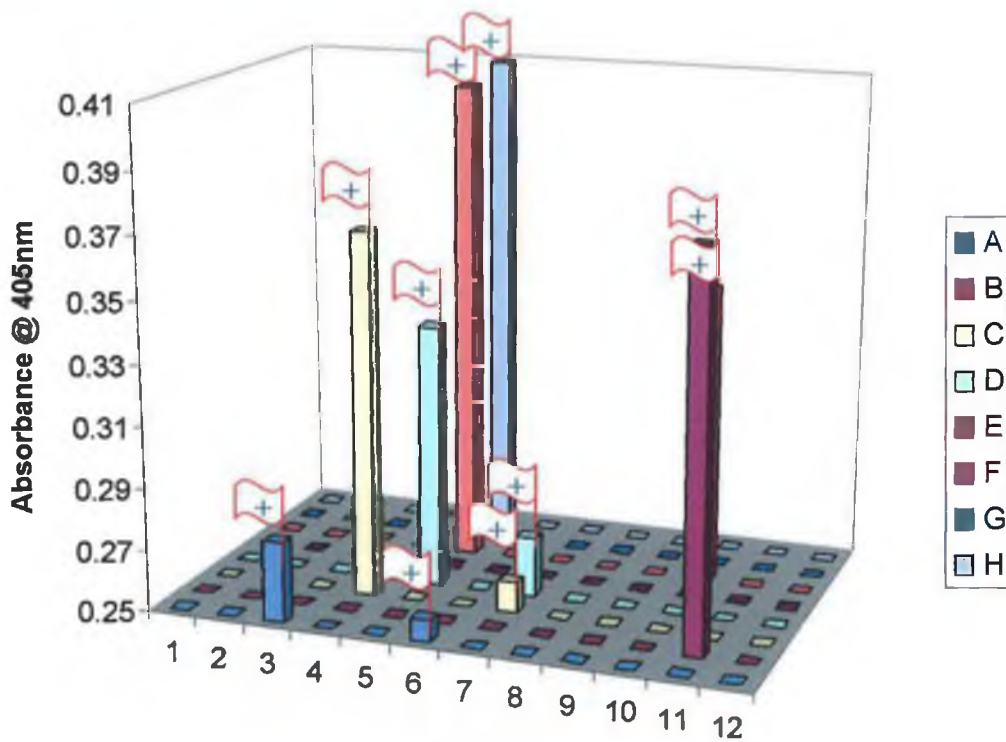


**Figure 5.15:** Bar graph represents the phage ELISA analysis on the 95 clones randomly selected following the sixth round of panning on the BMV library against p18. The flagged bars represent the positive phage clones that recognised immobilised p18.

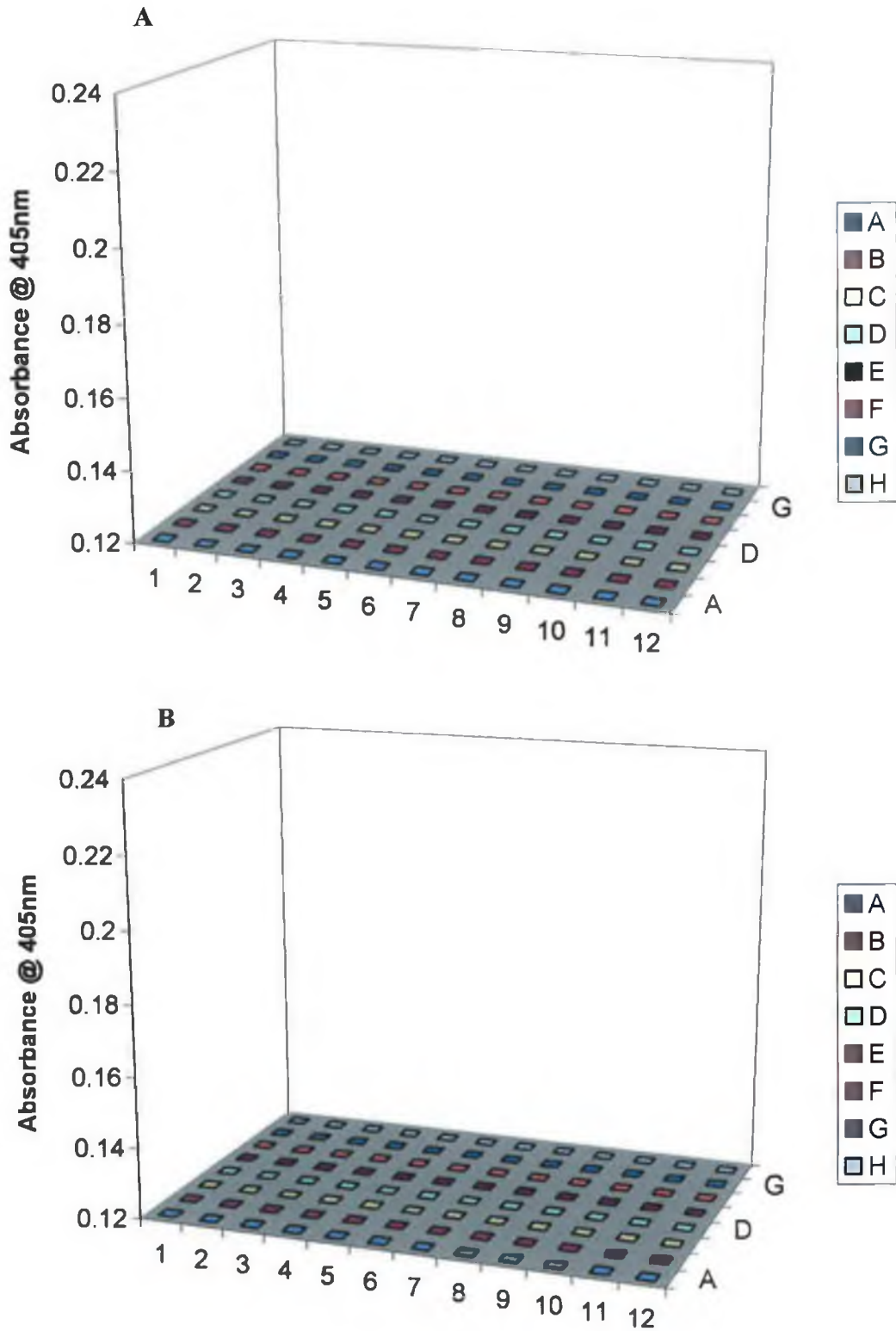


**Figure 5.16:** Bar graphs representing the soluble ELISA analysis on the 95 clones randomly selected following the sixth round of panning on the BMV library against p18. Following soluble scFv expression, upon addition of IPTG, the culture supernatants (A) and the periplasmic lysates (B) were analysed for the expression of p18-specific scFvs. However, no soluble scFvs directed against p18 were isolated.

### **5.2.2.2 Panning procedure for the detection of scFv phage display antibodies directed against bp26**

Six rounds of panning were also carried out on the BMV library stocks against the recombinant bp26. Table 5.7 gives a summary of the phage titres obtained and the number of positive clones isolated that recognised bp26.

The BMV library stocks consisting of  $1.4 \times 10^{10}$  cfu/ml of phage were used for the first round of panning against bp26. Phage particles produced from the first round stocks were then used for the second round of panning. A phage titre of  $1.5 \times 10^2$  cfu/ml was obtained following the second round of panning and the 95 random clones analysed did not recognise bp26. A third round of panning was then carried out, as before, and a phage titre of  $1.2 \times 10^4$  cfu/ml was obtained. 95 random clones were screened and no phage recognising bp26 were isolated. A fourth round of panning yielded a phage titre of  $4.4 \times 10^5$  cfu/ml of phage and following analysis, of 95 random clones, 12 positive phage recognising bp26 were isolated. However, attempts made to isolate soluble bp26-specific scFvs were unsuccessful. Therefore, a fifth and sixth round of panning was carried out with phage titres of  $1.3 \times 10^4$  and  $2.7 \times 10^5$  cfu/ml obtained, respectively. Phage ELISAs were carried out on 95 random clones from each round of panning and 2 positive clones recognising bp26 were isolated following the fifth round of panning and 9 were isolated following the sixth round (Fig. 5.17). Attempts made to isolate soluble bp26-specific scFvs were unsuccessful following the fifth round of panning. However, following the sixth round of panning soluble scFvs were isolated from the culture supernatant of 5 clones and from the periplasm of 5 clones (Fig. 5.18). The 5 positive clones B7, B11, B12, C12 and D9 expressed anti-bp26 scFvs into the supernatant and clones B7, B9, B11, B12 and D9 expressed soluble scFvs into the periplasm.

*Table 5.6: Data obtained following six rounds of panning on the naïve BMV library against bp26.*

Pan	Input Titre (cfu/ml)	Output Titre (cfu/ml)	# Clones assayed	# Positive phage clones	# Clones recognising free protein
1	$1 \times 10^{13}$	$5.1 \times 10^4$	-	-	-
2	$6.3 \times 10^{10}$	$1.5 \times 10^2$	95	0	0
3	$2.7 \times 10^8$	$1.2 \times 10^4$	95	0	0
4	$3.5 \times 10^8$	$4.4 \times 10^5$	95	12	0
5	$2.2 \times 10^8$	$1.3 \times 10^4$	95	2	0
6	$9.5 \times 10^7$	$2.7 \times 10^5$	95	9	6

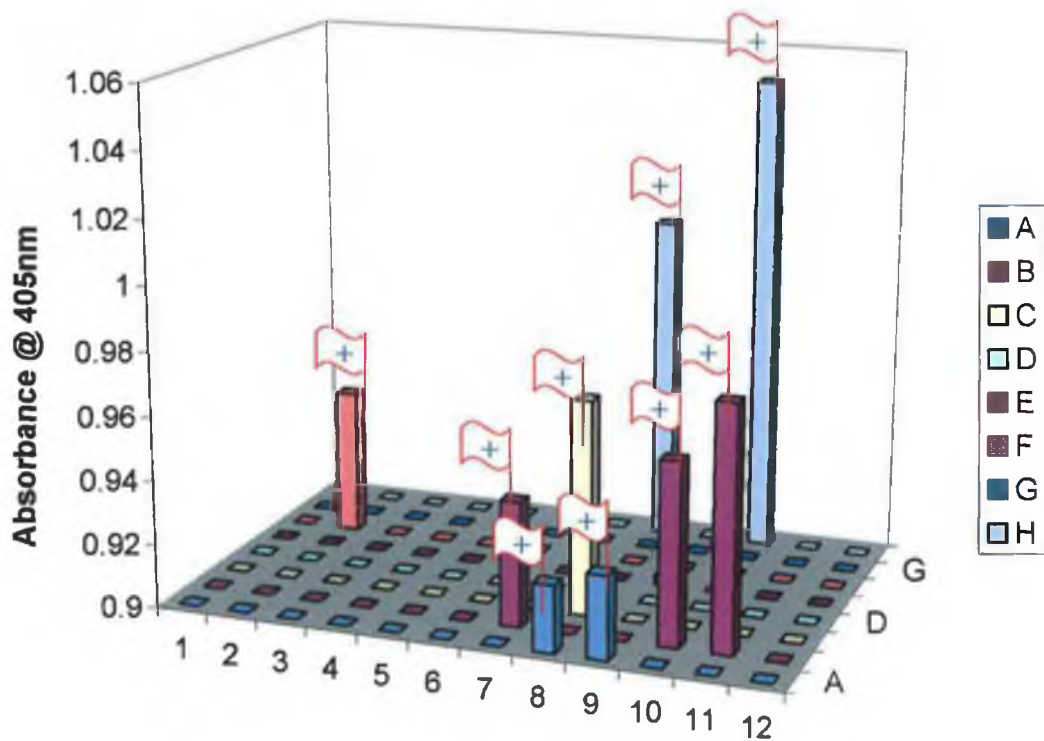


*Figure 5.17: Bar graph representing the phage ELISA analysis on the 95 clones randomly selected following the sixth round of panning on the BMV library against bp26. The flagged bars represent the positive phage clones that recognised immobilised bp26.*

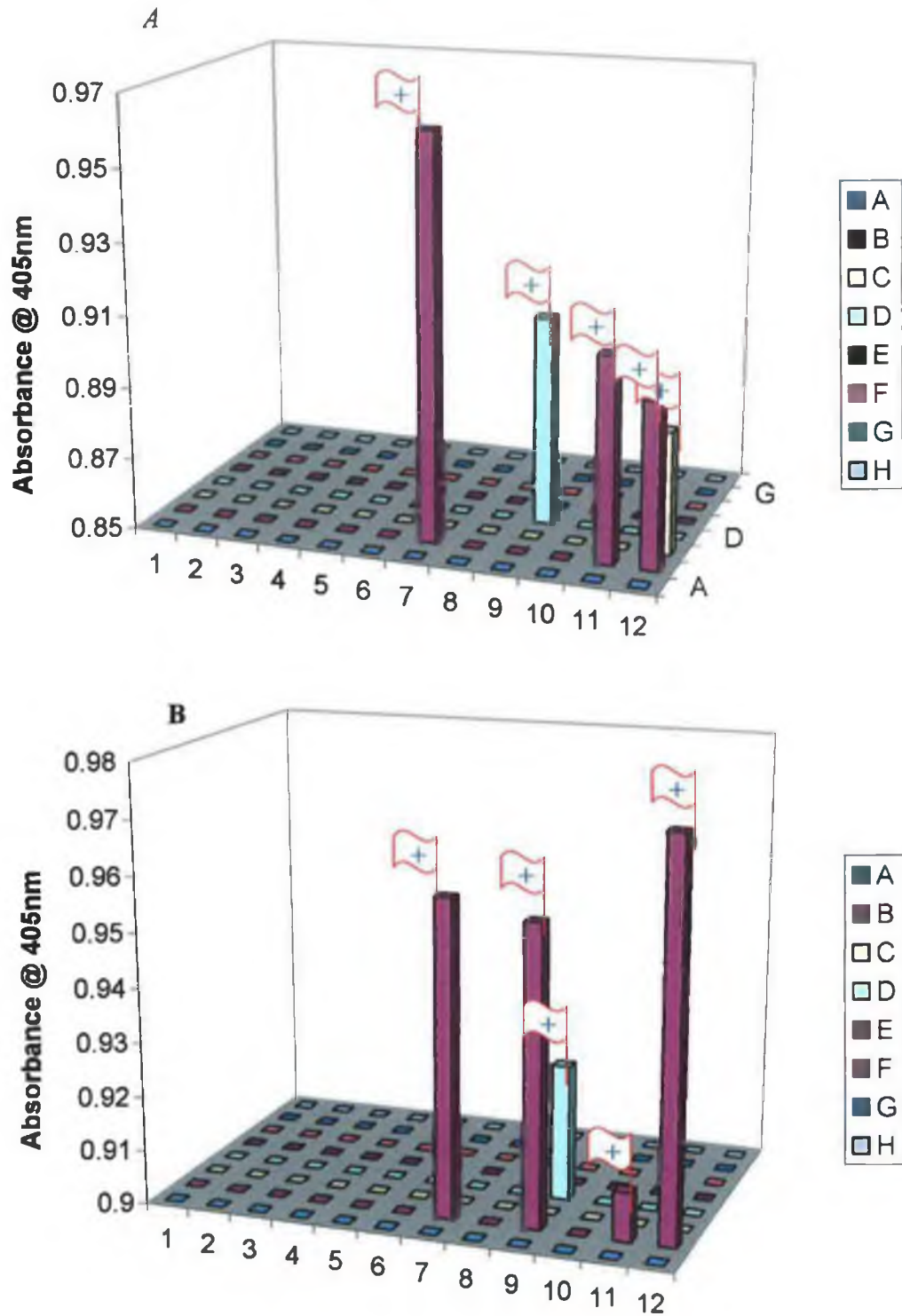


*Figure 5.18: Bar graphs representing the soluble ELISA analysis on the 95 clones randomly selected following the sixth round of panning on the BMV library against bp26. Following soluble scFv expression, upon addition of IPTG, the culture supernatants (A) and the periplasmic lysates (B) were analysed for the expression of bp26-specific scFvs. The flagged bars represent the soluble scFvs that recognised bp26.*

### **5.2.2.3 Analysis on the soluble anti-bp26 scFvs for recognition of free bp26**

Competitive ELISAs were then carried out on the soluble scFvs, expressed in the periplasm and culture supernatant. Different concentrations of bp26 were prepared in PBS, ranging from 0.39 – 100µg/ml and mixed with an equal volume of the periplasmic lysate or culture supernatant containing the expressed scFv. The mixture was then added to immunoplates coated with 10µg/ml of bp26 and the competitive ELISA completed as described in Section 2.5.9 Each of the 6 clones analysed were capable of expressing soluble scFvs into both the supernatant and periplasmic lysate, which exhibited affinity for free bp26 (Figs. 5.19 and 5.20).

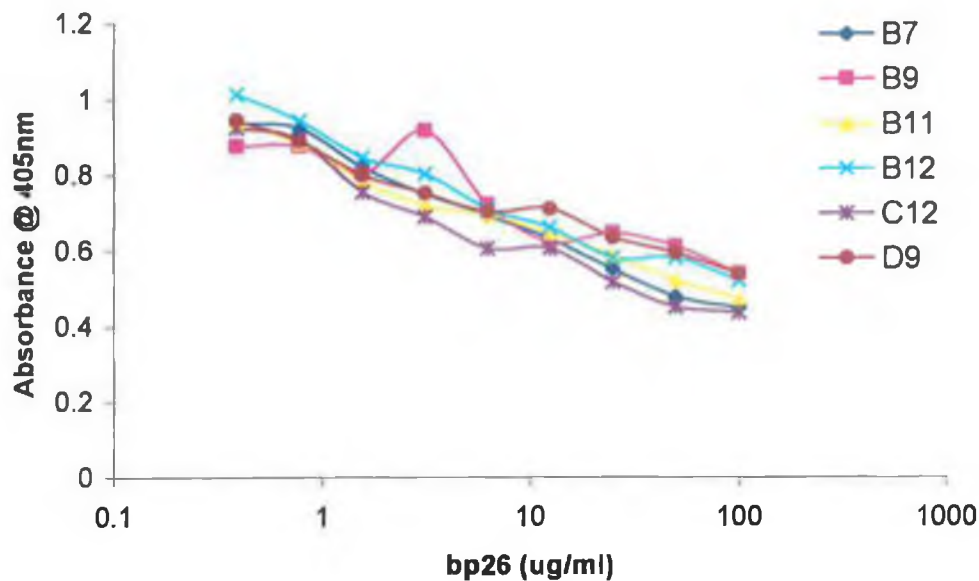


**Figure 5.19:** Competition ELISA on the clones B7, B9, B11, B12, C12 and D9 following soluble scFv expression into the culture supernatant. Free bp26 standards, ranging from 0.39 – 100µg/ml were assayed. Each of the six clones analysed clearly show competition for free bp26.

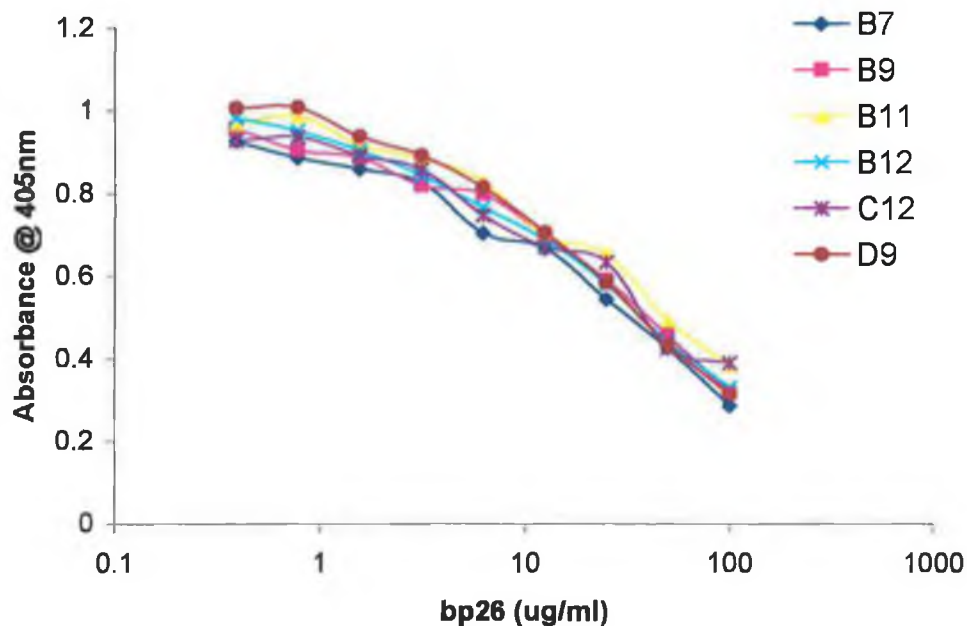


**Figure 5.20:** Competition ELISA on the clones B7, B9, B11, B12, C12 and D9 following soluble scFv expression into the periplasm. Free bp26 standards, ranging from 0.39 – 100µg/ml were assayed. Each of the six clones analysed clearly show competition for free bp26.

#### **5.2.2.4 Nucleotide and amino acid sequence analysis on clones B7, B11, C12 and D7**

Following confirmation that the soluble scFvs exhibited affinity for free bp26, 4 positive clones (B7, B11, D7 and C12) were selected for sequence analysis and comparisons. Plasmid DNA, encoding the bp26-specific scFvs, was purified from XL-1 Blue *E. coli*, as described in Section 2.2.2. The plasmid DNA was quantified and sent to MWG-Biotech (Germany) for sequencing. Comfort reads were obtained in both directions on the scFv inserts, using primers specific to the multiple cloning site of the pCANTAB6 vector. Nucleotide sequence alignments of the four scFv genes confirmed that clones B7, B11 and D9 were identical with clone C12 containing a one base pair substitution (Fig. 5.21). In comparison with clones B7, B11 and D9 clone C12 contained a G at base 496 instead of an A. The amino acid sequence of each scFv was then deduced from the nucleotide sequence. The amino acid sequences alignments on the four clones confirmed they were identical (Fig. 5.22).

Therefore, clone B7 was selected for further characterisation and analysis. The deduced amino acid sequence of clone B7 was compared with variable regions of immunoglobulins found in the SwissProt database and used along with the Kabat rules to identify the loops corresponding to the CDRs within the variable heavy and variable light domains (Fig. 5.23). The 3-D structure of the scFv was also predicated, using SwissModel, based on structurally related proteins (Fig. 5.24).

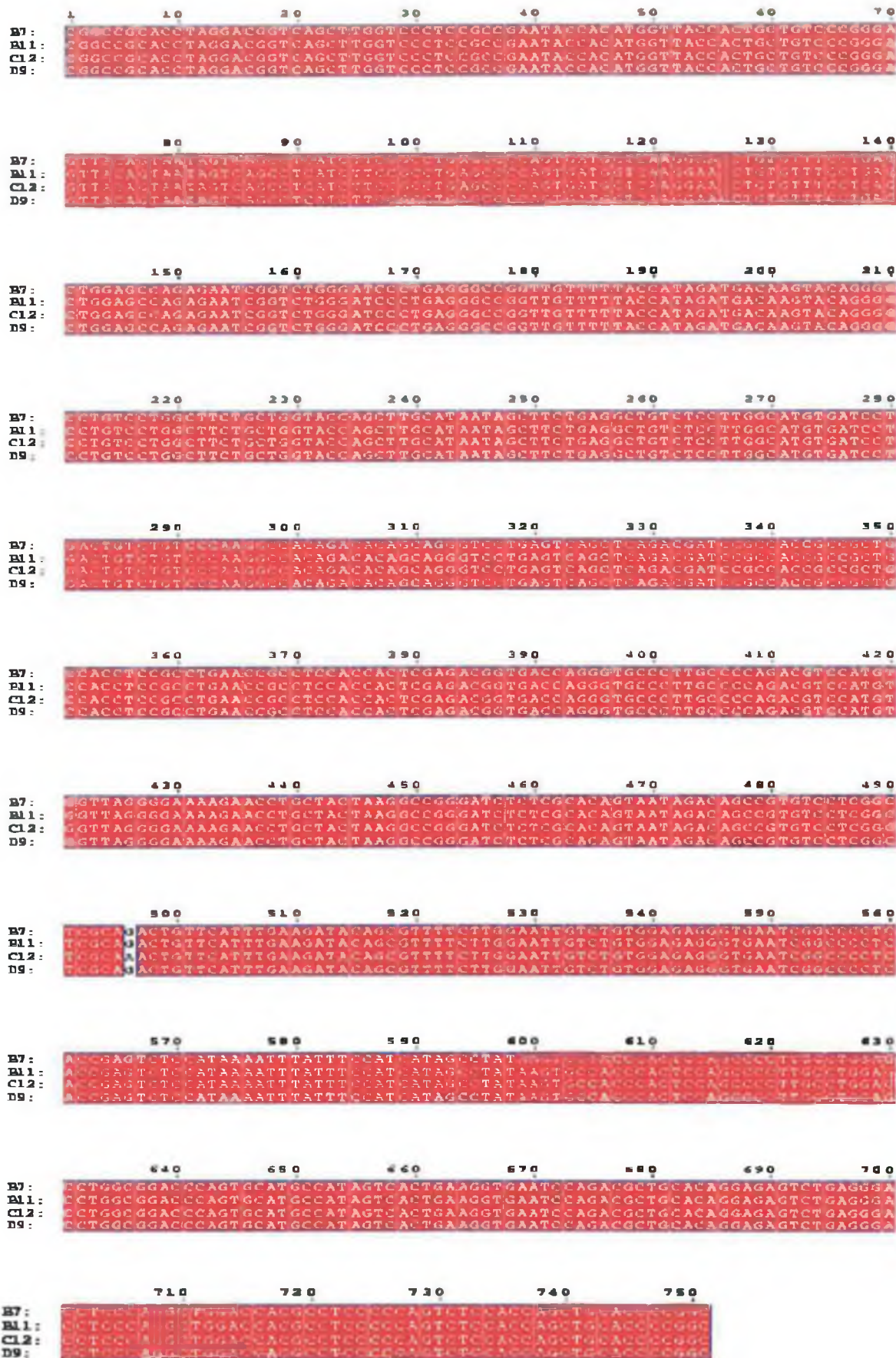


**Figure 5.21:** Nucleotide sequence alignment on the DNA encoding the 4 anti-bp26 scFvs, B7, B11, C12 and D9, which were isolated from the BMV phage display library. The one base-pair difference observed between the nucleotide sequences of B7, B11 and D9 and that of C12 is shown in white.

```

1      10      20      30      40      50      60      70
B7:  AGVQLVETGGGVVQPSRLRLSCAASGPTTFSDYGMHAYRQAPGKGLWVALIGYDGNRFYGGSVRGRFTL
B11: AGVQLVETGGGVVQPSRLRLSCAASGPTTFSDYGMHAYRQAPGKGLWVALIGYDGNRFYGGSVRGRFTL
C12: AGVQLVETGGGVVQPSRLRLSCAASGPTTFSDYGMHAYRQAPGKGLWVALIGYDGNRFYGGSVRGRFTL
D7:  AGVQLVETGGGVVQPSRLRLSCAASGPTTFSDYGMHAYRQAPGKGLWVALIGYDGNRFYGGSVRGRFTL

      80      90      100     110     120     130     140
B7:  STDNSEKLTLYLQNNSLRAEDTAVYYCARDFGLSRRFFSENNHMDVWGKGTLLVTVSSGGGGGGGGGGGGGGGGGGGG
B11: STDNSEKLTLYLQNNSLRAEDTAVYYCARDFGLSRRFFSENNHMDVWGKGTLLVTVSSGGGGGGGGGGGGGGGGGGGG
C12: STDNSEKLTLYLQNNSLRAEDTAVYYCARDFGLSRRFFSENNHMDVWGKGTLLVTVSSGGGGGGGGGGGGGGGGGGGG
D7:  STDNSEKLTLYLQNNSLRAEDTAVYYCARDFGLSRRFFSENNHMDVWGKGTLLVTVSSGGGGGGGGGGGGGGGGGGGG

      150     160     170     180     190     200     210
B7:  SELTQDFAVSVALGQTVRITCQGGSLRYYASWYQQKPGQAPVLLIYGKNNRPSGIPDRFSGSSGGNTAS
B11: SELTQDFAVSVALGQTVRITCQGGSLRYYASWYQQKPGQAPVLLIYGKNNRPSGIPDRFSGSSGGNTAS
C12: SELTQDFAVSVALGQTVRITCQGGSLRYYASWYQQKPGQAPVLLIYGKNNRPSGIPDRFSGSSGGNTAS
D7:  SELTQDFAVSVALGQTVRITCQGGSLRYYASWYQQKPGQAPVLLIYGKNNRPSGIPDRFSGSSGGNTAS

      220     230     240     250
B7:  LTITGAQAEDEADYYCNRRDSSGNHVVFGSGTLLTVLGAA
B11: LTITGAQAEDEADYYCNRRDSSGNHVVFGSGTLLTVLGAA
C12: LTITGAQAEDEADYYCNRRDSSGNHVVFGSGTLLTVLGAA
D7:  LTITGAQAEDEADYYCNRRDSSGNHVVFGSGTLLTVLGAA

```

*Figure 5.22: Amino acid sequence alignment on the DNA encoding the 4 anti-bp26 scFvs, B7, B11, C12 and D9, which were isolated from the BMV phage display library. The amino acid sequences alignments on the four clones proved they were identical.*

gccggggtgcagctggtggagactgggggaggcgtggtccagcctgggaggtccctcaga  
 A G V Q L V E T G G G V V Q P G R S L R  
 ctctcctgtgcagcgtctggattcaccttcagtgactatggcatgcactgggtccgccag  
 L S C\***A A S G F T F S D Y G M H**W V R Q  
**CDR-L1**  
 gctccaggcaaggggctggagtggtggcacttataggctatgatggaaataaattttat  
 A P G K G L E W V A L I G Y **D G N K F Y**  
**CDR-L2**  
 ggagactcggtgaggggccgattcacctctccacagacaattccaagaaaacgctgtat  
**G** D S V R G R F T L S T D N S K K T L Y  
 cttcaaatgaacagtctgcgagccgaggacacggctgtctattactgtgcgagagatccc  
 L Q M N S L R A E D T A V Y Y C\***A R D P**  
 ggccttagtagcaggttcttttcccctaaccacatggacgtctggggcaagggcacctcg  
**G L S S R** F F S P N H M D V W G K G T L  
**CDR-L3**  
 gtcaccgtctcagatggtggaggcgggttcaggcggaggtggcagcggcgggtggcggatcg  
 V T V S S G G G G S G G G G S G G G G S  
 tctgagctgactcaggaccctgctgtgtctgtggccttgggacagacagtcaggatcaca  
 S E L T Q D P A V S V A L G Q T V R I T  
 tgccaaggagacagcctcagaagctattatgcaagctggtaccagcagaagccaggacag  
 C\* Q G D **S L R S Y Y A S** W Y Q Q K P G Q  
**CDR-H1**  
 gccctgtacttgtcatctatggtaaaaacaaccggccctcagggatcccagaccgattc  
 A P V L V I Y G **K N N R P S G I P D** R F  
**CDR-H2**  
 tctggctccagctcaggaaacacagcttcccttgaccatcactggggctcaggcgggaagat  
 S G S S S G N T A S L T I T G A Q A E D  
 gaggctgactattactgtaactcccgggacagcagtggttaaccatgtggtattcggcgga  
 E A D Y Y C\* N S **R D S S G N H V V** F G G  
**CDR-H3**  
 gggaccaagctgaccgtcctaggtgcggccg  
 G T K L T V L G A A A

**Figure 5.23:** The nucleotide and deduced amino acid sequences of the gene encoding the bp26 specific scFv from clone B7. The amino acid sequences representing the CDRs were identified using the Kabat rules and are clearly visible underlined and in bold. The four conserved cystine residues are indicated with an asterisk.

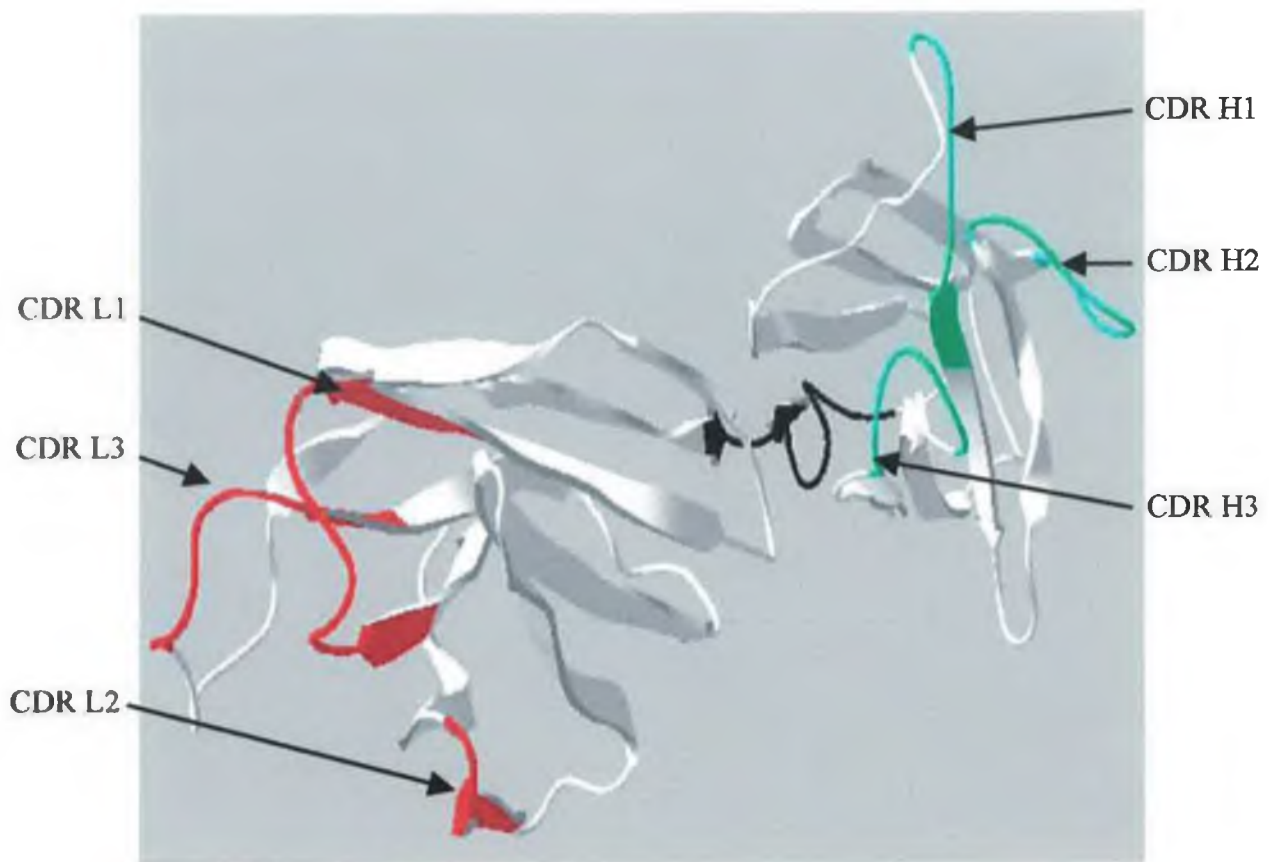


*Figure 5.24: The predicted 3-D structure of the anti-bp26 scFv from clone B7, which was obtained using SwissModel. The complementary determining regions (CDRs) are shown in red on the light chain and in green on the heavy chain.*

#### 5.2.2.5 Western blot analysis for the specific detection of bp26 using the B7 scFv

Following soluble expression of the scFv antibodies from pCANTAB6 a c-myc tag is incorporated at the C-terminus to aid in detection. During the course of the ELISA characterisation of the B7 scFv, the interaction between the bp26 and the B7 scFv will be indirectly detected using an anti-c-myc-HRP antibody. In order to confirm that the anti-c-myc-HRP antibody specifically binds the B7 scFv Western blot analysis was conducted.

Initially the specificity of the anti-c-myc HRP-labelled antibody for c-myc-tagged scFvs was determined. The supernatant containing the B7 scFv was electrophoresed along with a c-myc-tagged scFv, previously isolated from the BMV against a *Listeria monocytogenes* protein (Positive control) and a FLAG-tagged scFv, with no c-myc tag, isolated from a pre-immunised phage display library against AFB<sub>1</sub>-BSA (Negative control) using SDS-PAGE. The scFvs were then transferred to nitrocellulose, which was probed using the anti-c-myc-HRP antibody and colour developed following addition of chromogenic substrate (Figure 5.25 (A)). The anti-c-myc-HRP antibody was capable of specifically detecting the B7 scFv (Lane 3) and the *L. monocytogenes*-specific positive control scFv (Lane 2), with bands clearly visible at approximately 32kDa. However, the anti-c-myc antibody was unable to detect the anti-AFB<sub>1</sub> scFv (Lane 1), which lacked a c-myc tag.

Western blot analysis was also conducted to confirm the B7 scFv specifically recognised bp26. The recombinant p18 (Negative control) and bp26 proteins were electrophoresed using SDS-PAGE and then transferred to nitrocellulose. The nitrocellulose was probed using the B7 scFv, followed by the anti-c-myc-HRP antibody (Figure 5.25 (B)). The anti-c-myc-HRP antibody specifically detected the interaction between the recombinant bp26 and B7 scFv (Lane 2), with one band clearly visible at approximately 26kDa representing the bp26. However, the B7 scFv failed to detect the p18 protein (Lane 1) with no bands visible.

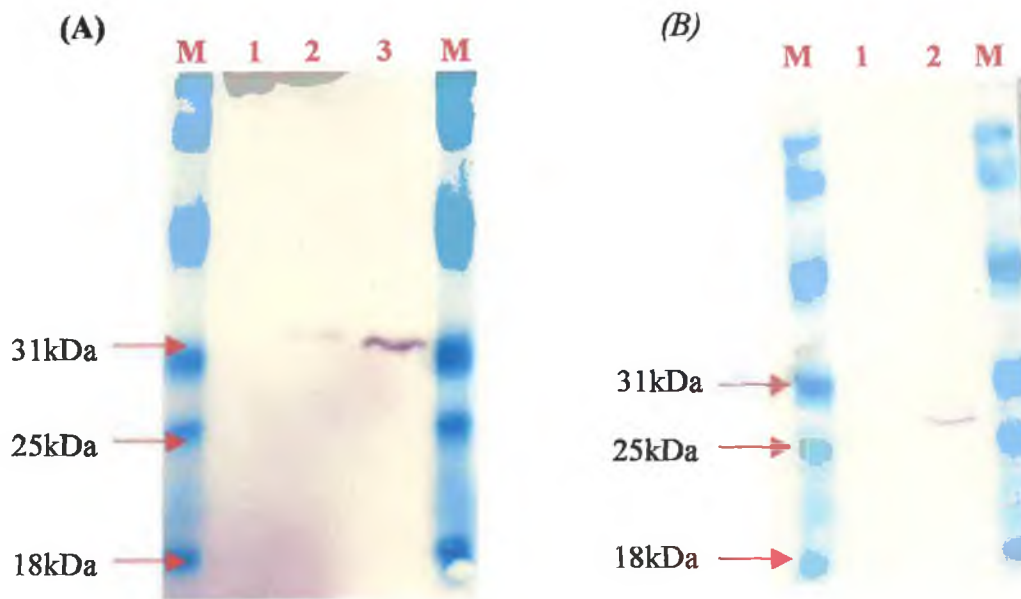


**Figure 5.25:** Western blot analysis on the specific detection of bp26 using the B7 scFv. **(A)** Represents Western blot analysis to determine the specificity of the anti-c-myc antibody for the detection of c-myc-tagged scFvs. Lane M: Pierce Blue Ranger prestained molecular weight markers; Lane 1: FLAG-tagged scFv, which was not detected using the anti-c-myc antibody; Lane 2: *L. monocytogenes*-specific scFv, which was specifically detected using the anti-c-myc antibody with a band clearly visible at 32kDa; Lane 3: The B7 scFv, which was specifically detected using the anti-c-myc antibody with a band clearly visible at 32kDa. **(B)** Represents the Western blot analysis to determine if the interaction between the bp26 and B7 scFv can be specifically detected using the anti-c-myc antibody. Lane M: Pierce Blue Ranger prestained molecular weight marker; Lane 1: Negative control consisting of p18 probed using the anti-bp26 scFv (B7) followed by the anti-c-myc antibody with no bands observed; Lane 2: The interaction between bp26 and the B7 scFv was indirectly detected using the anti-c-myc-HRP antibody with a band clearly visible at 26kDa.

#### **5.2.2.6 ELISA analysis of the soluble B7 scFv antibody directed against bp26**

Following selection of a soluble scFv that recognised the recombinant bp26 protein, both in solution and immobilised, competitive ELISA characterisation was carried out in order to give a further insight into the sensitivity, stability and reproducibility of the scFv.

##### **5.2.2.6.1 Checkerboard ELISA for the determination of the optimal scFv antibody dilution and bp26 concentration for use in a competitive ELISA**

A checkerboard ELISA was carried out in order to determine the optimal scFv antibody dilution and protein coating concentration for use in a competitive ELISA. Rows of wells on a 96-well microtitre plate were coated with concentrations of recombinant bp26 ranging from 0 to 50µg/ml and blocked with 4% (w/v) milk marvel powder. Dilutions of the B7 scFv antibody from undiluted to 1/1000 were prepared in PBS and each scFv dilution was added to each protein coating concentration on the plate. Figure 5.26 shows titre curves obtained for the B7 scFv antibody. The optimal protein coating concentration was found to be 12.5µg/ml and the optimal scFv dilution determined to be 1/8.

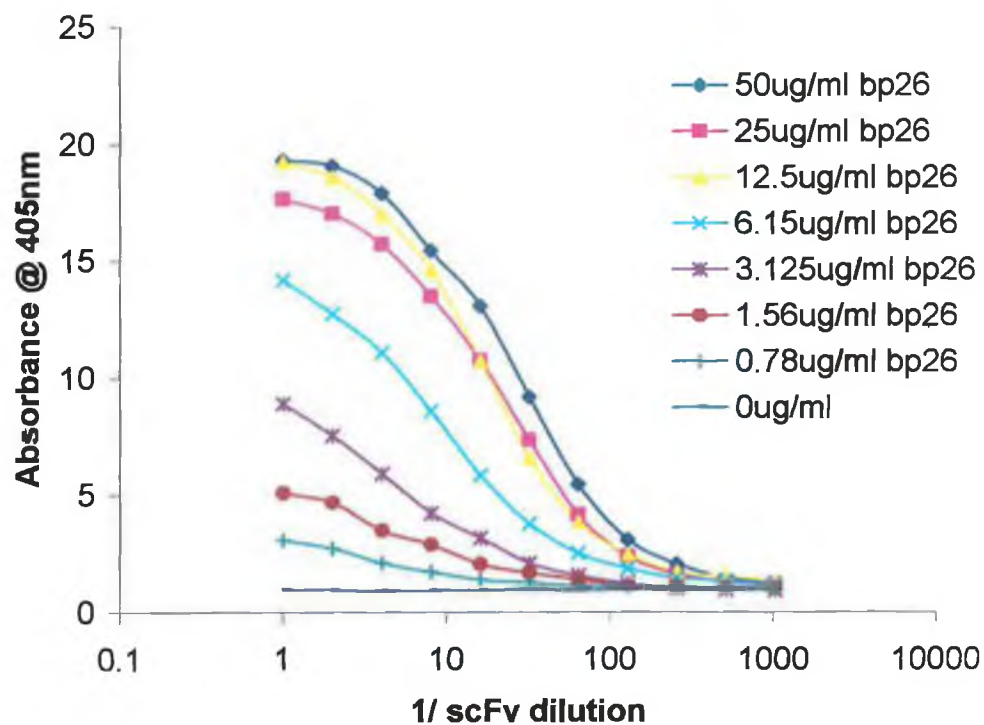


**Figure 5.26:** Checkerboard ELISA for determination of optimal bp26 protein coating concentration and scFv antibody dilution. The optimal bp26 protein coating concentration chosen was 12.5 $\mu$ g/ml and the optimal scFv dilution, which gave 70% of the maximum absorbance, was 1/8.

#### **5.2.2.6.2 Intra- and inter-day assay variability studies of the B7 scFv antibody**

Following optimisation of the various parameters for a competitive ELISA, intra- and inter-day assays were carried out. Immunoplates coated with 12.5µg/ml of bp26 were used to determine the range of detection for bp26 of the scFvs. Free bp26 standards, ranging in concentration from 24 – 25000ng/ml, were prepared in PBS and added to an equal volume of the optimal dilution of B7 scFv. Intra and inter-day variability studies were carried out on the scFv in order to estimate the sensitivity and reproducibility of the scFvs.

In order to determine intra-day assay variation, each concentration was assayed five times on one day and the mean absorbance of bound antibody for each bp26 concentration was plotted against the free bp26 concentration. The range of detection of the scFv antibody for free bp26 was 97 – 12500ng/ml and the coefficients of variation (C.V.'s) for the assay ranged from 1.51 – 8.39%.

Inter-day assay variability studies were also carried out on the scFv by performing the assays over five separate days. The coefficients of variation (CVs) were determined for each assay by expressing the standard deviation as a percentage function of the mean. The inter-day assay for the B7 scFv had a range of detection for free bp26 from 97 – 12500ng/ml (Fig. 5.27) and CVs ranged between 3.3 and 10.88% (Table 5.8), indicating that the assay were reproducible over five days.

*Table 5.8: Inter-day assay coefficients of variation for the detection of bp26 using the B7 scFv antibody fragment. Five sets of eight standards were assayed on five different days and the coefficients of variation calculated.*

<b>bp26 (ng/ml)</b>	<b>Calculated mean <math>\pm</math> S.D.</b>	<b>Coefficient of variation (%)</b>
12500	0.33 $\pm$ 0.035	10.88
6250	0.42 $\pm$ 0.039	9.21
3125	0.53 $\pm$ 0.050	9.30
1562	0.64 $\pm$ 0.021	3.30
781	0.71 $\pm$ 0.045	6.28
390	0.82 $\pm$ 0.044	5.37
195	0.89 $\pm$ 0.059	6.63
97	0.97 $\pm$ 0.046	4.71

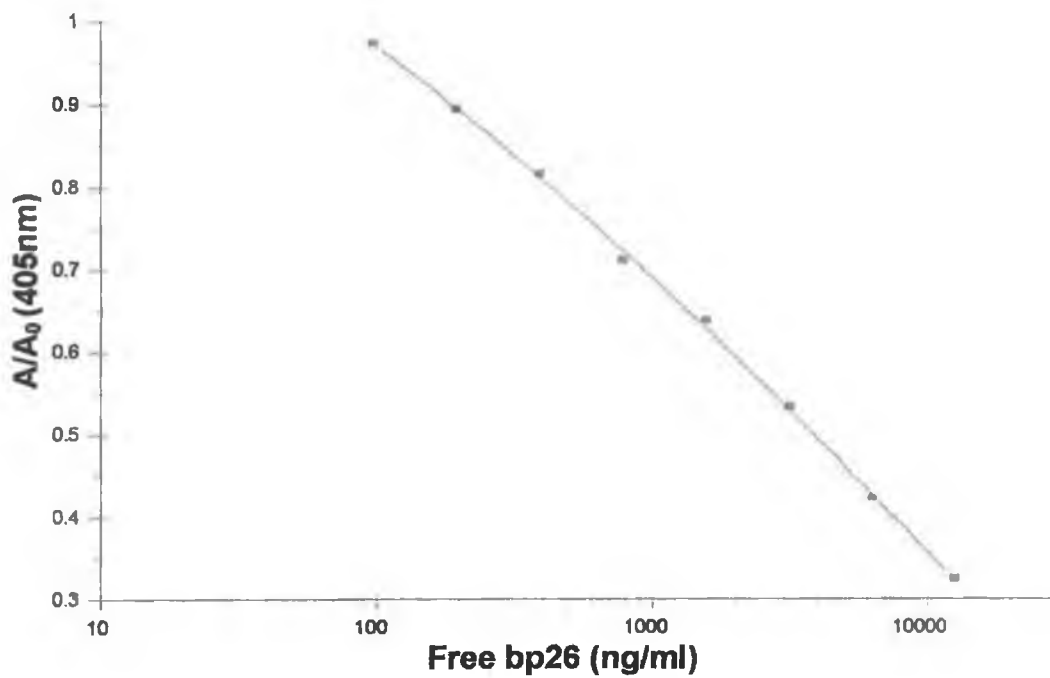


*Figure 5.27: Inter-day assay curve for the detection of bp26 using the B7 scFv in a competitive ELISA format. The range of detection of the antibody for free bp26 was between 97 and 12500ng/ml. The calibration curve was plotted using Biaevaluation software 3.1 and represents the average normalised ( $A/A_0$ ) results obtained over five individual days.*

### 5.2.2.6.3 Cross-reactivity studies on the anti-bp26 scFv

Cross-reactivity studies were then carried out on the bp26-specific scFv to determine the antibody specificity towards bp26 in relation to a panel of proteins (as described in Section 2.4.9). The assays were carried out as for the competitive ELISAs except the cross-reactants were added to the immunoplate with the bp26-specific scFv. Separate calibration curves were plotted for each protein and the least detectable dose (LDD) and IC<sub>50</sub> values were determined for each as 90% A/A<sub>0</sub> and 50% A/A<sub>0</sub>, respectively. The percentage cross reactivities were then estimated at the LDD (CR<sub>90</sub>) and at the IC<sub>50</sub> (CR<sub>50</sub>) by expressing 100-fold the ratio between values obtained for bp26 and those of the cross-reacting proteins.

Table 5.10 summarises the specificity and cross reactivity studies on the anti-bp26 scFv against the different proteins. Minimal levels of cross-reactivity (i.e. < 0.39) were observed between the anti-bp26 scFv and any of the 5 proteins tested at the LDD. Low levels of cross reactivity were also observed at the IC<sub>50</sub> with % cross-reactivity remaining below 8.

*Table 5.10: Cross-reactivity and specificity studies on the anti-bp26 B7 scFv against various proteins. The cross-reactivity potential was approximated at the least detectable dose (LDD) and at the IC<sub>50</sub> value.*

Protein	LDD <sup>a</sup> (ng/ml)	IC <sub>50</sub> <sup>b</sup> (ng/ml)	CR <sub>90</sub> <sup>c</sup> (%)	CR <sub>50</sub> <sup>d</sup> (%)
bp26	195	4000	100	100
p18	>50000	>50000	< 0.39	< 8
Bovine serum albumin (BSA)	>50000	>50000	< 0.39	< 8
Thyroglobulin (THY)	>50000	>50000	< 0.39	< 8
Ovalbumin (OVA)	>50000	>50000	< 0.39	< 8
Horse IgG	>50000	>50000	< 0.39	< 8

<sup>a</sup> Least detectable dose calculated at 90% A/A<sub>0</sub>

<sup>b</sup> 50% inhibition concentration (50% A/A<sub>0</sub>)

<sup>c</sup> Percentage cross-reactivity determined at IC<sub>50</sub>

<sup>d</sup> Percentage cross-reactivity determined at LDD

### **5.2.2.7 Investigations on the use of the anti-bp26 scFv in the development of an immunoassay for the detection of *Brucella abortus***

The initial aim of this chapter was the production of *Brucella*-specific antibodies and the subsequent development of immunoassay for the detection of *B. abortus*. A *Brucella*-specific scFv, directed against bp26, was isolated from a naïve phage display library. Attempts have been made to incorporate this scFv into an immunoassay for the detection of *B. abortus*.

Attempts have been made to develop a competitive ELISA, which would involve immobilised recombinant bp26 and cellular bp26 competing for binding to the scFv. The ELISA was carried out using an immunoplate coated with 12.5µg/ml of the recombinant bp26. A range of *B. abortus* cell concentrations, ranging from  $1.95 \times 10^6$  to  $1.6 \times 10^{10}$  cells/ml, were prepared in PBS and the cells lysed using a 1mg/ml solution of lysozyme. The lysed cells were centrifuged and an equal volume of the scFv added to the cellular supernatant. The mixture was added to the immunoplate and the ELISA completed. However, no competition was observed.

### 5.3 Discussion

The main focus of this chapter was the production and characterisation of *Brucella*-specific antibodies. Polyclonal and scFv antibodies were produced against *Brucella*-specific antigens and their sensitivity and specificity determined. The antibodies were then investigated for use in the development of an immunoassay for the detection of *Brucella abortus*. Their subsequent use in the development of an immunoassay for the detection of bovine brucellosis was also investigated (See Chapter 6).

Polyclonal antibodies were raised against *Brucella abortus* 45/20 cells in two rabbits, rabbit 1 and rabbit 2. Antibodies were raised against the crude cytoplasmic lysate from *B. abortus* 45/20 cells in rabbit 1 and against whole *B. abortus* 45/20 cells in rabbit 2. The rabbits were sacrificed 72 days after the initial immunisation and serum titres in excess of 1/163,8400 were obtained against the crude cytoplasmic lysate and whole *B. abortus* cells (Figs. 5.2 and 5.3). The polyclonal antibodies were purified from the rabbit serum by saturated ammonium sulphate precipitation, which involved the relatively crude precipitation of antibodies from the rabbit serum, followed by the more refined protein G affinity chromatography step in order to obtain pure IgG antibodies. The purification process was investigated using SDS-PAGE (Figs. 5.5 and 5.6). The level of purity obtained greatly increased when going from the serum, to the SAS precipitate to the protein G affinity purified antibodies, where ultimately a pure solution of IgG antibodies was obtained. The presence of the purified IgG antibodies in the protein G-purified sample was confirmed following Coomassie staining with two bands clearly visible at 25 and 50kDa, which represented the antibodies heavy and light chains, respectively. Western blots were then carried out in order to confirm that the bands present on the SDS-PAGE were in fact rabbit IgG antibodies. The proteins were transferred from the acrylamide gel to nitrocellulose, which was then probed with an alkaline phosphatase-labelled anti-rabbit antibody. Bands at 25 and 50kDa representing the heavy and light chains, respectively, confirmed the presence of the rabbit IgG antibodies in each sample (Figs. 5.7 and 5.8). The band representing the light chain appeared less intense, in comparison with the heavy chain, which was due to the smaller size and different amino acid composition of the light chain.

The purified polyclonal antibodies from rabbit 1 (pAB1) and rabbit 2 (pAB2) were then applied to the development of competitive ELISAs for the detection of *B.*

*abortus*. In order to develop a sensitive competitive ELISA for *B. abortus* several parameters were optimised. The limit of detection of a competitive ELISA can be affected by the affinity of an antibody and the equilibrium between free and immobilised antigen. If the concentration of the immobilised antigen were too high than there would be an unfair binding bias towards the immobilised antigen. For similar reasons the optimal antibody dilution used must be the limiting factor because excess would result in binding to both free and immobilised *B. abortus* cells to a higher degree affecting the limits of detection of the assays. Checkerboard ELISAs were carried on each polyclonal antibody to determine the optimal cell-coating concentration and antibody dilution for use in a competitive ELISA (Figs. 5.9 and 5.10). A cell-coating concentration of  $1.6 \times 10^8$  cells/ml was found to be optimal for pAB1 and pAB2. The optimal antibody dilution, which displayed 70% of maximum binding, was found to be 1/5000 for both pAB1 and pAB2.

Optimisation of the various assay parameters was then followed by the development of competitive ELISAs. The range of detection for free *B. abortus* 45/20 cells was found to be between  $1.95 \times 10^6$  and  $1.00 \times 10^9$  cells/ml for pAB1 and  $9.77 \times 10^5$  to  $1.00 \times 10^9$  cells/ml for pAb2 (Figs. 5.11 and 5.12). Intra- and inter-day variability studies were conducted to determine the reproducibility of the assays. The coefficients of variation (CVs) for the intra-day assay using pAb1 and pAb2 remained below 8.96 and 8.97%, respectively. Inter-day CVs for pAb1 ranged between 0.73 and 5.85% (Table 5.2) and for pAB2 ranged between 1.14 and 6.40% (Table 5.3). The results discussed above suggest that the competitive ELISAs are statistically viable and reproducible over a period of five days for the detection of *B. abortus*, within the defined range.

Cross-reactivity studies were then carried out on the polyclonal antibodies, in a competitive ELISA format, in order to determine the cross-reactivity potential of the antibodies against ubiquitous gram-negative and gram-positive bacteria (Tables 5.3 and 5.4). Hennion *et al.* (1998) recommends the comparison of two sets of values, the LDD and  $IC_{50}$ , in order to accurately estimate cross reactivity over the measurement range. The least detectable dose (LDD) is defined as the smallest concentration of analyte that produces a response that can be significantly distinguished from zero (Hennion *et al.*, 1998) and the  $IC_{50}$  is defined as the analyte concentration that results

in 50% inhibition. The cross-reactivity is then estimated at the LDD ( $CR_{90}$ ) and at the  $IC_{50}$  ( $CR_{50}$ ) as 100-fold the ratio between the LDD and  $IC_{50}$  values of the antigen and of the cross reactant, respectively. Minimal cross-reactivity (i.e. < 1%) was observed with pAb1 and pAb2 against the bacterial strains analysed (Tables 5.4 and 5.5). Therefore, confirming the specificity of pAB1 and pAB2 for *Brucella abortus* 45/20 cells.

The specificity of pAB1 and pAB2 towards the recombinant p18 and bp26 proteins and against the crude cell lysate from *B. abortus* 45/20 was then determined using Western blot analysis. *B. abortus* 45/20 cells were disrupted by sonication and the resulting supernatant electrophoresed using SDS-PAGE. The electrophoresed proteins were then transferred to nitrocellulose, which was probed using pAB1 and pAB2 (Fig. 5.13). The crude cell lysate probed with pAB1 detected two main bands one at 18kDa and the other at 45kDa. Four bands were detected using pAB2, at 16kDa, 18kDa, 38kDa and 45kDa. The band at 18kDa represents the 18kDa cytoplasmic protein (p18), which was previously discussed in Chapter 4. The antibody binding reactivity of pAb1 and pAb2 against the recombinant p18 and bp26 was also assessed using Western blotting. Purified recombinant p18 and bp26 were electrophoresed using SDS-PAGE and then transferred to nitrocellulose, which was probed using pAB1 and pAB2. Bound polyclonal antibodies directed against the recombinant proteins were then detected using an alkaline phosphatase-labelled anti-rabbit antibody. Figure 5.14 shows the Western blots obtained using pAB1 (A) and pAB2 (B). Both polyclonal antibodies recognised the p18 with band visible at 18kDa. However, they failed to detect bp26. These results were expected due to the cellular location of the native proteins, p18 is an 18kDa cytoplasmic protein and bp26 is a 26kDa periplasmic protein. The polyclonal antibodies were raised against whole *B. abortus* 45/20 cells and a crude cytoplasmic lysate. Therefore, reactivity of the antibodies would have been expected against a cytoplasmic protein (p18) and not against a periplasmic protein (bp26).

This chapter also focused on the isolation of *Brucella*-specific scFv antibody fragments from the BMV scFv phage display library. The BMV is a naive human library, which was constructed using functional V-gene segments from 43 non-

immunised donors and consisted of a repertoire of  $1.4 \times 10^{10}$  scFv fragments displayed on the surface of phage. This library has previously proven useful in the isolation of highly-specific monoclonal antibodies with high affinities against a variety of target antigens including carcinoembryonic antigen (CEA), doxorubicin, diethylenetriamine-pentaacetic acid (DTPA), fluorescein, merozoite surface protein 1 (MSP-1) of *Plasmodium falciparum* (malaria), human oestradiol and chicken very low density lipoprotein receptor (VDL-R) (Vaughan *et al.*, 1996).

The BMV library was panned against the two recombinant *Brucella*-specific proteins, p18 and bp26 (previously described in Chapter 4). In general, between four and six rounds of panning are required for the isolation of specific scFvs from naïve scFv repertoires (Vaughan *et al.*, 1996).

Six rounds of panning were carried out on the BMV library against p18. The first three rounds of panning against the p18 did not yield any positive clones. Following the sixth round of panning against p18 10 positive phage clones were isolated (Fig. 5.15). These phage clones expressed scFv fragments on their surface that were specific for the p18 protein. However, several attempts to isolate soluble scFvs failed (Fig. 5.16). Attempts made to express the respective soluble scFvs may have failed due to poor solubility or *in vivo* degradation of the c-myc tag used for the detection of the soluble scFvs. Similar problems were encountered when Hayhurst and associates (2003) reported the isolation of scFv antibody fragments against *B. melitensis*. Phage bound scFvs specific for *B. melitensis* were isolated from a pre-immunised phage-display library. However, attempts made to isolate the respective scFvs in a soluble form failed. Although, the expression of soluble functional specific-antibodies was achieved following (i) fusion of a human kappa light chain constant domain (Ck) chain to the scFv to generate a single chain antibody fragment (scAb) antibody fragments and (ii) co-expression of the periplasmic chaperone Skp, the phage bound scFvs offered greater sensitivity in an ELISA format.

Six rounds of panning were also carried out on the BMV against the bp26 recombinant protein. Following the sixth round of panning 9 positive clones were identified in phage that were capable of detecting the bp26 protein (Fig. 5.17). Following analysis on the sixth pan soluble scFvs were isolated from the culture

supernatant and periplasm of 5 clones (Fig. 5.18). Competitive ELISAs were then carried out on the soluble scFvs, directed against bp26, in order to estimate the specificity of the scFvs towards free recombinant bp26. Each of the 10 clones tested showed specificity towards the free bp26 (Figs. 5.19 and 5.20).

Nucleotide and amino acid sequence analysis were then conducted on four clones, B7, B11, D7 and C12. The pCANTAB6 plasmid DNA was purified from each clone and comfort reads were obtained on the scFv insert. Nucleotide sequence analysis on the four clones showed that the four clones were identical apart from a one base pair substitution in clone C11 at base 496, where a G was substituted with an A (Fig. 5.21). However, comparisons on the deduced amino acid sequences confirmed the four clones were identical (Fig. 5.22). Clone B7 was then selected for further characterisation. The complementary determining regions (CDRs) regions were identified on the heavy and light chains, of the B7 scFv, according to Kabat *et al.* (1991) (Fig. 5.23) and the 3-D structure of the B7 scFv was predicated using SwissModel (Fig. 5.24).

Western blot analysis was carried out to determine the specificity of the B7 scFv. The scFv-containing supernatant was electrophoresed along with an anti-*Listeria* and an anti-AFB<sub>1</sub> scFvs using SDS-PAGE and then transferred to nitrocellulose. The anti-*Listeria* scFv was previously isolated from the BMV library and following soluble expression had a c-myc tag incorporated. It served as a positive control. The anti-AFB<sub>1</sub> scFv was previously isolated from a pre-immunised phage display library and following soluble expression from pAK400 had a FLAG tag incorporated. The anti-AFB<sub>1</sub> scFv, lacking a c-myc tag, then served as a negative control. The nitrocellulose was probed with an anti-c-myc antibody and developed upon addition of the chromogenic substrate. The anti-c-myc antibody specifically detected the c-myc-tagged scFvs with the presence of a band at approximately 32kDa, representing the scFvs clearly visible in the lanes containing the anti-bp26 and anti-*Listeria* scFvs (Fig. 5.25 (A)). However, the anti-c-myc antibody failed to detect the FLAG-tagged scFv confirming the specificity of the anti-c-myc antibody for the c-myc-tagged scFvs. The ability of the anti-c-myc antibody to indirectly detect the interaction between the anti-bp26 scFv and bp26 was also confirmed using Western blotting. The bp26 and p18 (Negative control) proteins were electrophoresed using SDS-PAGE and transferred to

nitrocellulose. The nitrocellulose was probed with the B7 scFv, followed by the anti-c-myc antibody. The presence of a band at 26kDa in the lane containing bp26 confirmed that the scFv was specifically binding to the recombinant bp26 (Fig. 5.25 (B)). However, the absence of a band in the lane containing p18 confirms that the anti-c-myc antibody can be used to specifically detect the interaction between the anti-bp26 scFv and bp26.

ELISA characterisation was also carried out on the B7 scFv to give a further insight into the sensitivity, stability and reproducibility of the scFv, prior to application to a competitive assay format for the detection of either *B. abortus* or a bovine brucellosis infection. A checkerboard ELISA was carried out in order to determine the optimal scFv antibody dilution and protein coating concentration for use in a competitive ELISA. Various bp26 coating concentrations ranging from 0 to 50µg/ml and scFv dilutions ranging from undiluted to 1/1000 were tested to see which were optimal for use in a competitive ELISA for bp26 (Fig. 5.26). 12.5µg/ml was selected as the optimal coating concentration of the bp26 as it provided the highest absorbance values without depleting protein stocks and a 1/8 dilution of the bp26 was chosen because it displayed 70% of the total binding to the bp26. Following optimisation of the competitive ELISA parameters, intra/inter-day variability studies were carried out in order to determine the range of detection of the scFv and to establish the assay's reproducibility. The intra-day coefficients of variation for the detection of bp26 using the B7 scFv ranged between 1.51 – 8.39% and the range of detection for bp26 was between 97 – 12500ng/ml. Table 5.8 shows the inter-day coefficients of variation, which ranged between 3.30– 10.88%. Figure 5.27 shows the inter-day competitive ELISA where the range of detection for bp26 was also between 97 – 12500ng/ml. These results suggest that the ELISAs are reproducible over a period of five days, within the defined range.

A selection of proteins including bovine serum albumin (BSA), ovalbumin (OVA), thyroglobulin (THY), horse IgG and the recombinant p18 were used to determine the cross reactivity potential of the anti-bp26 scFv. The percentage cross reactivity was estimated for each protein at the LDD (CR<sub>90</sub>) and at the IC<sub>50</sub> (CR<sub>50</sub>). Minimal cross-reactivity (i.e. < 0.39%) was observed between the anti-bp26 scFv and the panel of

proteins analysed at the LDD with low levels of cross-reactivity (i.e. < 8%) also observed at the IC<sub>50</sub> (Table 5.10).

Attempts were then made to incorporate the anti-bp26 scFv in a competitive ELISA format for the detection of *B. abortus* cells. This assay format involved the immobilised recombinant bp26 and cellular bp26, from the periplasmic lysate of *B. abortus* 45/20 cells, competing for binding to the anti-bp26 scFv. Immunoplates were coated with the recombinant bp26 at 12µg/ml and the periplasmic lysate was isolated from various cell concentrations, ranging from 1.95x10<sup>6</sup> and 1.6x10<sup>10</sup> cells/ml, using lysozyme. However, no competition was observed between the cellular and recombinant bp26, which may have been due to a number of reasons. (i) The anti-bp26 scFv may have exhibited an unfair binding bias towards the recombinant protein inhibiting competition between the recombinant and cellular bp26. (ii) The anti-bp26 scFv was isolated from a naïve phage display library following six rounds of panning against the recombinant bp26, which was isolated from XL-Gold *E. coli* under denaturing conditions, indicating that only linear epitopes on the recombinant bp26 would have been exposed during the scFv selection process. This implies that the anti-bp26 scFv only recognised a linear epitope. However, during the competitive ELISA, described above, the competing cellular bp26, in its native 3-D conformation, may have masked the anti-bp26 specific-linear epitope, therefore, ruling out any chance of competition between the recombinant and cellular bp26 for binding with the anti-bp26 scFv. (iii) Although the bp26 protein has been described as highly immunogenic the levels of expression of the cellular bp26 have yet to be determined. Therefore, if the levels of expression were relatively low the cellular concentration of bp26 would not be sufficient to compete with the recombinant bp26. (iv) Although bp26 has been identified as an immunodominant antigen in *Brucella* infections in sheep, goats, cattle and humans (Lindler *et al.*, 1996; Rossetti *et al.*, 1996 and Debbarh *et al.*, 1996) its function has yet to be defined. The fact that bp26 is immunodominant during an infection may suggest it might play a role in *Brucella* virulence and may be upregulated in virulent strains of *Brucella* while being down regulated in non-virulent strains such as the *B. abortus* 45/20 rough strain, therefore, ruling out competition between the recombinant bp26 and cellular bp26 from the non-virulent *B. abortus* 45/20. However, until the function and intracellular behaviour of bp26 has been

identified no definite conclusion on the lack of competition between the recombinant and cellular bp26 for binding with the anti-bp26 can be reached.

Conventional methods for the detection of pathogenic bacteria include a morphological evaluation of the micro-organism and growth determination in various media under a variety of conditions. Traditional detection methods are laborious and time-consuming involving numerous steps such as pre-enrichment, selective enrichment, biochemical screening and serological confirmation (Invintski *et al.*, 1999). Polymerase chain reaction (PCR) has also been applied to amplify small quantities of species/strain-specific genetic material. Although PCR is a relatively quick procedure extensive sample clean up and processing maybe required.

More recently the use of immunoanalytical techniques have provided systems for the rapid sensitive detection of pathogenic bacteria. Immunoassays, incorporating both polyclonal and monoclonal antibodies, have been described for numerous highly toxic and infectious pathogenic bacteria. A fluorescence immunoassay (FIA), incorporating both monoclonal and polyclonal antibodies, has been developed for the detection of *Yersinia pestis*, which is the causative agent of the bubonic plague (Coo *et al.*, 1995). Immunoassays have also been developed for the detection of *Bacillus anthracis* (Wijesuriya *et al.*, 1994) and *E. coli* 0157:H7 (Pyle *et al.*, 1995).

Recombinant antibody technology has provided an alternative source of antibodies with desirable affinity and specificity. Large repertoire recombinant antibody libraries have been developed allowing the isolation of antibody fragments such as the antigen binding (Fab) and single chain variable fragments (scFv) displayed on the surface of phage particles. scFv antibody fragments have been isolated against numerous pathogenic bacteria and their spores. Immunised, non-immunised and semi-synthetic phage display libraries have been used for the isolation of specific-scFvs against several human and animal pathogens. A naïve human library was used for the isolation of scFvs against antigens associated with *Chlamydia trachomatis*, which causes trachoma (resulting in blindness) and sexually transmitted diseases (Lindquist *et al.*, 2002). scFvs specific for microcystin-LR a cyanobacterial hepatotoxins (McElhiney *et al.*, 2000), *Bacillus subtilis* spores (Zhou *et al.*, 2002) and *Candida albicans* (Haidaris *et al.*, 2001) has also been isolated from large human naïve

libraries. The Griffin 1 library, a semi-synthetic phage display library, has been used for the successful isolation of scFvs against *Streptococcus suis*, which causes severe infections in young pigs resulting in meningitis, septicemia and arthritis (de Greeff *et al.*, 2000). *B. melitensis*-specific scFv antibody fragments, capable of distinguishing between *Brucella melitensis* and several *Yersiniae*, were isolated from a pre-immunised phage display library (Hayhurst *et al.*, 2003).

Recent developments in biological warfare have highlighted the requirements for sensitive and specific detection systems for hazardous bacterial strains such as *Brucella*. To date, the majority of detection methods for *B. abortus* involve laborious and time-consuming cell-culture and biochemical techniques. Isolation of *B. abortus* involves taking multiple blood cultures, which are incubated under 10% CO<sub>2</sub>, at 35°C for up to six weeks. Special rich media is required, including blood, serum and haemin. Since *Brucella* is a class III pathogen strong biosafety measures need to be addressed, including at least level 3 containment facilities. Ideally, a sensitive and specific immunoanalytical technique would rule out the need for the laborious cell culture techniques and possibly reduce the dangers associated with growing up the bacterial cultures. However, immunoassays for the detection of *B. abortus* generally yield high levels of cross-reactivity with structurally related bacteria, such as *Yersinia*, that contain a similar 0.9 LPS epitope. Although, Hayhurst and associates (2003) have described the isolation of *B. melitensis*-specific phage-displayed scFv antibody fragments capable of distinguishing between *Brucella melitensis* and several *Yersiniae* difficulties were encountered when trying to isolate soluble scFvs. Therefore, *Brucella*-specific antibodies are generally applied to the development of immunoassays for the detection of a bovine brucellosis infection in serum samples. *Brucella*-specific antibodies have been successfully used in sandwich assay format as the capture antibody (Gornell *et al.*, 1984 and Al-Shamaly and Wright, 1998) or as a competing antibody in a competitive assay format (Gall and Nielsen, 1994, Uzal *et al.*, 1996, Stack *et al.*, 1999 and McGiven *et al.*, 2003) and this will be further addressed in Chapter 6.

This chapter, while focusing on the production of antibodies for the development of an immunoassay for the detection of a bovine brucellosis infection (See Chapter 6),

addresses the need for an immunoassay for the detection of *B. abortus* cells. Although, difficulties were encountered when trying to develop a competitive ELISA for the detection of *B. abortus* incorporating the anti-bp26 scFv the development of a competitive ELISA incorporating the anti-*Brucella* polyclonal antibodies was successful. Both polyclonal antibodies produced had a limit of detection for *B. abortus* cells at  $1.95 \times 10^6$  cells/ml. pAB1 was raised against the crude cytoplasmic lysate from *B. abortus* 45/20 cells and pAB2 was raised against whole *B. abortus* 45/20 cells, as previously discussed. Due to the rough morphology of the *B. abortus* 45/20 cells the polyclonal serum obtained will contain no antibodies against the 0.9 side chain. This rules out the cross-reactivity potential between the polyclonal antibodies and *Yersinia* cells.

## **CHAPTER 6**

**The development and validation of immunoassays for the  
detection of bovine brucellosis in serum samples**

## **6.1 Introduction**

### **6.1.1 Brucellosis**

Brucellosis is an infection caused by a gram-negative intracellular pathogen from the genus *Brucella*, which affects humans and domestic animals (Hemmen *et al.*, 1995). The disease is regarded as a major zoonosis in some parts of the world (Shamelian, 2000). In animals the infection is characterised by foetal abortions, lowered fertility and in some cases by reduced milk production (Toth *et al.*, 1995). In humans symptoms include undulant fever, arthritis and osteomyelitis (Rossetti *et al.* 1996). The disease usually presents as acute, sub-acute or localized, but in some cases chronic and sub-clinical infections are also common (Shamelian, 2000). *B. abortus* and *B. melitensis* are the most prevalent and economically significant because they cause infection in humans and ruminants (cows, sheep and goats) (Hemmen *et al.*, 1995). Brucellosis results in economic losses worldwide, having major impacts on underdeveloped and developing countries (Rossetti *et al.*, 1996) and it can also introduce limitations in the trade of animals and animal products internationally (Jacques *et al.*, 1998). Programs of control of brucellosis typically involve vaccination followed by diagnosis and elimination of reactors. However, some countries opt out of vaccination programs and are more in favour of regular routine testing programs followed by the slaughter of positive animals.

### **6.1.2 Brucellosis in Ireland**

Ireland is considered to be free of *Brucella melitensis* and is recognised as such under the EU Commission Decision 93/52/EC. However, *Brucella abortus* poses problems with reported cases of bovine brucellosis. In 1965 a milk ring test survey carried out on 105,000 dairy herds indicated that at least 12% of herds were infected with brucellosis. This survey also concluded that higher levels of infection were observed in the intensive dairying areas in the south of Ireland. This study promoted the initiation of a national program for bovine brucellosis eradication. This program involved a combination of vaccination using the 45/20 vaccine, serological testing and slaughter of positive reactors. By the mid 1980s the number positive reactor herds identified had been reduced to between 300 and 500 annually. Vaccination was then ceased in 1984, in 1986 annual serological testing of the National herd was suspended and the pre-movement test was then withdrawn in 1988. During this period the

number of positive reactors identified stayed between 300 and 400 per annum. However, the introduction of the suckler cow quota scheme led to a unusually high volumes of movement of older dairy cows, which is believed to have led to an increase dissemination of brucellosis infections throughout Ireland as the levels of brucellosis increased from 434 new reactors in 1994 to 1081 in 1998. The re-introduction of serological testing in 1998 (along with a range of measures discussed below) led to a significant decrease in the number of positive reactors identified. This national bovine brucellosis eradication program is in accordance with the requirements of Directive 64/52/EC. Numerous enhanced program measures have been introduced, which have collectively resulted in a marked improvement. These improvements include: (1) A 30-day compulsory pre-movement test is required for all eligible animals; (2) A full round of serological testing of all eligible animals (all females and males over 12 months of age); (3) Rapid depopulation of infected herds to prevent contiguous spread; (4) Slurry treatment, with hydrated lime in liquid form, in all brucellosis depopulated herds; (5) Diagnostic improvements have seen the introduction of newer blood tests including indirect ELISA and competitive ELISAs, the fluorescence polarization assay (FPA) and the brucellin skin test; (6) Improved milk testing has resulted in the milk ring test being replaced by the more specific and sensitive whey ELISA test; (7) District Veterinary Offices now have the option of extending the rest period following depopulation; (8) The Special Investigation Unit of the Department of Agriculture Food and Rural Development has focused considerable attention on tackling fraud and irregularities in relation to brucellosis; and (9) A cull cow-monitoring program has focused on blood sampling from cows in all slaughter plants for brucellosis testing.

Although vaccination can be a highly effective tool in relation to brucellosis eradication there are some significant drawbacks to the use of brucellosis vaccination in Ireland. Under current EU legislation any vaccinated herd would lose its Official Brucellosis Free (OBF) status for a three-year period and any herd containing animals from a previously vaccinated herd would also lose its OBF status. This would result in significant restrictions on live animal exports from such herds. However, the fact that some infected animals will not show positive in blood tests, particularly at certain stages of pregnancy, supports the need to develop new diagnostic assays that may

help to overcome this diagnostic defect that hinders brucellosis eradication both in Ireland and worldwide

### **6.1.3 Conventional methods for the detection of Brucellosis**

The diagnosis and control of brucellosis is generally based on the serological testing. Numerous serological assays have been described for the detection of brucellosis. With the more conventional methods including the Rose Bengal Plate Test (RBPT) (Davies, 1971), the Complement Fixation Test (CFT) (Alton *et al.*, 1988), the Buffered *Brucella* Plate Agglutination Test (BBAT), the Rapid Slide Agglutination Test (RSAT) and the Serum Agglutination Test (SAT), with the CFT and RBPT being the most accepted worldwide. These serological assays are generally used to detect antibodies directed against the rough lipopolysaccharide of *Brucella*.

#### **6.1.3.1 Rose Bengal Plate Test (RBPT)**

The Rose Bengal Plate test is a rapid agglutination used to detect acute *Brucella*-specific agglutins associated with previous exposure to *Brucella* organisms. An equal volume of serum and antigen is mixed on a white tile or enamel plate and rocked gently for 4 minutes and then observed for agglutination (Morgan *et al.*, 1969). This test is considered a valuable screening test (Farina 1985) and is very sensitive, especially in vaccinated animals. However, it is less effective than the CFT at detecting brucellosis in sheep (Joint FAO/WHO Expert Committee on Brucellosis, Technical report 740, 1986). Positive samples are usually retested using a confirmatory test such as the ELISA or CFT. However, false-negative reactions can occur. Cell concentration and standardisation procedure of the antigen can influence the efficiency of the test (Blasco *et al.*, 1994).

#### **6.1.3.2 Complement Fixation Test (CFT)**

The complement fixation test is a widely used and accepted confirmatory test and it is considered the most effective test for diagnosing brucellosis (Joint FAO/WHO Expert Committee on Brucellosis, Technical report 740, 1986). Numerous variations of the test are available and each is conventionally carried out using microtitre plates. The degree of haemolysis that has occurred in each well is compared with a set of known standards. The results are expressed in international CFT units (icftu). Although this test is highly sensitive and specific, false positive reactions have been reported in

animals vaccinated with the S19 vaccine. This complex technique requires good laboratory facilities and adequately trained staff to accurately titre and maintain the reagents. However, it has no particular advantage over the SAT performed in a hypertonic environment of 5 – 20% NaCl.

#### **6.1.3.3 Buffered *Brucella* Plate agglutination Test (BBAT)**

The Buffered *Brucella* plate agglutination test is a rapid agglutination test. The serum sample is mixed with the appropriate antigen, which is prepared from *B. abortus* strain 1119-3, and, following incubation, any visible signs of agglutination represent a positive result. This test has proven to be very sensitive especially in vaccinated animals. However, positive test results must be confirmed by ELISA or CFT.

#### **6.1.3.4 Rapid Slide Agglutination Test (RSAT)**

The rapid slide agglutination test is also a rapid agglutination test that is carried out on slides. A serum sample is mixed with a *Brucella* bacterial suspension in a circular spot on a slide. After approximately one minute a visible agglutination will appear if the serum contains specific anti-*Brucella* antibodies.

#### **6.1.3.5 Serum Agglutination Test (SAT)**

The serum agglutination test is used for the detection of acute *Brucella* infections and is based on the detection of IgM antibodies. The test can be performed in the presence of 2-mercaptoethanol (2-ME test) or dithiothreitol (SAT-DTT). This test can only be performed by skilled laboratory personnel and is not satisfactory for the detection of bovine brucellosis. The test can also fail to agglutinate in the presence of sheep sera and can result in a marked prozone phenomenon, whereby the specific antigen and antibody do not agglutinate or precipitate visibly because of an excess of either antibody or antigen.

### **6.1.4 Immunoassays for the diagnosis of brucellosis**

#### **6.1.4.2 ELISAs for the diagnosis of brucellosis**

ELISAs are also commonly used as screening tests for the diagnosis of brucellosis. The performance of ELISAs is comparable with that of the CF test, and since they are technically simpler to perform and more robust, their use may be preferred in many

laboratories as screening and confirmatory tests. Numerous indirect (Uzal *et al.*, 1996; Jacques *et al.*, 1998 and Vanzini *et al.*, 1998), sandwich (Al-Shamaly and Wright, 1998) and competitive (Gall and Nielsen, 1994, Stack *et al.*, 1999 and McGiven *et al.*, 2003) ELISAs have been described with the majority based on the detection of antibodies directed against the smooth lipopolysaccharide (LPS).

More recently, ELISAs incorporating cytosoluble proteins (Goldbaum *et al.*, 1992 and Debbarih *et al.*, 1995) and outer membrane proteins (OMPs) (Dubray and Bezar, 1980; Verstrete *et al.*, 1982; and Dubray and Charriaut, 1983) have been described for the detection of human (Goldbaum *et al.*, 1992), ovine (Debbarih *et al.*, 1996 and Cloeckaert *et al.*, 2001), canine (Baldi *et al.*, 1997) and caprine (Kittelberger *et al.*, 1995, 1998 and Zygmunt *et al.*, 2002) brucellosis.

The use of several cytosoluble proteins, including an 18kDa cytoplasmic protein (p18) (Goldbaum *et al.*, 1993 and Hemmen *et al.*, 1995) and a 26kDa periplasmic protein (bp26) (Debbarih *et al.*, 1996 and Rossetti *et al.*, 1996), were described as markers of an active *Brucella* infection in bovines. However, little research has focused on their use in the development of diagnostic assays for bovine brucellosis.

#### **6.1.4.2 Fluorescent polarisation assay (FPA) for the diagnosis of brucellosis**

The fluorescence polarization assay (FPA), described by Nielsen and associates (1996), is a homogeneous immunoassay based on the detection of serum antibodies directed against the LPS. The principal of an FPA is based on the fact that a molecule in solution rotates randomly at a rate inversely proportional to its size. The rate of rotation can be measured in the horizontal and vertical planes using a fluorescent label and polarized light. The rotational rate of a small-labelled antigen molecule will be altered if antibody is attached to it and this change in rotation can be measured. Therefore, the FPA assay only requires addition of labelled antigen to appropriately diluted test samples (so that the total time required is approximately 2 minutes). The FPA has been described for the diagnosis brucellosis in cattle (Nielsen *et al.*, 1996; and Dajer *et al.*, 1999), pigs (Nielsen *et al.*, 1999), bison (Gall *et al.*, 2000) and various species of deer (Gall *et al.*, 2001). The FPA was initially developed and validated in Canada, for the detection of antibodies to *Brucella abortus*, where brucellosis was eradicated (Nielsen *et al.*, 1996). The performance of the FPA was

then tested in areas of various incidences of brucellosis, which included Missouri, Texas, Chile, Mexico and Argentina (Nielsen *et al.*, 1998 and Dajer *et al.*, 1999).

#### **6.1.5 Proteins as serological diagnostic markers of brucellosis**

To date, the majority of serological tests for the detection of bovine brucellosis have targeted membrane-anchored lipopolysaccharides. However, such assays frequently yield false positive serological reactions due to cross reactivity with polysaccharide antigens of other micro-organisms such as *Yersinia enterocolitica* 0.9 (Garin-Bastuji *et al.*, 1999). Problems have also been encountered with these assays when trying to discriminate between actively infected and vaccinated cattle (Goldbaum *et al.*, 1993). Therefore, a greater emphasis is now being placed on the use of specific-proteins as serological diagnostic markers. Individual studies on the isolation of protein markers for brucellosis have yielded interesting results.

The major outer membrane proteins (OMPs) of *Brucella* species were initially identified in the early 1980s and identified as potential immunogenic and protective antigens (Dubray and Bezard, 1980; Verstrete *et al.*, 1982; and Dubray and Charriaut, 1983). They were classified as group 2 porin proteins, which consisted of proteins with a molecular mass of 36 – 38kDa, and group 3 proteins, which consisted of 31 – 34kDa and 25 – 27kDa OMPs. However, further studies using recombinant protein technology and monoclonal antibodies have shown major OMPs induce only low and heterogeneous antibody responses and thus constitute poor immunogens in *B. abortus*-infected cattle (Cloekaert *et al.*, 1992) and *B. melitensis*-infected sheep (Zygmunt *et al.*, 1994). However, group 3 OMPs appear to be immunodominant in the course of *B. ovis* infection in rams suggesting they may be useful for the development of a serological diagnostic test for ram brucellosis (Kittelberger *et al.*, 1995, 1998).

Attention then focused on the identification of sero-reactive cytosoluble proteins as diagnostic markers for brucellosis. Two interesting proteins, p18 (Goldbaum *et al.*, 1992) and bp26 (Debbarh *et al.*, 1995), were identified as possible serological diagnostic markers for *Brucella* infections.

Two research groups, working independently, on the identification of protein markers for the detection of brucellosis isolated the 26kDa periplasmic protein bp26,

previously identified as CP26 (Debbbarh *et al.*, 1996 and Rossetti *et al.*, 1996). Rossetti *et al.* were working on the isolation of a specific-protein marker for bovine brucellosis and Debbbarh *et al.* were focusing on the identification of protein markers for brucellosis in sheep. Sequence analysis of the cloned *B. melitensis* bp26 gene later revealed that it was nearly identical to the previously sequenced *B. abortus* bp26 gene (Debbbarh *et al.*, 1996). Comparison of the nucleotide and amino acid sequences of the bp26 protein also revealed no sequence homology with other bacterial proteins (Rossetti *et al.*, 1996). This 26kDa protein has proven useful in the discrimination between vaccinated and naturally infected animals. The bp26 protein was capable of discriminating between an antibody response from *B. melitensis* Rev.1 vaccinated and *B. melitensis*-infected sheep in a competitive ELISA (Debbbarh *et al.*, 1996). The protein also proved beneficial in discriminating between naturally infected and S19-vaccinated cattle (Rossetti *et al.*, 1996). This protein is also likely to elicit a strong immune response during early infection. Following experimental infection of sheep an antibody response to the bp26 protein was first recognised at 21 days and a high frequency of reactivity was also observed among naturally infected sheep following immunoblotting (Debbbarh *et al.*, 1996).

A group in Argentina have been investigating the 18kDa cytoplasmic protein (p18) as an alternative diagnostic marker for brucellosis (Goldbaum *et al.*, 1993; Baldi *et al.*, 1996 and Goldbaum *et al.*, 1999). Furthermore, Hemmen *et al.* (1995) cloned and sequenced a *Brucella abortus* cytoplasmic protein with an apparent molecular weight of 17kDa. It has been speculated that both these proteins are identical (Goldbaum *et al.*, 1999). This 18kDa protein has been successfully cloned and expressed in *E. coli* and the reactivity of animal and human sera was similar to that of the native protein contained in the cytoplasmic fractions of *Brucella* cells (Goldbaum *et al.*, 1999). Nucleotide and amino acid sequence comparisons have shown that this protein is also unique to *Brucella* spp. The protein is likely to be highly immunogenic due to its polymeric arrangement. Therefore, it is likely to elicit a strong immune response during early infection. This should greatly increase the pick-up efficiency during field-testing, and hence, reduce the numbers of false negative results. Furthermore, a detectable response may be elicited in pregnant cattle that are not identifiable by conventional tests. The protein is also capable of discriminating between S19-

vaccinated and naturally infected cattle (Goldbaum *et al.*, 1993). The protein has previously proven useful in the diagnosis of bovine, canine and human brucellosis.

#### **6.1.6 ELISA validation**

The ultimate aim of this research project was the development and validation of a sensitive and specific assay for the detection of bovine brucellosis in serum samples. This chapter focuses on the validation of indirect and sandwich ELISA assays using a process described by Jacobson (1998), who previously defined a validated assay as one that “consistently provides test results that identify animals as being positive or negative for an analyte or process, and, by inference, accurately predicts the infection status of animals with a predetermined degree of statistical certainty”.

There are several variables that may affect the performance of an assay and these must be addressed during the assay validation. Factors introducing assay variability can be categorised into three groups:

1. **The sample:** host/organ interaction affecting analyte concentration in the serum. Factors that may affect analyte concentration and composition in the serum sample include age, sex, breed, nutritional status, pregnancy and immunological responsiveness.
2. **The assay system:** physical, chemical biological and user-related factors, affecting assay performance in detecting the specific analyte in the serum sample. Interfering factors include instrumentation, operator error, reagent choice and calibration, reaction vessels, water quality, pH and ionicity of buffers and reagents, incubation temperatures and duration and cross reactants.
3. **The test result:** the ability of the assay results to determine the status of the host in relation to the analyte in question.

Therefore, there are many variables that need to be addressed during the validation of an assay. In order to try and address such issues assay validation was carried using an incremental process consisting of three steps:

- Step 1: Feasibility studies
- Step 2: Development and standardisation
- Step3: Characterisation of assay performance

## 6.2 Results

This chapter focuses on the development and validation of enzyme-linked immunosorbent assays for the diagnosis of bovine brucellosis in serum samples. Four indirect ELISAs and two sandwich ELISA formats were investigated as alternative sensitive and specific immunoassays for the detection of a *B. abortus* infection. The indirect and sandwich ELISAs were developed and validated using the incremental process described by Jacobson (1998) (See Section 6.1.6). Throughout the course of the assay development and validation process the *Brucella*-positive DeVeere Hunt Serum and the National Standard Serum (NSS) and the standard *Brucella*-negative serum were used to assess the discriminatory capabilities of the ELISAs and their selected reagents and protocols. The indirect and sandwich ELISAs were conducted as described in Sections 2.6.1 and 2.6.2, respectively.

### 6.2.1 Feasibility studies

Initially, feasibility studies were carried out in order to determine the discriminatory capabilities of the selected ELISA formats and reagents. These studies were intended to give an initial insight into the analytical sensitivity and specificity of the assay formats.

Feasibility studies were carried out on four indirect ELISAs incorporating the two recombinant proteins, p18 and bp26, the crude cytoplasmic lysate from *B. abortus* 45/20 and whole *B. abortus* 45/20 cells. Figure 6.1 (A) details the initial feasibility studies on the four indirect ELISA formats, which indicates that each antigen and assay format offered discriminatory capabilities in distinguishing between the *Brucella*-positive and negative sera.

Feasibility studies were also carried out on two sandwich ELISAs, which incorporated the two anti-*Brucella* polyclonal antibodies, pAB1 and pAB2 (Section 5.2.1). The feasibility studies were carried out using immunoplates coated with pAB1 and pAB2, as the capture antibody to immobilise the crude cytoplasmic lysate and whole *B. abortus* 45/20 cells, respectively. The pAB1 and pAB2 sandwich ELISAs were both capable of discriminatory between the *Brucella*-positive and negative sera (Fig. 6.1 (B)).

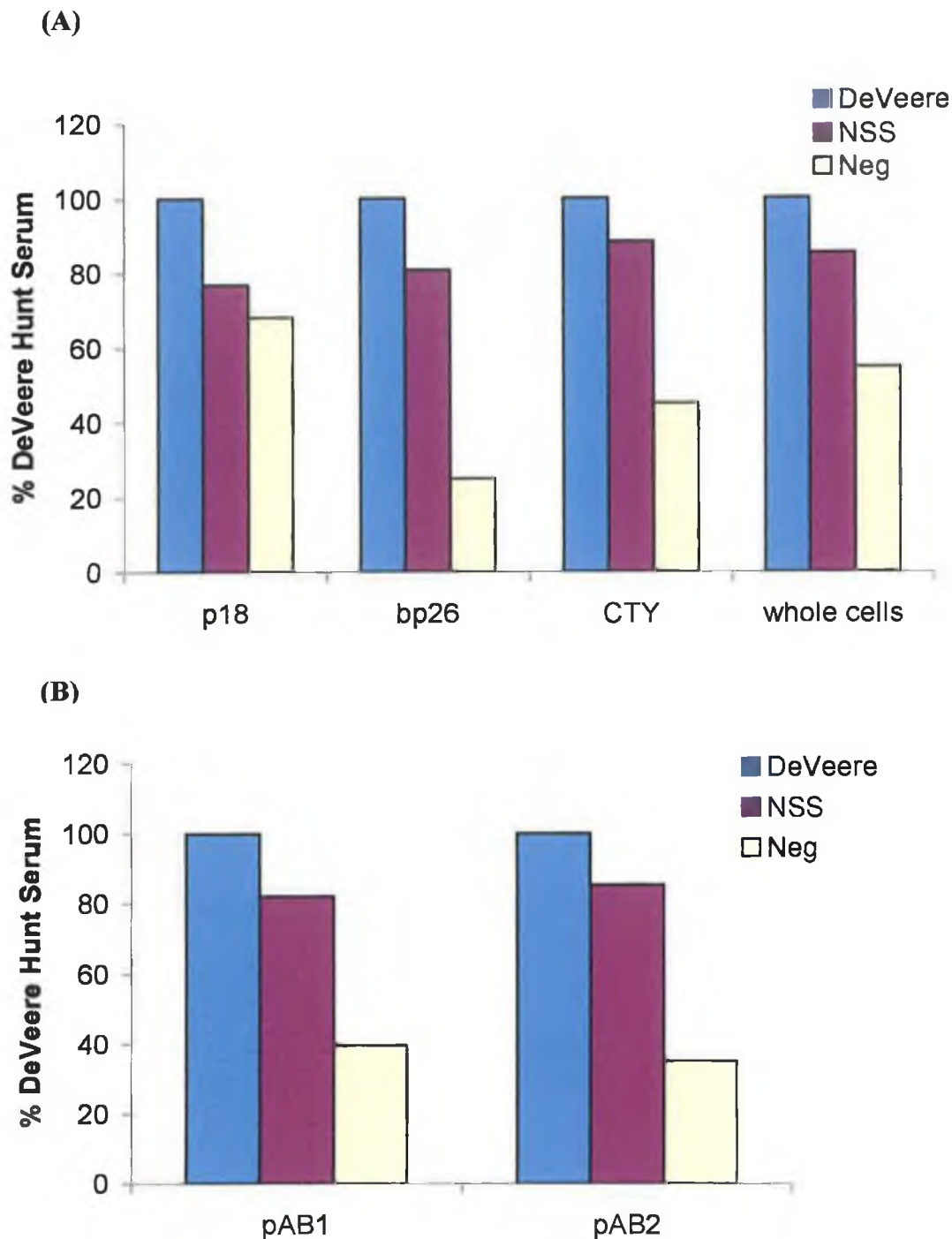


**Figure 6.1:** Initial feasibility studies on the indirect (A) and sandwich (B) ELISAs for the detection of bovine brucellosis. (A) Indirect ELISAs, incorporating p18, bp26, the crude cytoplasmic lysate and whole *B. abortus* cells, were investigated as diagnostic immunoassays for bovine brucellosis. (B) Sandwich ELISAs incorporating pAB1 and pAB2 polyclonal antibodies were developed using whole *B. abortus* and the crude cytoplasmic lysate, respectively. The feasibility studies were carried out using the standard positive serum samples, the DeVeere Hunt Serum, the National Standard Serum (NSS) and the standard negative serum. Each antigen and ELISA format was capable of discriminating between the *Brucella*-positive and negative serum samples.

## **6.2.2 Assay development and standardisation**

Following the initial feasibility studies on the indirect and sandwich ELISAs assay development and standardisation was conducted on each ELISA format. The ultimate aim of the assay development and standardisation was to obtain an optimised assay, which repeatedly achieved the same results for a standard serum. Development and standardisation of each ELISA assay involved the optimisation of the various assay parameters including antigen/antibody coating concentration/dilution and the serum and secondary antibody dilutions that were determined using checkerboard titrations. The optimal blocking reagents and antibody diluent were also determined along with preliminary estimates of the repeatability on the assays.

### **6.2.2.1 Optimisation of blocking reagents and antibody diluent**

Initial stages of assay development and standardisation involved the optimisation of the blocking solution and antibody diluent. The polyclonal nature of the bovine serum samples increases the chances of non-specific interactions between the serum antibodies and the blocking reagent. Optimisation of the blocking reagent and serum diluent would result in a reduction in levels of the non-specific interactions occurring.

The blocking reagent and antibody diluent were optimised for use in the indirect and sandwich ELISAs. Milk marvel, chicken egg albumin (ovalbumin) and bovine serum albumin (BSA) were investigated as the blocking reagent and antibody diluent. In order to establish the optimum blocking reagent and antibody diluent immunoplates were coated with 4% (w/v) milk marvel (Plate 1), 4% (w/v) ovalbumin (Plate 2) and 4% (w/v) BSA (Plate 3). A 1/50 dilution of each of the 3 standard serum samples were prepared using each of the following diluents; PBS containing 4% (w/v) milk marvel, PBS containing 4% (w/v) ovalbumin and PBS containing 4% (w/v) BSA. Each of the serum dilutions was then pre-incubated at 37°C for 1 hour and then added to the three immunoplates, in duplicate. A 1/2000 dilution of the HRP-labelled anti-bovine antibody was then prepared using the three different diluents, PBS containing 4% (w/v) milk marvel, PBS containing 4% (w/v) ovalbumin and PBS containing 4% (w/v) BSA. The three anti-bovine dilutions were then incubated for 1 hour at 37°C and then added to the three immunoplates. Bound serum antibodies were then

detected following the addition of the chromogenic substrate. The absorbance values obtained were then plotted on a bar graph.

Figures 6.2, 6.3 and 6.4 represent the results obtained from plate 1, plate 2 and plate 3, respectively. A high degree of non-specific interactions was observed between the plates coated with the milk marvel, ovalbumin and BSA, and the serum samples diluted and pre-incubated in the PBS containing both 4% (w/v) ovalbumin and 4% (w/v) BSA. Whereas, negligible non-specific interactions were observed between the plates coated with the milk marvel, ovalbumin and BSA, and the serum samples diluted and pre-incubated in the PBS containing 4% (w/v) milk marvel.

Therefore, in order to rule out any non-specific interactions 4% (w/v) milk marvel was selected as the optimal blocking reagent and antibody diluent for the serum samples and secondary antibody (following pre-incubation).

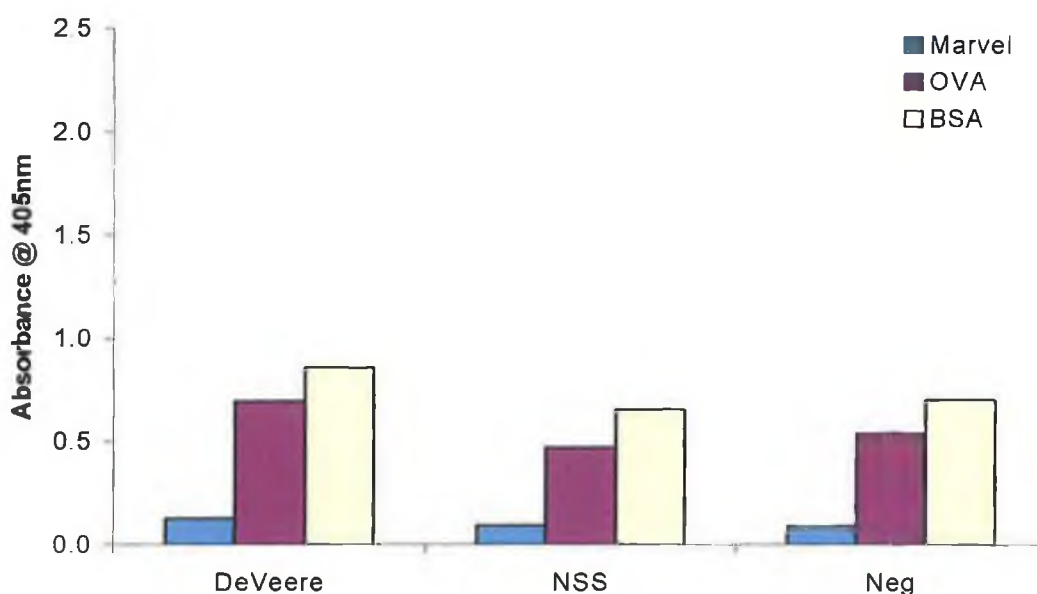


**Figure 6.2:** Optimisation of blocking reagent and antibody diluent. Results obtained for plate 1, which was coated with 4% (w/v) milk marvel. Each of the standard serum samples was added to the immunoplate, diluted to 1/50 with the 3 different diluents; PBS containing 4% (w/v) milk marvel, PBS containing 4% (w/v) ovalbumin and PBS containing 4% (w/v) BSA). A high degree of non-specific interactions was observed between the milk marvel blocking solution and serum samples diluted in ovalbumin and BSA. However, negligible non-specific interactions were observed between the milk marvel blocking solution and serum samples diluted in milk marvel.

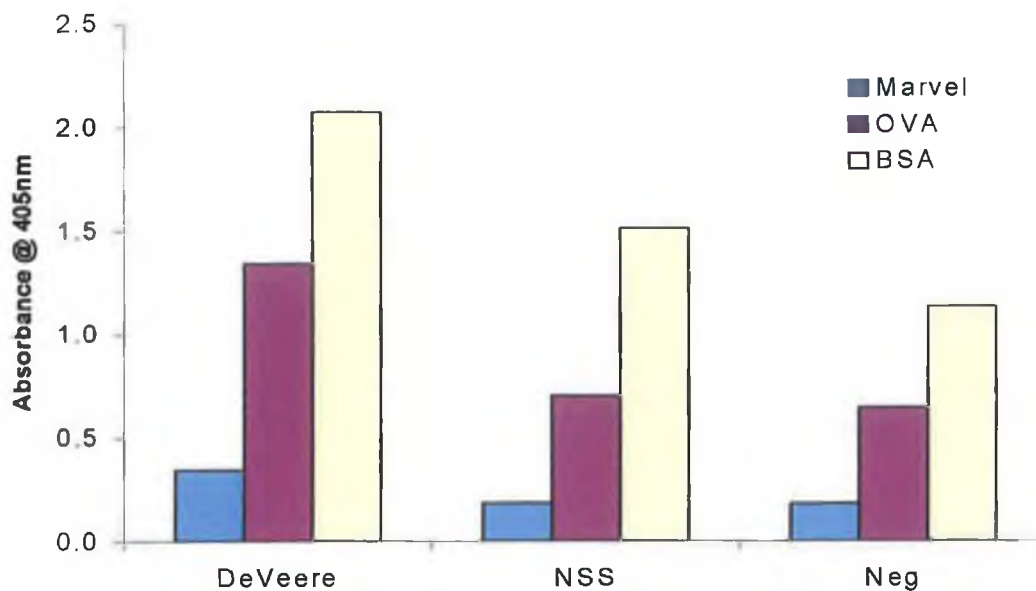


*Figure 6.3: Optimisation of blocking reagent and antibody diluent. Results obtained for plate 2, which was coated with 4% (w/v) ovalbumin. Each of the standard serum samples was added to the immunoplate, diluted to 1/50 with the 3 different diluents; PBS containing 4% (w/v) milk marvel, PBS containing 4% (w/v) ovalbumin and PBS containing 4% (w/v) BSA). A high degree of non-specific interactions was observed between the ovalbumin blocking solution and serum samples diluted in ovalbumin and BSA. However, negligible non-specific interactions were observed between the ovalbumin blocking solution and serum samples diluted in milk marvel.*

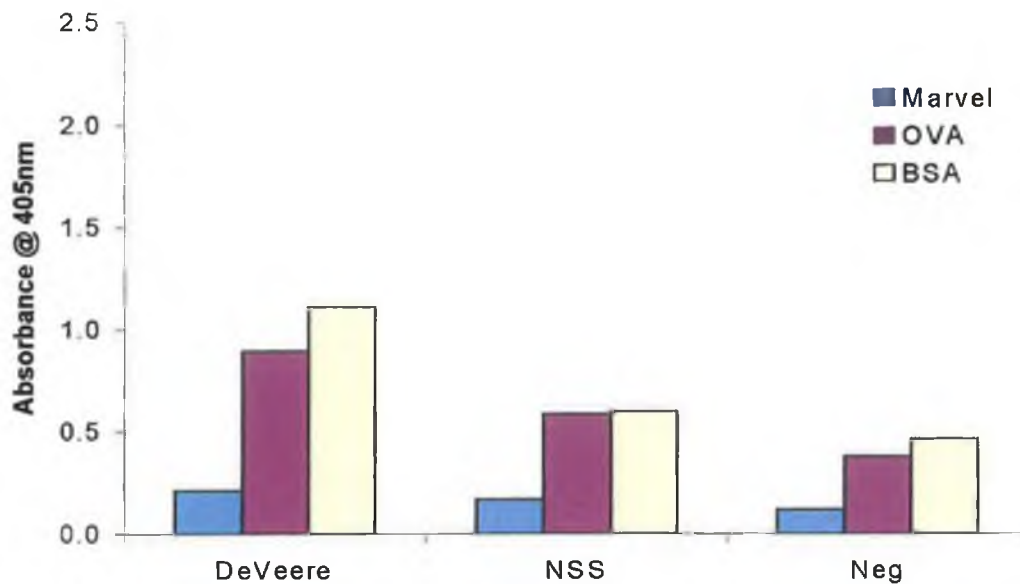


**Figure 6.4:** *Optimisation of blocking reagent and antibody diluent. Results obtained for plate 3, which was coated with 4% (w/v) BSA. Each of the standard serum samples was added to the immunoplate, diluted to 1/50 with the 3 different diluents; PBS containing 4% (w/v) milk marvel, PBS containing 4% (w/v) ovalbumin and PBS containing 4% (w/v) BSA). A high degree of non-specific interactions was observed between the BSA blocking solution and serum samples diluted in ovalbumin and BSA. However, negligible non-specific interactions were observed between the BSA blocking solution and serum samples diluted in milk marvel.*

#### **6.2.2.2 Optimisation of antigen coating concentrations/dilutions for use in the indirect ELISAs**

A panel of four coating antigens, the two recombinant proteins, p18 and bp26, the crude cytoplasmic lysate and whole *B. abortus* cells, were selected for the development of an indirect ELISA for the detection of bovine brucellosis. Following optimisation of the blocking reagent and antibody diluent assay development and standardisation focused on optimising the antigen coating concentration/dilution for each of the four antigens.

The indirect ELISAs were carried out as described in Section 2.6.1. Figure 6.5 shows the results obtained for the whole cell indirect ELISA. Cell coating concentrations ranging from  $1.6 \times 10^5$  –  $1.6 \times 10^9$  cells/ml were investigated and  $1.6 \times 10^8$  cells/ml offered the optimal discrimination capabilities when distinguishing between the standard *Brucella*-positive and negative sera (Fig. 6.5). p18 coating concentrations ranging from 0 - 25µg/ml were investigated for use with the p18 indirect ELISAs. A coating concentration of 25µg/ml enabled the optimal discrimination between the standard *Brucella*-positive sera, the DeVeere Hunt Serum and the NSS, and the standard negative serum (Data not shown). Varying bp26 coating concentrations, ranging from 0 - 25µg/ml, were investigated for use in the bp26 indirect ELISA. A bp26 coating concentration of 6.25µg/ml offered the optimal discrimination between the standard *Brucella*-positive and negative sera (Data not shown). CTY coating dilutions ranging from 1/2 – 1/64 were investigated for use in the CTY indirect ELISA, where a 1/4 dilution of the CTY enabled the optimal discrimination between the standard *Brucella*-positive and negative sera (Data not shown).

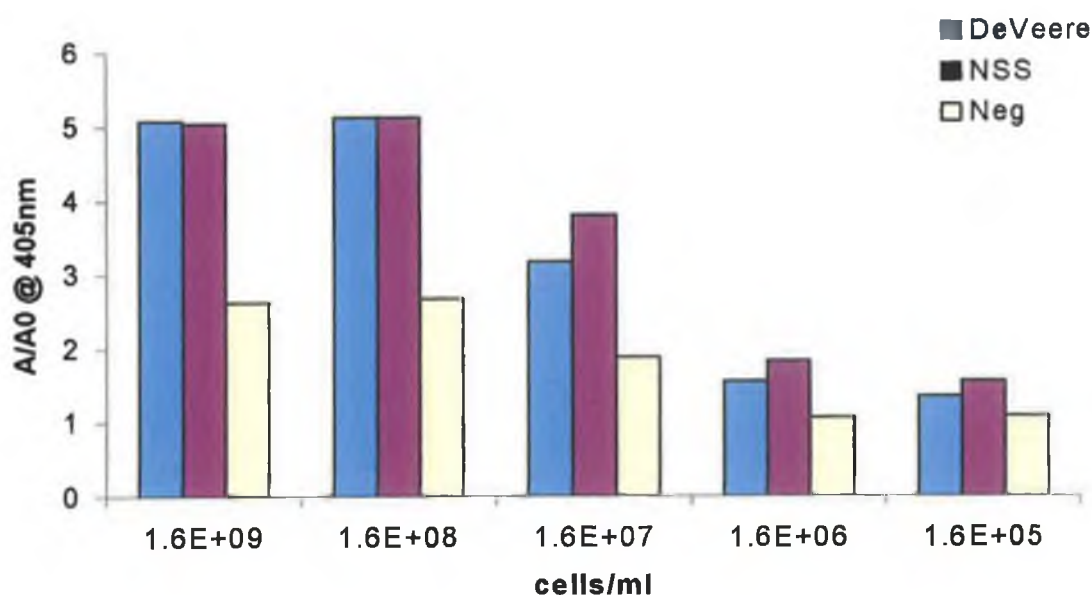


**Figure 6.5:** Optimisation of the whole *B. abortus* coating concentration for use in the whole cell indirect ELISA. Coating concentrations, ranging from  $1.6 \times 10^5$  –  $1.6 \times 10^9$  cells/ml, were tested in order to determine which concentration enabled optimal discrimination between the *Brucella*-positive and negative serum samples. A 1/500 dilution of pAB2 was selected as optimal.  $1.6 \times 10^8$  cells/ml was selected as the optimal cell concentration.

### 6.2.2.3 Optimisation of antibody coating dilutions for use in the sandwich ELISAs

Two sandwich ELISAs were developed incorporating the two polyclonal antibodies, pAB1 and pAB2, which were raised against the crude cytoplasmic lysate and whole *B. abortus* cells, respectively. Initially, development and standardisation of the sandwich ELISAs involved the optimisation of the polyclonal antibody coating dilution.

Figure 6.6 shows the results obtained for the sandwich ELISA incorporating pAB2 and whole *B. abortus* 45/20 cells, where pAB2 antibody coating dilutions ranging from 1/250 – 1/2000 were investigated. It was apparent that a 1/500 dilution of pAB2 enabled the optimal discrimination between the standard *Brucella*-positive and negative sera. Similarly, pAB1 antibody coating dilutions ranging from 1/250 – 1/2000 were investigated for use in the pAB1 sandwich ELISA, which incorporated the crude cytoplasmic lysate from *B. abortus* 45/20 cells as the capture antigen. In this

case a 1/500 dilution of pAB1 enabled optimal discrimination between the standard *Brucella*-positive and negative sera (Data not shown).

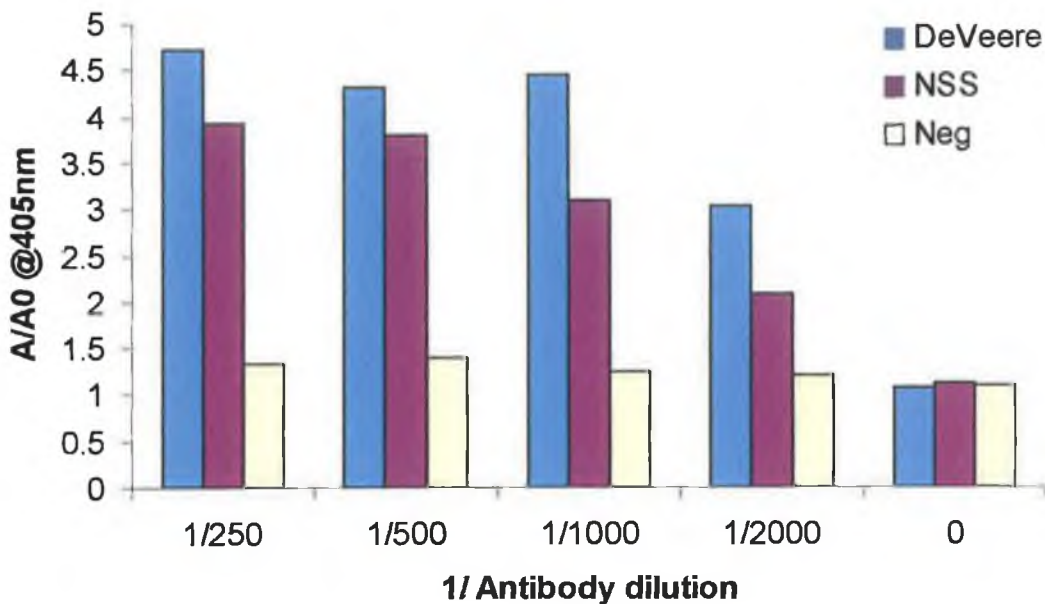


**Figure 6.6:** Optimisation of the pAB2 antibody coating dilution for use in the pAB2 sandwich ELISA. Antibody coating dilutions, ranging from 1/250 – 1/2000, were investigated to determine which dilution enabled optimal discrimination between the *Brucella*-positive and negative serum samples. A 1/500 dilution of pAB2 was selected as optimal.

#### 6.2.2.4 Optimisation of antigen concentrations/dilutions for use in the sandwich ELISAs

The development and standardisation of the sandwich ELISAs also involved optimisation of the crude cytoplasmic lysate (CTY) dilution and whole cell concentration for use in the pAB1 and pAB2 sandwich ELISAs, respectively.

Figure 6.7 shows the results obtained for the sandwich ELISA incorporating pAB2 and whole *B. abortus* 45/20 cells. Cell concentrations ranging from  $1.6 \times 10^5$  –  $1.6 \times 10^9$  were investigated.  $1.6 \times 10^8$  cells/ml offered the optimal discrimination between the standard *Brucella*-positive and negative sera. CTY dilutions ranging from neat – 1/16 were investigated for use in the sandwich ELISA incorporating pAB1 and CTY. A 1/16 dilution was chosen because it enabled discrimination between the standard

*Brucella*-positive sera, the DeVeere Hunt Serum and the NSS, and the standard negative serum.

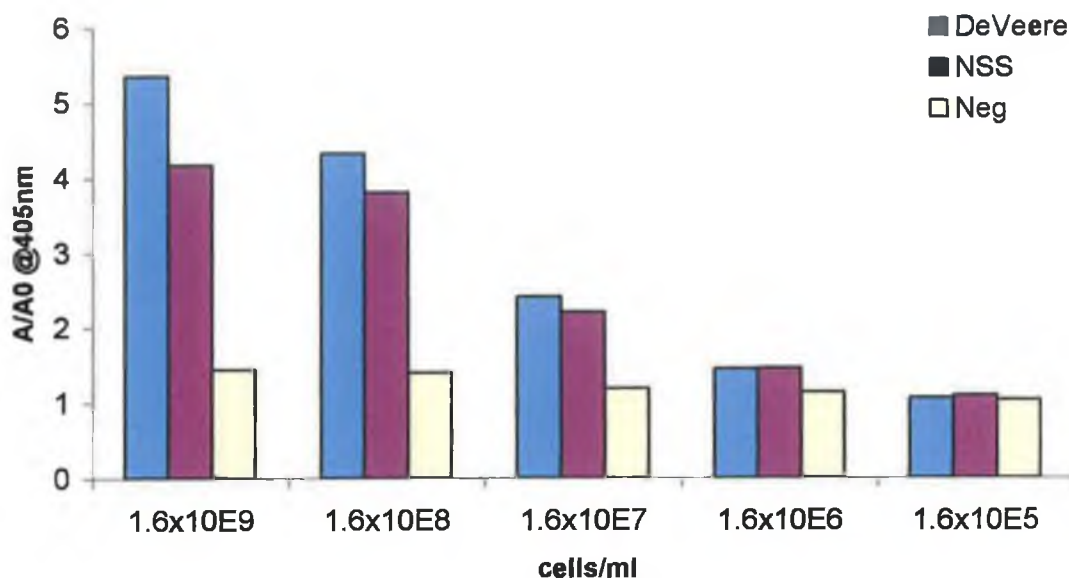


**Figure 6.7:** Optimisation of the whole cell concentration for use in the pAB2 sandwich ELISA. Cell concentrations, ranging from  $1.6 \times 10^5$  -  $1.6 \times 10^9$  cells/ml, were tested in order to determine which concentration enabled optimal discrimination between the *Brucella*-positive and negative serum samples.  $1.6 \times 10^8$  cells/ml was selected as the optimal cell concentration.

#### 6.2.2.5 Optimisation of bovine serum dilutions for use in the indirect and sandwich ELISAs

Following optimisation of the antigen / antibody coating concentrations and dilutions assay development and standardisation involved the determination of the optimal bovine serum dilution for use in the indirect and sandwich ELISAs.

Bovine serum dilutions, ranging from 1/25 – 1/2500, were investigated for use in the indirect and sandwich ELISAs to determine which allowed the greatest degree of discrimination between the positive and negative serum samples. Figure 6.8 shows the results obtained for the pAB2 sandwich ELISA, where it is apparent that a 1/50 serum dilution enabled the optimal discrimination between the standard *Brucella*-positive sera, the DeVeere Hunt Serum and the NSS, and the standard negative serum. Similar results were obtained for the p18, bp26, CTY and whole cell indirect ELISAs and the

pAB1 sandwich ELISA, where a 1/50 dilution of the serum samples enabled the optimal discrimination between the standard *Brucella*-positive and negative sera (Data not shown).

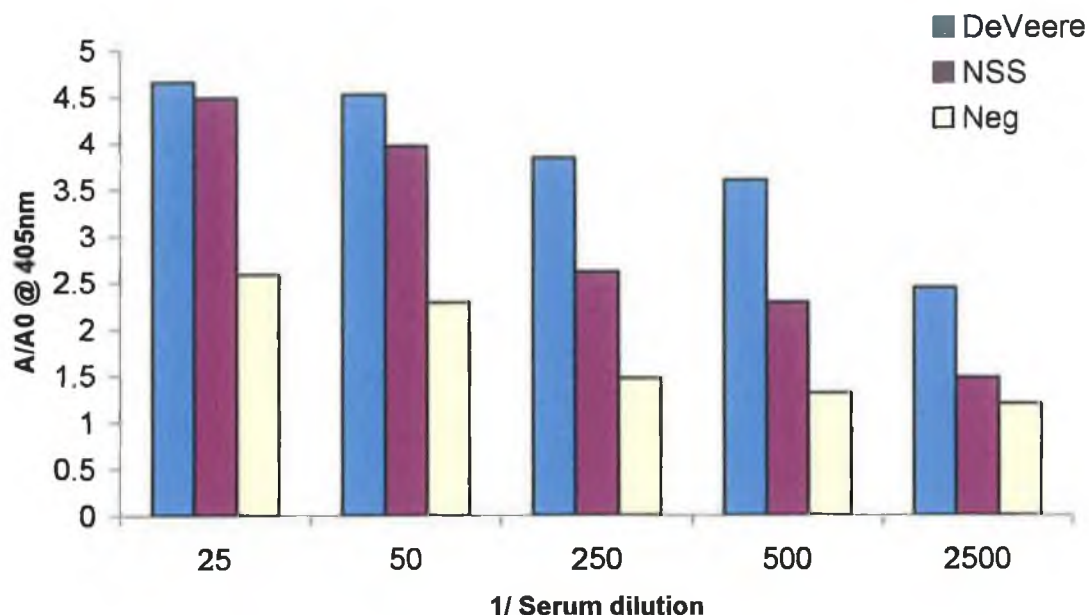


**Figure 6.8:** Optimisation of the serum dilution for use in the pAb2 sandwich ELISA. Serum dilutions, ranging from 1/25 – 1/2500, were tested in order to determine which concentration enabled optimal discrimination between the standard positive serum, the DeVeere Hunt Serum and the NSS, and the standard negative serum. A 1/50 dilution of the bovine serum samples was selected as optimal.

#### 6.2.2.6 Optimisation of anti-bovine secondary antibody dilution for use in the indirect and sandwich ELISAs

During assay development and standardisation it was also necessary to determine the optimal secondary anti-bovine antibody dilution for use in the indirect and sandwich ELISAs. The three standard serum samples, the DeVeere Hunt Serum, the NSS and the standard negative serum, were used with varying anti-bovine antibody dilutions in order to determine which serum dilution offered the best discriminatory capability.

Anti-bovine secondary antibody dilutions, ranging from 1/1000 – 1/16000, were investigated to determine which allowed the greatest degree of discrimination between the positive and negative serum samples. Figure 6.9 shows the results obtained for the pAB2 sandwich ELISA, where a 1/2000 dilution of the anti-bovine

secondary antibody enabled the optimal discrimination between the standard *Brucella*-positive and negative sera. A 1/2000 dilution of the anti-bovine secondary antibody also appeared to be optimum for use in the p18, bp26, CTY and whole cell indirect ELISAs and in the pAB1 sandwich ELISA (Data not shown).

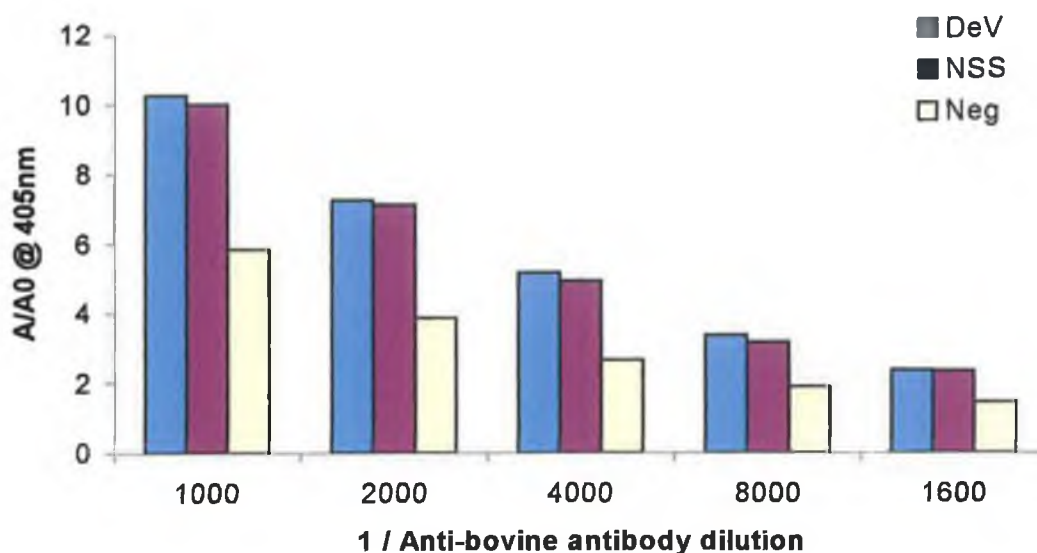


*Figure 6.9: Optimisation of the anti-bovine antibody, dilution for use in the pAb2 sandwich ELISA. Anti-bovine antibody dilutions, ranging from 1/1000 – 1/16000, were tested in order to determine which concentration enabled optimal discrimination between the standard positive serum, the DeVeere Hunt Serum and the NSS, and the standard negative serum. A 1/2000 dilution of the anti-bovine antibody was selected as optimal.*

#### 6.2.2.7 Initial estimates on the repeatability of the indirect and sandwich ELISAs

Following optimisation of the various assay parameters estimates on the repeatability of each indirect and sandwich ELISA were determined. This involved carrying out intra- and inter-day variability studies on the indirect and sandwich ELISAs. The three standard serum samples, the DeVeere Hunt Serum, the NSS and the standard negative serum, were used to estimate assay repeatability. Three replicates of each standard were assayed over ten individual days to provide estimates on repeatability. Coefficients of variation were determined by expressing the standard deviation of the replicates over the mean of the replicates, and generally values below 10% indicate adequate reproducibility (Jacobson, 1998). Estimates on the repeatability were

determined for the p18, bp26, CTY and whole cell indirect ELISAs and on the pAB1 and pAB2 sandwich ELISAs.

Intra-day variability studies were carried out on each ELISA where three replicates of each standard were assayed and the coefficients of variation determined, in order to estimate variation between replicates within a day. The intra-day coefficients of variation obtained for the p18, bp26, CTY and whole cell indirect ELISAs remained below 8.2%. Whereas, the intra-day coefficients of variation for the pAB1 and pAB2 sandwich ELISAs ranged between 0.7 and 9.8%.

Inter-day variability studies were then carried out on the indirect and sandwich ELISAs where three replicates of each standard were assayed over ten days and the coefficients of variation determined, in order to estimate variation between replicates over a ten day period. Table 6.1 summarises the inter-day coefficients of variation obtained for the p18, bp26, CTY and whole cell indirect ELISAs. The CVs for each indirect ELISA remained below 9.5%. Figure 6.10 shows the graphical representation of the inter-day variability studies on p18, bp26, CTY and whole cell indirect ELISAs. Table 6.2 summarises the inter-day coefficients of variation obtained for the pAB1 and pAB2 sandwich ELISAs. The CVs for each sandwich ELISA remained below 8.9%. Figure 6.11 shows the graphical representation of the inter-day variability studies on the pAB1 and pAB2 sandwich ELISAs.

**Table 6.1:** Inter-day assay coefficients of variation obtained for the p18, bp26, CTY and whole cell indirect ELISAs. Three sets of each standard were assayed on ten different days and the coefficients of variation calculated.

Serum	p18	bp26	CTY	Whole cell
DeVeere	9.5%	7.2%	8.6%	8.6%
NSS	8.4%	6.6%	7.7%	9.2%
Negative	4.6%	5.0%	7.2%	8.2%

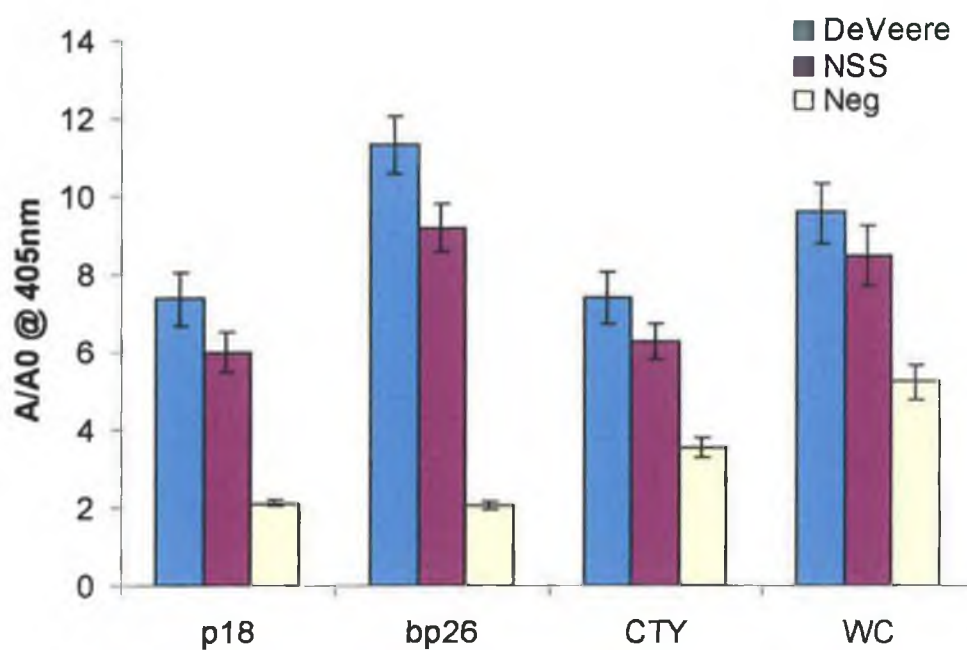


**Figure 6.10:** Inter-day assay graph obtained for the p18, bp26, CTY and whole cell (WC) indirect ELISAs. The optimised assay formats were capable of discriminating between the Brucella-positive and negative standard serum samples. The bar graph represents the average normalised ( $A/A_0$ ) results obtained over ten individual days. The error bars represent the standard deviation calculated between the ten-day replicates.

*Table 6.2: Inter-day assay coefficients of variation obtained for pAB1 and pAB2 sandwich ELISAs. Three sets of each standard were assayed on ten different days and the coefficients of variation calculated.*

Serum	pAB1	pAB2
DeVeere	8.1%	7.1%
NSS	8.9%	7.6%
Negative	7.5%	6.7%

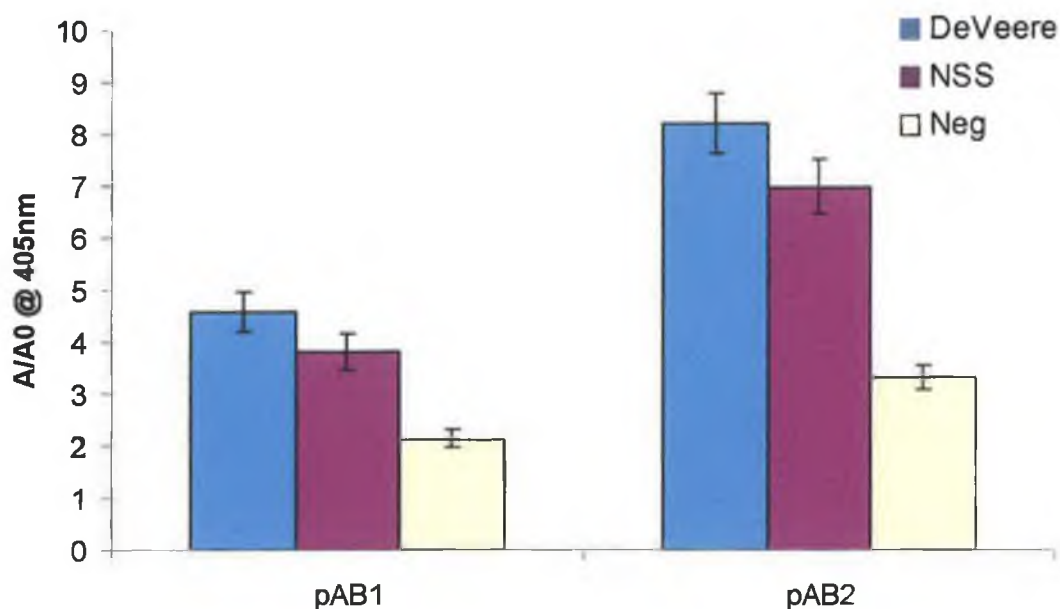


*Figure 6.11: Inter-day assay graph obtained for the pAB1 and pAB2 sandwich ELISAs. The optimised assay formats were capable of discriminating between the Brucella-positive and negative standard serum samples. The bar graph represents the average normalised (A/A<sub>0</sub>) results obtained over ten individual days. The error bars represent the standard deviation calculated between the ten-day replicates.*

## 6.2.3 Characterisation of assay performance

### 6.2.3.1 Performance characterisation on the indirect and sandwich ELISAs

Following optimisation of the various parameters required to successfully carry out the indirect and sandwich the performance of each assay was determined using a set of reference *Brucella*-positive and negative serum samples. The indirect and sandwich ELISAs were carried out on the standard positive sera, the DeVeere Hunt Serum and the National Standard Serum, on the 18 reference positive sera, on the standard negative serum, and on the 50 reference negative sera. The indirect and sandwich ELISAs were carried out incorporating the optimised parameters as described in sections 2.6.1 and 2.6.2, respectively.

Figure 6.12 shows the ELISA results obtained for the p18 indirect ELISA. A cut-off point of point of 30% was chosen to enable optimal discrimination between the *Brucella*-positive and *Brucella*-negative reference samples, suggesting that serum samples with a value above 30% were positive for a *Brucella* infection and serum samples with a value below 30% were regarded as negative. 13 out of the 20 positive serum samples tested, displayed greater than or equalled to 30% of the absorbance value obtained for the DeVeere Hunt Serum. Whereas, 7 had values lower than 30% suggesting 7 false negatives. 36 out of the 51 negative serum samples displayed values lower than 30% of the DeVeere Hunt Serum. Whereas, 15 of the negative reference samples had values above 30%, indicating 15 false positive results. The diagnostic sensitivity (DSn) and diagnostic specificity (DSp) were then calculated using a 2 x 2 table that associated infection status with test results from the 20 infected and 51 uninfected reference animals (Table 6.3). The p18 indirect ELISA yielded a diagnostic sensitivity of 62% and a diagnostic specificity of 70%.

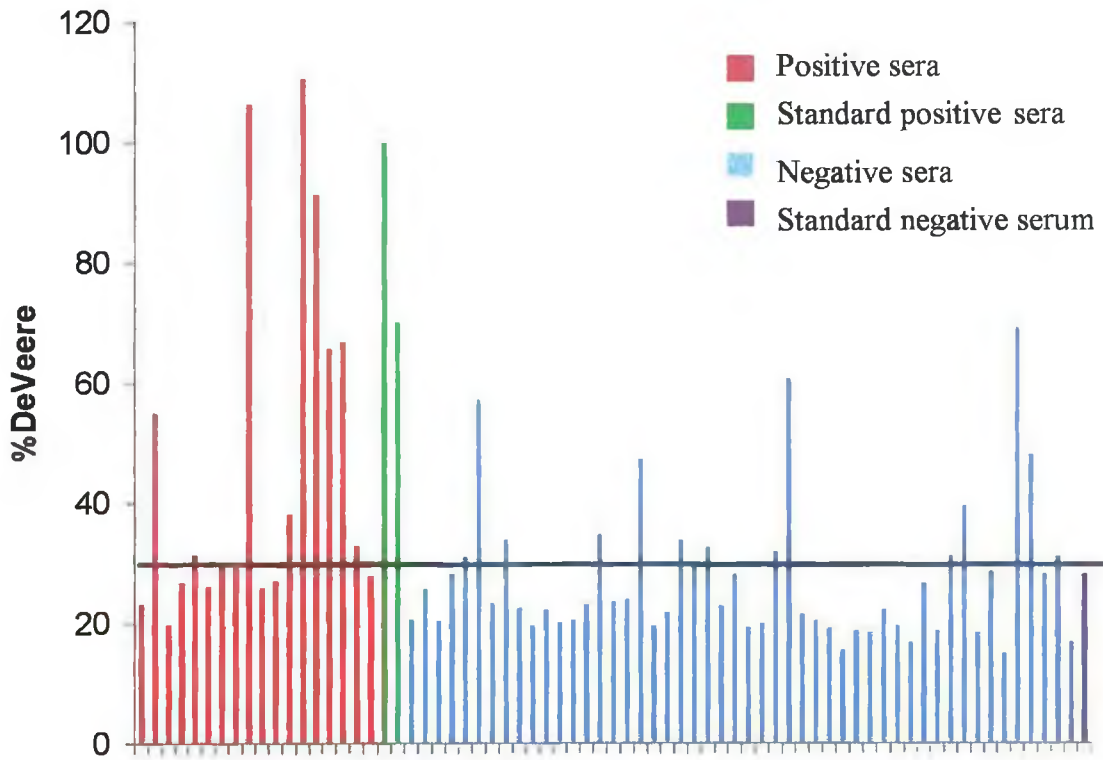


*Figure 6.12: Characterisation of the p18 ELISA performance. The p18 indirect ELISA was assessed for use as a diagnostic assay for bovine brucellosis in serum samples. The indirect ELISA was performed using a panel of 20 positive serum samples from animal infected with *Brucella* and 50 negative reference samples that were uninfected. The absorbance value for each sample was recorded at 405nm and the mean plotted as a percentage of the mean absorbance obtained for the DeVeere Hunt Serum. A stringent cut-off point of 30% was chosen to allow discrimination between the *Brucella*-positive and negative serum samples.*

**Table 6.3:** Calculations of diagnostic sensitivity (DSn) and diagnostic specificity (DSp) for the p18 indirect ELISA. A 2 x 2 table that associated infection status with test results from the 20 infected and 51 uninfected reference animals was used to calculate the DSn and DSp. The p18 indirect ELISA yielded a diagnostic sensitivity of 62% and a diagnostic specificity of 70%.

		Reference animals of known infected status			
		Infected		Uninfected	
Test result	Positive	13	A	B	15
	Negative	7	C	D	36
		<b>Diagnostic sensitivity</b> $\frac{A}{A + C} = \frac{13}{20} = 62\%$		<b>Diagnostic specificity</b> $\frac{D}{D + B} = \frac{36}{51} = 70\%$	

Figure 6.13 shows the ELISA results obtained for the bp26 indirect ELISA. A cut-off point of point of 35% was chosen to enable optimal discrimination between the *Brucella*-positive and *Brucella*-negative reference samples. 8 out of the 20 positive serum samples tested, displayed greater than or equalled to 35% of the absorbance value obtained for the DeVeere Hunt Serum. Whereas, 12 had values lower than 35% suggesting 13 false negatives. 45 out of the 51 negative serum samples displayed values lower than 35% of the DeVeere Hunt Serum. Whereas, 6 of the negative reference samples had values above 35%, indicating 6 false positive results. The diagnostic sensitivity (DSn) and diagnostic specificity (DSp) were then calculated using a 2 x 2 table that associated infection status with test results from the 20 infected and 51 uninfected reference animals aided the calculations (Table 6.4). The bp26 indirect ELISA yielded a diagnostic sensitivity of 38% and a diagnostic specificity of 88%.

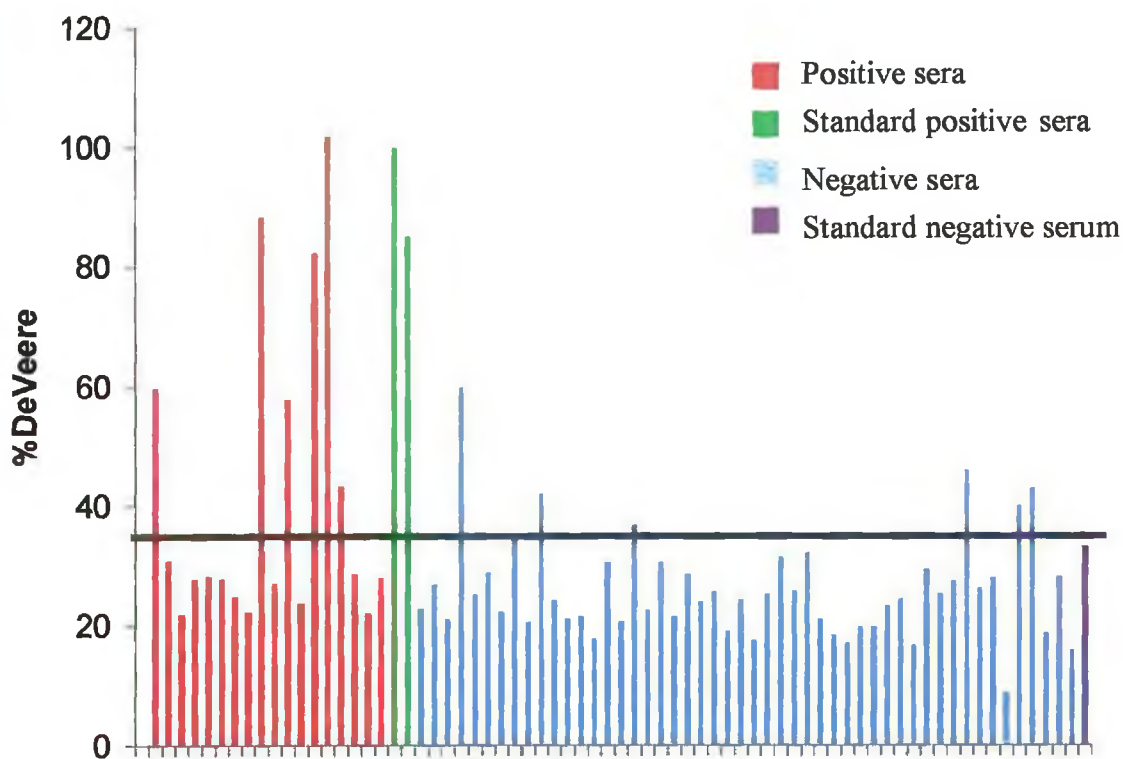


*Figure 6.13: Characterisation of the bp26 ELISA performance. The bp26 indirect ELISA was assessed for use as a diagnostic assay for bovine brucellosis in serum samples. The indirect ELISA was performed using a panel of 20 positive serum samples from animals infected with *Brucella* and 50 negative reference samples that were uninfected. The absorbance value for each sample was recorded at 405nm and the mean plotted as a percentage of the mean absorbance obtained for the DeVeere Hunt Serum. A stringent cut-off point of 35% was chosen to allow discrimination between the *Brucella*-positive and negative serum samples.*

**Table 6.4:** Calculations of diagnostic sensitivity (DSn) and diagnostic specificity (DSp) for the bp26 indirect ELISA. A 2 x 2 table that associated infection status with test results from the 20 infected and 51 uninfected reference animals was used to calculate the DSn and DSp. The bp26 indirect ELISA yielded a diagnostic sensitivity of 38% and a diagnostic specificity of 88%.

		Reference animals of known infected status	
		Infected	Uninfected
Test result	Positive	8	6
	Negative	12	45
		A	B
		C	D
		<i>Diagnostic sensitivity</i>	<i>Diagnostic specificity</i>
		$\frac{A}{A + C} = \frac{8}{20} = 38\%$	$\frac{D}{D + B} = \frac{45}{51} = 88\%$

Figure 6.14 shows the ELISA results obtained for the CTY indirect ELISA. A cut-off point of point of 45% was chosen to enable optimal discrimination between the *Brucella*-positive and *Brucella*-negative reference samples. Each of the 20 positive serum samples tested, displayed greater than or equalled to 45% of the absorbance value obtained for the DeVeere Hunt Serum and 46 out of the 51 negative serum samples displayed values lower than 45% of the DeVeere Hunt Serum. Whereas, 5 of the negative reference samples had values above 45%, indicating only 5 false positive results. The diagnostic sensitivity (DSn) and diagnostic specificity (DSp) were then calculated using a 2 x 2 table that associated infection status with test results from the 20 infected and 51 uninfected reference animals aided the calculations (Table 6.5). The CTY indirect ELISA yielded a diagnostic sensitivity of 100% and a diagnostic specificity of 90%.

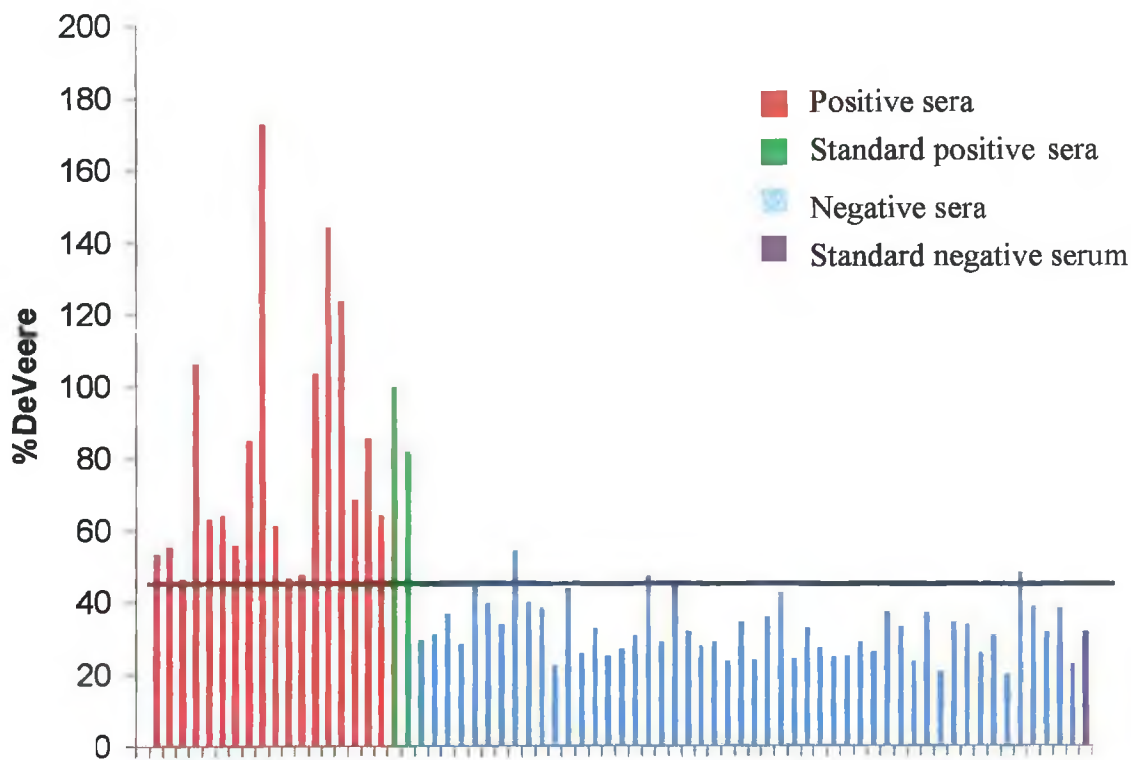


*Figure 6.14: Characterisation of the CTY ELISA performance. The CTY indirect ELISA was assessed for use as a diagnostic assay for bovine brucellosis in serum sample. The indirect ELISA was performed using a panel of 20 positive serum samples from animals infected with *Brucella* and 50 negative reference samples that were uninfected. The absorbance value for each sample was recorded at 405nm and the mean plotted as a percentage of the mean absorbance obtained for the DeVeere Hunt Serum. A stringent cut-off point of 45% was chosen to allow discrimination between the *Brucella*-positive and negative serum samples.*

**Table 6.5:** Calculations of diagnostic sensitivity (DSn) and diagnostic specificity (DSp) for the CTY indirect ELISA. A 2 x 2 table that associated infection status with test results from the 20 infected and 51 uninfected reference animals was used to calculate the DSn and DSp. The CTY indirect ELISA yielded a diagnostic sensitivity of 100% and a diagnostic specificity of 90%.

		Reference animals of known infected status			
		Infected		Uninfected	
Test result	Positive	20	A	B	5
	Negative	0	C	D	46
		<i>Diagnostic sensitivity</i> $\frac{A}{A + C} = \frac{20}{20} = 100\%$		<i>Diagnostic specificity</i> $\frac{D}{D + B} = \frac{46}{51} = 90\%$	

Figure 6.15 shows the ELISA results obtained for the whole cell indirect ELISA. A cut-off point of point of 55% was chosen to enable optimal discrimination between the *Brucella*-positive and *Brucella*-negative reference samples. 20 out of the 20 positive serum samples tested, displayed greater than or equalled to 55% of the absorbance value obtained for the DeVeere Hunt Serum and 48 out of the 51 negative serum samples displayed values lower than 55% of the DeVeere Hunt Serum. Whereas, only 3 values above 55%, indicating 3 false positive results. The diagnostic sensitivity (DSn) and diagnostic specificity (DSp) were then calculated using a 2 x 2 table that associated infection status with test results from the 21 infected and 51 uninfected reference animals aided the calculations (Table 6.6). The whole cell indirect ELISA yielded a diagnostic sensitivity of 100% and a diagnostic specificity of 94%.

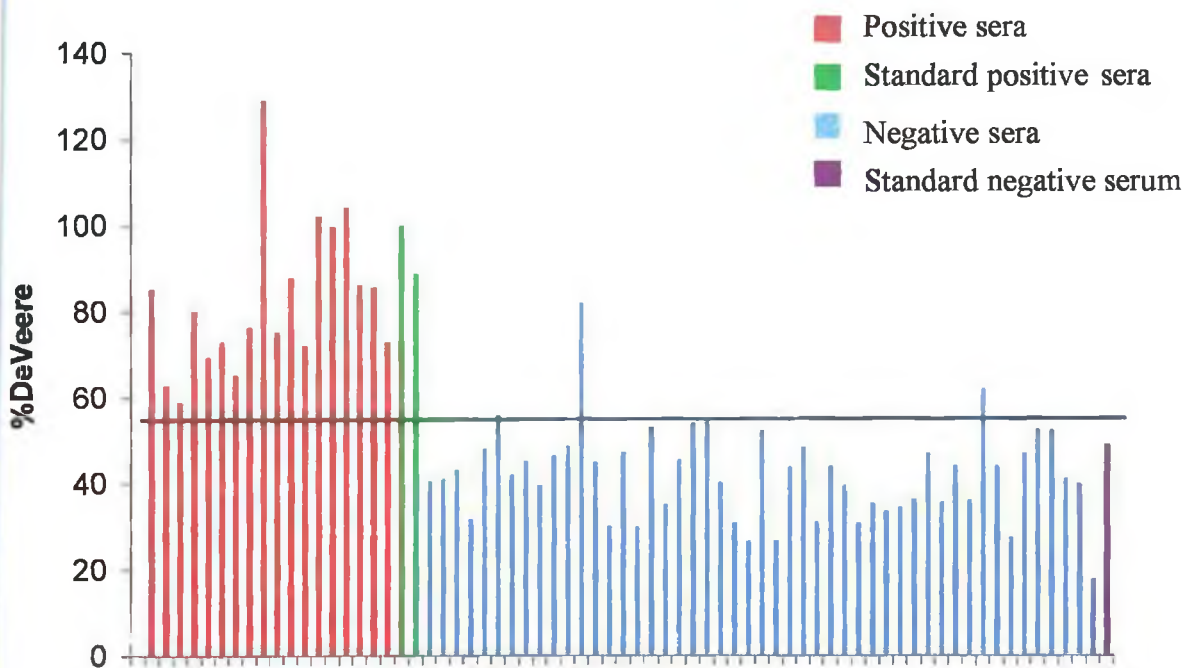


**Figure 6.15:** Characterisation of the whole cell indirect ELISA performance. The whole cell indirect ELISA was assessed for use as a diagnostic assay for bovine brucellosis in serum samples. The indirect ELISA was performed using a panel of 20 positive serum samples from animals infected with *Brucella* and 50 negative reference samples that were uninfected. The absorbance value for each sample was recorded at 405nm and the mean plotted as a percentage of the mean absorbance obtained for the DeVeere Hunt Serum. A stringent cut-off point of 55% was chosen to allow discrimination between the *Brucella*-positive and negative serum samples.

**Table 6.6:** Calculations of diagnostic sensitivity (DSn) and diagnostic specificity (DSp) for the whole cell indirect ELISA. A 2 x 2 table that associated infection status with test results from the 20 infected and 51 uninfected reference animals was used to calculate the DSn and DSp. The whole cell indirect ELISA yielded a diagnostic sensitivity of 100% and a diagnostic specificity of 94%.

		Reference animals of known infected status	
		Infected	Uninfected
Test result	Positive	20	3
	Negative	0	48
		A	B
		C	D
		<b>Diagnostic sensitivity</b>	<b>Diagnostic specificity</b>
		$\frac{A}{A + C} = \frac{20}{20} = 100\%$	$\frac{D}{D + B} = \frac{48}{51} = 94\%$

Figure 6.16 shows the ELISA results obtained for the pAB1 sandwich ELISA. A cut-off point of point of 55% was chosen to enable optimal discrimination between the *Brucella*-positive and *Brucella*-negative reference samples, suggesting that serum samples with a value above 55% were positive for a *Brucella* infection and serum samples with a value below 55% were regarded as negative. 20 out of the 20 positive serum samples tested, displayed greater than or equalled to 55% of the absorbance value obtained for the DeVeere Hunt Serum. 49 out of the 51 negative serum samples displayed values lower than 55% of the DeVeere Hunt Serum. Whereas, 2 of the negative reference samples had values above 55%, indicating 2 false positive results. The diagnostic sensitivity (DSn) and diagnostic specificity (DSp) were then calculated using a 2 x 2 table that associated infection status with test results from the 20 infected and 51 uninfected reference animals (Table 6.7). The pAB1 sandwich ELISA yielded a diagnostic sensitivity of 100% and a diagnostic specificity of 96%.

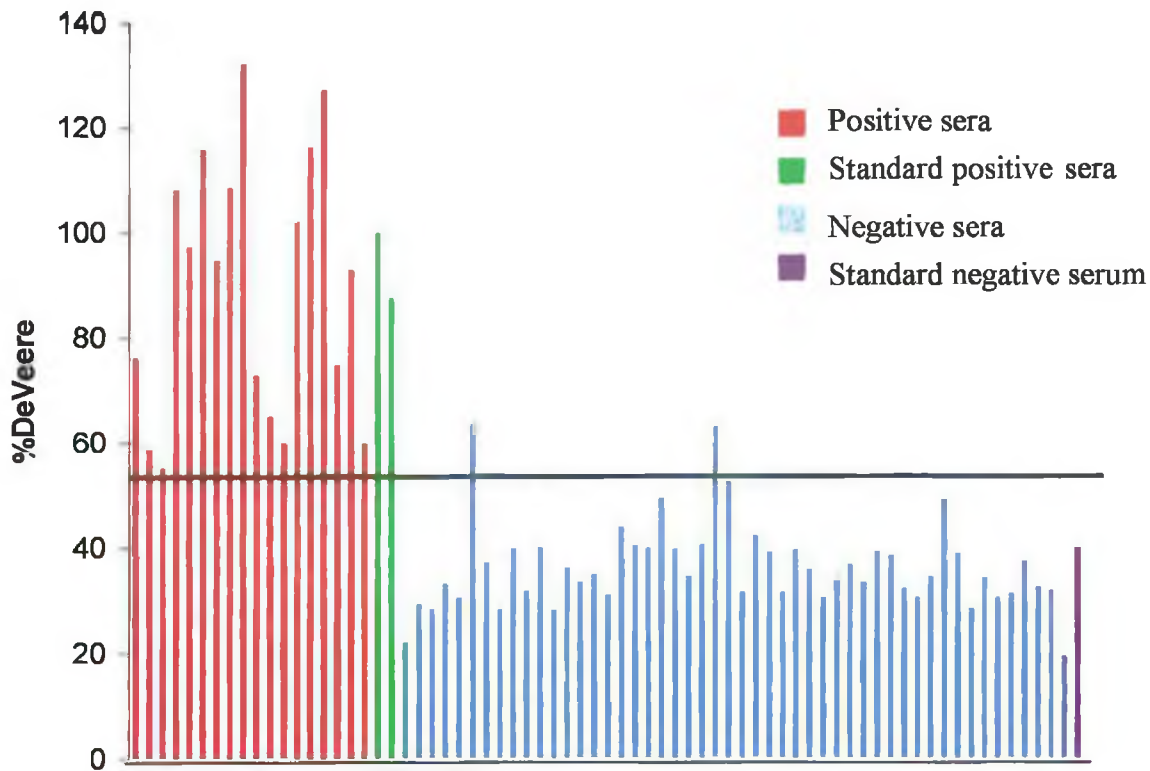


**Figure 6.16:** *Characterisation of the pAB1 sandwich ELISA performance. The pAB1 sandwich ELISA was assessed for use as a diagnostic assay for bovine brucellosis in serum sample. The sandwich ELISA was performed using a panel of 20 positive serum samples from animals infected with Brucella and 50 negative reference samples that were uninfected. The absorbance value for each sample was recorded at 405nm and the mean plotted as a percentage of the mean absorbance obtained for the DeVeere Hunt Serum. A stringent cut-off point of 55% was chosen to allow discrimination between the Brucella-positive and negative serum samples.*

**Table 6.7:** Calculations of diagnostic sensitivity (DSn) and diagnostic specificity (DSp) for the pAB1 sandwich ELISA. A 2 x 2 table that associated infection status with test results from the 20 infected and 51 uninfected reference animals was used to calculate the DSn and DSp. The pAB1 sandwich ELISA yielded a diagnostic sensitivity of 100% and a diagnostic specificity of 96%.

		Reference animals of known infected status					
		Infected	Uninfected				
Test result	Positive	20	2				
	Negative	0	49				
		<table border="1" style="margin: auto;"> <tr> <td style="padding: 2px;">A</td> <td style="padding: 2px;">B</td> </tr> <tr> <td style="padding: 2px;">C</td> <td style="padding: 2px;">D</td> </tr> </table>	A	B	C	D	
A	B						
C	D						
		<b>Diagnostic sensitivity</b> $\frac{A}{A + C} = \frac{20}{20} = 100\%$	<b>Diagnostic specificity</b> $\frac{D}{D + B} = \frac{49}{51} = 96\%$				

Figure 6.17 shows the ELISA results obtained for the pAB2 sandwich ELISA. A cut-off point of point of 50% was chosen to enable optimal discrimination between the *Brucella*-positive and *Brucella*-negative reference samples. 20 out of the 20 positive serum samples tested, displayed greater than or equalled to 50% of the absorbance value obtained for the DeVeere Hunt Serum. 49 out of the 51 negative serum samples displayed values lower than 50% of the DeVeere Hunt Serum. Whereas, 2 of the negative reference samples had values above 50%, indicating 2 false positive results. The diagnostic sensitivity (DSn) and diagnostic specificity (DSp) were then calculated using a 2 x 2 table that associated infection status with test results from the 20 infected and 51 uninfected reference animals aided the calculations (Table 6.8). The pAB2 sandwich ELISA yielded a diagnostic sensitivity of 100% and a diagnostic specificity of 96%.

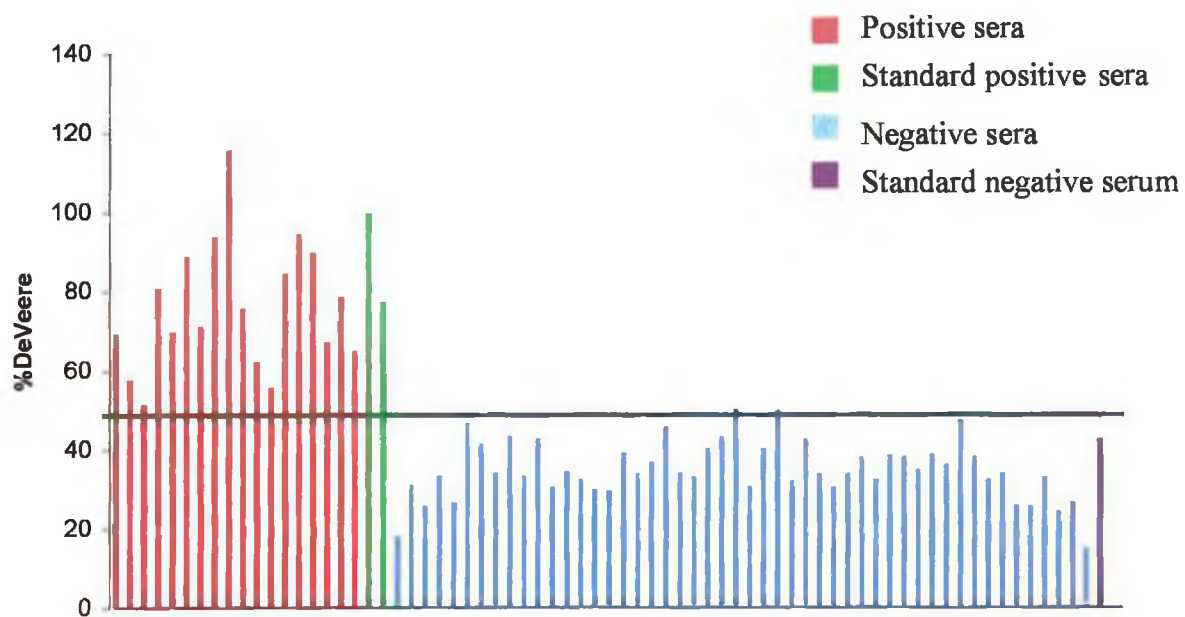


*Figure 6.17: Characterisation of the pAB2 sandwich ELISA performance. The pAB2 sandwich ELISA was assessed for use as a diagnostic assay for bovine brucellosis in serum sample. The sandwich ELISA was performed using a panel of 20 positive serum samples from animals infected with *Brucella* and 50 negative reference samples that were uninfected. The absorbance value for each sample was recorded at 405nm and the mean plotted as a percentage of the mean absorbance obtained for the DeVeere Hunt Serum. A stringent cut-off point of 50% was chosen to allow discrimination between the *Brucella*-positive and negative serum samples.*

**Table 6.8:** Calculations of diagnostic sensitivity (DSn) and diagnostic specificity (DSp) for the pAB2 sandwich ELISA. A 2 x 2 table that associated infection status with test results from the 20 infected and 51 uninfected reference animals was used to calculate the DSn and DSp. The pAB2 sandwich ELISA yielded a diagnostic sensitivity of 100% and a diagnostic specificity of 96%.

		Reference animals of known infected status			
		Infected		Uninfected	
Test result	Positive	20	A	B	2
	Negative	0	C	D	49
		<b>Diagnostic sensitivity</b> $\frac{A}{A + C} = \frac{20}{20} = 100\%$		<b>Diagnostic specificity</b> $\frac{D}{D + B} = \frac{49}{51} = 96\%$	

### 6.3 Discussion

This chapter focused on the development and validation of enzyme-linked immunosorbent assays for the diagnosis of bovine brucellosis. Four indirect and two sandwich ELISAs were investigated for use as a diagnostic assay for brucellosis. The assay should be highly sensitive and specific, reproducible, capable of discriminating between cattle vaccinated with attenuated *B. abortus* S19 and naturally infected cattle, and would also enable the detection of a *Brucella* infection shortly after infection. Ideally there would be no cross-reactivity with other gram-negative bacteria, e.g. *Yersinia enterocolitica* 0:9.

The indirect ELISAs were based on the detection of anti-*Brucella* serum antibodies specific for the recombinant p18 and bp26, the crude cytoplasmic lysate from *B. abortus* 45/20 and whole *B. abortus* 45/20 cells, directly adsorbed on immunoplates. The sandwich ELISAs were based on the detection of anti-*Brucella* serum antibodies specific for the crude cytoplasmic lysate from *B. abortus* 45/20 and whole *B. abortus* 45/20 cells, which were captured on the immunoplate using the polyclonal antibodies pAB1 and pAB2, respectively. The ELISA validation was carried out based on OIE standards, using a method previously described for the validation of serological assays for the diagnosis of infectious diseases (Jacobson, 1998).

The ELISA validation was based on an incremental process, whereby assay parameters were established and characterised through the following methods: (1) determining the feasibility of the method; (2) development of the assay through optimisation and standardisation of reagents and protocols; and (3) determining the performance characteristics of the assay.

The first stage in validating the indirect and sandwich ELISAs was the feasibility studies. Feasibility studies were carried out in order to determine if the selected reagents and protocols had the capacity to distinguish between *Brucella*-infected and uninfected samples. The feasibility studies were conducted on the p18, bp26, CTY and whole cell indirect ELISAs (Fig. 6.1 (A)) and on the pAB1 and pAB2 sandwich ELISAs (Fig. 6.1 (B)) using two positive control sera, the DeVere Hunt Serum and the National Standard Serum, and one standard negative serum. The four indirect and two sandwich ELISAs were capable of discriminating between the two standard

positive sera, the DeVeere Hunt serum and the NSS, and the standard negative serum. The raw test results (optical density) obtained were normalised by expressing the absorbance values as a percentage of the DeVeere Hunt Serum (Wright *et al.*, 1993). Normalisation of the raw test results accounts for variability that may be introduced by ambient temperatures, test parameters and the photometric instrument.

Following establishment of the feasibility of the p18, bp26, CTY and whole cell indirect ELISAs and the pBA1 and pAB2 sandwich ELISAs the next step in assay validation involved assay development and standardisation. Assay development and standardisation involved two main process: (1) Selection of optimal reagent concentrations and protocol parameters; and (2) Estimates on repeatability. Optimisation of the various assay parameters, including blocking reagent, optimal concentration /dilutions for antigen coating, serum samples and secondary antibody, was achieved through checkerboard titrations.

The choice of blocking reagent and serum / antibody diluent can greatly influence the sensitivity of an assay. The polyclonal nature of the bovine serum samples increases the possibility of non-specific interactions between serum antibodies and the blocking reagent. Ovalbumin, bovine serum albumin and milk marvel were investigated for use as the blocking reagent and serum / antibody diluent. The use of ovalbumin (Fig. 6.3) and BSA (Fig. 6.4) as the blocking reagent resulted in a high-degree of non-specific interactions with the bovine serum samples. However, the use of milk marvel as both blocking reagent and serum / antibody diluent (Fig. 6.2) resulted in negligible non-specific interactions. In order to keep the non-specific interactions to a minimum 4% milk marvel was selected as the blocking reagent and diluent for the serum samples and secondary antibody, which needed to be pre-incubated at 37°C for 1 hour (Data not shown).

The optimal antigen coating concentration/dilution, for use in the indirect ELISAs, was determined for p18, bp26, CTY and whole cells. The optimum concentration / dilution of the antigen adsorbed to the immunoplate was optimised using checkerboard titrations. The optimum coating concentration/ dilution was selected as the one that produced the best positive: negative ratio (i.e. the concentration / dilution

that enabled the greatest discrimination between the positive and negative serum samples). An optimum p18 coating concentration of 25µg/ml, a bp26 coating concentration of 6.25µg/ml, a CTY coating dilution of 1/4 and a whole cell coating concentration of  $1.6 \times 10^8$  cells/ml (Fig. 6.5) were selected because they enabled the greatest discrimination between the positive and negative control sera.

In order to develop a sensitive sandwich ELISA the capture antibody coating dilution and the captured antigen dilution / concentration was optimised. Polyclonal antibody dilutions ranging from 1/250 – 1/2000 were adsorbed onto immunoplates and assayed to determine the optimal antibody coating dilution. Results for the pAB1 and pAB2 (Fig. 6.6) sandwich ELISAs showed that a 1/500 dilution of the polyclonal antibodies enabled optimal discrimination between the standard positive and negative sera. The optimum antigen concentration / dilution was determined for use in the pAB1 and pAB2 sandwich ELISAs. A 1/16 dilution of the CTY and a *B. abortus* cell concentration of  $1.6 \times 10^8$  cells/ml (Fig. 6.7) enabled optimal discrimination between the standard positive and negative sera.

The next step involved in the incremental process for assay development and standardisation focused on the optimisation of the bovine serum sample dilution. The optimal serum dilution was independently determined for each of the four indirect ELISAs and the two sandwich ELISAs using the standard positive sera, DeVeere Hunt Serum and NSS, and standard negative serum. Bovine serum dilutions ranging from 1/25 – 1/2500 were assayed for the p18, bp26, CTY and whole cell indirect ELISAs and for the pAB1 and pAB2 (Fig. 6.8) sandwich ELISAs. In each case the serum samples diluted to 1/50 enabled the optimal discrimination between the standard positive sera, DeVeere Hunt Serum and NSS, and standard negative serum.

During assay development and standardisation it was also necessary to determine the optimal secondary anti-bovine antibody dilution for use in the indirect and sandwich ELISAs. A horseradish peroxidase-labelled anti-bovine secondary antibody was selected for use in the development of the indirect and sandwich ELISAs. The optimal working dilution was independently determined for each of the indirect and sandwich ELISAs using the standard positive sera, DeVeere Hunt Serum and NSS, and standard

negative serum. Anti-bovine secondary antibody dilutions ranging from 1/1000 – 1/16000 were assayed for the p18, bp26, CTY and whole cell indirect ELISAs and for the pAB1 and pAB2 (Fig. 6.9) sandwich ELISAs. In each case a 1/2000 dilution of the anti-bovine secondary antibody enabled the optimal discrimination between the standard positive sera, DeVere Hunt Serum and NSS, and standard negative serum.

Estimates on assay repeatability were also determined as one of the main processes involved in the assay development and standardisation. The repeatability studies involved carrying out intra- and inter-day variability studies on the indirect and sandwich ELISAs using the three standard serum samples. Three replicates of each standard were assayed over ten individual days to provide estimates on the repeatability. Coefficients of variation were determined by expressing the standard deviation of the replicates over the mean of the replicates. The intra-day coefficients of variation for the indirect ELISAs were calculated between the three replicates of each standard and all remained below 8.21%. The intra-day coefficients of variation calculated for the sandwich ELISAs remained below 9.82%. The inter-day variability studies on the p18, bp28, CTY and whole cell indirect ELISAs (Fig. 6.10) resulted in co-efficients of variation between 4.57 and 9.46% (Table 6.1). The inter-day co-efficients of variation for the pAB1 and pAB2 sandwich ELISAs (Fig 6.11) ranged between 6.70 and 8.90% (Table 6.2). Jacobson (1998) recommended that coefficients of variation for normalised data from the replicates of the standard serum should not exceed 10%. These results suggest that the indirect and sandwich ELISAs are reproducible over a period of ten days.

The final stage of the assay validation involved characterising the assays in accordance to performance in categorising predetermined serum samples as positive and negative. Estimates of diagnostic sensitivity (DSn) and diagnostic specificity (DSp) are used to determine assay performance. The DSn and DSp are derived from testing a panel of reference samples with predetermined infectious status and history relative to the disease/infection in question. The DSn is estimated as the proportion of known infected animals that give a positive result to infected animals that yield negative results (false negative (FN)). Whereas, the DSp is the proportion of uninfected animals that give negative results to uninfected animals that display positive results (false positives (FP)). The number of infected and uninfected

reference samples required can be calculated for determinations of DS<sub>n</sub> and DS<sub>p</sub> within statistically defined limits. It is recommended that a minimum of approximately 300 infected and 1000 – 5000 uninfected samples should be tested to provide added confidence in the estimates of DS<sub>n</sub> and DS<sub>p</sub> (Jacobson, 1998). However, in our case it was difficult to find a large number of infected and uninfected reference samples. Therefore, it was necessary to start the validation process with small panels of infected and uninfected sera.

The indirect and sandwich ELISAs were carried out on 20 known *Brucella*-positive and 51 known *Brucella*-negative serum samples using the optimised parameters discussed above. The results obtained were then used to calculate the diagnostic specificity (DS<sub>p</sub>) and diagnostic sensitivity (DS<sub>n</sub>) of each ELISA format. The p18 (Fig. 6.12) and bp26 (Fig. 6.13) indirect ELISAs appeared to be the least sensitive and specific, with the p18 indirect ELISA yielding a diagnostic sensitivity of 62% and a diagnostic specificity of 70% (Table 6.3) and the bp26 indirect ELISA yielding a diagnostic sensitivity of 38% and a diagnostic specificity of 88% (Table 6.4). The indirect ELISAs incorporating the *Brucella* cellular antigens appeared to offer improved diagnostic sensitivity and specificity over the recombinant proteins. The CTY indirect ELISA (Fig. 6.14) resulted in a diagnostic sensitivity of 100% and a diagnostic specificity of 90% (Table 6.5). The whole cell indirect ELISA (Fig. 6.15) yielded a diagnostic sensitivity of 100% and a diagnostic specificity of 94% (Table 6.6). The pAB1 and pAB2 sandwich ELISAs offered increased diagnostic sensitivity and specificity over the four indirect ELISAs. The pAB1 (Fig. 6.16) and pAB2 (Fig. 6.17) sandwich ELISAs both yielded diagnostic sensitivity of 100% and a diagnostic specificity of 96% (Tables 6.7 and 6.8, respectively).

These results would suggest that the crude cytoplasmic lysate from *B. abortus* 45/20 cells and the whole *B. abortus* 45/20 cells offer improved discriminatory capabilities over the recombinant p18 and bp26 *Brucella*-specific proteins. Based on an indirect ELISA format the whole *B. abortus* cells proved to be the most sensitive and specific antigen, out of the four antigens investigated, for the diagnosis of bovine brucellosis. The crude cytoplasmic lysate displayed a similar diagnostic sensitivity to the whole cells with a slightly reduced diagnostic specificity. Whereas, the pAB1 and pAB2

sandwich ELISAs offer improved discriminatory capabilities over the indirect ELISA when used for the diagnosis of bovine brucellosis in serum samples.

Published research has focused on the validation of a variety of ELISA formats for the diagnosis of bovine brucellosis in serum samples. An indirect ELISA based on the detection of serum antibodies directed against a hot water/hot phenol-extracted *B. abortus* smooth lipopolysaccharide was described by Vanzini and associates (1998). This indirect ELISA was validated using 562 infected and 2646 uninfected serum samples and yielded a relative sensitivity of 99.6% and specificity of 98.6%. A competitive ELISA utilising immobilised lipopolysaccharide and a monoclonal antibody specific for the O-polysaccharide epitope has also been described for the diagnosis of brucellosis (Nielsen *et al.*, 1995). The specificity and sensitivity of this ELISA were 99.7 and 100%, respectively, using 1464 uninfected and 261 infected serum samples. Evidently, these ELISAs appear to offer improved sensitivity and specificity over the indirect and sandwich ELISAs developed in this chapter. However, this may be due to the fact that a limited number of infected and uninfected reference samples were available during the ELISA development and validation.

The most commonly used immunoassays for the detection of bovine brucellosis target the O-side chain of membrane-anchored lipopolysaccharides on the surface of smooth *Brucella* strains. However, such assays frequently yield false positive serological reactions due to cross reactivity with polysaccharide antigens of other micro-organisms such as *Yersinia enterocolitica* 0.9 (Garin-Bastuji *et al.*, 1999). Problems have also been encountered with these assays when trying to discriminate between actively infected and vaccinated cattle (Goldbaum *et al.*, 1993). However, the CTY and whole cell indirect ELISAs and the pAB1 and pAB2 sandwich ELISAs described in this chapter incorporate whole *B. abortus* 45/20 whole cells or corresponding cellular extract. The *B. abortus* 45/20 are a non-virulent rough strain of *Brucella*. Therefore, they lack the O-side chain on membrane-anchored lipopolysaccharides. This would suggest that the CTY and whole indirect ELISAs and the pAB1 and pAB2 sandwich ELISAs would be less likely to exhibit false positive results, due to cross-reactivity with serum antibodies directed against *Yersinia* and other structurally related bacterial cells containing a similar O-side chain.

The 18kDa cytoplasmic protein, p18 (Goldbaum *et al.*, 1993 and Hemmen *et al.*, 1995) and the 26kDa periplasmic protein, bp26 (Debbarh *et al.*, 1996 and Rossetti *et al.*, 1996) were described as useful markers of an active *Brucella* infection. Research has focused on the incorporation of these proteins in immunoassays for the detection of human (Goldbaum *et al.*, 1992), ovine (Debbarh *et al.*, 1996 and Cloeckart *et al.*, 2001), canine (Baldi *et al.*, 1997) and caprine (Kittelberger *et al.*, 1995, 1998 and Zygmunt *et al.*, 2002) brucellosis. However, little research focused on their use in the development of diagnostic assays for bovine brucellosis. The research conducted in this chapter would therefore conclude that although the p18 and bp26 *Brucella*-specific proteins have proven useful as serological diagnostic markers for brucellosis they are unsuitable for the detection of a *B. abortus* infection.

## **CHAPTER 7**

**Overall conclusions and future work**

## 7.1 Overall conclusions and future work

The research discussed in this thesis focused on the development and characterisation of immunoassays for the detection of aflatoxin B<sub>1</sub> (AFB<sub>1</sub>) and for the diagnosis of bovine brucellosis.

Chapter 3 focused on the production and characterisation of three genetically derived aflatoxin B<sub>1</sub> (AFB<sub>1</sub>)-specific scFv antibody fragments. The gene encoding the AFB<sub>1</sub>-specific scFv was isolated from a pre-immunised phage display library and subsequently expressed as a monomeric, dimeric and alkaline phosphatase-labelled scFv. The three scFvs were applied to the development of competitive ELISAs for the detection of AFB<sub>1</sub>. The optimised competitive ELISAs were relatively sensitive with the dimeric and AP-labelled scFvs offering improved sensitivity over the monomeric scFv. The monomeric and dimeric scFvs displayed minimal cross reactivity towards structurally related aflatoxins. However, the AP-labelled scFv showed a relatively high-level of cross-reactivity towards aflatoxin B<sub>2</sub> and G<sub>1</sub>. The monomeric and dimeric scFvs were then applied to the development of Biacore inhibition immunoassays for the detection of AFB<sub>1</sub>. The inhibition assays were conducted using a CM-5 chip directly immobilised with an AFB<sub>1</sub> derivative and they offered improved sensitivity (0.39 and 0.19ng/ml for the monomeric and dimeric scFvs, respectively) over the competitive ELISAs (12 and 3ng/ml for the monomeric and dimeric, respectively). The monomeric and dimeric scFvs also exhibited minimal cross-reactivity towards the structurally related aflatoxins in the Biacore inhibition assay format. A rapid lateral flow immunoassay was also developed for the detection of AFB<sub>1</sub>, which incorporated an anti-AFB<sub>1</sub> rat monoclonal antibody (obtained from collaborators at IFR Norwich, UK). The monoclonal antibody was found to be relatively sensitive (1.5ng/ml) in the LFIA format.

The work described in Chapter 4 focused on the cloning and expression of two recombinant *B. abortus* proteins, p18 and bp26. The 18kDa cytoplasmic protein (p18) and the 26kDa periplasmic protein (bp26) were cloned using a two-step cloning strategy incorporating TA cloning and subsequent QIAexpress cloning. The recombinant proteins were successfully expressed from the high-level expression vector pQE-60 in XL-10 Gold *E. coli* cells. Several parameters affecting levels of recombinant protein expression were optimised and then applied to the large-scale

expression of the p18 and bp26 recombinant proteins. The His-tagged recombinant proteins were purified using immobilised metal affinity chromatography (IMAC) and the ability of the proteins to discriminate between *Brucella*-positive and negative serum samples was then confirmed using Western blotting and indirect ELISAs.

In Chapter 5 the production and characterisation of *Brucella*-specific antibodies for use in the development of immunoassays for the detection of *Brucella abortus* was examined in detail. Polyclonal antibodies were raised against the crude cytoplasmic lysate from *B. abortus* 45/20 and whole *B. abortus* 45/20 cells. Saturated ammonium sulphate precipitation and protein G affinity chromatography were used to isolate the polyclonal antibodies from the crude anti-serum. The purified polyclonal antibodies were applied to the development of competitive ELISAs for the detection of *B. abortus*. The polyclonal antibodies proved to be relatively sensitive and specific for the detection of *B. abortus* and the optimised ELISAs were highly reproducible. Research also focused on the isolation of *Brucella*-specific scFv antibody fragments from a naïve scFv phage display library. The BMV library (obtained from CAT, UK) was panned against the recombinant *Brucella*-specific proteins, p18 and bp26 (Chapter 4). Following six rounds of panning a bp26-specific scFvs were isolated from the BMV library. The scFvs proved to be relatively sensitive and specific for bp26 in a competitive ELISA format. Following six rounds of panning against p18, positive phage clones, expressing p18-specific scFvs, were isolated. However, several attempts to express the scFvs in a soluble form were unsuccessful. Attempts made to express the soluble, p18-specific, scFvs may have been unsuccessful due to poor solubility or *in vivo* degradation of the c-myc tag used for the detection of the soluble scFvs.

Chapter 6 focused on the development and validation of indirect and sandwich ELISAs, incorporating the recombinant p18 and bp26 proteins and the *B. abortus*-specific polyclonal antibodies, for the diagnosis of bovine brucellosis in serum samples. Four indirect ELISAs and two sandwich ELISAs were investigated as alternative sensitive and specific immunoassays for the diagnosis of bovine brucellosis. The indirect ELISAs were based on the detection of serum antibodies directed against the recombinant proteins p18 and bp26, the crude cytoplasmic lysate from *B. abortus* 45/20 and whole *B. abortus* 45/20 cells, which were directly adsorbed

onto immunoplates. Whereas, the sandwich ELISAs were based on the detection of serum antibodies towards the crude cytoplasmic lysate from *B. abortus* 45/20 and whole *B. abortus* 45/20 cells, which were captured on immunoplates using pAB1 and pAB2, respectively. The indirect and sandwich ELISAs were developed and validated based on Organisation Internationale des Epizootics (OIE) (World Organisation for Animal Health) standards, using a method described for the validation of serological assays for the diagnosis of infectious diseases (Jacobson, 1998). The diagnostic sensitivity and specificity of each ELISA was investigated using a panel of bovine sera with known infection status. The indirect ELISAs, incorporating the p18 and bp26 recombinant proteins, displayed poor discriminatory capabilities when distinguishing between the *Brucella*-positive and negative samples, whereas, the indirect and sandwich ELISAs incorporating the CTY and whole cells adequately discriminated between the *Brucella*-positive and negative serum samples.

In summary, this work highlights the potential use of immunoassays for the detection of food contaminants and the diagnosis of infectious diseases. It shows that a variety of genetically-derived antibody fragments can be engineered using appropriate expression vectors. The research also demonstrates the ease with which scFv fragments, and their derivatives, from a pre-immunised phage display library can be applied to a variety of sensitive and specific assay formats for the detection of AFB<sub>1</sub>. The use of a two-step cloning strategy also proved useful for the cloning, expression and purification of recombinant proteins. The relative ease with which large non-immunised phage display libraries could be used for the isolation of specific scFvs was also established. The use of an incremental process for the validation of immunoassays also proved successful in the development of highly sensitive and specific ELISAs for the detection of bovine brucellosis.

Future work could entail the application of the AFB<sub>1</sub> immunoassays to the specific detection of AFB<sub>1</sub> in grain samples, which could then be used for routine and reliable sample analysis. It may also be possible to increase expression levels of the AFB<sub>1</sub>-specific scFvs and subsequently apply them to a LFIA format. Research could also focus on the further validation of the indirect and sandwich ELISAs for the diagnosis of bovine brucellosis. This would involve monitoring the validity of the ELISAs using a pool of approximately 300 infected and 1000 – 5000 uninfected reference samples.

# CHAPTER 8

## References

- Abouzied, M.** (1999). High sensitive ELISA test for aflatoxins. *Agri-Food Antibodies*, Norwich, UK, Sep 14 – 17.
- Akamatsu, Y., Cole, M., Tso, J. and Tsurushita, N.** (1993). Construction of a human Ig combinatorial library from genomic V segments and synthetic CDR3 fragments. *J. Immunol.*, **151**, 4651 – 4659.
- Alcocer, M., Dillon, P., Manning, B., Doyen, C., Lee, H., Daly, S., O’Kennedy, R., Morgan, M.R.A.** (2000). Use of phosphonic acid as a generic hapten in the production of broad specificity anti-organophosphate pesticide antibody. *J. Agric. Food Chem.*, **48**, 2228 – 2233.
- Aldao, M., Carpinella, N., Corelli, M., Herrero, G.** (1995). Competitive ELISA for quantifying small amounts of aflatoxin B<sub>1</sub>. *Food Agric. Immunol.* **7**, 307 – 314.
- Al-Shamahy, H. and Wright, S.** (1998). Enzyme-linked immunosorbent assay for *Brucella* antigen detection in human sera. *J. Med. Microbiol.*, **47**(2), 169 – 172.
- Al-Shamahy, H. and Wright, S.** (1998). Enzyme-linked immunosorbent assay for *Brucella* antigen detection in human sera. *J. Med. Microbiol.*, **47**(2), 169 – 172.
- Alton, G., Jones, L., Angus, R. and Verger, J.** (1988). *Techniques for the brucellosis laboratory*. Institut National de la Recherche Agronomique, Paris, France.
- Alvi, A., Hu, W., Fulton, R., Coles, J., Long, M. and Nagata, L.** (2003). Functional enhancement of a partially active single-chain variable fragment antibody to Venezuelan equine encephalitis virus, *Viral Immunol.*, **16**(2), 213 – 222.
- Arakawa, F., Shibaguchi, H., Xu, Z. and Kuroki, M.** (2002). Targeting of T cells to CEA-expressing tumor cells by chimeric immune receptors with a highly specific single-chain anti-CEA activity. *Anticancer Res.*, **22**, 4285 - 4289.
- Arbabi Ghahroudi, M., Desmyter, A., Wyns, L., Hamers, R. and Muyldermans, S.** Selection and identification of single domain antibody fragments from camel heavy-chain antibodies. *FEBS Letters*, **414**(3), 521 – 526.
- Arnold, F.** (1991). Metal-affinity separations: a new dimension in protein processing. *Bio/Technology*, **9**, 151 – 156.

**Azzazy, H. and Highsmith, W. (2002).** Phage display technology: clinical applications and recent innovations. *Clinical Biochemistry*, **35**, 425 – 445.

**Baldari, C. and Cesareni, G. (1985).** Plasmids pEMBL Y: new single-stranded shuttle vectors for the recovery and analysis of yeast DNA sequences. *Gene*, **35**, 27 – 32.

**Baldi, P.C., Glambartolomei, G.H., Goldbaum, F.A., Abdon, L.F., Velikovskiy, C.A., Kittelberger, R. and Fossati, C.A. (1996).** Humoral immune response against lipopolysaccharide and cytoplasmic proteins of *Brucella abortus* in cattle vaccinated with *B. abortus* S19 or experimentally infected with *Yersinia enterocolitica* serotype 0:9. *Clin. Diagn. Lab. Immunol.* **3**, 472-476.

**Baldi, P.C., Wanke, M.M., Loza, M.E., Monachesi, N. and Fossati, C.A. (1997).** Diagnosis of canine brucellosis by detection of serum antibodies against an 18kDa cytoplasmic protein of *Brucella* spp. *Vet. Microbiol.* **51**, 273-281.

**Balint, R. and Larrick, J. (1993).** Antibody engineering by parsimonious mutagenesis. *Gene*, **137**, 109 – 118.

**Barbas, C., Kang, A., Lerner, R. and Benkovic, S. (1991).** Assembly of combinatorial antibody libraries on phage surfaces: the genIII site. *Proc. Natl. Acad. Sci. USA*, **88**, 7978 - 7981.

**Benjamini, E., Coico, R. and Sunshine, G. (2000).** Immunology: a short course, 4<sup>th</sup> edn. Wiley and Sons, New York, USA.

**Blasco, J., Garin-Bastuji, B., Marin, C., Gerbier, G., Fanlo, J., Jimenez de Bagues, M. and Cau, C. (1994).** Efficacy of different Rose Bengal and complement fixation antigens for the diagnosis of *Brucella melitensis* infection in sheep and goats. *Vet. Rec.*, **134**(16), 415 - 20.

**Blazek, D., Celer, V., Navratilova, I. and Skladal, P. (2003).** Generation and characterisation of single-chain antibody fragments specific against transmembrane envelope glycoproteins gp46 of the visna virus. *J. Virol. Methods*, **115**, 83 – 92.

**Boel, E., Verlaan, S., Poppelier, M., Westerdaal, N., Van Strijp, J. and Logtenberg, T. (2000).** Functional human monoclonal antibodies of all isotypes constructed from

phage display-derived single-chain Fv antibody fragments. *J. Immunol. Methods*, **26**(239), 153 – 166.

**Borrebaeck, C.** (1983). *In vitro* immunisation for the production of antigen-specific lymphocyte hybridomas. *Scand. J. Immunol.*, **18** (1), 9 – 12.

**Boschioli, M., Foulongne, V. and O'Callaghan, D** (2001). Brucellosis: a worldwide zoonosis. *Curr. Opin. Microbiol.*, **4**, 58 – 64.

**Boschioli, M., Ouachrani-Bettache, S., Foulongne, V., Michaux-Charachon, S., Bourg, G., Allardet-Servent, A., Cazevieille, C., Liautard, J., Ramuz, M. and O'Callaghan, D.** (2002). The *Brucella suis* virB operon is induced intracellularly in macrophages. *Proc. Natl. Acad. Sci. (USA)*, **99**(3), 1544 – 1549.

**Boussif, O., Lezoualch, F., Zanta, M., Mergny, M., Scherman, D., Demeneix, B. and Behir, J.** (1995). A versatile vector for gene and oligonucleotide transfer into cells in culture and *in vivo*: polyethylenimine. *Proc. Natl. Acad. Sci. (USA)*, **92**, 7297 – 7301.

**Bowden, G. and Georgiou, G.** (1990). Folding and aggregation of  $\beta$ -lactamase in the periplasmic space of *Escherichia coli*. *J. Biol. Chem.*, **28**, 16760 – 16766.

**Breitling, F., Dubel, S., Seehaus, T., Klewinghaus, I and Little, M.** (1991). A surface expression vector for antibody screening. *Gene*, **104**(2), 147 - 153.

**Brennan, J., Dillon, P., O'Kennedy, R.** (2002). Production, purification and characterisation of genetically derived scFv and bifunctional antibody fragments capable of detecting illicit drug residues. *J. Chromatogr. B*, **786**, 327 – 342.

**Brinkmann, U., Reiter, Y., Jung, S., Lee, B. and Pastan, I.** (1993). A Recombinant Immunotoxin Containing a Disulfide-Stabilized Fv Fragment. *Proc Natl Acad Sci. (USA)*, **90**(16), 7538 – 7542.

**Brooks, B., Rodes, H., Klein, M., Gerlach, E., Dubel, S., Little, M., Pfizenmaier, K. and Moosmayer, D.** (1997). TNF receptor antagonistic scFv, which is not secreted in mammalian cells, is expressed as a soluble mono- and bivalent scFv derivative in insect cells. *Immunotechnology*, **3**, 173 – 184.

**Bujard, H., Gentz, R., Lanzer, M., Stuebber, D., Mueller, M., Ibrahim, I., Haeuptle, M. and Dobberstein, B. (1987).** A T5 promoter-based transcription-translation system for the analysis of proteins *in vitro* and *in vivo*. *Methods in Enzymology*, **115**, 416 – 433.

**Cadwell, R. and Joyce, G. (1992).** Randomization of genes by PCR mutagenesis. *PCR Methods Appl.*, **2**, 28 – 33.

**Cadwell, R. and Joyce, G. (1994).** Mutagenesis PCR. *PCR Methods Appl.*, **3**, 136 – 140.

**Cai, X. and Garen, A. (1995).** Anti-melanoma antibodies from melanoma patients immunized with genetically modified autologous tumour cells: selection of specific antibodies from single-chain Fv fusion phage libraries. *Proc. Natl. Acad. Sci. (USA)*, **92**, 6537 – 6541.

**Candlish, A., Stimsin, W., Smith, J. (1985).** A monoclonal antibody to aflatoxin B<sub>1</sub>: detection of the mycotoxins by enzyme immunoassay. *Letters in Applied Microbiology*, **1**, 57 – 61.

**Carlson, M., Barger, C., Benson, R., Fraser, A., Phillips, T., Velky, J., Groopman, J., Strickland, P., Ko, H. (2000).** An automated, handheld biosensor for aflatoxin. *Biosens. Bioelectron.* **14**, 841 – 848.

**Caroff, M., Bundle, D. and Perry, M. (1984).** Structure of the O-chain of the phenol-phase soluble cellular lipopolysaccharide of *Yersinia enterocolitica* serotype O:9. *Eur. J. Biochem.*, **139**(1), 195 – 200.

**Casey, J., Keep, P., Chester, K., Robson, L., Hawkins, R. and Begent, R. (1995).** Purification of bacterially expressed single chain Fv antibodies for clinical applications using metal chelate chromatography. *J. Immunol. Methods*, **179**, 105 – 116.

**Charlton, K., Harris, W. and Porter, A (2001).** The isolation of super-sensitive anti-hapten antibodies from combinatorial antibody libraries derived from sheep. *Biosens. Bioelectron.*, **16**, 639 – 646.

**Cho, B., Kieke, M., Boder, E., Wittrup, K and Kranz, D. (1998).** A yeast surface display system for the discovery of ligands that trigger cell activation. *J. Immunol. Methods*, **220**, 179 – 188.

**Cho, W., Sohn, U. and Kwak, J. (2000).** Production and *in vitro* folding of a single chain antibody specific for human plasma apolipoprotein A-I. *J. Biotech.*, **77**, 169 – 178.

**Choi, G., Lee, D., Min, W., Cho, Y., Kweon, D., Son, D., Park, K. and Seo. (2004).** Cloning, expression and characterisation of single-chain variable fragment antibody against mycotoxin deoxynivalenol in recombinant *Escherichia coli*. *Protein expression and purification*, **35**(1), 84 – 92.

**Chu, G., Hayakawa, H and Berg, P. (1987).** Electroporation for the efficient transfection of mammalian cells with DNA. *Nuc. Acids Res.*, **15**, 1311 – 1326.

**Clackson, T., Hoogenboom, H.R., Griffiths, A.D. and Winter, G. (1991).** Making antibody fragments using phage display libraries. *Nature (London)* **352**, 624-628.

**Clare, J., Romanos, M., Rayment, F., Rowedder, J., Smoth, M., Payne, M., Sreekrishna, K. and Henwood, C. (1991).** Production of mouse epidermal growth factor in yeast: high-level secretion using *Pichia pastoris* strains containing multiple gene copies. *Gene*, **105**, 205 – 212.

**Cloeckaert, A, Grayon, M., Verger, J., Letesson, J. and Godfroid, F. (2001).** Conservation of seven genes involved in the biosynthesis of the lipopolysaccharide O-chain in *Brucella* spp. *Res. Microbiol.*, **151**, 209 – 216.

**Cloeckaert, A., Baucheron, S., Vizcaino, N. and Zygmunt, M. (2001).** Use of recombinant BP26 in serological diagnosis of *Brucella melitensis* infection in sheep. *Clin. Diagn. Lab. Immunol.*, **8**(4), 772 – 775.

**Cloeckaert, A., Baucheron, S., Vizcaino, N. and Zygmunt, M. (2001).** Use of recombinant BP26 protein in serological diagnosis of *Brucella melitensis* infection in sheep. *Clin. Diagn. Lab. Immunol.*, **8**(4), 772 – 775.

**Cloeckaert, A., Debbarh, H., Vizcaino, N., Saman, E., Dubray, G. and Zygmunt, M.** (1996). Cloning, nucleotide sequence, and expression of the *Brucella melitensis* bp26 gene encoding for a protein immunogenic in infected sheep. FEMS Microbiology Letters, **140**, 139 – 144.

**Cloeckaert, A., Kerkhofs, P. and Limet, J.** (1992). Antibody response to *Brucella* outer membrane proteins in bovine brucellosis: immunoblot analysis and competitive enzyme-linked immunosorbent assay using monoclonal antibodies. J. Clin. Microbiol., **30**, 3168 – 3174.

**Cloeckaert, A., Verger, J., Grayon, M and Grepinet, O.** (1995). Restriction site polymorphism of the genes encoding the major 25kDa and 36kDa outer membrane proteins of *Brucella*. Microbiol., **141**, 2111 – 2121.

**Cloeckaert, A., Verger, J., Grayon, M., Paquet, J., Garin-Bastuji, B., Foster, G. and Godfroid.** (2001). Classification of *Brucella* spp. isolated from marine mammals by DNA polymorphism at the omp2 locus. Microbes and Infection, **3**, 729 – 738.

**Creppy, E.** (2002). Update of survey, regulation and toxic effects of mycotoxins in Europe. Toxicology Letters **127**, 19 – 28.

**d'Anjou, M. and Daugulis, A.** (2001). A rational approach to improving productivity in recombinant *Pichia pastoris* fermentation. Biotechnol. Bioeng., **72**, 1- 11.

**Dajer, A., Luna-Martinez, E., Zapata, D., Villegas, S., Glutierrez, E., Pena, G., Gurria, F., Nielsen, K. Gall, D.** (1999). Evaluation of a fluorescence-polarization assay for the diagnosis of bovine brucellosis in Mexico. Prev. Vet. Med. **40**, 67-73.

**Daly, S., Dillon, P., Manning, B., Dunne, L., Killard, A., O'Kennedy, R.** (2002). Production and characterisation of murine single chain Fv antibodies to aflatoxin B<sub>1</sub> derived from a pre-immunised antibody phage display library system. Food Agric. Immunol. **14**, 155 – 274.

**Daly, S., Keating, G., Dillon, P., Manning, B., O'Kennedy, R., Lee, H., Morgan, R.** (2000). Development of surface plasmon resonance-based immunoassay for aflatoxin B<sub>1</sub>. J. Agric. Food Chem., **48**(11), 5097 – 5104.

**Das, C. and Mishra, H. (2000).** Effects of aflatoxin B<sub>1</sub> detoxification on the physiochemical properties and quality of ground nut meal. *Food Chemistry* **70**, 483 – 487.

**Daugherty, P., Chen, G., Iverson, B. and Georgiou, G. (2000).** Quantitative analysis of the effects of the mutation frequency on the affinity maturation of single chain Fv antibodies. *Proc. Natl. Acad. Sci. (USA)*, **97**(5), 2029 – 2034.

**Davies, E., Smith, J., Birkett, C., Manser, J., Anderson-Dear, D. and Young, J. (1995).** Selection of specific phage-display antibodies using libraries derived from chicken immunoglobulin genes. *J. Immunol. Methods*, **186**(1), 125 - 135.

**Davies, G. (1971).** The Rose Bengal test. *Vet. Rec.*, **88**, 447 - 449.

**Davies, H., Lomas, L. and Austen, B. (1999).** Profiling of amyloid beta peptide variants using SELDI protein chip arrays. *Biotechniques*, **27**, 1258 – 1261.

**Davis, G., Bedzyk, W., Voss, E. and Jacobs, T. (1991).** Single chain antibody (SCA) encoding genes: one-step construction and expression in eukaryotic cells. *Bio/Technology*, **9**, 165 – 169.

**De Boer, M., Ossendorp, F., Van Duijin, G., Ten Voorde, G. and Tager, J. (1989).** Optimal conditions for the generation of monoclonal antibodies using primary immunisation of mouse splenocytes *in vitro* under serum-free conditions. *J. Immunol. Meth.*, **121**, 253 – 260.

**De Bruin, R., Spelt, K., Mol, J., Koes, R. and Quattrocchio, F. (1999).** Selection of high-affinity phage antibodies from phage display libraries. *Nature Biotech.* **17**, 397-399.

**De Greeff, A., van Alphen, L. and Smith, H. (2000).** Selection of recombinant antibodies specific for pathogenic *Streptococcus suis* by subtractive phage display. *Infect. Immun.*, **68**(7), 3949 – 3955.

**De Haard, H., van Neer, N., Reurs, A., Hufton, S., Roovers, R., Henderikx, P., de Bruine, A., Arends, J. and Hoogenboom, H. (1999).** A large non-immunized human

Fab fragment phage library that permits rapid isolation and kinetic analysis of high affinity antibodies. *J Biol Chem.*, **274**(26), 18218 - 18230.

**De Kruif, J.**, Terstappen, L., Boel, E. and Logtenberg, T. (1995). Rapid selection of cell sub-population-specific monoclonal antibodies from a synthetic phage antibody library. *Proc. Natl. Acad. Sci. (USA)*, **92**, 3938 – 3942.

**De Saeger, S.** and van Peteghem, C. (1996). Dipstick enzyme immunoassay to detect *Fusarium* T-2 toxin in wheat. *Appl. Environ. Microbiol.*, **62**(6), 1880 – 1884.

**Debbarh, H.**, Cloeckaert, A., Zygmunt, M. and Dubray, G. (1995). Identification of sero-reactive *Brucella melitensis* cytosoluble proteins which discriminate between antibodies elicited by infection and Rev.1 vaccination in sheep. *Vet. Microbiol.*, **44**, 37 – 48.

**Debbarh, H.S-A.**, Zygmunt, M.S., Dubray, G., and Cloeckaert, A. (1996). Competitive enzyme-linked immunosorbent assay using monoclonal antibodies to the *Brucella melitensis* BP26 protein to evaluate antibody responses in infected and *B. melitensis* Rev.1 vaccinated sheep. *Vet. Microbiol.* **53**, 325-337.

**DelVecchio, V.**, Kapatral, V., Redkar, R., Patra, G., Mujer, C., Los, T., Ivanova, N., Anderson, I., Bhattacharyya, A., Lykidis, A., Rexnik, G., Jablonski, L., Larsen, N., Hagius, S., O'Callaghan, D., Letesson, J., Haselkorn, R., Kyripides, N. and Overbeek, R. (2002). The genome sequence of the facultative intracellular pathogen *Brucella melitensis*. *Proc. Natl. Acad. Sci. (USA)*, **99**(1), 443 – 448.

**Demartis, S.**, Tarli, L., Borsi, L., Zardi, L. and Neri, D. (2001). Selective targeting of tumour neovasculature by a radiohalogenated human antibody fragment specific for the ED-B domain of fibronectin. *Eur. J. Nuclear Med.*, **28**(4), 534 - 539.

**Detilleux, P.**, Deyoe, B. and Cheville, N. (1990). Penetration and intracellular growth of *Brucella abortus* in nonphagocytic cells in vitro. *Infect. Immun.*, **58**(7), 2320 – 2328.

**Dillon, P.**, Daly, S., Manning, B., O'Kennedy, R. (2003). Immunoassay for the determination of morphine-3-glucuronide using a surface plasmon resonance-based biosensor. *Biosens. Bioelectron.*, **18**, 217 – 227.

- Dillon, P., Manning, B., Daly, S., Killard, T., O’Kennedy, R. (2003).** Production of recombinant anti-morphine-3-glucuronide single-chain variable fragments (scFv) antibody for the development of a “real-time” biosensor-based immunoassay. *J. Immunol. Methods*, **276**, 151 – 161.
- Dooley, H., Flajnik, M. and Porter, A. (2003).** Selection and characterization of naturally occurring single-domain (IgNAR) antibody fragments from immunized sharks by phage display. *Mol. Immunol.*, **40**(1), 25 - 33.
- Dorai, H., Cartnay, J., Hudziak, R., Tai, M., Laminet, A., Houston, L., Huston, J. and Oppermann, H. (1994).** Mammalian cell expression of single-chain Fv (sFv) antibody proteins and their C-terminal fusions with interleukin-2 and other effector domains. *Bio/Technology*, **12**, 890 – 897.
- Dubray, G. and Bezard, G. (1980).** Isolation of three protective cell-wall antigens of *Brucella abortus* in experimental brucellosis in mice. *Ann. Rech. Vet.*, **11**, 367 – 373.
- Dubray, G. and Charriaut, C. (1983).** Evidence of three major polypeptide species and two major polysaccharide species in *Brucella* outer membrane. *Ann. Rech. Vet.*, **14**, 311 – 318.
- Eldin, P., Pauza, M., Hieda, Y., Lin, G., Murtaugh, M., Pentel, P. and Pennell, C. (1997).** High-level secretion of two antibody single chain Fv fragments by *Pichia pastoris*. *J. Immunol. Methods*, **201**, 67 – 75.
- Farina, R. (1985).** Current serological methods in *Br. melitensis*, p. 139–146. J. M. Verger, and M. Plommet (ed.), In *Brucella melitensis*. Martinus Nijhoff, Dordrecht, The Netherlands.
- Fiedler, U. and Conrad, U. (1995).** High-level production and long-term storage of engineered antibodies in transgenic tobacco seeds. *Bio/Technology*, **13**, 1090 – 1093.
- Foster, G. Jahans, K., Reid, R. and Ross, H. (1996).** Isolation of *Brucella* species from cetaceans, seals and otter. *Vet. Rec.*, **138**, 583 – 586.

**Franek, M., Kolar, V. and Eremin, S. (1995).** Enzyme immunoassays for s-triazine herbicides and their application in environmental and food analysis. *Anal. Chim. Acta.*, **311**, 349 – 356.

**French, D., Laskov, R. and Scharff, M. (1989).** The role of somatic hypermutation in the generation of antibody diversity. *Science*, **244**, 1152 - 1157.

**Freyre, F., Vazquez, J., Ayala, M., Canaan-Haden, L., Bell, H., Rodriguez, I., Gonzalez, A., Cintado, A., Gavilondo, J. (2000).** Very high expression of an anti-carcinoembryonic antigen single-chain Fv antibody fragment in yeast *Pichia pastoris*. *J. Biotech.*, **76**, 157 – 163.

**Gaberc-Porekar, V. and Menart, V. (2001).** Perspectives of immobilized-metal affinity chromatography. *J. Biochem. Biophys. Methods*, **49**, 335 – 360.

**Gall, D. and Nielsen, K. (1994).** Improvements to the competitive ELISA for detection of antibodies to *Brucella abortus* in cattle sera. *J. Immunoassay.*, **15**(3), 277 – 291.

**Gall, D. and Nielsen, K. (1994).** Improvements to the competitive ELISA for detection of antibodies to *Brucella abortus* in cattle sera. *J. Immunoassay.*, **15**(3), 277 – 291.

**Gall, D., Nielsen, K., Forbes, L., Cook, W., Leclair, D., Balsevicius, S., Kelly, L., Smith, P. and Mallory, M. (2001).** Validation of the fluorescence polarization assay and other serological tests for the detection of brucellosis in cervids. *J. Wildlife Dis.*, **37**, 110 – 118.

**Gall, D., Nielsen, K., Forbes, L., Davies, D., Elzer, P., Olsen, S., Balsevicius, S., Kelly, L., Smith, P., Tan, S. and Joly, D. (2000).** Validation of the fluorescence polarization assay and comparison to other serological tests for the detection of serum antibodies to *Brucella abortus* in bison. *J. Wildlife Dis.*, **36**, 469 – 476.

**Garin-Bastuji, B., Hummel, N., Gerbier, G., Cau, C., Pouillot, R., Da Costa, M. and Fontaine, J.J. (1999).** Non specific serological reactions in the diagnosis of bovine brucellosis: experimental oral infection of cattle with repeated doses of *Yersinia enterocolitica* 0:9. *Vet. Microbiol.* **66**, 223-233.

**Garrard, L. and Henner, D. (1993).** Selection of an anti-IGF-1 Fab from a Fab phage library created by mutagenesis of multiple CDR loops. *Gene*, **128**, 103 – 109.

**Garrard, L., Yang, M., O'Connell, M., Kelley, R. and Henner, DJ. (1991).** Fab assembly and enrichment in a monovalent phage display system. *Biotechnology* **9**(12), 1373 - 1377.

**Garrett, S.D., Appleford, D.J.A., Wyatt, G.M., Lee, H.A. and Morgan, M.R.A. (1997).** Production of a recombinant anti-parathion antibody (scFv); Stability in methanolic food extracts and comparison to an anti-parathion monoclonal antibody. *J. Agric. Food Chem.* **45**, 4183-4189.

**Georgiou, G and Valax, P. (1996).** Expression of correctly folded proteins in *Escherichia coli*. *Curr. Opin. Biotechnol.*, **7**, 190 – 197.

**Ghosh, S., Basu, S., Strum, J., Basu, S. and Bell, M. (1995).** Identification of conditions that facilitate the expression of GST fusions as soluble, full-length proteins. *Anal. Biochem.*, **225**, 376 – 378.

**Goding, J. (1996).** Monoclonal antibodies: principals and practice, 3<sup>rd</sup> edn., Chapter 3, p. 85. Academic Press, New York, USA.

**Goldbaum, F., Velikovsky, C., Baldi, P., Mortl, S., Bacher, A. and Fossati, C. (1999).** The 18-kDa cytoplasmic protein of *Brucella* species – an antigen useful for diagnosis – is a lumazine synthase. *J. Med. Microbiol.*, **48**, 833 - 839.

**Goldbaum, F.A., Leoni, J., Wallach, J.C. and Fossati, C.A. (1993).** Characterization of an 18-kilodalton *Brucella* cytoplasmic protein which appears to be a serological marker of active infection of both human and bovine brucellosis. *J. Clin. Microbiol.* **31**, 2141-2145.

**Goldbaum, F.A., Rubbi, C.P., Wallach, J.C., Miguel, S.E., Baldi, P.C. and Fossati, C.A. (1992).** Differentiation between active and inactive human brucellosis by measuring antiprotein humoral immune responses. *J. Clin. Microbiol.* **30**, 604-607.

**Goldbaum, F.A., Velikovsky, C.A., Baldi, P.C., Mortl, S., Bacher, A. and Fossati, C.A. (1999).** The 18-kDa cytoplasmic protein of *Brucella* species – an antigen useful for diagnosis – is a lumazine synthase. *J. Med. Microbiol.* **48**, 833-839.

**Goodrick, J., Xu, M., Finnegan, R., Schilling, B., Hoppe, H. and Wan. (2001).** High-level expression and stabilization of recombinant human chitinase produced in a continuous constitutive *Pichia pastoris* expression system. *Biotechnol. Bioengin.*, **74**, 492 – 497.

**Goodsell, D. (2001).** The molecular perspective: Cytochrome P450. *The Oncologist* **6**, 205 –206.

**Gorrell, M., Milliken, G., Anderson, B. and Pucci, A. (1984).** An enzyme immunoassay for bovine brucellosis using a monoclonal antibody specific for field strains of *Brucella abortus*. *Dev. Biol. Stand.*, **56**, 491 – 494.

**Gourama, H. and Bullerman, L. (1995).** *Aspergillus flavus* and *Aspergillus parasiticus*: Aflatoxigenic fungi of concern in foods and feeds: A review. *Journal of Food Protection* **58**(12), 1395 – 1404.

**Graham, F. and Van der Eb, A. (1973).** A new technique for the assay of infectivity of human adenovirus 5 DNA. *Virology*, **52**, 456 – 467.

**Griffiths, A., Williams, S., Hartley, O., Tomlinson, I., Waterhouse, P., Crosby, W., Kontermann, R., Jones, P., Low, N., Allison, T., Prospero, T., Hoogenboom, H., Nissim, A., Cox, J., Harrison, J., Zaccolo, M., Gherardi, E. and Winter, G. (1994).** Isolation of high affinity human antibodies directly from large synthetic repertoires. *EMBO*, **13**(14), 3245 – 3260.

**Haidaris, C., Malone, J., Sherrill, L., Bliss, J., Gaspari, A., Insel, R. and Sullivan, M. (2001).** Recombinant human antibody single chain variable fragments reactive with *Candida albicans* surface antigens. *J. Immunol. Methods*, **257**, 185 – 202.

**Hanes, J. and Pluckthun, A. (1997).** *In vitro* selection and evolution of functional proteins by using ribosome display. *Proc. Natl. Acad. Sci. (USA)*, **94**, 4937 – 4942.

**Hanes, J., Schaffitzel, C., Knappik, A. and Pluckthun, A. (2000).** Picomolar affinity antibodies from a fully synthetic naïve library selected and evolved by ribosome display. *Nature Biotechnol.*, **18**(12), 1287 – 1292.

**Hannig, G. and Makrides, S. (1998).** Strategies for optimising heterologous protein expression in *Escherichia coli*. *TIBTECH*, **16**, 54 –60.

**Harrison, R. (2000).** Expression of soluble heterologous proteins via fusion with NusA protein. *inNovations*, **11**, 4 – 7.

**Hartley, R., Nesbitt, B., O’Kelly, J.** Toxic metabolites of *Aspergillus flavus*. *Nature (London)*, **1963**, 198, 1056 – 1058.

**Harvey, (1991).** Optimisation of nitrocellulose membrane-based immunoassays. Keene, New Hampshire: Schleicher and Schuell.

**Hawkins, R., Russell, S. and Winter, G. (1992).** Selection of phage antibodies by binding affinity. Mimicking affinity maturation. *J. Mol. Biol.*, **226**, 889 – 896.

**Hayhurst, A., Happe, S., Mabry, R., Koch, Z., Iverson, B. and Georgiou, G. (2003).** Isolation and expression of recombinant antibody fragments to the biological warfare pathogen *Brucella melitensis*. *J. Immunol. Methods*, **276**, 185 – 196.

**He, M. and Taussig, M. (1997).** Antibody-ribosome-mRNA (ARM) complexes as efficient selection particles for *in vitro* display and evolution of antibody combining sites. *Nucleic Acids Res.*, **25**, 5132 - 5134.

**He, M., Menges, M., Groves, M., Corps, E., Liu, H., Bruggemann, M. and Taussig, M. (1999).** Selection of a human anti-progesterone antibody fragment from a transgenic mouse library by ARM ribosome display. *J. Immunol. Methods.*, **231**, 105 - 117.

**Hellwig, S., Emde, F., Raven, P., Henke, M., van der Logt, P and Fischer, R. (2001).** Analysis of single-chain antibody production in *Pichia pastoris* using on-line methanol control in fed-batch and mixed-feed fermentations. *Biotechnol. Bioeng.*, **74**, 344 – 352.

**Hemmen, F., Weynants, V., Scarcez, T., Letesson, J. and Saman, E. (1995).** Cloning and sequence analysis of a newly identified *Brucella abortus* gene and serological evaluation of the 17-kilodalton antigen that it encodes. *Clin. Diagn. Lab. Immunol.*, **2**, 263 - 267.

**Hendy, S., Chen, Z., Barker, H., Cruz, S., Chapman, S., Torrance, L., Cockburn, W. and Whitelam, G. (1999).** Rapid production of single-chain Fv fragments in plants using a potato virus X episomal vector. *J. Immunol. Methods*, **231**, 137 – 146.

**Hennion, M.C., Barcelo, D. (1998).** Strengths and limitations of immunoassays for effective and efficient use for pesticides in water sample: A review. *Anal. Chim. Acta* **362**, 3 – 34.

**Hochuli, E., Dobeli, H. and Schacher. (1987).** New metal chelate adsorbent selective for proteins and peptides containing neighbouring histidine residues. *J. Chromatogr.*, **411**, 177 – 184.

**Holliger, P., Prospero, T. and Winter, G. (1993).** “Diabodies:” small bivalent, and bispecific antibody fragments. *Proc. Natl. Acad. Sci. (USA)*, **90**, 6444 – 6448.

**Hoogenboom, H. and Winters, G. (1992).** By-passing immunisation: human antibodies from synthetic repertoires of germline V<sub>H</sub> gene segments rearranged *in Vitro*. *J. Mol. Biol.*, **227**, 381 – 388.

**Hoogenboom, H., de Bruine, A., Hufton, S., Hoet, R., Arends, J. and Roovers, R. (1998).** Antibody phage display technology and its applications. *Immunotechnology* **4**, 1-20.

**Hoover, D. and Friedlander, A. (1997)** Brucellosis. *Textbook of Military Medicine: Medical aspects of chemical and biological warfare: Chapter 5*, pp. 513 – 522.

**Hu, S., Shively, L., Raubitschek, A., Sherman, M., Williams, L., Wong, J., Shively, J. and Wu, A. (1996).** Minibody: A novel engineered anti-carcinoembryonic antigen antibody fragment (single-chain Fv-CH3) exhibits rapid, high-level targeting of xenografts. *Cancer Res.*, **56(13)**, 3055 - 3061.

**Hudson, P. and Kortt, A. (1999).** High avidity scFv multimers; diabodies and triabodies. *J. Immunol. Methods*, **231**, 177 - 189.

**Hunt, D., Bourdon, A., Wild, P and Crosby, N. (1978).** Use of high performance liquid chromatography combined with fluorescence detection for the identification and estimation of aflatoxins and ochratoxin in food. *J. Sci. Food Agric.* **29**, 234 – 238.

**Hussein, H. and Brasel, J. (2001).** Toxicity, metabolism and impact of mycotoxins on humans and animals. *Toxicology*, **167**, 101 – 134.

**Huston, J., Levinson, D., Mudgett-Hunter, M., Tai, M., Novotny, J., Margolies, M., Ridge, R., Brucoleri, R., Haber, E., Crea, R. and Oppermann, H. (1988).** Protein engineering of antibody binding sites: recovery of specific activity in an anti-digoxin single-chain Fv analogue produced in *Escherichia coli*. *Proc. Natl. Acad. Sci. (USA)*, **85**, 5879 – 5883.

**Ikonomou, L., Schneider, Y. and Agathos, S. (2003).** Insect cell culture for industrial production of recombinant proteins. *Appl. Microbiol. Biotechnol.*, **62**, 1 – 20.

**Iliades, P., Kortt, A. and Hudson, P. (1998).** Triabodies: single-chain Fv fragments without a linker form trivalent trimers. *FEBS letters*, **409**, 437 – 441.

**Ivnitske, D, Hamid, I., Atanasov, P. and Wilkins, E. (1999).** Biosensors for detection of pathogenic bacteria. *Biosensors Bioelectron.*, **14**, 599 – 624.

**Jacobson, R. (1998).** Validation of serological assays for the diagnosis of infectious diseases. *Rev. Sci. Tech. Off. Int. Epiz.*, **17(2)**, 469 – 486.

**Jacques, I., Olivier-Bernardin, V. and Dubray, G. (1998).** Efficacy of ELISA compared to conventional tests (RBPT and CFT) for the diagnosis of *Brucella melitensis* infection in sheep. *Vet. Microbiol.* **64**, 61-73.

**Jahans, K., Foster, G. and Broughton, E. (1997).** The characterisation of *Brucella* strains isolated from marine mammals. *Vet. Microbiol.*, **57**, 373 – 382.

**Jost, C., Kurucz, I., Jacobus, C., Titus, J., George, A. and Segal, D. (1994).** Mammalian expression and secretion of functional single-chain Fv molecules. *J. Biol. Chem.*, **269**, 26267 – 26273.

**Jumas-Bilak, E., Charachon, S., Bourg, G., O'Callaghan, D. and Ramuz, M. (1998).** Differences in chromosome number and genome rearrangements in the genus *Brucella*. *Mol. Microbiol.*, **27**, 99 – 106.

**Kabat, E., Wu, T., Reid-Miller, M., Perry, H., Gottesman, K., Foeller, C. (1991).** Sequences of proteins of immunological interest. US Department of Health and Human Services, Public Service, NIH, Washington, DC, USA (5<sup>th</sup> Edition).

**Keating, G.** Biosensor-based studies on coumarins. Ph.D. Thesis, Dublin City University, Dublin 9, Republic of Ireland, 1998.

**Kettleborough, C., Saldanha, J., Ansell, K. and Bendig, M. (1993).** Optimisation of primers for cloning libraries of mouse immunoglobulin genes using the polymerase chain reaction. *Eur. J. Immunol.*, **23**, 206 – 211.

**Killard, A.J., Deasy, B., O'Kennedy, R. and Smyth, M.R. (1995).** Antibodies: production, functions and applications in biosensors. *Trends Anal. Chem.* **14**, 257-267.

**Kipriyanov, S.M., Moldenhauer, G. and Little, M. (1997).** High level production of soluble single chain antibodies in small-scale *Escherichia coli* cultures. *J. Immunol. Methods* **200**, 69-77.

**Kittelberger, R., Diack, D., Vizcaino, N., Zygmunt, M. and Cloeckaert, A. (1998).** Characterisation of an immunodominant antigen in *Brucella ovis* and evaluation of its use in an enzyme-linked immunosorbent assay. *Vet. Microbiol.*, **59**, 213 – 227.

**Kittelberger, R., Hilbink, F., Hansen, M., Penrose, M., de Lisle, G., Lettesson, J., Garin-Bastuji, B., Searson, J., Fossati, C. and Cloeckaert, A. (1995).** Serological crossreactivity between *Brucella abortus* and *Yersinia enterocolitica* 0:9 I immunoblot analysis of the antibody response to *Brucella* protein antigens in bovine brucellosis. *Vet. Microbiol.*, **47**, 257 – 270.

**Kittelberger, R., Hilbink, F., Hansen, M., Ross, D., de Lisle, G., Cloeckaert, A. and de Bruyn, J. (1995).** Identification and characterisation of immunodominant antigens during the course of infection with *Brucella ovis*. *J. Vet. Diagn. Invest.*, **7**, 210 - 218.

**Kittelberger, R., Hilbink, F., Hansen, M., Ross, G., Joyce, M., Fenwick Heesemann, J., Wolf-Watz, H. and Nielsen, K (1995).** Serological cross-reactivity between *Brucella abortus* and *Yersinia enterocolitica* 0:9 II the use of *Yersinia* outer protein for the specific detection of *Yersinia enterocolitica* infections in ruminants. *Vet. Microbiol.*, **47**, 271 – 280.

**Kohler, G. and Milstein, C. (1975).** Continuous cultures of fused cells secreting antibody of predefined specificity. *Nature (London)*, **256**, 495 – 497.

**Korde, A., Pandey, U., Banerjee, S., Sarma, H., Hajare, S., Venkatesh, M., Sharma, A., Pillai, M. (2003).** Development of a radioimmunoassay procedure for aflatoxin B<sub>1</sub> measurement. *J. Agric. Food Chem.*, **51**(4), 843 – 846.

**Kortepeter, M. and Parker, G. (1999).** Potential biological weapons threats. *Emerg. Infect. Dis.*, **5**(4), 523 – 527.

**Krebber, A., Bornhauser, S., Burmester, J., Honegger, A., Willuda, J., Bosshard, H., Pluckthun, A. (1997).** Reliable cloning of functional antibody variable domains from hybridomas and spleen cell repertoires employing a reengineered phage display system. *J. Immunol. Methods*, **201**, 35 – 55.

**Kretzschmar, T., Aoustin, L., Zingel, O., Marangi, M., Vonach, B., Towbin, H. and Greiser, M. (1996).** High-level expression in insect cells and purification of secreted monomeric single-chain Fv antibodies. *J. Immunol. Methods*, **195**, 93 – 101.

**Kussak, A., Andersson, B., Andersson, K. (1995).** Immunoaffinity column clean-up for high-performance liquid chromatography determination of aflatoxins B<sub>1</sub>, B<sub>2</sub>, G<sub>1</sub>, G<sub>2</sub>, M<sub>1</sub> and Q<sub>1</sub> in urine. *J. Chromatogr. B Biomed. Appl.*, **672**(2), 253 – 259.

**La Vallie, E., DiBlasio, E., Kovacic, S., Grant, K., Schendel, P., and McCoy, J. (1993).** A thioredoxin gene fusion system that circumvents inclusion body formation in the *E. coli* cytoplasm. *Bio/Technology*, **11**, 187 – 193.

**Laemmli, U. (1970).** Cleavage of structural proteins during the assembly of the head of bacteriophage T4. *Nature (London)*, **227**, 680 – 685.

**Lang, I., Barbas, C. and Schleef, R. (1996).** Recombinant rabbit Fab with binding activity to type-1 plasminogen activator inhibitor derived from a phage display library against human alpha-granules. *Gene*, **172**, 295 – 298.

**Langone, J., Van Vunakis, H. (1976).** Aflatoxin B; Specific antibodies and their use in radioimmunoassay. *J. Natl. Cancer Inst.*, **56(3)**, 591 – 595.

**Lawrence, L., Kortt, A., Iliades, P., Tulloch, P. and Hudson, P. (1998).** Orientation of antigen binding sites in dimeric and trimeric single-chain Fv antibody fragments. *FEBS Letters*, **425**, 479 – 484.

**Leumelle, C., Chardes, T., Montavon, C., Chaabihi, H., Mani, J., Pungiere, Cerutti, M., Devauchelle, G., Pau, B. and Biard-Piechaczyk, M. (1998).** Anti-digoxin scFv fragments expressed in bacteria and in insect cells have different antigen binding properties. *FEBS Lett.*, **423**, 159 – 166.

**Leung, D., Chen, E. and Goeddel, D. (1989).** A method for random mutagenesis of a defined DNA segment using a modified polymerase chain reaction. *Technique*, **1**, 11 - 15.

**Lewis, S. (1994).** The mechanism of V(D)J joining: Lessons from molecular, immunological and comparative analyses. *Advances in Immunology*, **56**, 27 - 150.

**Liautard, J., Gross, A., Dornand, J. and Kohler, S. (1996).** Interactions between professional phagocytes and *Brucella* species. *Microbiologia.*, **12(2)**, 197 – 206.

**Liedberg, B., Nylander, C and Lundstrom I. (1995).** Biosensing with surface plasmon resonance--how it all started. *Biosens. Bioelectron.*, **10(8)**, 1 - 9.

**Lindner, P., Bauer, K., Krebber, A., Nieba, L., Kremmer, E., Krebber, C., Honegger, A., Klingler, B., Mocikat, R. and Pluckthun, A. (1997).** Specific detection of his-tagged proteins with recombinant anti-his tag scFv-phosphatase or scFv-phage fusions. *Bio/Techniques*, **22(1)**, 140 – 149.

**Lindquist, E., Marks, J., Kleba, B. and Stephens, R. (2002).** Phage-display antibody detection of *Chlamydia trachomatis*-associated antigens. *Microbiol.*, **148**, 443 – 451.

**Littlefield, J.** (1964). Selection of hybrids from matings of fibroblasts *in vitro* and their presumed recombinants. *Science* **145**, 709 – 710.

**Liu, X., Zhang, S., Pan, X. and Wang, C.** (1999). A novel method for increasing production of mature proteins in the periplasm of *Escherichia coli*. *Protein Science*, **8**, 2085 – 2089.

**Longstaff, M., Newell, C., Boonstra, B., Strachan, G., Learmonth, D., Harris, W., Porter, A., Hamilton, W.** (1998). Expression and characterisation of single-chain antibody fragments produced in transgenic plants against the organic herbicides atrazine and paraquat. *Anal. Biochem.*, **1381**, 147 – 160.

**Mahler, S., Marquis, C., Brown, G., Roberts, A. and Hoogenboom, H.** (1997). Cloning and expression of human V-genes derived from phage display libraries as fully assembled human anti-TNF $\alpha$  monoclonal antibodies. *Immunotechnology*, **3**, 31 – 43.

**Male, S., Cooke, A., Owen, M., Trowsdale, J. and Champion, B.** (1996). *Advanced Immunology*, Chapter 8, pp. 8.2 – 8.15. Mirror International Publishers, London, UK.

**Malmborg, A., Duenas, M., Ohlin, M., Soderlind, E. and Borrebaeck, C.** (1996). Selection of binding from phage-displayed antibody libraries using the Biacore biosensor. *J. Immunol. Meth.*, **198**, 51 – 57.

**Marks, J., Griffiths, A., Malmqvist, M., Clackson, T., Bye, J. and Winter, G.** (1992). By-passing immunisation: building high affinity human antibodies by chain shuffling. *Bio/Technology*, **10**, 779.

**Marks, J., Hoogenboom, H., Bonnert, T., McCafferty, J., Griffiths, A. and Winter, G.** (1991). By-passing immunisation: human antibodies from V-gene libraries displayed on phage. *J. Mol. Biol.*, **222**, 581 – 597.

**May, K.** (1991). Home tests to monitor fertility. *Am. J. Obstet. Gynecol.*, **165**, 2000 – 2002.

**McCafferty, J., Griffiths, A., Winter, G. and Chiswell, D. (1990).** Phage antibodies: filamentous phage displaying antibody variable domains. *Nature (London)*, **348**, 552 – 554.

**McElhiney, J., Lawton, L., Porter, A.** Detection and quantification of microcystins (cyanobacterial hepatotoxins) with recombinant antibody fragments isolated from a naïve human phage display library. *FEMS Microbiol. Lett.*, 2000, **193**, 83 – 88.

**McGiven, J.A., Tucker, J.D., Perrett, L.L., Stack, J.A., Brew, S.D., and MacMillan, A.P. (2003).** Validation of FPA and cELISA for the detection of antibodies to *Brucella abortus* in cattle sera and comparison to SAT, CFT, and iELISA. *J. Immunol. Methods*, **278**, 171 – 178.

**Michaux, S., Paillisson, J., Nurit, M., Bourg, G., Servent, A and Ramuz, M. (1993).** Presence of two independent chromosomes in the *Brucella melitensis* 16M genome. *J. Bacteriol.*, **175**, 701 – 705.

**Moghaddam, A., Løbersli, I., Gebhardt, K., Braunagel, M., Marvik, O.** Selection and characterisation of recombinant single-chain antibodies to the hapten aflatoxin B<sub>1</sub> from naïve recombinant antibody libraries. *J. Immunol. Methods*, 2001, **254**, 169 – 181.

**Moreno, W., Cloeckert, A. and Moriyon, I. (2002).** *Brucella* evolution and taxonomy. *Vet. Microbiol.*, **90**, 209 – 227.

**Morgan, W., Mackinnon, D., Lawson, J. and Culle, G. (1969).** The Rose Bengal plate agglutination test in the diagnosis of brucellosis. *Vet. Rec.*, **85**, 636-641.

**Müller, K., Arndt, K., Bauer, K. and Plückthun, A. (1998).** Tandem immobilised metal-ion affinity chromatography / immunoaffinity purification of His-tagged proteins – Evaluation of two anti-His-tag monoclonal antibodies. *Anal. Biochem.*, **259**, 54 – 61.

**Nawaz, S., Coker, R., Haswell, S. (1995).** HPTLC-A valuable chromatographic tool for the analysis of aflatoxins. *Planar Chromatogr.* **8**, 4 – 9.

**Nielsen, K., Gall, D., Jolley, M., Leishman, G., Balsevicius, S., Smith, P., Nicoletti, P. and Thomas, F. (1996).** A homogeneous fluorescence polarization assay for detection of antibody to *Brucella abortus*. *Jour. Immunol. Methods* **195**, 161-168.

**Nielsen, K., Gall, D., Smith, P., Vigliocco, A., Perez, B., Samartino, L., Nicoletti, P., Dajer, A., Elzer, P. and Enright, F. (1999).** Validation of the fluorescence polarization assay as a serological test for the presumptive diagnosis of porcine brucellosis. *Vet. Microbiol.* **68**, 245-253.

**Nielsen, K., Kelly, L., Gall, D., Nicoletti, P. and Kelly, W. (1995).** Improved competitive enzyme immunoassay for the diagnosis of bovine brucellosis. *Veterinary Immunology and Immunopathology*, **46**, 285 – 291.

**Niessen, M., Wichers, J., Lee, H., Alcocer, M., Morgan, M., van Amerongen, A.** Rapid sol particle immunoassay for the detection of aflatoxin in food products. European research towards safer and better food, Karlsruhe, Germany, Oct. 18 – 20, 1998.

**Nissim, A., Hoogenboom, H., Tomlinson, I., Flynn, G., Midgley, C., Lane, D. and Winter, G. (1994).** Antibody fragments from a single pot phage display library as immunochemical reagents. *EMBO*, **13**(3), 692 – 698.

**O’Kennedy, R. and Thornes, R. (1997).** Coumarins, Biology, Applications and Mode of Action, Chapter 2, pp. 23 – 67. Wiley: Chichester, UK.

**Oliveira, S., Soeurt, N. and Splitter, G. (2002).** Molecular and cellular interactions between *Brucella abortus* antigens and host immune responses. *Vet. Microbiol.*, **90**, 417 – 424.

**Owen, M., Gandecha, A., Cockburn, B. and Whitelam, G. (1992).** Synthesis of a functional anti-phytochrome single chain Fv protein in transgenic tobacco. *Bio/Technology*, **10**, 790 – 794.

**Pack, P. and Pluckthun, A. (1992).** Miniantibodies: use of amphipathic helices to produce functional, flexibly linked dimeric FV fragments with high avidity in *Escherichia coli*. *Biochemistry*, **31**(6), 1579 - 1584.

**Pack, P., Kujau, M., Schroeckh, V., Knupfer, U., Wenderoth, R., Riescnberg, D. and Pluckthun, A. (1993).** Improved bivalent miniantibodies with identical avidity as whole antibodies, produced by high cell density fermentation of *Escherichia coli*. *Bio/Technology*, **11**, 1271 – 1277.

**Pal, A. and Dhar, T. (2004).** An analytical device for on-site immunoassay. Demonstration of its applicability in semi quantitative detection of aflatoxin B<sub>1</sub> in a batch of samples with ultra high sensitivity. *Anal. Chem.* **76**, 98 – 104.

**Pasqualini, R. and Ruoslahti, (1996).** Organ targeting *in vivo* using phage display peptide libraries. *Nature (London)*, **380**, 364 – 366.

**Paulsen, I., Seshadri, R., Nelson, K., Eisen, J., Heidelberg, J., Read, T., Dodson, R., Umayam, L., Brinkac, L., Beenan, M., Daugherty, S., Deboy, T., Durkin, A., Kolonay, J., Madupu, R., Nelson, W., Ayodeji, B., Kraul, M., Shetty, J., Malek, J., Van Aken, S., Riedmuller, S., Tettelin, H., Gill, S., White, O., Salzberg, S., Hoover, D., Lindler, E., Halling, S., Boyle, S. and Fraser, C. (2002).** The *Brucella suis* genome reveals fundamental similarities between animal and plant pathogens and symbionts. *Proc. Natl. Acad. Sci. (USA)*, **99**(20), 13148 – 13153.

**Pelkonen, P., Lang, M., Negishi, M., Wild, C. and Juvonen, (1997).** R. Interaction of aflatoxin B<sub>1</sub> with cytochrome P450 2A5 and its mutants: Correlation with metabolic activation and toxicity. *Chem. Res. Toxicol.* **10**, 85 – 90.

**Persic, L., Roberts, A., Wilton, J., Cattaneo, A., Bradbury, A. and Hoogenboom, H. (1997).** An integrated vector system for the eukaryotic expression of antibodies or their fragments after selection from phage display libraries. *Gene*, **10**(187), 9 – 18.

**Pfund, W. and Bourdage, J. (1990).** The conformation-sensitive immunoassay: a membrane-based ELISA system for identifying antibodies sensitive to alterations of protein conformation. *Mol Immunol.*, **27**(6), 495 - 502.

**Porath, J., Carlsson, J., Olsson, I and Belfrage, G. (1975).** Metal chelate affinity chromatography, a new approach to protein fractionation. *Nature (London)*, **258**, 598 – 599.

**Porte, F., Liautard, J. and Kohler, S. (1999).** Early acidification of phagosomes containing *Brucella suis* is essential for intracellular survival in murine macrophages. *Infect. Immun.*, **67**(8), 4041 – 4047.

**Porter, R. (1991).** Lecture for the Nobel Prize for physiology or medicine 1972: Structural studies of immunoglobulins. *Scand. J. Immunol.*, **34**(4), 381 - 389.

**Pou, K., Ong, H., Adam, A., Lamothe, P. and Delahaut, P. (1994).** Combined immunoextraction approach coupled to a chemiluminescence enzyme immunoassay for the determination of trace levels of salbutamol and clenbuterol in tissue samples. *Analyst*, **119**(12), 2659 - 2662.

**Quinn, J. and O’Kennedy, R. (1999)** Transduction platforms and biointerfacial design of biosensors for ‘real-time’ biomolecular interaction analysis. *Anal. Letters*, **32**, 1475 – 1517.

**Raifie-Kolpin, M., Essenberg, R. and Wyckoff, J. (1996).** Identification and comparison of macrophage-induced proteins and proteins induced under various stress conditions in *Brucella abortus*. *Infect. Immun.*, **64**(12), 5274 – 5283.

**Rees, A.R., Staunton, D., Webster, D.M., Searle, S.J., Henry, A.H. and Pedersen, J.T. (1994).** Antibody design: beyond the natural limits. *Tibtech*, **12**, 199-206.

**Reiter, Y., Brinkmann, U., Kreitmann, R., Jung, S., and Lee, B. (1994).** Stabilisation of the Fv fragments in recombinant immunotoxins by disulphide bonds engineered into conserved framework regions. *Biochemistry*, **33**, 5451 - 5459.

**Ridder, R., Geisse, S., Kleuser, B., Kawalleck, P. and Gram, H. (1995).** A COS-cell-based system for rapid production and quantification of scFv:IgC kappa antibody fragments. *Gene*, **166**, 273 – 276.

**Riley, L. and Robertson, D. (1984).** Ingestion and intracellular survival of *Brucella abortus* in human and bovine polymorphonuclear leukocytes. *Infect. Immun.*, **46**(1), 224 – 230.

**Robinson-Dunn, B. (2002).** The microbiology laboratory’s role in response to bioterrorism. *Arch. Pathol. Lab. Med.*, **126**, 291 – 294.

**Roitt, I., Brostoff, J. and Male, D. (1989).** Immunology, 2<sup>nd</sup> edn., Gower Medical Publishing, London, UK.

**Rondot, S., Koch, J., Breitling, F. and Dubel, S. (2001).** A helper phage to improve single-chain antibody presentation in phage display. *Nature Biotechnology* **19**, 75-78.

**Rosen, R., Rosen, J. and DiProssimo, V. (1984).** Confirmation of aflatoxins B<sub>1</sub> and B<sub>2</sub> in peanuts by gas chromatography / mass spectrometry / selected ion monitoring. *J. Agric. Food Chem.* **32**, 276 – 278.

**Ross, H., Jahans, K., MacMillan, A., Reid, R., Thompson, P and Foster, G. (1996).** *Brucella* species infection in North Sea seal and cetacean populations. *Vet. Rec.*, **138**, 647 – 648.

**Rossetti, O.L., Arese, A.I., Boschioli, M.L. and Cravero, S.L. (1996).** Cloning of *Brucella abortus* gene and characterisation of expressed 26-kilodalton periplasmic protein: Potential use for diagnosis. *J. Clin. Microbiol.* **34**, 165-169.

**Rotz, L., Khan, A., Lilibridge, S., Ostroff, M. and Hughes, J. (2002).** Public health assessment of potential biological terrorism agents. *Emerg. Infect. Dis.*, **8**(2), 225 – 230.

**Salamon, Z., Brown, M. and Tollin G. (1999).** Plasmon resonance spectroscopy: probing molecular interactions within membranes. *Trends Biochem. Sci.*, **24**(6), 213 - 219.

**Sanchez, D., Zandomeni, R., Cravero, S., Verdun, R., Pierrou, E., Faccio, P., Diaz, G., Lanzavecchia, S., Agüero, F., Frasch, A., Andersson, S., Rossetti, O., Grau, O. and Ugalde, R. (2001).** Gene discovery through genomic sequencing of *Brucella abortus*. *Infect. Immun.*, **69**(2), 865 – 868.

**Sangari, F. and Agüero, J. (1996).** Molecular basis of *Brucella* pathogenicity: an update. *Microbiologia.*, **12**(2), 207 – 218.

**Schaffitzel, C., Hanes, J., Jermutus, L. and Pluckthun, A. (1999).** Ribosome display: an *in vitro* method for selection and evolution of antibodies from libraries. *J. Immunol. Methods*, **231**, 119 - 135.

**Schier, R., Bye, J. and Apell, G. (1996).** Isolation of high affinity monomeric human anti-c-erbB-2 single chain Fv using affinity driven selection. *J. Mol. Biol.*, **255**, 28 – 43.

**Schneider, E., Usleber, E., Martlbauer, E., Dietrich, R., Terplan, G. (1995).** Multimycotoxin dipstick enzyme immunoassay applied to wheat. *Food Additives and Contaminants*, **12**(3), 387 – 393.

**Schurig, G., Sriranganathan, N and Corbel, M. (2002).** Brucellosis vaccines: past, present and future. *Vet. Microbiol.*, **90**, 479 – 496.

**Shamelian, S.O.A. (2000).** Diagnosis and treatment of brucellosis. *The Netherlands Journal of Medicine* **56**, 198-199.

**Shusta, E., Raines, R. and Pluckthun, A. (1998).** Increasing the secretory capacity of *Saccharomyces cerevisiae* for production of single-chain antibody fragments. *Nature Biotechnol.*, **16**, 773 – 777.

**Sibanda, L., De Saeger, S. and Van Peteghem, C. (1999).** Development of a portable field immunoassay for the detection of aflatoxin M<sub>1</sub> in milk. *International Journal of Food Microbiology*, **48**, 203 – 209.

**Smela, M., Currier, S., Bailey, E. and Essigmann, J. (2001).** The chemistry and biology of aflatoxin B<sub>1</sub>: from mutational spectrometry to carcinogenesis. *Carcinogenesis* **22**(4), 535 – 545.

**Smith, D. and Johnson, K. (1988).** Single-step purification of polypeptides expressed in *Escherichia coli* as fusions with glutathione S-transferase. *Gene*, **67**, 31 – 40.

**Smith, G. (1985).** Filamentous fusion phage: novel expression vectors that display cloned antigens on the virion surface. *Science*, **228**, 1315 – 1316.

**Stack, J., Perrett, L., Brew, S. and MacMillan, A. (1999).** Competitive ELISA for bovine brucellosis suitable for testing poor quality samples. *Vet. Rec.*, **145**(25), 735 – 736.

**Stemmer, W. (1994).** Rapid evolution of a protein in vitro by DNA shuffling. *Nature (London)*, **370**, 389 – 391.

**Stenberg, E., Persson, B., Roos, H. and Urbaniczky, C. (1991).** Quantitative determination of surface concentration of protein with surface plasmon resonance using radiolabeled proteins. *J. Colloid Interface Sci.*, **143**, 513 - 526.

**Strachan, G., Whyte, J. Molloy, P., Paton, G., and Porter, A. (2000).** Development of robust, environmental, immunoassay formats for the quantification of pesticides in soil. *Environ. Sci. Technol.*, **34** (8), 1603 – 1608.

**Stuber, D., Bannwarth, W., Meloen, R. and Matile, H. (1990).** New B cell epitopes in the *Plasmodium falciparum* malaria circumsporozoite protein. *Eur. J. Immunol.*, **20**, 819 – 824.

**Sun, C., Wirsching, P. and Janda, K. (2002).** Enabling ScFvs as multi-drug carriers: a dendritic approach. *Bioorg. Med. Chem.*, **11**(8), 1761 - 1768.

**Suzuki, M., Takayanagi, A. and Shimizu, N. (2003).** Recombinant single-chain antibodies with various oligopeptide tails for targeted gene delivery. *Gene Ther.*, **10**(9), 781 - 788.

**Swartz, J. (2001).** Advances in *Escherichia coli* production of therapeutic proteins. *Curr. Opin. Biotechnol.*, **12**, 195 – 201.

**Toth, T.E., Cobb, J.A., Boyle, S.M., Roop, R.M. and Schurig, G.G. (1995).** Selective humoral immune response of Balb/C mice of *Brucella abortus* proteins expressed by vaccinia virus recombinants. *Vet. Microbiol.* **45**, 171-183.

**Uzal, F., Carrasco, A. and Nielsen, K. (1996)** Evaluation of a competitive ELISA for the diagnosis of bovine brucellosis. *Vet. Res. Commun.*, **20**(5), 421 – 426.

**Uzal, F., Carrasco, A. and Nielsen, K. (1996)** Evaluation of a competitive ELISA for the diagnosis of bovine brucellosis. *Vet. Res. Commun.*, **20**(5), 421 – 426.

**Van Amerongen, A., Loon, D., Berendsen, L. and Wichers, J. (1994).** Quantitative computer image analysis of a human chronic gonadotropin colloidal carbon dipstick assay. *Clin. Chim. Acta*, **229**, 67 – 75.

**Van Der Gaag, B., Wahlstrom, L., Burggraaf, R., Stigter, E., Burstoff-Asp, C.** Application development on the BIAcore for the detection of mycotoxins in food and feed). Seventh BIA symposium, Edinburgh, UK, Sep 2 – 4 1998.

**Van Emon, J.M., Seiber, J.N. and Hammock, B.D. (1989).** Immunoassay techniques for pesticide analysis. In: Sherma, J. (ed.), Analytical methods for pesticides and plant growth regulators (Volume XVII: Advanced analytical techniques), Academic Press, San Diego, 217-261.

**Vanzini, V., Aguirre, N., Lugaresi, C., de Echaide, S., Canavesio, V., Guglielmo, A., Marchesino, M. and Nielsen, K. (1998).** Evaluation of an indirect ELISA for the diagnosis of bovine brucellosis in milk and serum samples in dairy cattle in Argentina. Preventive Veterinary Medicine, **36**, 211 – 217.

**Vaughan, T., Williams, A., Pritchard, K., Osbourn, J., Pope, A., Earnshaw, J., McCafferty, J., Hodits, R., Wilton, J and Johnson, K. (1996).** Human antibodies with sub-nanomolar affinities isolated from a large non-immunised phage display library. Nature Biotechnol., **14**, 309 – 314.

**Verstrete, D., Creasy, M., Caveney, N., Baldwin, C., Blab, M. and Winter, A. (1982).** Outer membrane proteins of *Brucella abortus*: isolation and characterisation. Infect. Immun., **35**(3), 979 – 989.

**Wang, Y., Liang, Z., Zhang, Y., Yao, S., Xu, Y., Tang, Y., Zhu, S., Cui, D. and Feng, Y. (2001).** Human insulin from a precursor over-expressed in the methylotrophic yeast *Pichia pastoris* and a simple procedure for purifying the expression product. Biotechnol. Bioengin., **73**, 74 – 79.

**Ward, C.M., Wilkinson, A.P., Bramham, S, Lee, H.A., Chan, H., Butcher, G., Hutchings, A., Morgan, M.R.A. (1990).** Production and characterisation of polyclonal and monoclonal antibodies against aflatoxin B<sub>1</sub>-oxime-BSA in an enzyme-linked immunosorbent assay. Mycotoxin Res., **6**, 73 – 83.

**Ward, R., Clark, M., Lees, J. and Hawkins, N. (1996).** Retrieval of human antibodies from phage-display libraries using enzymatic cleavage. J. Immunol. Methods, **189**, 73 – 82.

**Waterhouse, P., Griffiths, A., Johnson, K. and Winter, G. (1993).** Combinatorial infection and *in vivo* recombination: a strategy for making large phage antibody repertoires. *Nucleic Acid Res.*, **21**, 2265 – 2266.

**Wennig, R., Moeller, M., Haguenoer, J., Marocchi, A., Zoppi, F., Smith, B., de la Torre, R., Carstensen, C., Goerlach-Graw, A., Schaeffler, J. and Leinberger R. (1998).** Development and Evaluation of Immunochromatographic Rapid Tests for Screening of Cannabinoids, Cocaine, and Opiates in Urine. *J. Anal. Toxicol.*, **22**, 148 – 155.

**Wild, D. and Davies, C. (1994).** Components. In: Wild, D. (ed), *The immunoassay handbook*, Stockton Press, New York, pp. 49-82.

**Woloshuk, C. and Prieto, R. (1998).** Genetic organisation and function of the aflatoxin B<sub>1</sub> biosynthetic genes. *FEMS Microbiol. Lett.*, **160**, 169 – 176.

**Wong, R., Mytych, D., Jacobs, S., Bordens, R., Swanson, S. (1997).** Validation parameters for a novel biosensor assay which simultaneously measures serum concentrations of a humanized monoclonal antibody and detects induced antibodies. *J. Immunol. Methods*, **209**, 1 – 15.

**Wright, A. and Morrison, S. (1997).** Effects of glycosylation on antibody function: implications for genetic engineering. *Tibtech*, **15**, 26 – 32.

**Wright, P., Nilsson, E., Van Rooij, E., Lelenta, M. and Jeggo, M. (1993).** Standardisation and validation of enzyme-linked immunosorbent assay techniques for the detection of antibody in infectious disease diagnosis. *Rev. Sci. Tech. Off. Int. Epiz.*, **12**, 435 – 450.

**Wurm, F. and Bernard, A. (1999).** Large-scale transient expression in mammalian cells for recombinant protein production. *Curr. Opin. Biotechnol.*, **10**, 156 – 159.

**Yalow, R. and Berson, S. (1959).** Assay of plasma insulin in human subjects by immunological methods. *Nature (London)*, **184**, 1648 – 1649.

**Yamanaka, H., Inoue, T. and Ikeda-Tanaka, O. (1996).** Chicken monoclonal antibody isolated from a phage display system. *J. Immunol.*, **157**, 1156 – 1162.

**Young, N., MacKenzie, C., Narang, S., Oomen, R. and Baenziger, J. (1995).** Thermal stabilization of a single-chain Fv antibody fragment by introduction of a disulphide bond. *FEBS Lett.*, **377**(2), 135 - 139.

**Yuan, Q., Clarke, J., Zhou, H., Lonz, J., Peska, J., Hart, L. (1997).** Molecular cloning, expression and characterisation of a functional single-chain Fv antibody to the mycotoxin zearalenone. *Appl. Environ. Microbiol.*, **63**, 263 – 269.

**Zahnd, C., Spinelli, S., Luginbuhl, B., Amstutz, P., Cambillau, C. and Pluckthun, A. (2004).** Directed *in vitro* evolution and crystallographic analysis of a peptide-binding single chain antibody fragment (scFv) with low picamolar affinity. *J. Biol. Chem.*, **279**(18), 18870 – 18877.

**Zhan, Y. and Cheers, C. (1993).** Endogenous gamma interferon mediates resistance to *Brucella abortus* infection. *Infect. Immun.*, **61**(11), 4899 – 4901.

**Zhan, Y., Kelso, A and Cheers, C. (1993).** Cytokine production in the murine response to *Brucella* infection or immunization with antigenic extracts. *Immunology*, **80**(3), 458 – 464.

**Zhan, Y., Yang, J. and Cheers, C. (1993).** Cytokine response to T-cell subsets from *Brucella abortus* infected mice to soluble *Brucella* proteins. *Infect. Immun.*, **61**(7), 2841 – 2847.

**Zhou, B., Wirsching, P and Janda, K. (2002).** Human antibodies against spores of the genus *Bacillus*: A model study for the detection of and protection against anthrax and the bioterrorist threat. *Proc. Natl. Acad. Sci. (USA)*, **99**(8), 5241 – 5246.

**Zygmunt, M., Baucheron, S., Vizcaino, N., Bowden, R. and Cloeckaert, A. (2002).** Single-step purification and evaluation of recombinant BP26 protein for serological diagnosis of *Brucella ovis* infection in rams. *Vet. Microbiol.*, **87**, 213 – 220.

**Zygmunt, M., Cloeckaert, A. and Dubray, G. (1994).** *Brucella melitensis* cell envelope protein and lipopolysaccharide epitopes involved in humoral immune response of naturally and experimentally infected sheep. *J. Clin. Microbiol.*, **32**, 2514 – 2522.

## APPENDIX A

## **Safety precautions**

### **Aflatoxin B<sub>1</sub>**

Aflatoxin B<sub>1</sub> is a potent carcinogen that can cause heritable genetic damage. It is very toxic by inhalation, in contact with skin and if swallowed. All aflatoxin related work must be conducted within a fumehood. Personal protective clothing including gloves, safety goggles and a lab coat must be worn at all times. Spillages should be cleaned up immediately using 12% (v/v) hypochlorite. All aflatoxin B<sub>1</sub> contaminated waste must be decontaminated as follow:

- An equal volume of 12% (v/v) hypochlorite is added to the contaminated waste and left standing for 30 mins.
- The pH of the waste is then adjusted to 8.0 and left standing for 30 mins.
- Then 5% (v/v) acetone is added and the waste left standing for 30 mins.
- The decontaminated waste can then be disposed.

### ***Brucella abortus***

*B. abortus* is a class III pathogen and live cultures must only be handled in a certified biological safety cabinet. Therefore, all *B. abortus* cells used during this research were received heat-killed from the Blood Testing Laboratory, Department of Agriculture, Food and Fisheries, Cork.